Expanding the Scope of Poly(ethylene glycol)s for Bioconjugation to Squaric Acid-Mediated PEGylation and pH-Sensitivity

Dissertation zur Erlangung des Grades eines
`Doktor rerum naturalium (Dr. rer. nat.)' der Fachbereiche:

Physik, Mathematik und Informatik (FB 08),
Chemie, Pharmazie und Geowissenschaften (FB 09),
Biologie (FB 10),
Universitätsmedizin

der Johannes Gutenberg-Universität

Carsten Dingels

Mainz 2013

JOHANNES GUTENBERG UNIVERSITÄT MAINZ

Max Planck Graduate Center
mit der Johannes Gutenberg-Universität Mainz

Reviewer 1:

Reviewer 2:

Date of oral examination: January 21, 2013

I hereby declare that I wrote the dissertation submitted without any unauthorized external assistance and used only sources acknowledged in the work. All textual passages which are appropriated verbatim or paraphrased from published and unpublished texts as well as all information obtained from oral sources are duly indicated and listed in accordance with bibliographical rules. In carrying out this research, I complied with the rules of standard scientific practice as formulated in the statutes of Johannes Gutenberg-University Mainz to insure standard scientific practice.

Meinen Eltern

"*There are two possible outcomes: If the result confirms the hypothesis, then you've made a measurement. If the result is contrary to the hypothesis, then you've made a discovery.*"

Enrico Fermi

Danksagung

Table of Contents

Motivation and Objectives

One of the most common polymers found in everyday products and produced on a multi-million-ton scale per annum is poly(ethylene glycol) (PEG), also known as poly(ethylene oxide) (PEO) and poly(oxyethylene) (POE). Although this synthetic polymer consists of a simple, linear polyether structure, it exhibits a unique combination of properties which attracts the interest in a broad range of fields of applications in both academia as well as in industry. PEG is chemically inert, non-toxic, almost non-immunogenic, soluble in a wide range of organic solvents and highly water-soluble, which is unexpected when regarding the aliphatic polyether structure. In result, the polymer is most suitable to serve as the hydrophilic segment in nonionic surfactants for products getting closest to its user, such as body-care products and edibles. Other fields of applications include breathable fabrics, the conservation of waterborne wooden artifacts and biomedical applications.

Among the latter, PEG is known as a shielding component in drug delivery systems. The socalled "PEGylation", i.e., the covalent attachment of PEG chains, to therapeutically active proteins has gathered immense attention and has become a multi-billion-dollar market in the last three decades, with several polymer therapeutics approved by the Food and Drug Administration (FDA). Direct application of the respective proteins suffers from their inherent disadvantages, such as their rapid proteolytic degradation and frequently found immunogenicity. The PEGylation of therapeutically active proteins slows down their proteolytic degradation, reduces their renal filtration rate and lowers their immunogenicity. In summary, these effects lead to significantly prolonged blood circulation times. Since the polyether impedes protein/ligand or protein/receptor interactions, a reduction of the protein's *in vitro* bioactivity commonly is observed upon PEGylation. In numerous cases, the use of branched PEG architectures instead of linear chains has been proven to be advantageous: The resulting polymer/protein conjugates are less immunogenic, undergo slower proteolysis, exhibit higher *in vitro* bioactivities, and show highly prolonged body residence times compared to their linear derivatives.

Despite these valuable characteristics, some important drawbacks remain: PEG is not biodegradable and parenterally applied, PEG conjugates must consist of polyether chains that do not exceed a certain molecular weight limit (usually 30,000 g/mol). Otherwise the polymer

cannot be excreted and accumulates in the liver, leading to storage diseases and potentially liver cancer. Furthermore, the PEG derivatives used in PEGylation usually are employed as poly(ethylene glycol) monomethyl ethers (mPEGs) in multi-step processes and the polymers lack an additional functional group that could be used for further derivatization, such as the attachment of labels or targeting moieties. Also, the loss of efficiency of PEGylated proteins due to the accelerated clearance induced by anti-PEG antibodies has been observed to be more severe for conjugates prepared from mPEGs than from α-activated ω-hydroxyl-PEGs.

The objectives of the current thesis were:

(i) The establishment of diethyl squarate, a successful coupling agent for the generation of neoglycoproteins that is highly selective for amines in the presence of multiple hydroxyl groups, as a linker for the attachment of α-amino PEGs to proteins and the development of novel heterofunctional poly(ethylene glycol) structures suitable for bioconjugation.

(ii) Generation of novel heteromultifunctional polyether structures, in particular α-amino ω_2-dihydroxyl star-shaped three-arm PEG, which is a promising candidate for the squaric acid mediated PEGylation with branched polymer architecture.

(iii) Generation of novel heterobifunctional, linear PEGs with a single acid-labile moiety either at the conjugation site to enable the detachment of the polymer from the protein at the place of action or at a controlled position in the main chain to obtain biodegradable PEGs.

(iv) The synthetic strategies to these heterofunctional PEGs should be straightforward, involve only a few steps and result in well-defined polyethers, which required full conversion in all postpolymerization reactions and narrowly distributed molecular weights of the polydisperse products.

The systematic exploration of the squaric acid mediated PEGylation was carried out using amino mPEGs, protected lysine derivatives and bovine serum albumin (BSA) as model compounds. The reactivity of the activated PEGs was investigated employing reaction kinetics followed by ^{1}H NMR spectroscopy and sodium dodecyl sulfate - polyacrylamide gel electrophoresis (SDS-PAGE). Further, preliminary studies on the biocompatibility of the novel conjugates were carried out.

For the syntheses of acid-labile PEGs, a universal strategy for the implementation of acetals into initiators for the anionic ring-opening polymerization of epoxides was developed and tested by the modification of various established initiators, i.e., cholesterol, *N*,*N*-dibenzylamino ethanol, and mPEG. All polymers were examined regarding their degradability under acidic conditions.

The heterofunctional star-shaped PEG was synthesized by polymerizing ethylene oxide (EO) from a divalent macroinitiator carrying a primary and a secondary hydroxyl group. To investigate the influence of the chemical nature of the initiating site, a novel divalent initiator was developed, which consisted of a primary and a secondary hydroxyl group separated by an acetal moiety.

In the appendix, several chapters summarize contributions to other areas of polyether chemistry that evolved out of the topics treated in this thesis in the context of collaborations with colleagues in the Frey group.

Supporting Informations quoted in the text always refer to the Supporting Information found at the end of the respective chapter.

Abstract

Poly(ethylene glycol) (PEG) is used in a broad range of applications due to its unique combination of properties and approved use in formulations for body-care products, edibles and medicine. This thesis aims at the synthesis and characterization of novel heterofunctional PEG structures and the establishment of diethyl squarate as a suitable linker for the covalent attachment to proteins.

Chapter 1 is an introduction on the properties and applications of PEG as well as the fascinating chemistry of squaric acid derivatives. In **Chapter 1.1**, the synthesis and properties of PEG are described, and the versatile applications of PEG derivatives in everyday products are emphasized with a focus on PEG-based pharmaceuticals and nonionic surfactants. This chapter is written in German, as it was published in the German Journal *Chemie in unserer Zeit*. **Chapter 1.2** deals with PEGs major drawbacks, its non-biodegradability, which impedes parenteral administration of PEG conjugates with polyethers exceeding the renal excretion limit, although these would improve blood circulation times and passive tumor targeting. This section gives a comprehensive overview of the cleavable groups that have been implemented in the polyether backbone to tackle this issue as well as the synthetic strategies employed to accomplish this task. **Chapter 1.3** briefly summarizes the chemical properties of alkyl squarates and the advantages in protein conjugation chemistry that can be taken from its use as a coupling agent.

In **Chapter 2**, the application of diethyl squarate as a coupling agent in the PEGylation of proteins is illustrated. **Chapter 2.1** describes the straightforward synthesis and characterization of squaric acid ethyl ester amido PEGs with terminal hydroxyl functions or methoxy groups. The reactivity and selectivity of theses activated PEGs are explored in kinetic studies on the reactions with different lysine and other amino acid derivatives, followed by ^{1}H NMR spectroscopy. Further, the efficient attachment of the novel PEGs to a model protein, i.e., bovine serum albumin (BSA), demonstrates the usefulness of the new linker for the PEGylation with heterofunctional PEGs. In **Chapter 2.2**, initial studies on the biocompatibility of polyether/BSA conjugates synthesized by the squaric acid mediated PEGylation are presented. No major cytotoxic effects on very sensitive primary human umbilical vein endothelial cells exposed to various concentrations of the conjugates were observed in a WST-1 assay. A cell

adhesion molecule - enzyme immunosorbent assay did not reveal the expression of E-selectin or ICAM-1, important cell adhesion molecules involved in inflammation processes.

The focus of **Chapter 3** lies on the syntheses of novel heterofunctional PEG structures which are suitable candidates for the squaric acid mediated PEGylation and exhibit superior features compared to established PEGs applied in bioconjugation. **Chapter 3.1** describes the synthetic route to well-defined, linear heterobifunctional PEGs carrying a single acid-sensitive moiety either at the initiation site or at a tunable position in the polyether backbone. A universal concept for the implementation of acetal moieties into initiators for the anionic ring-opening polymerization (AROP) of epoxides is presented and proven to grant access to the degradable PEG structures aimed at. The hydrolysis of the heterofunctional PEG with the acetal moiety at the initiating site is followed by ^{1}H NMR spectroscopy in deuterium oxide at different pH. In an exploratory study, the same polymer is attached to BSA via the squarate acid coupling and subsequently cleaved from the conjugate under acidic conditions. Furthermore, the concept for the generation of acetal-modified AROP initiators is demonstrated to be suitable for cholesterol, and the respective amphiphilic cholesteryl-PEG is cleaved at lowered pH. In **Chapter 3.2**, the straightforward synthesis of α-amino ω_2-dihydroxyl star-shaped three-arm PEGs is described. To assure a symmetric length of the hydroxyl-terminated PEG arms, a novel AROP initiator is presented, who's primary and secondary hydroxyl groups are separated by an acetal moiety. Upon polymerization of ethylene oxide for these functionalities and subsequent cleavage of the acid-labile unit no difference in the degree of polymerization is seen for both polyether fragments.

Zusammenfassung

Aufgrund der einzigartigen Kombination nützlicher Eigenschaften und der Zulassung für die Verarbeitung in Körperpflegeprodukten, Lebensmitteln und Medikamenten wird Poly(ethylenglykol) (PEG) in einer Vielzahl verschiedener Anwendungen eingesetzt. Diese Dissertation beschäftigt sich mit der Synthese und Charakterisierung neuer heterofunktioneller PEG-Strukturen und der Etablierung von Diethoxycyclobutendion (Quadratsäurediethylester) als Kupplungsreagenz zur kovalenten Verknüpfung von PEG und PEG-Derivaten mit Proteinen.

Kapitel 1 stellt eine Einleitung zu den Eigenschaften und Anwendungen von PEG sowie der faszinierenden Chemie der Quadratsäurederivate dar. Im **Unterkapitel 1.1** werden die Synthese und die Eigenschaften von PEG vorgestellt, sowie dessen vielseitige Anwendung im alltäglichen Gebrauch. Insbesondere wird die Verwendung in der Medizin und Pharmazie sowie für nichtionische Tenside erörtert. Der Text dieses Unterkapitels ist in deutscher Sprache verfasst, da er als Artikel in der deutschsprachigen Zeitschrift Chemie in unserer Zeit veröffentlicht wurde. Das **Unterkapitel 1.2** behandelt die größte Schwachstelle von PEG, seine Biopersistenz. Diese behindert den Einsatz parenteral verabreichter PEG-Konjugate mit Polyetherketten, deren hydrodynamische Volumina die Ausschlussgrenze der Nieren überschreiten. Solche Konjugate würden verlängerte Blutzirkulationszeiten und ein effektiveres passives Tumor-Targeting aufweisen. Das Unterkapitel gibt einen vollständigen Überblick über die verschiedenen spaltbaren Gruppen, die als Sollbruchstellen in PEG eingeführt wurden und lässt die Synthesestrategien zu deren Einbau in das Polymerrückgrat Revue passieren. Das **Unterkapitel 1.3** fasst schließlich die chemischen Eigenschaften von Qaudratsäurealkylestern und die sich daraus resultierenden Vorzüge als Kupplungsreagenz für Proteinkonjugationen kurz zusammen.

In **Kapitel 2** wird die Verwendung von Qaudratsäuredieethylester als Kupplungsreagenz für die PEGylierung von Proteinen vorgestellt. Das **Unterkapitel 2.1** beschreibt die direkte Synthese und Charakterisierung von Quadratsäureethylesteramido-PEGs mit terminalen Hydroxyl- oder Methoxygruppen. Die Reaktivität und Selektivität dieser aktivierten PEGs gegenüber unterschiedlichen Lysin- und weiteren Aminosäurederivaten werden anhand von mit Hilfe der 1H NMR Spektroskopie erstellten Kinetiken untersucht. Ferner demonstriert die effiziente Verknüpfung der neuen PEGs mit einem Modellprotein, bovines Serumalbumin

(BSA), die Nützlichkeit des Diethoxycyclobutendions für die PEGylierung mit heterofunktionellen PEGs. Im **Unterkapitel 2.2** werden erste Untersuchungen zur Biokompatibilität der durch die quadratsäurevermittelte PEGylierung hergestellten Polyether/BSA-Konjugate präsentiert. Bei der Exposition sehr sensibler menschlicher Nabelschnurendothelzellen gegenüber verschiedenen Konzentrationen der Konjugate konnten in einem WST-1-Assay keine größeren zytotoxischen Effekte festgestellt werden. Eine Expression der wichtigen, an Entzündungsprozessen beteiligten Zelladhäsionsmoleküle E-Selektin und ICAM-1 konnte mittels Immunoassay nicht nachgewiesen werden.

Der Schwerpunkt von **Kapitel 3** liegt auf der Synthese neuer heterofunktioneller PEG-Strukturen, die mögliche Kandidaten für die quadratsäurevermittelte PEGylierung darstellen und im Vergleich zu den gegenwärtig in der Biokonjugation etablierten PEGs vorteilhafte Merkmale aufweisen. Das **Unterkapitel 3.1** beschreibt die Syntheseroute zu wohldefinierten, linearen heterobifunktionellen PEGs mit einer säurelabilen Gruppe, die sich entweder am Initiatorterminus oder an einer frei wählbaren Position innerhalb des Polyetherrückgrats befindet. Ein universelles Konzept zur Einführung eines Acetals in etablierte Initiatoren für die anionische Ringöffnungspolymerisation (AROP) wird vorgestellt und verwendet, um die angestrebten abbaubaren PEG-Strukturen darzustellen. Die Hydrolyse des heterofunktionellen PEGs mit initiatorseitigem Acetal wird mittels ^{1}H NMR Spektroskopie in Deuteriumoxid bei verschiedenen pH-Werten verfolgt. Dieses Polymer wird ferner mittels der Quadratsäurekupplung an BSA gebunden und anschließend unter sauren Bedingungen wieder von ihm abgespalten. Darüber hinaus wird gezeigt, dass das Konzept für die Einführung von Acetalen in AROP-Initiatoren auch zur Modifikation von Cholesterin herangezogen werden kann und das entsprechende amphiphile Cholersteryl-PEG bei erniedrigtem pH gespalten wird. Im **Unterkapitel 3.2** wird die direkte Synthese von dreiarmigen α-Amino-ω_2-dihydroxyl-PEG-Sternpolymeren beschrieben. Um sicherzustellen, dass beide hydroxylterminierten PEG-Arme die gleiche Länge aufweisen, wird ein neuer AROP-Initiator eingesetzt, dessen primäre und sekundäre Hydroxylgruppe durch ein Vollacetal getrennt sind. Nach der Ethoxylierung dieser Funktionalitäten und der anschließenden Spaltung des Acetals konnte kein Unterschied im Polymerisationsgrad beider Polyetherfragmente festgestellt werden.

Graphical Abstract

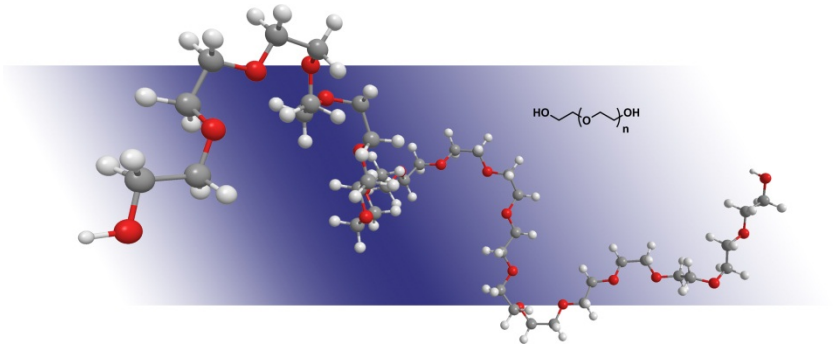

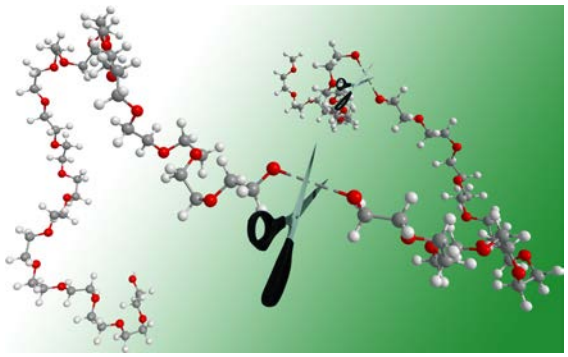

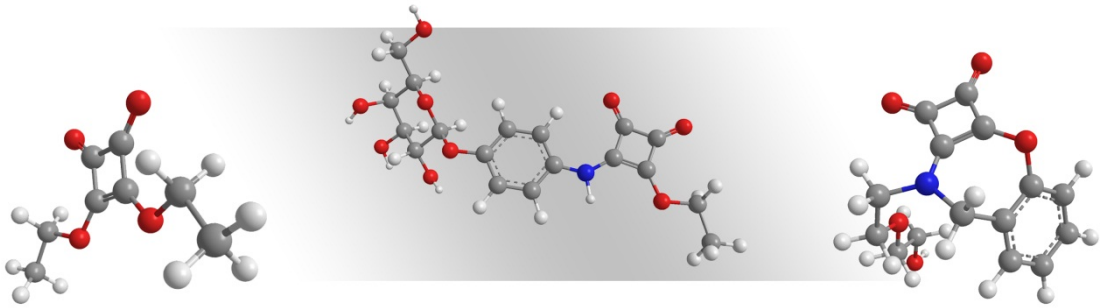

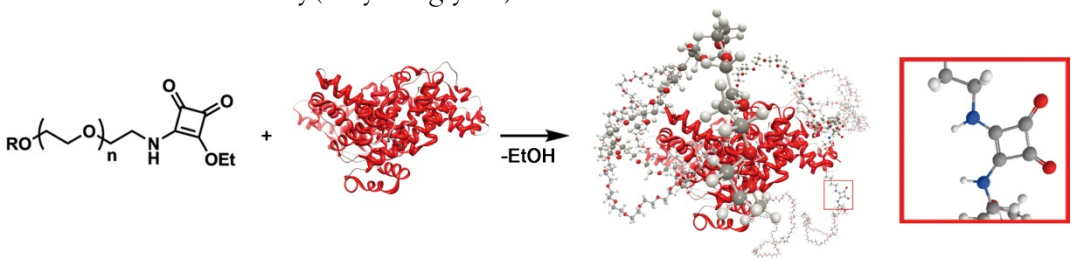

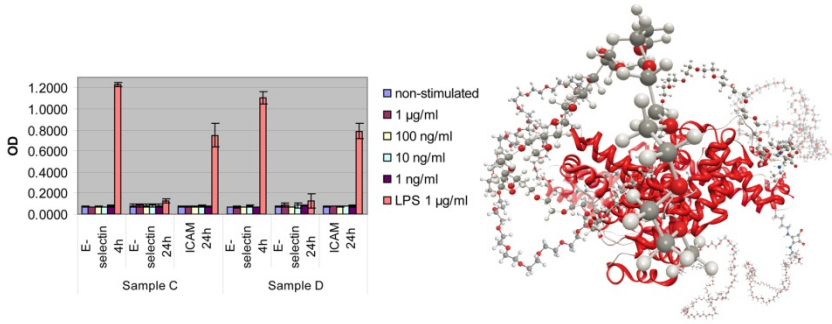

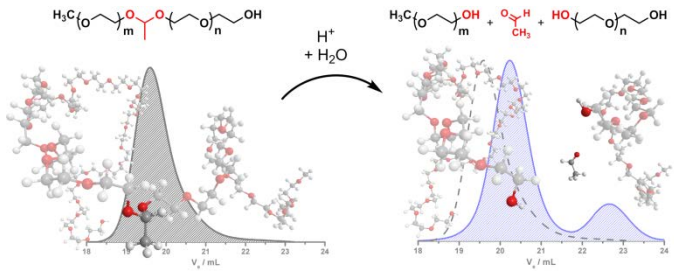

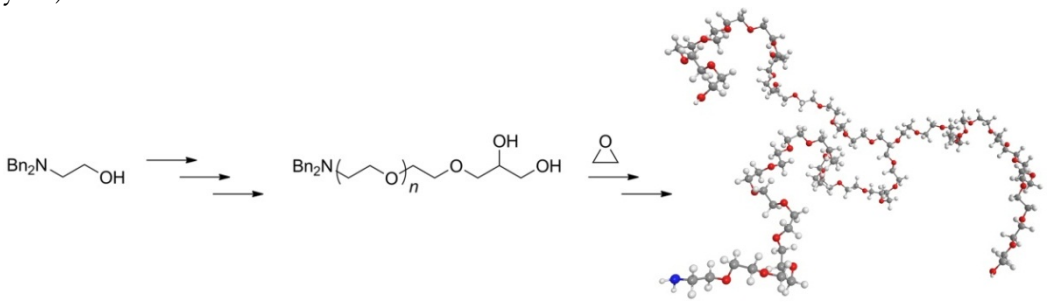

1 Introduction

1.1 Die vielen Gesichter des Poly(ethylenglykol)s

Carsten Dingels, Martina Schömer, Holger Frey

Johannes Gutenberg-Universität Mainz, Institut für Organische Chemie, Duesbergweg 10–14, 55099 Mainz, Germany.

Published in: *Chem. unserer Zeit* **2011**, 45, 338-349.

Abstract

Poly(ethylenglykol): Wohl kein anderes Polymer spielt eine so vielfältige Rolle in unserem täglichen Leben und ist daraus kaum mehr wegzudenken, obwohl uns dies meist nicht bewusst ist. Poly(ethylenglykol), kurz „PEG", hat eine denkbar einfache, aliphatische Polyether-Struktur (Abbildung 1). Im Bereich der Pharmazie und Medizin stellt es den Goldstandard für viele Anwendungen dar, ist aber auch in fast allen Kosmetikprodukten für die Haut omnipräsent. Überdies spielt es eine Rolle in Li-Ionen-Akkus moderner Notebooks.

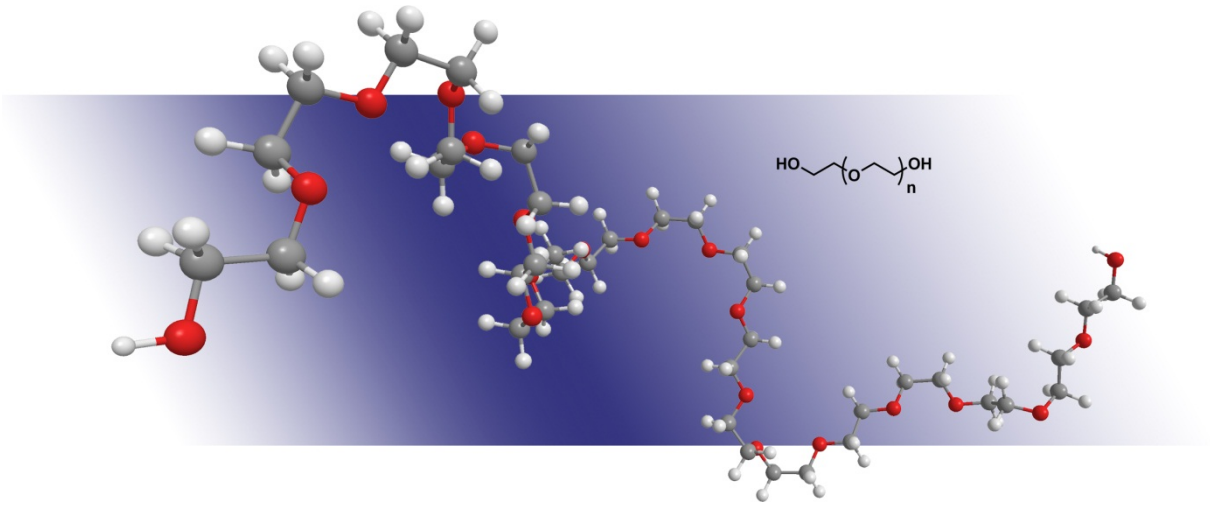

ABB. 1 Poly(ethylenglykol) – das Molekül mit der einfachen Polyetherstruktur spielt nicht nur in unserem täglichen Leben eine vielfältige Rolle.

Einleitung

Poly(ethylenglykol)e werden seit Jahrzehnten in pharmazeutischen Zubereitungen verwendet. PEG-Segmente sind in vielen nichtionischen Tensiden essentieller Bestandteil und bilden dort den hydrophilen Teil. PEG-haltige nichtionische Tenside kontrollieren den Aufbau vieler Schäume, so beispielsweise von PU-Schäumen, wie sie sich in Sitzpolstern für Automobile finden. Viele der Einsatzgebiete von PEG oder PEG-Tensiden erfordern keine großen Mengen, aber ohne diese PEG-Derivate als gleichsam „magische Komponenten" könnten die gewünschten Materialien gar nicht erhalten werden.

Hinter einer Reihe von Handelsnamen verbirgt sich PEG unterschiedlichen Molekulargewichts: „Macrogol", „Pegoxol", „Carbowax™" und „Polyox™". Im vorliegenden Artikel soll zum einen auf die Herstellungsrouten von PEG eingegangen werden, zum anderen sollen die ungewöhnlichen Eigenschaften dieser auf den ersten Blick denkbar einfachen Polyetherstruktur vorgestellt werden. Die nachfolgenden Abschnitte widmen sich dann ausgewählten Anwendungsgebieten von PEG, die einen Eindruck von der Breite des Applikationsspektrums dieses Polymers geben. Zuletzt sollen auch neue Entwicklungen und Fragestellungen aus der aktuellen Forschung zur Sprache kommen.

Herstellung von Poly(ethylenglykol) aus Ethylenoxid

Die Herstellung von Poly(ethylenglykol) basiert nicht auf der direkten Polymerisation des Ethylenglykols, denn die Herstellung eines Polyethers auf der Basis eines Diols ist aufgrund der schlechten Abspaltbarkeit der Hydroxylgruppe nicht möglich. Auch eine Williamson-artige Polymersynthese führt nicht zu den gewünschten Molekulargewichten. Als Monomer kommt somit bei allen Routen zur Herstellung das Ethylenoxid (EO) zum Einsatz, das bei 300 °C und erhöhtem Druck durch kontrollierte Oxidation von Ethylen unter Zuhilfenahme von Silberkatalysatoren gewonnen wird (Abbildung 2). Weltweit werden auf diesem Weg jährlich 19 Mio. Tonnen Ethylenoxid erzeugt (Weltproduktion im Jahr 2009), wovon der Großteil (ca. 70%) allerdings gleich wieder hydrolysiert wird, um Ethylenglykol, ein weitverbreitetes Frostschutzmittel bzw. eine Monomerkomponente für die Polykondensation von Poly(ethylenterephthalat), PET, herzustellen.

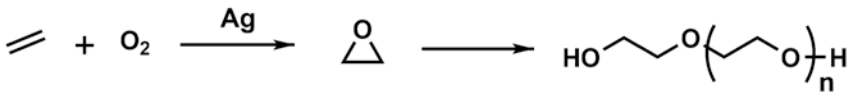

Abb. 2 Synthese von PEG: Monomer für die Herstellung von Poly(ethylenglykol)en ist Ethylenoxid (EO), das technisch durch Oxidation von Ethylen synthetisiert wird.

Ethylenoxid ist außerdem ein wichtiges Zwischenprodukt in der chemischen Industrie zur Herstellung von Dioxan und Ethylenglykolether (beides wichtige Lösungsmittel), Ethanolamin sowie Acrylnitril. Ethylenoxid siedet bei 11 °C, ist also bei Raumtemperatur ein Gas und ist sowohl elektrophil wie auch nukleophil sehr gut angreifbar, da die große Ringspannung des kleinen Heterozyklus (113 kJ/mol)[1] eine Triebkraft für eine Fülle an Folgereaktionen darstellt. Durch seine hohe Reaktivität in Kombination mit seiner Leichtflüchtigkeit ist Ethylenoxid eine Verbindung, die mit Vorsicht gehandhabt werden muss. Bei der Verwendung und dem Umgang mit Ethylenoxid muss dessen extrem hohe Toxizität und Kanzerogenität bedacht werden, die es jedoch wiederum ermöglichen, EO zur Niedertemperatursterilisation von hitzeempfindlichen Materialien zu verwenden. EO tötet zuverlässig Bakterien, Schimmel und Pilzsporen jeder Art ab. Insbesondere wird es zur Sterilisation von empfindlichen Materialien wie Kunststoffprodukten (z. B. Verbandmaterial, Spritzen, Katheter) in der Klinik verwendet, da in diesen Fällen keine Möglichkeit zur Dampfsterilisation bei hohen Temperaturen besteht. Für den Umgang im Labor mit EO ist eine sichere Verpackung und Handhabung unerlässlich. Ein vollständiger Umsatz bei der Polymerisation bzw. die rückstandslose Entfernung sind sicherzustellen.

Poly(ethylenglykol)e (PEGs) sind Polymere des Ethylenoxids mit der allgemeinen Formel $HO(CH_2CH_2O)_n$-H, wobei *n* die durchschnittliche Anzahl an Wiederholungen der Oxyethylen-Gruppe angibt. Der Wert *n* entspricht somit dem Polymerisationsgrad. Die offizielle IUPAC-Bezeichnung des PEG lautet „Poly(oxyethylene)-α-hydro-ω-hydroxy“, bezogen auf die chemische Struktur der Wiederholungseinheit. Auch der geläufigere Name „Poly(ethylene oxide)“ ist nach den IUPAC-Regeln erlaubt, da er das Polymer anhand der Struktur der Ausgangsverbindung beschreibt.

Die ersten Poly(ethylenglykol)e und Poly(ethylenglykol)acetate erhielt 1859 Wurtz durch Reaktion von Ethylenoxid mit Wasser, Ethylenglykol und Essigsäure. Als er Ethylenoxid mit Alkali- oder Zinkchlorid umsetzte, fand er kristallines Poly(ethylenglykol) als Produkt. Bereits 1929 untersuchte Hermann Staudinger die Polymerisation von Ethylenoxid mit verschiedenen Katalysatoren und erhielt Poly(ethylenglykol)e unterschiedlicher Molmassen.[2] In der Folge

wurden Poly(ethylenglykol)e durch Basenkatalyse bzw. Initiierung durch Alkoholate kommerziell nutzbar gemacht und nach und nach der genaue Polymerisationsmechanismus aufgeklärt.

Die Herstellung von PEG ist über verschiedene ringöffnende Polymerisationsmechanismen möglich – sowohl anionische und kationische als auch koordinative Strategien. Für die Synthese von wohldefinierten Polymerstrukturen mit enger Polydispersität wird die oxyanionische Polymerisation bevorzugt, da sie ohne Nebenreaktionen abläuft, vorausgesetzt alle Reaktionspartner werden sorgfältig gereinigt und getrocknet. Bei der kationischen Polymerisation von EO lassen sich als Initiatoren Lewis-Säuren, beispielsweise BF_3 oder SbF_3 verwenden. Wählt man einen kationischen Weg zur ringöffnenden Polymerisation von EO, so ist der Weg über den „aktivierter-Monomer-Mechanismus“ anstelle des Kettenenden-Mechanismus zu bevorzugen, da hierbei „Back-biting“-Vorgänge, die zu zyklischen Oligomeren führen können, unwahrscheinlicher sind. Die verschiedenen Mechanismen der Ringöffnungspolymerisation von Ethylenoxid zeigt Abbildung 3.

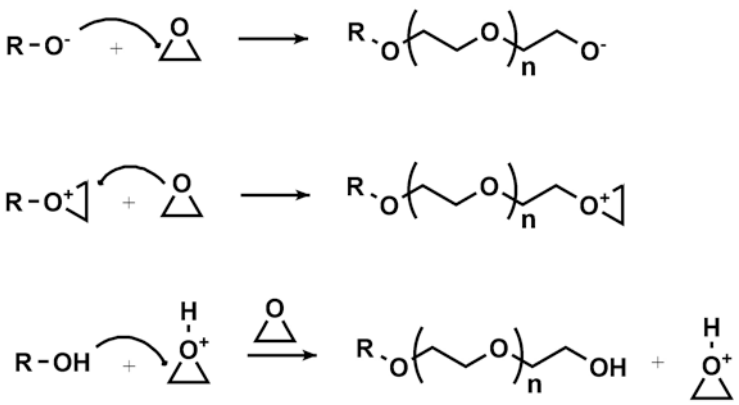

Abb. 3 Mechanismen: Anionischer, kationischer Kettenenden- und kationischer „aktivierter-Monomer-Mechanismus“ der ringöffnenden Polymerisation von Ethylenoxid (EO).

Auch mit Hilfe der Doppelmetallcyanid (DMC)-Katalyse lässt sich PEG herstellen. Der Polymerisationsmechanismus ist hier koordinativer Art, wobei Katalysatoren wie $Zn_3[Co(CN)_6]_2$ verwendet werden. Da diese Herstellungsart allerdings sehr kostenintensiv und die nachträgliche Abtrennung des Katalysators aufwändig ist, verwendet man das Verfahren großtechnisch hauptsächlich zur Poly(propylenoxid)-Synthese. Die bei diesem Monomer sonst auftretenden Nebenreaktionen (Umlagerungen, die zu Allyl- bzw. Propenyl-funktionalisierten Ketten führen) können durch die DCM-Katalyse erfolgreich unterdrückt werden, sodass der Nutzen bei der PPO-Herstellung den zusätzlichen Aufwand rechtfertigt.

Da die anionische Ringöffnungspolymerisation eine sehr gute Kontrolle der Struktur und des Molekulargewichts bietet, ist sie seit langem im Labor wie auch in der Technik die Methode der Wahl zur Herstellung von PEG bzw. PEO (Abbildung 4). Die anionisch ringöffnende Polymerisation von Epoxiden gelingt prinzipiell mit einer Reihe von Alkyl- oder Oxyanion-Initiatoren, beispielsweise Kalium- und Cäsiumalkoholaten. Lithiumalkyle und Lithium-alkoholate, die bei carbanionischen Polymerisationen von Vinylmonomeren wie Styrol eingesetzt werden, eignen sich generell nicht zur Polymerisation von Epoxiden, da in diesem Fall ein sehr stabiles Kontaktionenpaar am Alkoholat-Kettenende ausgebildet wird. Ist das Gegenion des propagierenden Makroanions ein Li^+-Kation, so findet lediglich eine einmalige Ringöffnung statt, aber keine weitere Anlagerung von Epoxiden. Dies nutzt man, um carbanionische Polymerisationen gezielt durch Zugabe von Epoxiden abzubrechen.

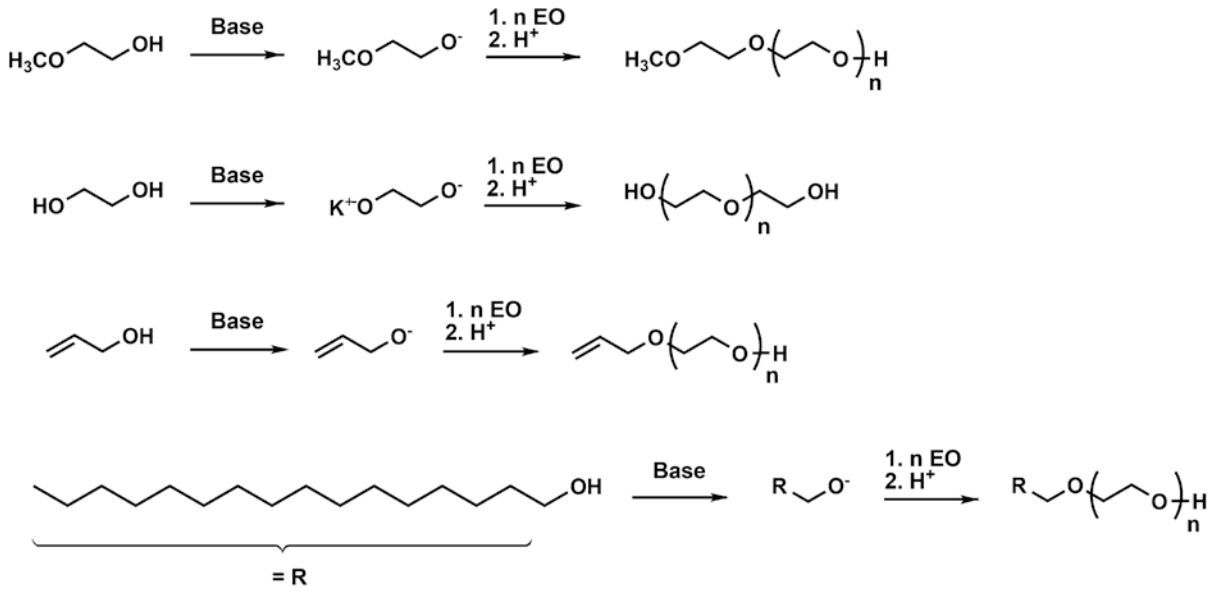

Abb. 4 Synthese verschiedener PEG-Strukturen durch anionische Polymerisation.

Auf diesem Weg lassen sich durch Zugabe von Ethylenoxid zu lebenden Polystyrolanionen (vgl. Infokasten[1]) beispielsweise hydroxylfunktionelle Polystyrole herstellen.[3] Die Geschwindigkeit der oxyanionischen Polymerisation ist abhängig vom Gegenion des wachsenden Kettenendes. Je größer („weicher“) das Gegenion ist, desto weniger stark wird es an das propagierende Oxyanion gebunden. Dies bedeutet im Fall der Alkalimetalle, dass Li^+-Organyle keine Polymerisation zeigen, während die größeren Homologen der Gruppe, also K^+ und Cs^+, das wachsende Kettenende weniger blockieren und eine hohe Polymerisationsgeschwindigkeit möglich ist. Weiterhin besteht die Möglichkeit, Chelatliganden wie Kronenether zur Komplex-

ierung des Kations einzusetzen, was ebenfalls die Bindungsfähigkeit des Kations an das wachsende Kettenende verringert.

Auch im industriellen Maßstab wird PEG hauptsächlich anionisch ringöffnend aus Ethylenoxid dargestellt. Als Initiator wird hier Natrium- oder Kaliumhydroxid verwendet, und es wird bevorzugt ohne Lösungsmittel gearbeitet.

Für PEG mit einer geringen und mittleren Molmasse von 200 bis 35.000 g/mol hat sich die Bezeichnung „Poly(ethylenglykol)“ eingebürgert. Für Polymere mit höherer Molmasse hat sich die Bezeichnung „Poly(ethylenoxid)“ (PEO) etabliert. Grundsätzlich wird PEG jedoch in allen Bereichen, in denen es um Biokompatibilität geht, nicht als „Poly(ethylenoxid)“ bezeichnet, nicht zuletzt auch, um das Mitschwingen der bekannten und für biomedizinische oder kosmetische Anwendungen unerwünschten Toxizität von Ethylenoxid schon im Namen zu vermeiden.

Ungewöhnliche Eigenschaften von PEG

PEG bildet keine Fasern, trägt lediglich zwei endständige Funktionalitäten, es weist im Festkörper keine außergewöhnlichen mechanischen Eigenschaften auf, kurz, es besitzt als Material selbst keine besonderen Eigenschaften und ist somit auf den ersten Blick eigentlich

1) **Lebende Polymeranionen** Mit Hilfe der anionischen Polymerisation lassen sich prinzipiell Polymere mit sehr engen Molekulargewichtsverteilungen herstellen. Voraussetzungen hierfür sind Monomere, die unter den anionischen Bedingungen keinerlei Nebenreaktionen eingehen können und Initiatoren, welche eine funktionelle Gruppe tragen, die mindestens genauso reaktiv ist wie das entstehende Kettenende während des Kettenwachstums. Dies ist ein entscheidendes Kriterium für die spätere Molekulargewichtsverteilung, da nach der Zugabe des Initiators möglichst alle Ketten gleichzeitig starten sollten, um bis zum Ende der Polymerisation in etwa gleich lang zu werden. Sind alle Monomermoleküle verbraucht, ist das Kettenende immer noch reaktiv, da ja keine Nebenreaktionen ablaufen können. Man spricht in diesem Fall von lebenden Polymeranionen. Es kann nun weiteres Monomer zugegeben werden. Möglich ist auch der Abbruch der Reaktion durch die Zugabe eines Terminierungsreagenz. Mit einigen Reagenzien lassen sich an den Kettenenden funktionelle Gruppen einführen. Neben Epoxiden lassen sich auch Monomere mit völlig anderen reaktiven Gruppen anionisch zu Polymeren umsetzen. Das prominenteste Beispiel ist das Vinylbenzol, welches unter dem Namen Styrol wesentlich bekannter ist. Lösungen lebender Polystyrolanionen weisen eine rötliche Farbe auf.

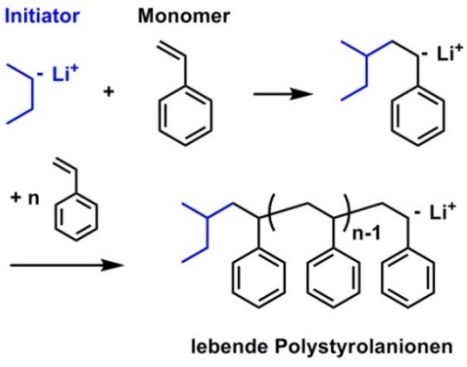

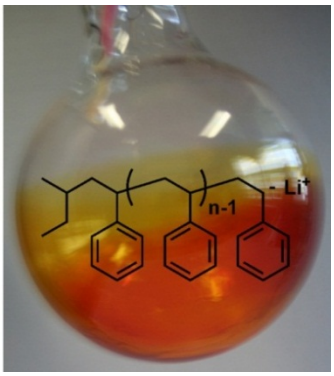

„eine graue Maus“ unter den Polymermaterialien. Was macht nun dieses Material so wichtig und vielseitig?

Das Erscheinungsbild von PEG hängt stark vom Molekulargewicht ab. Poly(ethylenglykol)e mit einer mittleren Molmasse bis zu 400 g/mol sind bei Raumtemperatur nichtflüchtige Flüssigkeiten, was für eine Reihe von Anwendungen von Vorteil ist. PEG 600 hingegen weist einen Schmelzbereich von 17 bis 22 °C auf, woraus eine flüssige Konsistenz bei Raumtemperatur und eine pastenartige Konsistenz bei tieferen Temperaturen resultiert. Für Molekülmassen über 2000 g/mol wird PEG dann als feste Substanz erhalten, entweder als Flocken oder als feines Pulver. Härte und Schmelzpunkt steigen mit dem Molekulargewicht an, bis der Schmelzpunkt bei höheren Molekulargewichten einen konstanten Wert von etwa 60 °C erreicht. Durch Mischung von niedermolekularen mit festen PEGs lassen sich wasserlösliche Produkte von salbenartiger Konsistenz herstellen, d. h. durch Abmischen von PEGs mit unterschiedlichem Molekulargewicht lässt sich der Schmelzpunkt der Mischung präzise im physiologisch relevanten Bereich einstellen. Niedermolekulares PEG wirkt somit wie ein Weichmacher für die höhermolekulare Komponente. Dies hat zentrale Bedeutung für viele Anwendungen in der Pharmazie.[4]

Die wichtigsten und tatsächlich einzigartigen Eigenschaften von PEG, die im folgenden Abschnitt diskutiert werden sollen, sind seine Wasserlöslichkeit und die fast nicht vorhandene bzw. extrem geringe Toxizität. Niedermolekulare PEGs sind in jedem Verhältnis mit Wasser mischbar. Mit steigendem Molekulargewicht nimmt die Wasserlöslichkeit etwas ab. Selbst von einem PEG 35000 können jedoch bei Raumtemperatur noch 50%ige homogene Lösungen hergestellt werden! Die hervorragende Wasserlöslichkeit von Poly(ethylenglykol) ist bei näherer Betrachtung vor allem im Vergleich zu anderen aliphatischen Polyethern verblüffend und auf den ersten Blick für den Polymerchemiker nicht verständlich. Tatsächlich existiert nur ein einziges weiteres wasserlösliches Polymer unter den Polyethern, und zwar Poly(vinylmethylether). Alle anderen aliphatischen Polyether wie Polyoxymethylen und Polymere der höheren Ether sind absolut wasserunlöslich (Tabelle 1).

Fast alle der in Tabelle 1 aufgelisteten aliphatischen Polyether spielen in der Technik eine wichtige Rolle und werden im großen Maßstab hergestellt, mit der Ausnahme von Polyacetaldehyd und Polytrimethylenoxid. Das Homologe mit nur einer Methylengruppe, Poly(oxymethylen) (POM), das Polymer des Formaldehyds, das zugleich das einfachste Polyacetal darstellt, wird wegen seiner extrem guten und schnellen Kristallisation und den

daraus resultierenden hervorragenden mechanischen Eigenschaften als Konstruktionswerkstoff eingesetzt. Es findet sich beispielsweise in Zahnrädern, in Automobilen oder im Modellbau, und jeder Chemiker hatte es in Form von Keck-Kegelschliffklemmen schon in den Händen.

Tab. 1 Die wichtigsten aliphatischen Polyetherstrukturen.[5]

Polymer	Formel	wasserlöslich (l) / unlöslich (u)
Polymethylenoxid (POM)	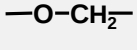	u
Polyacetaldehyd	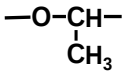	u
Poly(ethylenoxid) (PEG)	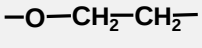	l
Polypropylenoxid (PPO)	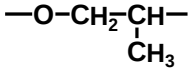	u
Polytrimethylenoxid	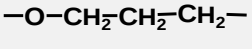	u
Polytetrahydrofuran	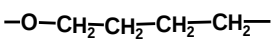	u

Die erstaunliche und einzigartige Wasserlöslichkeit von PEG ist auf den Abstand der sich wiederholenden Sauerstoffatome in der Polymerkette zurückzuführen, der etwa dem Abstand der Sauerstoffatome in flüssigem Wasser entspricht und so die Ausbildung eines ausgedehnten (ungespannten) Wasserstoffbrücken-Netzwerks zwischen der PEG-Kette und den Wassermolekülen erlaubt, also eine sehr effektive Hydrathülle ermöglicht. Dies konnte durch Molekularsimulationen und theoretische Arbeiten belegt werden.[5]

Beim Polyoxymethylen, das zwar anteilsmäßig mehr Sauerstoff in der Polymerkette trägt, ist der Abstand zweier benachbarter Sauerstoffatome zu gering, um die für die Wasserlöslichkeit nötige Hydrathülle auszubilden. Im Polypropylenoxid, das ja denselben Abstand der Sauerstoffatome entlang der Kette aufweist, wird die Anlagerung der Wassermoleküle durch die aus der Polymerhauptkette herausragenden unpolaren Methylgruppen so sehr gestört, dass auch Poly(propylenoxid), PPO, wasserunlöslich und recht lipophil ist. Dieser Sachverhalt wird bei den technisch hergestellten amphiphilen Copolymeren von PEG und PPO ganz gezielt genutzt (s.u.).

Im Gegensatz zu den meisten anderen Substanzen lässt sich die Wasserlöslichkeit von PEG bzw. seiner Derivate durch Erwärmung nicht unbegrenzt steigern. PEG gehört zur Gruppe der thermoresponsiven Polymere, die bei Erhöhung der Temperatur weniger gut löslich in Wasser

werden. Nur unterhalb einer kritischen Entmischungstemperatur (LCST, engl.: lower critical solution temperature) kann die hydrophile Oberfläche des Polymers die oben beschriebene Hydrathülle ausbilden und die Polymerkette liegt relativ gestreckt vor. Über der kritischen Entmischungstemperatur liegt dann Unlöslichkeit in Wasser vor.[5]

Die zweite herausragende Eigenschaft von PEGs sind ihre außergewöhnlich niedrigen Toxizitätswerte, sowohl was die akute als auch die chronische Toxizität bei oraler und intravenöser Aufnahme betrifft, als auch im Hinblick auf die Embryotoxizität und Hautverträglichkeit. Bei einer Reihe von Untersuchungen wurde zudem festgestellt, dass die Aufnahme von PEG im Magen-Darm-Trakt mit steigender Molmasse sinkt. In Experimenten an Ratten wurde beispielsweise gezeigt, dass PEG mit einer Molmasse von 5000 g/mol innerhalb von 5 h nicht aus dem Darm resorbiert wird, während PEG mit 1000 g/mol bis zu 2% aufgenommen wird. Die mittlere letale Dosis bei oraler Verabreichung (LD50) einer 50%igen Lösung in Wasser liegt für Mäuse bei mehr als 50 g PEG pro kg Körpergewicht! Selbst bei intravenöser Verabreichung beträgt der LD50-Wert für Mäuse immerhin noch 6 g pro kg Körpergewicht! Die Ausscheidung von PEG erfolgt bei Molekulargewichten unter 30.000 g/mol immer über die Nieren. Nierentoxizität konnte nur für PEG mit niedrigen Molmassen von 200–600 Da festgestellt werden. Die WHO („World Health Organisation“) legte für PEG einen ADI-Wert („akzeptable tägliche Aufnahme“) von 0–10 mg/kg Körpergewicht fest. Für die in PEG möglicherweise aus der Ringöffnungspolymerisation von EO enthaltenen niedermolekularen Verunreinigungen gelten für den Einsatz in kosmetischen Produkten die folgenden, strengen Grenzwerte: 1,4-Dioxan: 10 mg/kg, Ethylenglykol und Diethylenglykol: insgesamt 3 g/kg), Ethylenoxid: 1 mg/kg.[6]

PEG in nichtionischen Tensiden

Aufgrund seiner sehr guten Wasserlöslichkeit wird Poly(ethylenglykol) zur Darstellung vieler bedeutender nichtionischer, also ungeladener Tenside verwendet. Tenside sind oberflächenaktive Stoffe, weshalb sie in Englisch auch als Surfactants (**surf**ace **act**ive **a**ge**nts**) bezeichnet werden, die überall dort zum Einsatz kommen, wo es um die Verringerung von Oberflächenspannungen geht. Als waschaktive Substanzen (Detergentien) lösen sie beispielsweise fettigen Schmutz von Textilfasern oder Geschirr im Waschwasser auf, und als Emulgatoren sorgen sie

dafür, dass Emulsionen und Suspensionen stabil bleiben und sich nicht wieder in ihre Bestandteile zerlegen.

Im Allgemeinen bestehen die Moleküle solcher Substanzen aus einem hydrophilen und einem lipophilen Teil. Der hydrophile Teil kann entweder anionischer (z. B. Carboxylat-, Sulfonatgruppen), kationischer (z. B. quartärnere Ammoniumgruppen) oder nichtionischer Natur sein.

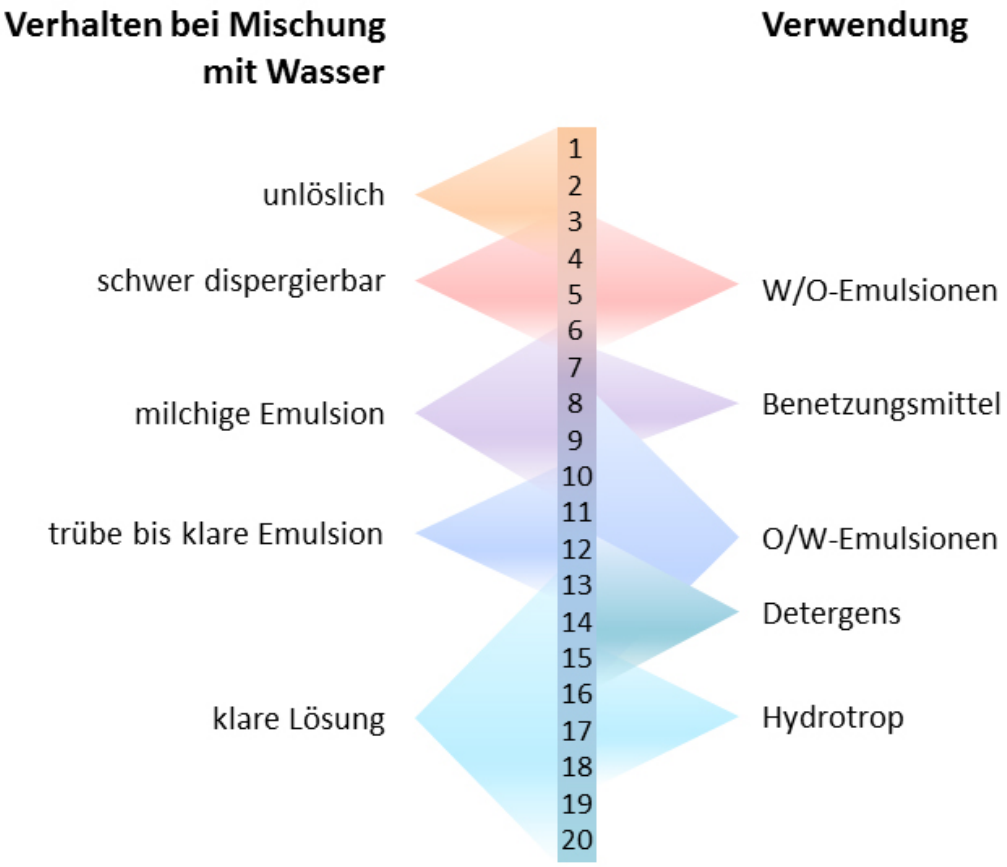

Abb. 5 HLB-Werte und Einsatzgebiete von Tensiden.[7]

Bei nichtionischen Tensiden beruht die Wasserlöslichkeit auf der Anwesenheit nichtionischer polarer Funktionen wie Hydroxylgruppen oder eben dem Einsatz von PEG. Das Polymer ist hierbei meist über Ester- oder Etherbindungen an den lipophilen Block gebunden, welcher gewöhnlich aus langkettigen Alkylresten wie Fettsäuren oder Fettalkoholen besteht. Zu den wichtigsten Vertretern dieser nichtionischen Tenside zählen PEG-Monoalkylether, PEG-Monoalkylphenylether (Alkylphenolethoxylate), PEG-Fettsäureester, PEG-Glycerylfettsäureester, PEG-Sorbitanfettsäureester und Poloxamere, d. h. Blockcopolymere von Poly(propylenoxid) und PEG. Die wichtigsten Strukturen sind in Abbildung 6 dargestellt.

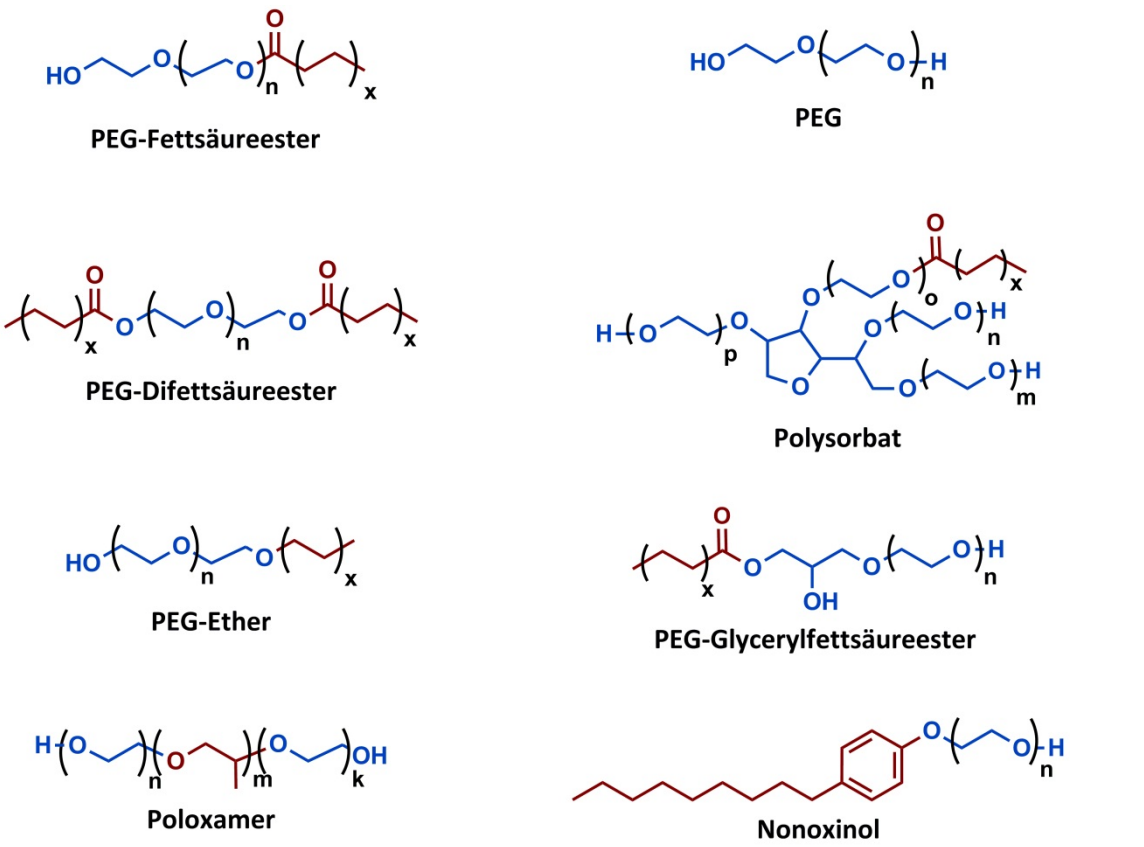

ABB. 6 Wichtigste PEG-Tenside, die vielfach in kosmetischen und pharmazeutischen Produkten zum Einsatz kommen; blau: hydrophiles PEG-Segment.

Die Kettenlängen der einzelnen Teile haben dabei einen entscheidenden Einfluss auf die Eigenschaften des Tensids: Ist der PEG-Block groß, weist das Tensid einen hohen HLB-Wert auf (**HLB** – **H**ydrophilic-**L**ipophilic **B**alance, vgl. Abbildung 5), und eignet sich zur Darstellung von O/W-Emulsionen („Öl in Wasser"). Nichtionische Emulgatoren für W/O-Emulsionen haben hingegen nur wenige Ethylenoxideinheiten und weisen einen geringen HLB-Wert auf. Für jedes nichtionische Tensid kann der HLB-Wert chromatographisch oder aus dessen Dielektrizitätskonstante bestimmt werden. Die Skala orientiert sich an der Wasserlöslichkeit der oberflächenaktiven Substanz. Kleine Werte bedeuten eine geringe Löslichkeit in Wasser, hohe dagegen eine gute. Aus dem für ein Tensid ermittelten HLB-Wert lässt sich auch ein möglicher Verwendungszweck ableiten. Zur Stabilisierung von W/O-Emulsionen werden zum Beispiel Tenside mit HLB-Werten von 3–6 benötigt, Tenside für O/W-Emulsionen sollten HLB-Werte im Bereich von 8–18 aufweisen.

So hat PEG-2-Stearylether beispielsweise einen HLB-Wert von 4,9, während PEG-23-laurylether einen HLB-Wert von 16,9 aufweist. Der Laurylether findet Anwendung in der Biochemie, da er Proteine aus Lipidmembranen lösen kann, ohne diese dabei zu denaturieren.

Bedeutend in der Reihe der Alkylphenolethoxylate sind vor allem Nonoxinol-9 und Nonoxinol-40, 4-Nonylphenylethoxylate mit durchschnittlich 9 und 40 Ethylenoxideinheiten. Nonoxinol-9 war lange Zeit Bestandteil vieler Reinigungsmittel, wurde jedoch aufgrund der toxischen Wirkung von 4-Nonylphenol, einem Abbauprodukt des Tensids, auf Lebewesen in kontaminierten Gewässern von der EU zum Einsatz in Reinigungsmitteln verboten. Wegen seiner spermiziden Wirkung ist es Bestandteil einiger Verhütungsmittel. Nonoxinol-40 spielt in der Biochemie bei der Solubilisierung von Lipidmembranen eine Rolle.

Im Gegensatz zu den bisher vorgestellten nichtionischen Tensiden, besteht der lipophile Teil der Poloxamere, auch unter dem Handelsnamen Pluronics® bekannt, nicht aus Fettsäureresten oder Fettalkoholen, sondern aus einem vollsynthetischen Polypropylenoxidblock. Dieser wird von zwei PEG-Blöcken flankiert, so dass es sich bei Poloxameren um ABA-Triblock-Copolymere handelt, deren Eigenschaften als oberflächenaktive Substanzen durch Veränderung der einzelnen Blocklängen sehr gut eingestellt werden können.

Was macht PEG in Kosmetikprodukten?

Schauen wir uns doch einmal einige der kosmetischen Produkte unseres Alltags an, mit denen wir täglich in Berührung kommen (Abbildung 7): Shampoo, Zahnpasta, Cremes, Lotionen, Haarstyling- und Make-Up-Produkte. In so gut wie allen wird man ein oder mehr Bestandteile finden, die PEG enthalten. Auch dessen anionische oder nichtionische Derivate werden in Kosmetika vielfach als Tenside, Emulgatoren und Feuchthaltemittel verwendet.

In Kosmetika wird entweder PEG selbst eingesetzt oder seine vielfältigen Derivate, in denen PEG als wasserlöslicher Block fungiert. Mit ihren zwei terminalen Hydroxylgruppen ist eine PEG-Kette in der Lage, sowohl Mono- als auch Diester oder -ether zu bilden, und zwar entweder durch Verwendung von langkettigen Carbonsäuren (meist Fettsäuren) oder Alkoholen als Initiator für die Polymerisation von Ethylenoxid oder durch nachträgliche Veresterung oder Veretherung dieser mit PEG.

Zu den wichtigsten PEG-Derivaten zählen daher PEG-Fettsäureester (z. B. PEG-Laurat, Dilaurat, Stearat oder Distearat), PEG-Ether (z. B. PEG-Laureths, Ceteths, Ceteareths oder Oleths), PEG-Aminether (z. B. PEG-Cocoamine) sowie PEG-Rizinusöl, PEG-Bienenwachs oder PEG-Sojasterin. Die Namen der PEG-Ester und -Ether leiten sich jeweils von den Trivialnamen der enthaltenen gesättigten und ungesättigten Fettsäuren (für die PEG-Ester) bzw.

Fettsäurealkohole (bei den PEG-Ethern) ab: Laurin- (C12, gesättigt), Cetin/Palmiton- (C16, gesättigt), Stearin- (C18, gesättigt), Öl- (C18, einfach ungesättigt), Cetearin- (Mischung aus C16 und C18). Die Ziffer im Namen gibt die Anzahl der Ethylenglykol-Wiederholungseinheiten im Molekül an. Oleth-20 beispielsweise besteht aus einem C18-Alkohol, verethert mit einem PEG-Molekül mit durchschnittlich 20 Wiederholungseinheiten, was etwa PEG-900 entspricht.

Auch Copolymere von PEG mit Silikonen (hauptsächliche Polydimethylsiloxane, Dimethicone genannt) finden Anwendung in Kosmetikprodukten, vor allem in Haarpflegeprodukten zur Glättung und Kämmbarkeitsverbesserung.

Abb. 7 PEG-haltige Produkte (1: Haarwachs, 2: Duschgel, 3: Rasierschaum, 4: Flüssigseife, 5: Zahnpasta) im Alltagsgebrauch; auf der rechten Seite der Abbildung sind die auf den jeweiligen Verpackungen angegebenen Handelsnamen der enthaltenen PEG-Derivate aufgelistet. Vor allem nichtionische PEG-Tenside spielen eine wichtige Rolle.

Unmodifiziertes PEG, vor allem solches mit relativ niedrigen Molekulargewichten, wird häufig als gut bioverträgliches Lösungsmittel in Cremes verwendet oder auch als Feuchthaltemittel zugegeben. Bei höheren Molekulargewichten (ab 2000 g/mol) kann PEG auch zur Einstellung einer gewünschten Viskosität (d. h. der Zähflüssigkeit) bzw. zur Stabilisierung von Emulsionen zugesetzt werden (siehe auch Abschnitt zu PEG-Tensiden).

Von noch größerer Bedeutung im Kosmetikbereich als PEG selbst sind seine Derivate. Die schon angesprochenen Tensideigenschaften von Molekülen mit ihrem hydrophilen PEG-Rückgrat und hydrophoben, langkettigen Kohlenwasserstoffresten sind aus den meisten Kosmetikprodukten nicht mehr wegzudenken. Speziell in Hautpflegeprodukten bilden Tenside

die wichtigste Komponente, um Wasser und Fette zu vermischen und so z. B. fetthaltige Cremes herzustellen. In Reinigungsmitteln wie Duschgel oder Seife finden Tenside Verwendung, um die „Löslichkeit“ von Fett- oder Schmutzpartikeln, die am Körper haften, in Wasser zu verbessern. Die wichtigsten Tensidstrukturen auf PEG-Basis sind in Abbildung 6 dargestellt.

PEG in der Pharmazie

Durch Mischen eines festen und eines flüssigen PEG, beispielsweise 50% PEG 1500 und 50% PEG 300, kann eine wasserlösliche Salbengrundlage erzeugt werden, die sich wegen ihrer breiten Löseeigenschaften für viele aktive Substanzen eignet. So wird PEG in allen Gebieten der pharmazeutischen Technologie als Wirkstoffträger verwendet. PEGs werden weiterhin zur Herstellung flüssiger Zubereitungen – wie Tropfen oder Injektionspräparate – sowie zur Füllung von Gelatinekapseln verwendet, da sie diese nicht anlösen oder verspröden. Suppositorien („Zäpfchen“) auf der Basis von PEG (in diesem Anwendungsgebiet oft als „Macrogol“ bezeichnet) können genau auf die Körpertemperatur eingestellt werden. Das Freisetzen der Wirksubstanzen erfolgt jedoch nicht durch Schmelzen, sondern durch das Auflösen der PEG-Matrix in der Darmflüssigkeit im Rektum. PEGs werden ganz allgemein als Lösevermittler und Hilfsmittel beim Tablettieren und Dragieren eingesetzt.

Darmspiegelungen stellen in fortgeschrittenem Lebensalter eine zunehmend wichtige Vorsorgemaßnahme dar, um Frühstadien des Darmkrebs zu diagnostizieren, einer der häufigsten Krebsarten. PEG wird zur Reinigung des Darmes vor einer solchen Untersuchung eingesetzt. Dazu werden im Vorfeld der Untersuchung 2 L einer konzentrierten PEG Elektrolyt-Lösung (PEG-EL) getrunken, was eine stark abführende Wirkung hat. In Analogie wird zur Behandlung einer Verstopfung Macrogol 4000 angewendet. In diesem Fall werden pro Tag 10–20 g eines PEG-Pulvers eingenommen.

Darüber hinaus gibt es eine Fülle weiterer Spezialanwendungen von PEG in der Pharmazie und Medizin, die hier nicht alle behandelt werden können. So werden PEGs beispielsweise in der Augenheilkunde als Bestandteil künstlicher Tränenflüssigkeiten zur Behandlung von Augentrockenheit verwendet. Weiche Kontaktlinsen beinhalten PEG-Blöcke, um Hydrophilie und damit Benetzbarkeit bzw. Quellbarkeit durch die Tränenflüssigkeit zu erzielen.

Am Ende dieses Abschnitts soll noch ein kritischer Punkt vermerkt werden: PEG kann penetrationsfördernd wirken, d.h. die Darmwand bzw. die Haut wird durchlässiger für Wirkstoffe, aber ebenso für Gifte, die somit leichter in den Körper gelangen können. Aus diesem Grund wird die Verwendung in einigen Produkten kontrovers diskutiert.

Kovalente Biokonjugation: „PEGylierung“

Die kovalente Verknüpfung von monofunktionellen PEG-Ketten (mPEG) mit Wirkstoffen oder Proteinen wird als „Pegylierung“ (bzw. „PEGylierung“) bezeichnet. Für die Konjugation niedermolekularer Wirkstoffmoleküle, Oligonucleotide und siRNA wird vorrangig PEG mit Molmassen von 20–40 kDa eingesetzt. Außer der Molmasse spielt auch der Polydispersitätsindex (PDI, Breite der Molekulargewichtsverteilung) von PEG eine wesentliche Rolle für pharmazeutische und medizinische Anwendungen dieser Art.

Ein PDI unter 1,1 gilt als Grundvoraussetzung, um eine akzeptable Homogenität des Polymers und damit eine reproduzierbare Aufenthaltsdauer im Körper und Immunogenität des Transportsystems zu gewährleisten. PEG erfüllt diese Voraussetzungen, da die Synthese des Polymers durch anionische Polymerisation von Ethylenoxid einen PDI um 1,01 ermöglicht. Bei 20–50 kg/mol Molekulargewicht erreichen die Konjugate eine Größe, die über der Nierenschwelle liegt und die rasche Ausscheidung verhindert, also eine verlängerte Zirkulationszeit im Blutkreislauf ermöglicht.

Durch die rasanten Fortschritte in der Bio- und Gentechnologie sind viele Proteine in wirtschaftlich interessanten Mengen zugänglich geworden. Einige davon eignen sich aufgrund ihrer Wirkungen im menschlichen Körper prinzipiell als Arzneimittel, wie das allgemein als Antidiabetikum bekannte Hormon Insulin. Einer allgemeinen Anwendung solcher Peptide als Therapeutika stehen allerdings deren rascher Abbau durch Peptidasen (Enzyme zur Verdauung von Proteinen) sowie die häufig beobachtbaren Immunreaktionen auf die körperfremden Biomoleküle entgegen. In den letzten Jahrzehnten hat sich die kovalente PEGylierung als hervorragende Methode zur Verlangsamung des beschriebenen Abbaus und zur Verringerung der Immunogenität beziehungsweise Allergenität dieser Peptide herauskristallisiert.[8] Das hochflexible, wasserlösliche Polymer schirmt dabei das PEGylierte Protein ab und erschwert so den Zugang zu dessen Oberfläche für Peptidasen und Antikörper. Letztere können bestimmte Strukturen der Proteine (sogenannte Epitope) identifizieren und anschließend eine

Immunreaktion auslösen. Durch die verringerte Abbaugeschwindigkeit verlängert sich der Zeitraum, in dem sich das Protein, in diesen Fällen das Protein-Polymer-Konjugat, in therapeutisch relevanten Konzentrationen in der Blutbahn befindet, wodurch das entsprechende Medikament in größeren Zeitabständen verabreicht werden kann.

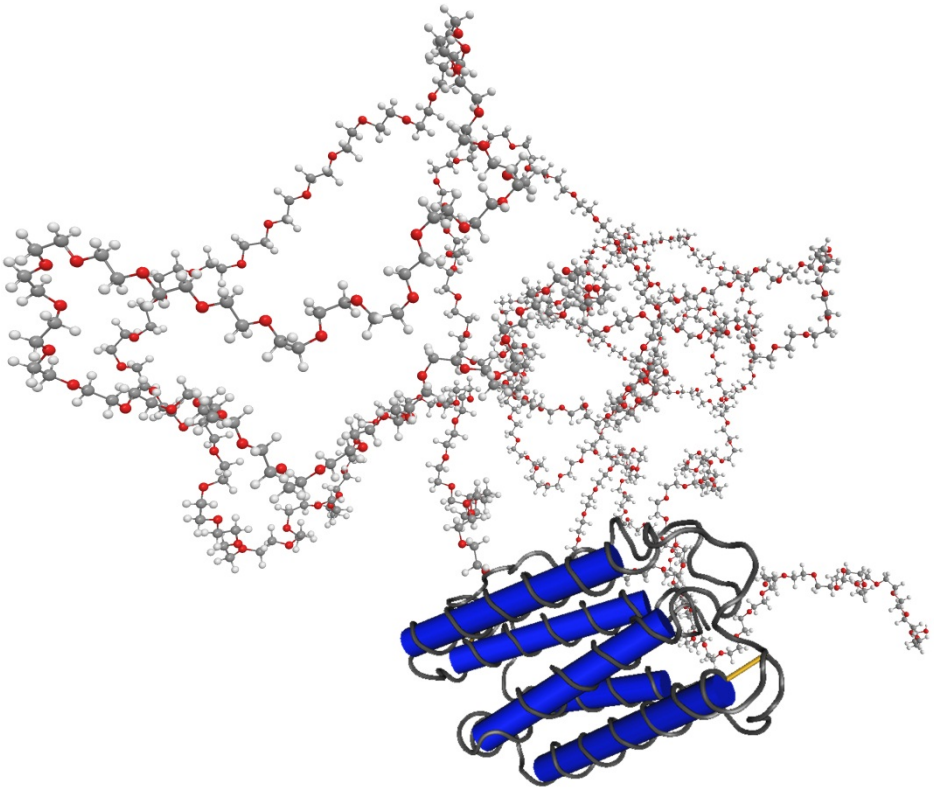

Abb. 8 Pegyliertes Interferon: Die PEG-Ketten (grau/rot) schirmen das Protein gegen Phagozytenangriff und schnellen Abbau ab.

Ein gravierender Nachteil der PEGylierung äußert sich in der zum Teil drastisch reduzierten Bioaktivität des modifizierten Proteins in vitro, da auch das aktive Zentrum durch das Polymer abgeschirmt wird, wodurch die Rezeptor-Ligand-Wechselwirkung geschwächt wird. Zudem können Polymerketten, die in der Nähe des aktiven Zentrums an das Protein gebunden sind, eine Änderung der räumlichen Anordnung dieses Zentrums bewirken, was ebenfalls in einer geringeren Bioaktivität resultiert. Obwohl dieser Effekt in vivo durch die längeren Zirkulationszeiten überkompensiert wird, sind natürlich weniger stark reduzierte Bioaktivitäten wünschenswert, da so die zu verabreichende Dosis verringert werden kann. In einigen Fällen wurden durch die Verwendung eines Poly(ethylenglykol)s mit verzweigter Struktur im Vergleich zu den Konjugaten mit den meistverwendeten linearen mPEGs höhere Bioaktivitäten und längere Zirkulationszeiten beobachtet. Auch das auf dem Markt befindliche Pegasys®

besteht aus einem mit einem verzweigten PEG konjugierten Protein (Interferon-α-2a, wirksam gegen Hepatitis C, Abbildung 8). Einige bereits auf dem Markt befindliche, PEGylierte Proteine sind in Tabelle 2 aufgelistet.[9]

Nicht nur Proteine lassen sich mit PEG nutzbringend konjugieren, sondern auch Liposomen (vesikuläre Lipidstrukturen), die zur Verkapselung und zum Transport von Wirkstoffen eingesetzt werden. Liposomen aus gängigen Phospholipiden werden im Blutkreislauf schnell durch Makrophagen angegriffen und abgebaut. Eine Modifikation von Liposomen mit PEG lässt sich durch die Zugabe von PEG-haltigen Lipiden zu Phospholipiden erreichen. Dies führt zu stark verminderter Aufnahme und Abbau durch die Leber und verlängerten Zirkulationszeiten der Liposomen im Blutkreislauf, wodurch die Abgabe und Wirkungsdauer des verkapselten Pharmakons wesentlich verlängert werden können. Solche durch PEG abgeschirmten Liposomen werden als „Stealth-Liposomen“ bezeichnet, weil PEG hier die Funktion einer Tarnkappe übernimmt und so Erkennungs- und Abbaumechanismen des Körpers getäuscht werden können, in Analogie zum „Stealth-Tarnkappenbomber“, der nicht von Radarsystemen erfasst werden kann.[10]

Tab. 2 Beispiele für PEGylierte Proteine auf dem Markt.

Handelsname	Protein	Jahr	Krankheit
Adagen®	Adenosindeaminase	1990	Schwerer kombin. Immundefekt
Oncaspar®	Asparaginase	1994	Akute lymphatische Leukämie
PEG-Intron®	Interferon-α-2b	2001	Hepatitis C
Pegasys®	Interferon-α-2a	2002	Hepatitis C
Neulasta®	G-CSF	2002	Neutropenie nach Chemotherapie
Somavert®	Antagonist des GHR	2003	Akromegalie
Cimzia®	Fab-Fragment eines TNF-α-Antikörpers	2008	Morbus Crohn

PEG in Lebensmitteln?

Tenside erfüllen in Lebensmitteln wichtige Funktionen (Abbildung 9). Sie dienen zur Stabilisierung von W/O-Emulsionen wie Butter und Mayonnaise, von O/W-Emulsionen wie Milch und Sahne, sie verhindern einen Fettaustritt bei Wurstwaren oder Schokolade und helfen

bei der Solubilisierung von Instantpulvern. Während in Milchprodukten und eihaltigen Waren wie Mayonnaise natürliche Emulgatoren wie oberflächenaktive Proteine oder Lecithine vorhanden sind, müssen zur Einstellung der gewünschten Eigenschaften mancher Lebensmittelprodukte Tenside zugesetzt werden.

Abb. 9 PEG in Lebensmitteln mit den auf den Verpackungen angegebenen E-Nummern der enthaltenen PEG-Derivate. Wiederum spielen nichtionische PEG-Tenside eine wichtige Rolle.

Schaut man sich die Liste der in der EU zugelassenen Lebensmittelzusatzstoffe genauer an, findet man auch einige PEG enthaltende Substanzen. So verbirgt sich hinter der Nummer E 431 ein PEG-Stearat mit 40 Ethylenoxideinheiten; die bereits vorgestellten PEG-Sorbitanester finden sich unter den Nummern E 432-436 (Tabelle 3). E 433 (Polysorbat 80) ist in vielen Backmischungen zu finden. Polysorbat 60 findet sich beispielsweise in Eiscreme.

Tab. 3 Polysorbate.

Name	Struktur	Fettsäurerest	E-Nummer
Polysorbat 20	PEG-Sorbitanmonoester	Laurat	E 432
Polysorbat 40	PEG-Sorbitanmonoester	Palmitat	E 434
Polysorbat 60	PEG-Sorbitanmonoester	Stearat	E 435
Polysorbat 65	PEG-Sorbitantriester	Stearat	E 433
Polysorbat 80	PEG-Sorbitanmonoester	Oleat	E 436

PEG-Sorbitanfettsäureester werden durch die Umsetzung von Sorbitanfettsäureestern mit Ethylenoxid unter alkalischen Reaktionsbedingungen hergestellt (Abbildung 10). Das erhaltene Produkt ist ein Gemisch von PEG-Sorbitanmolekülen mit unterschiedlicher Anzahl an Fettsäureresten an allen möglichen PEG-Kettenenden. Da neben dem 1,4-Sorbitanester im ersten Schritt der Reaktion noch weitere Isomere erhalten werden, und die eingesetzten Fettsäuren durch andere Fettsäuren kontaminiert sind, erhöht sich die Zahl der in den PEG-Sorbitanfettsäureestern vorhandenen Spezies weiter.[11]

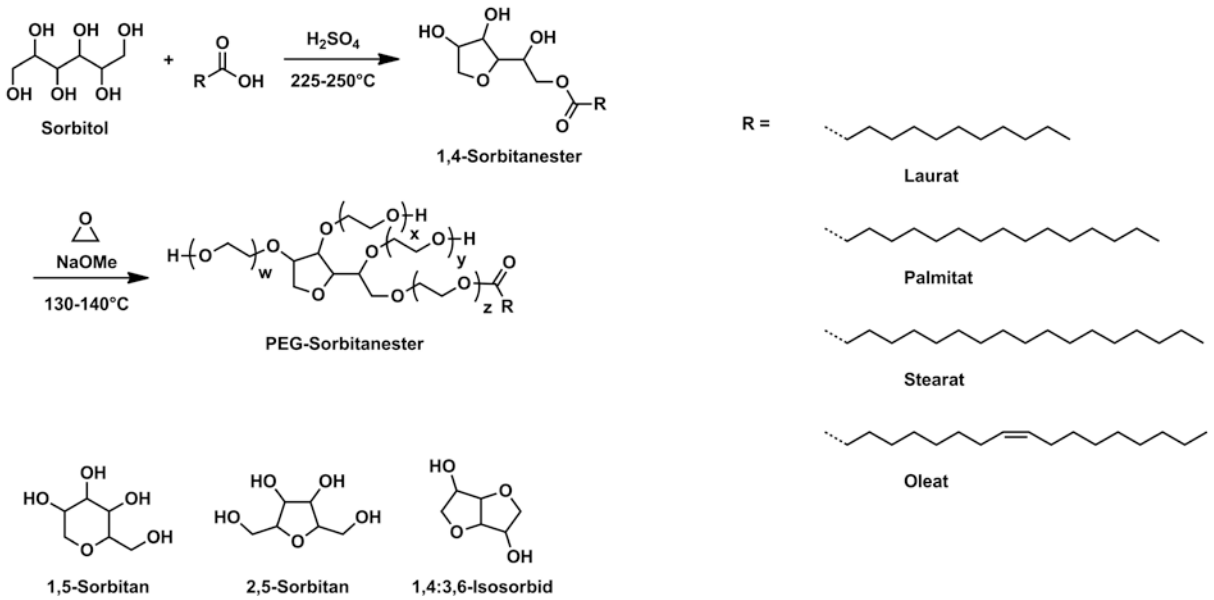

Abb. 10 Darstellung und Strukturen der Polysorbate.

Je nach hauptsächlich eingesetzter Fettsäure werden diese Tenside unter verschiedenen Bezeichnungen gehandelt (Tabelle 3). So bezeichnet man PEG-Sorbitanmonooleat als Polysorbat 80 oder Tween 80, wobei sich die Zahl in diesem Fall nicht auf die Anzahl der durchschnittlich im Molekül vorhandenen Ethylenoxideinheiten bezieht, welche in allen Fällen 20 beträgt, sondern Art und Anzahl der eingesetzten Fettsäurereste codiert (Tabelle 3). Die Polysorbate eignen sich mit HLB-Werten von 10 bis 15 zur Darstellung von O/W-Emulsionen und finden sowohl in Kosmetika als auch in Arzneimitteln und Lebensmitteln Verwendung.

PEG als Ionenleiter für Batterien

Die Sauerstoffe in der PEG-Kette können sehr gut mit Li-Ionen wechselwirken und werden aus diesem Grund als Festelektrolyte verwendet. Die effiziente Speicherung von elektrischer

Energie wird in Zukunft immer mehr an Bedeutung gewinnen. Notwendig hierfür sind Akkumulator-Systeme, die den Anforderungen an eine sichere und effektive Stromspeicherung genügen. Vorreiter hierbei sind Lithium-Ionen-Akkumulatoren, bei denen Lithium-Ionen zwischen den Elektroden hin- und herwandern. Um diese Wanderung zu ermöglichen, benötigt man einen Elektrolyten, der Lithium-Ionen leitet. Dies können aprotische organische Lösungsmittel wie Ethylencarbonat sein. Der Nachteil hierbei liegt in der Entflammbarkeit dieser Flüssigkeiten und dem fehlenden Auslaufschutz.

Eine Weiterentwicklung dieser Lithium-Ionen-Akkumulatoren mit flüssigen Elektrolyten sind die Lithium-Polymer-Akkus, bei denen der Elektrolyt ein auslaufsicheres (weil festes) und schwer entflammbares Polymer ist. Dazu sind PEG und verschiedene seiner Derivate hervorragend geeignet.

Die Ionenleitfähigkeit beruht hierbei auf der Kronenether-artigen Struktur einzelner kurzer PEG-Segmente, die die Wanderung der Lithium-Ionen zwischen den Elektroden ermöglichen. Allerdings kommen die so erzielbaren Lithium-Ionen-Leitfähigkeiten noch nicht an die der flüssigen Elektrolyte heran, da die Kristallisierfähigkeit des PEGs die Bewegung der Lithium-Ionen wiederum behindert, sodass derzeit auf einen Mittelweg, die Quellung des Polymers in flüssiger Elektrolytlösung, zurückgegriffen werden muss. Die Entwicklung eines sicheren Polymer-Elektrolyten, der eine ausreichende Leitfähigkeit ohne Zugabe von organischen Lösungsmitteln garantiert, bleibt also eine Herausforderung für die aktuelle Forschung, bei der PEG und seine Derivate mit Sicherheit eine entscheidende Rolle spielen werden.

Unerwartetes

PEG bei der Restaurierung von Grabungsfunden oder alten Holzobjekten

Bei der Konservierung von Grabungsfunden (Fossilien, archäologische Lederfunde oder Holzobjekte, die lange unter Wasser oder in feuchter Umgebung lagen) stellt die Austrocknung ein Grundproblem dar, da diese zu Schrumpfung und in der Folge zur Entstehung von Spannungen führt, die letztendlich im Zerfall der Fundobjekte resultieren. Mit Hilfe von PEG ist die Umwandlung solcher feuchter Objekte in langzeitstabile Trockenpräparate möglich. Die Konservierung erfolgt, indem man die Objekte entweder in einer PEG-Lösung tränkt oder mit einer solchen besprüht. Dabei wird das eingeschlossene Wasser schonend gegen PEG-Moleküle ausgetauscht, ohne dass es bei diesem Prozess zu größeren Volumenänderungen kommt. Je nach

Zustand des zu konservierenden Objekts kann hierfür PEG unterschiedlichen Molekulargewichts verwendet werden.

Abbildung 11 zeigt ein berühmtes Holzobjekt, das auf diesem Wege für die Nachwelt erhalten wurde: Das Wrack der legendären Vasa, das prunkvolle Kriegsschiff des Schwedenkönigs Gustav II. Adolf von Schweden, das 1628 bereits bei seiner Jungfernfahrt sank und nach mehreren Jahrhunderten unter Wasser erst 1961 geborgen wurde. Nachdem verschiedene Materialien zur Konservierung des Schiffswracks getestet wurden, entschloss man sich dazu, die Vasa mit einer wässrigen Lösung von PEG zu besprühen, das ins Holz eindringen und das enthaltene Wasser verdrängen sollte. Ab 1965 wurde das Wrack aus 500 Düsen mit verschiedenen wässrigen PEG-Lösungen besprüht. Die PEG-Konzentration wurde dabei mit der Zeit von 10 auf 45% erhöht. Die Konservierung mit PEG war erst nach 17 Jahren abgeschlossen![12] Interessanterweise wurde selbst nach 30 Jahren kein wesentlicher Abbau des zur Konservierung eingesetzten PEGs beobachtet.[13]

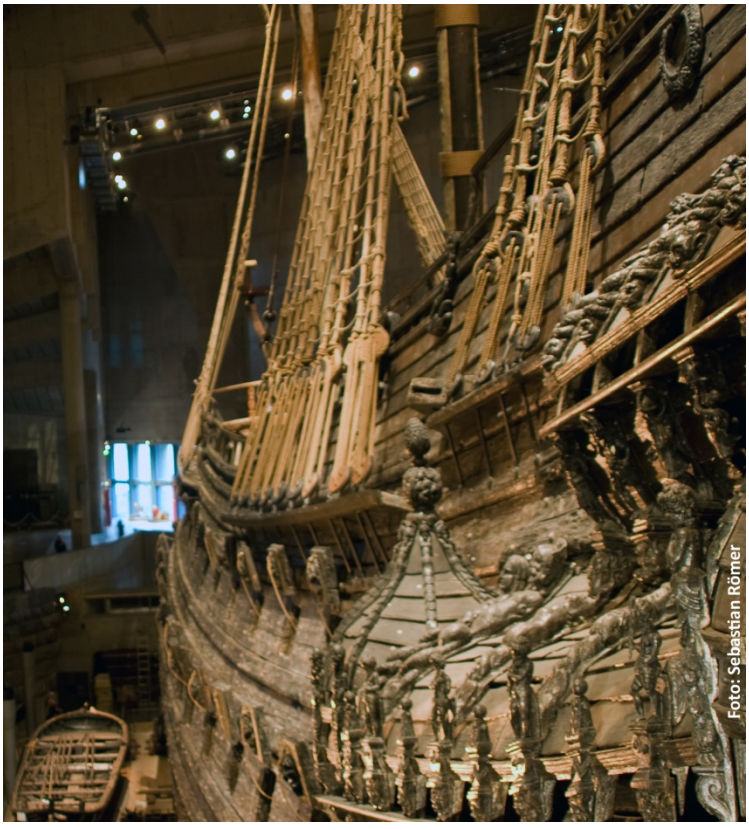

Abb. 11 Legendäres Schiffswrack aus dem 17. Jahrhundert: Das königliche Schiff „Vasa“, mit PEG konserviert.

PEG in U-Booten und für Textilien

Auch in der maritimen Kriegsführung spielt PEG überraschenderweise eine Rolle. Wird es durch seitlich an Schiffskörpern installierte Düsen ausgebracht, reduziert es die Viskosität des das Fahrzeug umströmenden Wassers und somit den hydrodynamischen Widerstand. Ferner werden Turbulenzen verringert, wodurch die propellerantriebsbedingten Geräusche gedämpft werden. Der Effekt ist abhängig vom Molekulargewicht des eingesetzten Polymers, weshalb besonders hochmolekulare PEGs ($M \geq 2 \cdot 10^6$ g/mol) zum Einsatz kommen.[14] Diese Technologie ist insbesondere für Unterseeboote hochinteressant und wurde von der US Navy erfolgreich getestet.

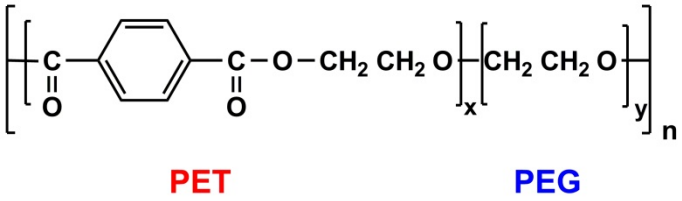

Abb. 13 Blockstruktur des Sympatex® Poly(etherester)s mit alternierenden PET und PEG Bausteinen.

Nach diesen ungewöhnlichen Einsatzgebieten noch ein Anwendungsfeld, das allen Sportbegeisterten bestens bekannt sein dürfte: Funktionsbekleidung für schweißtreibende Aktivitäten im Freien (Skisport, Mountainbike, Trekking, etc.) enthält oft die bekannte „Sympatex®"-Membran, ein Textilgewebe, das für Wasser und Wind undurchlässig ist, Wasserdampf jedoch von innen nach außen transportiert. Auch diesen Effekt verdankt das Material dem PEG. Hydroxylfunktionelle PEG-Diole werden als hydrophiler und flexibler Baustein für Multiblockcopolymere mit abwechselnden hydrophilen und hydrophoben Segmenten verwendet. Wird ein hydrophober und vergleichsweise steifer Poly(ethylenterephthalat) Block mit solchen hydrophilen und flexiblen Blöcken verknüpft, so entstehen durch die Unmischbarkeit der Blöcke hydrophile PEG-Domänen (mithin keine echten Poren!) im Material, die Wasserdampf aufnehmen und transportieren können (Abbildung 13). Eine solche „atmungsaktive" Sympatex®-Membran muss zur Erzielung der gewünschten Transport- und Barrierewirkung nur 5–10 µm dick sein und wird mit einem Oberstoff aus Polyester laminiert, d.h. verklebt. Je größer der Temperatur- und Feuchtigkeitsunterschied zwischen innen und außen, umso mehr gasförmiges Wasser wird durch die Membran geleitet.

Weiterentwicklung von PEG: Wo liegen die aktuellen Herausforderungen?

Am Ende dieses Artikels stellt sich die Frage, wo die aktuellen Fragestellungen zur Weiterentwicklung von PEG für den Chemiker liegen. Hierfür einige Beispiele: Verzweigte und damit polyfunktionelle PEG-Strukturen weisen einige vielversprechende Charakteristika auf. So besitzen sie eine große Anzahl von Endgruppen, die eine partielle oder vollständige weitere Funktionalisierung zulassen. Zudem behindern Verzweigungsstellen die Kristallisation, so dass komplett amorphes, nichtkristallines PEG erhalten werden sollte, wenn eine bestimmte Verzweigungsdichte überschritten ist. Kürzlich gelang so erstmals die Herstellung von baumartig folgeverzweigtem, also dendritischen PEG-Strukturen in einem Schritt. Dies lässt sich durch die direkte, einstufige Copolymerisation von EO mit Anteilen des Monomers Glycidol erreichen, das nach Ringöffnung zwei reaktive Funktionalitäten freisetzt, und so zur Entstehung der in Abbildung 14 dargestellten, dendritisch verzweigten PEG Struktur führt.[15] Die Biokompatibilität dieser Strukturen ist vergleichbar der des linearen PEG. Die Prüfung des Potentials solcher Strukturen in den nächsten Jahren kann zu weiteren, bislang unbekannten Anwendungsfeldern führen.

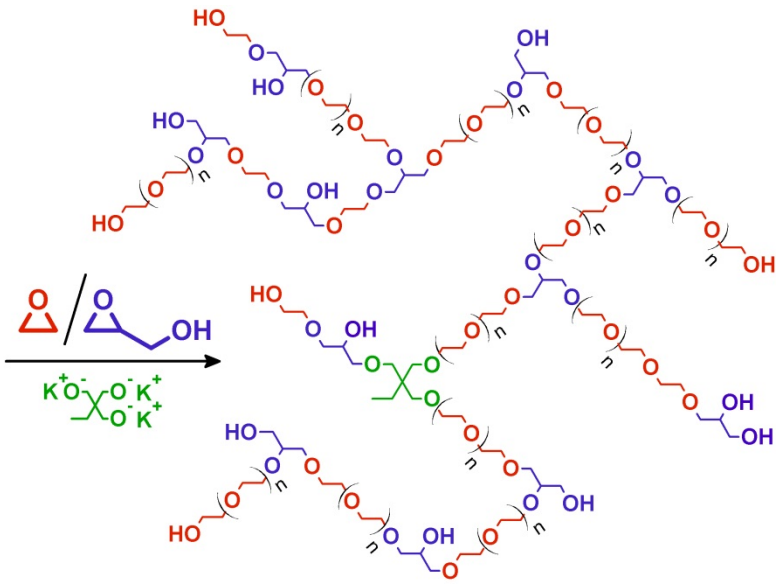

Abb. 14 Hochverzweigtes und biokompatibles PEG durch Einbau von Glycerin-Verzweigungseinheiten.

Innovative PEG-Strukturen spielen ferner eine große Rolle für die Weiterentwicklung der Biokonjugation mit Proteinen und Lipiden. In diesem Zusammenhang werden heterobifunktionelle PEG-Strukturen entwickelt, die zwei unterschiedliche Endgruppen tragen, die von

orthogonalen Umsetzungen angesprochen werden können. Auch die Synthese von PEG-Copolymeren mit weiteren Funktionalitäten innerhalb der Polyether-Kette stellt eine wichtige Aufgabe dar. Die Beschichtung von Oberflächen von Implantaten mit schwach vernetzten PEG-Hydrogelnetzwerken ist ein weiteres wichtiges Thema, da so eine unerwünschte Proteinablagerung verhindert werden kann. Auf weitere Entdeckungen und Anwendungsperspektiven für PEG-basierte Strukturen darf man also gespannt sein!

Zusammenfassung

Poly(ethylenglykol) ist in unserem Leben allgegenwärtig. Wir begegnen diesem biokompatiblen und hervorragend wasserlöslichen Polymer, meist ohne dass uns dies bewusst ist, in fast allen Bereichen des alltäglichen Bedarfs: Von Haut- und Haarpflegeartikeln, über Kosmetik- und Styling-Produkten bis hin zu Lebensmitteln und Medikamenten. Selbst in der maritimen Militärtechnologie und bei der Konservierung geborgener Kulturgüter wird es eingesetzt. Dieser Artikel beschäftigt sich mit der Darstellung, den teils überraschenden Eigenschaften und der Anwendung dieses strukturell simplen, aber faszinierend vielseitigen Polymers.

Summary

Today, a life without poly(ethylene glycol) is hardly imaginable. One encounters PEG in nearly every aspect of our daily needs: from cosmetics to hairstyling products and from medicines to food. Even in maritime military technology and the preservation of recovered cultural possessions PEG can be found. This article deals with the synthesis, the surprising properties, and the application of this structurally simple yet fascinating and important polymer.

Schlagwörter: *Poly(ethylenglykol), biokompatibel, nichtionische Tenside, Kosmetik, PEGylierung, Polymerelektrolyt.*

Literatur

[1] T. Dudev, C. Lim, „Ring Strain Energies from ab Initio Calculations“ J. Am. Chem. Soc. **1998**, *120*, 4450.

[2] H. Staudinger, O. Schweitzer, „Über hochpolymere Verbindungen, 20. Mitteil.: Über die Polyäthylenoxyde“ *Ber. Dtsch. Chem. Ges. A und B* **1929**, *62*, 2395.

[3] C. Tonhauser, D. Wilms, F. Wurm, E. B. Nicoletti, M. Maskos, H. Löwe, H. Frey, „Multihydroxyl-Functional Polystyrenes in Continuous Flow“ *Macromolecules* **2010**, *43*, 5582.

[4] T. Henning, „Polyethylene glycols (PEGs) and the pharmaceutical industry“ *SOFW J.* **2001**, *127*, 28.

[5] R. Kjellander, E. Florin, „Water structure and changes in thermal stability of the system poly(ethylene oxide)-water“ *J. Chem. Soc., Faraday Trans. 1* **1981**, *77*, 2053.

[6] C. Fruijtier-Pölloth, „Safety assessment on polyethylene glycols (PEGs) and their derivatives as used in cosmetic products“ *Toxicology* **2005**, *214*, 1.

[7] Nach: T. Hargreaves, Chemical formulation: an overview of surfactant-based preparations used in everyday life, 1. Aufl., Royal. Soc. Chemistry, Cambridge, **2003**, 81.

[8] A. Abuchowski, T. van Es, N. C. Palczuk, F. F. Davis, „Alteration ofImmunological Properties of Bovine Serum Albumin by CovalentAttachment of Polyethylene Glycol“ *J. Biol. Chem.* **1977**, *252*, 3578.

[9] F. M. Veronese, G. Pasut, „PEGylation, successful approach to drugdelivery“ *Drug Discovery Today* **2005**, *10*, 1451.

[10] D. D. Lasic, D. Needham, „The „Stealth“ Liposome: A Prototypical Biomaterial“ *Chem. Rev.* **1995**, *95*, 2601.

[11] S. Frison-Norrie, P. Sporns, „Investigating the Molecular Heterogeneity of Polysorbate Emulsifiers by MALDI-TOF MS“ *J. Agric. Food Chem.* **2001**, *49*, 3335.

[12] Website des offiziellen Vasa-Museums in Stockholm: www.vasamuseet.se/en/Preservation--Research/Conservation-1962-1979/ (16.03.2011).

[13] J. Glastrup, Y. Shashoua, H. Egsgaard, M. N. Mortensen, *Macromol. Symp.* **2006**, *238*, 22.

[14] V. T. Truong, „Drag reduction technologies“, **2001**, DSTO-GD-0290; http://hdl.handle.net/1947/3846.

[15] D. Wilms, M. Schömer, F. Wurm, M. I. Hermanns, C. J. Kirkpatrick, H. Frey, „Hyperbranched PEG by Random Copolymerization of Ethylene Oxide and Glycidol“ *Macromol. Rapid Commun.* **2010**, *31*, 1811.

Die Autoren

Carsten Dingels, geb. 1983, studierte Chemie an der Johannes Gutenberg-Universität Mainz mit einem halbjährlichen Aufenthalt an der University of Toronto. Seit Ende 2009 beschäftigt er sich im Rahmen seiner Dissertation im Arbeitskreis von Prof. Holger Frey mit der Darstellung neuer multifunktioneller PEG-Strukturen zur Biokonjugation. Er wird durch ein Stipendium des interdisziplinären Max Planck Graduate Center (MPGC) mit der Johannes Gutenberg-Universität gefördert.

Martina Schömer, geb. 1984, studierte Biomedizinische Chemie an der Johannes Gutenberg-Universität Mainz und der University of Durham/UK. Seit 2009 promoviert sie im Rahmen des interdisziplinären Max Planck Graduate Center (MPGC) mit der Johannes Gutenberg-Universität in der Arbeitsgruppe von Prof. Holger Frey am Institut für Organische Chemie. Sie arbeitet auf dem Gebiet der multifunktionellen, verzweigten Polyether, wobei das hyperverzweigte Poly(ethylenglykol) und dessen Einsatz in der Medizin und Pharmazie einen besonderen Schwerpunkt bilden.

Holger Frey, geb. 1965, studierte Chemie an der Universität Freiburg/Breisgau. Nach der Diplomarbeit und einem Aufenthalt an der Carnegie-Mellon University (Pittsburgh, USA) schloss er seine Promotion 1993 an der Universiteit Twente in den Niederlanden ab. Nach der Habilitation an der Universität Freiburg 1998 erhielt er 2002 einen Ruf an die Johannes Gutenberg-Universität Mainz auf eine Professur für Organische und Makromolekulare Chemie. Sein Hauptinteresse ist die Synthese neuer Funktionspolymere, insbesondere Polyether, Polyester und Silicium-haltiger Polymere. Ein weiterer Schwerpunkt liegt auf der Herstellung und Charakterisierung verzweigter Polymerstrukturen sowie auf der Nutzung von Mikroreaktoren für die Polymerherstellung.

Alle Autoren haben zu gleichen Anteilen zu diesem Artikel beigetragen.

1.2 From Biocompatible to Biodegradable: Poly(ethylene glycol)s With In-Chain Cleavable Linkages

*Carsten Dingels and Holger Frey**

Johannes Gutenberg-University Mainz, Institute of Organic Chemistry, Duesbergweg 10-14, 55099 Mainz, Germany.

Submitted for publication to Angewandte Chemie as a minireview.

Abstract

Due to the success of polymer therapeutics in the last decades and several launched polymer-based drugs, the scientific interest in these "nanopharmaceutics" is unbroken. Especially, when it comes to synthetic polymer/protein conjugates, poly(ethylene glycol) (PEG) is the gold standard polymer. However, like other synthetic polymers in the field, PEG suffers from its non-biodegradability, limiting its use in parental formulations to a molecular weight range with a specific upper limit, the renal excretion limit, to avoid polyether accumulation in human tissue. Therefore, several routes for the implementation of in-chain biocleavable moieties, such as acetals or disulfides, into PEG have been investigated. The strategies range from coupling reactions of commercial telechelic PEGs to custom-made PEG copolymers.

Keywords: *Biodegradation, poly(ethylene glycol), acetals, PEGylation, drug delivery*

Introduction

Since the late 1970s, when Davis and coworkers covalently attached poly(ethylene glycol) (PEG) to bovine proteins,[1, 2] this versatile polyether has become the gold standard polymer in drug delivery systems. It exhibits a unique combination of desirable properties rarely found for any other synthetic or natural polymer. PEG is non-toxic, mostly non-immunogenic, chemically inert and soluble in water.[3] Further, it is inexpensive and can be produced in a wide range of molecular weights in a well-defined manner with very low polydispersity indices (PDI, M_w/M_n). The polyether is soluble in a variety of organic solvents, which gives access to a vast variety of chemical transformations of its terminal hydroxyl groups. Hence, its functionalities can easily be adjusted to the purpose of its application.[4-6] Besides the field of drug delivery, PEG is also an important component in some textiles, laxatives, and surfactants found in daily products, such as cosmetics and edibles.[7]

Several different PEG-based drug delivery systems are subject to current pharmaceutical research, the most prominent being protein PEGylation,[3, 8-12] stealth liposomes,[13] and PEG-based polymeric carriers for low molecular weight drugs.[9, 12, 14] While all of these methods use PEG because of its non-toxicity, non-immunogenicity and water solubility, they are based on different concepts. Therapeutically active proteins, although acting highly specific and effective, exhibit some inherent difficulties. They undergo fast proteolytic degradation and are often immunogenic, which results in very short body residence times and a fast decrease below the effective concentration. The covalent attachment of PEG (PEGylation) decreases renal elimination lowers enzymatic degradation rates and reduces the immunogenicity of the protein/synthetic polymer conjugate compared to the native protein. Altogether, these effects result in prolonged blood circulation times and bioavailability of the conjugates. The success of this concept is underlined by the fact that several PEG-protein conjugate drugs have already been approved by the Food and Drug Administration (FDA).[15] “Stealth liposomes” consist of phospholipid vesicles decorated with PEG chains, anchored to the vesicle`s membrane via lipid anchor groups, and designed as transporters for low molecular weight drugs. Similar to the PEGylation of proteins, the fastening of PEG chains prolongs blood circulation times of the liposomes.[13, 16] Polymeric carriers for small molecular weight drugs rely on Ringsdorf’s drug delivery concept[17], which describes the use of a multifunctional, biocompatible synthetic polymer to transport pharmacons along with targeting moieties. These systems became even

more important when Maeda described the enhanced permeability and retention (EPR) effect for passive tumor targeting with large molecules,[18, 19] a central concept in today's anti-cancer research. PEG has been studied in this context, but suffers from its lack of polyfunctionality which results in low drug payloads.[9, 12, 14, 20] Therefore, several different strategies have been explored to synthesize PEGs with increased numbers of functional groups, such as multiarm PEGs,[21-23] dendrimer-like PEGs,[24-29] dendronized PEGs,[30, 31] and multifunctional PEGs.[32]

The benefits and drawbacks of the use of PEG in drug delivery systems along with those of possible alternative polymeric structures have recently been reviewed.[33, 34] One of the major concerns regarding the application of PEG in the human body is its non-biodegradability. As the blood circulation times rise with increasing molecular weight of PEG,[35] the use of high molecular weight polyethers appears to be advantageous. However, the hydrodynamic volume of PEG must not exceed the kidney excretion limit (40-60 kDa) to prevent accumulation of the polymer in the liver.[36] Consequently, degradable high molecular weight PEG derivatives which carry frangible joints in the backbone, but retain all of PEG's valuable properties, are highly desirable. To avoid toxic effects, the degradation products of such systems must not fall below400 $g \cdot mol^{-1}$.[33, 34] This review focuses on the different synthetic approaches for the incorporation of labile moieties into the PEG chain. Although highly interesting, PEGs with cleavable linkers[37] or lipids,[38-47] which were found to decrease the reduction in bioactivity of PEGylated proteins or increase the bioavailability of pharmacons transported in stealth liposomes, respectively, will not be discussed on the following pages.

Synthetic Approaches

The synthetic strategies for the incorporation of cleavable moieties into the backbone of PEG that have been employed up to date (Table 1) mirror the inherent challenges related to this task. The most appreciated approach would be the direct synthesis via the AROP of EO and an oxirane comonomer providing the additional functionality, analogous to the synthesis of multifunctional PEGs (*mf*-PEGs),[32] since copolymers can be obtained via AROP in a well-defined manner with low polydispersity. In contrast to the *mf*-PEGs, an oxirane co-monomer for the degradable PEGs can, if at all, hardly be synthesized. The degradable moiety would have to resist the harsh basic conditions of the AROP, limiting the choices to acetals, ketals,

Table 1. Cleavable units in degradable PEGs: Structures, implementation and degradation conditions.

Cleavable Unit	Structure	Synthetic Approach	Degradation[a]	Ref.
Acetals	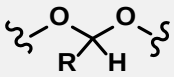	PEG coupling	pH < 7.4	[48-61]
Acetals/ ketals	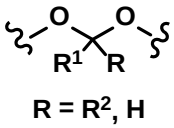 R = R^2, H	Cleavable AROP initiator	pH < 7.4	[62, 63]
Acetals/ ketals	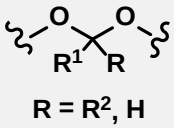 R = R^2, H	Cleavable AROP inimer[b]	pH ≤ 7.4	[64, 65]
Aconitic acid diamides	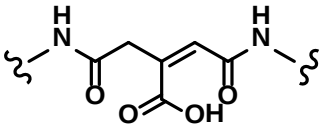	PEG coupling	pH < 7.4	[66]
Azo groups	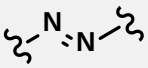	PEG coupling	enzymatic	[67, 68]
Carbonates	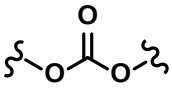	PEG coupling	basic hydrolysis	[69-79]
Carboxylates	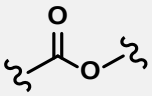	PEG coupling	hydrolytic, enzymatic	[24, 67, 68, 80-99]
Disulfides	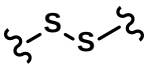	PEG coupling	reductive	[84, 100-103]
Hemiacetals	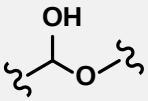	PEG oxidation	acidic or basic	[104]
Orthoesters	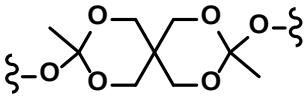	PEG coupling	pH < 7.4	[105]
Peptides	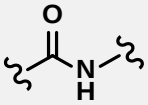	PEG coupling	enzymatic	[25, 106-117]
Phosphoesters	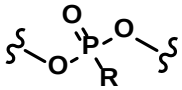	PEG coupling	acidic or basic	[118-131]
Urethane	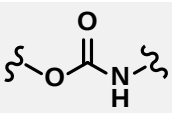	PEG coupling	(hydrolytic)	[84, 132-140]
Vinyl ethers	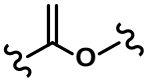	Elimination from chloromethyl functionalized PEG	pH < 7.4 @ 37 °C	[141]

[a] Conditions may vary for the same cleavable unit due to different adjacent moieties. [b] Concept results in hyperbranched architectures.

disulfides, ortho esters, and vinyl ethers. Three-membered cycles including these groups are highly energetic and have not been synthesized or are stable only at very low temperatures, as, for example, allene oxide[142] or *cyc*-S_2O.[143, 144] The direct synthesis of polyethers with in-chain acetals by cationic copolymerization EO and 1,3,5-trioxane is of course known, but the degradation of the resulting polymeric formaldehyde acetals require low pH conditions, the resulting formaldehyde is toxic, the *PDI*s are higher than those of anionically synthesized polymers, and the acetal content in the reported works is rather high, as the ethylene oxide units serve as stabilizing fractions to stop the unzipping of terminal oligoacetal blocks.[145-147]

Modification of Commercial PEGs

The majority of all cleavable groups incorporated into the backbone of PEG (summarized in Table 1 along with the corresponding synthetic approaches) were introduced by coupling of homotelechelic PEGs via addition or condensation reaction. A detailed discussion of the applicable labile units, as well as the synthesis and properties of the obtained materials will be presented in the next section. The main drawbacks common for all of these telechelics-based coupling strategies are the broad molecular weight distributions (M_w/M_n = 1.6 to >10) and poor control of the degree of polymerization. These issues are avoided if just two PEG chains are linked to one (multi)functional degradable coupling unit,[54, 85, 99, 107, 108, 114] resulting in cleavable PEGs with a single (functional) cleavable joint, but low yields are obtained when none of the termini is blocked as a methyl ether.[56] The PEG coupling approaches are popular because the required dihydroxy PEG telechelics are inexpensive and soluble in many organic solvents, enabling a variety of coupling reactions. In cases where the telechelic PEGs are coupled via a multihetero functional unit, degradable multifunctional PEGs can be synthesized as presented by Ulbrich and Říhová,[84, 102, 108] Lee,[80, 81] and Brocchini,[48, 50] for example. Furthermore, PEG is, as mentioned before, non-toxic and non-immunogenic and thus easy to handle, whereas all of the strategies that involve the synthesis of the polyether require polymerization of the gaseous ethylene oxide under anhydrous conditions. A one-step synthetic route to acid-degradable PEGs that relies neither on EO polymerization nor on a PEG coupling reaction was presented by Elisseeff and coworkers.[104] Some of the methylene groups of commercial PEG were oxidized to hemiacetals using Fenton's reagent. Unfortunately, degradation of the hemiacetals occurred already during the synthesis at low degrees of oxidation, which is a drawback that will have to be overcome.

EO polymerization methods

Synthetic approaches to degradable PEGs which do not rely on postpolymerization reactions of commercial PEGs have evolved just very recently and involve the initiation from a macroinitiator with a cleavable moiety,[62, 63] elimination of HCl from EO/ epichlorohydrin copolymers[141] and copolymerization of EO with a cleavable AROP inimer.[64] In 2011, Gnanou, Taton and coworkers presented an elegant synthetic route to acid-degradable dendrimer-like PEOs (poly(ethylene oxide)s, i.e., high molecular weight PEGs) with ketal branching units (Scheme 1).[62] All of the degradable dendritic PEOs from the second (G2, $M_{n,\,NMR}$ = 10,600 g·mol^{-1}) to the seventh generation (G7, $M_{n,\,NMR}$ = 446,000 g·mol^{-1}) were well-defined with *PDI*s below 1.10. Degradation of these materials was proven under different conditions. In extremely acidic media, three samples of different generations (G2, G3 and G7) degraded completely to PEG derivatives with molecular weights of around 2,000 g·mol^{-1}. At 37 °C and *pH* 5.5 65% of all ketal groups of G7 were degraded in 80 h, while the cleavage of 90% took one week. Of course, the shortcoming of these remarkable and promising structures is their time-consuming synthesis.

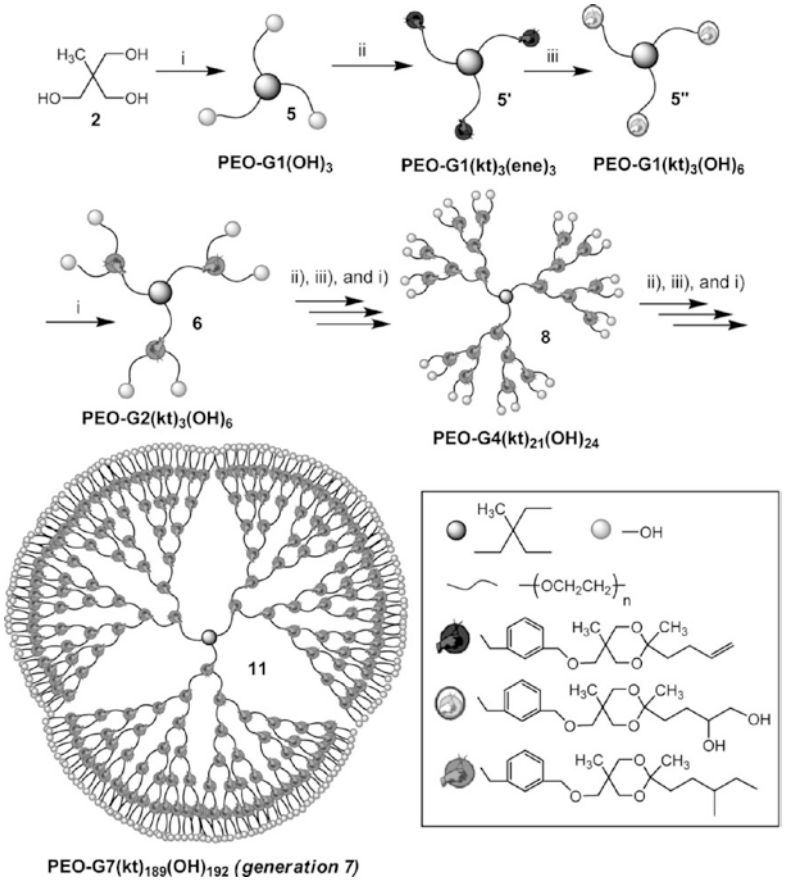

Scheme 1. Synthesis of acid-degradable dendrimer-like PEO. (From Ref. [62]).

With the copolymerization of EO and an inimer for the AROP that carried an acetal moiety, GEGE, our group presented an one-step synthesis to acid-degradable long-chain branched PEGs (Scheme 2).[64] Similar to the dendrimer-like PEOs, these structures carry acid-labile moieties at each branching unit and were decorated with hydroxyl groups. The prize paid for the rapid synthesis is the less defined, i.e., not perfectly branched, architecture, and the fact that the labile moieties do not separate both arms of each branching point from the initiation site, which results in broadly distributed degradation products. Other cleavable AROP inimers were solely presented in recent work by the group of Kizhakkedathu to generate degradable polyglycerol (PG).[65] In an elegant approach they synthesized a series of different ketal inimers and found a much slower degradation for ketals derived from vicinal diols than for ketals of two separated alcohol synthons. These inimers could possibly also be copolymerized with EO to tailor the degradation kinetics of degradable long-chain branched PEGs.

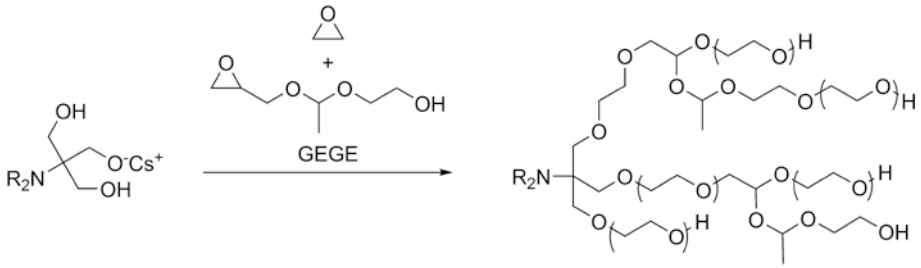

Scheme 2. Single-step synthesis of acid-degradable long-chain branched PEG according to Ref. [64].

The aforementioned polymerization methods resulted all in branched PEG architectures, but linear degradable PEGs have also been reported. A very promising pathway was reported by Lynd, Hawker et al. who copolymerized EO with epichlorohydrin via activated monomer ring-opening polymerization to obtain PEGs functionalized with chloromethyl groups and *PDI*s below 1.4.[141] Subsequent elimination of HCl resulted in PEGs with hydrolysis-sensitive vinyl ether units distributed along the backbone (Scheme 3). The degradation of the polyether occurred at *pH* 7.4 and 37 °C to approximately $M_n(t)/M_n(0) = 20\%$ after $t = 72$ h. However, no information on the nature of the terminal functionalities of the degradable polymer, the extent of substitution during the elimination step, and the intended coupling strategy to pharmacons were presented.

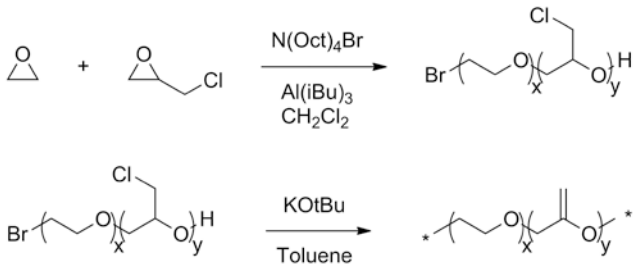

Scheme 3. Linear degradable PEGs according to Lynd, Hawker et al. (Ref. [141]).

Poly(ethylene glycol) monomethyl ether (mPEG) with a single acid-labile acetal unit in the backbone can be synthesized by turning the terminal hydroxyl group of mPEG with a lower molecular weight into a hydroxyethyl acetal, following a two-step protocol and subsequent polymerization of EO on this macroinitiator (Scheme 4).[63] The molecular weight of the macroinitiator and the number of added EO units determined the defined position of the acetal in the backbone. Figure 1 shows the SEC traces of the degradable mPEG before and after acidic degradation as well as its precursor. The two well-defined distributions of different molecular weights were attributed to the used low molecular weight PEG and the added PEG block. These degradable mPEGs might be applicable as substitutes for commercial mPEGs, relying on established protocols for conjugation to proteins or low molecular weight drugs in order to increase the maximum molecular weight of the polyether that can be used in the human body, avoiding the risk of accumulation of PEG in the liver.

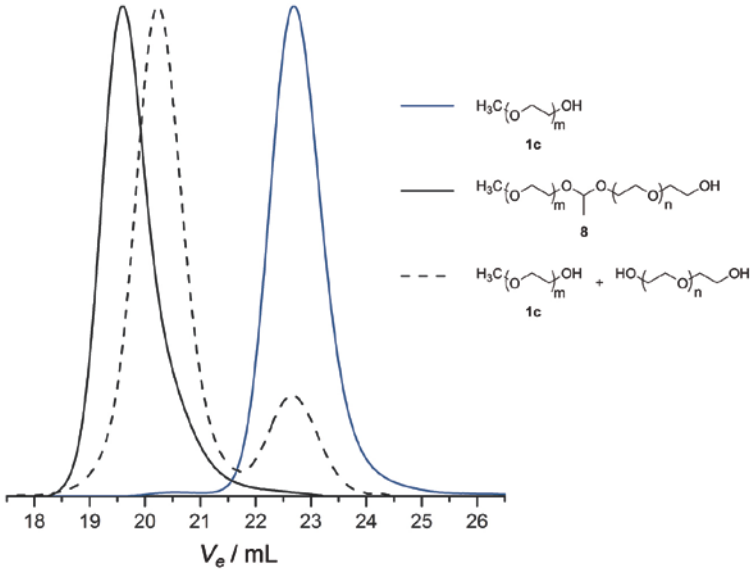

Figure 1. Size-exclusion chromatograms of degradable mPEG before and after degradation as well as its precursor. Reprinted with permission from Ref. [63]. Copyright (2012) American Chemical Society.

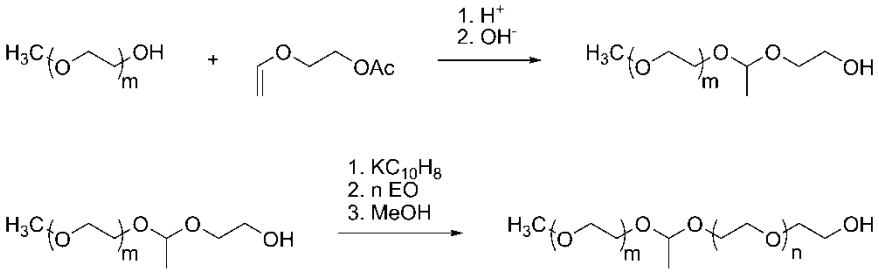

Scheme 4. Synthesis of mPEG with a single cleavable unit at a defined position according to Ref. [63].

Different Labile Units for Different Triggers

Acid Sensitive PEGs

The majority of the labile units listed in Table 1, including most of the PEGs synthesized by previously discussed EO polymerization methods, are cleaved at acidic pH. Acidity is a popular degradation trigger, especially for polymeric carriers of anticancer drugs making use of passive targeting of tumors (EPR effect) and the potentially increased acidity of such tissue.[148, 149] Reduced pH is further found in lysosomes (pH 5.5) and endosomes (pH 6.5), extending the possible application of acid sensitive polymer therapeutics beyond antitumor therapies.

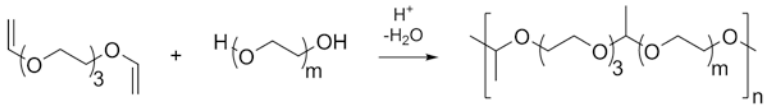

Scheme 5. Synthesis of acid-degradable PEGs from divinyl TEG according to Ref. [48].

The first attempt to synthesize acid sensitive PEGs based on a PEG coupling approach capitalized on *cis*-aconitic acid linkers. The obtained polymer was acid-degradable and most likely biocompatible. However, decarboxylation and cross-linking reactions led to non-degradable linkages.[66] Better results were achieved with the incorporation of acetal moieties in PEGs. Pioneering work by Duncan and Brocchini used the copolymerization of triethylene glycol (TEG) divinyl ether with dihydroxyl PEGs (Figure 5) and functional diols, such as protected serinol[48] and diphenols[51, 52]. The former diol allows postpolymerization modification of the resulting amino-pendent polyacetals (APEGs) with pendent doxorubicin (DOX) moieties,[50] whereas among the latter, drugs can be incorporated directly in the main chain.[51, 61] Using telechelic PEG with M_w = 3400, degradable PEGs with molecular weights up to 100,000 g·mol^{-1} and *PDI*s of 1.6-2.0 can be synthesized. Other synthetic routes to PEG polyacetals involve

condensation of PEG diols with the corresponding aldehyde[55, 60] or Williamson ether synthesis from an acetal-containing diol and PEG ditosylate.[53, 58, 59] Although conceptually interesting, these routes do not lead to high-molecular-weight polyethers, but result in polydisperse (PDIs > 2) or, in case of the etherification, ill-defined (5.8 < PDI < 11.6) polymers.

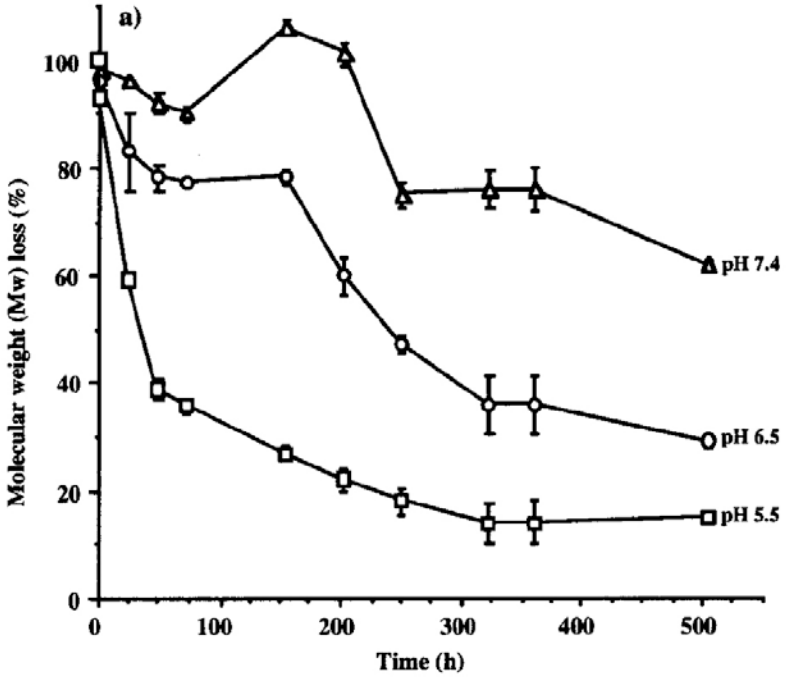

Figure 2. pH-dependent degradation of the aliphatic PEG poly(acetaldehyde acetal) described in Scheme 5. Adapted with permission from Ref. [48]. Copyright (2002) American Chemical Society.

The degradation of acetals in PEG is strongly pH and temperature dependent and, not surprisingly, faster in more acidic media.[48, 51, 52, 54, 59-61, 63, 64] At pH 5.5 and 37 °C, total degradation of PEG acetaldehyde acetals requires approximately three weeks, but also at pH 7.4 (pH of blood), a significant amount of the labile groups are hydrolyzed (Figure 2).[48] Further, the chemical composition of the acetal, i.e., the nature of the aldehyde and alcohols influence the rate of its hydrolysis: Benzaldehyde acetals degrade faster than aliphatic aldehydes (compare Ref. [54] and Ref. [60]), and phenolic acetaldehyde acetals are hydrolyzed faster than purely aliphatic ones.[51, 52] Cyclic acetals require harsher conditions than linear ones[53] (also true for PG-based polyketals[65]) and basic moieties, such as amino groups adjacent to the acetal also lead to decreased hydrolysis rates.[63] Biocompatibility and pharmacokinetic tests of acetal-containing PEGs and polymeric prodrugs have been promising so far. APEG, its derivative without pendent functions (Scheme 5), and the degradation products of the latter were non-cytotoxic in an MTT assay using B169F10 cells and non-hemolytic within 24 h.[48] Furthermore, doxorubicin-loaded

high molecular-weight APEGs outperformed *N*-(2-hydroxypropyl)methacrylamide copolymer DOX conjugates with prolonged blood circulation times, increased passive tumor targeting, and reduced DOX deposition in liver and spleen.[50] Besides their application as degradable polymeric carriers for low molecular weight molecules, acid-labile PEGs are also used for the synthesis of gene delivery vectors[54, 56] as well as precursors for degradable hydrogels[53, 57, 58] and triblock copolymers.[55, 59, 105]

Enzymatically Degradable PEGs

The pool of biodegradable units incorporated in PEG of course also contains enzymatically cleavable moieties. Most prominent among these are amino acid or oligopeptide linkages, which were applied for the coupling of monofunctional PEG derivatives[25, 107, 108, 114] and as monomers for polycondensation with difunctional PEGs.[106, 110-114] Depending on the inserted amino acid or sequence, the polymers can be cleaved by different proteases such as chymotrypsin or cathepsin B. Of course, PEG-based polypeptides can be degraded under simple hydrolysis conditions.[106, 114] First studies on such systems exposed the strong dependence of the degradation rate on the length and structure of the peptide linker.[106-108] While chymotrypsin requires a single in-chain phenylalanine residue for the PEG degradation,[106] cathepsin B does not cleave PEGs with just a glutamic acid linker.[108] In the latter case the degradation rate increases by adding a phenylalanine at the glutamic acids C terminus and is even higher by coupling it to the N terminal site. Further, the corresponding pendent benzylesters undergo proteolysis much faster than the free acid derivatives.[108] The degradable PEGs of this type are also suitable carriers for DOX, which can be bound via likewise enzymatically cleavable oligopeptides[109-112] or an acid sensitive hydrazone.[113] In contrast to free DOX, these polymer therapeutics exhibited no signs of toxicity in *in vivo* studies on mice and seemed to inhibit tumor growth.[111] However, no PDI values have been published for most of the PEG copolymers derived from polycondensation, but the available SEC traces indicate broad molecular weight distributions, which is an obstacle for eventual FDA approval.[111-113] PEGs with in-chain amino acid peptide bonds have also been prepared, mainly to add pending functionalities to the polyether rather than labile joints[115-117] and can be generated in a monodisperse fashion by multistep protection/deprotection protocols.[25]

If the required enzyme is solely available at the desired site of drug release, enzymatically degradable PEGs can be applicable for site-specific drug delivery. Azo compounds of 5-

aminoscalicylic acid (5ASA), a non-steroidal anti-inflammatory drug, are potent prodrugs for colon-specific delivery of this pharmacon. The free drug would be absorbed in the small intestine, whereas corresponding azo compounds can reach the colon, where reductive enzymes release 5ASA form its carriers.[150] The copolymerization of PEG diacids of various molecular weights with an Olsalazin (OLZ, *5,5'*-azodiscalicylic acid) derivative resulted in PEG-based prodrugs with molecular weights up to 47,000 $g \cdot mol^{-1}$ and in-chain carboxylates as well as enzymatically cleavable azo bonds. 5ASA release from the polymeric prodrugs in presence of reductive enzymes was confirmed (Figure 3). The comparison of the degradation rates in presence or absence of rat cecum content indicated that enzymatic azo reduction occurred prior to the cleavage of the ester. The ester hydrolysis rates at pH 6.8 (37 °C) were dependent on the size of the PEG precursors and higher for larger polyether segments.[67] Oral administration of the PEG prodrugs to rats confirmed colon-specific drug delivery *in vivo*.[68]

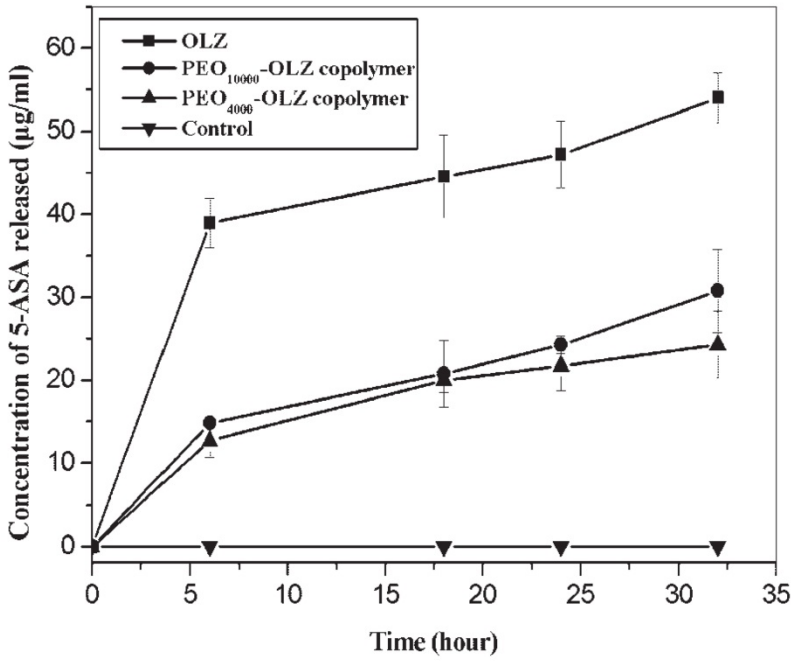

Figure 3. Release of 5ASA from OLZ and OLZ PEG copolymers in presence of reductive colon enzymes and benzyl viologen at 37 °C. (From Ref. [67]).

Several different polycondensation routes can be applied for the installation of carboxylates in PEG: DCC-promoted esterification[67, 68, 82-84], Michael addition to acrylates, as well as reactions of PEG with the corresponding acids,[92] acid anhydrides,[81] acyl chlorides,[85-89] and methyl carboxylates.[24, 93-97] Commonly, the polycondensation is conducted during the esterification step, but also the thiol oxidation of PEG cysteine diesters[84] and Michael addition of dithiols to

PEG di(meth)acrylates[90, 91] were used to synthesize PEG polyesters. Due to the numerous PEG-based polyesters synthesized for a wide range of applications, we will focus on the works that studied the PEG polyester degradability. Depending on the synthetic pathway and the size of the batched telechelic PEGs, polyesters with molecular weights in the range of 1,000-104,500 $g \cdot mol^{-1}$ and typical PDIs (1.4-2.7) were generated. The ester-containing PEGs can undergo enzymatic degradation, but just a few of them were examined regarding this property.[82, 86-88, 99] Mero et. al. observed almost no ester cleavage in a pH 7.4 buffer at 37 °C in 24 h, but rapid degradation in mouse plasma within the same time.[88] Typically, the enzymatic degradation at 37 °C and neutral pH takes a few days to complete, but comparison of the results is difficult because to many parameters vary (enzymes, linkers, PEG content, size of the PEG segments, observed quantity, type of sample). Carboxylates can further be degraded by simple hydrolysis under both, acidic and basic conditions. In theory, degradation rates are expected to be lowest under neutral conditions, but in presence of basic moieties, the hydrolysis can be slower in more acidic media (Figure 4).[81, 84, 99] Not surprisingly, hydrophilic poly(ether ester)s are hydrolyzed faster than hydrophobic derivatives under the same conditions.[67, 83]

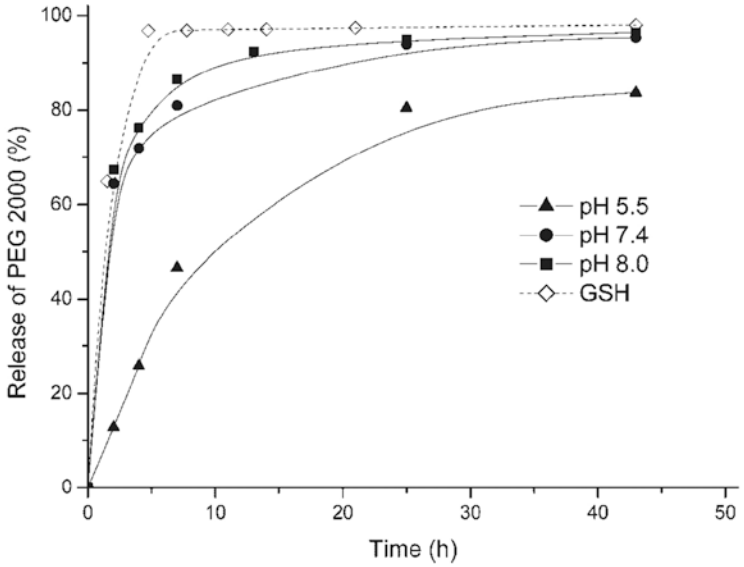

Figure 4. Degradation of PEG cystine polyester at 37 °C: Hydrolytic cleavage of ester moieties at different pH values. Reduction of disulfides at pH 5.5 (cGCH = 5 mm). (From Ref. [84]).

Alternative Labile Groups and Triggers

As azo bonds, disulfide linkages have been studied as reductively cleavable joints for the reversible connection of PEG telechelics.[84, 100-103] In contrast to the former, disulfides are

reduced by a reduced glutathione (GSH) derivative in the cytosol. The disulfide containing polyethers can either be synthesized from PEG dithiol precursors under oxidative conditions[84, 100-102] or by a polycondensation of telechelic PEGs and a suitable difunctional disulfide.[84] Depending on the synthetic route, size of the telechelic PEGs, and the reaction conditions, poly(ether sulfide)s with molecular weights up to 180,000 $g \cdot mol^{-1}$ were obtained. In contrast to poly(ether sulfide)s with degrees of polymerization exceeding 12, those prepared from tri-, tetra-, or hexa(ethylene glycol) were almost insoluble in water. Pendent functionalities have been incorporated in these polymers by coupling PEG chains to cystine via urethane or ester bonds. The reductive degradation rate is dependent on the hydrophobicity of the pendent functional groups. While the disulfides of a polyester from PEG and cystine at cytosolic glutathione concentrations (5 mm) are reduced even faster than the ester moieties are hydrolyzed at pH 8.0 (Figure 4), reductive degradation of a corresponding polymer with pendent *p*-nitrophenyl succinates is rather slow under the same conditions (<50% within 2 d).[84] As poly(ether sulfide)s also undergo reductive degradation when incubated with EL4 T-cells[102] and were non-toxic to HepG2 cells,[100] these polymers appear to be promising drug carriers.

Besides carboxylates, esters of other biologically relevant acids have been used to synthesize PEG-based polyesters. Physical properties of PEG-derived polycarbonates have been explored since the 1960s.[69-73] More recent studies have focused on the degradability and cell interactions of these materials, but the PEG contents were low (< 25%).[75-78] Water-soluble polymers with higher PEG fractions have been prepared, but no degradation data has been reported for these.[151, 152] PEGs with a single carbonate linker were solely mentioned in patent literature.[74, 79] Poly(H-phosphonate)s from PEG diols are generated by the polycondensation of the telechelic polyethers and dialkyl H-phosphonates.[118-129] The degradation of PEG polyphosphonates occurs randomly along the polymer chain under slightly basic conditions (pH 8.8, 40% degradation in 12 h) and is more rapid at low pH (pH 1.66, almost completed in 11 h). The degradation rate is further influenced by the polymer concentration, because the degradation yields in acidic products.[128, 131] These polymers might also undergo enzymatic degradation.[131] Poly(PEG H-phosphonate)s carry highly reactive P-H bonds that allow further functionalization, such as the attachment of pharmaceutically active compounds or linker moieties for the conjugation to such molecules[118, 129] as well as oxidation to the corresponding poly(PEG phosphate)s.[120-127] Another synthetic pathway to such polyphosphates is the

condensation of PEG diols and alkyl dichlorophosphates.[130] Further information on these interesting materials and their applicability in drug delivery systems can be found in a substantial monograph on polyphophoesters published recently.[131]

Various PEG-based polyurethanes (PUs) have been synthesized, mainly, to introduce pendent functionalities along the polymer backbone,[132-137] and are usually considered non-degradable under physiological conditions. Biodegradability has been described for numerous polyurethane materials, but seems to occur predominantly at additionally present cleavable units. Therefore, poly(ester urethane)s degrade faster than poly(ether urethane)s.[153] Similar findings were reported for PEG-based PU films using α-chymotrypsin in aqueous, buffered solution. A sample containing enzymatically cleavable trypsin chain extender eroded much faster than a PU-film without such a moiety.[138] The hydrolytic degradation of PEG-based PUs is slow and was investigated on samples synthesized without any chain extender at pH 7.4 (37 °C) (15% reduction of M_w within 12 days).[139]

Conclusions and Outlook

To tackle PEG's most important disadvantage in biomedical applications, its non-biodegradability, various synthetic pathways have been investigated to install several different degradable moieties in the backbone of PEG (Table 1) that can be cleaved under conditions found in organisms: Acidic, basic, enzymatic, and reductive. The rates of degradation strongly depend on the constitution and chemical environment of the linker as well as the size of the PEG segments for each of these classes. Care has to be taken, when comparing the degradation data of different methods. Main parameters that have to be taken into account are the temperature, pH, type of enzyme, concentrations (in case pseudo-first-order kinetics does not apply), and the measured quantity (number of remaining linkers, amount of released telechelic PEG, residual molecular weight). Although many of the presented PEGs gave promising results as biodegradable drug carriers, most of these polymers were synthesized in polycondensation reactions and exhibit certain deficits, such as broad molecular weight distributions. Well-defined degradable PEGs are obtained by coupling monofunctional PEGs to a (multi)functional labile unit, but the resulting polymers are limited in their payload, unless synthesized by multistep protection/deprotection protocols. Very recently, a number of strategies have been employed which base on custom-made PEGs by EO polymerization either from cleavable initiators or with

proper comonomers. However, none of the EO-based polymers has been tested regarding their biocompatibilities, their degradations *in vivo*, or their suitability as drug carriers, to date. In conclusion, the development of biodegradable PEGs has become a fast evolving field of research that will eventually contribute to a new generation of polymer therapeutics.

C.D. is grateful to the Max Planck Graduate Center with the Johannes Gutenberg-Universität Mainz (MPGC) for a fellowship and financial support.

References

[1] A. Abuchowski, T. van Es, N. C. Palczuk, F. F. Davis, *J. Biol. Chem.* **1977**, *252*, 3578.

[2] A. Abuchowski, J. R. McCoy, N. C. Palczuk, T. van Es, F. F. Davis, *J. Biol. Chem.* **1977**, *252*, 3582.

[3] F. M. Veronese, G. Pasut, *Drug Discovery Today* **2005**, *10*, 1451.

[4] S. Zalipsky, *Bioconjugate Chem.* **1995**, *6*, 150.

[5] J. Li, W. J. Kao, *Biomacromolecules* **2003**, *4*, 1055.

[6] M. S. Thompson, T. P. Vadala, M. L. Vadala, Y. Lin, J. S. Riffle, *Polymer* **2008**, *49*, 345.

[7] C. Dingels, M. Schömer, H. Frey, *Chem. unserer Zeit* **2011**, *45*, 338.

[8] P. Caliceti, F. M. Veronese, *Adv. Drug Del. Rev.* **2003**, *55*, 1261.

[9] R. B. Greenwald, Y. H. Choe, J. McGuire, C. D. Conover, *Adv. Drug Del. Rev.* **2003**, *55*, 217.

[10] J. M. Harris, R. B. Chess, *Nat. Rev. Drug Discov.* **2003**, *2*, 214.

[11] G. Pasut, M. Sergi, F. M. Veronese, *Adv. Drug Del. Rev.* **2008**, *60*, 69.

[12] G. Pasut, F. M. Veronese, *Adv. Drug Del. Rev.* **2009**, *61*, 1177.

[13] D. D. Lasic, D. Needham, *Chem. Rev.* **1995**, *95*, 2601.

[14] R. B. Greenwald, *J. Controlled Release* **2001**, *74*, 159.

[15] S. N. S. Alconcel, A. S. Baas, H. D. Maynard, *Polym. Chem.* **2011**, *2*, 1442.

[16] M. L. Immordino, F. Dosio, L. Cattel, *Int. J. Nanomed.* **2006**, *1*, 297.

[17] H. Ringsdorf, *J. Polym. Sci., Polym. Symp.* **1975**, *51*, 135.

[18] Y. Matsumura, H. Maeda, *Cancer Res.* **1986**, *46*, 6387.

[19] L. W. Seymour, Crit. Rev. Ther. Drug Carrier Syst. **1992**, 9, 135.

[20] R. Duncan, *Nat Rev Drug Discov* **2003**, *2*, 347.

[21] R. Knischka, P. J. Lutz, A. Sunder, R. Mülhaupt, H. Frey, *Macromolecules* **2000**, *33*, 315.

[22] D. Taton, M. Saule, J. Logan, R. Duran, S. Hou, E. L. Chaikof, Y. Gnanou, *J. Polym. Sci., Part A: Polym. Chem.* **2003**, *41*, 1669.

[23] H. Zhao, B. Rubio, P. Sapra, D. Wu, P. Reddy, P. Sai, A. Martinez, Y. Gao, Y. Lozanguiez, C. Longley, L. M. Greenberger, I. D. Horak, *Bioconjugate Chem.* **2008**, *19*, 849.

[24] C. J. Hawker, F. Chu, P. J. Pomery, D. J. T. Hill, *Macromolecules* **1996**, *29*, 3831.

[25] M. Berna, D. Dalzoppo, G. Pasut, M. Manunta, L. Izzo, A. T. Jones, R. Duncan, F. M. Veronese, *Biomacromolecules* **2006**, *7*, 146.

[26] X.-S. Feng, D. Taton, E. L. Chaikof, Y. Gnanou, *J. Am. Chem. Soc.* **2005**, *127*, 10956.

[27] X. Feng, D. Taton, R. Borsali, E. L. Chaikof, Y. Gnanou, *J. Am. Chem. Soc.* **2006**, *128*, 11551.

[28] X. Feng, D. Taton, E. L. Chaikof, Y. Gnanou, Biomacromolecules 2007, 8, 2374.

[29] D. Wilms, M. Schömer, F. Wurm, M. I. Hermanns, C. J. Kirkpatrick, H. Frey, Macromol. Rapid Commun. 2010, 31, 1811.

[30] Y. H. Choe, C. D. Conover, D. Wu, M. Royzen, Y. Gervacio, V. Borowski, M. Mehlig, R. B. Greenwald, J. Controlled Release 2002, 79, 55.

[31] G. Pasut, S. Scaramuzza, O. Schiavon, R. Mendichi, F. M. Veronese, *J. Bioact. Compat. Polym.* **2005**, *20*, 213.
[32] B. Obermeier, F. Wurm, C. Mangold, H. Frey, *Angew. Chem. Int. Ed.* **2011**, *50*, 7988.
[33] K. Knop, R. Hoogenboom, D. Fischer, U. S. Schubert, *Angew. Chem. Int. Ed.* **2010**, *49*, 6288.
[34] K. Knop, R. Hoogenboom, D. Fischer, U. S. Schubert, *Angew. Chem.* **2010**, *122*, 6430.
[35] T. Yamaoka, Y. Tabata, Y. Ikada, *J. Pharm. Sci.* **1994**, *83*, 601.
[36] G. Pasut, F. M. Veronese, *Prog. Polym. Sci.* **2007**, *32*, 933.
[37] D. Filpula, H. Zhao, *Adv. Drug Del. Rev.* **2008**, *60*, 29.
[38] J. A. Boomer, D. H. Thompson, *Chem. Phys. Lipids* **1999**, *99*, 145.
[39] X. Guo, F. C. Szoka, *Bioconjugate Chem.* **2001**, *12*, 291.
[40] J. A. Boomer, H. D. Inerowicz, Z.-Y. Zhang, N. Bergstrand, K. Edwards, J.-M. Kim, D. H. Thompson, *Langmuir* **2003**, *19*, 6408.
[41] C. Masson, M. Garinot, N. Mignet, B. Wetzer, P. Mailhe, D. Scherman, M. Bessodes, *J. Controlled Release* **2004**, *99*, 423.
[42] H. Hatakeyama, H. Akita, K. Kogure, M. Oishi, Y. Nagasaki, Y. Kihira, M. Ueno, H. Kobayashi, H. Kikuchi, H. Harashima, *Gene Ther.* **2006**, *14*, 68.
[43] R. M. Sawant, J. P. Hurley, S. Salmaso, A. Kale, E. Tolcheva, T. S. Levchenko, V. P. Torchilin, *Bioconjugate Chem.* **2006**, *17*, 943.
[44] H. Xu, Y. Deng, D. Chen, W. Hong, Y. Lu, X. Dong, *J. Controlled Release* **2008**, *130*, 238.
[45] J. A. Boomer, M. M. Qualls, H. D. Inerowicz, R. H. Haynes, V. S. Patri, J.-M. Kim, D. H. Thompson, *Bioconjugate Chem.* **2009**, *20*, 47.
[46] R. Kuai, W. Yuan, Y. Qin, H. Chen, J. Tang, M. Yuan, Z. Zhang, Q. He, *Mol. Pharm.* **2010**, *7*, 1816.
[47] D. Chen, X. Jiang, Y. Huang, C. Zhang, Q. Ping, *J. Bioact. Compat. Polym.* **2010**, *25*, 527.
[48] R. Tomlinson, M. Klee, S. Garrett, J. Heller, R. Duncan, S. Brocchini, *Macromolecules* **2002**, *35*, 473.
[49] J. Cheng, K. T. Khin, G. S. Jensen, A. Liu, M. E. Davis, *Bioconjugate Chem.* **2003**, *14*, 1007.
[50] R. Tomlinson, J. Heller, S. Brocchini, R. Duncan, *Bioconjugate Chem.* **2003**, *14*, 1096.
[51] M. J. Vicent, R. Tomlinson, S. Brocchini, R. Duncan, *J. Drug Target.* **2004**, *12*, 491.
[52] J. Rickerby, R. Prabhakar, M. Ali, J. Knowles, S. Brocchini, *J. Mater. Chem.* **2005**, *15*, 1849.
[53] S. Kaihara, S. Matsumura, J. P. Fisher, *Macromolecules* **2007**, *40*, 7625.
[54] V. Knorr, L. Allmendinger, G. F. Walker, F. F. Paintner, E. Wagner, *Bioconjugate Chem.* **2007**, *18*, 1218.
[55] W. Cui, M. Qi, X. Li, S. Huang, S. Zhou, J. Weng, *Int. J. Pharm.* **2008**, *361*, 47.
[56] J. B. Wong, S. Grosse, A. B. Tabor, S. L. Hart, H. C. Hailes, *Mol. BioSyst.* **2008**, *4*, 532.
[57] M. W. Betz, J. F. Caccamese, D. P. Coletti, J. J. Sauk, J. P. Fisher, *J. Biomed. Mater. Res., Part A* **2009**, *90A*, 819.

[58] S. Kaihara, S. Matsumura, J. P. Fisher, *J. Biomed. Mater. Res., Part A* **2009**, *90A*, 863.
[59] S. Kaihara, J. P. Fisher, S. Matsumura, *Macromol. Biosci.* **2009**, *9*, 613.
[60] Y. Wang, H. Morinaga, A. Sudo, T. Endo, *J. Polym. Sci., Part A: Polym. Chem.* **2011**, *49*, 596.
[61] R. M. England, E. Masiá, V. Giménez, R. Lucas, M. J. Vicent, *J. Controlled Release* **2012**, DOI: 10.1016/j.jconrel.2012.08.017.
[62] X. Feng, E. L. Chaikof, C. Absalon, C. Drummond, D. Taton, Y. Gnanou, *Macromol. Rapid Commun.* **2011**, *32*, 1722.
[63] C. Dingels, S. S. Müller, T. Steinbach, C. Tonhauser, H. Frey, *Biomacromolecules* **2013**, DOI: 10.1021/bm3016797.
[64] C. Tonhauser, C. Schüll, C. Dingels, H. Frey, *ACS Macro Lett.* **2012**, *1*, 1094.
[65] R. A. Shenoi, J. K. Narayanannair, J. L. Hamilton, B. F. L. Lai, S. Horte, R. K. Kainthan, J. P. Varghese, K. G. Rajeev, M. Manoharan, J. N. Kizhakkedathu, *J. Am. Chem. Soc.* **2012**, *134*, 14945.
[66] M.-C. DuBois Clochard, S. Rankin, S. Brocchini, *Macromol. Rapid Commun.* **2000**, *21*, 853.
[67] J. Lai, L.-Q. Wang, K. Tu, C. Zhao, W. Sun, *Macromol. Rapid Commun.* **2005**, *26*, 1572.
[68] J. Lai, K. Tu, H. Wang, Z. Chen, L.-Q. Wang, *J. Appl. Polym. Sci.* **2008**, *108*, 3305.
[69] E. P. Goldberg, J. Polym. Sci., Part C: Polym. Symp. **1963**, 4, 707.
[70] T. Suzuki, T. Kotaka, *Macromolecules* **1980**, *13*, 1495.
[71] T. Suzuki, T. Kotaka, *Polym. J.* **1983**, *15*, 15.
[72] T. Suzuki, H. Chihara, T. Kotaka, *Polym. J.* **1984**, *16*, 129.
[73] H. Tanisugi, H. Ohnuma, T. Kotaka, *Polym. J.* **1984**, *16*, 633.
[74] J. M. Harris, M. D. Bentley, X. Zhoa, X. Shen (Shearwater Corporation), US6348558B1, **2002**.
[75] E. Tziampazis, J. Kohn, P. V. Moghe, *Biomaterials* **2000**, *21*, 511.
[76] S. L. Bourke, J. Kohn, *Adv. Drug Del. Rev.* **2003**, *55*, 447.
[77] R. I. Sharma, J. Kohn, P. V. Moghe, *J. Biomed. Mater. Res., Part A* **2004**, *69A*, 114.
[78] A. Sousa, J. Schut, J. Kohn, M. Libera, *Macromolecules* **2006**, *39*, 7306.
[79] A. Kozlowski, J. McKannan, S. P. McManus (NEKTAR THERAPEUTICS), WO2007016560A2, **2007**.
[80] C.-Y. Won, C.-C. Chu, J. D. Lee, *Polymer* **1998**, *39*, 6677.
[81] C.-Y. Won, C.-C. Chu, J. D. Lee, *J. Polym. Sci., Part A: Polym. Chem.* **1998**, *36*, 2949.
[82] T. Padmaja, B. S. Lele, M. C. Deshpande, M. G. Kulkarni, *J. Appl. Polym. Sci.* **2002**, *85*, 2108.
[83] K. Nagahama, M. Hashizume, H. Yamamoto, T. Ouchi, Y. Ohya, *Langmuir* **2009**, *25*, 9734.
[84] A. Braunová, M. Pechar, R. Laga, K. Ulbrich, *Macromol. Chem. Phys.* **2007**, *208*, 2642.
[85] J. M. Harris (Shearwater Corporation), US6214966B1, **2001**.
[86] M. Nagata, S. Hizakae, *J. Polym. Sci., Part A: Polym. Chem.* **2003**, *41*, 2930.
[87] M. Nagata, S. Hizakae, *Macromol. Biosci.* **2003**, *3*, 412.

[88] A. Mero, O. Schiavon, G. Pasut, F. M. Veronese, E. Emilitri, P. Ferruti, *J. Bioact. Compat. Polym.* **2009**, *24*, 220.
[89] S. Unal, Q. Lin, T. H. Mourey, T. E. Long, *Macromolecules* **2005**, *38*, 3246.
[90] N. Wang, A. Dong, H. Tang, E. A. Van Kirk, P. A. Johnson, W. J. Murdoch, M. Radosz, Y. Shen, *Macromol. Biosci.* **2007**, *7*, 1187.
[91] N. Wang, A. Dong, M. Radosz, Y. Shen, *J. Biomed. Mater. Res., Part A* **2008**, *84A*, 148.
[92] S. Chen, Y. Wang, Y. Fan, J. Ma, *J. Biomed. Mater. Res., Part A* **2009**, *88A*, 769.
[93] R. Kumar, M.-H. Chen, V. S. Parmar, L. A. Samuelson, J. Kumar, R. Nicolosi, S. Yoganathan, A. C. Watterson, *J. Am. Chem. Soc.* **2004**, *126*, 10640.
[94] S. Dou, S. Zhang, R. J. Klein, J. Runt, R. H. Colby, *Chem. Mater.* **2006**, *18*, 4288.
[95] W. Wang, W. Liu, G. J. Tudryn, R. H. Colby, K. I. Winey, *Macromolecules* **2010**, *43*, 4223.
[96] S. Bhatia, A. Mohr, D. Mathur, V. S. Parmar, R. Haag, A. K. Prasad, *Biomacromolecules* **2011**, *12*, 3487.
[97] H.-Y. Wang, Y.-J. Zhou, Z. Wang, N. Wang, K. Li, X.-Q. Yu, *Macromol. Biosci.* **2011**, *11*, 595.
[98] W. Wang, G. J. Tudryn, R. H. Colby, K. I. Winey, *J. Am. Chem. Soc.* **2011**, *133*, 10826.
[99] A. Braunová, M. Pechar, K. Ulbrich, *Collect. Czech. Chem. Commun.* **2004**, *69*, 1643.
[100] Y. Lee, H. Koo, G.-w. Jin, H. Mo, M. Y. Cho, J.-Y. Park, J. S. Choi, J. S. Park, *Biomacromolecules* **2005**, *6*, 24.
[101] J. Lee, M. K. Joo, J. Kim, J. S. Park, M.-Y. Yoon, B. Jeong, *J. Biomater. Sci. Polym. Ed.* **2009**, *20*, 957.
[102] T. Etrych, L. Kovár, V. Šubr, A. Braunová, M. Pechar, P. Chytil, B. Říhová, K. Ulbrich, *J. Bioact. Compat. Polym.* **2010**, *25*, 5.
[103] T. Hernandez-Mireles, M. Rito-Palomares, *J. Chem. Technol. Biotechnol.* **2006**, *81*, 997.
[104] B. Reid, S. Tzeng, A. Warren, K. Kozielski, J. Elisseeff, *Macromolecules* **2010**, *43*, 9588.
[105] M. Qi, X. Li, Y. Yang, S. Zhou, *Eur. J. Pharm. Biopharm.* **2008**, *70*, 445.
[106] K. Ulbrich, J. Strohalm, J. Kopeček, *Makromol. Chem.* **1986**, *187*, 1131.
[107] M. Pechar, J. Strohalm, K. Ulbrich, *Collect. Czech. Chem. Commun.* **1995**, *60*, 1765.
[108] M. Pechar, J. Strohalm, K. Ulbrich, E. Schacht, *Macromol. Chem. Phys.* **1997**, *198*, 1009.
[109] K. Ulbrich, M. Pechar, J. Strohalm, V. Šubr, B. Říhová, *Macromol. Symp.* **1997**, *118*, 577.
[110] K. Ulbrich, V. Šubr, M. Pechar, J. Strohalm, M. Jelínková, B. Říhová, *Macromol. Symp.* **2000**, *152*, 151.
[111] M. Pechar, K. Ulbrich, V. Šubr, L. W. Seymour, E. H. Schacht, *Bioconjugate Chem.* **2000**, *11*, 131.
[112] M. Pechar, K. Ulbrich, M. Jelínková, B. Říhová, *Macromol. Biosci.* **2003**, *3*, 364.
[113] M. Pechar, A. Braunová, K. Ulbrich, M. Jelínková, B. Říhová, *J. Bioact. Compat. Polym.* **2005**, *20*, 319.
[114] M. Pechar, A. Braunová, K. Ulbrich, *Collect. Czech. Chem. Commun.* **2005**, *70*, 327.
[115] S. Ramanathan, B. Qiu, S. Pooyan, G. Zhang, S. Stein, M. J. Leibowitz, P. J. Sinko, *J. Controlled Release* **2001**, *77*, 199.

[116] F. d'Acunzo, J. Kohn, *Macromolecules* **2002**, *35*, 9360.
[117] F. d'Acunzo, T.-Q. Le, J. Kohn, *Macromolecules* **2002**, *35*, 9366.
[118] R. Tzevi, P. Novakov, K. Troev, D. M. Roundhill, *J. Polym. Sci., Part A: Polym. Chem.* **1997**, *35*, 625.
[119] J. Pretula, S. Penczek, *Makromol. Chem.* **1990**, *191*, 671.
[120] J. Pretula, S. Penczek, *Makromol. Chem., Rapid Commun.* **1988**, *9*, 731.
[121] S. Penczek, J. Pretula, *Macromolecules* **1993**, *26*, 2228.
[122] R. Tzevi, G. Todorova, K. Kossev, K. Troev, E. M. Georgiev, D. M. Roundhill, *Makromol. Chem.* **1993**, *194*, 3261.
[123] J. Pretula, K. Kaluzynski, R. Szymanski, S. Penczek, *Macromolecules* **1997**, *30*, 8172.
[124] J. Wang, R. Zhuo, *Eur. Polym. J.* **1999**, *35*, 491.
[125] R. Georgieva, R. Tsevi, K. Kossev, R. Kusheva, M. Balgjiska, R. Petrova, V. Tenchova, I. Gitsov, K. Troev, *J. Med. Chem.* **2002**, *45*, 5797.
[126] K. Troev, I. Tsatcheva, N. Koseva, R. Georgieva, I. Gitsov, *J. Polym. Sci., Part A: Polym. Chem.* **2007**, *45*, 1349.
[127] S. Stanimirov, A. Vasilev, E. Haupt, I. Petkov, T. Deligeorgiev, *J. Fluoresc.* **2009**, *19*, 85.
[128] I. Gitsov, F. E. Johnson, *J. Polym. Sci., Part A: Polym. Chem.* **2008**, *46*, 4130.
[129] I. Kraicheva, A. Bogomilova, I. Tsacheva, G. Momekov, D. Momekova, K. Troev, *Eur. J. Med. Chem.* **2010**, *45*, 6039.
[130] D.-a. Wang, C. G. Williams, Q. Li, B. Sharma, J. H. Elisseeff, *Biomaterials* **2003**, *24*, 3969.
[131] K. D. Troev, *Polyphosphoesters*, Elsevier, Oxford, **2012**.
[132] A. Nathan, D. Bolikal, N. Vyavahare, S. Zalipsky, J. Kohn, *Macromolecules* **1992**, *25*, 4476.
[133] A. Nathan, S. Zalipsky, S. I. Ertel, S. N. Agathos, M. L. Yarmush, J. Kohn, *Bioconjugate Chem.* **1993**, *4*, 54.
[134] A. Nathan, S. Zalipsky, J. Kohn, *J. Bioact. Compat. Polym.* **1994**, *9*, 239.
[135] S.-Y. Huang, S. Pooyan, J. Wang, I. Choudhury, M. J. Leibowitz, S. Stein, *Bioconjugate Chem.* **1998**, *9*, 612.
[136] X.-M. Liu, A. Thakur, D. Wang, *Biomacromolecules* **2007**, *8*, 2653.
[137] X.-M. Liu, L.-d. Quan, J. Tian, F. C. Laquer, P. Ciborowski, D. Wang, *Biomacromolecules* **2010**, *11*, 2621.
[138] D. Sarkar, S. T. Lopina, *Polym. Degrad. Stab.* **2007**, *92*, 1994.
[139] H. Fu, H. Gao, G. Wu, Y. Wang, Y. Fan, J. Ma, *Soft Matter* **2011**, *7*, 3546.
[140] X. Sun, H. Gao, G. Wu, Y. Wang, Y. Fan, J. Ma, *Int. J. Pharm.* **2011**, *412*, 52.
[141] P. Lundberg, B. F. Lee, S. A. van den Berg, E. D. Pressly, A. Lee, C. J. Hawker, N. A. Lynd, *ACS Macro Lett.* **2012**, *1*, 1240.
[142] T. H. Chan, B. S. Ong, *J. Org. Chem.* **1978**, *43*, 2994.
[143] W.-J. Lo, Y.-J. Wu, Y.-P. Lee, *J. Chem. Phys.* **2002**, *117*, 6655.
[144] W.-J. Lo, Y.-J. Wu, Y.-P. Lee, *J. Phys. Chem. A* **2003**, *107*, 6944.
[145] H. Nagahara, K. Kagawa, T. Iwaisako, J. Masamoto, *Ind. Eng. Chem. Res.* **1995**, *34*, 2515.

[146] H. Nagahara, K. Kagawa, K. Hamanaka, K. Yoshida, T. Iwaisako, J. Masamoto, *Ind. Eng. Chem. Res.* **2000**, *39*, 2275.
[147] N. Yamasaki, K. Kanaori, J. Masamoto, *J. Polym. Sci., Part A: Polym. Chem.* **2001**, *39*, 3239.
[148] J. L. Wike-Hooley, J. Haveman, H. S. Reinhold, *Radiother. Oncol.* **1984**, *2*, 343.
[149] I. F. Tannock, D. Rotin, *Cancer Res.* **1989**, *49*, 4373.
[150] M. Roldo, E. Barbu, J. F. Brown, D. W. Laight, J. D. Smart, J. Tsibouklis, *Expert Opin. Drug Delivery* **2007**, *4*, 547.
[151] C. Yu, J. Kohn, *Biomaterials* **1999**, *20*, 253.
[152] C. Yu, S. S. Mielewczyk, K. J. Breslauer, J. Kohn, *Biomaterials* **1999**, *20*, 265.
[153] A. Lendlein, A. Sisson, Editors, *Handbook of Biodegradable Polymers: Synthesis, Characterization And Applications*, Wiley-VCH Verlag GmbH & Co. KGaA, Weinheim, **2011**.

Carsten Dingels (born 1983) studied chemistry at the Johannes Gutenberg-Universität Mainz and the University of Toronto until 2009 when he received his diploma degree. Currently, he is writing his PhD thesis in the research group of Prof. Holger Frey on novel poly(ethylene glycol) derivatives for biomedical applications. His work was supported by a scholarship of the Max Planck Graduate Center (MPGC).

Holger Frey (born 1965) studied Chemistry at the University of Freiburg. Following a stay at Carnegie Mellon-University (Pittsburgh, USA) he obtained his PhD at the University of Twente (NL). After his Habilitation (University of Freiburg, 1998) on polycarbosilanes, he moved to the Johannes Gutenberg-Universität Mainz in 2001. Since 2003 he has held a full professorship there in organic and macromolecular chemistry. His research is directed at novel linear and branched functional polymer structures, microreactor-based syntheses, and biomedical materials in general.

1.3 Proteins squared: Squaric Acid Derivatives for Bioconjugation

A brief introduction to squarate chemistry.

Introduction

Squaric acid (3,4-dihydroxy-3-cyclobutene-1,2-dione) can be considered as two connected vinylogous carboxylic acid moieties that share a carbon-carbon double bond. It was synthesized first by Cohen and coworkers by the hydrolysis of both, 1,3,3-triethoxy-2-chloro-4,4-difluorocyclobutene and 1,2-diethoxy-3,3,4,4-tetrafluorocyclobutene (Scheme 1A).[1] However, of more relevance became a synthetic route starting from perchloro-butadiene, an unneeded by-product in the industrial perchloration of hydrocarbons. The hexachloro-butadiene is reacted to 1-ethoxy-pentachloro-budatiene which undergoes a catalyzed thermal cyclization to perchloro-cyclobuteneone. Finally, the latter is hydrolyzed to squaric acid (Scheme 1B).[2-4]

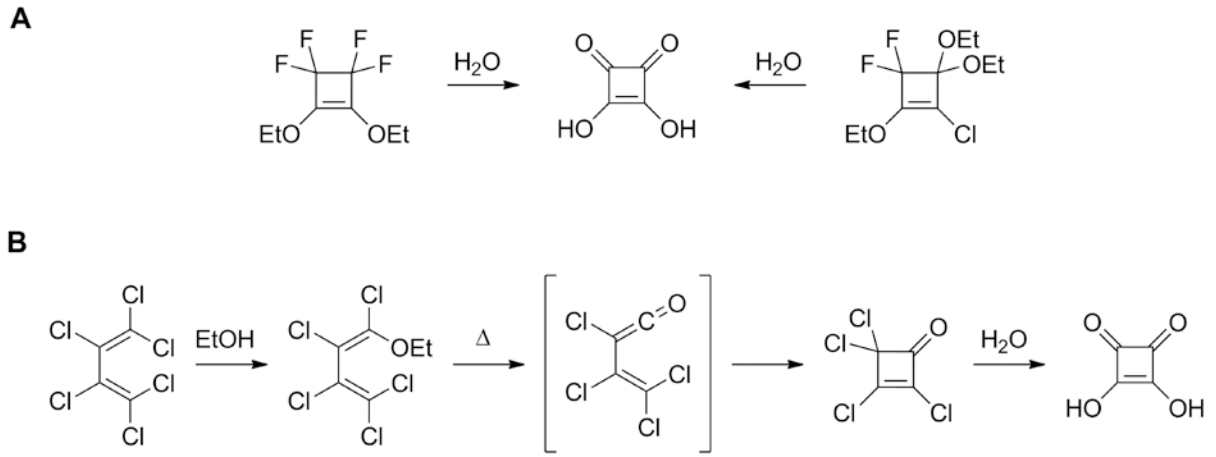

Scheme 1. Synthetic routes to squaric acid. **A** Synthesis according to Cohen and coworkers. **B** Industrially relevant pathway.

The acidic strength of the divalent squaric acid is extraordinarily high for an organic acid. Its pK_1 and pK_2 values are 1.2 and 3.5, respectively.[5] These values result from the high resonance stabilization of the corresponding dianion squarate ($C_4O_4^{2-}$). While the lengths of the carbon-

carbon bonds of the free acid differ, the carbons of the squarate form a perfect square. In consequence, all oxygen atoms of ^{17}O-labeled squarate exhibit the same chemical shift in ^{17}O NMR spectroscopy.[6] The squarate is a member of cyclic oxocarbon dianions with the empirical formula $(C_nO_n)^{2-}$ and, as the deltate ($n = 3$), can be regarded aromatic, while the aromaticity of the higher analogues (croconate: $n = 5$, rhodizonate: $n = 6$) decreases with increasing size of the cycle.[7, 8]

The wide range of squaric acid derivatization reactions has been reviewed by Schmidt.[9] In the following, a brief summary of the dialkyl squarates and their role as coupling agents for the attachment of amino group-containing organic compounds, especially carbohydrates, to proteins will be given. A comprehensive review on this topic and further, biomedically relevant aspects of squarate chemistry is currently in preparation.[10]

From Squaric Acid Esters to Asymmetrical Squaramides

Some of the dialkyl squarates, such as the diethyl, dibutyl,[3] and didecyl[11] derivative can be synthesized by refluxing squaric acid in the corresponding alcohol. In contrast, the similar reaction carried out in methanol just yields the monomethyl ester and also dipropyl squarate cannot be prepared by this method.[9] However, squaric acid can be directly converted into its dimethyl ester in a reaction with diazomethane.[12] A universal route to dialkyl squarates is the alcoholysis of the squaric acid dichloride, which can be prepared from the free acid and thionyl chloride.[13]

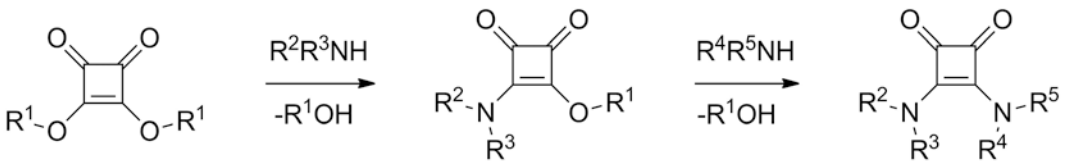

Scheme 2. Aminolysis of dialkyl squarate to the ester amide and subsequently to the squaramide.

From the dialkyl squarates, most frequently the dimethyl or diethyl derivative, squaric acid diamides (also known as squaramides) can be obtained by aminolysis. The symmetric diamides are formed in various solvents, when more than two equivalents of the amine (ammonia, primary amines, secondary amines, hydrazines or anilines) are applied under basic conditions.[12, 14-16] In all cases, primarily the symmetric 1,2-diamide is formed (Scheme 2, $R^2 = R^4$, $R^3 = R^5$) whereas the 1,3-diamide is the main product when squaric acid is used

directly.[17, 18] The latter can also be synthesized from the analogous 1,2-diamides in presence of sulfuric acid.[19, 20]

As shown in Scheme 2, the synthesis of the diamides requires the previous formation of the corresponding squaric acid ester amides. Due to a faster amine addition of the squaric acid diesters compared to the resulting ester amides under neutral conditions, the latter can be isolated in excellent yields for most amines. Tietze and coworkers were the first to realize the potential in the generation of asymmetric squaramides from these substances and synthesized a library of different ester amides and symmetrical as well as asymmetrical diamides of squaric acid.[21] To generate the latter, the second amine is reacted to the squaric acid ester amide under more basic conditions: While the first amidation of the dialkyl squarate is conducted at pH 7, the amidation of the ester amide requires pH 9.

The lower reactivity of the ester amide is explained by the higher electron density that impedes the nucleophilic attack of the amine. Further, squaric acid derivatives were calculated to be more aromatic when they are protonated at the carbonyl oxygen atoms,[8] and the resulting reduced aromaticity in basic media might be the reason for the higher reactivity of the squaric acid ester amides under more basic conditions.

Luk and coworkers reported a slow, but highly selective reaction of squaric acid ethyl ester derivatives toward cysteine's amino group in neutral aqueous solutions. Out of a mixture of 5 different L-amino acids, including cysteine and lysine, the ethyl ester reacted selectively with cysteine. According to the mechanism proposed by the authors, first squaric acid thioester is formed and undergoes a subsequent S → N acyl transfer to form the squaramide.[22] The reaction rates were increased significantly (full conversion within 5 min) by using cyclic amino squarates (Scheme 3). These derivatives also reacted with amino groups of amino acids in water under neutral conditions. The enhanced reactivity reportedly results from the ring-strain released during the amidation (thioesterification).[23]

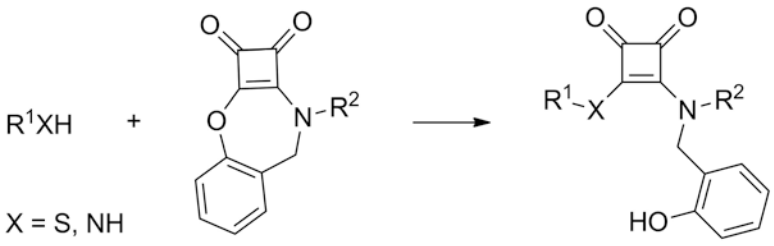

Scheme 3. Reaction of amines and thiols with cyclic amino squarates according to Ref. [23].

Squaric Acid mediated Protein Conjugation

Due to their assembly from a variety of different amino acids, most of which carry additional functionalities besides the essential carboxylate and amino group, proteins are biomolecules with a large number of functional moieties that can be addressed for the attachment of a ligand, such as synthetic polymers or carbohydrates. In most syntheses of protein conjugates the aliphatic amino groups of lysine residues and the N-terminus are chosen as target sites because they usually can be found and reacted at protein surfaces.[24] An efficient coupling agent for a selective protein derivatization at the lysine moieties must not interfere with the other numerous functionalities of the polypeptide, such as the hydroxyls of serines, threonines, and tyrosines or the thiol group of cysteines. In addition, the activation of ligands carrying further functional moieties should also be selective to avoid the time-consuming use of protective groups. These criteria are met by dialkyl squarates, since an eligible ligand is selectively converted to the squaric acid ester amide, which subsequently reacts solely at the protein's amino residues.

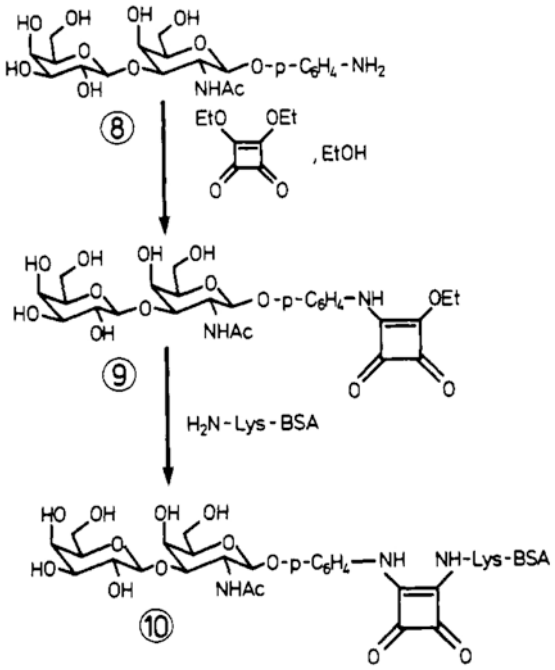

Scheme 4. Squaric acid mediated glycosylation of BSA. Reprinted with permission from Ref. [25]). Copyright (1991) American Chemical Society.

Especially for the synthesis of neoglycoproteins, i. e. synthetic sugar protein conjugates, squaric acid mediated coupling has been successfully employed due to the squarates high tolerance towards hydroxyl groups, which is demanded in glycosylation chemistry to prevent crosslinking reactions. In 1991, Tietze and coworkers were the first to establish protein glycosylation using

diethyl squarate as a linker (Scheme 4).[25] They reported excellent yields of the coupling of a disaccharide to bovine serum albumin (BSA) and demonstrated that the degree of conversion could be followed by UV-Vis spectroscopy. The high value of this linker was confirmed in various additional studies on squaric acid mediated protein glycosylation[26-32] and particularly by Hashimoto and coworkers, who compared various commercially available linkers for the attachment of mannose to BSA. Due to its selectivity, low costs, and the possible retrieval of the ester amide excess used in the conjugation step, diethyl squarate was chosen as one of the most useful linkers.[33]

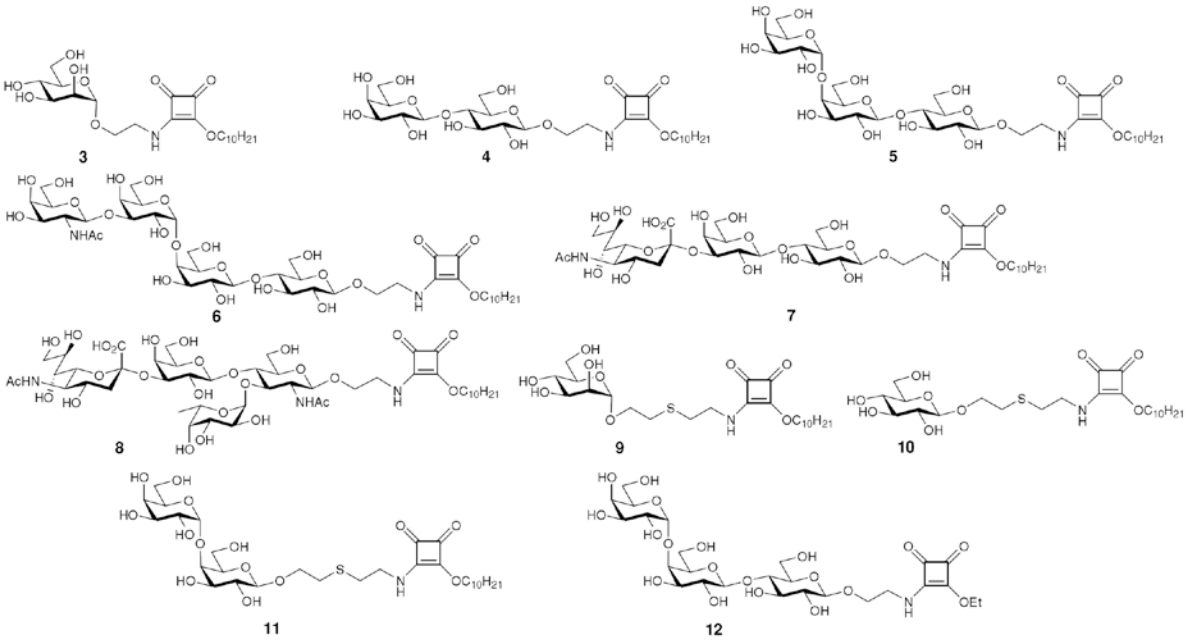

Figure 1. Various glycosylation agents prepared from didecyl squarate (from Ref. [11]).

Despite of the success of the squaric acid diethyl ester, in some cases the use of its derivative might be advantageous. In contrast to diethyl squarate, the corresponding dimethyl ester is water-soluble and a crystalline solid at room temperature. Upon amidation with amino functional glycosides, the didecyl squarate yields squaric acid ester amides which are more hydrophobic due to the larger alkyl chain and can conveniently be purified. Further, the excess of this glycosylation agent necessary in the conjugation step can be recovered by C18 solid phase extraction. This procedure was tested for various glycosides (Figure 1) and found to be efficient, independent of the sugar structure.[11] A direct comparison of the dimethyl, diethyl, dibutyl, and didecyl squarate as glycoside/protein coupling reagents revealed no substantial differences in the conversion of the glycosides to the corresponding squaric acid ester amides.[34] However, the

resulting ester amides differed significantly in their hydrolysis rates, depending on the size of the alkyl chain: In line with the expectation, the decyl derivative was hydrolyzed the slowest, while the methyl ester amide was inactivated the fasted in buffered aqueous medium.[34]

Besides oligosaccharides, suitable oligopeptides, i.e., peptides bearing a single addressable amino group, have also been coupled to proteins via squarate linkages. Kunz and coworkers demonstrated the attachment of squaric acid esters amides of various MUC1 glycopeptides to BSA and tetanus toxoid to investigate the conjugates applicability in immunotherapy.[35-39] While all the previously described examples of squaric acid mediated protein conjugation were carried out at elevated pH, Luk and coworkers coupled an lysine-containing oligopeptide, whose ε-amino group was activated by the conversion with diphenyl squarate to another peptide bearing a N-terminal cysteine at neutral pH in water.[22] They also used the same reaction to immobilize peptides with N-terminal cysteines on a squaric acid phenyl ester amide surface.[40]

Conclusion

Since the pioneering work of Tietze et al., the squaric acid derivatives have been recognized and established as powerful tools for the covalent attachment of ligands to proteins. Compared to other methods, squaric acid derivatives exhibit several advantages: (i) the most common derivatives are commercially available; (ii) the dialkyl squarates react selectively with amino groups without interference of other functional groups, such as esters and hydroxyl groups (reaction with thiols is possible under specific conditions); (iii) the activation of the ligand does not require harsh conditions; (iv) ligand-to-ligand coupling during the ligand activation step does not occur due to the lower reactivity of the resulting ester amides; (v) the degree of protein modification can be detected using UV-Vis spectroscopy; (vi) in comparison to other coupling agents, the squarate-activated ligands are more stable towards hydrolysis.

The solubility, morphology, reactivity, selectivity and other properties of the linkers as well as the activated ligands can be tuned by either simple transesterification reactions or further modifications, such as the synthesis of the cyclic amino squarates introduced by the group of Luk. So far, squarate mediated coupling is mainly used in protein glycosylation, but the due to the linker's unique combination of properties, other biomedical fields of protein research may benefit from its application. Surprisingly, the valuable squarate coupling has not been used for the generation of synthetic polymer/protein conjugates. Due to its high potential and especially

its tolerance towards hydroxyl groups, diethyl squarate was chosen for the mediation of the attachment of novel heterofunctional poly(ethylene glycol) stuctures to proteins and the coupling chemistry of squarate modified PEGs was closely investigated in this thesis.

Referenzes

[1] S. Cohen, J. R. Lacher, J. D. Park, *J. Am. Chem. Soc.* **1959**, *81*, 3480.

[2] G. Maahs, *Angew. Chem.* **1963**, *75*, 982.

[3] G. Maahs, Justus Liebigs Ann. Chem. **1965**, 686, 55.

[4] A. Roedig, P. Bernemann, *Justus Liebigs Ann. Chem.* **1956**, *600*, 1.

[5] D. J. MacDonald, *J. Org. Chem.* **1968**, *33*, 4559.

[6] G. Cerioni, R. Janoschek, Z. Rappoport, T. T. Tidwell, *J. Org. Chem.* **1996**, *61*, 6212.

[7] P. v. R. Schleyer, K. Najafian, B. Kiran, H. Jiao, *J. Org. Chem.* **2000**, *65*, 426.

[8] D. Quinonero, A. Frontera, P. Ballester, P. M. Deyá, *Tetrahedron Lett.* **2000**, *41*, 2001.

[9] A. H. Schmidt, *Synthesis* **1980**, 961.

[10] F. Wurm, H.-A. Klok, *in preparation*.

[11] A. Bergh, B. G. Magnusson, J. Ohlsson, U. Wellmar, U. J. Nilsson, *Glycoconjugate J.* **2001**, *18*, 615.

[12] S. Cohen, S. G. Cohen, *J. Am. Chem. Soc.* **1966**, *88*, 1533.

[13] R. C. De Selms, C. J. Fox, R. C. Riordan, *Tetrahedron Lett.* **1970**, *11*, 781.

[14] G. Maahs, P. Hegenberg, *Angew. Chem.* **1966**, *78*, 927.

[15] G. Manecke, J. Gauger, *Makromol. Chem.* **1969**, *125*, 231.

[16] G. Seitz, H. Morck, *Synthesis* **1971**, 146.

[17] E. Neuse, B. Green, Justus *Liebigs Ann. Chem.* **1973**, *1973*, 619.

[18] E. Neuse, B. Green, *Justus Liebigs Ann. Chem.* **1973**, *1973*, 633.

[19] G. Manecke, J. Gauger, *Tetrahedron Lett.* **1967**, *8*, 3509.

[20] J. Gauger, G. Manecke, *Chem. Ber. Recl.* **1970**, *103*, 3553.

[21] L. F. Tietze, M. Arlt, M. Beller, K.-H. Glüsenkamp, E. Jähde, M. F. Rajewsky, *Chem. Ber.* **1991**, *124*, 1215.

[22] P. Sejwal, Y. Han, A. Shah, Y.-Y. Luk, *Org.* Lett. **2007**, *9*, 4897.

[23] D. Cui, D. Prashar, P. Sejwal, Y.-Y. Luk, *Chem. Commun.* **2011**, *47*, 1348.

[24] S. Moelbert, E. Emberly, C. Tang, *Protein Sci.* **2004**, *13*, 752.

[25] L. F. Tietze, C. Schroeter, S. Gabius, U. Brinck, A. Goerlach-Graw, H. J. Gabius, *Bioconjugate Chem.* **1991**, *2*, 148.

[26] V. P. Kamath, P. Diedrich, O. Hindsgaul, *Glycoconjugate J.* **1996**, *13*, 315.

[27] A. Chernyak, A. Karavanov, Y. Ogawa, P. Kovac, *Carbohydr. Res.* **2001**, *330*, 479.

[28] P. I. Kitov, D. R. Bundle, *J. Chem. Soc., Perkin Trans. 1* **2001**, 838.

[29] A. A. Karelin, Y. E. Tsvetkov, L. Paulovicová, S. Bystrický, E. Paulovicová, N. E. Nifantiev, *Carbohydr. Res.* **2010**, *345*, 1283.

[30] J.-W. Wang, A. Asnani, F.-I. Auzanneau, *Biorg. Med. Chem.* 2010, *18*, 7174.

[31] P. Xu, M. M. Alam, A. Kalsy, R. C. Charles, S. B. Calderwood, F. Qadri, E. T. Ryan, P. Kováč, *Bioconjugate Chem.* **2011**, *22*, 2179.

[32] F. Jahouh, S.-j. Hou, P. Kováč, J. H. Banoub, *Rapid Commun. Mass* Spectrom. **2012**, *26*, 749.

[33] M. Izumi, S. Okumura, H. Yuasa, H. Hashimoto, *J. Carbohydr. Chem.* **2003**, *22*, 317.

[34] S.-j. Hou, R. Saksena, P. Kováč, *Carbohydr. Res.* **2008**, *343*, 196.

[35] U. Westerlind, A. Hobel, N. Gaidzik, E. Schmitt, H. Kunz, *Angew. Chem. Int. Ed.* **2008**, *47*, 7551.

[36] A. Kaiser, N. Gaidzik, U. Westerlind, D. Kowalczyk, A. Hobel, E. Schmitt, H. Kunz, *Angew. Chem. Int. Ed.* **2009**, *48*, 7551.

[37] A. Hoffmann-Röder, A. Kaiser, S. Wagner, N. Gaidzik, D. Kowalczyk, U. Westerlind, B. Gerlitzki, E. Schmitt, H. Kunz, *Angew. Chem. Int. Ed.* **2010**, *49*, 8498.

[38] N. Gaidzik, A. Kaiser, D. Kowalczyk, U. Westerlind, B. Gerlitzki, H. P. Sinn, E. Schmitt, H. Kunz, *Angew. Chem. Int. Ed.* **2011**, *50*, 9977.

[39] H. Cai, Z.-H. Huang, L. Shi, Z.-Y. Sun, Y.-F. Zhao, H. Kunz, Y.-M. Li, *Angew.* Chem. *Int. Ed.* **2012**, *51*, 1719.

[40] P. Sejwal, S. K. Narasimhan, D. Prashar, D. Bandyopadhyay, Y.-Y. Luk, *J. Org. Chem.* **2009**, *74*, 6843.

2 Squaric Acid Mediated PEGylation

2.1 Squaric Acid Mediated Chemoselective PEGylation of Proteins: Reactivity of Single-Step-Activated α-Amino Poly(ethylene glycol)s

Carsten Dingels,[a] Frederik Wurm,[b, c] Manfred Wagner,[c] Harm-Anton Klok,[b] and Holger Frey[a]*

[a] Institut für Organische Chemie, Johannes Gutenberg-Universität Mainz, Duesbergweg 10–14, 55099 Mainz (Germany)

[b] Institut des Materiaux and Institut des Sciences et Ingénierie Chimiques, Laboratoire des Polymères, Ecole Polytechnique Fédérale de Lausanne (EPFL), Bâtiment MXD, Station 12, 1015 Lausanne (Switzerland)

[c] Max-Planck-Institut für Polymerforschung, Ackermannweg 10, 55128 Mainz (Germany)

Published in: *Chem. Eur. J.* **2012**, *18*, 16828.

Abstract:

The covalent attachment of poly(ethylene glycol) (PEG) to therapeutically active proteins (PEGylation) has become an important method to deal with the pharmacological difficulties of these polypeptides, such as short body-residence times and immunogenicity. However, the derivatives of PEG used for PEGylation lack further functional groups that would allow the addition of targeting or labeling moieties. Squaric acid diethyl ester was used for the chemoselective single-step activation of poly(ethylene glycol)s into the respective ester amides. The resultant selective protein-reactive poly(ethylene glycol)s were investigated with respect to their selectivity towards amino acid residues in bovine serum albumin (as a model protein). The presented procedure relies on a robust two-step protocol and was found to be selective towards lysine residues; the activated polyethers are efficient and stoichiometric PEGylation agents with a remarkable hydrolytic stability over a period of several days. By adjusting the pD value of the conjugation mixture, the chemoselectivity of the activated PEGs towards the α- and ε-amino groups of lysine methyl ester was effectively changed.

Keywords: *Chemoselectivity, kinetics, PEGylation, proteins, squaric acid.*

Introduction

The application of therapeutically active proteins such as insulin, interferons, and granulocyte-colony-stimulating factor as pharmaceuticals suffers from their immunogenicity and susceptibility towards degradation in vivo. Therefore, different strategies for protein modification have been developed to reduce these effects, such as the addition, removal, substitution, or chemical modification of amino acids and the attachment of synthetic polymers.[1] Abuchowski et al. linked poly(ethylene glycol) (PEG) to bovine serum albumin (BSA) and bovine liver catalase through a cyanuric chloride coupling route[2] and laid the cornerstone for PEGylation, that is, the covalent attachment of PEG to (poly)peptides and proteins. PEG exhibits a unique combination of properties valuable for bioconjugation: It is highly soluble in water, chemically inert, nontoxic, mostly nonimmunogenic, and soluble in many organic solvents.[3a] PEGylation is the most important strategy to reduce immunogenicity and to increase the blood circulation times of drugs. In addition, due to the increased molecular weight and hydrodynamic volume of the PEGylated therapeutic in comparison with those of the native protein, renal excretion is reduced. Furthermore, the polyether chains shield the protein and hinder antibodies from recognizing the determinants on the surface of the therapeutic, thus reducing its immunogenicity. Also, the shielding impedes proteases in catalyzing the hydrolytic degeneration of the polypeptides.[3] Today, a number of PEGylated enzymes, cytokines, antibodies, and growth factors are approved by the US Food and Drug Administration.[4]

In the last decades, a variety of strategies were established to covalently bind PEG to proteins. Commonly, the monomethyl ether of PEG (mPEG) is used for PEGylation after (usually multistep) activation of the hydroxy group with a protein-reactive moiety. Most of the protein-reactive PEG derivatives that have been used so far, however, are susceptible towards a range of functional groups (for example, amines, alcohols, and thiols), and the PEGylation chemistries that have been developed so far are not easily extended towards alternative synthetic polymers that contain functional groups other than the one that is used for the protein conjugation. This obviously impedes the development of synthetic polymer–peptide/protein conjugates in which the synthetic polymer contains functional groups that can be used for further functionalization, for example, to introduce labels or target ligands. A potentially interesting reagent that could help to overcome these problems is diethyl squarate (**1**). Diethyl squarate has been previously used for the amine-selective, hydroxy-orthogonal attachment of carbohydrates[5] and

glycopeptides[6] to proteins. Diethyl squarate consists of two connected vinylogous carboxylic acid esters sharing a carbon–carbon double bond (Scheme 1). Due to this connection, derivatization of one ester moiety affects the reactivity of the other. The reactivity of the diester towards amidation is high. At neutral pH values, it can be converted selectively into the analogous ester amide, without formation of the coupled product, that is, the diamide (squaramide), because the resulting ester amide has a reduced reactivity.[7] Thus, the ester amide can be isolated, and at higher pH values, usually around pH 9, it can react with a second amine to result in an asymmetric squaric acid di amide. Squaric acid derivatives were calculated to be weakly aromatic,[8] so the amidation of **1** can be viewed as a nucleophilic substitution in an aromatic system. In comparison to **1**, the squaric acid ester amide possesses a higher electron density in the carbon cycle, which makes a second nucleophilic attack less favorable. Moreover, squaramides exhibit high proton affinity and enhanced aromaticity when protonated,[8] which might also apply for the ester amides and explain the increased reactivity in basic media.

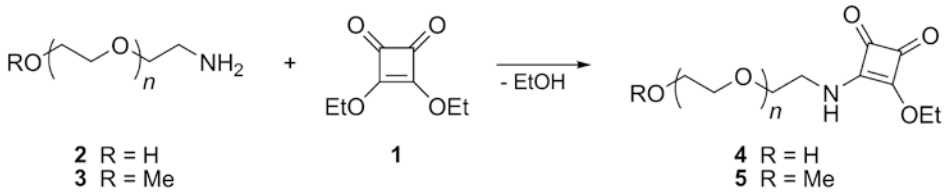

2 R = H
3 R = Me

1

4 R = H
5 R = Me

Scheme 1. One-step activation of α-amino-PEGs with diethyl squarate.

Herein, we report the activation of α-amino PEGs with **1** in a single step that tolerates the presence of hydroxy and other functional groups, which allows for subsequent derivatization of the polymer. In addition, we demonstrate efficient PEGylation with the novel activated PEGs under different conditions and their stability towards hydrolysis. Selectivity of the PEGylation towards the α- and ε-amino groups of lysine was investigated in detail, and it was proven that the chemoselectivity can be adjusted selectively towards either of the amines at different pH values.

Results and Discussion

Synthesis of protein-reactive PEGs: α-Amino-ω-hydroxy PEG (**2**) and the respective methoxy-PEGs, **3**, with number-averaged molecular weights (M_n) of **2** and **5** kDa, were modified with **1**, and the properties of the resulting protein-reactive polymers were investigated. The amino mPEGs, synthesized according to a known protocol,[9] were activated with diethyl squarate in ethanol with triethylamine as an additive. The size exclusion

chromatography (SEC) elugrams of the squaric acid ester amido mPEGs (SEA-mPEGs, **5**) showed narrow molecular-weight distributions (polydispersity index (PDI) = 1.05), and no dimers, that is, diamides, were detectable, for either the 2.1 kDa sample (Figure 1) or the 5.1 kDa sample (see the Supporting Information, Figure S14). In addition, the presence of the squaramide was also detected by strong UV absorption during the SEC measurements. Quantitative end-group functionalization was proven by MALDI-TOF MS and ^{1}H NMR spectroscopy. The MALDI-TOF mass spectra of **5** with molecular weights of 2.1 kDa and 5.1 kDa displayed the expected single mass distribution. No unreacted amino mPEG or coupled products were detected. Besides the distribution of the polymer cationized with potassium, a second distribution with lower intensity was observed in some cases, which was assigned to the sodium-cationized species (Figure 2 and Figure S8 in the Supporting Information). Full conversion was also confirmed by comparison of the ^{1}H NMR integrals of the peaks assigned to the methyl groups at both polymer termini (Figure S3 and S4 in the Supporting Information). The signal of the single amide proton splits into two broad peaks at approximately $\delta = 6.6$ ppm. This has already been reported for low-molecular-weight compounds[10] and is a result of the rotational barrier along the cyclobutene carbon–nitrogen bond, which leads to the presence of *syn* and *anti* conformers.

The tolerance of the diethyl squarate activation of PEG towards hydroxy groups was further demonstrated by the synthesis of α-squaric acid ester amido ω-hydroxy-PEG (**4**; Scheme 1). The necessary α-amino ω-hydroxy PEG was synthesized by *N*,*N*-dibenzyl amino ethoxide initiated anionic ring-opening polymerization of ethylene oxide (EO) and subsequent cleavage of the protecting groups by hydrogenation (Scheme 2), analogous to protocols for the synthesis of copolymers of EO with different comonomers that were published recently.[11] Successful synthesis of **7** with narrow molecular-weight distributions (PDI 1.06) was confirmed by NMR spectroscopy, MALDI-TOF MS, and SEC (see the Supporting Information). Removal of the benzyl protecting groups by catalytic hydrogenation[12] was complete after 24 h (at 30–40 bar), as determined by NMR spectroscopy. Conversion of **2** into the analogous squaric acid ester amide **4** was accomplished by the reaction of **1** in ethanol/water (1/1) with triethylamine as an additive (Scheme 1). ^{1}H NMR spectroscopy and MALDI-TOF MS confirmed full derivatization of the amino group and preservation of the hydroxy moiety. As for the SEA-mPEGs, the formation of the corresponding squaramide was suppressed and no coupled product was found by SEC analysis.

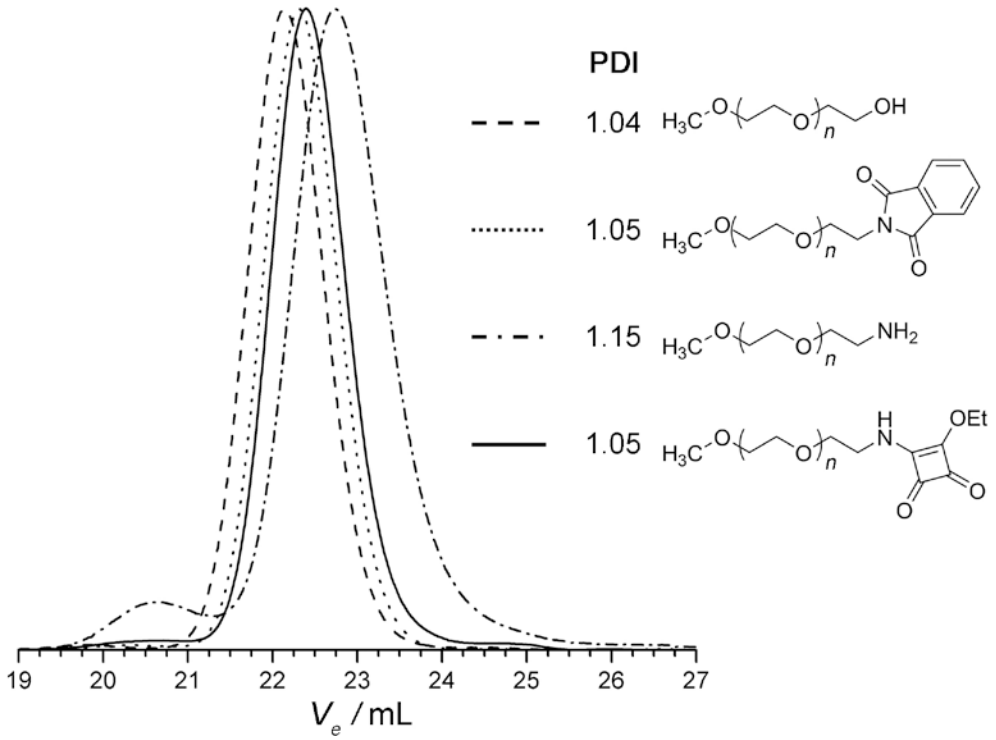

Figure 1. SEC elugrams of **4** (2.1 kDa) and its precursors (eluent: DMF; refractive index (RI) detector signal). The amino-PEGs often revealed a broadening of the mass distribution in the SEC analysis that led to an increase in the M_w/M_n ratio (the polydispersity index). Sometimes, even bimodal SEC traces were observed. This effect was attributed to interactions of the amino moiety with the poly(hydroxyethyl-methacrylate) columns of the chromatograph. Upon derivatization, the PDI values decreased significantly again.

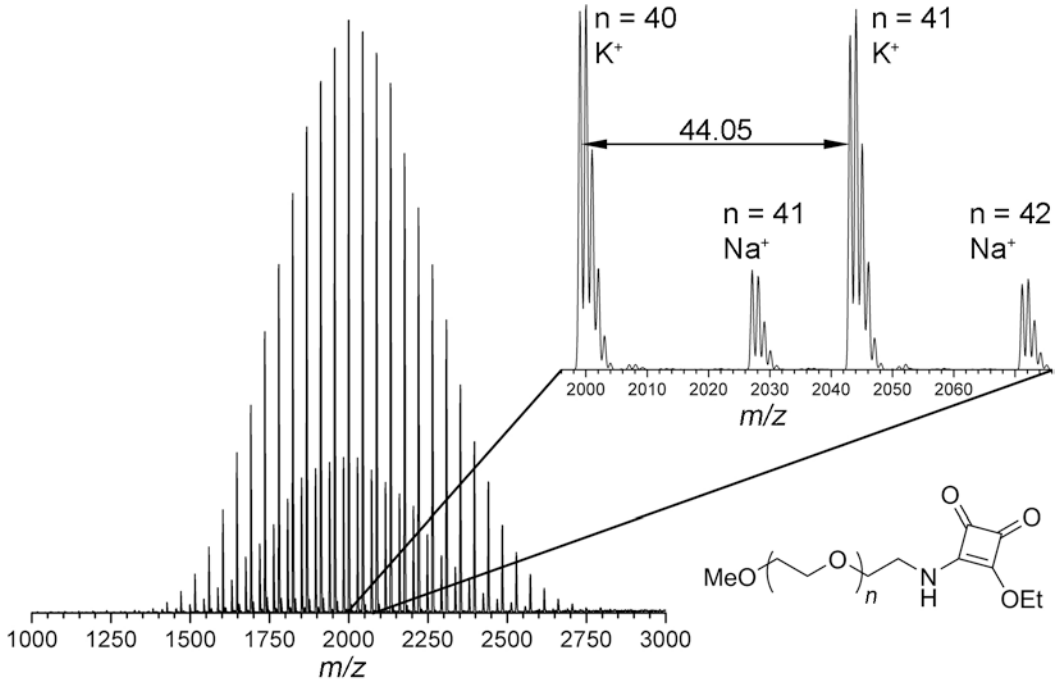

Figure 2. MALDI-TOF mass spectrum of **5** (2.1 kDa).

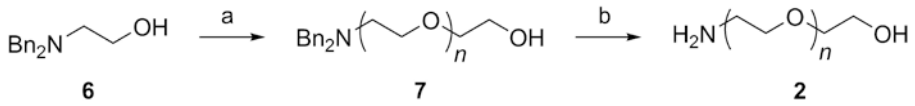

6 7 2

Scheme 2. Synthetic route to α-amino-ω-hydroxy-PEG. a) 1) C_6H_6, 90 °C, vacuum; 2) $KC_{10}H_8$, THF, *n*EO; 3) MeOH; b) H_2, $Pd(OH)_2/C$, MeOH/THF/water (2:1:1), 80 bar. Bn: benzyl; THF: tetrahydrofuran.

Reactivity of the squaric acid ester amide at the polymer terminus: In a next step, the reactivity of the terminal squaric acid ester amide towards the ε-amino group of lysine was investigated by following the reaction kinetics with ^{1}H NMR spectroscopy. As a model substrate, N_α-acetyl-L-lysine methyl ester hydrochloride (Ac-Lys-OMe), a lysine derivative with protected α-amino and carboxylic acid groups, was chosen. The solvent was a 0.1 M sodium borate buffer in deuterium oxide that provided a stable pD value of about 9.6 (0.4 added to the corresponding pH value of 9.2)[13] throughout the reaction, which was sufficiently high to enable the diamide formation. As the resonances of the ester amide's ethyl group were superimposed by other signals and the amide protons were not observable under these conditions, the resonance of the methyl group of ethanol, which is released during the reaction, was monitored at a chemical shift value of $\delta = 1.16$ ppm. Figure 3 shows the intensity of the methyl signal of the recorded spectra plotted against time for the reaction of a 2 kDa SEA-mPEG with 1.8 equivalents of Ac-Lys-OMe. All signals were normalized to the singlet resonance of the methoxy group of mPEG at $\delta = 3.36$ ppm. The resonance of the N-acetyl protons of the polymer-bound lysine ($\delta = 2.02$ ppm, Figure 3) was shifted by $\delta = 0.02$ ppm to higher field relative to the analogous signal of the substrate. However, these signals superimposed and, hence, were not suitable for the kinetic data analysis but could qualitatively show the progress of the reaction. As shown in Figure 3, after approximately four hours, the reaction was complete and the signal ratios remained constant. The reaction was carried out at room temperature in an NMR tube and mixing was merely provided by the spinning of the tube. Under the reaction conditions, the lysine methyl ester protecting group was hydrolyzed slowly (18% cleavage after 12 h). Obviously, hydrolysis of the polymer s terminal ethyl ester is a possible side reaction that has to be taken into account. It was monitored under the same conditions as the experiment described above but without the substrate by monitoring the decreasing intensity of the methyl resonance of the ethyl ester (see Figure S18 in the Supporting Information). The half-life of **5** in deuterated borate buffer (pD 9.6) was found to be three days, which evidenced very slow hydrolysis relative to the fast diamide formation. The hydrolysis of **5** was further studied at pD 8.4 in an

analogous ^{1}H NMR experiment by using a deuterated phosphate buffer solution. Within three days, 4.5% of the squaric acid ester was degraded (see Figure S20 in the Supporting Information). When it is considered that the reported hydrolytic half-lives of the commonly used PEG carboxylic acid *N*-hydroxysuccinimide esters are in the order of 0.75–23.3 min at pH 8,[14] this hydrolytic stability of 5 is remarkable and underlines the potential of this reagent to enable amino-selective protein conjugation of functional synthetic polymers.

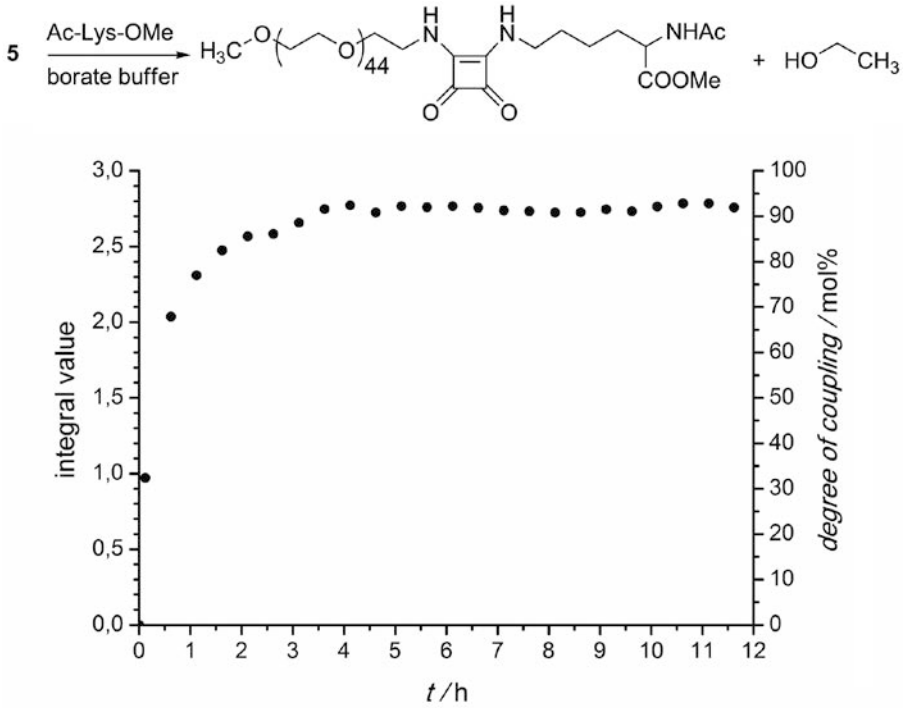

Figure 3. Reaction kinetics of SEA-mPEG (2.1 kDa) with N_a-acetyl-L-lysine methyl ester (2 eq.) in deuterated borate buffer (pD 9.6) monitored by ^{1}H NMR spectroscopy.

The reaction rate was increased significantly by adding dimethylsulfoxide (DMSO) to the reaction. When 2 equivalents of substrate were used and the solvent consisted of 70% deuterated borate buffer and 30% [D6]DMSO, the reaction was completed after approximately 40 min (Figure 4). As before, the increasing signal intensity of the released ethanol was monitored. The more pronounced data-point fluctuation in the case of the larger polymers is attributed to the lower signal-to-noise ratio. Interestingly, the degree of polymerization, that is, 44 or 112, had no considerable influence on the reactivity of the ethyl squarate. The reaction rates of the second amidation step can be influenced by the amount of substrate. As expected, adding equimolar amounts of Ac-Lys-OMe resulted in slightly lower reaction rates than those with a twofold excess (Figure 4). Again, the rates did not depend on the molecular weight of the PEG derivatives that were used. The hydrolysis of **5** in the presence of DMSO was also found to

be faster: 50% of the macromolecular ester was hydrolyzed in 1.5 days (see Figure S19 in the Supporting Information). However, in comparison to the timescale of the diamide formation, the hydrolysis can be neglected, which should allow for stoichiometric control over the degree of PEGylation (see below).

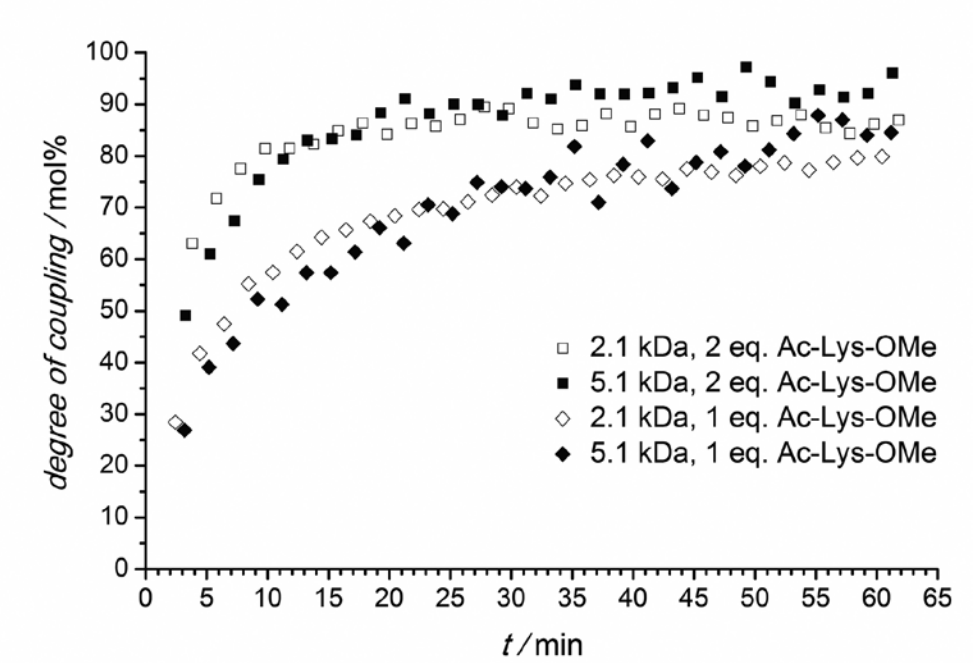

Figure 4. Diamide formation in borate buffer/DMSO (7:3) for two SEA-mPEGs with different molecular weights and two different concentrations of N_{α}-acetyl-L-lysine.

Chemoselectivity: The selectivity of SEA-mPEG towards the α- and the ε-amino group of lysine was investigated by following the reaction of 5 with one equivalent of L-lysine methyl ester dihydrochloride (H-Lys-OMe) in detailed ^{1}H NMR spectroscopy experiments. Figure 5 A shows selected regions of a series of NMR spectra recorded in a borate buffer (pD 9.6)/[D6]DMSO solution (the full spectra can be found in Figure S21 in the Supporting Information). The evolving triplet at δ = 1.21 ppm, which can be assigned to the ethanol released during the reaction, was used to monitor the total conversion by amidation and is plotted against the reaction time in Figure 5 B (black circles). Full conversion was achieved after approximately three hours, which is also confirmed by the decaying peak of the terminal methyl group of the squaric acid ester amide at δ = 1.5 ppm. The conversion of the lysine ε-amino group was calculated from the decreasing signal of the adjacent methylene group at δ = 2.9 ppm and is also shown in Figure 5 B (open squares). After an initial phase, the degree of N_{ε}-amide formation, which was obtained by dividing the ε-amino group conversion by the total conversion

was found to be constantly 70%. Hence, under these conditions, the ε-amino group is more reactive than the sterically more hindered α-amino group, which would suggest preferred PEGylation of the ε-amino groups in a protein. During the reaction time of three hours, the hydrolysis of the polyether s terminal ethyl ester in this solvent is negligible (see above).

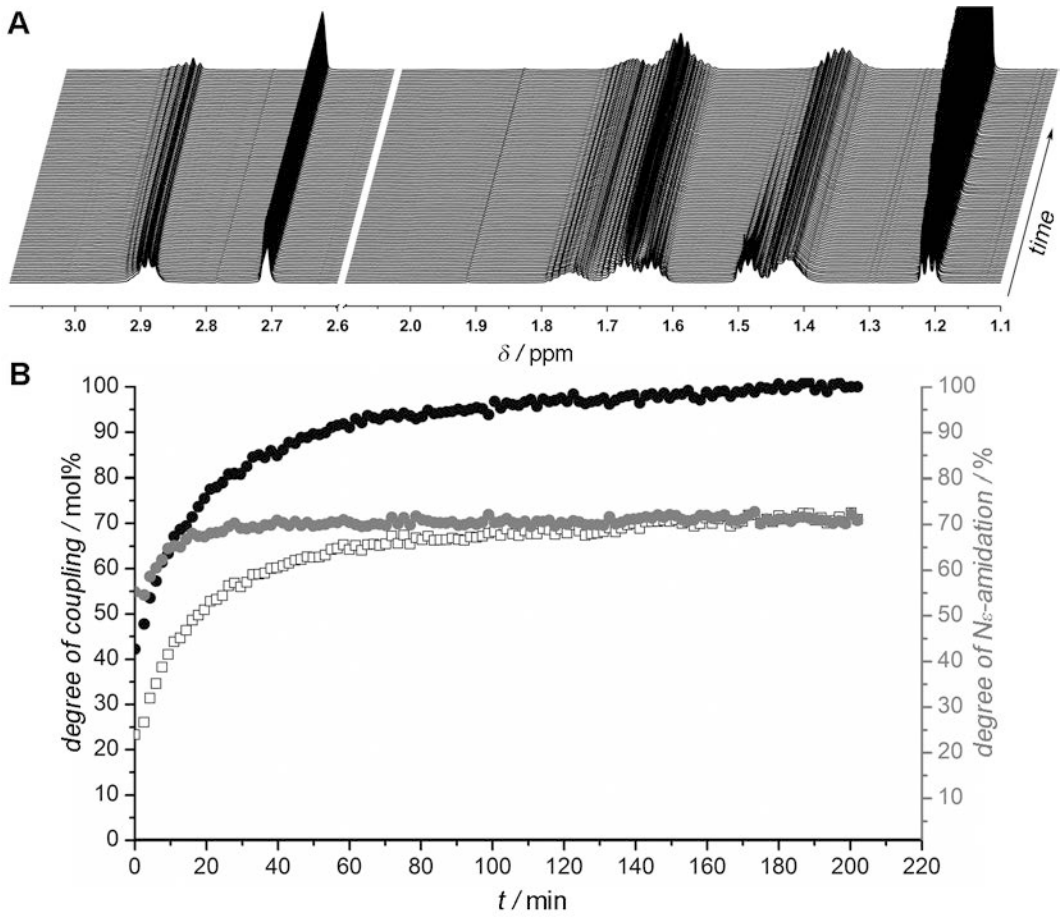

Figure 5. Reaction kinetics of SEA-mPEG (2.1 kDa) with L-lysine methyl ester (1 eq.) in borate buffer (pD 9.6)/[D6]DMSO (7:3). A) Selected regions of the ^{1}H NMR spectra (700 MHz; T = 294 K). B) Normalized signal intensities (left scale; black circles: EtOH; open squares: N_{ε}-amide) and the degree of N_{ε}-amidation (right scale; gray circles) plotted against reaction time.

When the same reaction was carried out in a deuterated phosphate buffer at pD 8.4, the reaction time increased significantly. The amidation was monitored continuously for the first 28 h and selected regions of the spectra are shown in Figure 6 A (the full spectra are shown in Figure S22 in the Supporting Information). As determined from the released ethanol, approximately 70% of the SEA-mPEG undergoes amidation during this period of time; after storage of the reaction mixture for six days, the conversion increased to 92%. Data derived from two spectra recorded after 63 h and 139 h are marked with asterisks in Figure 6 B and only can be regarded as a trend

because the sample was stored at room temperature in between the measurements, whereas it was kept constantly at 294 K within the spectrometer for the first 28 h.

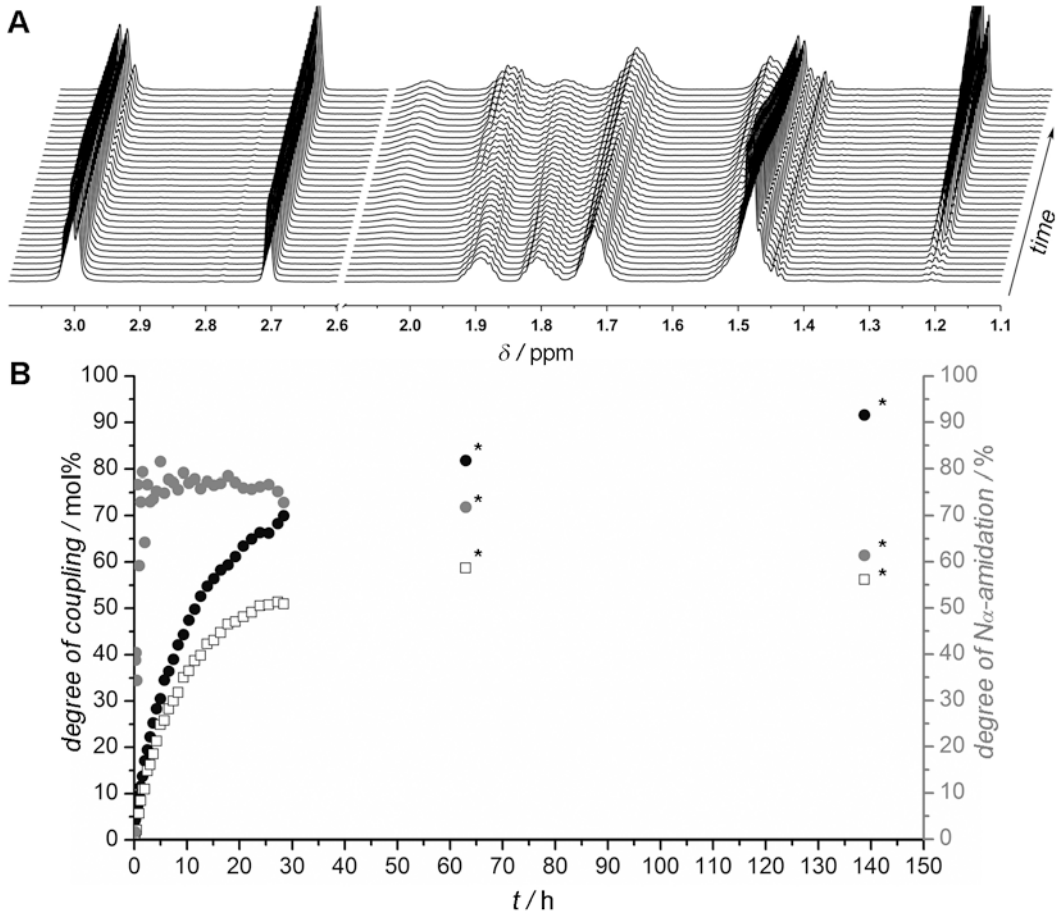

Figure 6. Reaction kinetics of SEA-mPEG (2.1 kDa) with L-lysine methyl ester (1 eq.) in phosphate buffer (pD 8.4)/[D6]DMSO (7:3). A) Selected regions of ^{1}H NMR spectra (700 MHz; T = 294 K) obtained in the first 28 h. B) Normalized signal intensities (left scale; black circles: EtOH; open squares: N_α-amide) and the degree of N_α-amidation (right scale; gray circles) plotted against reaction time. Data points marked with asterisks were recorded after resting of the sample at room temperature, whereas the reaction was followed at T = 294 K for the first 28 h.

Most interestingly, the chemoselectivity of the SEA-mPEG changes at this pD value compared with that in the experiment at pD 9.6. A major fraction of the amino-reactive PEG reacts with the α-amino group of lysine. To our knowledge, this is the first time that such behavior has been observed for a squaric acid alkyl ester amide. Whereas the signal of the methylene group adjacent to the ε-amino group of the lysine derivative exhibited a significant decrease in the experiments described above, only a slight decrease occurred during the reaction at the lower pD value. Instead, a signal at δ = 2.05 ppm was detected and was assigned to one of the diastereotopic protons of the β-carbon atom of lysine, which was PEGylated through the α-

amino group. After 28 h, 50% of the α-amino groups had been converted; after 63 h, it was 59%. However, 76 h later, the signal had decreased by 3%. Whether this observation should be assigned to a hydrolytic cleavage of the squaramide or to solvent effects is under current investigation. The assignment of this signal to one of the β-protons of N_α-PEGylated lysine was validated by DOSY (diffusion-ordered spectroscopy) and TOCSY (total correlation spectroscopy) NMR experiments on the sample. The TOCSY spectrum (see Figure S26 in the Supporting Information) revealed the affiliation of the signal at $\delta = 2.05$ ppm to the spin system of the lysine's alkyl chain and coupling to a signal superimposed by the HDO signal at $\delta = 4.8$ ppm, which was assigned to the α-proton of N_α-PEGylated lysine. According to the DOSY spectrum (see Figure S27 in the Supporting Information), the aforementioned signals belong to a species with the lowest diffusion constant of the system ($1\times10^{-10}\,m^2s^{-1}$), which indicates a PEGylated lysine. The degree of N_α-amidation was found to be approximately 75% within the first 28 h and diminished during the course of the reaction. One of the reasons is the hydrolysis of the SEA-mPEG, which has to be taken into account because the total conversion took longer than 140 h. As the lysine derivative can be seen as a model for the N terminus of a protein, it might be possible to use SEA-PEGs for the selective PEGylation of a protein's N terminus at a specific pH value which is currently under investigation. The reaction of 5 with H-Lys-OMe in the deuterated borate buffer/DMSO solution was also carried out at a lower temperature (283 K). Apart from a prolonged reaction time (total conversion was achieved after 9 h), no significant differences to the experimental results illustrated in Figure 5 were observed. Again, the lysine derivative was PEGylated mainly at the ε-amino group and the degree of N_ε-amidation was around 70% (see Figure S23 in the Supporting Information). These experiments clearly prove the versatility and the superior hydrolytic stability of squaric acid ester amides over the conventional activated esters used in protein PEGylation.

Besides the amino groups of the lysine residues or the N terminus, other nucleophilic amino acids may potentially react with the activated polyethers **4** and **5**, such as the hydroxy group of serine, the guanidine group of arginine, and histidine's imidazole moiety. To evaluate the selectivity of the squaric acid modified PEGs towards amine groups, the reactivity of 5 towards arginine and histidine residues was investigated in ^{1}H NMR experiments analogous to those described earlier. *N-tert*-Butoxycarbonyl-L-histidine methyl ester (Boc-His-OMe) served as the histidine model compound with protected α-amino and carboxylic acid groups, and a solution of 70% deuterated borate buffer with 30% [D6]DMSO was used as the solvent. As before, the

signal intensity of the methyl group of ethanol released in the course of the reaction was monitored for 12 h (1.5 equivalents of protected amino acid were used; see Figure S25 in the Supporting Information). The NMR experiments revealed the release of only 5% ethanol over this time period, which is identical to the loss of ethyl ester groups that was observed during the experiments that were carried out to assess the hydrolytic stability of **5** (see above). This clearly indicates that **5** is essentially nonreactive towards histidine. A similar result was obtained from experiments with N_{α}-*p*-tosyl-L-arginine methyl ester hydrochloride (Ts-Arg-OMe). Even after 2.5 h, the expected resonance of the methyl group of ethanol was barely visible (see Figure S24 in the Supporting Information). Thus, undesired PEGylation of histidine and arginine residues with **5** under these conditions can be ruled out. In addition to reaction with arginine and histidine residues, another possible side-reaction during protein conjugation could involve transesterification with hydroxy side chain functional amino acids, such as serine. In principle, however, the reaction of 4 or 5 with serine, or another hydroxy-containing amino acid, would merely generate another PEG squaric acid monoester derivative, which would still be reactive towards amine groups and, as a consequence, would not be expected to compromise the chemoselectivity of the SEA-PEG derivatives. To evaluate this hypothesis, a mixture of two equivalents each of Ac-Lys-OMe and *N*-benzyloxycarbonyl-L-serine methyl ester (Z-Ser-OMe) was treated with 5 in a solution of ethanol with triethylamine as an additive. MALDI-TOF MS analysis of the reaction products only indicated the formation of the diamide (see Figure S9 in the Supporting Information). This clearly proves that the novel SEA-PEGs can chemoselectively PEGylate proteins at the amino groups of lysine residues and probably the N terminus without interference by arginine, histidine, or serine moieties. The reaction of squaric acid ester amides with low molecular weights towards cysteine has already been studied and was found to result exclusively in the corresponding squaramide because the thioester formation is reversible.[15] Therefore, in the presence of amino groups, squaric acid mediated PEGylation at cysteine residues is unlikely.

Bioconjugation: The bioconjugation of the novel activated PEGs was investigated with a model protein, namely bovine serum albumin (BSA), the primary structure of which consists of 59 lysine residues,[16] from which 30–35 are available for covalent attachment.[17] 10-, 20-, 50-, and 100-fold excesses of **5** were fed to solutions of the protein in an aqueous borate buffer (pH 10). These amounts correspond to 0.29, 0.57, 1.4, and 2.9 equivalents of the available

lysine residues, respectively. Two series of conjugates with varying molecular weights of **5**, that is, a 2.1 kDa polymer (Table 1, conjugates **A–D**) and a 5.1 kDa polymer (Table 1, conjugates **E–H**), were prepared. All PEGylated proteins were purified by dialysis and isolated after freeze–drying in almost quantitative yields (with respect to the amount of BSA used). Figure 7 shows the sodium dodecylsulfate polyacrylamide gel electrophoresis (SDS-PAGE) results for the obtained conjugates (lanes 3 to 10) and the unmodified BSA (lane 2), as well as a molecular-weight size marker (lane 1). The absence of free unmodified BSA in all of the lanes indicates complete conversion of the native protein. All conjugates exhibit significantly increased molecular weights compared to BSA, which evidences modification of the protein in all cases.

Table1. Sizes and degrees of PEGylation for the mPEG–protein conjugates.

Conjugate	M_{PEG} [kDa]	n_{PEG}/n_{BSA}[a]	M_{Con} [kDa][b,c]	n_{PEG}/n_{BSA}[c]
A	2.1	10	87.0	10.0
B	2.1	20	106.5	19.4
C	2.1	50	117.5	24.7
D	2.1	100	136.0	33.5
E	5.1	10	112.3	9.1
F	5.1	20	157.4	18.0
G	5.1	50	226.0	31.5
H	5.1	100	240.0	34.2

[a] Ratio applied. [b] Determined by SEC-RALS analysis. [c] Ratio found.

The samples prepared by adding a 10- and 20-fold molar excess of the polymer show a clear difference in their apparent size, whereas the conjugates obtained from the batches treated with 50 and 100 equivalents displayed only slight differences. The PEGylated BSA synthesized with 100 equivalents of the 5.1 kDa polymer barely moved through the gel (Figure 7, lane 10). These results were in very good agreement with the results obtained by SEC and measured with a right-angle light-scattering detector (SEC-RALS), which provided a more specific size analysis of the synthesized protein–polymer conjugates. The SEC traces of all samples including the unmodified protein tailed to higher molecular weights, which indicates the presence of a small fraction of dimeric BSA in the commercial protein; this is also visible in the SDS-PAGE result

for the unmodified BSA (Figure 7, lane 2). From the absolute number-averaged molecular weights determined by the SEC-RALS analysis, the average number of PEG chains attached to a protein was calculated (Table 1).

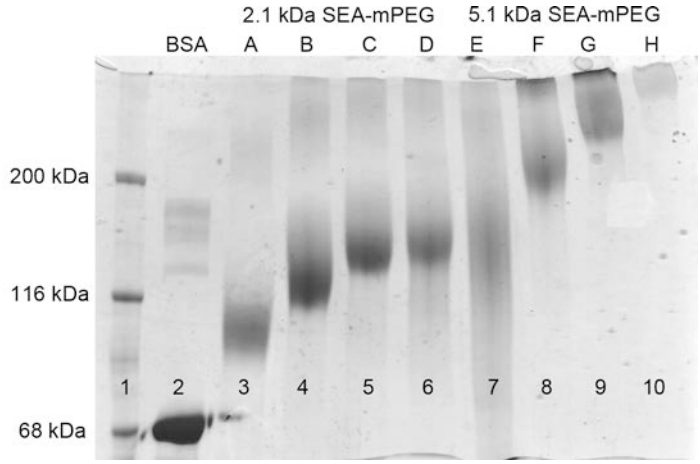

Figure 7. SDS-PAGE (6 %) results of BSA (lane 2) and BSA–polymer conjugates prepared by different feeds of either 2.1 kDa SEA-mPEG (lanes 3–6) or 5.1 kDa SEA-mPEG (lanes 7–10) in aqueous borate buffer (pH 10).

For the conjugates synthesized with low feeds of **5** (**A**, **B**, **E**, and **F**), the average number of polymers bound to BSA corresponded well to the targeted ratio of polymer/protein and confirmed stoichiometric PEGylation of BSA without loss of active polymer. This is rationalized by the extreme hydrolytic stability of the reactive ester amide at the polymer chain end. **D** and **H** carry approximately 34 polymer chains, respectively, which indicated quantitative PEGylation of the surface-available lysines. In order to investigate the influence of the PEGylation reaction conditions, especially the elevated pH value, on the protein structure, circular dichroism (CD) spectra of both BSA and the PEGylated BSA samples were recorded. The CD spectroscopy experiments demonstrated that the structure of the model protein BSA was not changed by the squaric acid mediated PEGylation with 5 (M_n = 2.1 kDa), regardless of the degree of PEGylation (CD spectra of BSA, **B**, and **D** are provided in Figure S29 in the Supporting Information). The high pH protocol is probably not suitable for all proteins. However, some proteins like rabbit kidney cytokinase and catechol 1,2-dioxygenase exhibit maximal activity at pH 8.5 or 9, for example.[18] For the production of PEGASYS, one of the most prominent PEGylated therapeutics on the market, human interferon α-2a is PEGylated in a borate buffer at pH 9 at 4 °C.[19] The results of kinetic studies on the reaction of SEA-mPEGs with L-lysine methyl ester at pD 8.4 suggest a promising outcome for the squaric acid mediated

PEGylation under less basic conditions. Furthermore, Luk and coworkers demonstrated the reactivity of low-molecular-weight squaric acid ethyl ester alkyl derivatives towards peptides with N-terminal cysteines under very mild conditions (neutral pH value).[15] The applicability of these procedures to our PEGylation agents is under current investigation.

The hydroxy-functionalized SEA-PEGs, **4**, were found to be equally suitable for the PEGylation of BSA as the methyl ether derivatives (see Figure S28 in the Supporting Information).

Conclusions

We have demonstrated the single-step activation of α-amino PEGs with commercially available diethyl squarate (**1**). This general protocol proved to be highly selective for PEGylation of lysine residues, without side reactions at other nucleophilic amino acid residues, on the model protein BSA in aqueous systems at room temperature. In comparison with standard PEGylation agents, the squaric acid ester amide activated polyethers proved to have prolonged hydrolytic stability (half-life of several days at pD 9.6), which broadens the applicability of PEGylation reactions in biologically interesting media and guarantees efficient PEGylation even over a long reaction time. Furthermore, the squaric acid mediated PEGylation tolerates hydroxy-functionalized PEG derivatives and, as shown recently, even polyglycerol derivatives,[11d] which gives the opportunity for labeling or attachment of targeting functions to the polymer chains in subsequent reactions.

Detailed NMR investigations proved a remarkable change in the chemoselectivity of the squaric acid activated PEG: Whereas mainly the ε-amino group of lysine is PEGylated at elevated pD values, the major product in a less basic environment is the N_α-amide of lysine. This selectivity and high hydrolytic stability renders the squaric acid mediated PEGylation superior over many other activated ester techniques for protein modification. The chemoselectivity of the SEA-PEGs will be explored in further studies.

Experimental Section

Materials: All reagents and solvents were purchased from Acros Organics or Sigma–Aldrich and used without further purification unless stated otherwise. Diisopropylazodicarboxylate was purchased from Apollo Scientific and aqueous borate buffer (pH=10) from Fisher Scientific. N_α-

acetyl-L-lysine methyl ester hydrochloride and *N-tert*-butoxycarbonyl-L-histidine methyl ester were bought from Bachem. The dialysis membranes (Spectra/Por 1, MWCO = 68 kDa, 40 mm flat width, Spectra/Por 6, MWCO = 50 kDa, 34 mm flat width) were obtained from Spectrum Laboratories. Deuterated solvents were purchased from Deutero GmbH and except for deuterium oxide were stored over molecular sieves (3Å). Dibenzylamino ethanol was synthesized according to a known protocol.[20]

Instrumentation: ^{1}H NMR spectra were recorded at 294 K, unless stated otherwise, either on a Bruker ARX 400 with a 5mm BBO probe (400 MHz spectra) or a Bruker Avance III 700 (16,4 T) with a 5 mm z-gradient BBI invers ^{1}H/X probe (700 MHz spectra). Spectra recorded on the 700 MHz spectrometer were regulated by a standard ^{1}H methanol NMR sample using the topspin 3.0 software (Bruker). The spectra were referenced against the residual HDO at $\delta(^{1}H)$ = 4,80 ppm. All 1D spectra were processed with MestReNova 6.1.1-6384 software. The 2D-TOCSY program was run with the MLEV17 sequence for the homonuclear Hartman–Hahn transfer with a "tocsy" mixing time of 100 ms. For the 700 MHz probe, the spectrum was obtained with π/2-pulse length of 9.3 µs (^{1}H) and a sweep width of 8400 Hz (12 ppm) for both dimensions. A relaxation delay of 3s was chosen for the 2D experiment. The DOSY experiments were recorded with a 5 mm BBI ^{1}H/X z-gradient probe and a gradient strength of 5.516 G mm^{-1} on the 700 MHz spectrometer by using a double-stimulated echo for convection compensation. The relaxation time was 2 s, the diffusion delay was kept at 90 ms and the gradient pulse with a length of 1600 µs. For the calibration of the gradient strength, a sample of $^{2}H_2O/^{1}H_2O$ was measured at a defined temperature and compared with the literature diffusion coefficient of $^{2}H_2O/^{1}H_2O$.[21] 2D spectra were processed with Topspin 3.0. For SEC measurements, a 9:1 mixture of phosphate buffer (0.1 M, pH 6.5)/methanol was used at a flow rate of 0.5 mL min^{-1} on Shodex OHpak 804 and 805 columns in a Viscotek TDA 300 instrument with triple detection at 25°C, equipped with a MetaChem degasser, a Viscotek VE 1121 GPC solvent pump, and a VE 5200 GPC autosampler. SEC measurements in *N*,*N*-dimethyl-formamide (DMF) containing 0.25 g L^{-1} of lithium bromide as an additive were performed on an Agilent 1100 Series as an integrated instrument with a Polymer Standards Service (PSS) hydroxyethyl methacrylate column (106/105/104 g mol^{-1}), an RI detector, and a UV detector operating at 275 nm. Calibration was executed using poly(ethylene oxide) standards from PSS. MALDI-TOF MS measurements of all polymers were recorded on a Shimadzu Axima CFR

MALDI-TOF mass spectrometer, equipped with a nitrogen laser delivering 3 ns laser pulses at 337 nm. α-Cyanohydroxycinnamic acid was used as a matrix and potassium trifluoroacetate was added for ion formation. SDS-PAGE was carried out with 4–8% Tris-HCl gels (Biorad, 0.75 mm, 10 wells). Circular dichroism (CD) spectra were recorded on a JASCO J-815 CD spectrometer equipped with a PTC-423S Peltier type temperature-control system at 20.0 °C in a 1 mm cell in water with analyte concentrations of 1.5 μmol L^{-1} and a band width of 1.0 nm at a scanning speed of 50 nm s^{-1} (data pitch: 0.1 nm). Spectra presented are accumulations of 10 individual measurements each. IR spectra were recorded on a Thermo Scientific Nicolet iS10 FT-IR spectrometer, equipped with a diamond attenuated-total-reflectance unit and were processed with OMNIC 8.1.210 software.

α-Amino-ω-hydroxy-poly(ethylene glycol) (2): Hydrogenation of α-dibenzylamino-ω-hydroxy-PEG (**7**) was carried out analogously to a known protocol.[12] Details are given in the Supporting Information.

α-Squaric acid ester amido ω-hydroxy-poly(ethylene glycol) (4): A solution of **2** (500 mg, 0.222 mmol), diethyl squarate (340 mg, 1.99 mmol), and triethylamine (230 mg, 2.27 mmol) was stirred in a mixture of water (6.3 mL) and ethanol (6.3 mL) for 4 h. After removal of the ethanol with a rotational evaporator, the solution was extracted with dichloromethane three times. The combined organic phases were dried over sodium sulfate, and the product was precipitated several times from methanol in cold diethyl ether. After confirmation of complete removal of the diethyl squarate by thin layer chromatography, the SEA-PEG was dried in vacuo and eventually lyophilized from distilled water to give a colorless powder; ^{1}H NMR (400 MHz, [D_6]DMSO, 21°C): δ = 8.81 (br s, 0.52H; NH), 8.63(br s, 0.47H; NH), 4.65 (q, ^3J (H,H) = 6.9 Hz, 2H; CH_2-CH_3), 4.57 (t, ^3J (H,H) = 5.4 Hz, 1H; OH) 3.87–3.35 (m, 203H; $(CH_2CH_2O)_n$), 1.37 ppm (t, ^3J (H,H) = 7.0 Hz, 3H; CH_2–CH_3); IR (ATR): $\tilde{\nu}$ = 3435, 2882, 1802 $(C{=}O)_s$, 1706 $(C{=}O)_{as}$, 1609 (C=C), 1466, 1454, 1359, 1341, 1279, 1241, 1147, 1099, 1059, 960, 841 cm^{-1}.

α-Squaric acid ester amido poly(ethylene glycol) ω-methyl ether (5): α-Amino-mPEG[9] (1 mmol), triethylamine (1.02 g, 10.1 mmol), and diethyl squarate (860 mg, 5.05 mmol) were dissolved in ethanol (50 mL). After the mixture had been stirred for 24 h at room temperature, the solvent was removed under reduced pressure. The crude product was precipitated several times from dichloromethane in cold diethyl ether. After confirmation of

complete removal of the diethyl squarate by thin layer chromatography, the SEA-mPEG was dried in vacuo and eventually lyophilized from distilled water to give a colorless powder; yield: 57–63 %; ^{1}H NMR (400 MHz, [D6]DMSO, 21 °C): δ = 8.80 (br s, 0.56 H; NH), 8.62 (br s, 0.44H; NH), 4.65 (q, ^3J(H,H) = 7 Hz, 2H; CH_2–CH_3), 3.80–3.25 (m, 215H; $(CH2CH2O)_n$), 3.24 (s, 3H; O–CH_3), 1.37 ppm (t, ^3J(H,H) = 7 Hz, 3H; CH_2–CH_3); IR (ATR): $\tilde{\nu}$ = 2883, 1803 (C=O)s, 1710 (C=O)as, 1612 (C=C), 1466, 1454, 1359, 1340, 1279, 1240, 1146, 1103, 1060, 947, 841 cm^{-1}.

α-Dibenzylamino-ω-hydroxy-poly(ethylene glycol) (7): Under argon, dibenzylaminoethanol (6, 603.3 mg, 2.50 mmol) was placed in a dry Schlenk flask and dissolved in benzene (10 mL). Traces of moisture were removed by azeotropic distillation of benzene and subsequent drying at 333 K under high vacuum for 14 h. After dry THF (20 mL) had been cryo-transferred into the Schlenk flask, it was flooded with argon and, under vigorous stirring, a 1 M solution of potassium naphthalenide in THF (2 mL; prepared from potassium (235 mg, 6.0 mmol), naphthalene (770 mg, 6.0 mmol), and dry THF (6 mL) in a glove box) was added slowly. The hydrogen released and half of the amount of THF were removed by distillation under reduced pressure. After ethylene oxide (5.0 g, 0.11 mol) had been cryo-transferred through a graduated ampule into the initiator solution, the flask was closed tightly and stirred overnight at 323 K. Methanol (2 mL) was added and the polymer was precipitated twice in cold diethyl ether. Filtration and subsequent drying under reduced pressure gave 7 in quantitative yields; ^{1}H NMR (400 MHz, $CDCl_3$, 21 °C): δ = 7.38–7.14 (m, 10H; CH_{Ar}), 3.95–3.25 (m, 219H; $PhCH_2$, $(CH_2CH_2O)_n$), 2.65 ppm (t, ^3J(H,H) = 8.2 Hz, 2H; CH_2–NBn_2). Attention must be paid when working with the gaseous, toxic, and flammable ethylene oxide.

Typical protocol for the PEGylation of BSA: Solutions of BSA (25 mg, 379 nmol) in an aqueous borate buffer (250 µL, pH 10) were treated with various amounts of SEA-mPEG (2.1 kDa) and stirred for 2 days. The solutions were dialyzed against distilled water (MWCO = 50 kDa). Upon lyophilization, the conjugates were obtained quantitatively. Further information is available in the Supporting Information.

The reaction of 5 with Ac-Lys-OMe in the presence of Z-Ser-OMe: Ac-Lys-OMe (11.9 mg, 50 µmol), Z-Ser-OMe (12.7 mg, 50 µmol), and 5 (50.0 mg, 24 µmol) were stirred in ethanol (2 mL) with triethylamine (100 µL) as an additive for 12 h. After the solvent had been

evaporated, the product was precipitated from dichloromethane in cold diethyl ether three times; yield: 48.3 mg (89 %).

Kinetic studies: Typical reaction kinetics protocol for the reaction of 5 with H-Lys-OMe in borate buffer with DMSO. H-Lys-OMe (4.4 mg, 19 µmol) and 5 (40.0 mg, 19 µmol) were dissolved in a 7:3 mixture of a 0.1 M deuterated borate buffer and [D6]DMSO (600 µL) in an NMR tube. After locking and shimming, a ^{1}H NMR spectrum (700 MHz) was recorded with 32 scans and a relaxation delay of 10 s at T = 294 K every 1.69 min for 3.4 h. All spectra were processed (Fourier transformation, phase correction, baseline correction) and referenced to the solvent signal (DMSO). All signals were integrated in the same limits.

Reaction kinetics protocols for all reactions monitored by ^{1}H NMR spectroscopy are described in the Supporting Information.

Acknowledgements

C.D. is grateful to the Max Planck Graduate Center (MPGC) with the Johannes Gutenberg-Universität Mainz for a fellowship and financial support. F.W. thanks the Alexander-von-Humboldt Foundation for a fellowship.

References

[1] a) K. Hermansen, P. Fontaine, K. K. Kukolja, V. Peterkova, G. Leth, M.-A. Gall, *Diabetologia* **2004**, *47*, 622; b) R. Tugyi, K. Uray, D. Iv n, E. Fellinger, A. Perkins, F. Hudecz, *Proc. Natl. Acad. Sci. USA* **2005**, 102, 413; c) M. Bakke, C. Setoyama, R. Miura, N. Kajiyama, *Biotechnol. Bioeng.* **2006**, *93*, 1023; d) M. A. Gauthier, H.-A. Klok, *Chem. Commun.* **2008**, 2591; e) M. A. Gauthier, H.-A. Klok, *Polym. Chem.* **2010**, *1*, 1352; f) H.-A. Klok, *Macromolecules* **2009**, *42*, 7990.

[2] a) A. Abuchowski, T. v. Es, N. C. Palczuk, F. F. Davis, *J. Biol. Chem.* **1977**, *252*, 3578; b) A. Abuchowski, J. R. McCoy, N. C. Palczuk, T. Vanes, F. F. Davis, J. *Biol. Chem.* **1977**, *252*, 3582.

[3] a) F. M. Veronese, G. Pasut, *Drug Discovery Today* **2005**, *10*, 1451; b) G. Pasut, F. M. Veronese, *Prog. Polym. Sci.* **2007**, *32*, 933.

[4] S. N. S. Alconcel, A. S. Baas, H. D. Maynard, *Polym. Chem.* **2011**, *2*, 1442.

[5] a) V. P. Kamath, P. Diedrich, O. Hindsgaul, *Glycoconjugate J.* **1996**, *13*, 315; b) L. F. Tietze, C. Schroeter, S. Gabius, U. Brinck, A. Goerlach-Graw, H. J. Gabius, *Bioconjugate Chem.* **1991**, *2*, 148; c) A. Chernyak, A. Karavanov, Y. Ogawa, P. Kovac, *Carbohydr. Res.* **2001**, *330*, 479; d) A. Bergh, B. G. Magnusson, J. Ohlsson, U. Wellmar, U. J. Nilsson, *Glycoconjugate J.* **2001**, *18*, 615; e) S.-j. Hou, R. Saksena, P. Kovác, *Carbohydr. Res.* **2008**, *343*, 196.

[6] U. Westerlind, A. Hobel, N. Gaidzik, E. Schmitt, H. Kunz, *Angew. Chem.* **2008**, *120*, 7662; *Angew. Chem. Int. Ed.* **2008**, *47*, 7551.

[7] L. F. Tietze, M. Arlt, M. Beller, K.-H. Glüsenkamp, E. Jähde, M. F. Rajewsky, *Chem. Ber.* **1991**, *124*, 1215.

[8] D. QuiÇonero, A. Frontera, P. Ballester, P. M. Dey , *Tetrahedron Lett.* **2000**, *41*, 2001.

[9] P. Mongondry, C. Bonnans-Plaisance, M. Jean, J. F. Tassin, *Macromol. Rapid Commun.* **2003**, *24*, 681.

[10] M. C. Rotger, M. N. Pina, A. Frontera, G. Martorell, P. Ballester, P. M. Dey , A. Costa, *J. Org. Chem.* **2004**, *69*, 2302.

[11] a) C. Mangold, C. Dingels, B. Obermeier, H. Frey, F. Wurm, *Macromolecules* **2011**, *44*, 6326; b) F. Wurm, A. M. Hofmann, A. Thomas, C. Dingels, H. Frey, *Macromol. Chem. Phys.* **2010**, *211*, 932; c) F. Wurm, J. Klos, H. J. Räder, H. Frey, *J. Am. Chem. Soc.* 2009**,** *131*, 7954; d) F. Wurm, C. Dingels, H. Frey, H.-A. Klok, *Biomacromolecules* **2012**, *13*, 1161.

[12] B. Obermeier, F. Wurm, H. Frey, *Macromolecules* **2010**, *43*, 2244.

[13] P. K. Glasoe, F. A. Long, *J. Phys. Chem.* **1960**, *64*, 188.

[14] J. M. Harris, A. Kozlowski (Shearwater Polymers Inc.), US-A 000005672662, **1997**.

[15] P. Sejwal, Y. Han, A. Shah, Y.-Y. Luk, *Org. Lett.* **2007**, *9*, 4897.

[16] K. Hirayama, S. Akashi, M. Furuya, K.-i. Fukuhara, *Biochem. Biophys. Res. Commun.* **1990**, *173*, 639.

[17] M. H. V. Van Regenmortel, J. P. Briand, S. Muller, S. Plaué in *Laboratory techniques in biochemistry and molecular biology: Synthetic polypeptides as antigens*, Vol. 19 (Eds.: R. H. Burdon, P. H. van Knippenberg), Elsevier, Amsterdam, **1988**, p. 227.

[18] a) S. Y. Ali, L. Evans, *Biochem. J.* **1968**, *107*, 293; b) P. D. Strachan, A. A. Freer, C. A. Fewson, *Biochem. J.* **1998**, *333*, 741.

[19] P. Bailon, A. Palleroni, C. A. Schaffer, C. L. Spence, W.-J. Fung, J. E. Porter, G. K. Ehrlich, W. Pan, Z.-X. Xu, M. W. Modi, A. Farid, W. Berthold, *Bioconjugate Chem.* **2001**, *12*, 195.

[20] D. Dix, P. Imming, *Arch. Pharm.* **1995**, *328*, 203.

[21] a) A. Jerschow, N. Müller, J. *Magn. Reson., Ser. A* **1996**, *123*, 222; b) A. Jerschow, N. Müller, *J. Magn. Reson.* **1997**, *125*, 372.

Supporting Information

Squaric Acid Mediated Chemoselective PEGylation of Proteins: Reactivity of Single-Step-Activated α-Amino Poly(ethylene glycol)s

Carsten Dingels, Frederik Wurm, Manfred Wagner, Harm-Anton Klok, and Holger Frey

Table of contents

1. Synthetic protocols

1.1 α-Amino ω-hydroxy-poly(ethylene glycol) **2**

Hydrogenation of α-Dibenzylamino ω-hydroxy-PEG (**7**) was carried out analogous to a known protocol.[1] **7** (3.96 g, 1.65 mmol) and Pearlman's catalyst (400 mg) were stirred under hydrogen atmosphere (80 bar) for 3 days in a solution of water (20 mL), THF (20 mL), and methanol (40 mL) in a stainless steel reactor. The solution was filtered through celite and the filter cake washed with 2 L of methanol. After removal of the solvent the crude product was precipitated from dichloromethane (DCM) in cold diethyl ether twice. Lyophilization from distilled water yielded 2.80 g (1.24 mmol, 75%) as a colorless powder. *^{1}H NMR* (400 MHz, $CDCl_3$): δ [ppm] = 3.92-3.34 (m, 215H, $(CH_2CH_2O)_n$), 2.82 (t, 0.7H, J = 5.4 Hz; $-CH_2-NH_3^+$), 2.63 (t, 1.3H, J = 6.0 Hz; $-CH_2-NH_2$).

1.2 PEGylation of BSA with SEA–mPEG of 2100 g·mol^{-1}(conjugates **A** – **D**)

Solutions of BSA (25 mg, 379 nmol) in an aqueous borate buffer (250 µL, pH = 10) were treated with various amounts of SEA-mPEG (details provided in Table S1) and stirred for 2

days. The solutions were dialyzed against distilled water (MWCO = 50 kDa). Upon lyophilization the conjugates were yielded quantitatively.

Table S1. Amounts of SEA-mPEG (2.1 kDa) batched in PEGylation and found in the conjugates.

Sample	m_{PEG}[a] / mg	n_{PEG}[a] / µmol	M_n[b] / kDa	n_{PEG} / n_{BSA}[b,c]
A	8.0	3.79	87.0	10.0
B	15.9	7.58	106.5	19.4
C	39.8	18.9	117.5	24.7
D	79.5	37.9	136.0	33.5

[a]fed, [b]determined by SEC-RALS, [c]found

1.3 PEGylation of BSA with SEA–mPEG of 5100 g·mol^{-1} (conjugates **E** – **H**)

Solutions of BSA (12.5 mg, 189 nmol) in an aqueous borate buffer (250 µL, pH = 10) were treated with various amounts of SEA-mPEG (details provided in Table S2) and stirred for 2 days. The solutions were dialyzed against distilled water (MWCO = 50 kDa). Upon lyophilization the conjugates were yielded quantitatively.

Table S2. Amounts of SEA-mPEG (5.1 kDa) batched in PEGylation and found in the conjugates.

Sample	m_{PEG}[a] / mg	n_{PEG}[a] / µmol	M_n[b] / kDa	n_{PEG} / n_{BSA}[b,c]
E	9.7	1.89	112.3	9.1
F	19.3	3.79	157.4	18.0
G	38.6	7.58	226.0	31.5
H	96.6	18.9	240.0	34.2

[a]fed, [b]determined by SEC-RALS, [c]found

1.4 PEGylation of BSA with α-squaric acid ester amido ω-hydroxy-PEG (**4**)

The PEGylations of BSA using **4** as reagent were carried out analogous to those with 2.1 kDa SEA-mPEGs as described under 1.2.

2. Reaction kinetics protocols

2.1 Hydrolysis of **5** in borate buffer (pD = 9.6)

5 (50.0 mg, 24 µmol) was dissolved in 600 µL of a 0.1 M solution of sodium tetraborate decahydrate in deuterium oxide in a NMR tube. Time was recorded when the polymer had dissolved completely. ^{1}H NMR spectra (400 MHz) were recorded with 32 scans and a relaxation delay of 1 s at T = 294 K on a daily basis. All spectra were processed (Fourier transformation, phase correction, baseline correction) and referenced to the solvent signal. All signals were integrated in the same limits and normalized to the singlet of the methoxy group of mPEG at 3.36 ppm.

2.2 Hydrolysis of **5** in phosphate buffer (pD = 8.4)

5 (42.0 mg, 20 µmol) was dissolved in 600 µL of a deuterated phosphate buffer (18.6 mg (137 µmol) KH_2PO_4 and 150.1 mg (862 µmol) K_2HPO_4 dissolved in D_2O (10.0 mL)) in a NMR tube. Time was recorded when the polymer had dissolved completely. ^{1}H NMR spectra (400 MHz) were recorded with 32 scans and a relaxation delay of 10 s at T = 294 K on a daily basis. All signals were integrated in the same limits and normalized to the singlet of the methoxy group of mPEG at 3.36 ppm.

2.3 Hydrolysis of **5** in borate buffer with DMSO

5 (30.0 mg, 14 µmol) was dissolved in 600 µl of a 7:3 mixture of a 0.1 M deuterated borate buffer and DMSO-d_6 in a NMR tube. Time was recorded when the polymer had dissolved completely. ^{1}H NMR Spectra (400 MHz) were recorded with 32 scans and a relaxation delay of 1 s at T = 294 K on a daily basis. All spectra were processed (Fourier transformation, phase

correction, baseline correction) and referenced to the solvent signal (DMSO). All signals were integrated in the same limits and normalized to the singlet of the methoxy group of mPEG at 3.36 ppm.

2.4 Hydrolysis of **5** in phosphate buffer with DMSO

5 (42.0 mg, 20 µmol) was dissolved in 600 µl of a 7:3 mixture of deuterated phosphate buffer (18.6 mg (137 µmol) KH_2PO_4 and 150.1 mg (862 µmol) K_2HPO_4 dissolved in D_2O (10.0 mL)) and DMSO-d_6 in a NMR tube. Time was recorded when the polymer had dissolved completely. ^{1}H NMR spectra (400 MHz) were recorded with 32 scans and a relaxation delay of 10 s at T = 294 K on a daily basis. All signals were integrated in the same limits and normalized to the singlet of the methoxy group of mPEG at 3.36 ppm.

2.5 Reaction of **5** with Ac-Lys-OMe in borate buffer (pD = 9.6)

Ac-Lys-OMe (11.4 mg, 48 µmol) and **5** (50.0 mg, 24 µmol) were dissolved in 600 µL of a 0.1 M solution of sodium tetraborate decahydrate in deuterium oxide in a NMR tube. Time was recorded when both, substrate and polymer, had dissolved completely. After locking and shimming a ^{1}H NMR spectrum (400 MHz) was recorded with 8 scans and a relaxation delay of 1 s at T = 294 K every 30 min for 12 h. All spectra were processed (Fourier transformation, phase correction, baseline correction) and referenced to the solvent signal. All signals were integrated in the same limits and normalized to the singlet of the methoxy group of mPEG at 3.36 ppm. The reaction kinetics was followed by monitoring the resonance of the methyl group of the released ethanol at 1.16 ppm.

2.6 Reaction of **5** with Ac-Lys-OMe in borate buffer with DMSO

The polymer (40.0 mg) and Ac-Lys-OMe (either 1 or 2 equivalents) were dissolved 600 µl of a 7:3 mixture of a 0.1 M deuterated borate buffer and DMSO-d_6 in a NMR tube. Time was recorded when both, substrate and polymer, had dissolved completely. After locking and shimming a ^{1}H NMR spectrum (400 MHz) was recorded with 8 scans and a relaxation delay of 1 s at T = 294 K every 2 min for 1 h. All spectra were processed (Fourier transformation, phase

correction, baseline correction) and referenced to the solvent signal (DMSO). All signals were integrated in the same limits and normalized to the singlet of the methoxy group of mPEG at 3.36 ppm. The reaction kinetics was followed by monitoring the resonance of the methyl group of the released ethanol at 1.16 ppm.

2.7 Reaction of **5** with Ts-Arg-OMe in borate buffer with DMSO

Ts-Arg-OMe (18.0 mg, 48 µmol) and **5** (50.0 mg, 24 µmol) were dissolved 600 µl of a 7:3 mixture of a 0.1 M deuterated borate buffer and DMSO-d_6 in a NMR tube. Time was recorded when both, substrate and polymer, had dissolved completely. After locking and shimming a ^{1}H NMR spectrum (400 MHz) was recorded with 8 scans and a relaxation delay of 1 s at $T = 294$ K every 5 min for 2.5 h. All spectra were processed (Fourier transformation, phase correction, baseline correction) and referenced to the solvent signal (DMSO). All signals were integrated in the same limits and normalized to the singlet of the methoxy group of mPEG at 3.44 ppm. The reaction kinetics was followed by monitoring the resonance of the methyl group of the released ethanol at 1.24 ppm.

2.8 Reaction of **5** with Boc-His-OMe in borate buffer with DMSO

Boc-His-OMe (12.8 mg, 48 µmol) and **5** (50.0 mg, 24 µmol) were dissolved 600 µl of a 7:3 mixture of a 0.1 M deuterated borate buffer and DMSO-d_6 in a NMR tube. Time was recorded when both, substrate and polymer, had dissolved completely. After locking and shimming a ^{1}H NMR spectrum (400 MHz) was recorded with 8 scans and a relaxation delay of 1 s at $T = 294$ K every minute for 30 min. Afterwards, 24 further spectra were recorded every 30 min. All spectra were processed (Fourier transformation, phase correction, baseline correction) and referenced to the solvent signal (DMSO). All signals were integrated in the same limits and normalized to the singlet of the methoxy group of mPEG at 3.41 ppm. The reaction kinetics was followed by monitoring the resonance of the methyl group of the released ethanol at 1.23 ppm.

2.9 Reaction of **5** with H-Lys-OMe in borate buffer with DMSO

5 (40.0 mg, 19 µmol) were dissolved in 600 µl of a 7:3 mixture of a 0.1 M deuterated borate buffer and DMSO-d_6 in a NMR tube. After locking and shimming a ^{1}H NMR spectrum (700 MHz) was recorded with 32 scans and a relaxation delay of 10 s at T = 294 K every 1.69 min for 3.4 h. All spectra were processed (Fourier transformation, phase correction, baseline correction) and referenced to the solvent signal (DMSO). All signals were integrated in the same limits.

2.10 Reaction of **5** with H-Lys-OMe in phoshate buffer with DMSO

5 (40.0 mg, 19 µmol) were dissolved in 600 µl of a 7:3 mixture of a deuterated phosphate buffer (18.6 mg (137 µmol) KH_2PO_4 and 150.1 mg (862 µmol) K_2HPO_4 dissolved in D_2O (10.0 mL)) and DMSO-d_6 in a NMR tube. After locking and shimming a ^{1}H NMR spectrum (700 MHz) was recorded with 32 scans and a relaxation delay of 10 s at T = 294 K every 1.69 min for 28 h. 63 h and 139 h after the reaction was started two more spectra of the sample were recorded. All spectra shown were processed (Fourier transformation, phase correction, baseline correction) and referenced to the solvent signal (DMSO). All signals were integrated in the same limits.

2.11 Reaction of **5** with H-Lys-OMe in borate buffer with DMSO, T = 283 K

5 (35.2 mg, 16.8 µmol) were dissolved in 530 µl of a 7:3 mixture of a 0.1 M deuterated borate buffer and DMSO-d_6 in a NMR tube. After locking and shimming a ^{1}H NMR spectrum (700 MHz) was recorded with 32 scans and a relaxation delay of 10 s at T = 283 K every 1.69 min for 12 h at 283 K. All spectra shown were processed (Fourier transformation, phase correction, baseline correction) and referenced to the solvent signal (DMSO). All signals were integrated in the same limits.

3. ^{1}H NMR spectra

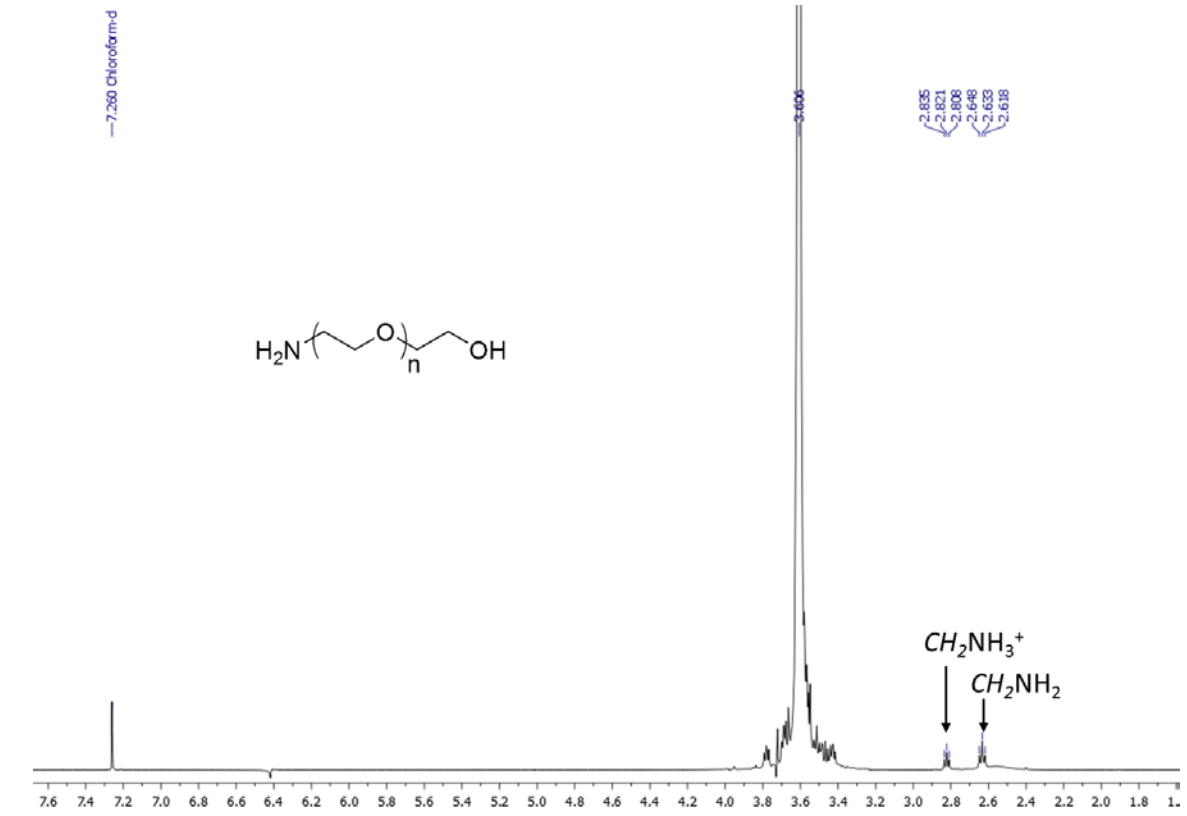

Figure S1. ^{1}H NMR spectrum (400 MHz) of **2** (with n = 53, 2.4 kDa) in DMSO-d_6 at T = 294 K.

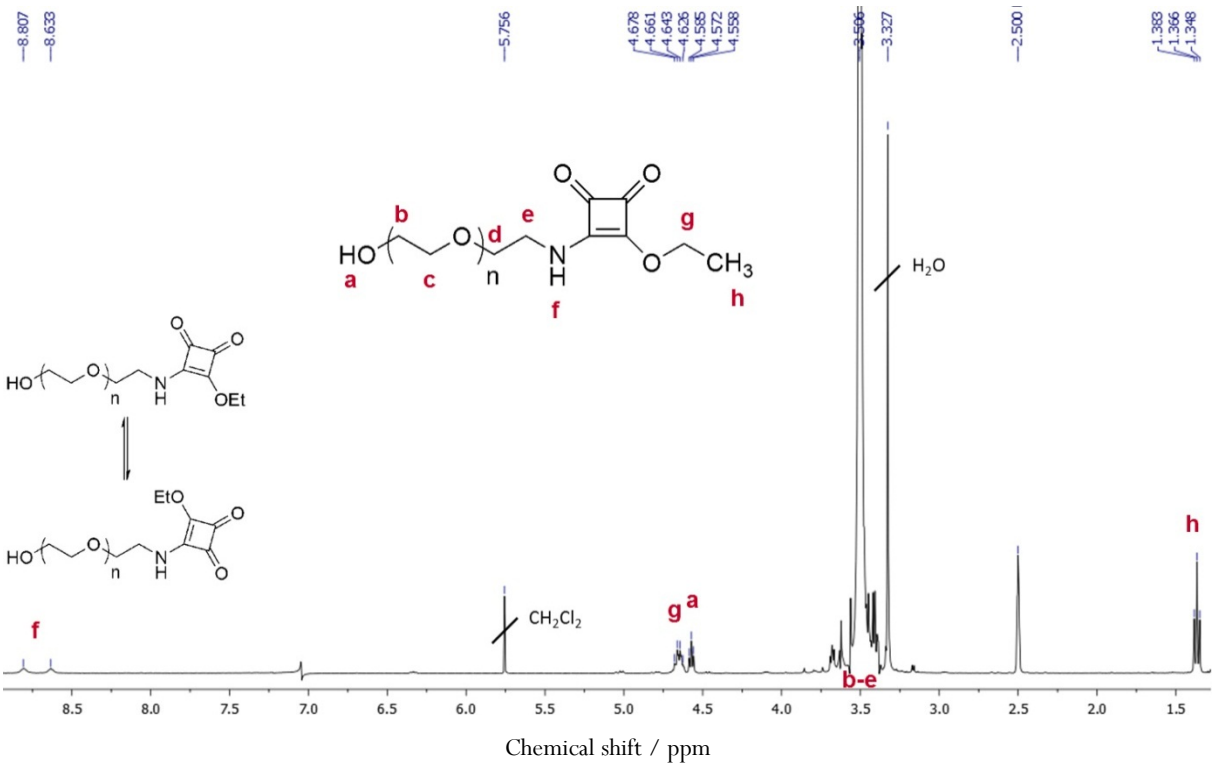

Figure S2. ^{1}H NMR spectrum (400 MHz) of **4** (with n = 53, 2.5 kDa) in DMSO-d_6 at T = 294 K.

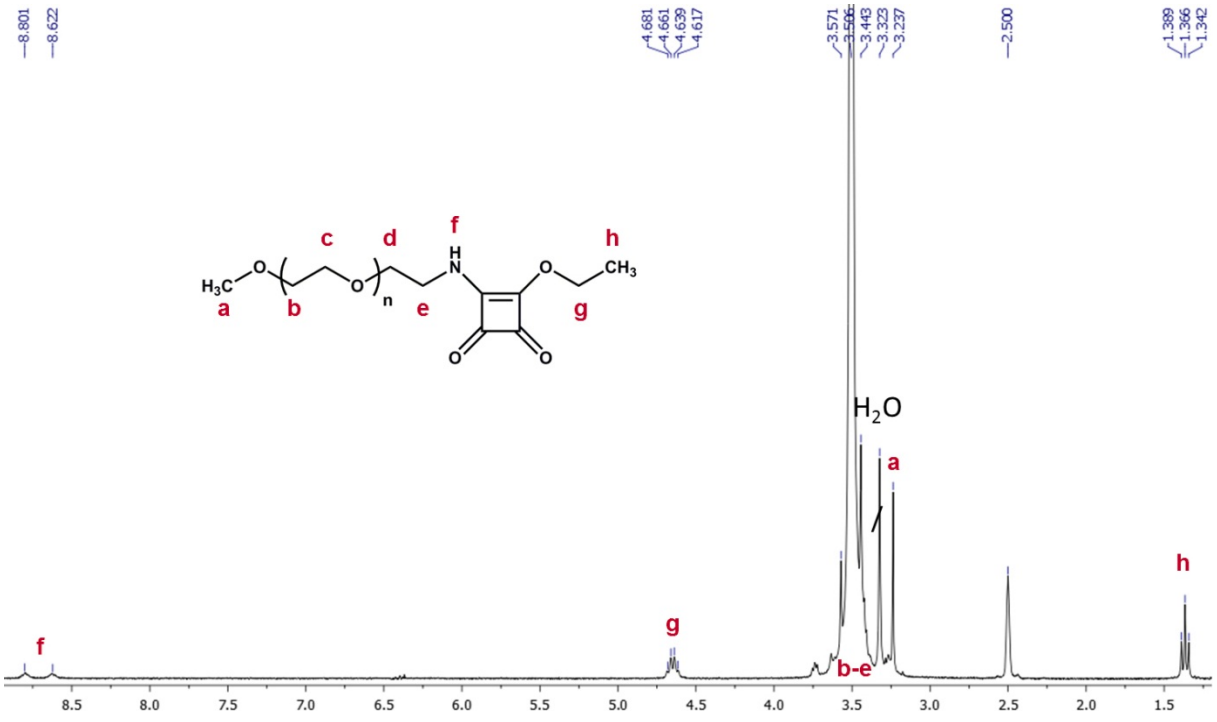

Figure S3. ^{1}H NMR spectrum (400 MHz) of **5** (with n = 44, 2.1 kDa) in DMSO-d_6 at T = 294 K.

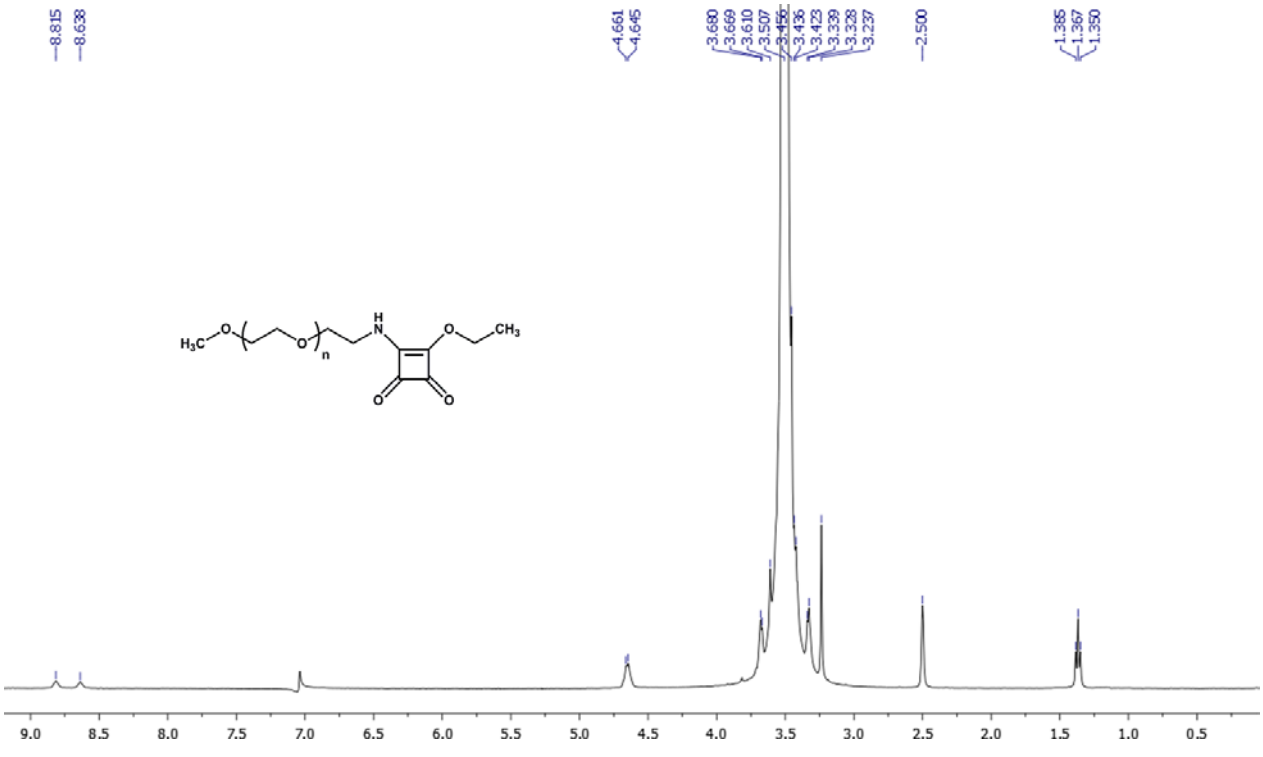

Figure S4. ^{1}H NMR spectrum (400 MHz) of **5** (with n = 113, 5.1 kDa) in DMSO-d_6 at T = 294 K.

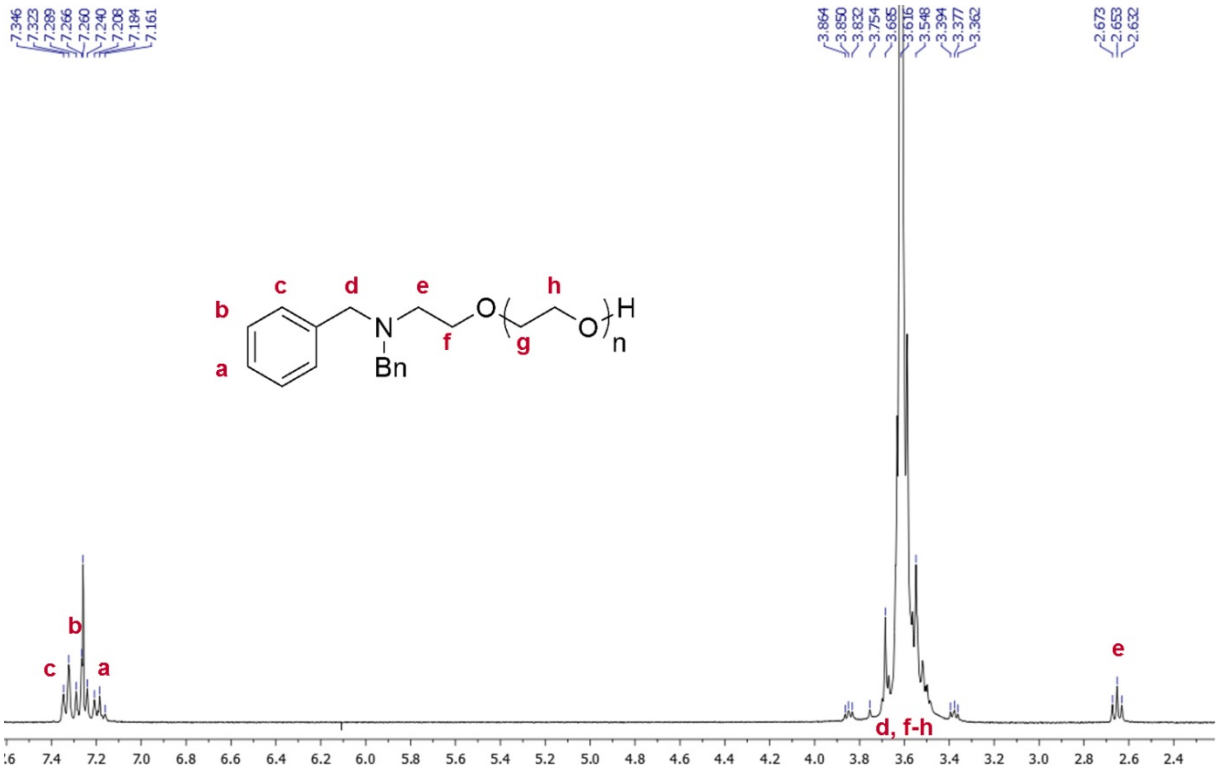

Figure S5. ^{1}H NMR spectrum (400 MHz) of **7** (n = 53, 2.6 kDa) in DMSO-d_6 at T = 294 K.

4. MALDI-ToF mass spectra

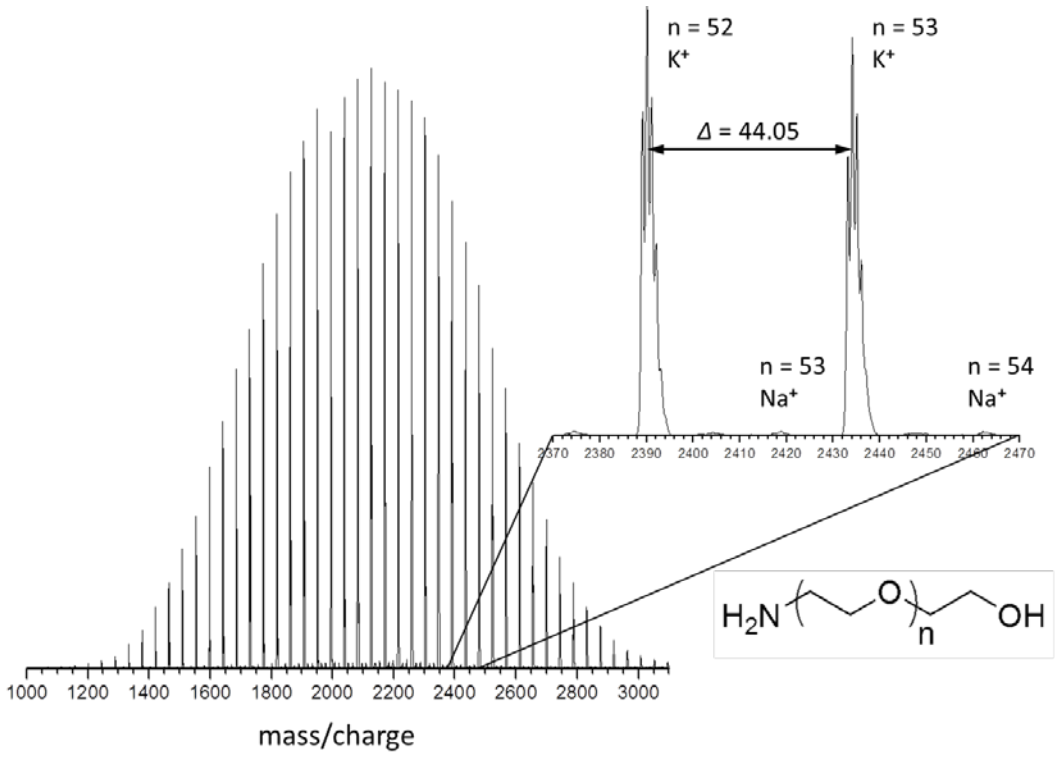

Figure S6. MALDI-ToF mass spectrum of **2** (2.4 kDa). Matrix: CHCA, Salt: KTFA.

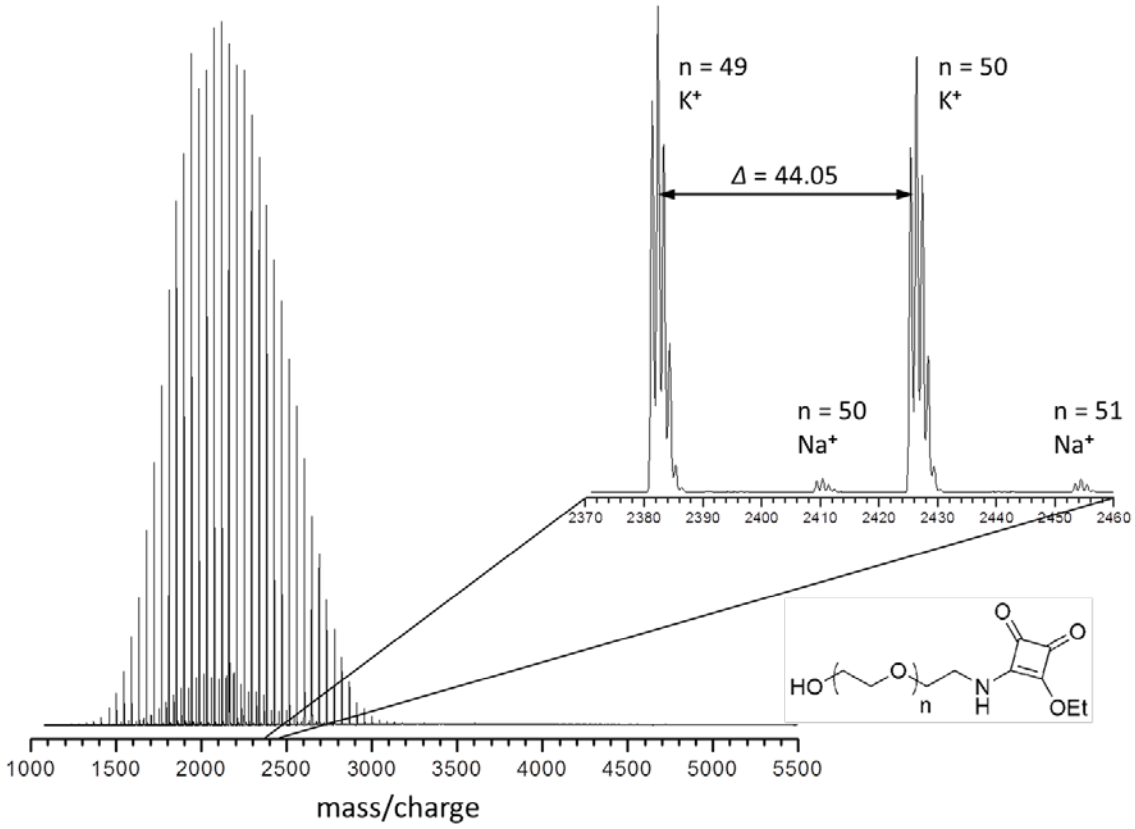

Figure S7. MALDI-ToF mass spectrum of **4** (2.5 kDa). Matrix: CHCA, Salt: KTFA.

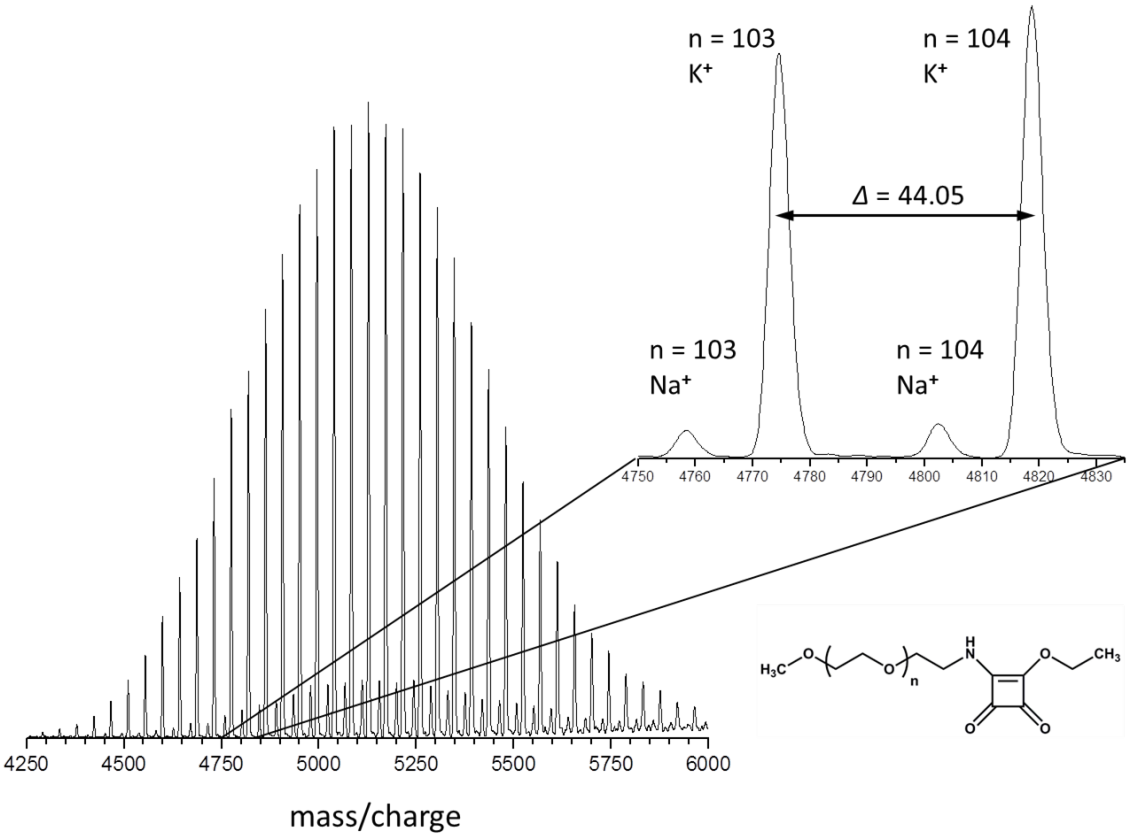

Figure S8. MALDI-ToF mass spectrum of **5** (5.1 kDa). Matrix: CHCA, Salt: KTFA.

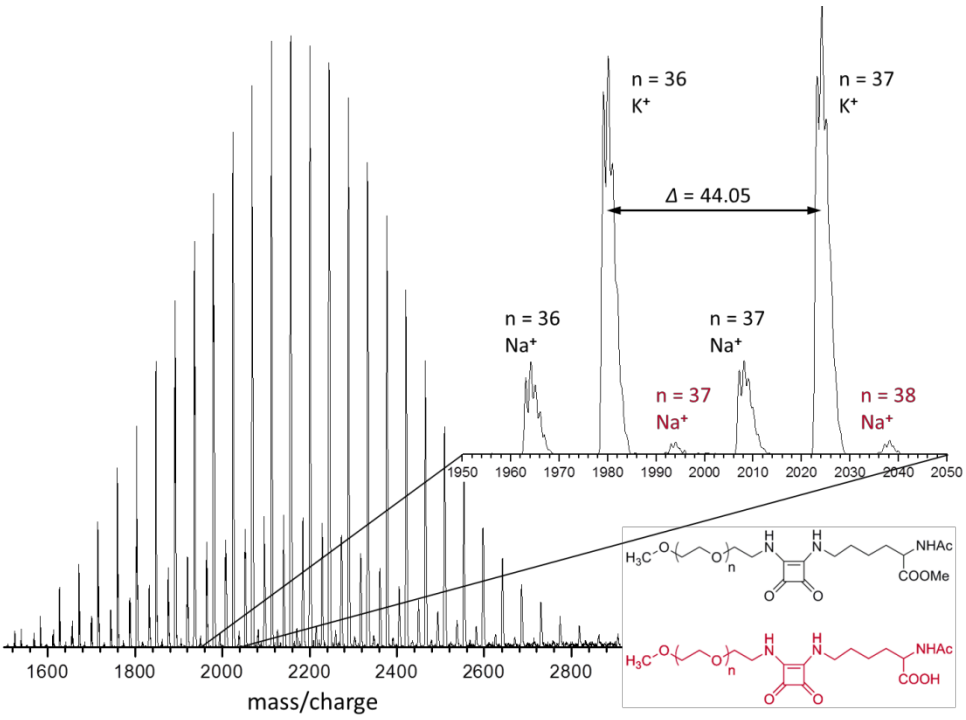

Figure S9. MALDI-ToF mass spectrum of **5** (2.1 kDa) after reaction with 2 eq. of Ac-Lys-OMe and Z-Ser-OMe, respactively. Matrix: CHCA, Salt: KTFA. *Note: A very small amount of species with hydrolyzed methyl ester can be detected in some cases (red).*

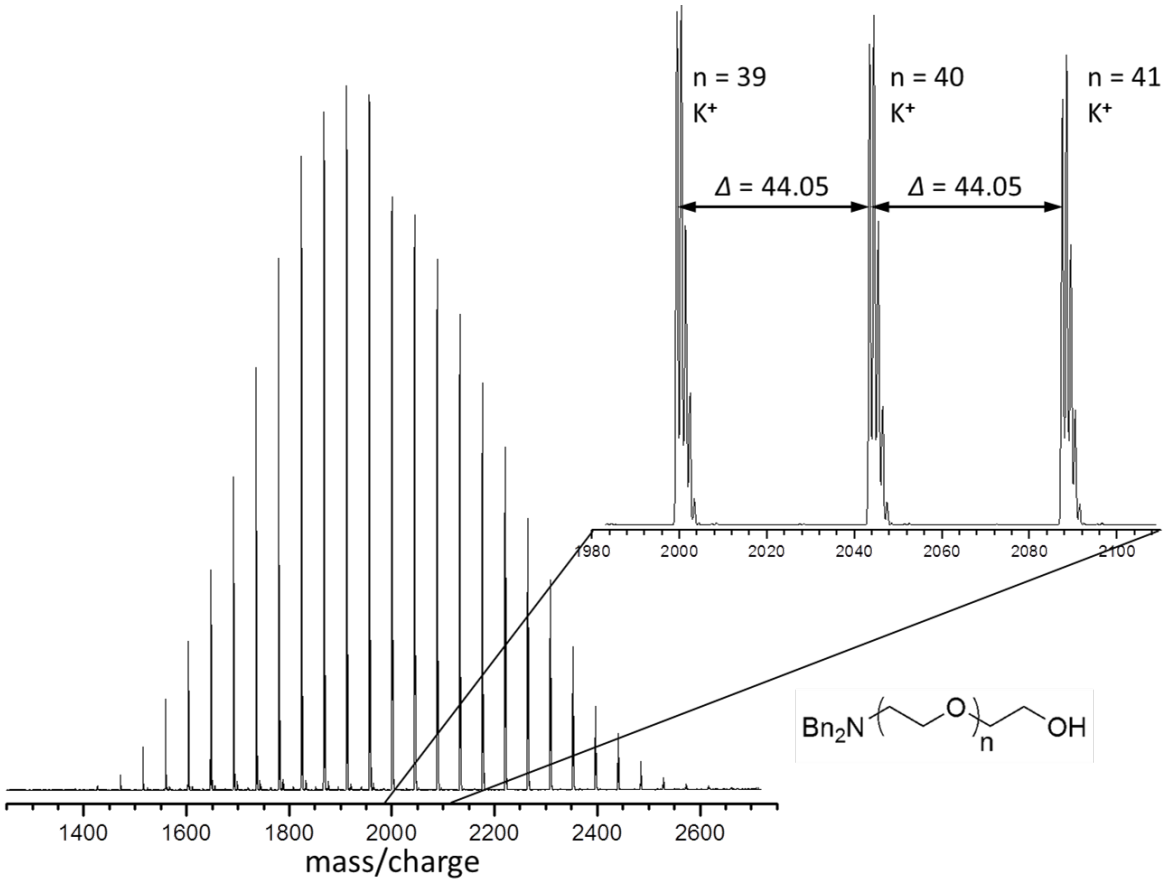

Figure S10. MALDI-ToF mass spectrum of **7** (2.6 kDa). Matrix: CHCA, Salt: KTFA.

5. IR spectra

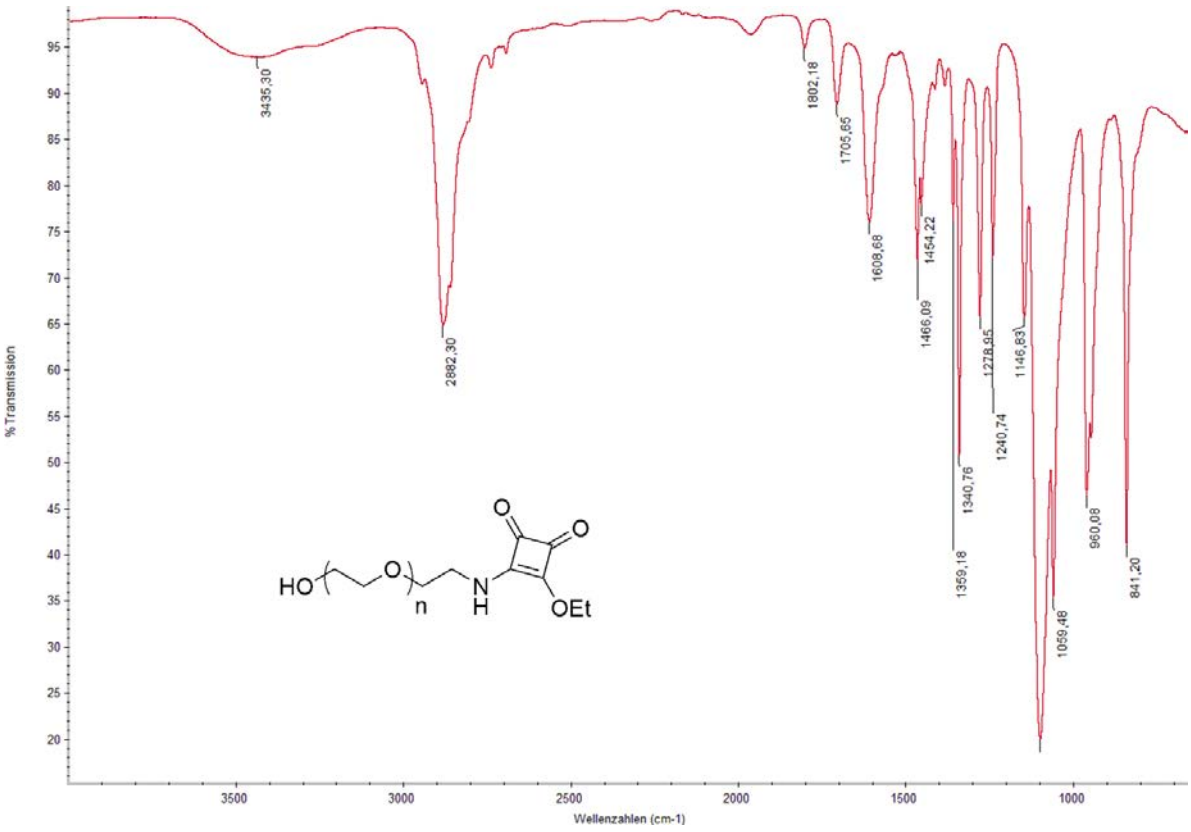

Figure S11. IR spectrum of **4** (with n = 53, 2.5 kDa).

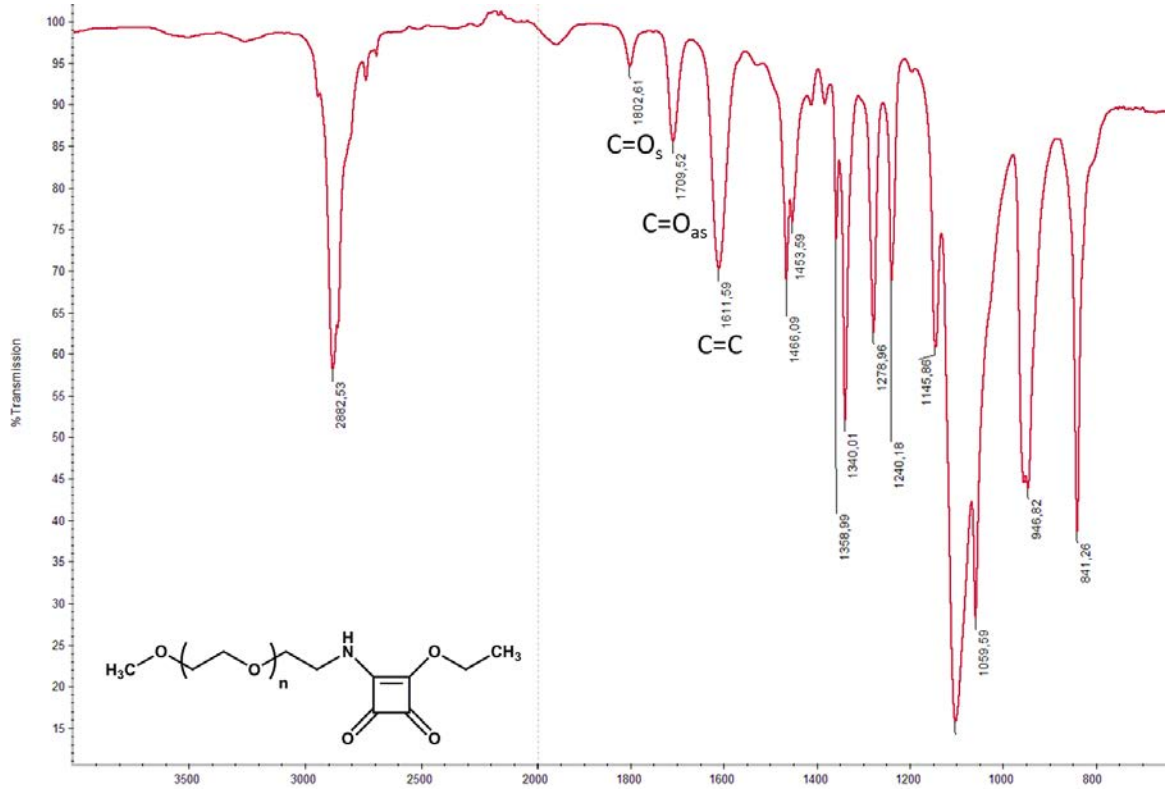

Figure S12. IR spectrum of **5** (with n = 44, 2.1 kDa).

6. SEC elugrams

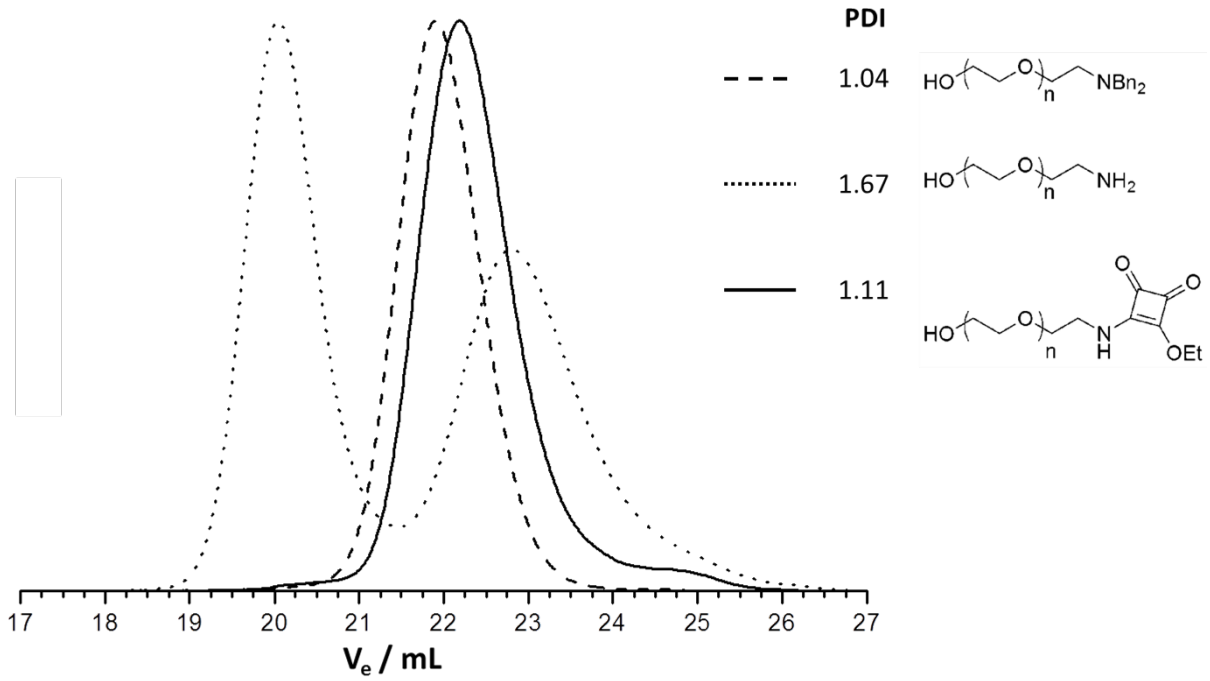

Figure S13. SEC elugrams of **2** (2.5 kDa) and its precursors (from SEC in DMF, RI detector signal). *Note: The amino PEGs often revealed a broadening of the mass distribution in the SEC analysis (on our system) leading to an increase in the apparent M_w/M_n ratio (polydispersity index, PDI). Sometimes, even bimodal SEC traces were observed. This effect was attributed to interactions of the amino moiety with the poly(HEMA) columns of the chromatograph. Upon derivatization the PDIs decreased significantly, confirming that the enhanced PDI-values were an artifact of the SEC-method.*

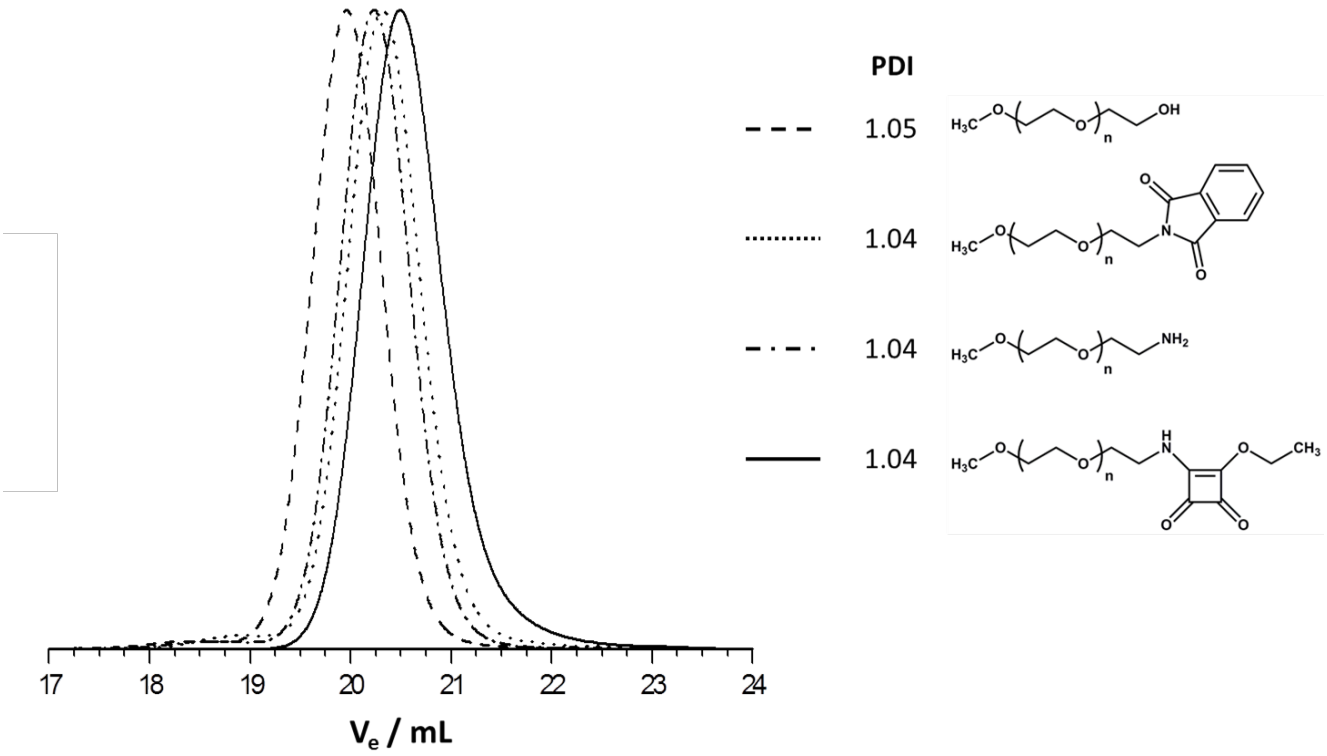

Figure S14. SEC elugrams of **4** (5.1 kDa) and its precursors, RI detector, eluent: DMF.

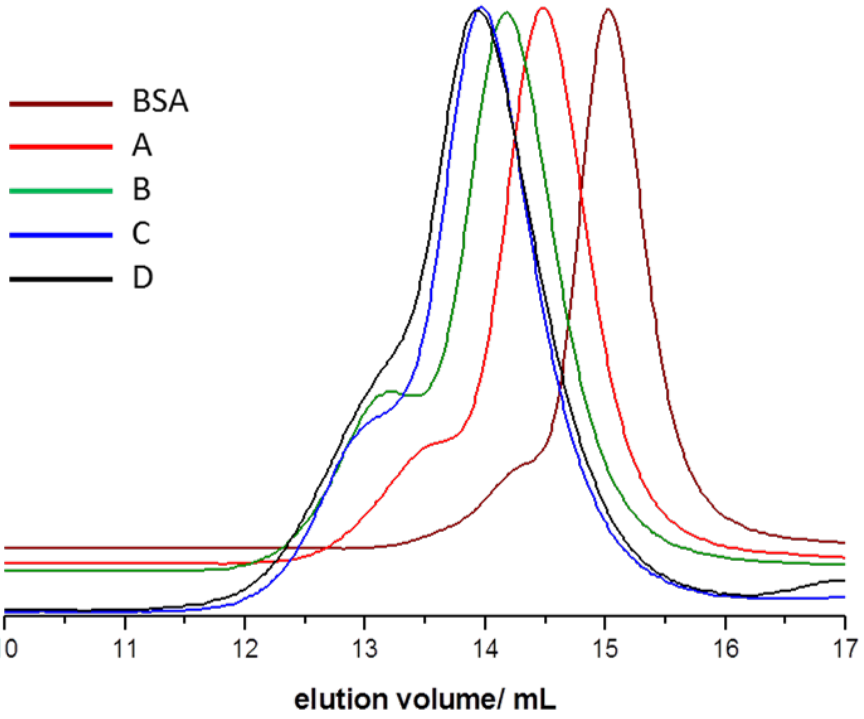

Figure S15. SEC elugrams of BSA and the conjugates **A – D**, RI detector, eluent: aqueous PBS 0.1 M, pH = 6.5 with 10% MeOH. *Note: The high molecular weight "shoulder" indicates the presence of BSA-dimers in the commercial batch.*

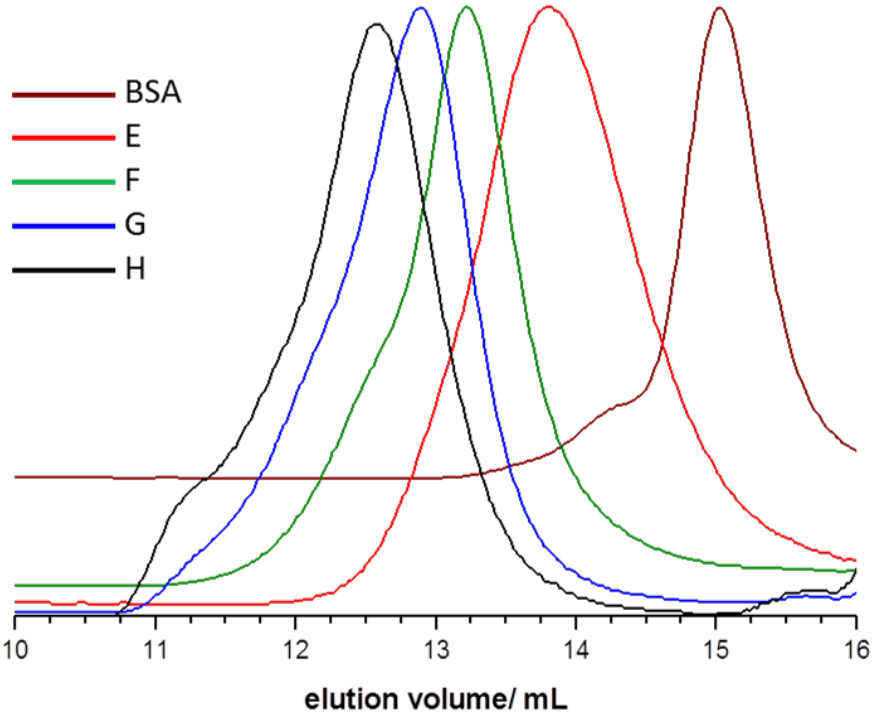

Figure S16. SEC elugrams of BSA and the conjugates **E – H**, RI detector, eluent: Aqueous PBS 0.1 M, pH = 6.5 with 10% MeOH.

7. Reaction kinetics monitored by ^{1}H NMR spectroscopy

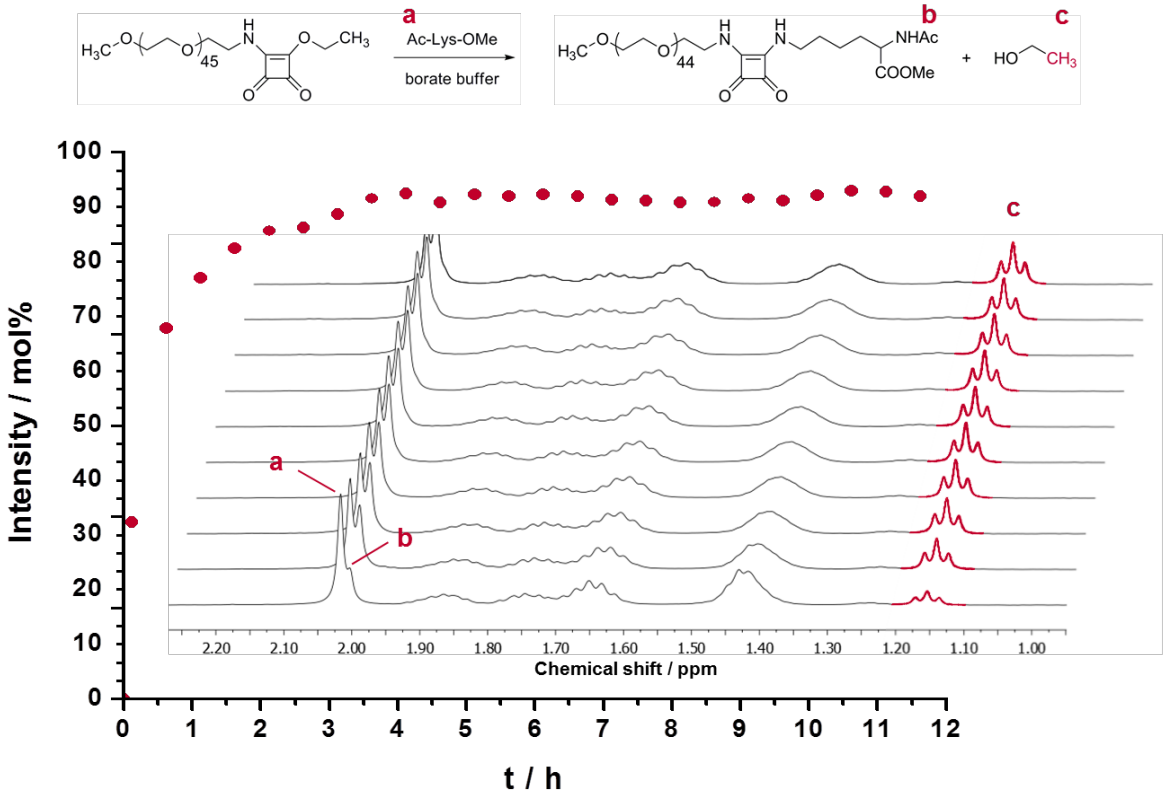

Figure S17. Reaction of SEA-mPEG (2.1 kDa) with Ac-Lys-OMe in deuterated 0.1 M borate buffer. The reaction was followed by ^{1}H NMR spectroscopy (400 MHz) at $T = 294$ K. Methyl resonance intensity of released ethanol plotted vs. time, normalized to resonance of **a**. Monitored peak highlighted in ^{1}H NMR spectra (detail, last spectra omitted for clarity).

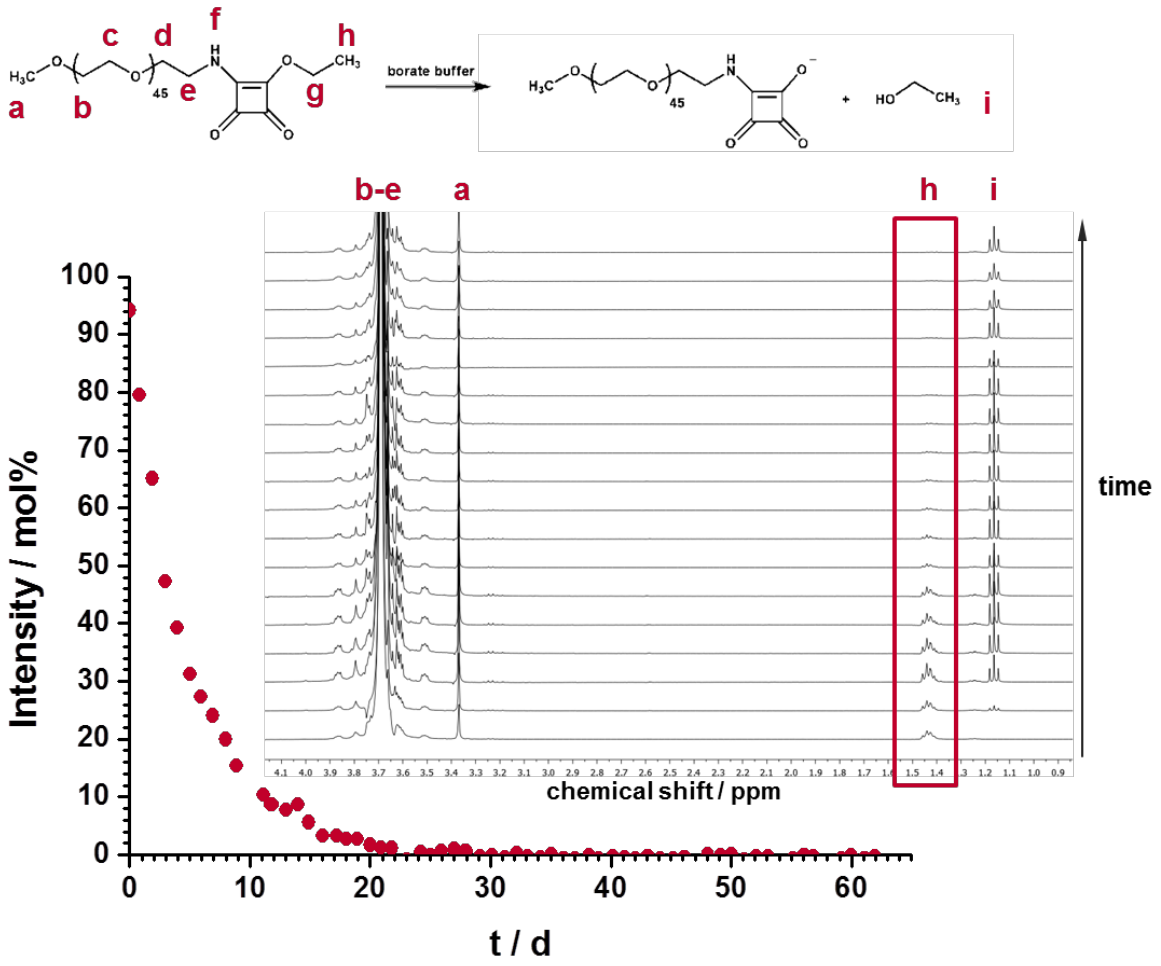

Figure S18. Hydrolysis of SEA-mPEG (2.1 kDa) in deuterated borate buffer (pD = 9.6). The reaction was followed by ^{1}H NMR spectroscopy (400 MHz) at T = 294 K. Resonance intensity of **h** plotted vs. time and normalized to resonance of **a**.

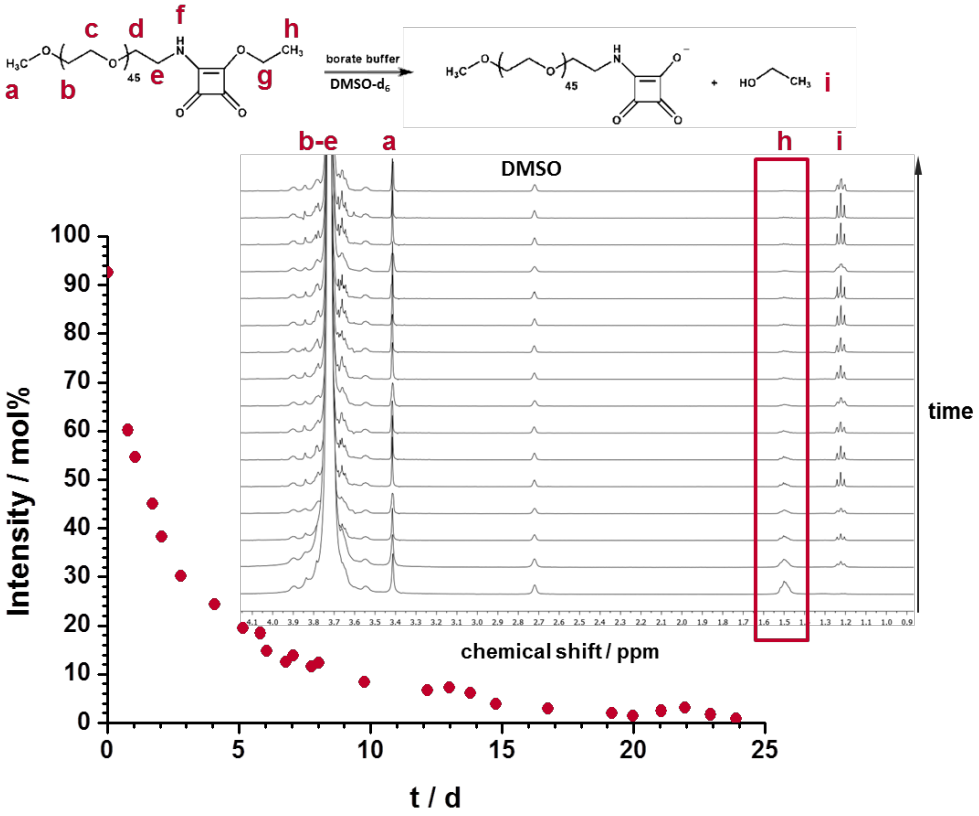

Figure S19. Hydrolysis of SEA-mPEG (2.1 kDa) in deuterated borate buffer (pD = 9.6)/DMSO-d_6 (7/3). The reaction was followed by ^{1}H NMR spectroscopy (400 MHz) at T = 294 K. Resonance intensity of **h** plotted against time, normalized to resonance of **a**.

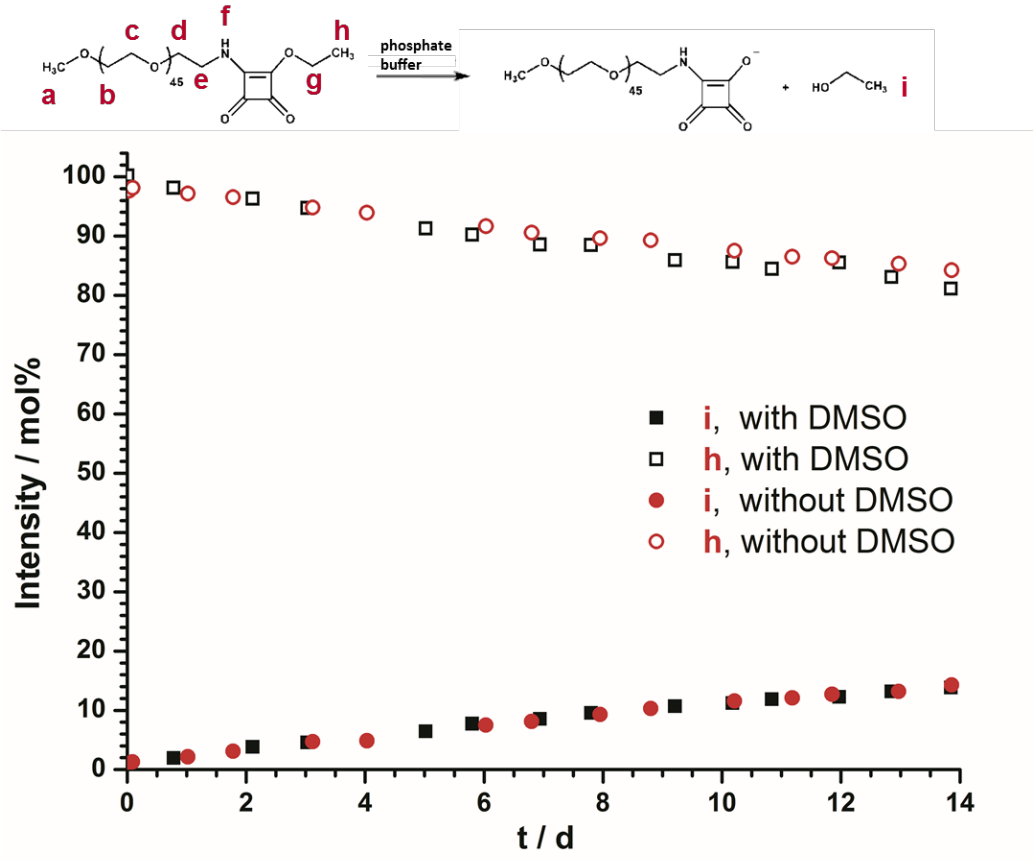

Figure S20. Hydrolysis of SEA-mPEG (2.1 kDa) in deuterated phosphate buffer (pD = 8.4) (red circles) and deuterated phosphate buffer (pD = 8.4)/DMSO-d_6 (7/3) (black squares). The reaction was followed by ^{1}H NMR spectroscopy (400 MHz) and spectra recorded at T = 294 K. Resonance intensities of **h** and i plotted against time, normalized to resonance of **a**.

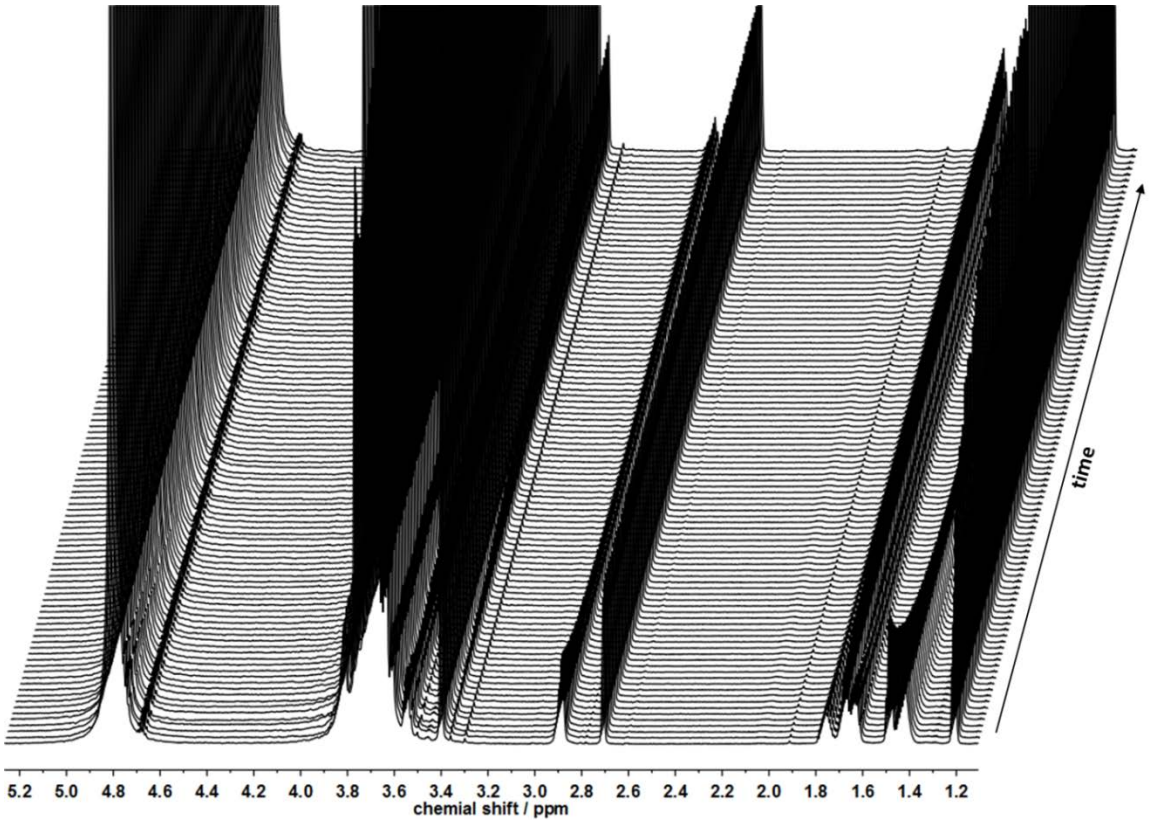

Figure S21. ^{1}H NMR spectra (700 MHz) of the reaction of SEA-mPEG (2.1k Da) with 1 eq. of L-lysine methyl ester in borate buffer (pH = 9.6)/DMSO (7/3) at T = 294 K.

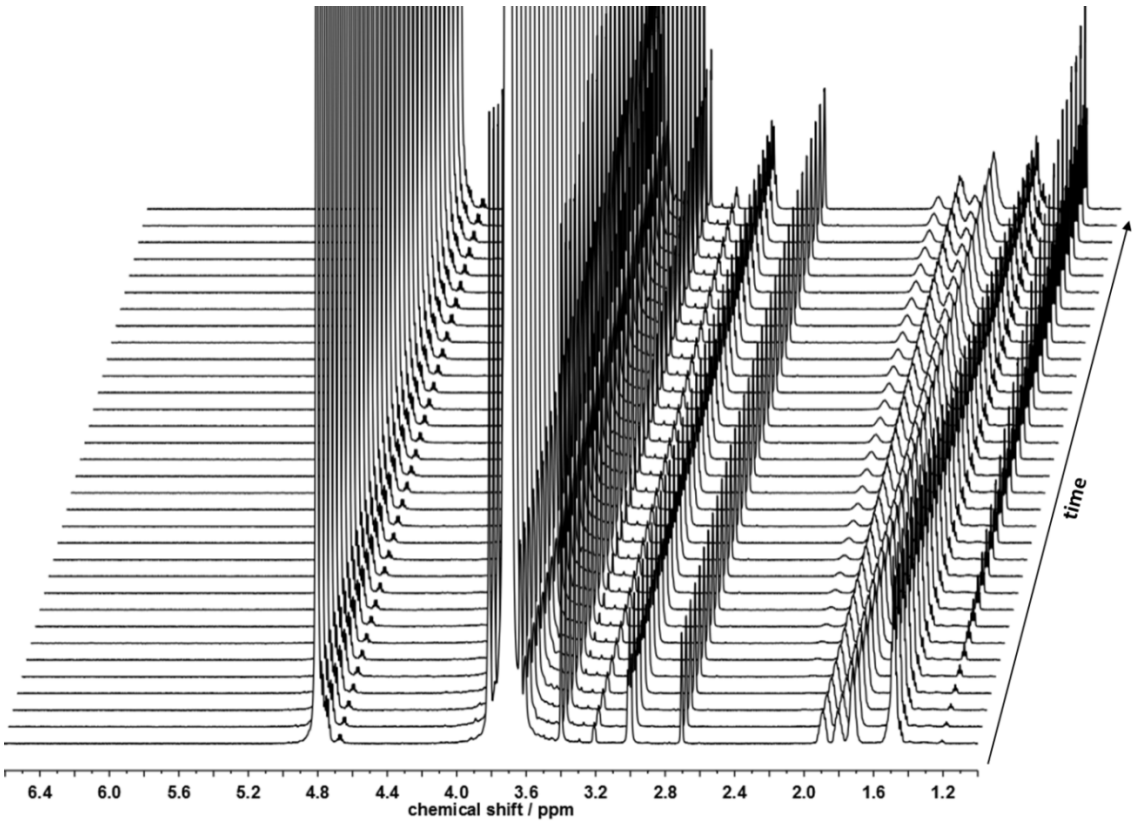

Figure S22. ^{1}H NMR spectra (700 MHz) of the reaction of SEA-mPEG (2.1k Da) with 1 eq. of L-lysine methyl ester in phosphate buffer (pH = 8.4)/DMSO (7/3) at T = 294 K (first 28 h).

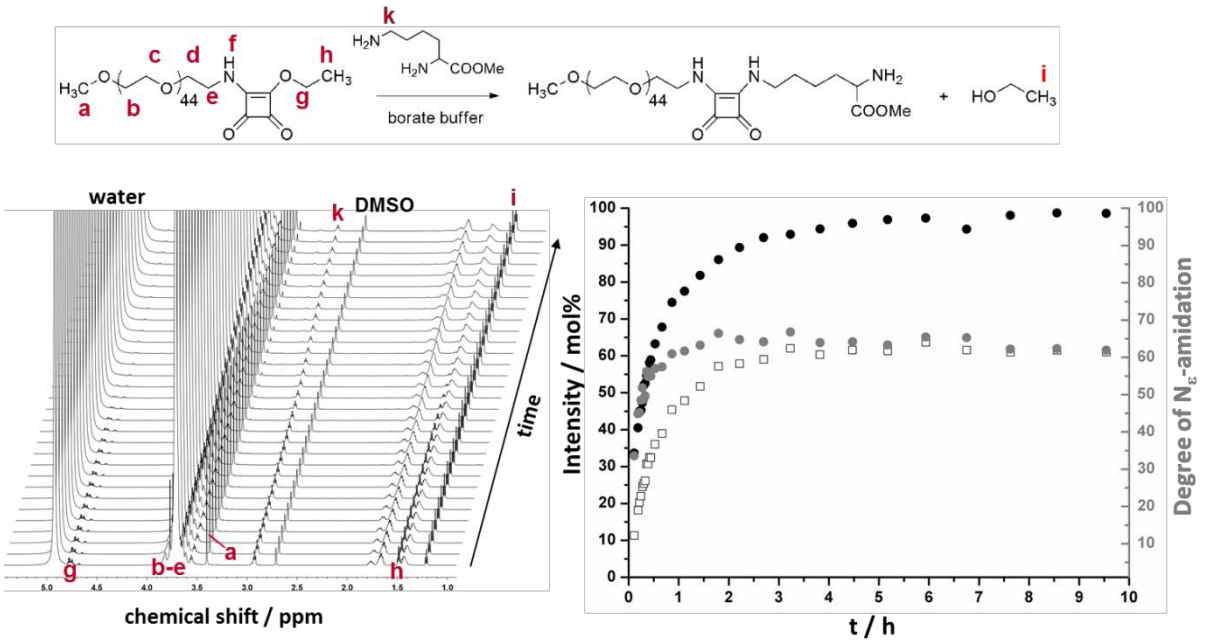

Figure S23. Reaction of SEA-mPEG (2.1k Da) with 1 eq. of l-lysine methyl ester in borate buffer (pH = 9.6)/DMSO (7/3) at $T = 283$ K. Left: ^{1}H NMR spectra (700 MHz). Right: Normalized signal intensities (black, left scale. Full circles: EtOH. Open squares: N_α-amide) and the degree of N_α-amidation (grey, right scale) plotted against reaction time.

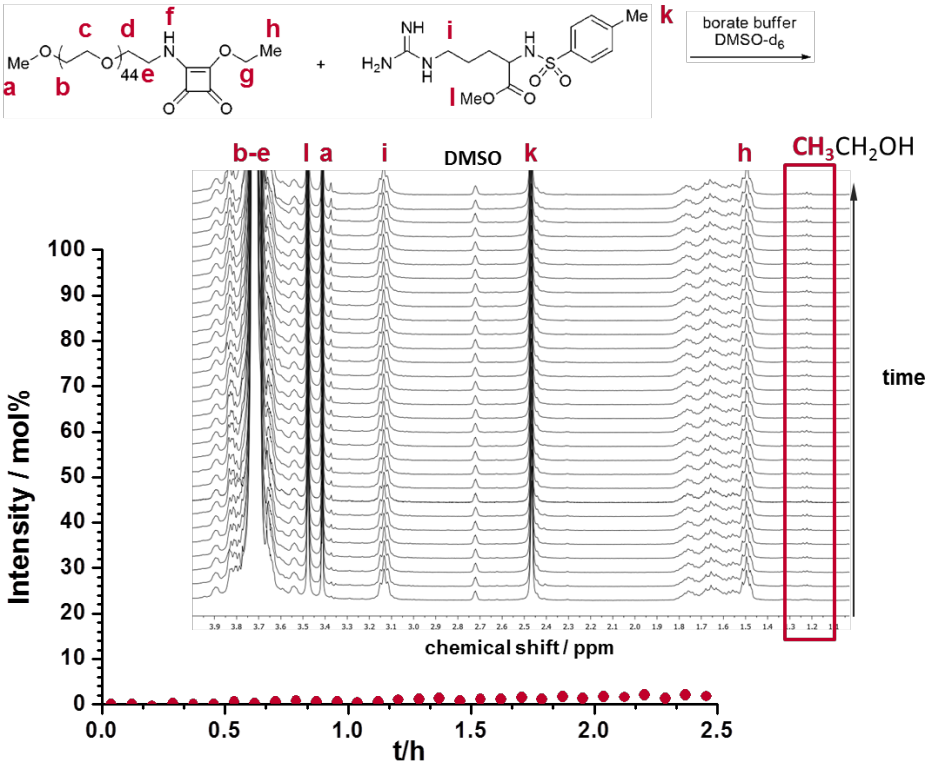

Figure S24. Reaction of SEA-mPEG (2.1 kDa) with Ts-Arg-OMe in deuterated borate buffer (pD = 9.6)/DMSO-d_6 (7/3). Methyl resonance intensity of released ethanol plotted against time, normalized to resonance of **a**.

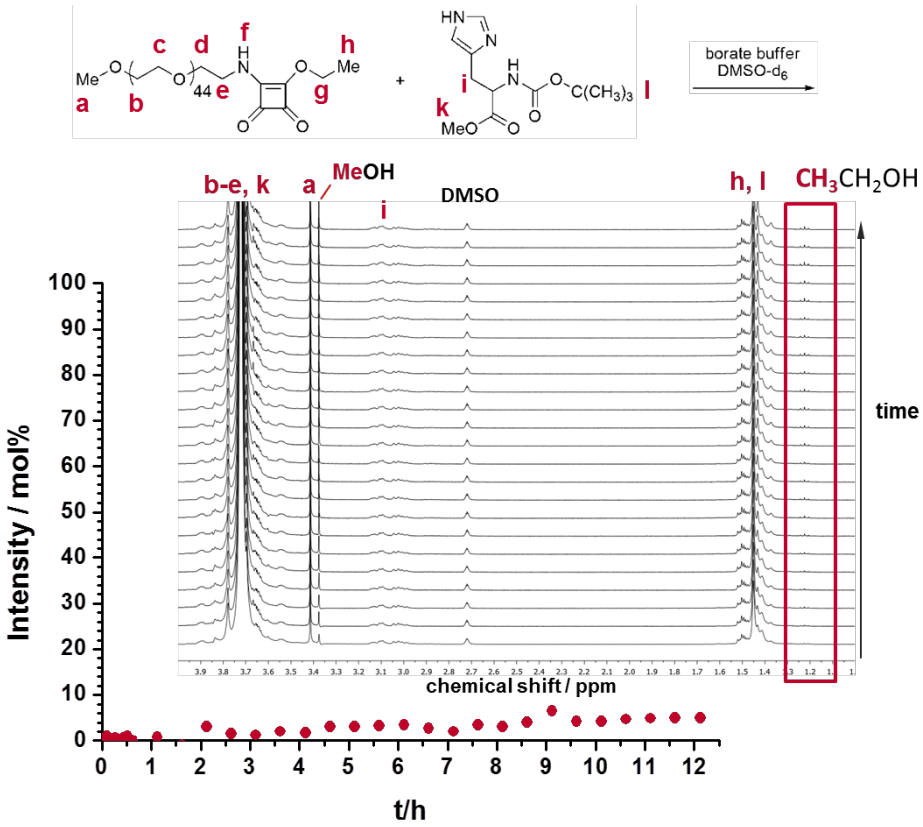

Figure S25. Reaction of SEA-mPEG (2.1 kDa) with Boc-His-OMe in deuterated borate buffer (pD = 9.6)/DMSO-d_6 (7/3). Methyl resonance intensity of released ethanol plotted against time, normalized to resonance of **a**. Note slow cleavage of methyl ester **k**.

8. 2D NMR spectra

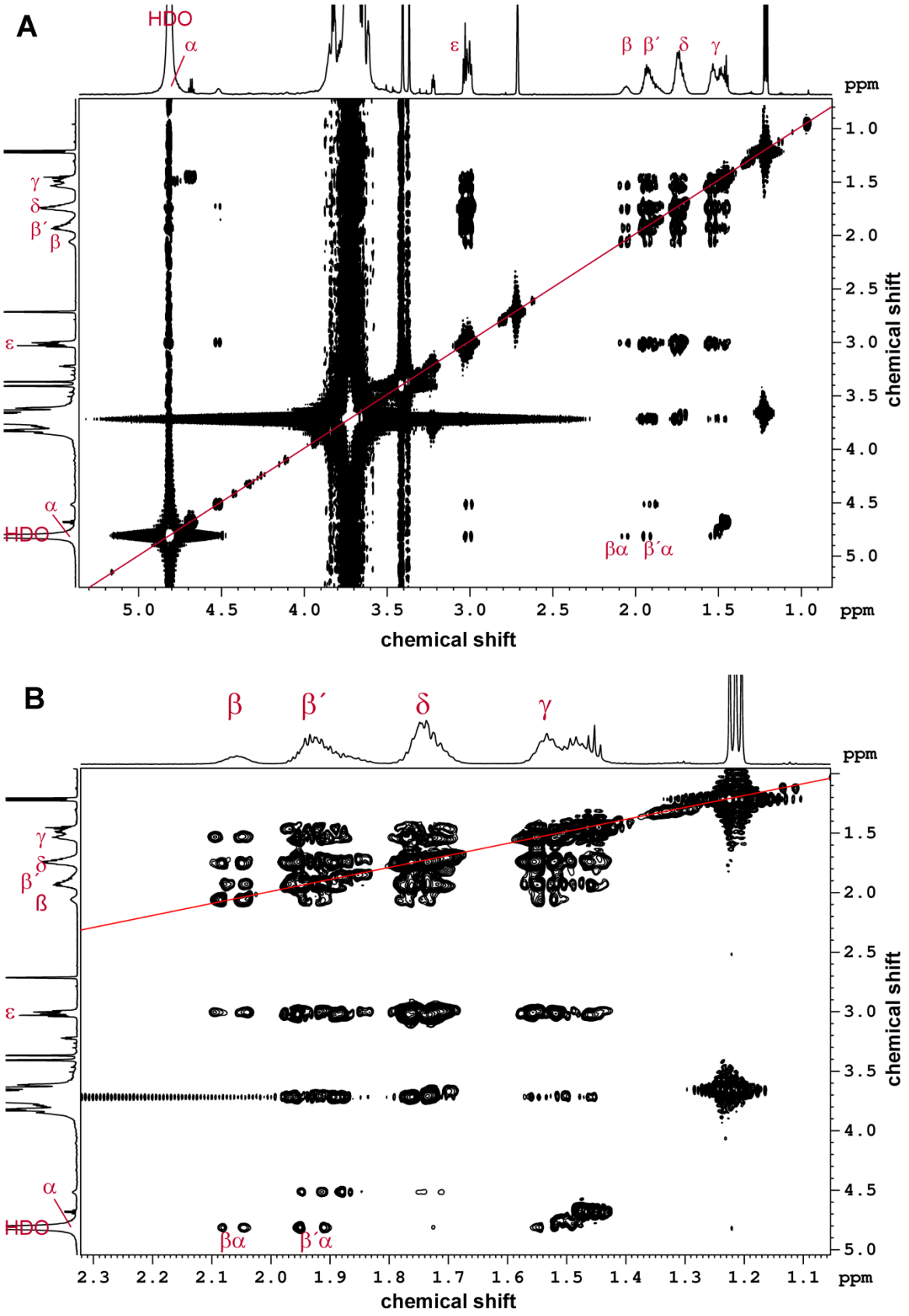

Figure S26. ^{1}H TOCSY spectrum (700 MHz) of reaction mixture of SEA-mPEG (2.1k Da) with 1 eq. of L-lysine methyl ester in phosphate buffer (pH = 8.4)/DMSO (7/3) at T = 294 K. **A**: Full spectrum. **B**: Detail.

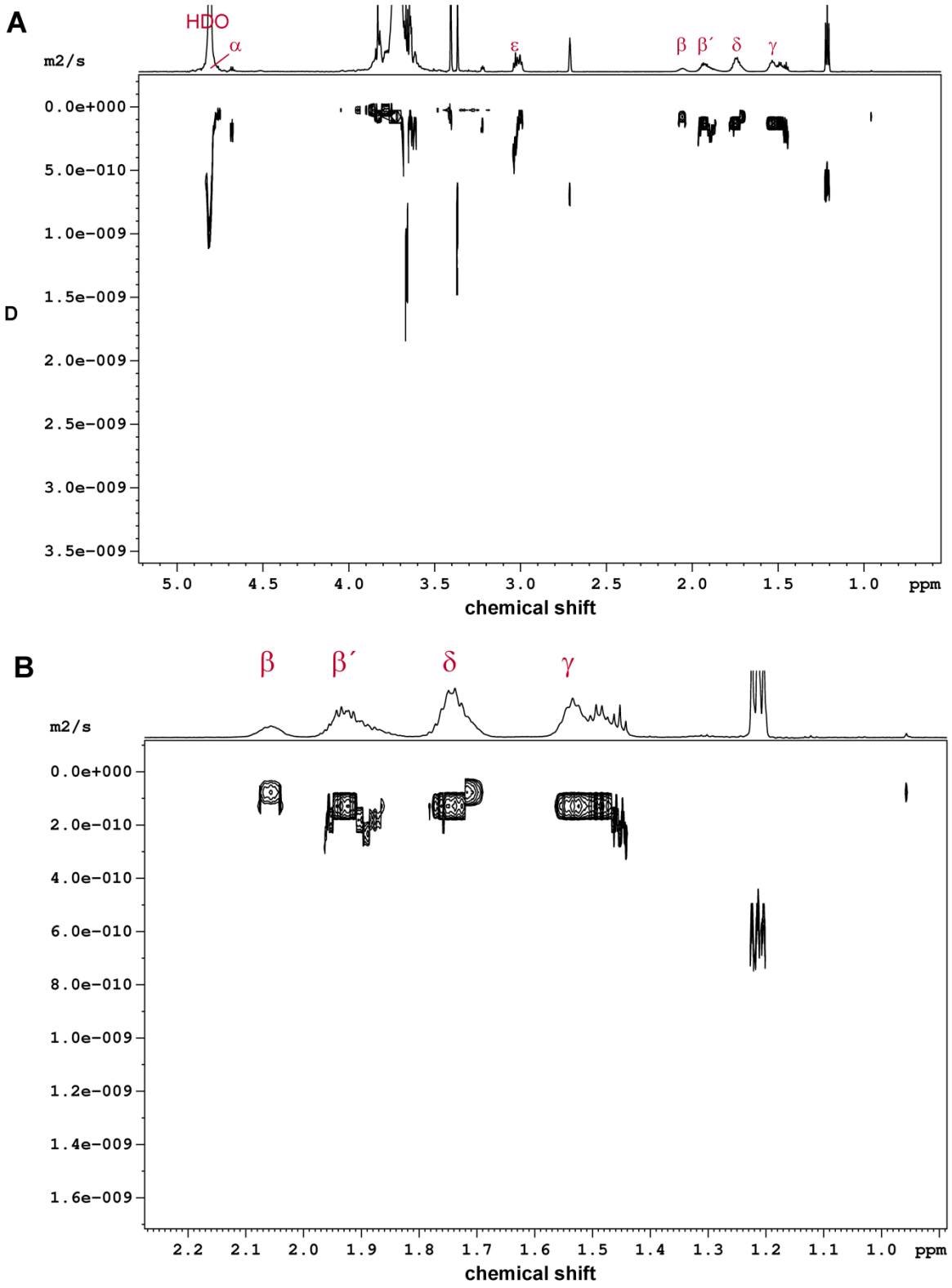

Figure S27. ^{1}H DOSY spectrum of the reaction mixture of SEA-mPEG (2.1k Da) with 1 eq. of L-lysine methyl ester in phosphate buffer (pH = 8.4)/DMSO (7/3) at T = 294 K recorded after 139 h. **A**: Full spectrum. **B**: Detail.

9. SDS PAGE

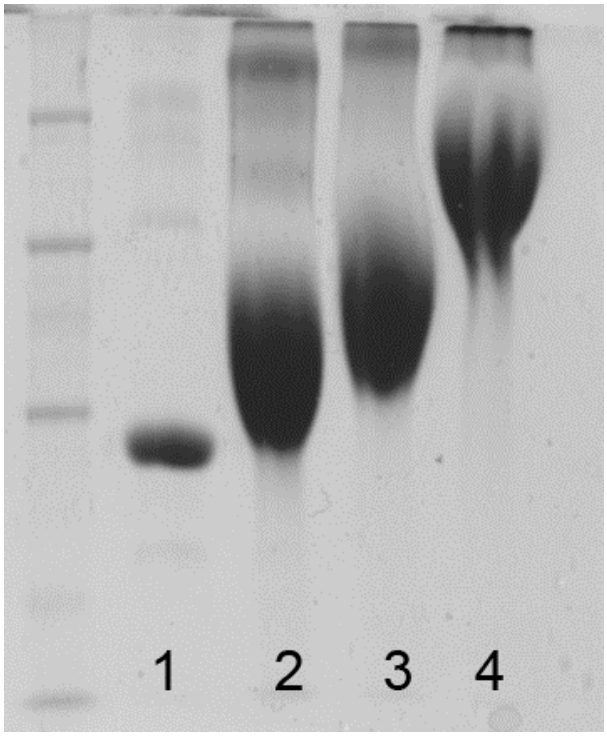

Figure S28. SDS-PAGE (8%) of BSA (lane 1) and BSA-polymer conjugates obtained by PEGylation with α-squaric acid ester amido ω-hydroxy-PEG (lanes 2-4; 10, 20, and 50 equivalents polymer added, respectively).

10. CD spectra

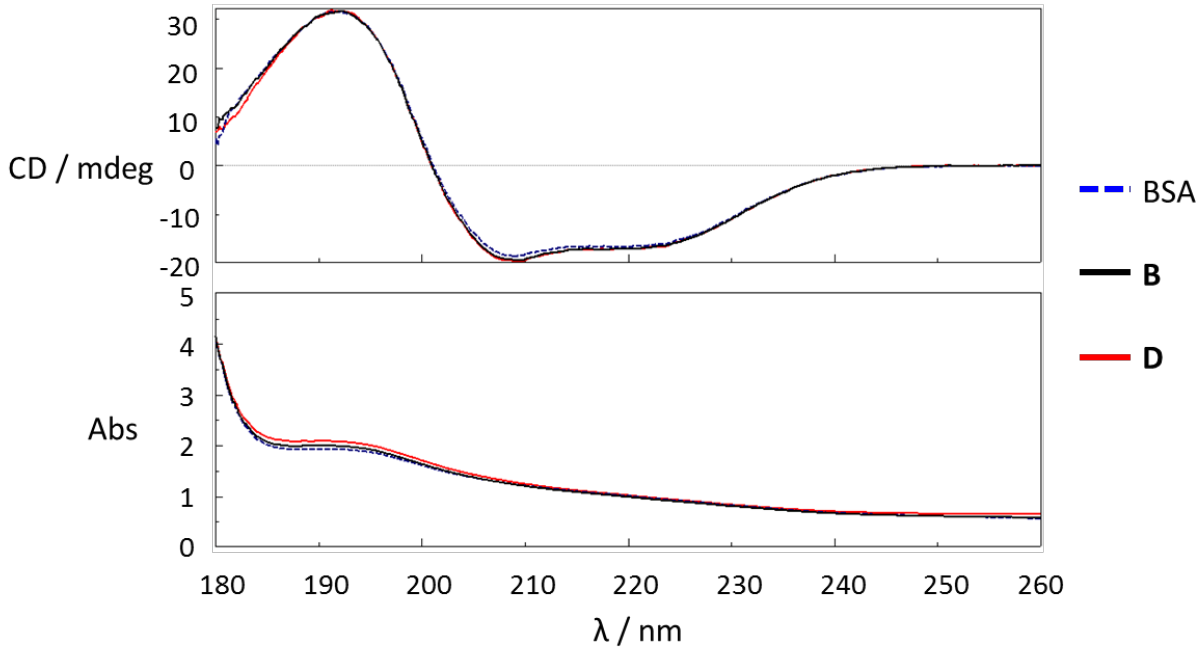

Figure S29. CD spectra of BSA and the conjugates **B** and **D**. Absorption spectra shown were recorded simultaneously.

11. References

[1] B. Obermeier, F. Wurm, H. Frey, *Macromolecules* **2010**, *43*, 2244.

2.2 Initial Studies on the Biocompatibility of Squaric Acid Coupled PEG/Protein Conjugates

Carsten Dingels,[1] Ronald E. Unger,[2] Holger Frey,[1] and C. James Kirkpatrick[2,]*

[1]Department of Organic Chemistry, Johannes Gutenberg-Universität Mainz, Duesbergweg 10–14, D-55099 Mainz (Germany)

[2]Institute of Pathology, Johannes Gutenberg-Universität Mainz, Langenbeckstraße 1, D-55101 Mainz (Germany)

The WST-1 assay and the CAM-EIA were carried out by Dr. R. E.Unger, REPAIR Lab, Institute of Pathology, Johannes Gutenberg-Universität Mainz. The data presented in the following represent preliminary results, since the studies were carried out with just one donor.

Motivation

For the intended application of the squaric acid-mediated PEGylation in the preparation of polymer therapeutics, the biocompatibility and non-immunogenicity of the resulting protein/PEG conjugates must be assured. In an initial study, cytotoxic effects of squaric acid-PEGyated bovine serum albumin (BSA) as a model conjugate on human endothelial cells were investigated as well as the expression of cell adhesion molecules involved in inflammation processes by the cells exposed to these conjugates. The knowledge of the influence of such potential polymer therapeutics on human endothelial cells is of particular interest, since the conjugates come in close contact with these in the circulatory system.

Results and Discussion

BSA was PEGylated with 50 equivalents (sample **C**) and 100 equivalents (sample **D**) of squaric acid ethyl ester amido mPEG (2.1 kDa) resulting in conjugates with 27 to 34 PEG chains per BSA. The samples were prepared in analogy to the previously described protocols for the

synthesis of BSA/PEG conjugates **C** and **D** (*vide supra*). To insure the production of sterile conjugates, minor alterations were made (*vide infra*). The dialysis on on the system was carried out against methanol, which impeded the isolation of conjugates with lower degrees of PEGylation, since these precipitated in the dialysis tubing.

Initial studies on the biocompatibility of BSA/PEG conjugates synthesized by squaric acid-mediated PEGylation were carried out by the exposition of various concentrations of the samples to human umbilical vein endothelial cells (HUVECs) for 4 h and 24 h. The cell viability was investigated by microscopic examination of the cell morphology as well as using a WST-1 assay. Furthermore, the expression of cell adhesion molecules (CAMs) involved in inflammation, i.e., E-selectin and intercellular adhesion molecule-1 (ICAM-1), was determined by a cell adhesion molecule - enzyme immunosorbent assay (CAM-EIA). Cells that were not exposed to PEGylated BSA served as a negative control for all experiments. Lipopolysaccharide (LPS), which is known to be a powerful inducer of the expression of the CAMs was used as a positive control in the CAM-EIA.

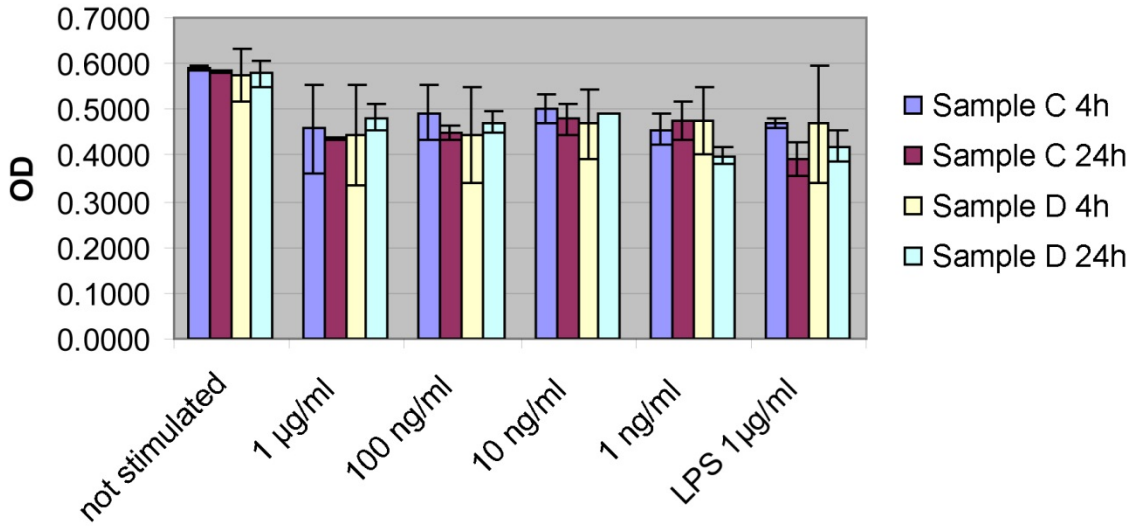

Figure 1. Cell viability of HUVECs exposed to PEGylated BSA samples **C** and **D** at different concentrations as well as LPS after 4 h and 24 h, respectively. Spectrophotometric analysis on the final reaction mixture of the metabolic assay (WST-1) given as optical density (OD).

No differences in the cell morphology were observed after 4 h and 24 h of exposition of HUVECs to the PEGylated proteins at all examined concentrations and LPS. Since there was no change in the appearance of the cells, no images were taken. The positive results were confirmed by the WST-1 assay, which showed no significant decrease in proliferation of the cells exposed to the protein conjugates and LPS, since no marked differences in the bioreduction of

2-(4-Iodophenyl)-3-(4-nitrophenyl)-5-(2,4-disulfophenyl)-2H-tetrazolium (WST-1)[1] were seen after 4 h and 24 h (Figure 1). However, a slight decrease was observed for all cells exposed to the protein conjugates and LPS compared to the control. In summary, these results indicate that both of the BSA/PEG conjugates in the concentration range of 1 ng/mL to 1 mg/mL and LPS (1 mg/mL) had no major toxic effect on HUVECs.

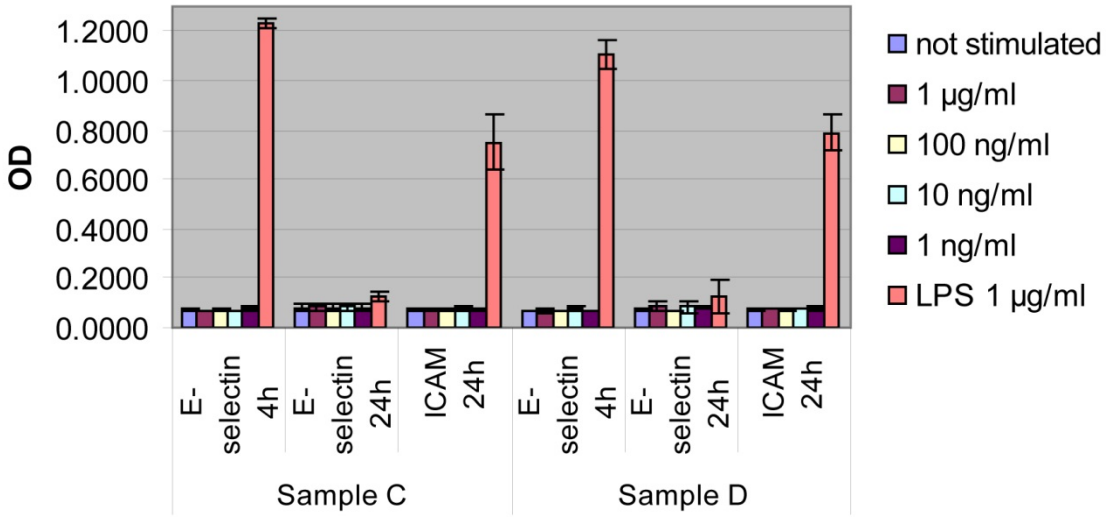

Figure 2. Expression of E-selectin and ICAM-1 by HUVECs exposed to PEGylated BSA samples **C** and **D** at various concentrations as well as LPS after 4 h and 24 h of stimulation.

In the CAM-EIA, the LPS-induced expression of E-selectin after 4 h and ICAM-1 after 24 h can be seen in Figure 2. E-selectin expression is falling off after 24 h as expected. Since the induction of ICAM-1 is slower, its expression was not studied after 4 h. Both of the squaric acid-PEGylated BSA samples did not activate the human endothelial cells within the investigated period of time at the specified concentrations. No significant differences to the E-selectin and ICAM-1 levels of the controls were observed, whereas the HUVECs stimulated by LPS clearly showed an expression of these cell adhesion molecules after 4 h and 24 h, respectively (Figure 2).

Due to the high degree of PEGylation for both protein/polymer conjugates, the surface of BSA can be assumed to be completely decorated with PEG chains, and therefore the positive initial results on the biocompatibility of the conjugates are closely related to the biocompatibility of PEG.

Conclusion

Initial studies on the biocompatibility of BSA/PEG conjugates synthesized via squaric acid mediated PEGylation showed no cytotoxic effects of the compounds on the sensitive human endothelial cells in the investigated concentration range between 1 ng/mL and 1 mg/mL. Furthermore, no expression of important cell adhesion molecules involved in inflammation was induced by the PEGylated BSA samples in the mentioned concentrations during 24 h.

However, these results can be regarded as being preliminary only, since merely one donor was involved, and the investigated concentrations were rather low. The outcome of the studies has to be further confirmed by investigating the effects of the compounds on cells from various donors and at higher concentrations. In addition, the effects on other cell types and blood compatibility will have to be examined before claiming these protein/synthetic polymer conjugates biocompatible. Studies in this direction are in progress and will be reported in due course. Nevertheless, these preliminary investigations on a very sensitive, human cell type, namely the endothelial cell, indicate that there is no evidence to date of a massive cytotoxic effect.

Experimental Part

Cell assays. Primary human umbilical vein endothelial cells (HUVECs) were seeded in a 96-well microplate and after at least 4 h of adherence were stimulated for either 4 h or 24 h with different concentrations of PEGylated BSA ranging from 1 ng/mL to 1 µg/mL or lipopolysaccharide (LPS, 1 µg/mL). As a negative control cells were not stimulated. 30 min before the expiration of the stimulation time, the cell viability was investigated using a WST-1 assay, which measures cellular enzymatic activity. Subsequently, the cells were fixed with methanol and ethanol and their activation was examined by a cell adhesion molecule - enzyme immunosorbent assay (CAM-EIA), which uses specific antibodies to the CAMs.

Protein/PEG conjugates. Two samples of BSA (25 mg) were PEGylated with squaric acid ethyl ester amido mPEG (2.1 kDa) according to the slightly altered protocol for the conjugates **C** and **D** described under *2.1 Squaric Acid Mediated Chemoselective PEGylation of Proteins: Reactivity of Single-Step-Activated α-Amino Poly(ethylene glycol)s*.[2] In contrast to the previously described protocol, the aqueous borate buffer was prepared from a freshly uncapped bottle of sterile water directly before use and filtered through a sterile disposable bottle top filter (Millipore Stericup,

Durapore Membrane, 0.22 µm pore site rating). Further, all labware was either treated with methanol (micro test tubes, pipette tips) or heated above 150 °C (glassware, spatula). The conjugates were purified by extensive dialysis against methanol using dialysis tubing with a molecular weight cut off of 50,000 Da (Cellu Sep H1, 34 mm flat width) and subsequent removal of the solvent under reduced pressure. While sample **C** was isolated quantitatively (46.8 mg), most of **D** had become insoluble upon removal of the methanol. 43.7 mg of **C** and 7.1 mg of **D** were transferred in sterile conical tubes for the cell assays.

References

[1] M. Ishiyama, M. Shiga, K. Sasamoto, M. Mizoguchi, P.-g. He, *Chem. Pharm. Bull.* **1993**, *41*, 1118.

[2] C. Dingels, F. Wurm, M. Wagner, H.-A. Klok, H. Frey, *Chem. Eur. J.* **2012**, *18*, 16828.

3 Novel Poly(ethylene glycol) Structures for Biomedical Applications

3.1 A Universal Concept for the Implementation of a Single Cleavable Unit at Tunable Position in Functional Poly(ethylene glycol)s

Carsten Dingels,[1] *Sophie S. Müller,*[1, 2] *Tobias Steinbach,*[1, 2] *Christine Tonhauser,*[1, 2] *and Holger Frey**[1]

[1]Department of Organic Chemistry, Johannes Gutenberg-Universität Mainz, Duesbergweg 10–14, D-55099 Mainz, Germany

[2]Graduate School Materials Science in Mainz, Staudingerweg 9, D-55128 Mainz, Germany

Accepted for publication in: *Biomacromolecules* **2013**, DOI: 10.1021/bm3016797.

KEYWORDS: *Acetal, Amphiphile, cleavable PEG, Hydrolysis, PEGylation.*

Abstract

Poly(ethylene glycol) (PEG) with acid-sensitive linkers, lipids, or backbones gained attention particularly for various biomedical applications, such as the covalent attachment of PEG (PEGylation) to protein therapeutics, the synthesis of stealth liposomes, and polymeric carriers for low-molecular-weight drugs. These PEGs are favored over their inert analogues because of superior pharmacodynamic and/or pharmacokinetic properties of their formulations. However, synthetic routes to acetal-containing PEGs published up to date either require enormous efforts or result in ill-defined materials with a lack of control over the molecular weight. Herein, we describe a novel methodology to implement a single acetaldehyde acetal in well-defined (hetero)functional poly(ethylene glycol)s with total control over its position. To underline its general applicability, a diverse set of initiators for the anionic polymerization of ethylene oxide (cholesterol, dibenzylamino ethanol, and poly(ethylene glycol) monomethyl ether (mPEG)) was modified and used to synthesize the analogous labile PEGs. The polyether bearing the cleavable lipid had a degree of polymerization of 46, was amphiphilic and exhibited a critical micelle concentration of 4.20 mg·L^{-1}. From dibenzylamino ethanol three heterofunctional PEGs with different molecular weights and labile amino termini were generated. The transformation of the amino functionality into the corresponding squaric acid ester amide demonstrated the accessibility of the cleavable functional group and activated the PEG for protein PEGylation, which was exemplarily shown by the attachment to bovine serum albumin (BSA). Furthermore, turning mPEG into a macroinitiator with a cleavable hydroxyl group granted access to a well-defined poly(ethylene glycol) derivative bearing a single cleavable moiety within its backbone. All the acetal-containing PEGs and PEG/protein conjugates were proven to degrade upon acidic treatment.

Introduction

Since the pioneering work of Davis and co-workers in the 1970's[1, 2] PEGylation, i.e., the covalent attachment of poly(ethylene glycol) (PEG) to a substrate, has become one of the most important strategies to overcome the inherent disadvantages of protein therapeutics.[3-7] Pharmaceutically interesting proteins undergo proteolytic degradation as well as renal clearance and often are immunogenic or antigenic. Hence, they usually exhibit short body-residence times and a fast decrease from therapeutically effective concentrations to ineffective doses. The attachment of a water-soluble, synthetic polymer such as PEG to the protein leads to decreased renal filtration, decreased proteolytic degradation and reduced immunogenicity of the conjugate in comparison to the unmodified protein. These effects result in prolonged body-residence times of the PEGylated proteins.

However, often decreased bioactivity of protein pharmaceuticals is observed when PEG chains are attached to their surface.[8] The attachment of PEG via a cleavable linker can be advantageous for some protein-therapeutics.[9, 10] PEGs with cleavable coupling units[11] or lipids[12-21] have also been investigated for other pharmaceutical applications where reversible PEGylation of the desired substrate is favorable, such as the shielding of polyplexes and liposomes.

Besides a reduction in the PEG conjugates' bioactivity in most cases, PEGylation suffers from another disadvantage regardless of the substrate: Its application is limited to polyethers with average molecular weights below 40-60 kDa, since PEG is not biodegradable and otherwise will not be excreted, but accumulate in the liver.[22] However, the circulation time of PEGylated proteins improve by increasing the average molecular weight of the synthetic polymer.[23] In consequence, biodegradable poly(ethylene glycol)s carrying cleavable moieties in the backbone are of great interest. This statement is also true for pharmaceutical applications other than the PEGylation of proteins, polyplexes or liposomes: Biocompatible and biodegradable polymers are well suited to carry low molecular weight drugs into tumor tissue making use of Ringsdorf's drug delivery concept[24] and the enhanced permeability and retention (EPR) effect.[25, 26]

Various strategies have been employed to incorporate cleavable moieties into the backbone of PEG, such as cis-aconityl linkages,[27] acetals,[28-31], as well as esters and disulfides.[32] Unfortunately, neither of the aforementioned materials is well-defined since all of them were synthesized from telechelic PEGs via step-growth mechanisms. Nevertheless, promising results

in terms of drug delivery and *in vivo* degradation were, for example, obtained by Tomlinson et al. who synthesized PEG-based polyaceteals loaded with doxorubicin, a potent anti-cancer drug[28] and demonstrated that acetaldehyde, which is formed by the degradation of acetaldehyde acetal-containing PEGs, is not cytotoxic.[29] Elisseeff and co-workers partially oxidized the ether bonds of PEG with Fenton's reagent to generate hemiacetals at the polyether backbone and demonstrated their degradability. [33] However, no degradation kinetics data was provided. Very recently, Lundberg et al. published a promising strategy to synthesize more defined degradable PEG derivatives via monomer-activated copolymerization of ethylene oxide and epichlorohydrin and subsequent elimination of hydrogen chloride.[34] The obtained vinyl ether-containing polymers exhibited polydispersity indices (*PDI*, M_w/M_n) below 1.4, but unfortunately, no concept for the attachment of therapeutics was presented.

Due to their stability in extremely basic media[35] acetals and ketals tolerate the harsh conditions of the anionic ring-opening polymerization (AROP) of oxiranes and have been established as protecting groups for aldehyde and hydroxyl groups in AROP initiators[36-40] and monomers.[41, 42] Further, these groups have been employed to generate degradable, water-soluble polyethers by epoxide AROP. Based on a ketal-containing branching unit Feng et al. demonstrated the synthesis of degradable dendrimer-like PEGs up to the seventh generation with a molecular weight of almost half a million $g \cdot mol^{-1}$.[43] Although these polyethers are well-defined, the synthetic effort necessary for their production will probably hinder widespread applications. Hyperbranched poly(ethylene glycol)s with acetal groups at each branching point that can be synthesized by the copolymerization of ethylene oxide (EO) with the inimer glycidyloxyethyl ethylene glycol ether (GEGE) in a one-pot reaction were recently presented by our group.[44] In this context the recent work of the group of Kizhakkedathu has to be mentioned, who used ketal-containing inimers for the oxyanionic polymerization[45] analogous to GEGE and multifunctional, ketal-containing initiators for the ring-opening multibranching polymerization of glycidol[46] to produce cleavable hyperbranched polyether polyols.

Acetal-functionalized PEGs are not solely interesting for biomedical applications. For instance, poly(ethylene glycol) bearing an acetaldehyde chloroethyl acetal terminus has been used to generate scissile PEG polystyrene block-copolymers, which were investigated as precursors for porous films.[47]

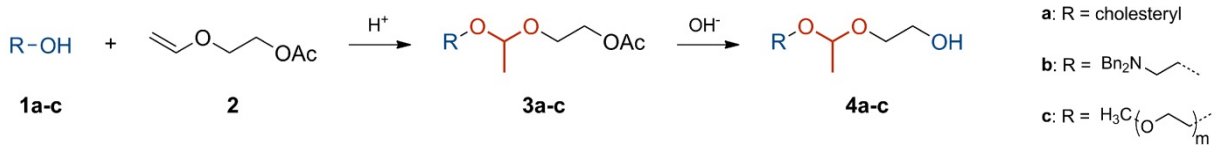

Scheme 1. Synthetic route to AROP initiators containing a single acetal moiety.

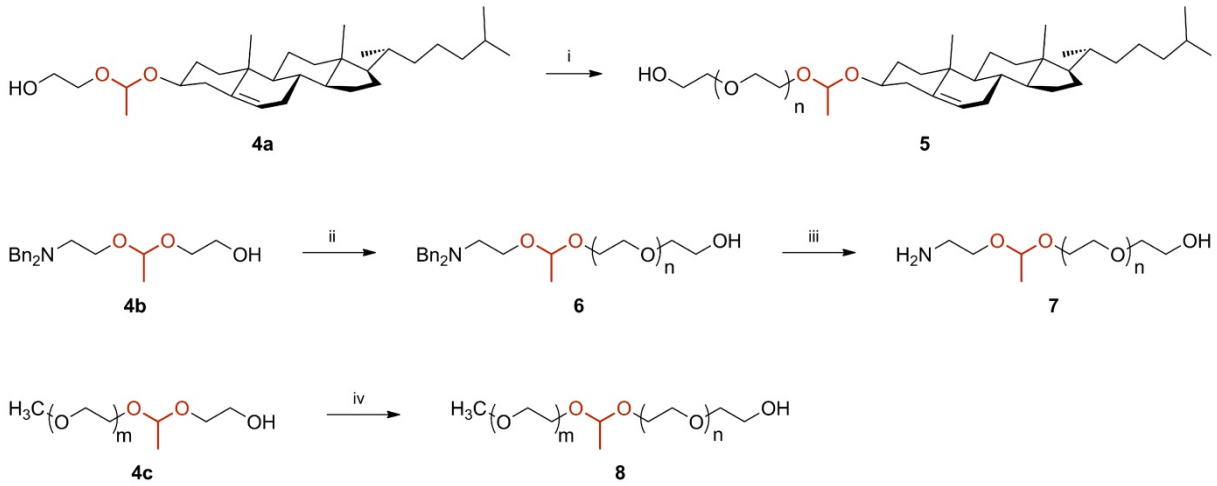

Scheme 2. Synthesis of scissile PEGs with different termini. i) 1. $CsOH{\cdot}H_2O$, C_6H_6, 90 °C, vacuum 2. Tetrahydrofuran (THF), *n* EO, 60 °C 3. MeOH. ii) 1. $CsOH{\cdot}H_2O$, C_6H_6, 90 °C, vacuum 2. THF/dimethylsulfoxide (DMSO), n EO. 3. MeOH iii) H_2, $Pd(OH)_2/C$, dioxane/water 1:1, 80 bar, 40 °C. iv) 1. C_6H_6, 90 °C, vacuum 2. $KC_{10}H_8$, THF/DMSO, *n* EO 3. MeOH.

Depending on the desired application of degradable PEG the cleavable moieties have to be located either in the backbone or at (one of) the functional terminus (termini). Herein, we present the implementation of a single, cleavable acetal moiety into conventional initiators for the anionic ring-opening polymerization of epoxides using a straight-forward two-step protocol (Scheme 1), which gives access to both types of PEG, either cleavable in the backbone or at one of the terminal sites (Scheme 2). First, the original initiators, alcohols **1a-c**, are added to 2-acetoxyethyl vinyl ether[48] (AcVE, **2**) under acidic conditions to form the asymmetric acetaldehyde acetals **3a-c**. Subsequently, the products are saponified to release the desired acetal-containing initiators **4a-c**.

The developed methodology is in principle applicable to all acid stable AROP initiators and was proven for a diverse set of alcohols to underline its general usefulness: Cholesterol (**1a**) as an apolar initiator, dibenzylamino ethanol (**1b**), which carries an additional, orthogonally protected functional group, and poly(ethylene glycol) monomethyl ether (mPEG, **1c**) as a macroinitiator. The scissile macroinitiator granted access to PEGs carrying a single acetal moiety in the backbone of the polymer. The specific position of this acid labile group can be controlled

by the molecular weight of the macroinitiator and the number of ethylene oxide (EO) units added.

Experimental Section

Materials. All reagents and solvents were purchased from Acros Organics, Fluka or Sigma-Aldrich and were used without further purification unless stated otherwise. Ethylene glycol monovinyl ether was purchased from TCI Europe. Deuterated solvents were purchased from Deutero GmbH and stored over molecular sieves (except for deuterium oxide). 2-Acetoxyethyl vinyl ether[48] (**2**) and dibenzylamino ethanol[49] (**1b**) were prepared according to known protocols. Dry THF used for the anionic ring-opening polymerization of ethylene oxide was dried and stored over sodium. Care must be taken when handling the toxic, flammable, and gaseous ethylene oxide.

Methods. ^{1}H NMR spectra (400 MHz) were recorded on a Bruker ARX 400 with a 5mm BBO probe. 2D and ^{13}C NMR spectra were recorded on a Bruker Avance-II 400 (400 MHz, 5 mm BBO probe, and B-ACS 60 auto sampler) if not stated otherwise. All spectra were recorded with 32 scans at 294 K using a relaxation delay of 1 s, unless stated otherwise and processed with MestReNova v6.1.1 software. Size-exclusion chromatography (SEC) measurements in DMF containing 0.25 g·L^{-1} of lithium bromide as additive were performed on an Agilent 1100 Series as an integrated instrument using PSS (Polymer Standards Service) HEMA column (106/105/104 g/mol), RI-detector, and UV-detector operating at 275 nm. Calibration was executed using poly(ethylene oxide) (PEO) standards from PSS. Matrix-assisted laser desorption/ionization time-of-flight mass spectrometry (MALDI-ToF MS) measurements of all polymers were recorded on a Shimadzu Axima CFR MALDI-ToF MS mass spectrometer, equipped with a nitrogen laser delivering 3 ns laser pulses at 337 nm. α-Cyano hydroxyl cinnamic acid (CHCA) or dithranol was used as a matrix and potassium triflouroacetate (KTFA) was added for ion formation. The analytes were dissolved in methanol at a concentration of 10 g·L^{-1}. An aliquot (10 µL) was added to 10 µL of a solution (10 g·L^{-1}) of the matrix and 1 µL of a solution of the cationization agent. 1 µL of the mixture was applied on a multistage target, methanol evaporated, and a thin matrix/analyte film was formed.

Sodium dodecyl sulfate polyacrylamide gel electrophoresis (SDS-PAGE) was carried out with Tris-HCl gels (Biorad, 1.0 mm, 10 well, 8% resolving gel, 4% stacking gel). IR spectra were

recorded on a Thermo Scientific Nicolet iS10 FT-IR spectrometer, equipped with a diamond ATR unit and were processed with OMNIC 8.1.210 software. Mass spectra were either measured on a Finnigan MAT 95 (field desorption, FD-MS) or a Waters/Micromass QToF Ultima 3 (electrospray ionization, ESI-MS). Surface tension measurements to determine the critical micelle concentrations (CMC) were performed on a Dataphysics DCAT 11 EC tensiometer equipped with a TV 70 temperature control unit, a LDU 1/1 liquid dosing and refill unit, as well as a RG 11 Du Noüy ring. Surface tension data was processed with SCAT v3.3.2.93 software. The CMC presented is a mean value of three experiments. All solutions for surface tension measurements were stirred for 120 s at a stir rate of 50%. After a relaxation period of 400 s three surface tension values were measured. The mean values of the three measurements were plotted against the logarithm of the concentration. The slopes of the traces at high concentrations as well as in the low concentration range were determined by linear regression. The concentration at the fits' intersection was the CMC. The Du Noüy ring was rinsed thoroughly with water and annealed in a butane flame. Turbidimetry was performed in a Jasco V-630 UV-VIS spectrometer at a wavelength of $\lambda = 528$ nm and the data was processed with the Time Course Measurement program of Spectra Manager v2.08 software.

Synthesis procedures. *Acetoxyethyl 1-(cholesteryloxy)ethyl ether (**3a**).* Cholesterol (5.0 g, 13 mmol) and 2-Acetoxyethyl vinyl ether (2.53 g, 19.4 mmol) were stirred for 45 min in dichloromethane with *p*-toluene sulfonic acid monohydrate (*p*TSA, 25 mg, 0.13 mmol). The solution was treated with triethylamine (250 µL) and washed with 1 N aqueous sodium hydroxide solution. After drying over sodium sulfate the organic phase was evaporated to small volume. Pure product (4.80 g, 9.29 mmol, 72%) was obtained by column chromatography (eluent: petrol ether/ethyl acetate 8:1) over silica. *^{1}H NMR* (400 MHz, $CDCl_3$): δ [ppm] = 5.32 (s, 1H, H-6), 4.85 (q, 1H, J_{AB} = 5.3 Hz, H_3CCHO_2), 4.26-4.12 (m, 2H, AcO-CH_2), 3.78-3.58 (m, 2H, $AcOCH_2$-CH_2), 3.65-3.36 (m, 1H, H-3α), 2.38-2.12 (m, 2H, H-4), 2.05 (s, 3H, H_3C-CO-), 2.03-1.94 (m, 1H, H-12α), 1.99-1.89 (m, 1H, H-7β), 1.87-1.79 (m, 2H, H-1β and H-2α), 1.87-1.74 (m, 1H, H-16β), 1.63-0.81 (m, 22H), 1.30 (d, 3H, J_{AB} = 5.3 Hz, H_3C-CHO_2), 0.99 (s, 3H, H_3-19), 0.90 (d, 3H, J_{AB} = 6.5 Hz, H_3-21), 0.84 (d, 3H, J_{AB} = 6.6 Hz, H_3-26), 0.83 (d, 3H, J_{AB} = 6.6 Hz, H_3-27), 0.65 (s, 3H, H_3-18). *^{13}C NMR* (100.6 MHz, $CDCl_3$): δ [ppm] = 170.1 (1C, Me*C*OO), 140.9 and 140.8 (1C, C-5) 121.9 and 121.8 (1C, C-6), 98.0 and 97.9 (1C, Me-CHO_2), 75.9 and 75.8 (1C, C-3), 63.9 (1C, AcO-CH_2) 61.6

(1C, $AcOCH_2$-CH_2-), 50.3 (1C, C-9), 42.4 (1C, C-13), 40.1 and 39.5 (1C, C-4), 39.8 (1C, C-12), 39.6 (1C, C-24), 37.5 and 37.3 (1C, C-1), 36.8 (1C, C-10), 36.3 (1C, C-22), 35.9 (1C, C-20), 32.0 (2C, C-7 and G-8), 29.5 and 28.7 (1C, C-2), 28.3 (1C, C-16), 28.1 (1C, C-25), 24.4 (1C, C-15), 23.9 (1C, C-23), 22.9 (1C, C-27), 22.7 (1C, C-26), 21.1 (2C, C-11 and CH_3-COO), 20.6 (1C, CH_3-CHO_2), 19.5 (1C, C-19), 18.8 (1C, C-21), 12.0 (1C, C-18). MS (ESI-MS, MeOH): m/z = 539.42 $[M+Na]^+$, 1055.86 $[2M+Na]^+$.

*Acetoxyethyl 1-(2-dibenzylamino ethoxy)ethyl ether (**3b**)*. Dibenzylamino ethanol (5.0 g, 21 mmol) and 2-Acetoxyethyl vinyl ether (5.0 g, 38 mmol) were stirred for 30 min in dichloromethane with trifluoroacetic acid (TFA, 7.1 g, 62 mmol). The solution was treated with triethylamine (1.5 mL) and washed with 1 N aqueous sodium hydroxide solution. After drying over sodium sulfate the organic phase was evaporated to small volume. Pure product was obtained by column chromatography (eluent: petrol ether/ethyl acetate 6:1) over silica. Yield: 85%. *^{1}H NMR* (400 MHz, $CDCl_3$): δ [ppm] = 7.42 (d, 4H, J_{AB} = 7.2 Hz, 4 meta CH_{Ar}), 7.34 (t, 4H, J_{AB} = 7.4 Hz, 4 ortho CH_{Ar}), 7.26 (d, 2H, J_{AB} = 7.4 Hz, 2 para CH_{Ar}), 4.75 (q, 1H, J_{AB} = 5.4 Hz, H_3C-CHO_2), 4.21 (t, 2H, J_{AB} = 4.9 Hz, AcO-CH_2), 3.77-3.67 (m, 1H, NCH_2-CH_a), 3.76-3.67 (m, 1H, $AcOCH_2$-CH_a), 3.69 (s, 4H, 2 Ph-CH_2), 3.65-3.57 (m, 1H, $AcOCH_2$-CH_b), 3.61-3.52 (m, 1H, NCH_2-CH_b), 2.72 (t, 2H, J_{AB} = 6.3 Hz, N-CH_2-CH_2), 2.07 (s, 3H, H_3C-CO), 1.31 (d, 3H, J_{AB} = 5.4 Hz, H_3C-CHO_2). *^{13}C NMR* (100.6 MHz, $CDCl_3$): δ [ppm] = 171.0 (1C, Me-*CO*-O), 139.7 (2C, 2 quaternary C_{Ar}), 128.8 (4C, ortho CH_{Ar}), 128.2 (4C, meta CH_{Ar}), 126.9 (2C, para CH_{Ar}), 99.7 (1C, H_3C-CHO_2), 64.0 (1C, NCH_2-CH_2), 63.8 (1C, AcO-CH_2), 62.2 (1C, $AcOCH_2$-CH_2), 59.0 (2C, 2 Ph-CH_2), 52.9 (1C, N-CH_2-CH_2), 21.0 (1C, H_3C-CO), 19.5 (1C, H_3C-CHO_2).

*1-(2-Acetoxyethoxy)ethoxy mPEG (**3c**)*. Poly(ethylene glycol) monomethyl ether (**1c**, 4.0 g, 2.0 mmol), 2-Acetoxyethyl vinyl ether (1.3 g, 10 mmol), and *p*TSA (3.8 mg 0.2 mmol) were placed in a round-bottom flask, dissolved in dichloromethane (DCM, 20 mL), and stirred for 30 min. The reaction was quenched with triethylamine (0.2 mL) and washed with 1 N aqueous sodium hydroxide solution. The organic phase was dried over sodium sulfate and subsequently concentrated to small volume. Pure product was obtained by precipitation in cold diethyl ether. Yield: 87%. *^{1}H NMR* (400 MHz, $CDCl_3$): δ [ppm] = 4.77 (q, 1H, J_{AB} = 5.4 Hz, H_3C-CHO_2), 4.16 (t, 2H, J_{AB} = 4.8 Hz, AcO-CH_2), 3.86-3.36 (m, 180H, CH_2O), 3.33 (s, 3H, OCH_3), 2.03 (s, 3H, H_3C-CO), 1.28 (d, 3H, J_{AB} = 5.4 Hz, H_3C-CHO_2).

*Glycol 1-(cholesteryloxy)ethyl ether (**4a**).* Potassium hydroxide (1.00 g, 17.8 mmol) and Acetoxyethyl 1-(cholesteryloxy)ethyl ether (**3a**, 1.00 g, 1.93 mmol) were stirred under reflux in a solution of ethanol (12 mL) and water (0.5 mL) for 3 h. After cooling, brine was added and the solution was extracted with DCM three times. After drying over sodium sulfate the organic phase was evaporated to small volume. Pure product (536 mg, 1.13 mmol, 59%) was obtained by column chromatography (eluent: petrol ether/ethyl acetate 2:1) over silica. *^{1}H NMR* (400 MHz, $CDCl_3$): δ [ppm] = 5.32 (s, 1H, H-6), 4.81 (q, 1H, J_{AB} = 5.3 Hz, H_3C-*C*HO_2), 3.75-3.64 (m, 2H, HO-*C*H_2), 3.71-3.53 (m, 2H, $HOCH_2$-*C*H_2), 3.94-3.34 (m, 1H, H-3α), 2.53 (t, 1H, J_{AB} = 5.8 Hz, OH), 2.35-2.12 (m, 2H, H-4), 2.04-1.94 (m, 1H, H-12α), 1.99-1.90 (m, 1H, H-7β), 1.90-1.78 (m, 2H, H-1β and H-2α), 1.88-1.73 (m, 1H, H-16β), 1.63-0.80 (m, 22H), 1.32 (d, 3H, J_{AB} = 5.3 Hz, *H*$_3$*C*-CHO_2), 0.98 (s, 3H, H_3-19), 0.89 (d, 3H, J_{AB} = 6.5 Hz, H_3-21), 0.84 (d, 3H, J_{AB} = 6.6 Hz, H_3-26), 0.84 (d, 3H, J_{AB} = 6.6 Hz, H_3-27), 0.65 (s, 3H, H_3-18). *^{13}C NMR* (100.6 MHz, $CDCl_3$): δ [ppm] = 170.1 (1C, Me-*C*O-O), 140.9 and 140.8 (1C, C-5) 121.9 and 121.8 (1C, C-6), 98.0 and 97.9 (1C, Me-*C*HO_2), 75.9 and 75.8 (1C, C-3), 63.9 (1C, AcO-*C*H_2) 61.6 (1C, $AcOCH_2$-*C*H_2-), 50.3 (1C, C-9), 42.4 (1C, C-13), 40.1 and 39.5 (1C, C-4), 39.8 (1C, C-12), 39.6 (1C, C-24), 37.5 and 37.3 (1C, C-1), 36.8 (1C, C-10), 36.3 (1C, C-22), 35.9 (1C, C-20), 32.0 (2C, C-7 and G-8), 29.5 and 28.7 (1C, C-2), 28.3 (1C, C-16), 28.1 (1C, C-25), 24.4 (1C, C-15), 23.9 (1C, C-23), 22.9 (1C, C-27), 22.7 (1C, C-26), 21.1 (2C, C-11 and *C*H_3CO), 20.6 (1C, *C*H_3-CHO_2), 19.5 (1C, C-19), 18.8 (1C, C-21), 12.0 (1C, C-18). MS (ESI-MS, MeOH): *m/z* = 497.42 $[M+Na]^+$, 971.81 $[2M+Na]^+$.

*Glycol 1-(2-dibenzylamino ethoxy)ethyl ether (**4b**).* Potassium hydroxide (3.2 g, 57 mmol) and Acetoxyethyl 1-(2-dibenzylamino ethoxy)ethyl ether (**3b**, 6.0 g, 16 mmol) were stirred under reflux in a solution of ethanol (8.4 mL) and water (4.2 mL) for 3 h. After cooling, brine was added and the solution was extracted with DCM three times. After drying over sodium sulfate the organic phase was evaporated to small volume. Pure product was obtained by column chromatography (eluent: petrol ether/ethyl acetate 2:1) over silica. Yield: 58%. *^{1}H NMR* (400 MHz, DMSO-d_6): δ [ppm] = 7.41-7.27 (m, 8H, 4 meta CH_{Ar} and 4 ortho CH_{Ar}), 7.22 (t, 2H, J_{AB} = 7.1 Hz, 2 para CH_{Ar}), 4.63 (q, 1H, J_{AB} = 5.2 Hz, H_3C-*CHO*$_2$), 4.61 (t, 1H, J_{AB} = 4.7 Hz, *HO*-CH_2), 3.68-3.57 (m, 1H, NCH_2-*C*H_a), 3.60 (s, 4H, 2 Ph-*C*H_2), 3.53-3.43 (m, 1H, NCH_2-*C*H_b), 3.52-3.43 (m, 1H, $HOCH_2$-*C*H_a), 3.51 (m, 2H, HO-*C*H_2), 3.42-3.32 (m, 1H, $HOCH_2$-*C*H_b), 2.56 (t, 2H, J_{AB} = 6.2 Hz, N-*C*H_2-CH_2), 1.17 (d, 3H, J_{AB} = 5.3 Hz, *H*$_3$*C*-CHO_2). *^{13}C NMR* (100.6 MHz, DMSO-d_6): δ [ppm] = 139.5 (2C, 2 quaternary C_{Ar}), 128.5 (4C, ortho

CH_{Ar}), 128.2 (4C, meta CH_{Ar}), 126.8 (2C, para CH_{Ar}), 99.3 (1C, H_3C-*CHO*$_2$), 66.7 (1C, $HOCH_2$-*CH*$_2$), 63.1 (1C, NCH_2-*CH*$_2$), 60.4 (1C, HO-*CH*$_2$), 58.0 (2C, 2 Ph-*CH*$_2$), 52.4 (1C, N-*CH*$_2$-CH_2), 19.8 (1C, *H*$_3$*C*-CHO_2). MS (FD-MS, MeOH): *m/z* = 329.4 $[M]^+$, 569.6 $[2M\text{-}Bn+2H]^+$, 659.7 $[2M+H]^+$, 691.7 $[2M+MeOH+H]^+$.

*1-(2-Hydroxyethoxy)ethoxy mPEG (**4c**).* Potassium hydroxide (1.2 g, 21 mmol) and **3c** (3.7 g, 1.9 mmol) were stirred under reflux in a solution of ethanol (3.0 mL) and water (1.5 mL) for 3 h. After cooling the solution was extracted with DCM three times and the combined organic phases were dried over sodium sulfate. DCM was evaporated and pure product was obtained by precipitation in cold diethyl ether. Yield: 67%. *^{1}H NMR* (400 MHz, $CDCl_3$): δ [ppm] = 4.77 (q, 1H, J_{AB} = 5.5 Hz, H_3C-*CH*O_2), 3.84-3.385 (m, 180H, ($CH_2CH_2O)_n$), 3.32 (s, 3H, OCH_3), 1.28 (d, 3H, J_{AB} = 5.2 Hz, *H*$_3$*C*-CHO_2).

α-*(1-(Cholesteryloxy)ethoxy)* ω-*hydro PEG (5).* **4a** (427 mg, 0.900 mmol), cesium hydroxide monohydrate (134 mg, 0.798 mmol), and benzene were placed in a Schlenk flask. The mixture was stirred at RT for about 30 min to generate the cesium alkoxide (degree of deprotonation 89%). The salt was dried under vacuum at 90 °C for 24 h, dry THF was added via cryo-transfer, and ethylene oxide (2 mL, 51 mmol) was cryo-transferred first to a graduated ampule and then to the Schlenk flask containing the initiator solution. The mixture was allowed to warm up to room temperature, heated to 60 °C, and the polymerization was performed for 12 h at this temperature under vacuum. The reaction was quenched with methanol, the solvent was evaporated and the crude product was precipitated into cold diethyl ether. *^{1}H NMR* (400 MHz, $CDCl_3$): δ [ppm] = 5.31 (s, 1H, H-6), 4.83 (q, 1H, J_{AB} = 5.3 Hz, H_3C-*CH*O_2), 4.10-3.21 (m, 190H, CH_2O and H-3α), 2.35-2.12 (m, 2H, H-4), 2.04-1.89 (m, 2H, H-12α and H-7β), 1.88-1.73 (m, 3H, H-1β, H-2α, and H-16β), 1.63-0.80 (m, 22H), 1.30 (d, 3H, J_{AB} = 5.3 Hz, *H*$_3$*C*-CHO_2), 0.98 (s, 3H, H_3-19), 0.89 (d, 3H, J_{AB} = 6.6 Hz, H_3-21), 0.85 (d, 3H, J_{AB} = 6.6 Hz, H_3-26), 0.84 (d, 3H, J_{AB} = 6.6 Hz, H_3-27), 0.65 (s, 3H, H_3-18).

α-*(1-(2-Dibenzylamino ethoxy)ethoxy)* ω-*hydro PEG (**6**).* **6** was synthesized similar to protocols for *N*,*N*-dibenzylamino ethoxide initiated anionic ring-opening polymerization of ethylene oxide known in the literature.[50, 51] The following protocol is typical and describes the example of **6** with a degree of polymerization (*Pn*) of 50 (**6**$_{50}$). Cesium hydroxide monohydrate (150 mg, 893 µmol) was added to a solution of **4b** (322.7 mg, 0.9796 mmol) dissolved in benzene (7 mL) in a dry Schlenk flask. The mixture was stirred for 30 min at 60 °C under slightly reduced pressure with closed stop cock. Moisture was removed by azeotropic distillation of benzene and

subsequent drying at 80 °C under high vacuum for 3.5 h. After cooling to room temperature dry THF (7 mL) was cryo-transferred into the Schlenk flask and dry DMSO (2 mL) was added via syringe. Subsequently, ethylene oxide (1.95 g, 44.3 mmol) was cryo-transferred via a graduated ampule to the initiator solution and the flask was closed tightly. The reaction mixture was stirred overnight at 40 °C and finally quenched by the addition of methanol (2 mL). The polymer was precipitated from methanol in cold diethyl ether twice and subsequently dried under reduced pressure. Yield: 2.07 g (91%). *^{1}H NMR* (400 MHz, $CDCl_3$): δ [ppm] = 7.32 (d, 4H, J_{AB} = 7.3 Hz, 4 ortho CH_{Ar}), 7.52 (t, 2H, J_{AB} = 7.4 Hz, 2 meta CH_{Ar}), 7.17 (t, 1H, J_{AB} = 7.2 Hz, para CH_{Ar}), 4.65 (q, 1H, J_{AB} = 5.3 Hz, H_3C-*CHO_2*), 3.97 (m, 208H, CH_2O), 2.62 (t, 2H, J_{AB} = 6.3 Hz, N-*CH_2*-CH_2), 1.23 (d, 3H, J_{AB} = 5.3 Hz, *H_3C*-CHO_2).

α-*(1-(2-Amino ethoxy)ethoxy)* ω-*hydro PEG (***7***).* Hydrogenation of α-(1-(2-dibenzylamino ethoxy)ethoxy) ω-hydro PEG (**6**) was carried out similar to the protocol described for α-dibenzylamino ω-hydroxy-PEG.[51] The following protocol describes the synthesis of **7** with a degree of polymerization of 50 (**7$_{50}$**). **6$_{50}$** (700 mg, 0.313 mmol) was dissolved in a water/dioxane 1:1 mixture and stirred with palladium(II)-hydroxide on activated charcoal (150 mg) under hydrogen (80 bar) for 3 days in a stainless steel reactor. After the solution had been filtered through Celite® the filter cake was washed with methanol (2 L). The transparent solution was reduced to small volume and precipitated in cold diethyl ether. A second precipitation from DCM in cold diethyl ether yielded 457 mg (0.222 mmol, 71%) of **7$_{50}$**. *^{1}H NMR* (400 MHz, DMSO-d_6): δ [ppm] = 4.68 (q, 1H, J_{AB} = 5.2 Hz, H_3C-*CHO_2*), 4.59 (s, 1H, OH), 3.80-3.37 (m, 210H, CH_2O), 2.65 (t, 2H, J_{AB} = 5.8 Hz, H_2N-*CH_2*), 1.20 (d, 3H, J_{AB} = 5.2 Hz, *H_3C*-CHO_2).

α-*(1-mPEG ethoxy)* ω-*hydro PEG (***8***).* **4c** (1.00 g, 0.476 mmol) was dissolved in benzene (10 mL) in a dry Schlenk flask. The solution was stirred for 30 min at 90 °C under slightly reduced pressure with closed stop cock. Moisture was removed by azeotropic distillation of benzene and subsequent drying at 90 °C under high vacuum overnight. After cooling to room temperature dry THF (20 mL) was cryo-transferred into the Schlenk flask and potassium naphthalenide in THF (1 mL, c = 0.5 mol·L^{-1}, prepared under argon from potassium (235 mg, 6.0 mmol), naphthalene (770 mg, 6.0 mmol), and dry THF (12 mL) in a glove box) was added via syringe. Subsequently, the generated hydrogen was evaporated including half the amount of THF and ethylene oxide (3.0 g, 68 mmol) was cryo-transferred via a graduated ampule to the macroinitiator solution. The reaction mixture was stirred for 3 h at 60 °C first and overnight at

40 °C. After the polymerization had been quenched by the addition of methanol (1.3 mL) the polymer was precipitated from methanol in cold diethyl ether twice and subsequently dried under reduced pressure. Yield: 3.64 g (91%). *^{1}H NMR* (400 MHz, $CDCl_3$): δ [ppm] = 4.75 (q, 1H, J_{AB} = 5.3 Hz, H_3C-*CH*O_2), 3.99-3.37 (m, 714H, CH_2O), 3.33 (s, 3H, OCH_3), 1.27 (d, 3H, J_{AB} = 5.4 Hz, *H_3C*-CHO_2).

*α-(1-(2-(squaric acid ethyl ester amido)ethoxy)ethoxy) ω-hydro PEG (**10**).* Diethyl squarate (**9**, 60.7 mg, 357 µmol), $\mathbf{7}_{75}$ (100 mg, 29.2 µmol), and triethylamine (43 µL, 310 µmol) were stirred in a 1:1 water /ethanol solution (2 mL) for 4 h. After the ethanol had been removed by distillation, the solution was extracted with DCM four times. Subsequently, the organic phase was evaporated to small volume and precipitated in cold diethyl ether. The resulting polymer was precipitated several times from methanol in cold diethyl ether until no more diethyl squarate was detected by thin layer chromatography (TLC). *^{1}H NMR* (400 MHz, $CDCl_3$): δ [ppm] = 4.82-4.68 (m, 3H, H_3C-*CH_2*-O and H_3C-*CH*O_2), 3.99-3.37 (m, 311H, CH_2O and CH_2N), 1.50-1.38 (m, 3H, *H_3C*-CH_2O), 1.35-1.22 (m, 3H, *H_3C*-CHO_2).

Results and Discussion

A.1 Addition of Conventional AROP Initiators to AcVE. The key step in the implementation of an acetaldehyde moiety between the hydroxyl group and the residue of established AROP initiators is the acid catalyzed addition of the alcohol to AcVE (Scheme 1). This vinyl ether was chosen for three reasons: First, upon the addition reaction the acetate can be saponified with little effort under basic conditions that every possible initiator for the AROP and the generated acetal will tolerate. Second, upon saponification a new hydroxyl group is generated, which is essential for the initiation of the anionic epoxide polymerization. And, finally, upon deprotonation the generated alkoxide is structurally related to the growing chain end, i.e., an alkyloxyethoxide, which is favorable for the initiation kinetics. The amount of acid necessary to promote the addition of the alcohol across the vinyl ether double bond varied depending on the nature of the alcohol (*vide infra*). Hence, the applied conventional initiators have to be more or less stable under acidic conditions. In contrast to the aforementioned and doubtless innovative, multifunctional, ketal-containing initiators used by Kizhakkedathu and coworkers,[46] our methodology yields asymmetric acetals from established initiators in a rapid two-step synthesis.

Cholesterol (**1a**) was chosen as a model compound to demonstrate the applicability of our acetal insertion protocol to apolar, monofunctional initiators for the oxyanionic ROP of epoxides. The addition of the steroid to AcVE was catalyzed by 1 mol% of *p*-toluene sulfonic acid. The conditions of the vinyl ether addition had to be adjusted for dibenzylamino ethanol (**1b**), since catalytic amounts of acid solely protonated the basic tertiary amine, but did not activate the vinyl ether double bond. The excess of trifluoroacetic acid which was necessary to provide a satisfactory reaction rate was determined by following the reaction kinetics via ^{1}H NMR spectroscopy. Figure S46 displays the reaction kinetics of the addition reaction in deuterated chloroform when 1.8 equivalents of AcVE and three equivalents of TFA were batched (for spectra see SI, Figure S47). 85% conversion was achieved after 44 min, whereas under identical conditions except for less acid fed to the reaction mixture (i.e., 2 eq. TFA batched with respect to **1b**), 90% conversion was reached after 18 h (data not shown).

According to our protocol, a PEG macroinitiator opens up the synthesis of well-defined poly(ethylene glycol)s carrying a single acetal moiety in the backbone (Scheme 2). mPEG was chosen as the simplest precursor for this system, since it is chemically inert except for the mandatory hydroxyl group. The necessary amount of acid was higher than in the analogous reaction with **1a**, reflecting the lower reactivity of the polymeric alcohol, but significantly lower than in the reaction with **1b**, since no basic residue was competing for protons with the double bond.

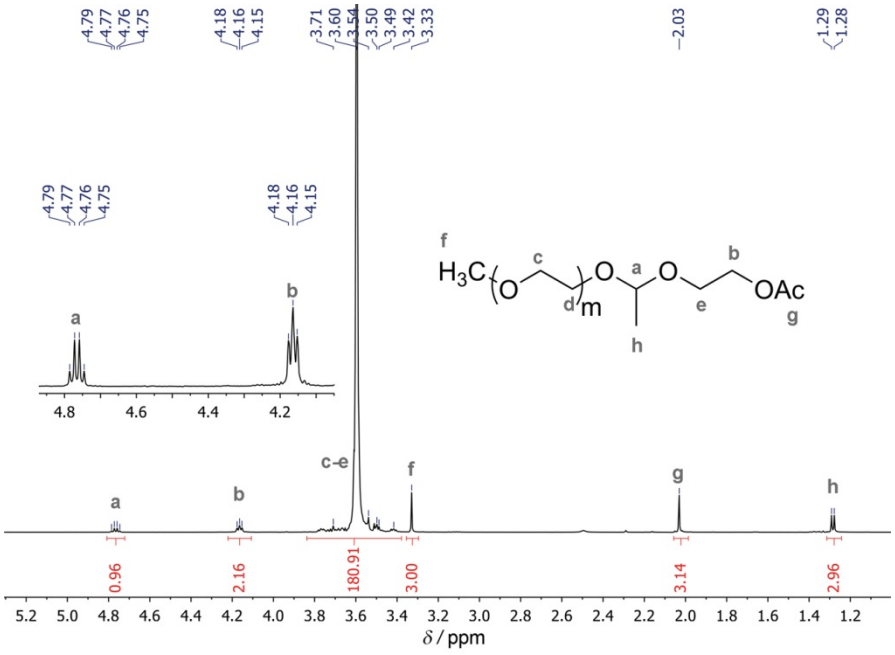

Figure 1. ^{1}H NMR spectrum (400 MHz) of **3c** in $CDCl_3$ at T = 294 K.

Complete conversion of the alcohols **1a-c** to the corresponding acetal acetates **3a-c** was confirmed by NMR spectra recorded in deuterated chloroform (Figure 1 and SI, Figures S1-S12). To assign all peaks in the ^{13}C and ^{1}H NMR spectra of the purified acetal acetates **3a** and **3b** 2D NMR experiments were carried out, i.e., COSY (correlated spectroscopy), HSQC (heteronuclear single quantum coherence), and HMBC (heteronuclear multiple bond correlation) experiments (find 2D NMR spectra in the Supporting Information, Figures S3-S7 (**3a**) and S10-S12 (**3b**)). Additionally, the chemical shifts of the cholesteryl derivative **3a** were compared to those of steroids known in the literature.[52, 53]

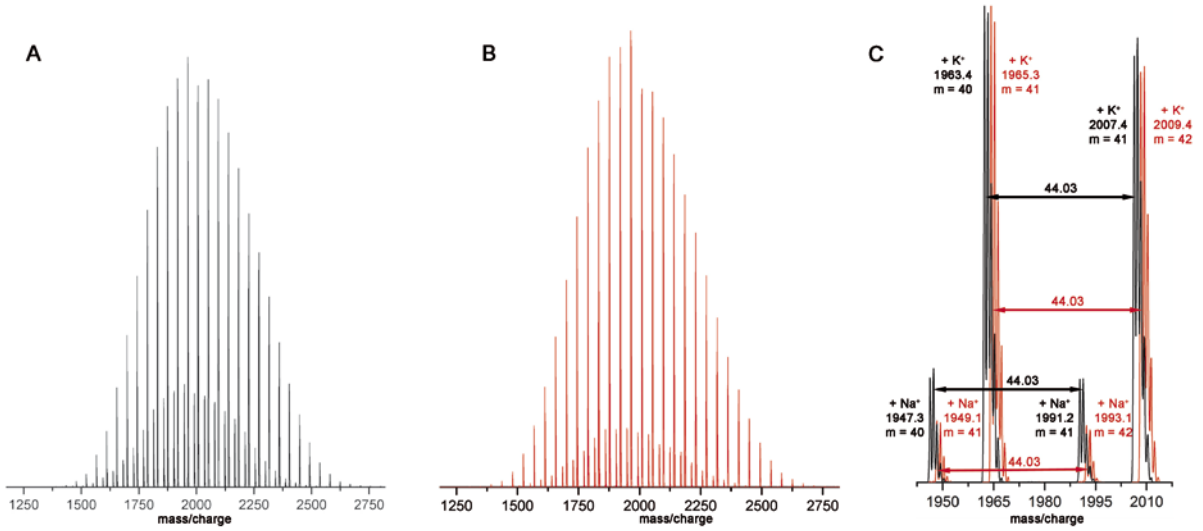

Figure 2. MALDI-ToF mass spectra of derivatized mPEGs. **A** Mass spectrum of **3c**. **B** Mass spectrum of **4c**. C Detail of overlay of mass spectra of **3c** (black) and **4c** (red). Masses given for averaged signals, mass differences calculated from monoisotopic peaks. All spectra were recorded in reflectron mode.

In the ^{1}H NMR spectra the conversion was determined from the ratio of the peaks assigned to the acetal methine protons (**3a**: 4.85 ppm, **3b**: 4.75 ppm, **3c**: 4.77 ppm) and protons of the former alcohol residues. These were the cholesteryl carbon-carbon double bond (H-6, 5.32 ppm), the aromatic protons (7.50-7.20 ppm), and the methoxy group of mPEG (3.33 ppm), respectively. Successful addition of the alcohols across the double bond of AcVE was further indicated by the carbonyl stretch vibrations of the acetates at 1741.2 cm^{-1} (**3a**), 1738.4 cm^{-1} (**3b**), and 1739.0 cm^{-1} (**3c**) in the IR spectra of the acetals (SI, Figures S32-S34). Full conversion of mPEG to 1-(2-acetoxyethoxy)ethoxy mPEG (**3c**) was also confirmed by MALDI-ToF MS. The mass spectrum (Figure 2A) revealed a single distribution of the desired polymeric species cationized either with sodium or potassium. Within the limits of the error the

mass peaks satisfied the following equation with $M_{C+} = M_{Na+} = 23.0\ \mathrm{g{\cdot}mol^{-1}}$ for sodium cationized molecules and $M_{C+} = M_{K+} = 39.1\ \mathrm{g{\cdot}mol^{-1}}$ for those cationized with potassium:

$$\mathrm{M_8(n) = M_{CH_3} + M_{CH_3CO} + (n+2)\cdot M_{EO} + M_{C^+} = 74.08\frac{g}{mol} + (2+n)\cdot 44.05\frac{g}{mol} +}$$

$$\mathrm{M_{C^+}}M_{\mathbf{3c}}(n) = M_{CH_3O} + M_{CH_3CO} + (2+n)\cdot M_{EO} + M_{C^+} = 74.1\frac{g}{mol} + (2+n)\cdot 44.05\frac{g}{mol} + M_{C^+}$$

The SEC elugram of **3c** (Figure 3) shows a monomodal distribution and a slight increase in both, the number-averaged molecular weight ($M_n = 1700\ \mathrm{g{\cdot}mol^{-1}}$ to $M_n = 1900\ \mathrm{g{\cdot}mol^{-1}}$) and the polydispersity index (1.06 to 1.07) in comparison to the batched mPEG (**1c**). Data derived from SEC analysis can be regarded as trend only, since all samples were referenced to a PEG standard. The most important factor for the synthesis of **3c** is the reaction time, since slow transacetalization may take place. Upon longer exposure of the produced acetal to the acidic reaction conditions, the symmetric polymeric acetal, which is shown in Scheme 3, is formed. This side reaction can be followed by SEC as a second mode evolving at twice the molecular weight of the product (find elugrams in the Supporting Information, Figure S53). Therefore, quenching the reaction with triethylamine in time is important to yield quantitative conversion and avoid transacetalization reactions.

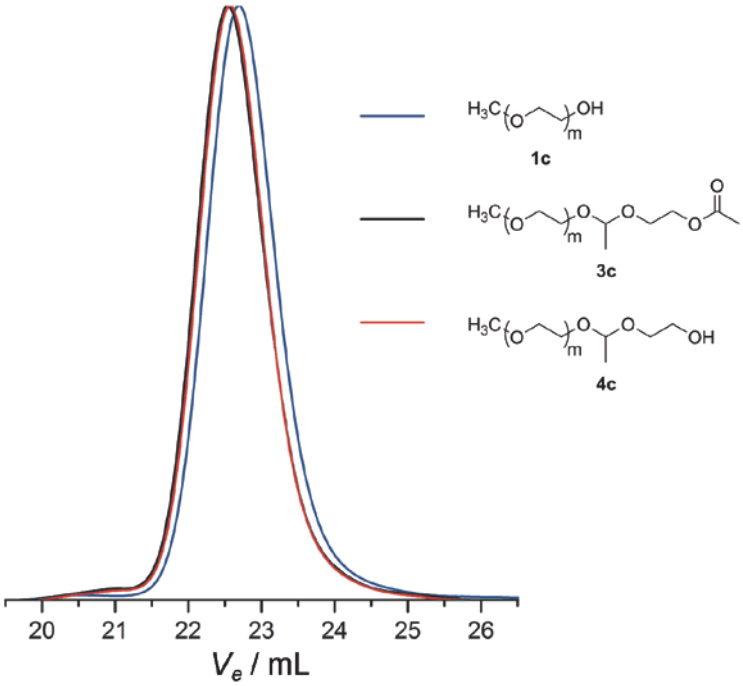

Figure 3. SEC elugrams of **3c** (black), **4c** (red), and the corresponding mPEG precursor (blue).

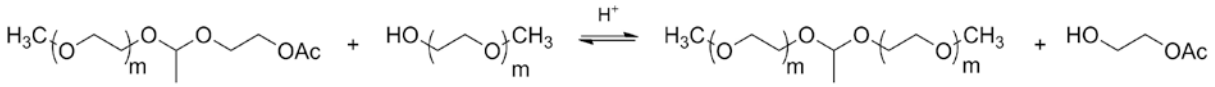

Scheme 3. Possible transacetalization during synthesis of **3c**.

A.2 Saponification of Acetal Acetates. The acetal acetates **3a-c** were saponified to yield the scissile initiators **4a-c**, respectively, and the removal of the acetate was confirmed by NMR and IR spectroscopy. For the assignment of all peaks in both ^{1}H and ^{13}C NMR spectra recorded of **4a** and **4b** additional 2D NMR experiments (COSY, HSQC, and HMBC) were carried out (Supporting Information). In the ^{1}H NMR spectra of all cleavable initiators (SI, Figures S13, S20, and S25) the characteristic acetyl peak at around 2.0 ppm of the corresponding precursors had disappeared. Further, the resonance of the methylene protons adjacent to the hydroxyl group exhibited a clear high-field shift compared to the corresponding signals of their analogous acetates. In the ^{13}C NMR spectra (SI, Figures S14, and S21), the carbonyl peaks had vanished completely as well as the bands of the carbonyl stretches at around 1740 cm^{-1} in the IR spectra (SI, Figures S35-S37). In return, all IR spectra exhibited broad hydroxyl bands at wavenumbers of ca. 3400 cm^{-1}.

The mPEG derivative **4c** was further characterized by MALDI ToF MS and SEC. In the mass spectrum of **4c** (Figure 2B) the observed mass-averaged peaks satisfied the following equation:

$$M_{\mathbf{4c}}(n) = M_{CH_3O} + M_H + (2+n)\cdot M_{EO} + M_{C^+} = 32.0\frac{g}{mol} + (2+n)\cdot 44.05\frac{g}{mol} + M_{C^+}$$

The difference of the molecular masses of $M_{4c}(n+1)$ and its reactant $M_{3c}(n)$ was calculated and found to be just 2 g·mol^{-1} (Figure 2C). Fortunately, the isotopic resolution obtained in the investigated measuring range allowed to clearly distinguish between the two series of polyether masses. The SEC trace of 1-(2-hydroxyethoxy)ethoxy mPEG was monomodal and shifted to a smaller hydrodynamic volume in comparison to the acetate derivative **3c** (Figure 3). Also, the *PDI* increased slightly to 1.08 upon the saponification.

B.1 Use of Cleavable Initiators for EO Polymerization: PEG with Cleavable Cholesterol Initiator. Cholesteryl PEGs were subject to various studies for very different purposes: They are amphiphilic, can be utilized in the synthesis of stealth liposomes,[54-56] and exhibit liquid-crystalline behavior, if the degree of polymerization is low.[57, 58] Insertion of a scissile unit between the polymer and the initiating unit will lead to pH-responsive materials,

which lose their amphiphilic or mesogenic properties upon acidic treatment. PEGs attached to cholesterol via an acid labile linker are known already (*vide supra*), but the synthetic pathways presented are laborious or the overall yield limited.[13, 14, 19] According to our protocol, PEGs with a scissile terminal cholesterol unit can be synthesized rapidly in three steps. The resulting α-(1-(cholesteryloxy)ethoxy) ω-hydro PEG (**5**) was characterized by NMR spectroscopy, SEC, and MALDI-ToF MS. The mass spectrum of **5** (SI, Figure S39) displayed the distribution of the desired polydisperse compound cationized with potassium.

Successful initiation of the oxyanionic polymerization of EO with **4a** was also confirmed by the ^{1}H NMR spectrum of **5** (Figure 4) in which, besides the acetal peaks, the H-3 and H-6 resonance s as well as the characteristic pattern of the cholesteryl's methyl groups were clearly identified. The degree of polymerization and the number-averaged molecular weight were calculated from the area under the backbone peak (reduced by five protons arising from the initiator) related to the integral of a cholesteryl methyl resonance (H_3-18).

$$P_n = \frac{3}{4} \cdot \frac{I_{PEG} - 5}{I_{Me}} = 46$$

$$M_n = P_n \cdot M_{EO} + M_{4a} = 46 \cdot 44 \frac{g}{mol} + 475 \frac{g}{mol} \approx 2500 \frac{g}{mol}$$

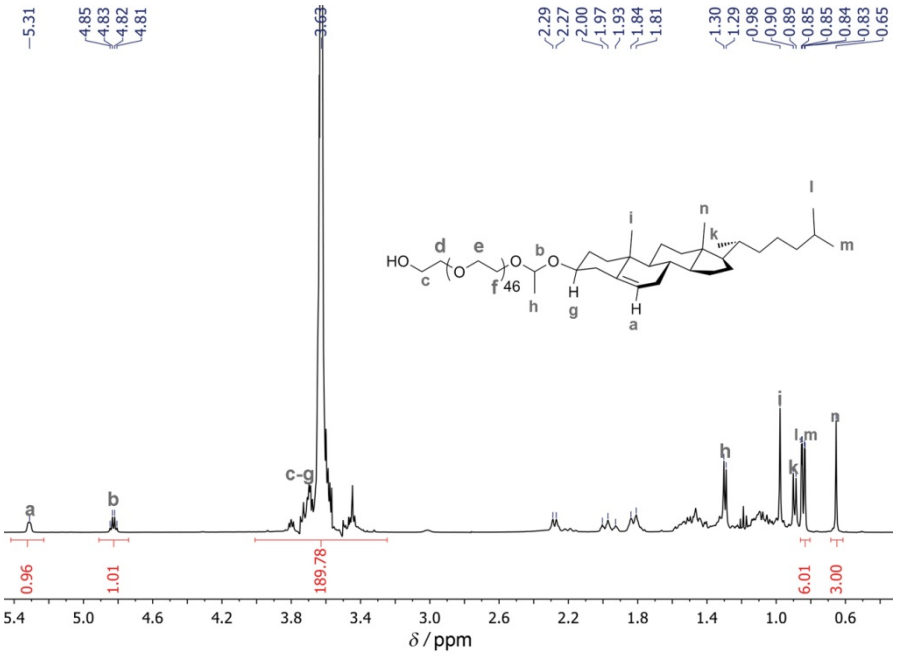

Figure 4. ^{1}H NMR spectrum (400 MHz) of **5** in $CDCl_3$ at T = 294 K. Peak assignment of cholesteryl moiety shown solely for characteristic protons for clarity.

These values are in very good agreement with the theoretically expected ones ($P_n = 45$, $M_n = 2450\ g{\cdot}mol^{-1}$), whereas the M_n derived from SEC analysis (find SEC elugram in the SI, Figure S44) was smaller ($1690\ g{\cdot}mol^{-1}$). The underestimation of M_n found by SEC results from the rather large apolar initiating moiety, which leads to a contraction of the polyether coil to reduce initiator/solvent interactions. Nevertheless, the SEC elugram corresponded to a well-defined polymer with a polydispersity index of 1.08. Since cholesteryl PEGs are known to be amphiphilic and form micelles in aqueous solutions, the critical micelle concentration of **5** was determined by measuring the surface tension of aqueous solutions of the scissile cholesteryl PEG with a ring tensiometer. **5** has a CMC of $4.20 \pm 0.39\ mg{\cdot}L^{-1}$, which is in the order of CMCs expected for amphiphilic polyethers of similar molecular weights.[54, 59]

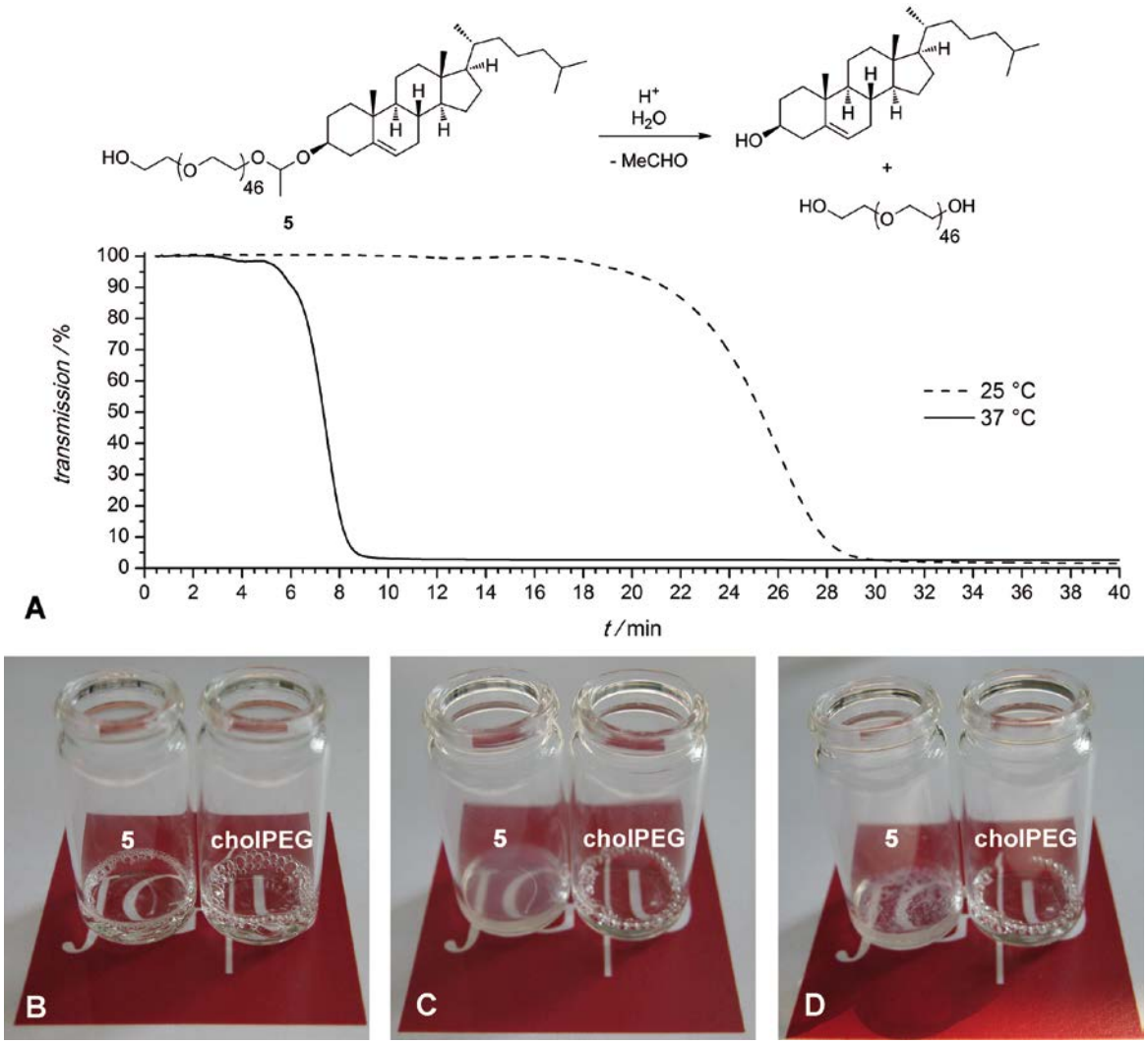

Figure 5. Acidic cleavage of scissile cholesteryl PEG **5**. **A** Cleavage followed by turbidimetry ($\lambda = 528$ nm) at pH 1 for two different temperatures (25°C and 37°C). **B-D** Photographs of **5**'s cleavage in comparison to regular cholesteryl PEG (cholPEG). **B** Aqueous polymer solutions. **C** Onset of cholesterol precipitation after addition of hydrochloric acid. **D** Precipitated cholesterol in case of scissile cholesteryl PEG **5**.

The degradability of **5** was demonstrated by acidic hydrolysis of the acetal, followed by turbidimetry at pH 1. In Figure 5A the relative transmission is plotted against the reaction time for two different temperatures (T = 25 °C and T = 37 °C). After an initial period the solutions started to turn turbid, as the released cholesterol precipitated and the transmission began to decrease. Finally, so much cholesterol had precipitated that almost all light was scattered. As expected, cholesterol was released faster at higher reaction temperature as indicated by the shorter initial phase and the more negative slope of the trace.

Complete removal of the steroid was confirmed by ^{1}H NMR spectra recorded of both, the precipitate as well as the residue of the aqueous phase of a similar experiment (Photographs of this experiment are shown in Figure 2B-D, find protocol in the SI).The former shows a clean cholesterol spectrum, despite of some water (SI, Figure S29), whereas the latter just exhibits pure PEG diol (SI, Figure S30).

B.2 Scissile heterofunctional PEGs. Poly(ethylene glycol)s with cleavable terminal functionalities can be used to covalently bind PEG to different substrates such as other synthetic polymers, proteins, or small molecular weight drug molecules and subsequently release the substrate upon a suitable trigger. As mentioned before, such materials have been described in the past, but most of these approaches are based on the extensive modification of monofunctional mPEGs and do not allow any further modification of the polyether, such as the addition of a labeling or targeting moiety.

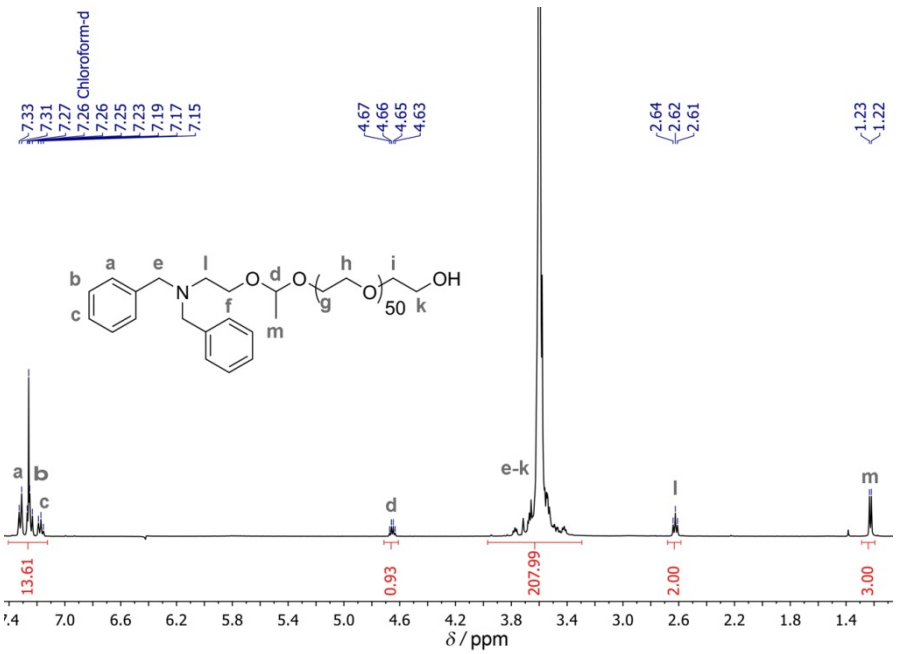

Figure 6. ^{1}H NMR spectrum (400 MHz) of $\mathbf{6}_{50}$ recorded in $CDCl_3$.

Three cleavable heterofunctional polymers $\mathbf{6}_{Pn}$ were synthesized with varying degrees of polymerization and characterized by standard methods. The proton NMR spectrum (Figure 6) was referenced to the methyl group of the acetal and exhibits full incorporation of the initiator. The degree of polymerization and the number-averaged molecular weights were calculated from the integral values using the following equation, where I_{PEG} is the integral of the backbone peak.

$$P_n = \frac{3}{4} \cdot \frac{I_{PEG} - 10}{I_{Me}}$$

$$M_{\boldsymbol{n}} = P_n \cdot M_{EO} + M_{\boldsymbol{4b}} = P_n \cdot 44\frac{g}{mol} + 329\frac{g}{mol}$$

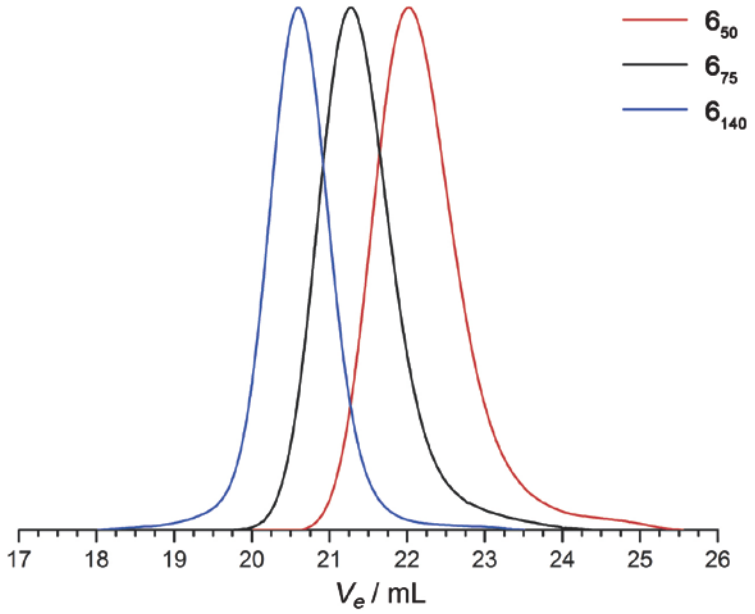

Figure 7. SEC elugrams of **6** with various degrees of polymerization; RI detector signal.

All molecular weights found were in good agreement with the calculated theoretical values as well as those determined by SEC (elugrams shown in Figure 7) and are summarized in Table 1. , The SEC elugrams of all samples (Figure 7) revealed monomodal traces of well-defined polymers with *PDI*s lower than 1.08. Full incorporation of the initiator was further confirmed by the MALDI-ToF MS (Figure 8). All mass-averaged peaks satisfied the following equation:

$$M_{\mathbf{6}}(n) = M_{\mathbf{4b}} + n \cdot M_{EO} + M_{K^+} = 329.4\frac{g}{mol} + n \cdot 44.05\frac{g}{mol} + 39.1\frac{g}{mol}$$

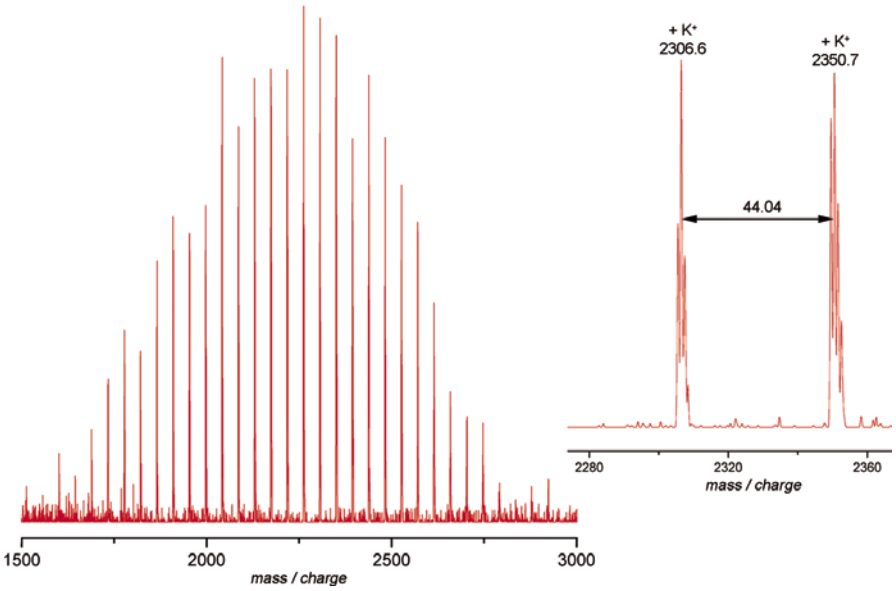

Figure 8. MALDI-ToF mass spectrum of $\mathbf{6_{50}}$ and detail. Masses given for averaged signals, mass difference calculated from monoisotopic peaks. Spectrum was recorded in reflectron mode.

In conclusion, we successfully applied **4b** as an initiator for the oxyanionic polymerization of ethylene oxide and confirmed its full incorporation into well-defined poly(ethylene glycol)s with adjustable molecular weights.

To obtain heterofunctional polyethers, all samples of **6** were hydrolyzed to the corresponding α-amino-ω-hydro PEGs $\mathbf{7_{50}}$, $\mathbf{7_{75}}$, and $\mathbf{7_{140}}$. Complete removal of the benzyl groups was verified by the absence of aromatic signals in the ^{1}H NMR spectrum (exemplary spectrum of $\mathbf{7_{50}}$ shown in the Supporting Information, Figure S26). The residual initiator proton signals (quadruplet of methine at 4.68 ppm, triplet of methylene adjacent to the amino group at 2.65 ppm, and doublet of methyl group at 1.20 ppm) were still observed. The degrees of polymerization, determined by the following equation, were in good agreement with those of the corresponding precursors (Table 1). Hence, no cleavage of the acetal occurred during the hydrogenation step.

$$P_n = \frac{3}{4} \cdot \frac{I_{PEG} - 6}{I_{Me}}$$

The MALDI-ToF mass spectra of **7** (SI, Figures S40-S42) supported this result, as each of them revealed the distribution of mass peaks of the desired species. .

As mentioned in a previous study, PEGs carrying a terminal amino group exhibit an apparent broadening of the molecular weight distributions in SEC analysis with our system.[51] This effect was also observed for all samples of **7** (exemplary SEC elugram of $\mathbf{7_{50}}$ shown in SI, Figure S45)

which is why no reasonable molecular weight average and thus no *PDI* could be determined by SEC. However, upon derivatization of the amino group SEC revealed a well-defined PEG with narrow molecular weight distribution (*vide infra*).

Table 1. Characteristic data of scissile heterofunctional PEGs **6**, **7**, and **10**.

Polymer	M_n[a] / g·mol^{-1}	M_n[b] / g·mol^{-1}	M_n[c] / g·mol^{-1}	M_w[c] / g·mol^{-1}	P_n[b]	*PDI*[c]
$\mathbf{6}_{50}$	2320	2510	2140	2320	50	1.08
$\mathbf{6}_{75}$	3330	3630	3040	3260	75	1.07
$\mathbf{6}_{140}$	5730	6490	5590	5900	140	1.06
$\mathbf{7}_{50}$	2330	2400	-[d]	-[d]	51	-[d]
$\mathbf{7}_{75}$	3450	3470	-[d]	-[d]	75	-[d]
$\mathbf{7}_{140}$	6310	6500	-[d]	-[d]	144	-[d]
10	3570	3610	3160	3360	76	1.06

[a] Calculated. [b] Determined by ^{1}H NMR. [c] Determined by SEC, referenced to PEG standards. [d] Not determined, due to apparent broadening of molecular weight distribution in SEC analysis.

In order to confirm the accessibility of **7**'s cleavable terminal amino group for further derivatization reactions and activate the polyether for the bioconjugation with proteins, the recently established conversion of α-amino-ω-hydroxyl PEGs into the corresponding squaric acid ester amides[51] was carried out. $\mathbf{7}_{75}$ was reacted with diethyl squarate to yield **10** (Scheme 4).

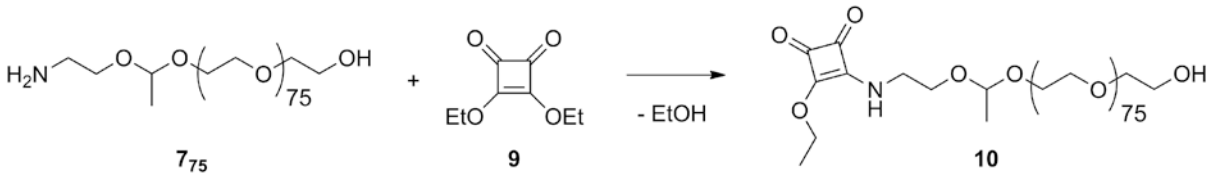

$\mathbf{7}_{75}$ **9** **10**

Scheme 4. Synthetic route to scissile squaric acid ester amido PEGs.

In Figure 9 the superimposed SEC traces of **10** and its precursors $\mathbf{6}_{75}$ and $\mathbf{7}_{75}$ are shown. The SEC elugrams of **10** and $\mathbf{6}_{75}$ exhibited monomodal traces of well-defined polymers with corresponding molecular weight distributions. The *PDI* of **10** (1.06) was slightly lower than the *PDI* found for $\mathbf{6}_{75}$ (1.07) which was attributed to a loss of a small low-molecular weight fraction of the polymer upon repetitive precipitation of **10** in cold diethyl ether during the work-up. Full

conversion of the amino terminus to the squaric acid ester amide and complete retention of the acetal was verified by MALDI-ToF MS. The mass spectrum (SI, Figure S43) shows the expected distribution of potassium cationized polymer peaks. In the ^{1}H NMR spectrum of **10** (SI, Figure S28), the methyl protons showed an isolated signal around 1.28 ppm, whereas the corresponding methylene signal was superimposed by the acetal methine resonance at 4.76 ppm. The P_n determined from the NMR spectrum is in very good agreement with the values calculated for the amino PEG precursor. However, a small amount (< 5 mol%) of acetaldehyde was detected in the proton NMR spectrum. Since the ethyl ester's methyl group integrated to the expected value, the MALDI-ToF MS detected a single distribution, and TLC of **10** showed a single UV-active compound, the detected partial acetal cleavage had occurred in the NMR tube.

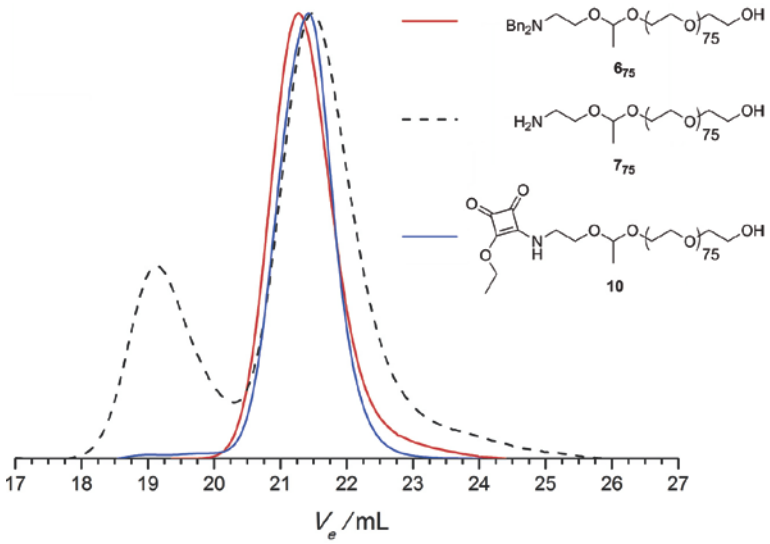

Figure 9. SEC elugrams of $\mathbf{6}_{75}$ (red, RI detector), $\mathbf{7}_{75}$ (dotted black, RI detector) and **10** (blue, UV detector). Note, that amino PEGs often revealed a broadening of the mass distribution in the SEC analysis (on our system) leading to a seeming increase of the *PDI*.

A closer look was taken on the acidic cleavage of the acetals by following the hydrolysis of the α-(1-(2-dibenzylamino ethoxy)ethoxy) ω-hydro PEG $\mathbf{6}_{75}$ at 37 °C in acidic D_2O solutions with various pD values (pD 2.4, pD 4.4, pD 4.9, and pD 5.4) with ^{1}H NMR spectroscopy. All integrals were referenced to the aromatic resonances of the benzyl groups and the integral of the acetal methyl signal was monitored to determine the residual acetal. The acidic acetal cleavage was also investigated for **10** at pD 4.9 in an experiment analogous to those described before. In Figure 10 the normalized integral values of the residual acetals of $\mathbf{6}_{75}$ and **10** are plotted against time (find corresponding NMR spectra in the SI, Figures S48-S52). Since the solvent served as a

reagent in the degradation and the samples were diluted ($c_6 = 5.74$ mM, $c_{10} = 2.38$ mM), it was assumed that acetal hydrolysis followed pseudo-first order kinetics and therefore, the experimental data was fitted with an exponential decay function:

$$I_{\mathbf{6_{75}}}(\mathrm{pD}, t) = e^{-k_{D_2O}t} \cdot I_{\mathbf{6_{75}}}(\mathrm{pD}, t = 0).$$

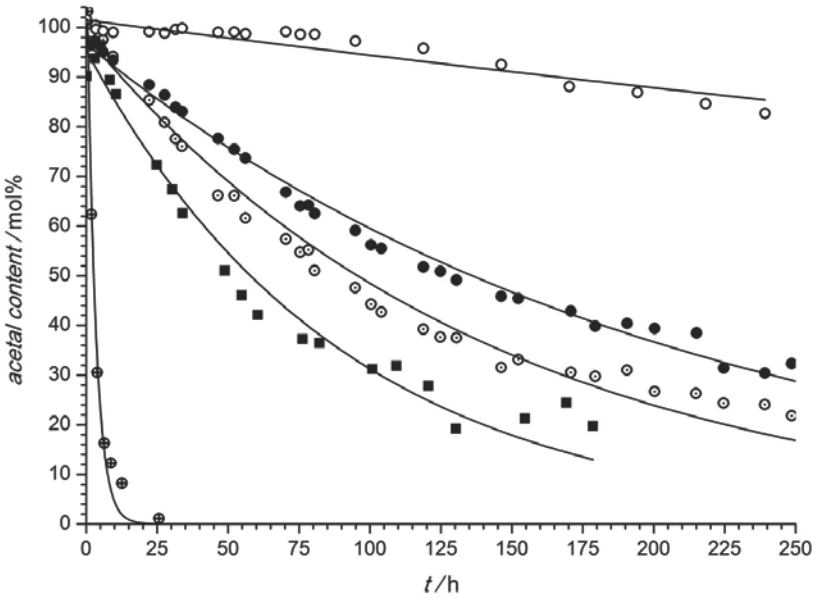

Figure 10. Acidic cleavage of scissile PEGs $\mathbf{6_{75}}$ (circles) and **10** (squares) in deuterium oxide followed by ^{1}H NMR spectroscopy at various pD values at $T = 37$ °C. Crossed circles: pD 2.4. Dotted circles: pD 4.4. Full circles/squares: pD 4.9. Open circles: pD 5.4. Solid lines: Exponential fits.

The cleavage rate constants in deuterium oxide kD2O and corresponding half-lives t1/2 of all hydrolyses were calculated from the exponential fits and are listed in Table 2. Similar to the acidic degradation of recently presented poly(glycidyloxyethyl ethylene glycol ether) (PGEGE) copolymers,[44] a strong pH-dependence of the degradation kinetics was observed. At pD 2.4 half the amount of $\mathbf{6_{75}}$ had been hydrolyzed after two hours, whereas at pD 5.4 the polymer exhibited a half-life of over a month ($t_{1/2} = 40 \pm 4$ d). Most interestingly, **10** degrades much faster than $\mathbf{6_{75}}$ under the same conditions. The basic tertiary amino group adjacent to the acetal of $\mathbf{6_{75}}$ is protonated and carries a positive charge in acidic media. Hence, the pre-equilibrium protonation of one of the acetal oxygens (due to the Coulomb forces most probably the one at the PEG side), which occurs prior to the cleavage of the acetal carbon-oxygen bond,[60] is hindered, and therefore the hydrolysis rate of $\mathbf{6_{75}}$ is comparably low. The corresponding nitrogen of **10** will not be protonated, since its electron lone pair is delocalized in the squaric

acid amide bond, resulting in a faster acetal cleavage. Nevertheless, squaric acid amides are known to be protophilic[61] and **10** will be protonated at its squaric acid moiety to some extent. This is why under comparable conditions the half-life of **10** is longer than that of Bn_2NTrisP(G-*co*-GEGE), whose focal amino group is spatially separated from most of its acetaldehyde acetals.[44] Unfortunately, these values cannot be transferred directly to protic systems, as it has to be taken into account that the kinetic deuterium isotope effect for the hydrolysis of (simple) non-cyclic acetals in water is around $k_{D+}/k_{H+} = 2.6\text{-}2.7$.[60]

Table 2. Acetal cleavage rate constants and half-lives of scissile PEGs in acidic deuterium oxide.

Polymer	pD	k_{D2O} / s^{-1}	$t_{1/2}$ / h
$\mathbf{6}_{75}$	2.4	1180 ± 100	2.12 ± 0.18
$\mathbf{6}_{75}$	4.4	25.4 ± 0.7	98.2 ± 2.9
$\mathbf{6}_{75}$	4.9	17.4 ± 0.3	143.1 ± 2.9
$\mathbf{6}_{75}$	5.4	2.60 ± 0.23	961.4 ± 86.2
10	4.9	40.2 ± 1.9	62.1 ± 3.0

B.3 PEG with scissile backbone. Well-defined functional PEGs with a cleavable group in the backbone can be synthesized rapidly with our methodology using an AROP macroinitiator such as 1-(2-hydroxyethoxy)ethoxy mPEG (**4c**). The amount of EO batched in the polymerization was calculated to add a PEG block with a number-averaged molecular weight of 6.0 kg·mol^{-1}, allowing separation and distinction of this block from the macroinitiator precursor (2.0 kg·mol^{-1}) via SEC upon acidic cleavage of the acetal. For the interpretation of the ^{1}H NMR spectrum of the scissile mPEG **8** (SI, Figure S27) the peak integrals were again referenced to the signal of the methoxy group. Except for the larger backbone signal the spectrum was almost identical to that of the precursor. In agreement with the expected theoretical value the M_n was calculated from the ^{1}H NMR spectrum to be 7.9 kg·mol^{-1} using the following equation:

$$M_n = P_n \cdot M_{EO} + M_{CH_3OH} = \frac{3}{4} \cdot \frac{I_{PEG}}{I_{CH_3}} \cdot 44 \frac{g}{mol} + 32 \frac{g}{mol}$$

This value also corresponds well to the M_n determined from the SEC trace (7.5 kg·mol^{-1}, elugram shown in Figure 11). Note, that the trace was referenced to a PEG standard. Compared to the macroinitiator the molecular weight distribution became broader and the polydispersity index increased to 1.09, still indicating a well-defined polyether. The cleavability of the in-chain acetal in acidic media was demonstrated by stirring the scissile mPEG **8** in aqueous 0.11 M *p*-toluene sulfonic acid for 3 h at room temperature. In Figure 11 the normalized SEC elugrams of **8** before and after degradation as well as its mPEG precursor **1c** are shown. Note, that the degraded sample exhibits a bimodal trace and the mode corresponding to a smaller hydrodynamic radius fits well to that of **1c**. The second mode is clearly shifted to a lower molecular weight in comparison to the SEC trace of **8** and was clearly assigned to the PEG block polymerized onto **4c**. Both modes of the degraded sample corresponded to narrowly distributed PEGs with number-averaged molecular weights of about 1.8 kg·mol^{-1} and 5.7 kg·mol^{-1}, respectively, which is in very good agreement with the expected values. Hence, we successfully demonstrated the incorporation of a single acetal into the backbone of well-defined poly(ethylene glycol) monomethyl ether with full control over its position in the chain and the final cleavability of that moiety under acidic conditions.

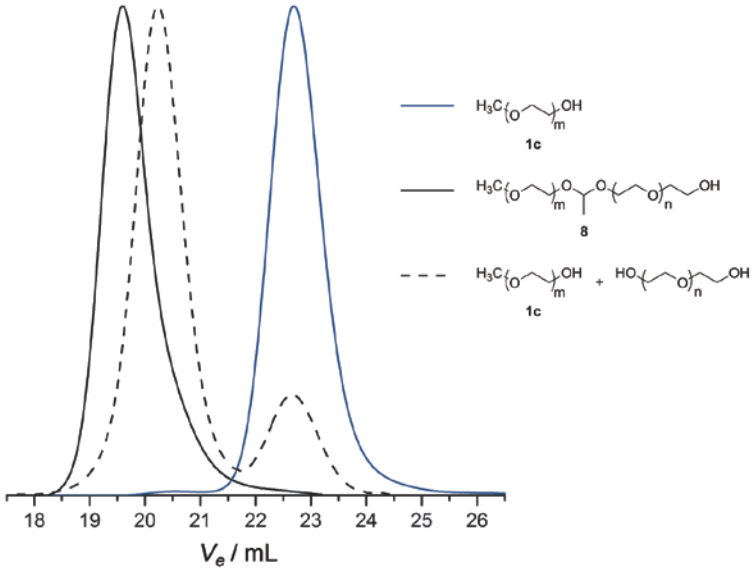

Figure 11. SEC elugrams of mPEG **1c** (blue), and scissile mPEG **8** (black) before and after acetal cleavage. RI detector channel.

C. Exploratory Results on Bioconjugation to BSA. 13 equivalents of **10** were coupled to BSA using a protocol for the squaric acid mediated PEGylation recently published by our group.[51] Successful covalent attachment of the acetal-containing squaric acid amido PEGs was

evidenced by SDS-PAGE. In Figure 12 the Coomassie Blue-stained gel obtained from the electrophoresis is shown. Compared to BSA (lane 2) the BSA-PEG conjugate (lane 6) exhibits a clear shift towards higher molecular masses. Lane 2 further reveals the presence of a fraction of dimerized BSA, which also was PEGylated completely (high-molecular weight band in lane 6). The polydispersity of both the molecular weight of the synthetic polyether and the number of polymer chains attached to the protein result in the clear broadening of the protein-polymer conjugate band.

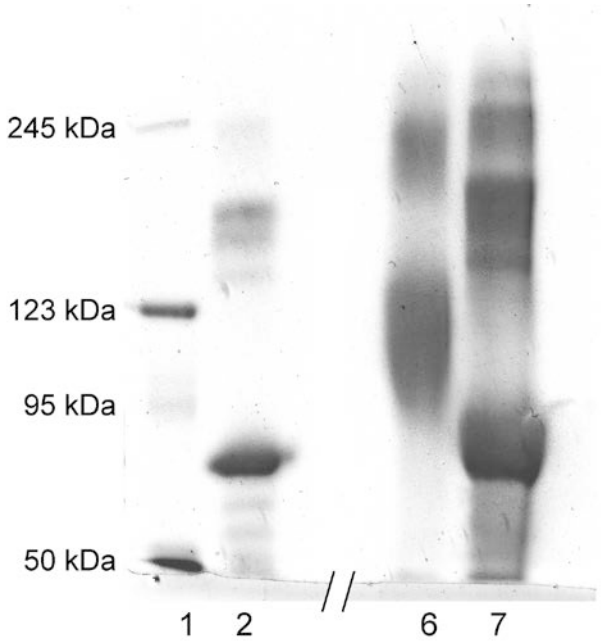

Figure 12. SDS-PAGE of PEGylated BSA. Lane1: MW marker. Lane 2: BSA. Lane 6: BSA PEGylated with **10**. Lane 7: PEGylated BSA after acidic treatment.

To proof the cleavability of the acetals and the resulting release of BSA, the synthesized BSA-PEG conjugate was hydrolyzed in 1 N hydrochloric acid. SDS-PAGE of the product (Figure 12, lane 7) exhibits complete release of the protein, which migrated the same distance through the gel as the unmodified BSA. This is also true for the dimer. The slight broadening of the bands was attributed to the polydisperse number of squaramide linkers still attached to the protein. In conclusion, we successfully demonstrated that the incorporation of an acetal moiety into squaric acid amido PEGs does not decrease their applicability as PEGylation agents, but gives access to acid sensitive protein-PEG conjugates. The detachment of the polyether from the conjugate under physiologically more relevant conditions is under current investigation.

Conclusion

We have developed the implementation of an acetaldehyde acetal into initiators for the anionic ring-opening polymerization of oxiranes, following a straightforward two-step protocol. Its general applicability to a variety of acid stabile AROP initiators has been demonstrated by the conversion of a diverse set of chemically different alcohols: Cholesterol, dibenzylamino ethanol and poly(ethylene glycol) monomethyl ether. Upon polymerization of EO onto the obtained low molecular weight initiators, polyethers with cleavable initiator moieties, but completely different properties were generated.

The PEG carrying the scissile cholesterol unit is an amphiphile with a CMC of 4.20 $mg \cdot L^{-1}$, whereas the cleavable heterofunctional PEGs obtained from dibenzylamino ethanol could be subsequently derivatized and activated for the recently described squaric acid mediated PEGylation. The latter was proven in a first exploratory model reaction to BSA. In the case of the scissile macroinitiator, PEG carrying a single acetal moiety in the backbone of the polymer was synthesized. All PEGs were characterized by NMR spectroscopy, MALDI ToF mass spectrometry and size-exclusion chromatography (SEC). The incorporation of a single acetal unit at the desired position was verified for each of the well-defined polyethers (*PDI*s $\leq$ 1.09). All of the obtained polymers and the PEGylated BSA were proven to be cleaved at the acetal moieties in acidic media.

In conclusion, we established a rapid methodology to incorporate a single acid labile moiety at a desired position in well-defined functional poly(ethylene glycol)s. These materials are highly interesting for the development of new pharmaceuticals as well as for materials science. Possible applications of the acid sensitive cholesteryl PEGs, e. g. for the reversible stabilization of liposomes or acid sensors are subjects to ongoing studies. Also, the PEGylation of other proteins than BSA with the scissile polyethers, the pharmaceutical properties of the conjugates, especially the *in vivo* bioactivities, as well as their toxicities are under current investigation.

Acknowledgment

The authors are thankful to Jacky Thill, Eric Hoffmann, Alina Mohr, and Margarete Deptolla for technical support. C.D. is grateful to the Max Planck Graduate Center with the Johannes Gutenberg-Universität Mainz (MPGC) for a fellowship and financial support.S.S.M., and T.S. are recipients of a fellowship through funding of the Excellence Initiative (DFG/GSC 266) in the context of the graduate school of excellence "MAINZ" (Materials Science in Mainz).

References

[1] A. Abuchowski, T. van Es, N. C. Palczuk, F. F. Davis, *J. Biol. Chem.* **1977**, *252*, 3578.

[2] A. Abuchowski, J. R. McCoy, N. C. Palczuk, T. van Es, F. F. Davis, *J. Biol. Chem.* **1977**, *252*, 3582.

[3] P. Caliceti, F. M. Veronese, *Adv. Drug Del. Rev.* **2003**, *55*, 1261.

[4] J. M. Harris, R. B. Chess, *Nat. Rev. Drug Discov.* **2003**, *2*, 214.

[5] F. M. Veronese, G. Pasut, *Drug Discovery Today* **2005**, *10*, 1451.

[6] G. Pasut, M. Sergi, F. M. Veronese, *Adv. Drug Del. Rev.* **2008**, *60*, 69.

[7] S. N. S. Alconcel, A. S. Baas, H. D. Maynard, *Polym. Chem.* **2011**, *2*, 1442.

[8] S. Zalipsky, *Adv. Drug Del. Rev.* **1995**, *16*, 157.

[9] M. J. Roberts, J. Milton Harris, *J. Pharm. Sci.* **1998**, *87*, 1440.

[10] D. Filpula, H. Zhao, *Adv. Drug Del. Rev.* **2008**, *60*, 29.

[11] V. Knorr, L. Allmendinger, G. F. Walker, F. F. Paintner, E. Wagner, *Bioconjugate Chem.* **2007**, *18*, 1218.

[12] J. A. Boomer, D. H. Thompson, *Chem. Phys. Lipids* **1999**, *99*, 145.

[13] X. Guo, F. C. Szoka, *Bioconjugate Chem.* **2001**, *12*, 291.

[14] C. Masson, M. Garinot, N. Mignet, B. Wetzer, P. Mailhe, D. Scherman, M. Bessodes, *J. Controlled Release* **2004**, *99*, 423.

[15] H. Hatakeyama, H. Akita, K. Kogure, M. Oishi, Y. Nagasaki, Y. Kihira, M. Ueno, H. Kobayashi, H. Kikuchi, H. Harashima, *Gene Ther.* **2006**, *14*, 68.

[16] R. M. Sawant, J. P. Hurley, S. Salmaso, A. Kale, E. Tolcheva, T. S. Levchenko, V. P. Torchilin, *Bioconjugate Chem.* **2006**, *17*, 943.

[17] H. Xu, Y. Deng, D. Chen, W. Hong, Y. Lu, X. Dong, *J. Controlled Release* **2008**, *130*, 238.

[18] J. B. Wong, S. Grosse, A. B. Tabor, S. L. Hart, H. C. Hailes, *Mol. BioSyst.* **2008**, *4*, 532.

[19] J. A. Boomer, M. M. Qualls, H. D. Inerowicz, R. H. Haynes, V. S. Patri, J.-M. Kim, D. H. Thompson, *Bioconjugate Chem.* **2008**, *20*, 47.

[20] R. Kuai, W. Yuan, Y. Qin, H. Chen, J. Tang, M. Yuan, Z. Zhang, Q. He, *Mol. Pharm.* **2010**, *7*, 1816.

[21] D. Chen, X. Jiang, Y. Huang, C. Zhang, Q. Ping, *J. Bioact. Compat. Polym.* **2010**, *25*, 527.

[22] G. Pasut, F. M. Veronese, *Prog. Polym. Sci.* **2007**, *32*, 933.

[23] T. Yamaoka, Y. Tabata, Y. Ikada, *J. Pharm. Sci.* **1994**, *83*, 601.

[24] H. Ringsdorf, *J. Polym. Sci., Polym. Symp.* **1975**, *51*, 135.

[25] Y. Matsumura, H. Maeda, *Cancer Res.* **1986**, *46*, 6387.

[26] L. W. Seymour, *Crit. Rev. Ther. Drug Carrier Syst.* **1992**, *9*, 135.

[27] M.-C. DuBois Clochard, S. Rankin, S. Brocchini, *Macromol. Rapid Commun.* **2000**, *21*, 853.

[28] R. Tomlinson, J. Heller, S. Brocchini, R. Duncan, *Bioconjugate Chem.* **2003**, *14*, 1096.

[29] R. Tomlinson, M. Klee, S. Garrett, J. Heller, R. Duncan, S. Brocchini, *Macromolecules* **2002**, *35*, 473.

[30] J. Rickerby, R. Prabhakar, M. Ali, J. Knowles, S. Brocchini, *J. Mater. Chem.* **2005**, *15*, 1849.

[31] Y. Wang, H. Morinaga, A. Sudo, T. Endo, *J. Polym. Sci., Part A: Polym. Chem.* **2011**, *49*, 596.
[32] A. Braunová, M. Pechar, R. Laga, K. Ulbrich, *Macromol. Chem. Phys.* **2007**, *208*, 2642.
[33] B. Reid, S. Tzeng, A. Warren, K. Kozielski, J. Elisseeff, *Macromolecules* **2010**, *43*, 9588.
[34] P. Lundberg, B. F. Lee, S. A. van den Berg, E. D. Pressly, A. Lee, C. J. Hawker, N. A. Lynd, *ACS Macro Lett.* **2012**, *1*, 1240.
[35] T. W. Greene, P. G. M. Wuts, *Protective groups in organic synthesis*, 3rd ed., Wiley, New York, **1999**.
[36] K. B. Wagener, S. Wanigatunga, *Macromolecules* **1987**, *20*, 1717.
[37] Y. Akiyama, H. Otsuka, Y. Nagasaki, M. Kato, K. Kataoka, *Bioconjugate Chem.* **2000**, *11*, 947.
[38] Y. Akiyama, Y. Nagasaki, K. Kataoka, *Bioconjugate Chem.* **2004**, *15*, 424.
[39] X. Feng, D. Taton, E. L. Chaikof, Y. Gnanou, *Biomacromolecules* **2007**, *8*, 2374.
[40] X. Fan, B. Huang, G. Wang, J. Huang, *Macromolecules* **2012**, *45*, 3779.
[41] D. Taton, A. Le Borgne, M. Sepulchre, N. Spassky, *Macromol. Chem. Phys.* **1994**, *195*, 139.
[42] F. Wurm, J. Nieberle, H. Frey, *Macromolecules* **2008**, *41*, 1909.
[43] X. Feng, E. L. Chaikof, C. Absalon, C. Drummond, D. Taton, Y. Gnanou, *Macromol. Rapid Commun.* **2011**, *32*, 1722.
[44] C. Tonhauser, C. Schüll, C. Dingels, H. Frey, *ACS Macro Lett.* **2012**, *1*, 1094.
[45] R. A. Shenoi, J. K. Narayanannair, J. L. Hamilton, B. F. L. Lai, S. Horte, R. K. Kainthan, J. P. Varghese, K. G. Rajeev, M. Manoharan, J. N. Kizhakkedathu, *J. Am. Chem. Soc.* **2012**, *134*, 14945.
[46] R. A. Shenoi, B. F. L. Lai, J. N. Kizhakkedathu, *Biomacromolecules* **2012**, *13*, 3018.
[47] K. Satoh, J. E. Poelma, L. M. Campos, B. Stahl, C. J. Hawker, *Polym. Chem.* **2012**, *3*, 1890.
[48] B. W. Greenland, S. Liu, G. Cavalli, E. Alpay, J. H. G. Steinke, *Polymer* **2010**, *51*, 2984.
[49] D. Dix, P. Imming, *Arch. Pharm.* **1995**, *328*, 203.
[50] F. Wurm, A. M. Hofmann, A. Thomas, C. Dingels, H. Frey, *Macromol. Chem. Phys.* **2010**, *211*, 932.
[51] C. Dingels, F. Wurm, M. Wagner, H.-A. Klok, H. Frey, *Chem. Eur. J.* **2012**, *18*, 16828.
[52] J. W. Blunt, J. B. Stothers, *Org. Magn. Reson.* **1977**, *9*, 439.
[53] P. Muhr, W. Likussar, M. Schubert-Zsilavecz, *Magn. Reson. Chem.* **1996**, *34*, 137.
[54] H. Ishiwata, A. Vertut-Doi, T. Hirose, K. Miyajima, *Chem. Pharm. Bull.* **1995**, *43*, 1005.
[55] A. Vertut-Doi, H. Ishiwata, K. Miyajima, *Biochim. Biophys. Acta, Biomembr.* **1996**, *1278*, 19.
[56] A. M. Hofmann, F. Wurm, E. Hühn, T. Nawroth, P. Langguth, H. Frey, *Biomacromolecules* **2010**, *11*, 568.
[57] M. A. López-Quintela, A. Akahane, C. Rodríguez, H. Kunieda, *J. Colloid Interface Sci.* **2002**, *247*, 186.
[58] J.-T. Xu, L. Xue, Z.-Q. Fan, Z.-H. Wu, J. K. Kim, *Macromolecules* **2006**, *39*, 2981.

[59] A. M. Hofmann, F. Wurm, H. Frey, *Macromolecules* **2011**, *44*, 4648.
[60] E. H. Cordes, *Prog. Phys. Org. Chem.* **1967**, *4*, 1.
[61] D. Quinonero, A. Frontera, P. Ballester, P. M. Deyá, *Tetrahedron Lett.* **2000**, *41*, 2001.

Supporting Information

A Universal Concept for the Implementation of a Single Cleavable Unit in Functional Poly(ethylene glycol)s

Carsten Dingels, Sophie S. Müller, Tobias Steinbach, Christine Tonhauser, and Holger Frey

Table of contents

1. Synthetic protocols

1.1 Reaction kinetics of the synthesis of Acetoxyethyl 1-(2-dibenzylamino ethoxy)ethyl ether (**3b**) followed by ^{1}H NMR spectroscopy.

AcVE (**2**, 50 mg, 0.38 mmol) and dibenzylamino ethanol (**1b**, 50 mg, 0.21 mmol) were dissolved in $CDCl_3$ (350 µL each) in separate vials. Trifluoroacetic acid (71 mg, 0.62 mmol) was added to the amine containing vial and the reaction was started by combining both solutions in a NMR tube ($t = 0$). After locking and shimming a spectrum was recorded every minute at 294 K with 13 scans and a relaxation delay of 1 s for 40 min. To analyze the mixture of AcVE and **1b** before the beginning of the reaction, an identical reaction solution without TFA was prepared and measured using the described parameters. All signals were integrated in the same limits and all integral values were referenced to the aromatic resonances.

1.2 Reaction kinetics of acidic cleavage of α-(1-(2-Dibenzylamino ethoxy)ethoxy)-ω-hydro PEG $\mathbf{6}_{75}$ followed by 1H NMR spectroscopy.

$\mathbf{6}_{75}$ (25.0 mg, 6.89 µmol) was dissolved in a vial containing 1.200 mL acidic deuterium oxide solution[1] (pD 2.4: diluted D_2SO_4, pD 4.4 and pD 4.9: acetate buffers, pD 5.4: phosphate buffer) and stirred at 310 K. For each ^{1}H NMR measurement an aliquot of 600 µL was placed in a NMR tube and returned to the corresponding stock solution after the spectrum had been recorded. The spectra were recorded at 294 K with 32 scans (16 scans for the sample degraded at pD 2.4) and a relaxation delay of 1 s. All signals were integrated in the same limits and all integral values were referenced to the aromatic resonances. The acetal methyl group was monitored to follow the degradation.

1.3 Reaction kinetics of acidic cleavage of α-(1-(2-(squaric acid ethyl ester amido)ethoxy)ethoxy)-ω-hydro PEG (**10**) followed by 1H NMR spectroscopy.

10 (10.2 mg, 2.85 µmol) was dissolved in a vial containing a deuterated[1] acetate buffer solution (1.200 mL, pD 4.9) and stirred at 310 K. For each ^{1}H NMR measurement an aliquot of 600 µL was placed in a NMR tube and returned to the stock solution after the spectrum had been recorded. All spectra were recorded at 294 K with 32 scans and a relaxation delay of 1 s. The

signals were integrated in the same limits and all integral values were referenced to the polyether backbone signal. The acetal methyl group was monitored to follow the degradation.

1.4 Reaction kinetics of the addition of mPEG (2 kg·mol-1) to AcVE followed by SEC.

The reaction was carried out analogous to a 1.5-fold batch of the described synthesis of 1-(2-Acetoxyethoxy)ethoxy mPEG (**3c**). Every 30 min an aliquot of 5 mL was quenched with sufficient triethylamine. All samples were washed with 1 N NaOH, dried over sodium sulfate and evaporated to small volume. The polymers were precipitated in cold diethyl ether, filtered, and subsequently dried *in vacuo*. Finally, all samples were analyzed via size exclusion chromatography.

1.5 Acidic cleavage of α-(1-(Cholesteryloxy)ethoxy)-ω-hydro PEG (**5**) monitored by turbidimetry.

An aqueous solution of the scissile amphiphile **5** (10 mg·L^{-1}) kept at either $T = 25$ °C or $T = 37$ °C in a cuvette with a width of 10 mm was acidified to pH 1 by adding concentrated hydrochloric acid and subsequently placed in a UV-VIS spectrometer with a tempered measuring cell. Time measurement was started on acidifying the solution and the relative light transmission ($\lambda = 528$ nm) through the cell was recorded.

1.6 Acidic cleavage of α-(1-(Cholesteryloxy)ethoxy)-ω-hydro PEG (**5**) for NMR studies.

2.0 mL of a solution of the scissile cholesteryl PEG **5** (10 g·L^{-1}) and an analogous solution of a poly(ethylene glycol) monocholesteryl ether with comparable molecular weight (2300 g·mol^{-1}) as a control were acidified by the addition of 20 µL of concentrated hydrochloric acid. The solution was centrifuged and the phases separated by decantation. The precipitate was washed with water, dissolved in chloroform-d, and dried over sodium sulfate. The water of the aqueous phase was removed by distillation. Afterwards, the residue was dried in high vacuum at 60 °C and dissolved in chloroform-d. ^{1}H NMR spectra of both, the precipitate as well as the residue of the aqueous phase were recorded.

1.7 Acidic cleavage of α-(1-mPEG ethoxy)-ω-hydro PEG (**8**).

8 (0.20 g, 25µmol) and pTSA (20 mg, 0.11 mmol) were stirred for 3 h in water (1 mL). After the solution had been extracted with DCM three times the organic phases were combined and dried over sodium sulfate. The solution was evaporated to small volume and precipitated in cold diethyl ether.

1.8 Covalent attachment of **10** to BSA.

PEGylation of BSA was carried out analogous to a published protocol for squaric acid mediated PEGylation.[2] BSA (10.2 mg, 155 nmol) and **10** (7.2 mg, 2.0 µmol) were dissolved in aqueous borate buffer (pH 10, 200 µL) and DMSO (85.5 µL) and stirred overnight at room temperature. BSA-PEG conjugate was obtained in quantitative yields after dialysis in water ($MWCO$ = 25 kDa) and subsequent lyophilization.

2. NMR spectra

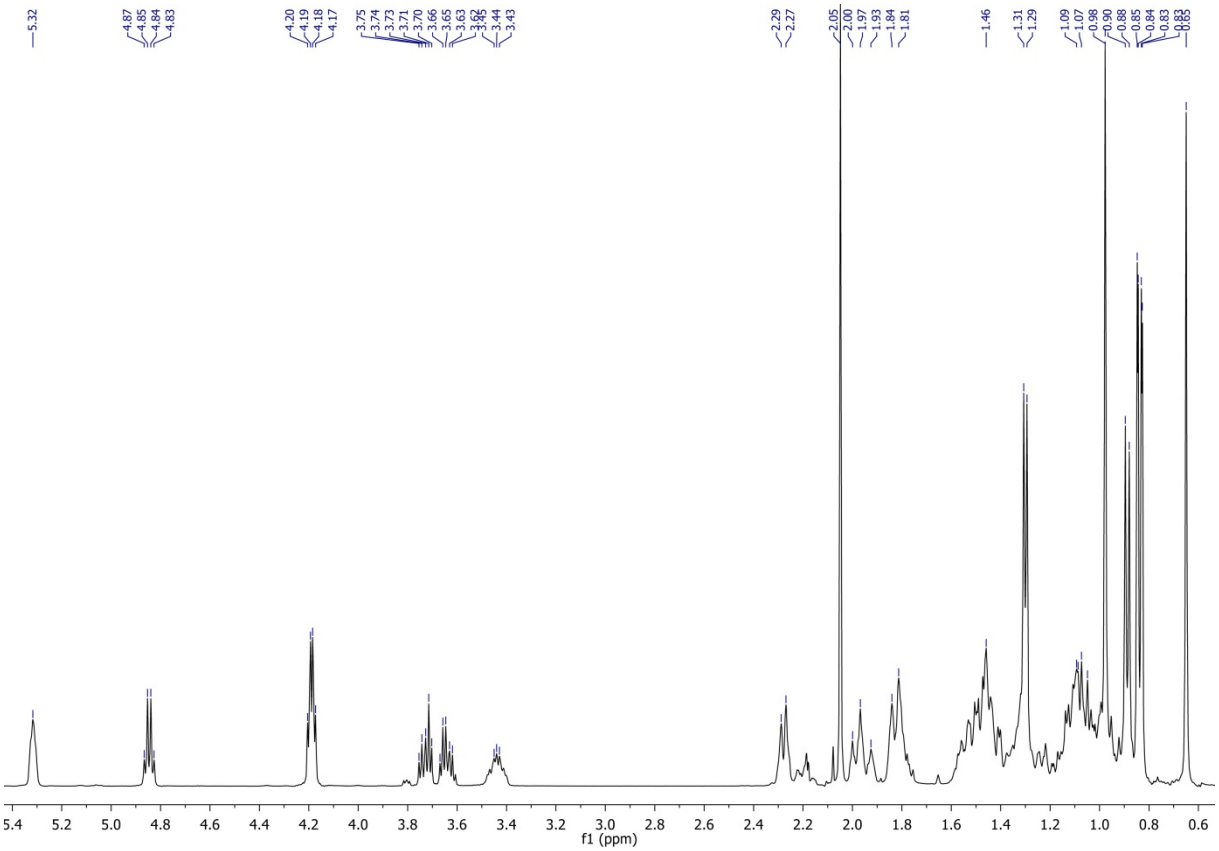

Figure S1. ^{1}H NMR spectrum (400 MHz) of **3a** in $CDCl_3$ at T = 294 K.

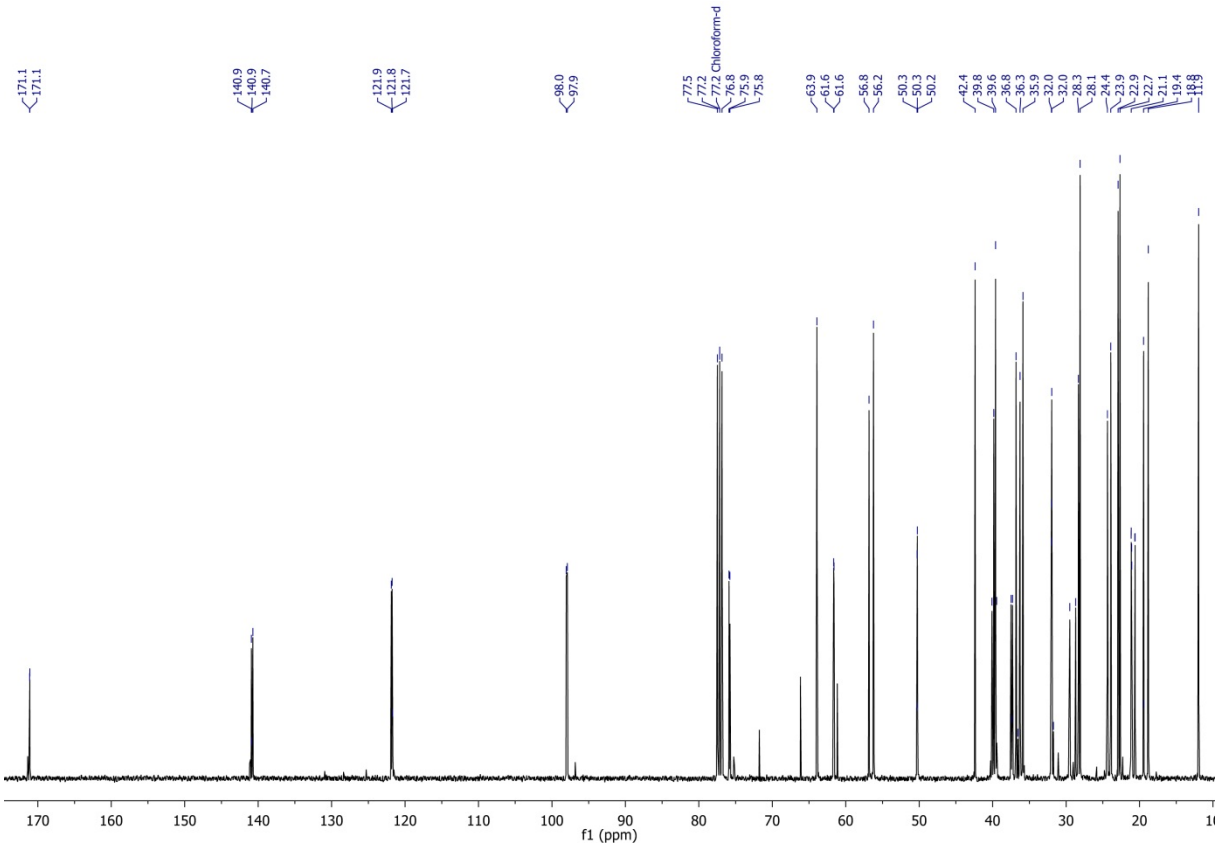

Figure S2. ^{13}C NMR spectrum (100.6 MHz) of **3a** in $CDCl_3$ at T = 294 K.

Note to Figure S2. As AcVE is a prochiral compound, the addition of the diastereopure cholesterol led to the formation of two diastereomers, which were not separated by column chromatography. In the broadband decoupled ^{13}C NMR experiments on 3a, several carbon atoms, mainly those of the steroid's A ring and the acetaldehyde acetal unit, exhibited slightly different chemical shifts in dependence on the configuration of the acetal. In the ^{13}C NMR spectrum of the mixture of diastereomers these carbon atoms appeared as two signals with no significantly different integration values. Hence, none of the two diastereomers was formed in favor over the other. A separation of both diastereomers was not intended, as subsequent to saponification, both will serve as initiators for the polymerization of ethylene oxide equally. Whether a separation becomes necessary for possible applications is under current investigation.

While a proton spectrum of pure **3a** could be recorded (Figure S1), the carbon NMR spectrum revealed a few additional peaks assigned to cholesterol resulting from acetal degradation of the sample in the deuterated chloroform during the much more time-consuming ^{13}C experiments. Acetal cleavage in chloroform-*d* was also observed during proton NMR experiments on α-(1-(2-(squaric acid ethyl ester amido)ethoxy)ethoxy) ω-hydro PEG **10** (Figure S28).

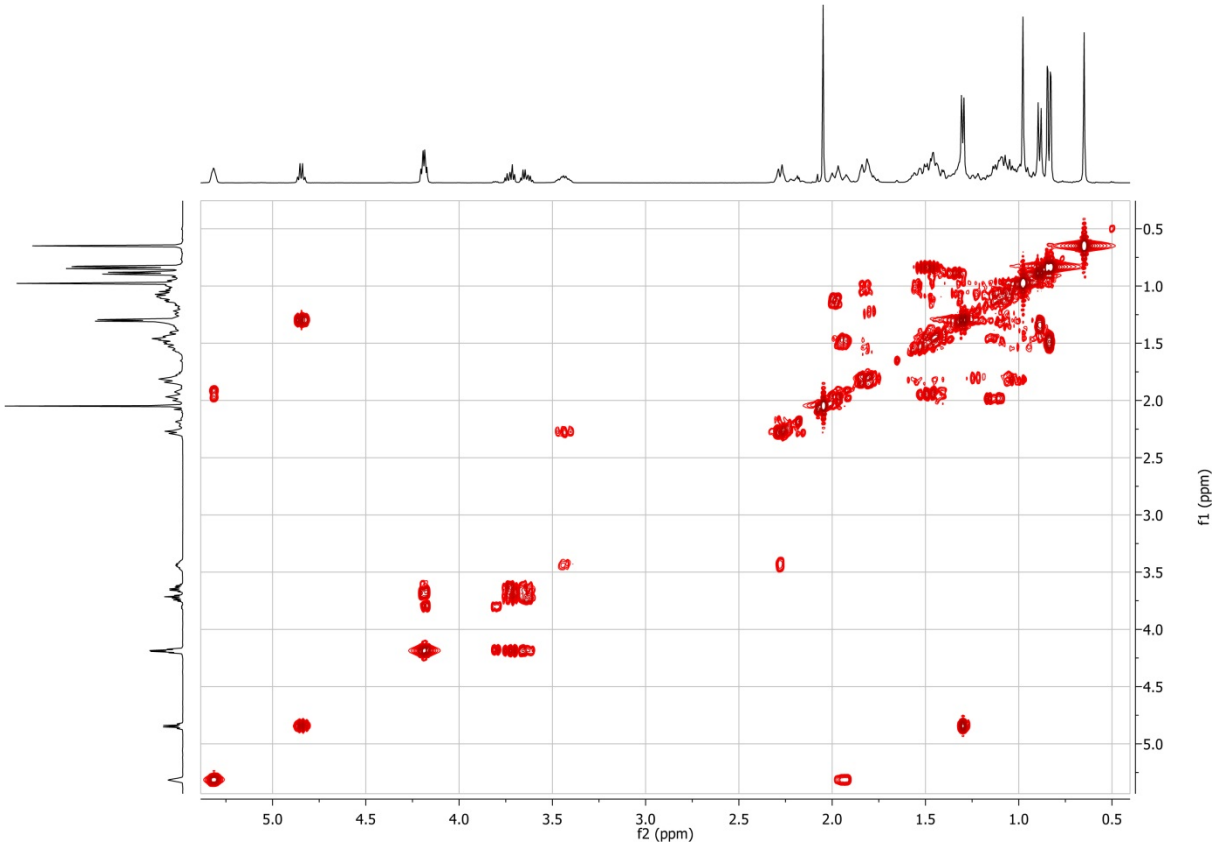

Figure S3. ^{1}H COSY NMR spectrum (400 MHz) of **3a** in $CDCl_3$ at T = 294 K.

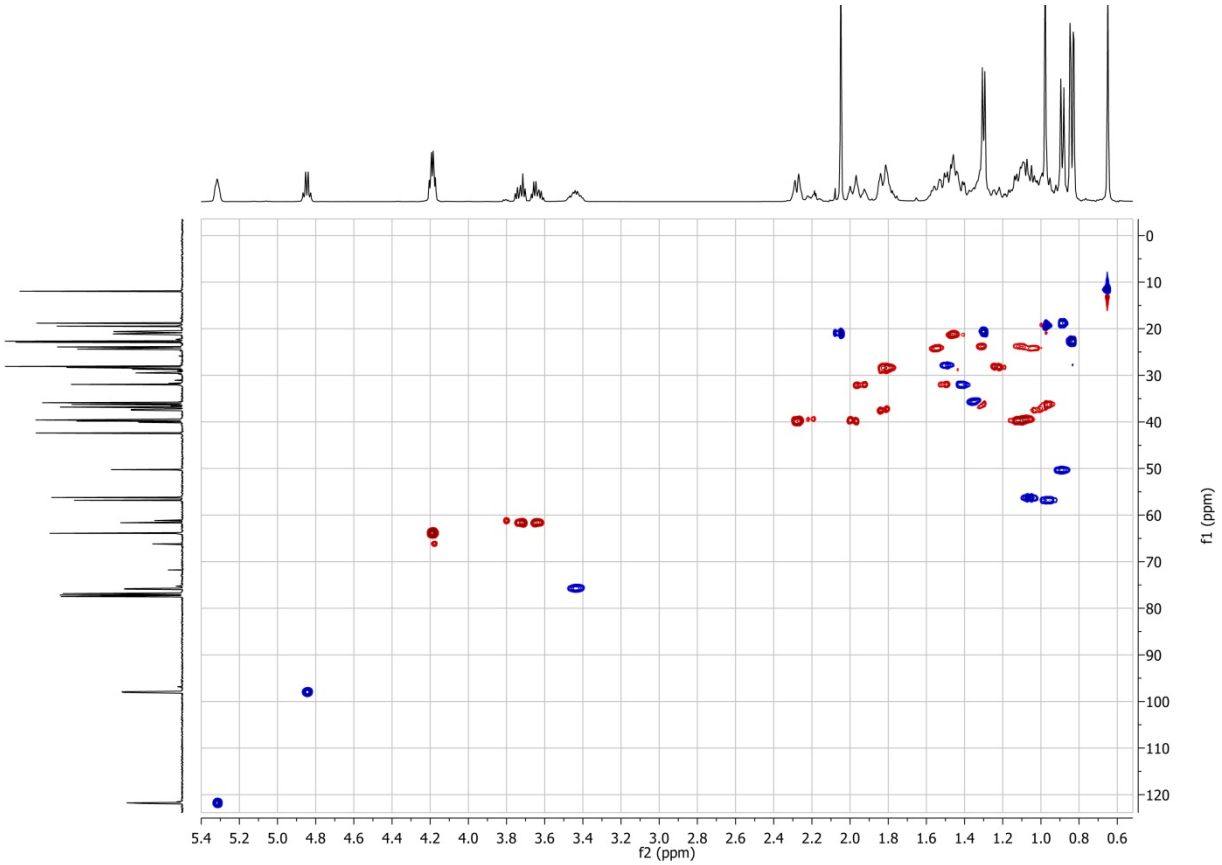

Figure S4. HSQC NMR spectrum (400 MHz) of **3a** in $CDCl_3$ at $T = 294$ K.

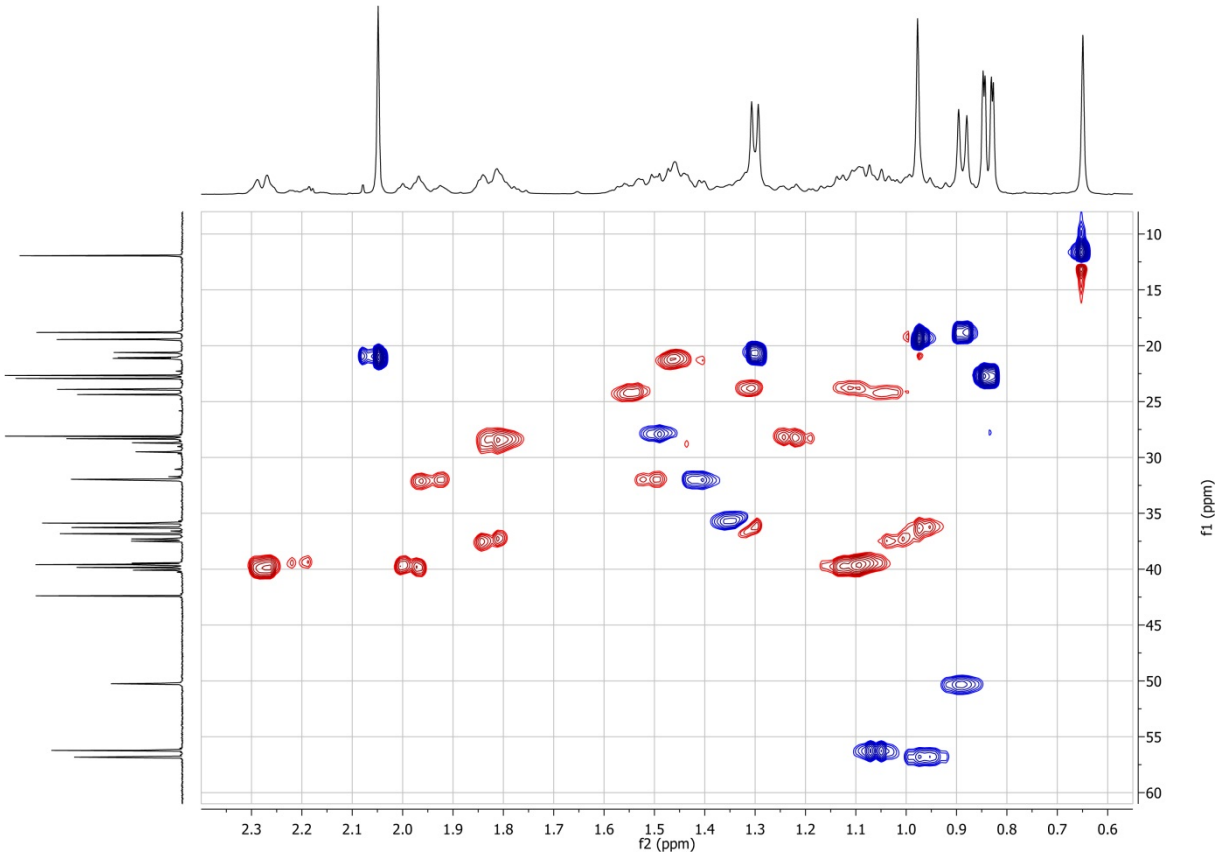

Figure S5. HSQC NMR spectrum (400 MHz) of **3a** in $CDCl_3$ at $T = 294$ K (detail of Figure S4).

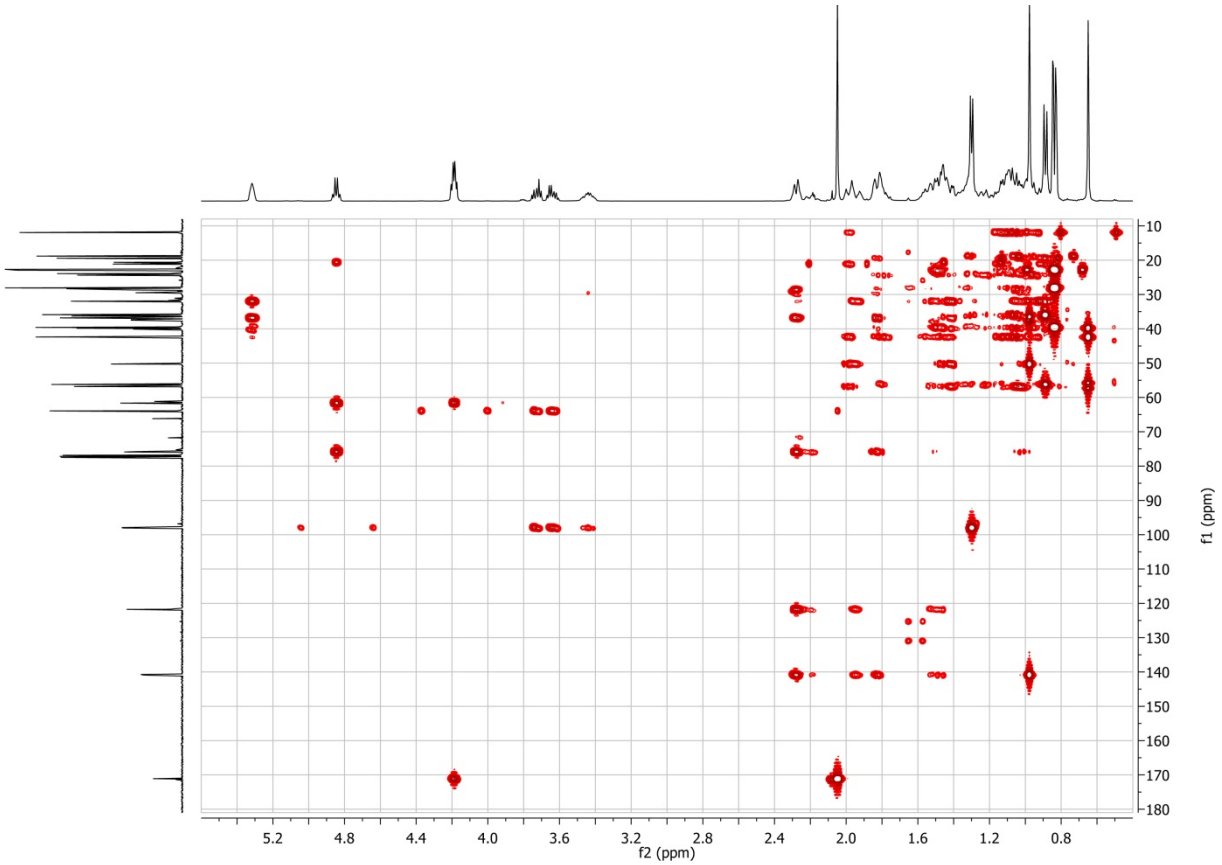

Figure S6. HMBC NMR spectrum (400 MHz) of **3a** in $CDCl_3$ at T = 294 K.

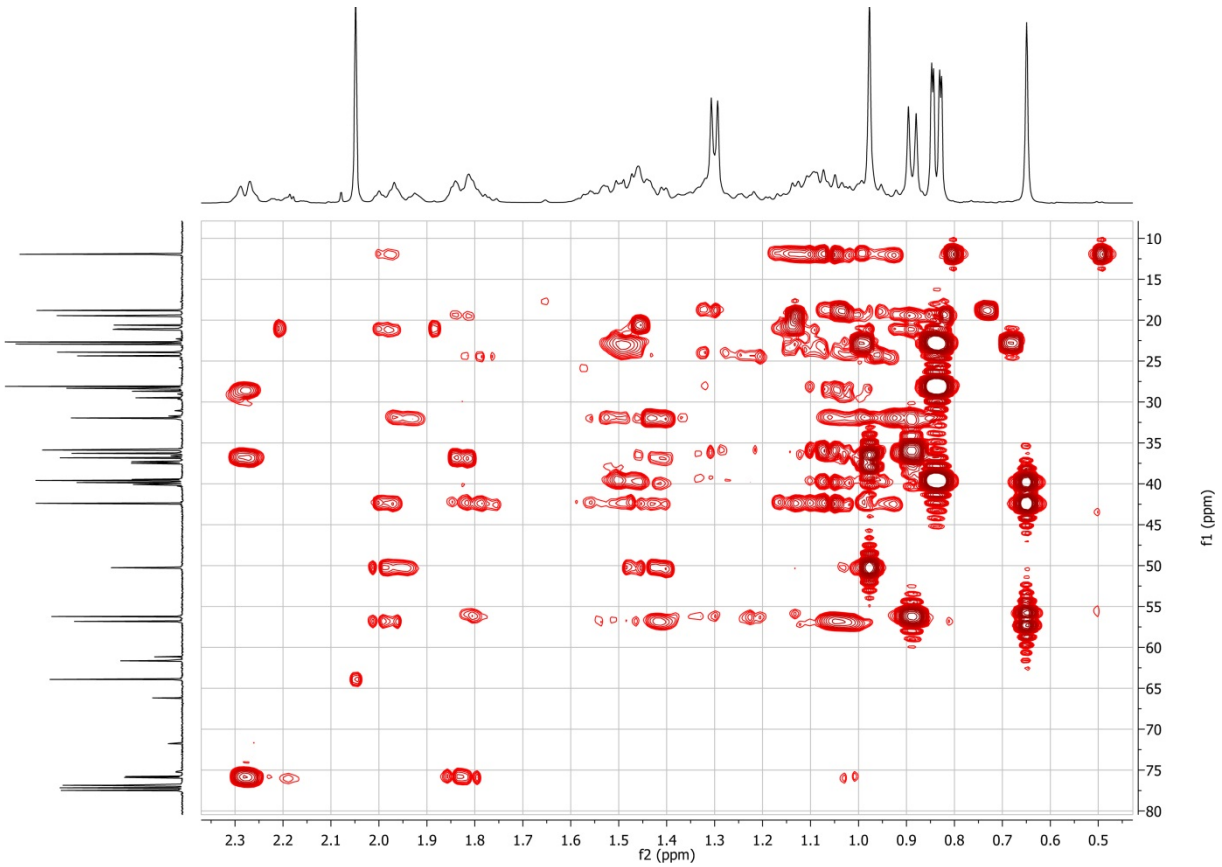

Figure S7. HMBC NMR spectrum (400 MHz) of **3a** in $CDCl_3$ at T = 294 K (detail of Figure S6).

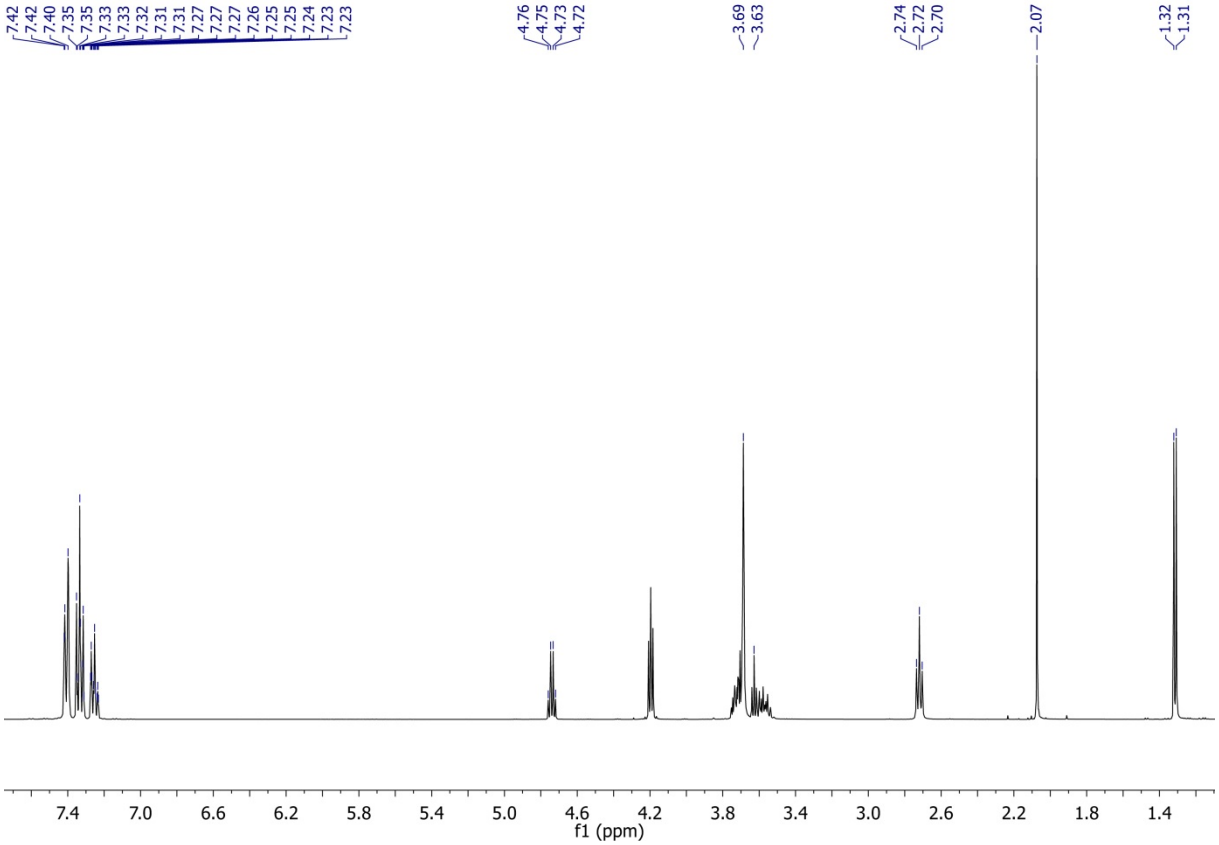

Figure S8. ^{1}H NMR spectrum (400 MHz) of **3b** in $CDCl_3$ at T = 294 K.

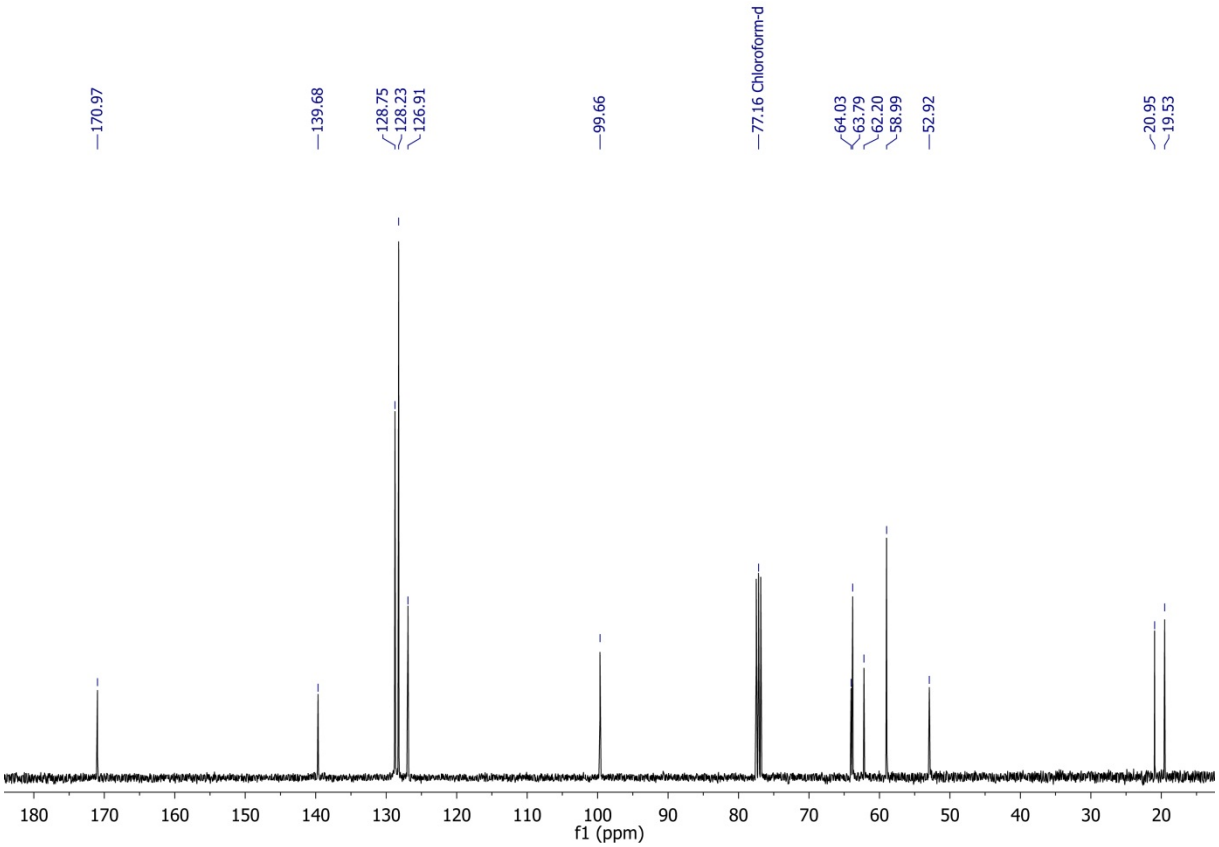

Figure S9. ^{13}C NMR spectrum (100.6 MHz) of **3b** in $CDCl_3$ at T = 294 K recorded on a Bruker ARX 400.

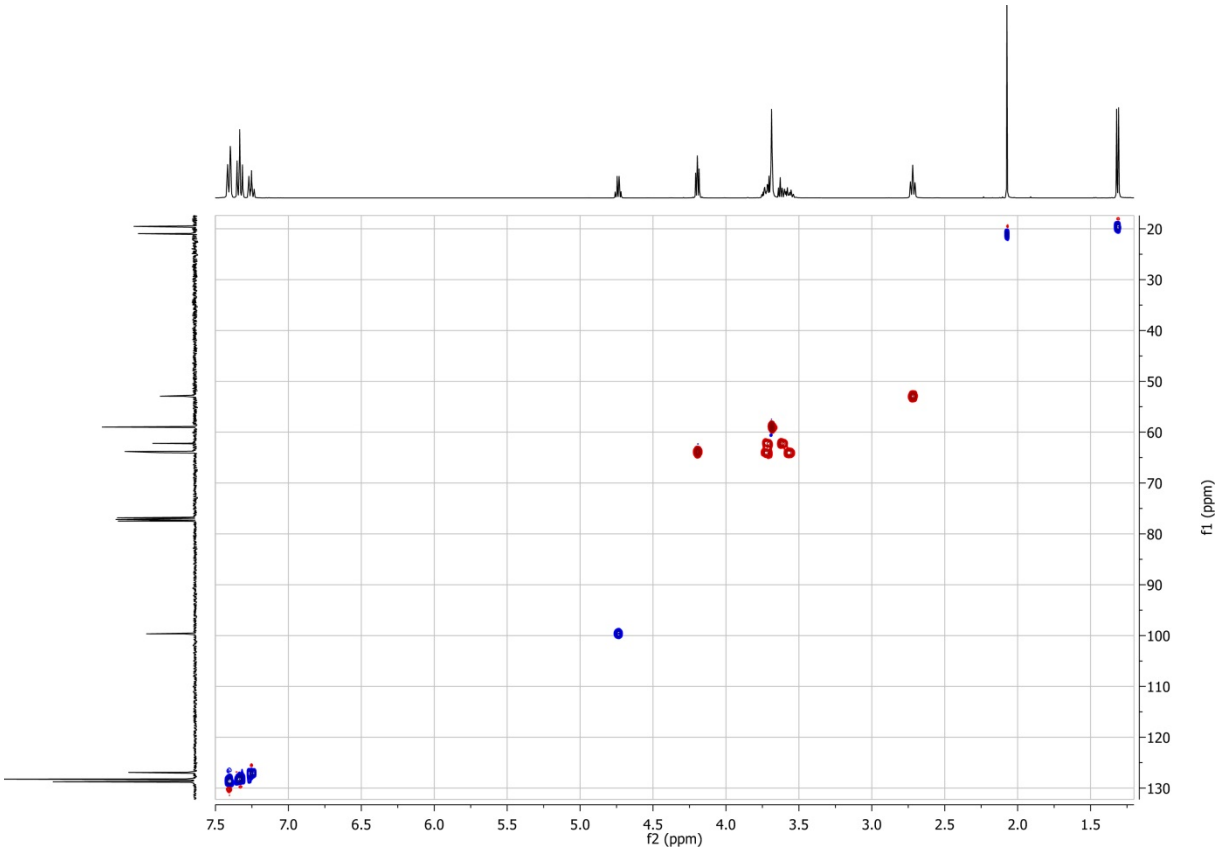

Figure S10. HSQC NMR spectrum (400 MHz) of **3b** in $CDCl_3$ at $T = 294$ K.

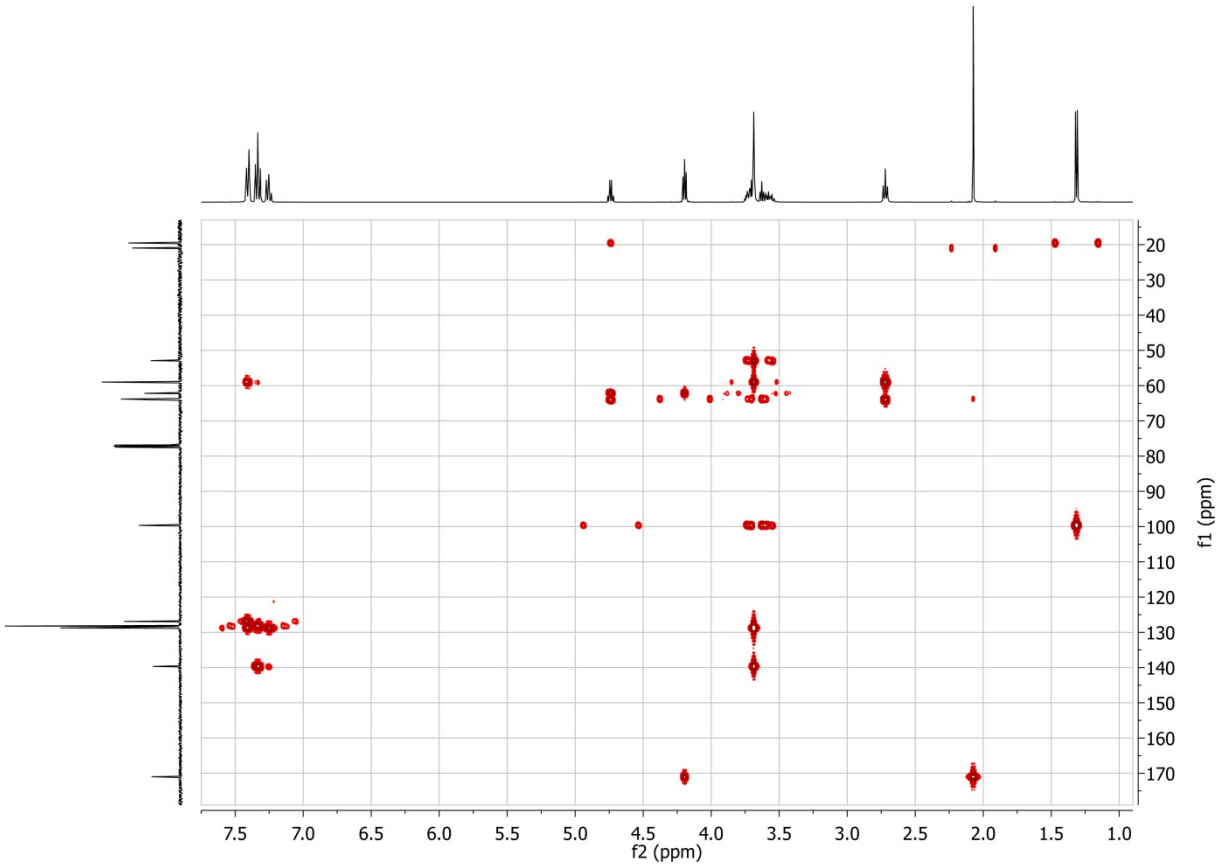

Figure S11. HMBC NMR spectrum (400 MHz) of **3b** in $CDCl_3$ at $T = 294$ K.

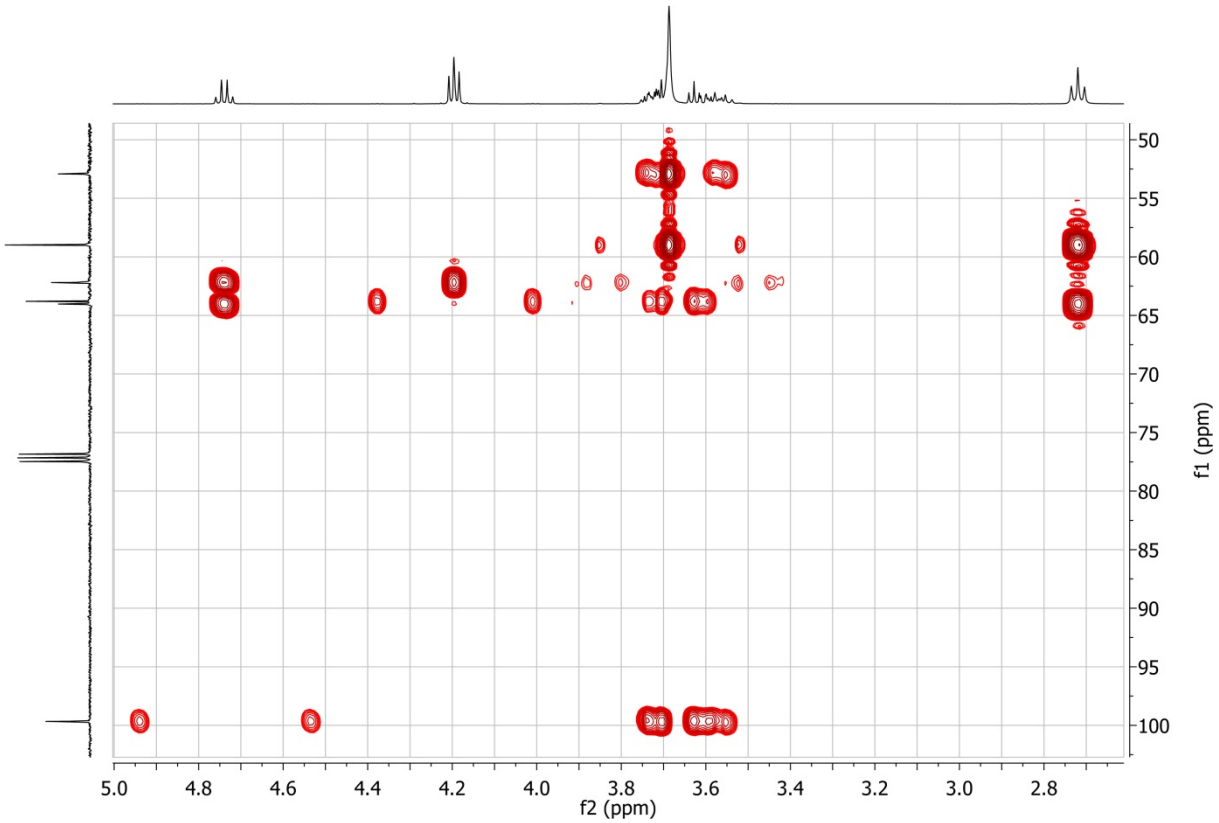

Figure S12. HMBC NMR spectrum (400 MHz) of **3b** in $CDCl_3$ at T = 294 K (detail of Figure S11).

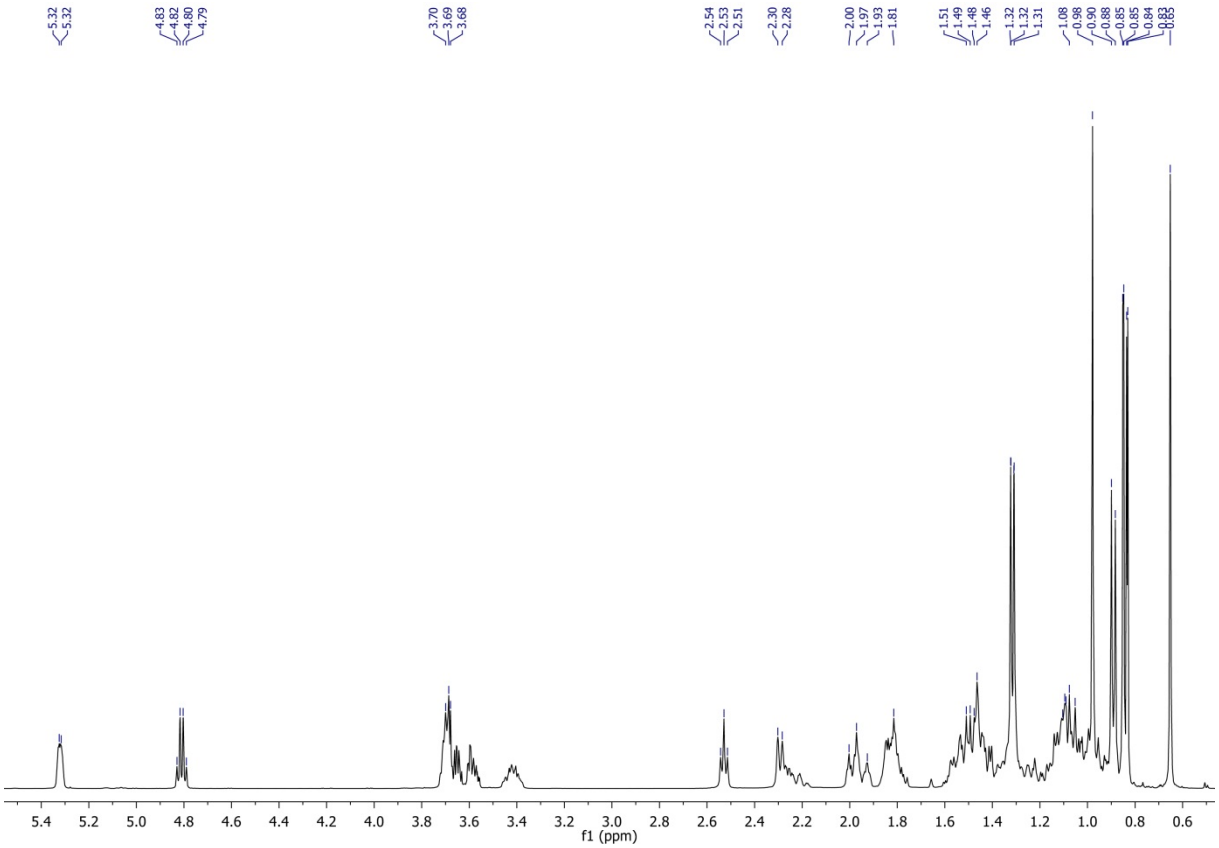

Figure S13. ^{1}H NMR spectrum (400 MHz) of **4a** in $CDCl_3$ at T = 294 K.

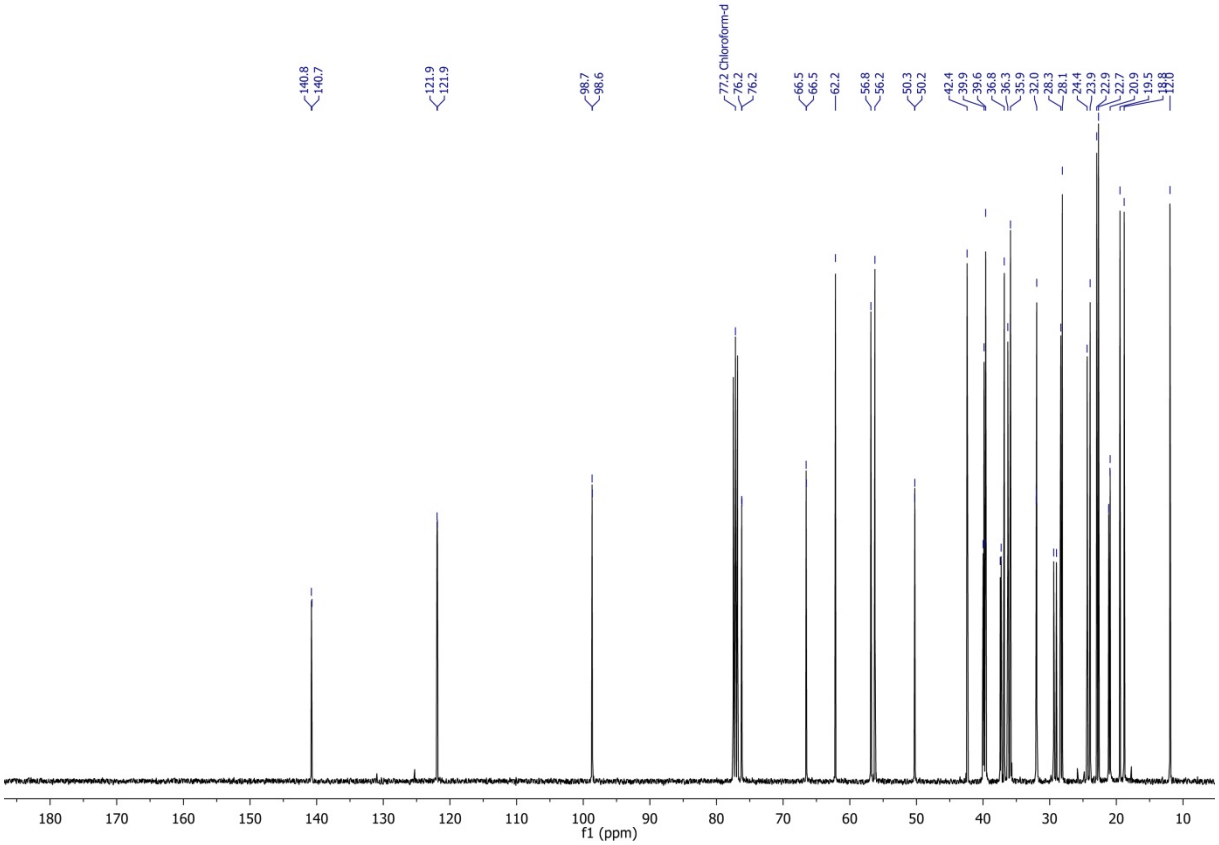

Figure S14. ^{13}C NMR spectrum (100.6 MHz) of **4a** in $CDCl_3$ at T = 294 K.

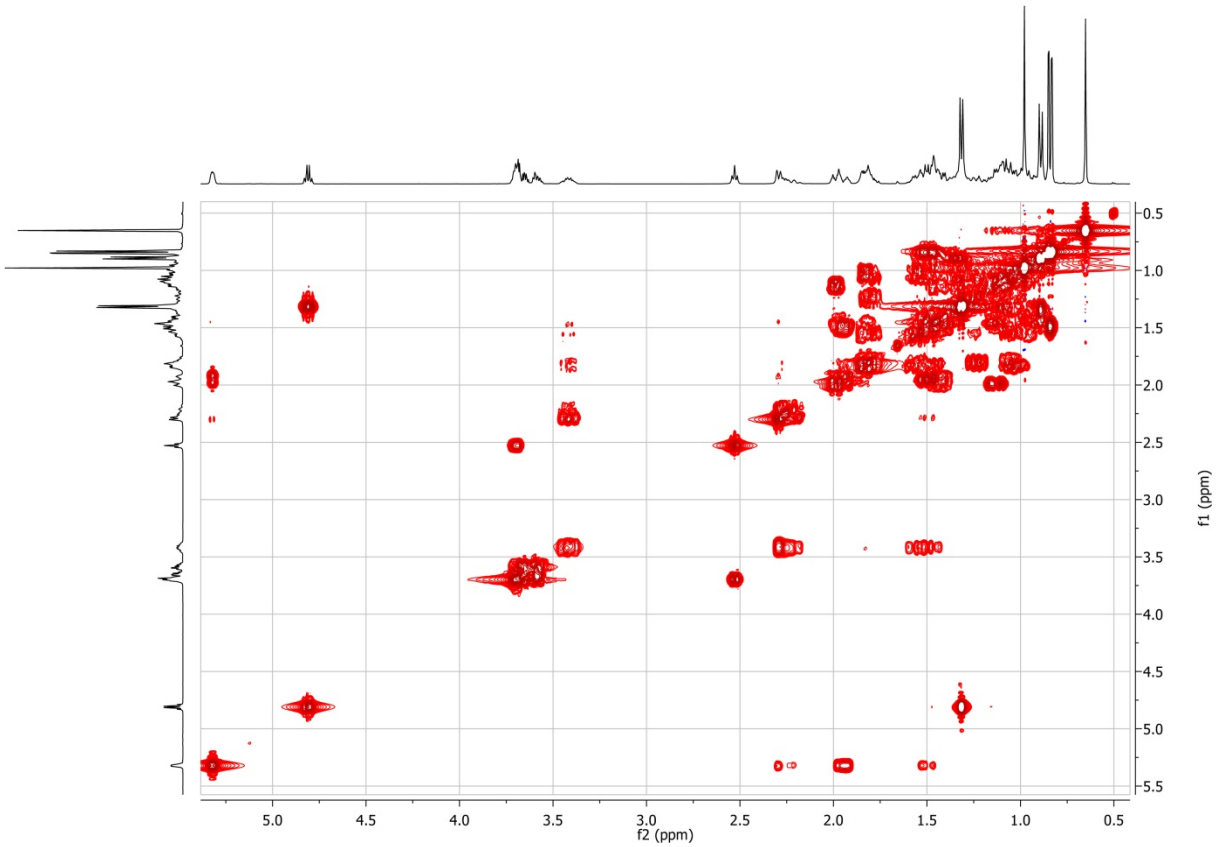

Figure S15. ^{1}H COSY spectrum (400 MHz) of **4a** in $CDCl_3$ at T = 294 K.

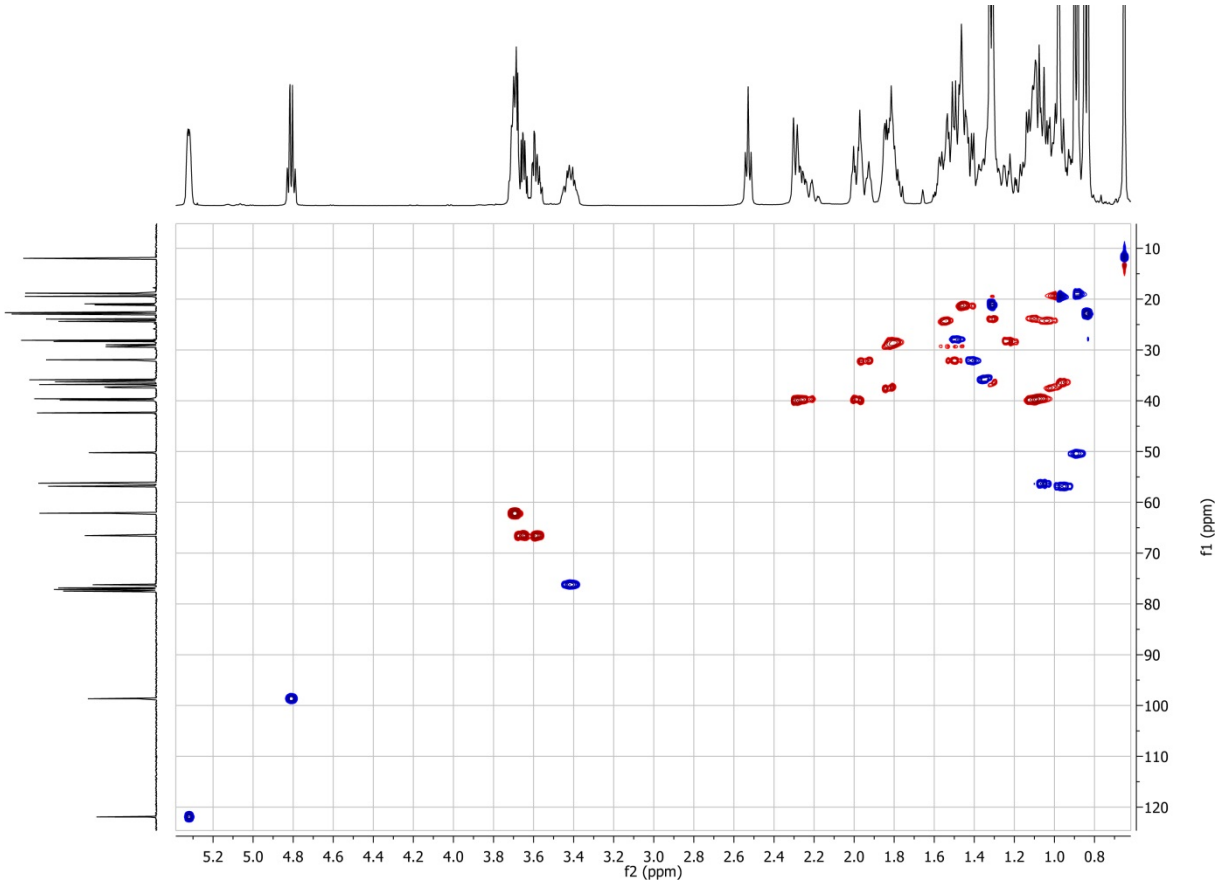

Figure S16. HSQC spectrum (400 MHz) of **4a** in $CDCl_3$ at T = 294 K.

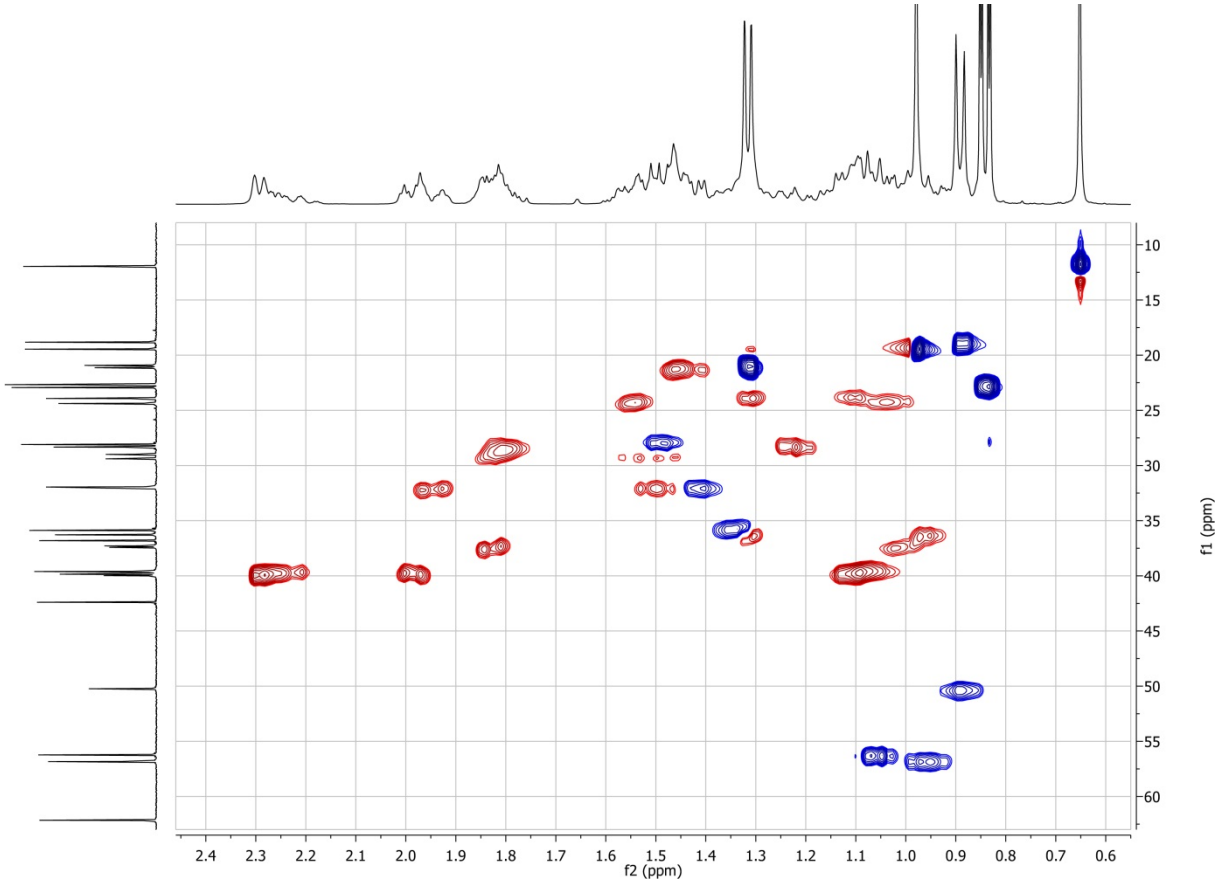

Figure S17. HSQC spectrum (400 MHz) of **4a** in $CDCl_3$ at T = 294 K (detail of Figure S16).

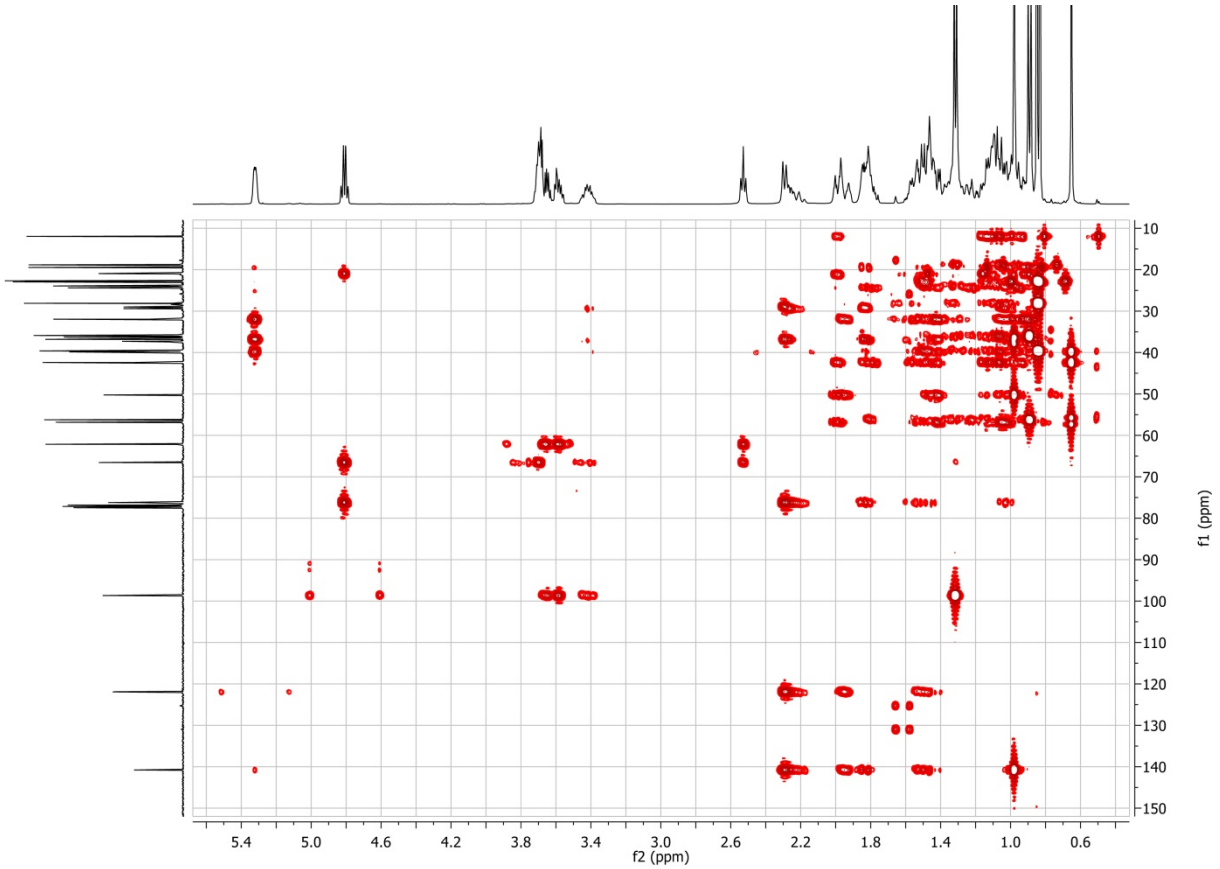

Figure S18. HMBC spectrum (400 MHz) of **4a** in $CDCl_3$ at T = 294 K.

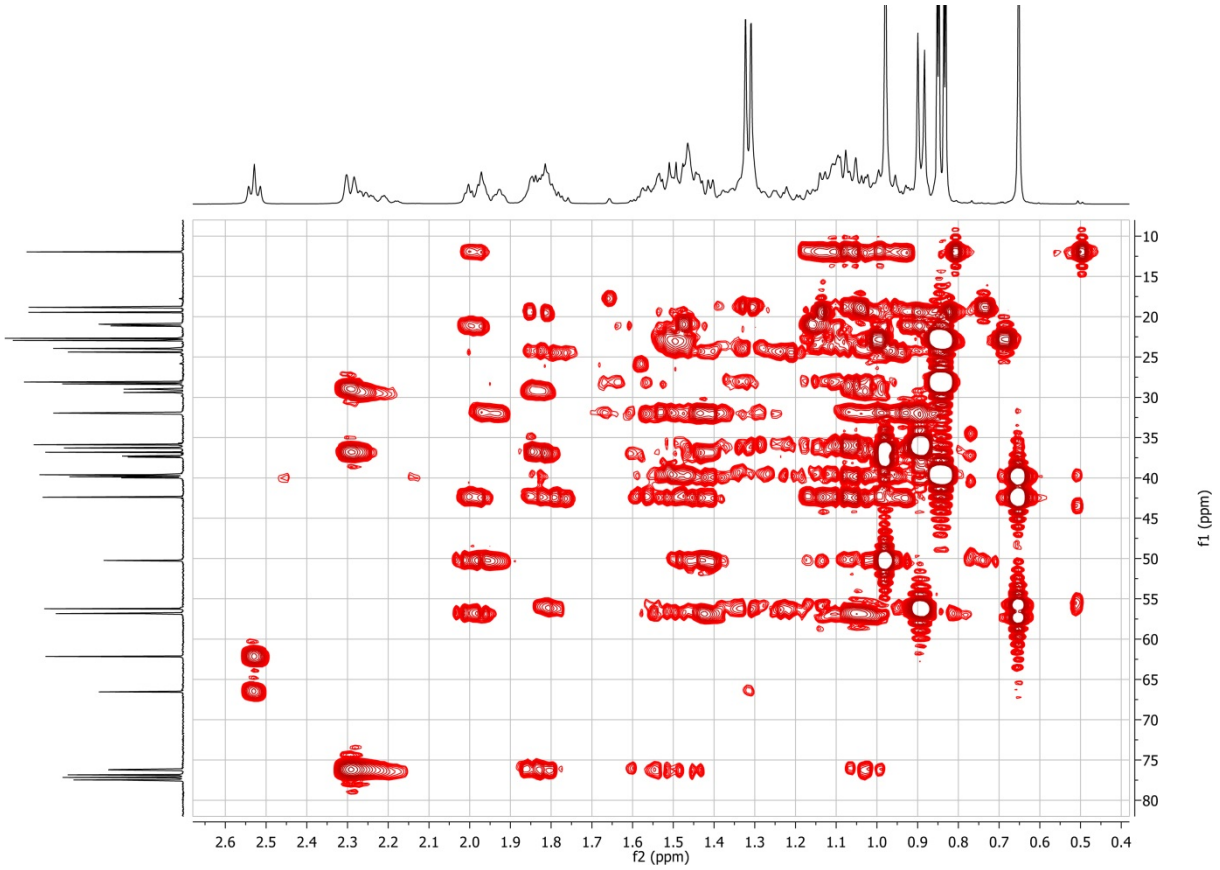

Figure S19. HMBC spectrum (400 MHz) of **4a** in $CDCl_3$ at T = 294 K (detail of Figure S18).

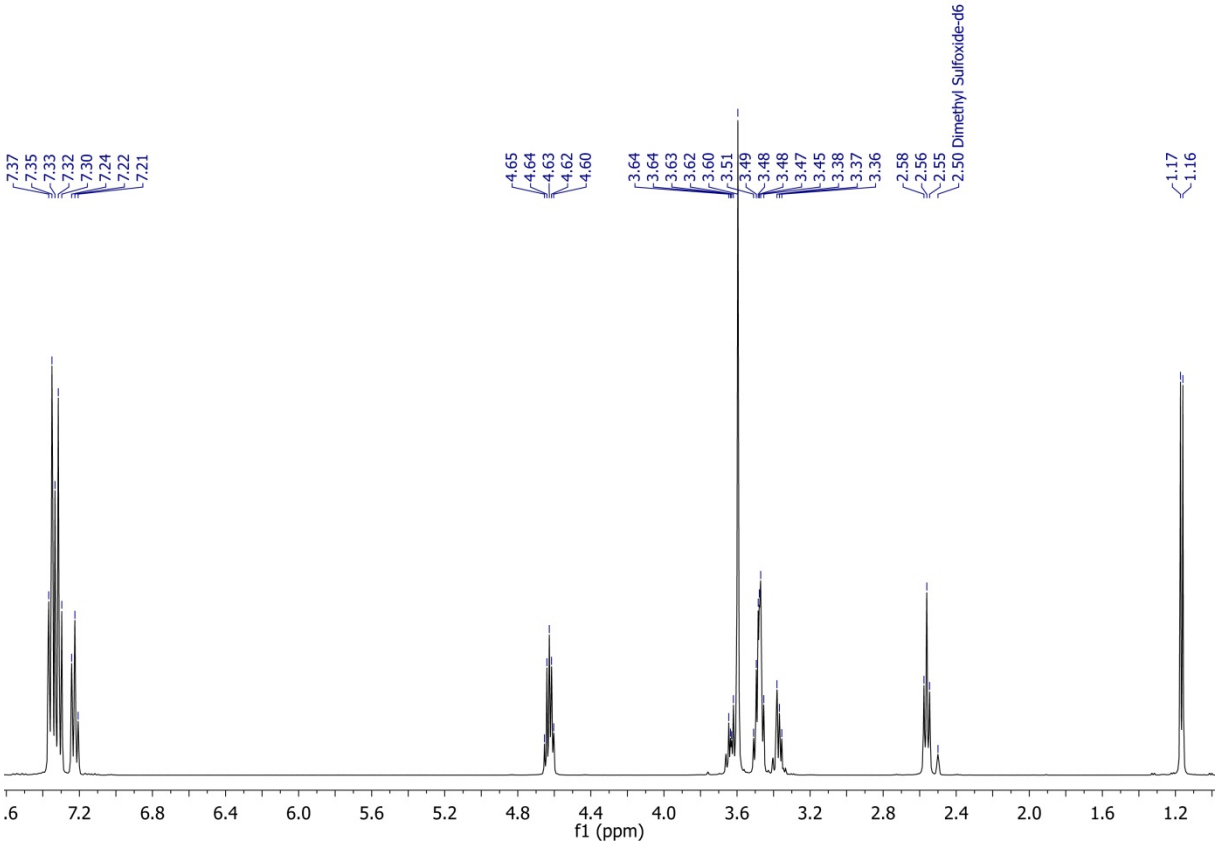

Figure S20. ^{1}H NMR spectrum (400 MHz) of **4b** in DMSO-d$_6$ at T = 294 K.

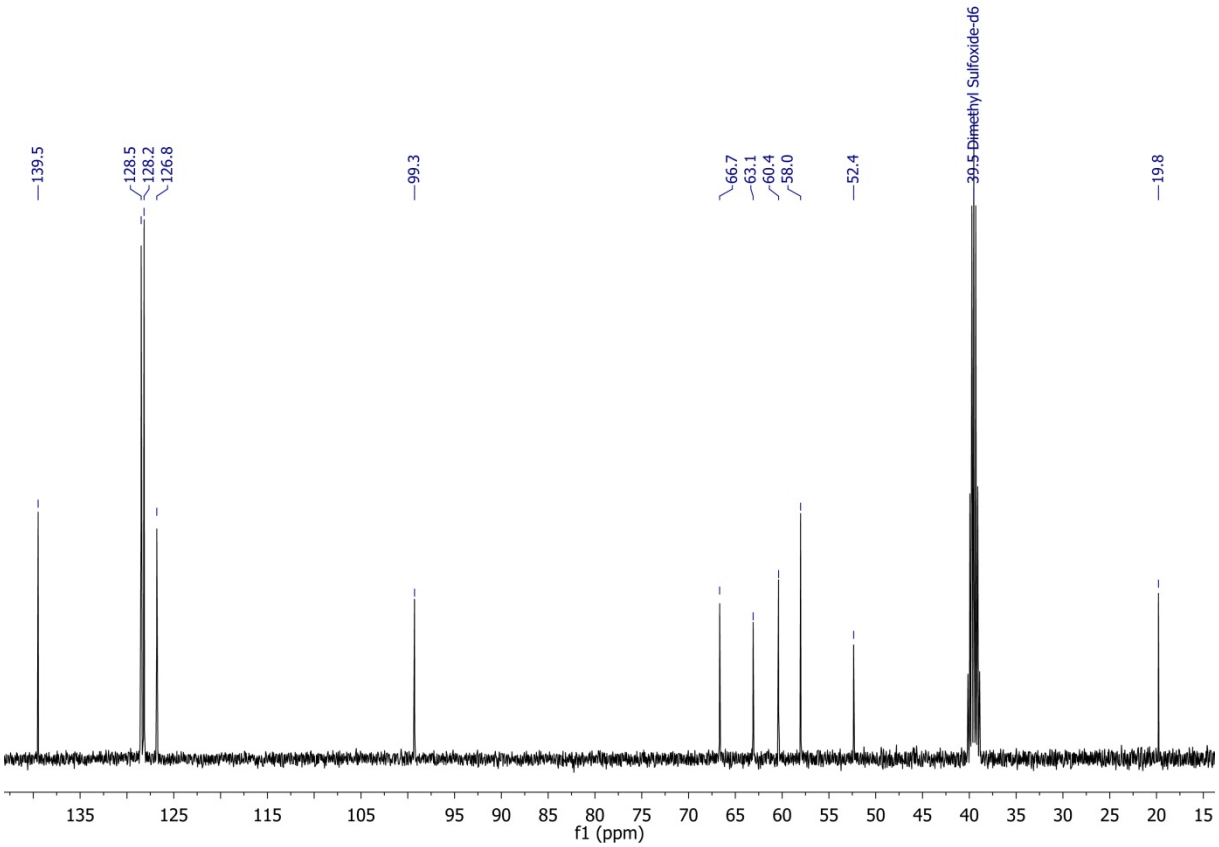

Figure S21. ^{13}C NMR spectrum (100.6 MHz) of **4b** in DMSO-d$_6$ at T = 294 K recorded on a Bruker ARX 400 with a 5mm BBO probe.

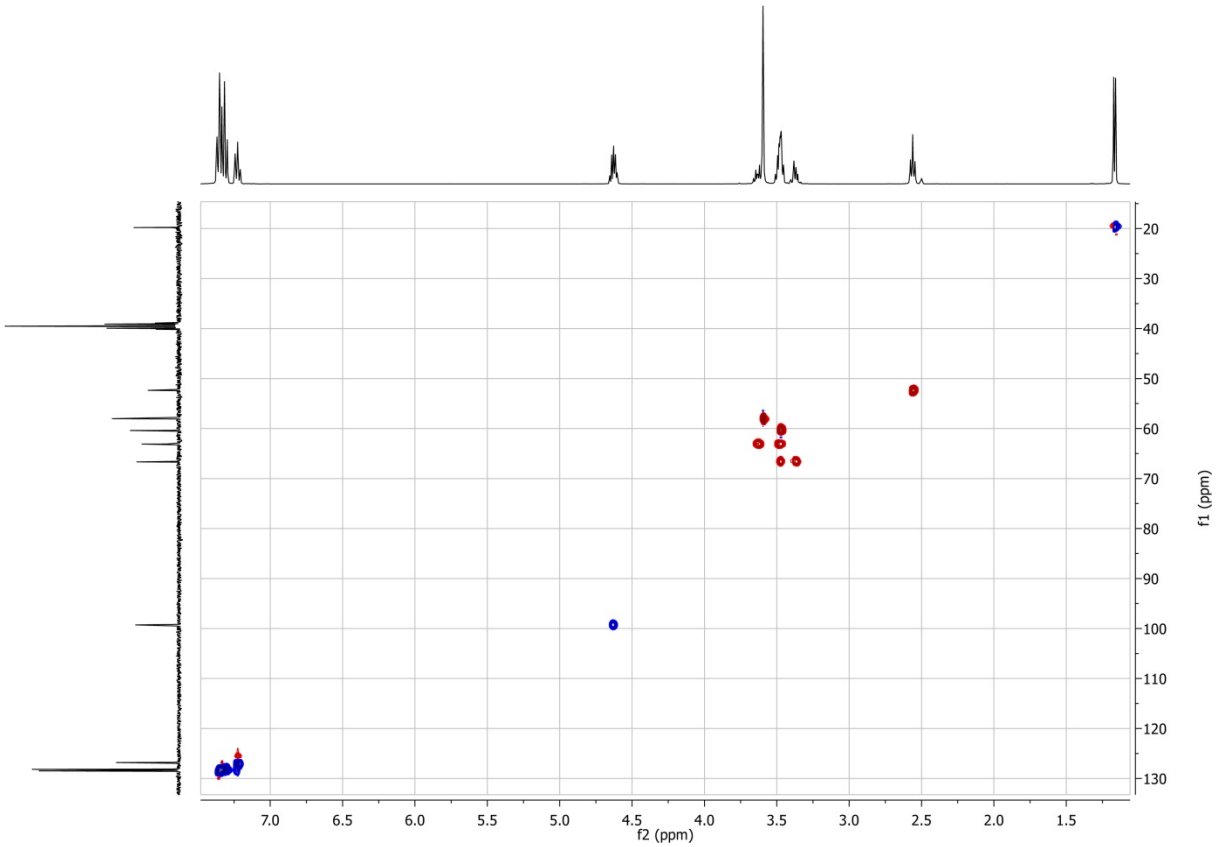

Figure S22. HSQC NMR spectrum (400 MHz) of **4b** in DMSO-d_6 at T = 294 K.

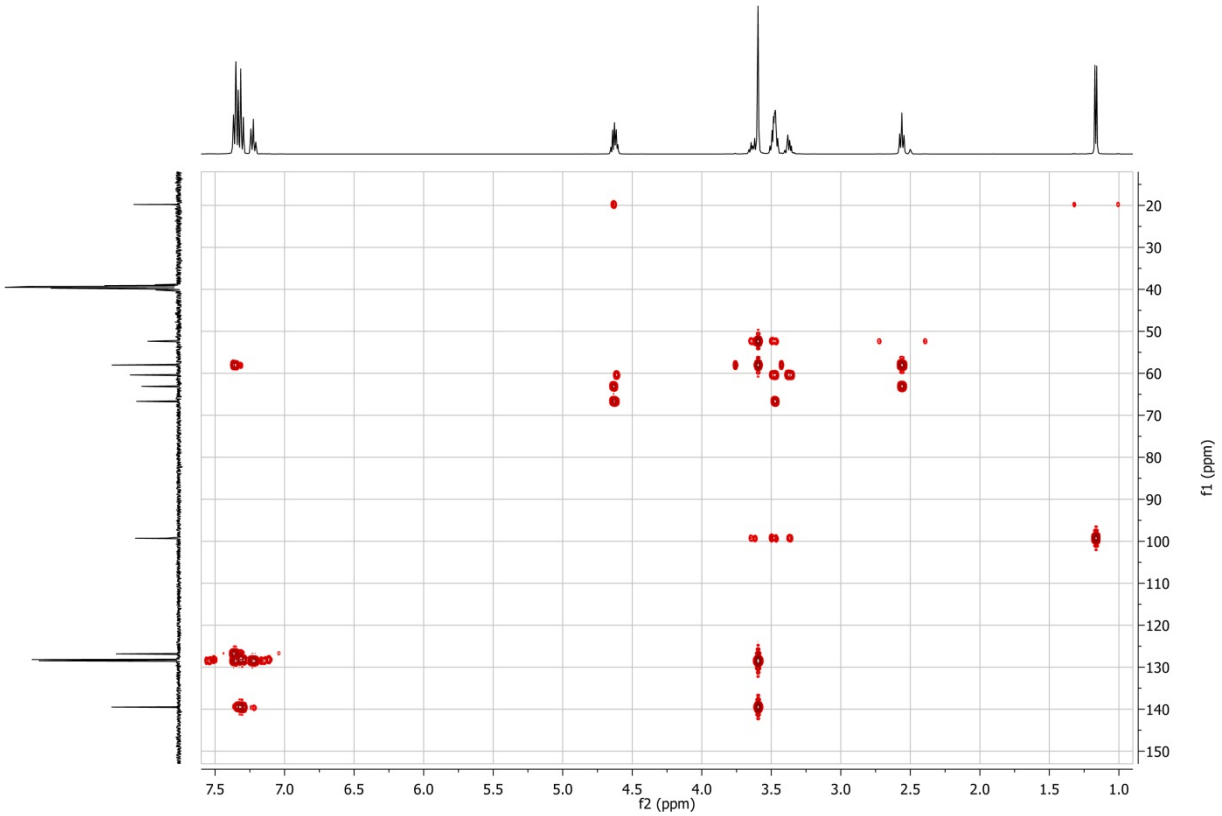

Figure S23. HMBC NMR spectrum (400 MHz) of **4b** in DMSO-d_6 at T = 294 K.

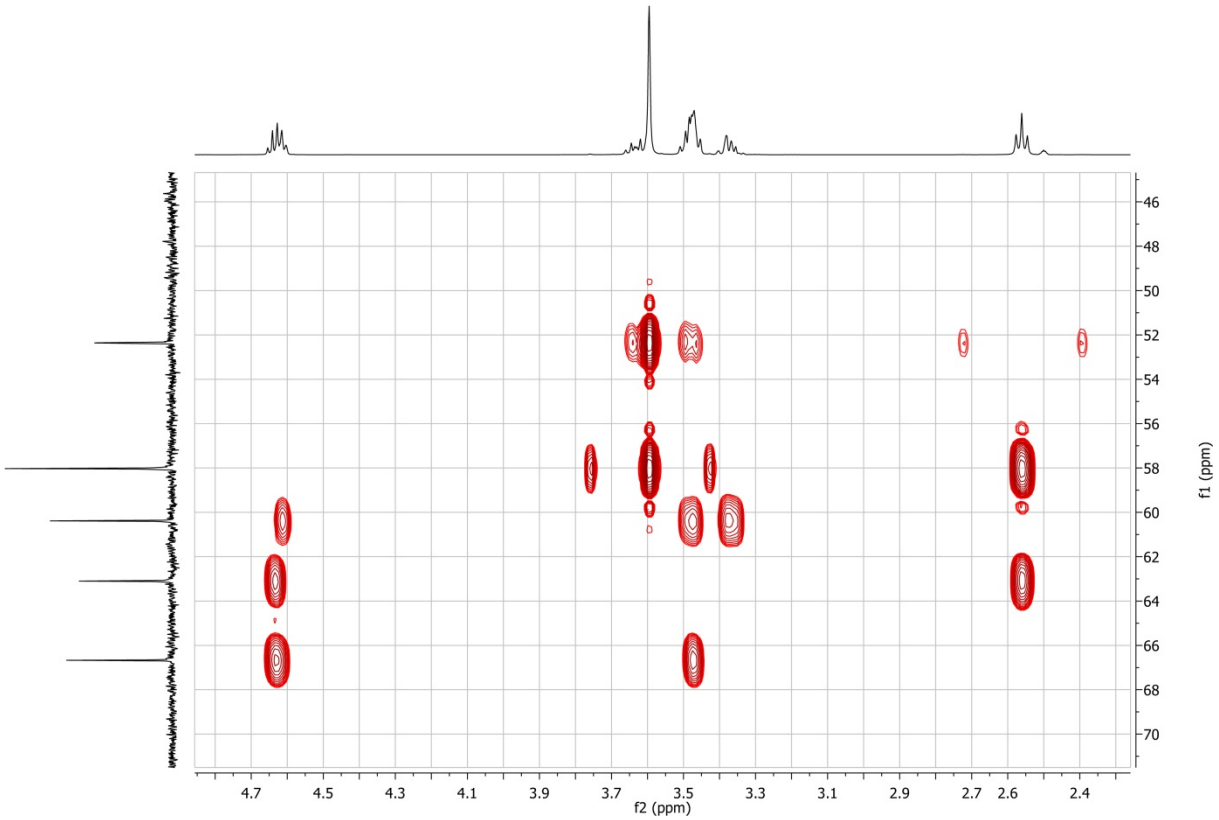

Figure S24. HMBC NMR spectrum (400 MHz) of **4b** in DMSO-d_6 at T = 294 K (detail of Figure S23).

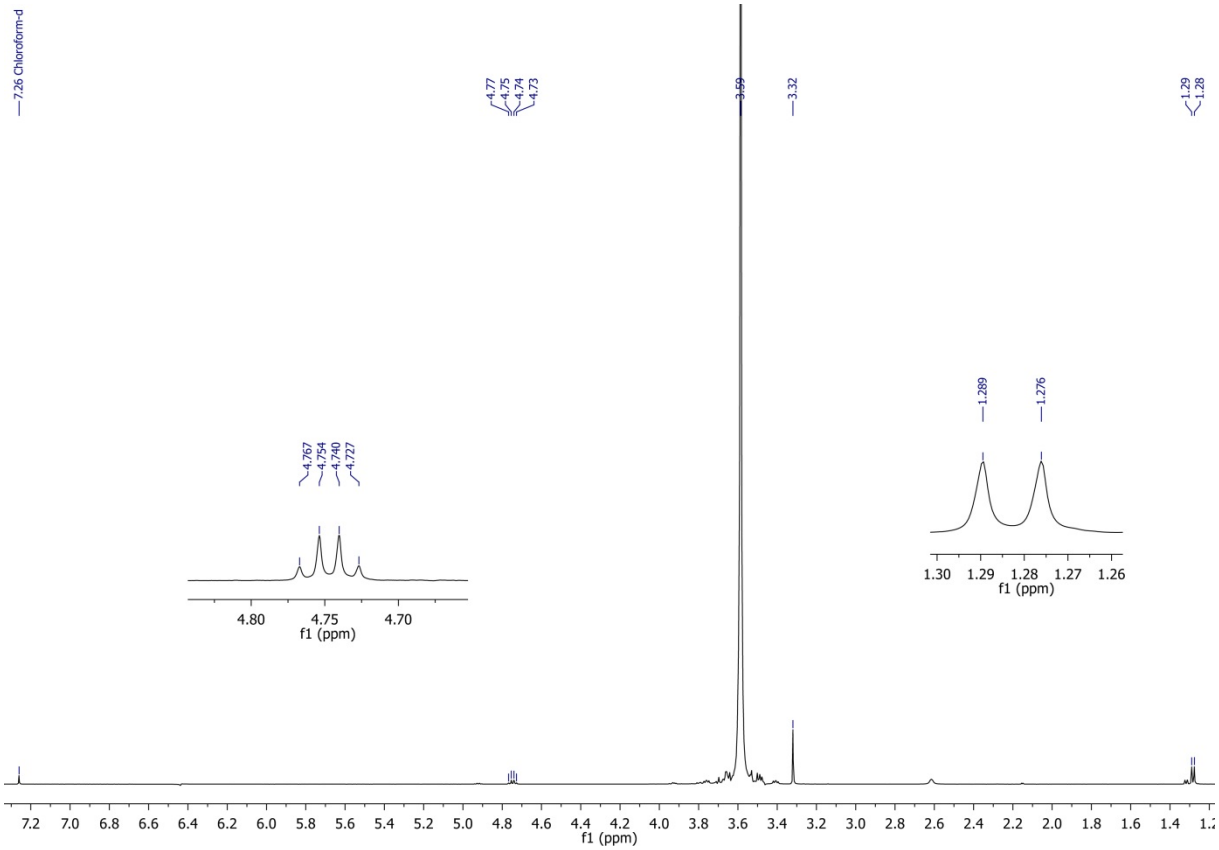

Figure S25. ^{1}H NMR spectrum (400 MHz) of **4c** in $CDCl_3$ at T = 294 K.

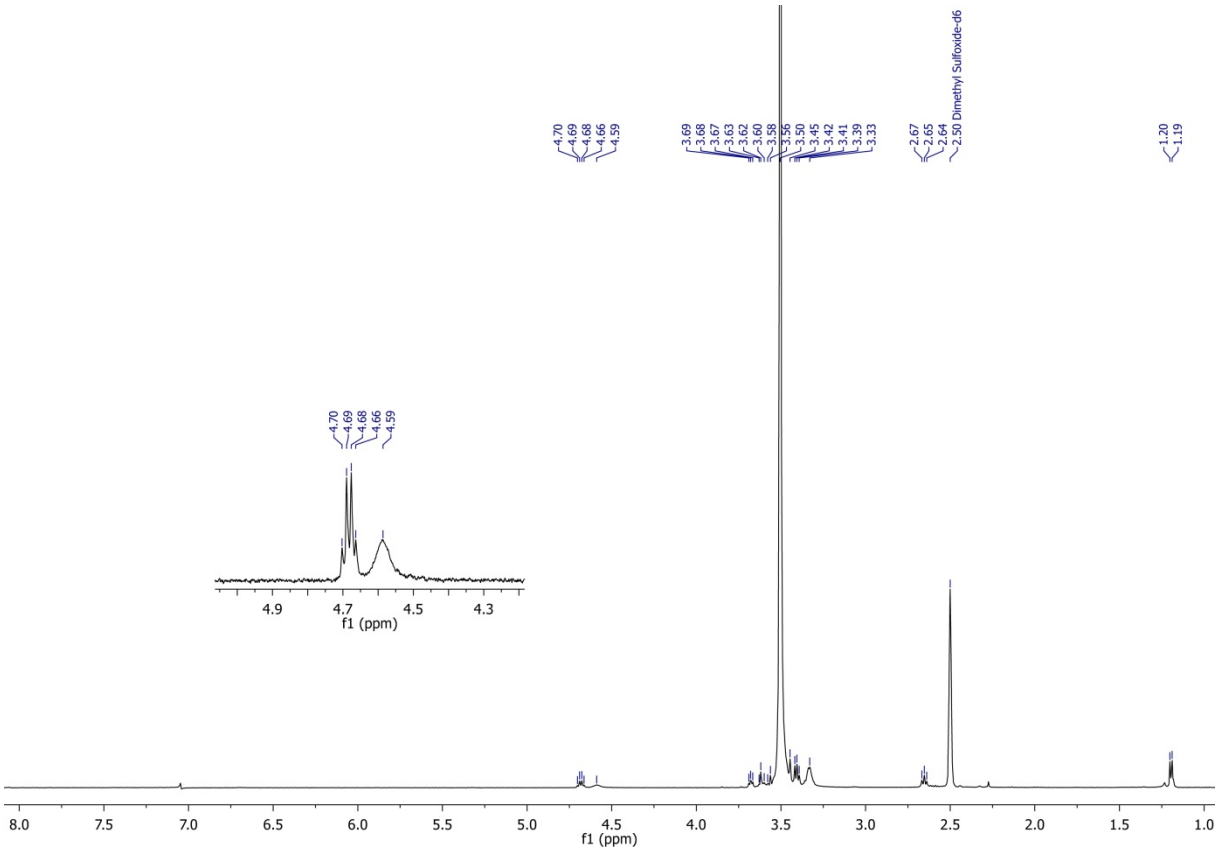

Figure S26. ^{1}H NMR spectrum (400 MHz) of $\mathbf{7}_{50}$ in DMSO-d_6 at T = 294 K.

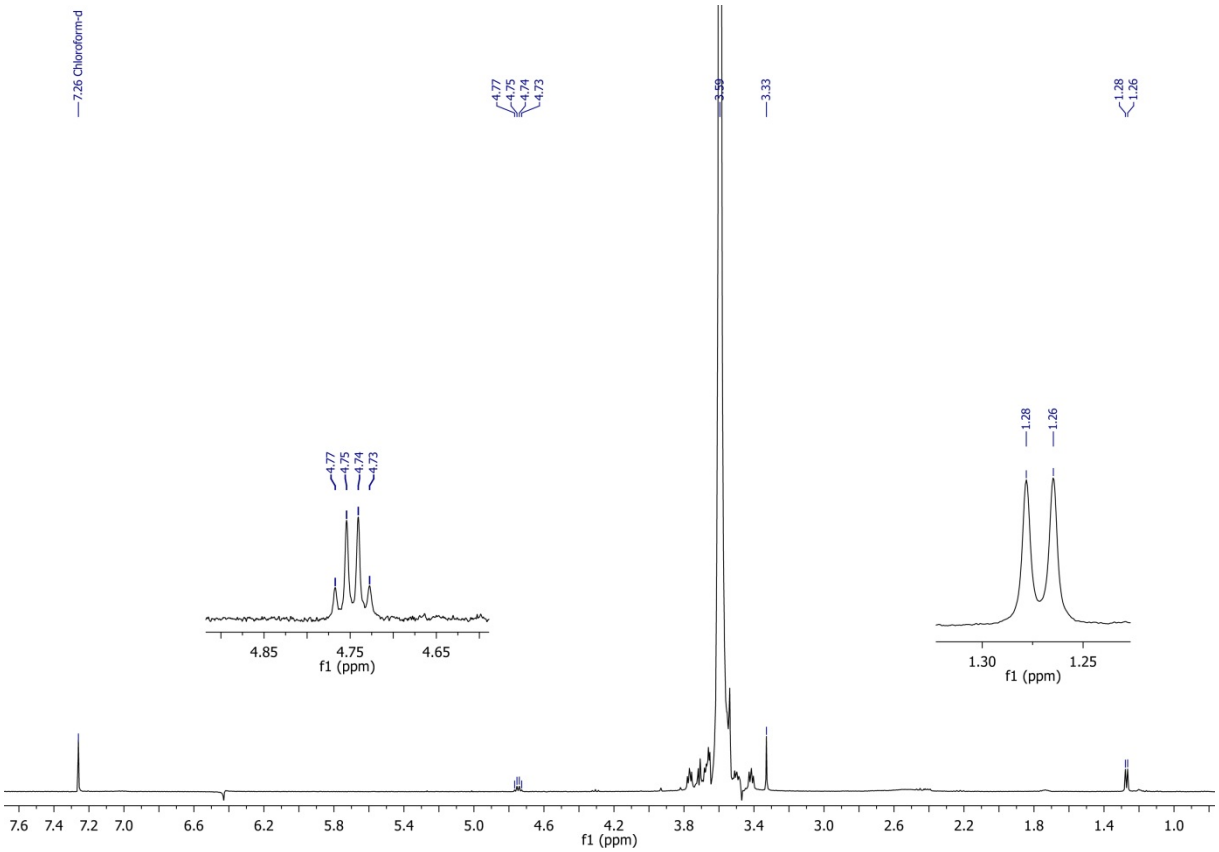

Figure S27. ^{1}H NMR spectrum (400 MHz) of **8** in $CDCl_3$ at T = 294 K.

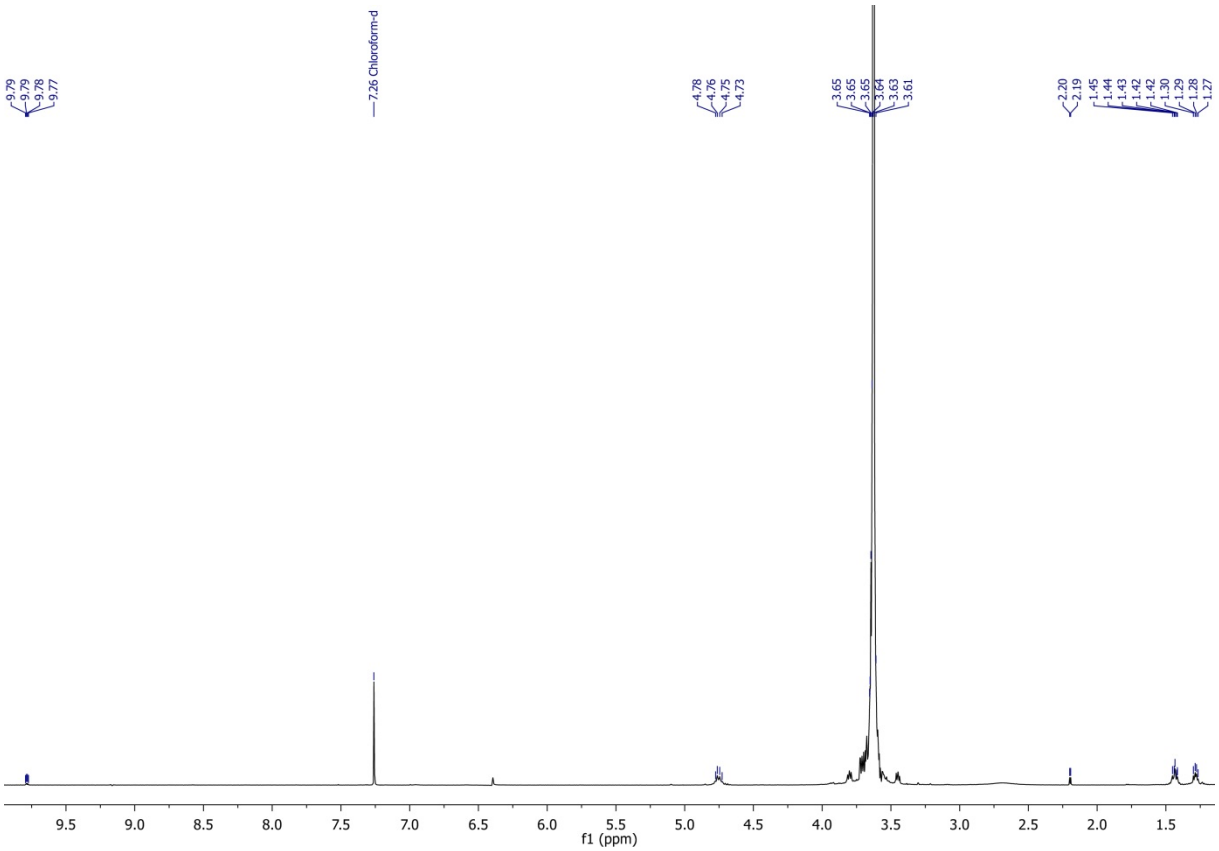

Figure S28. ^{1}H NMR spectrum (400 MHz) of **10** in $CDCl_3$ at $T = 294$ K.

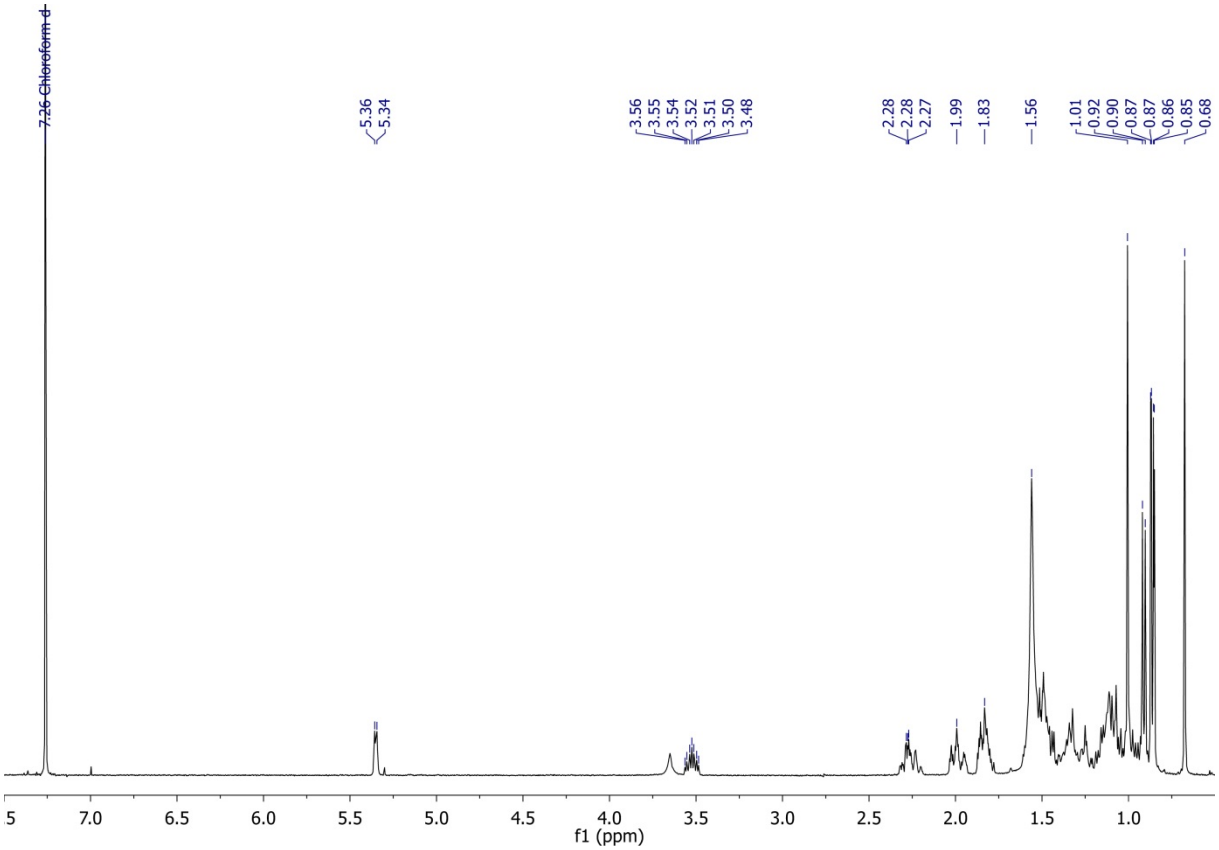

Figure S29. ^{1}H NMR spectrum (400 MHz) of precipitate of **5**'s cleavage, recorded in $CDCl_3$ at $T = 294$ K.

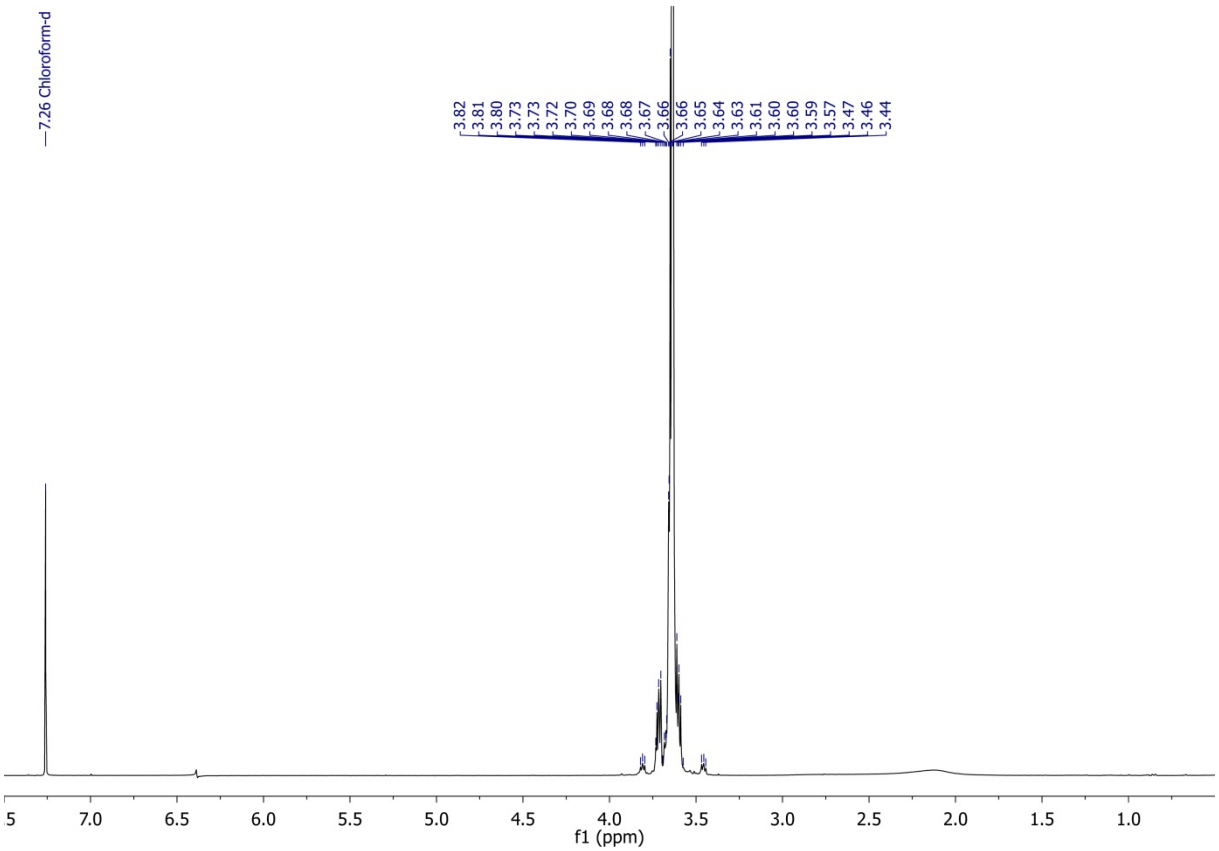

Figure S30. ^{1}H NMR spectrum (400 MHz) of PEG diol isolated from aqueous phase of **5**'s cleavage, recorded in $CDCl_3$ at $T = 294$ K.

3. IR spectra

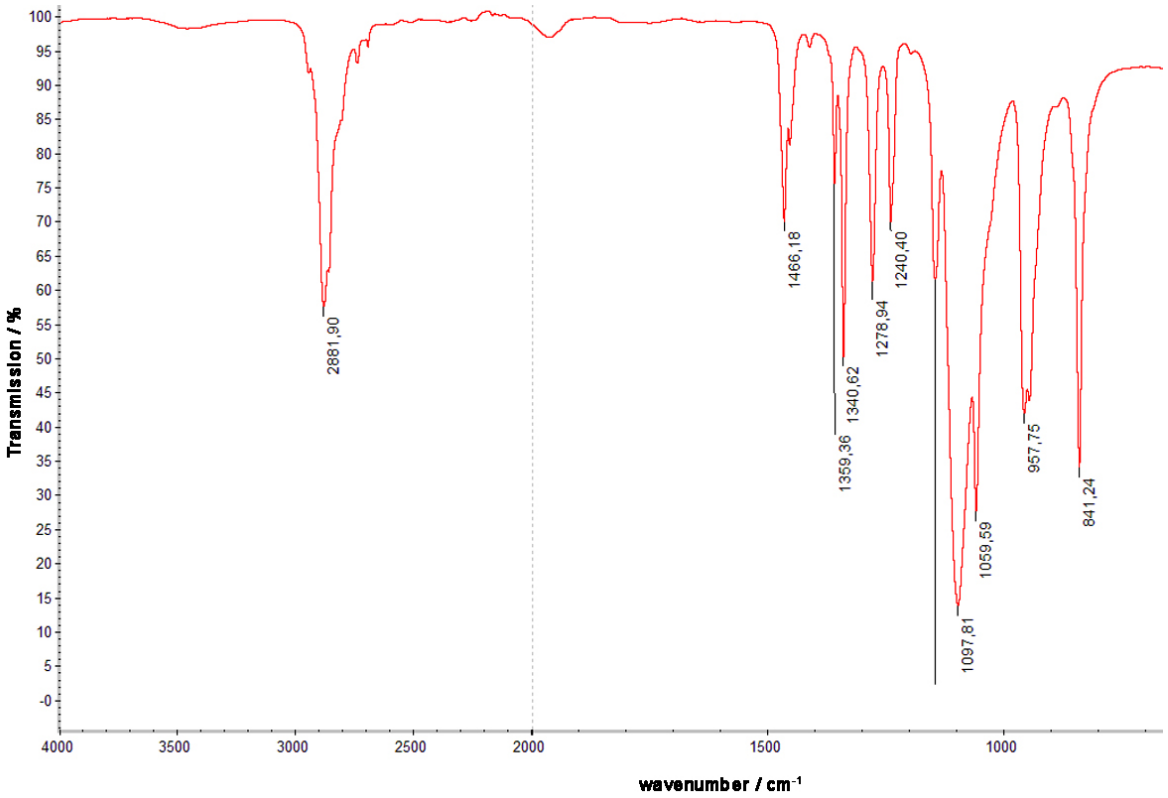

Figure S31. IR-spectrum of commercially available 2.0 kg·mol^{-1} mPEG (**1c**).

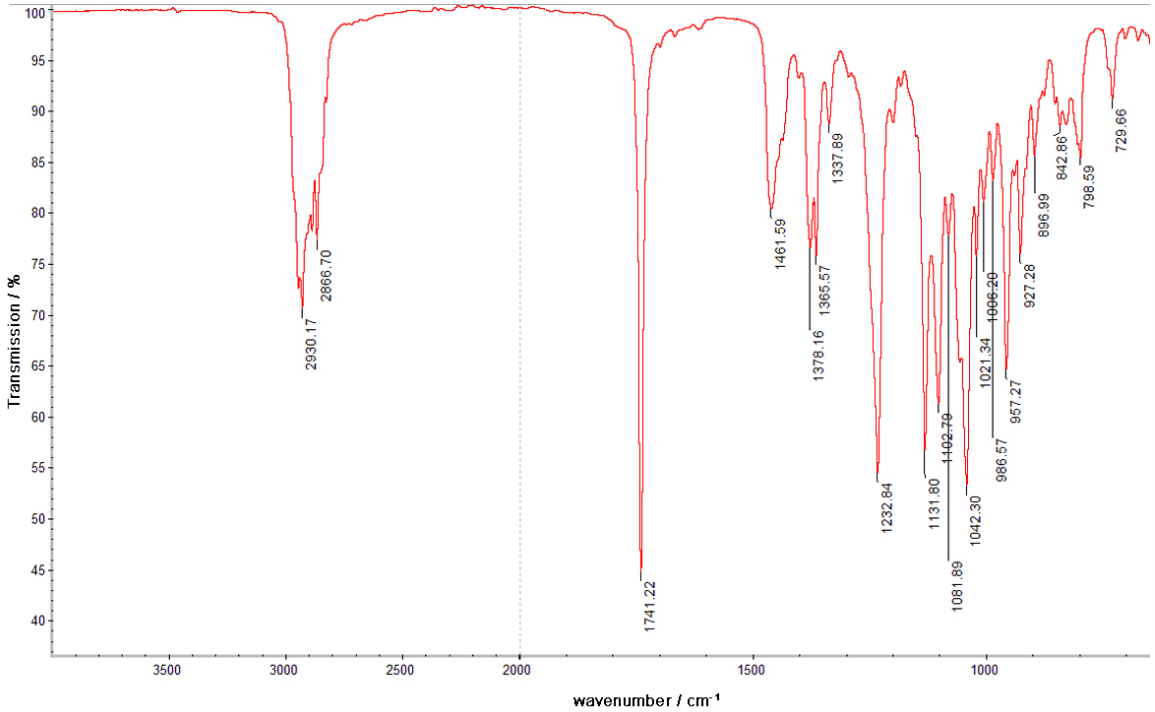

Figure S32. IR-spectrum of **3a**.

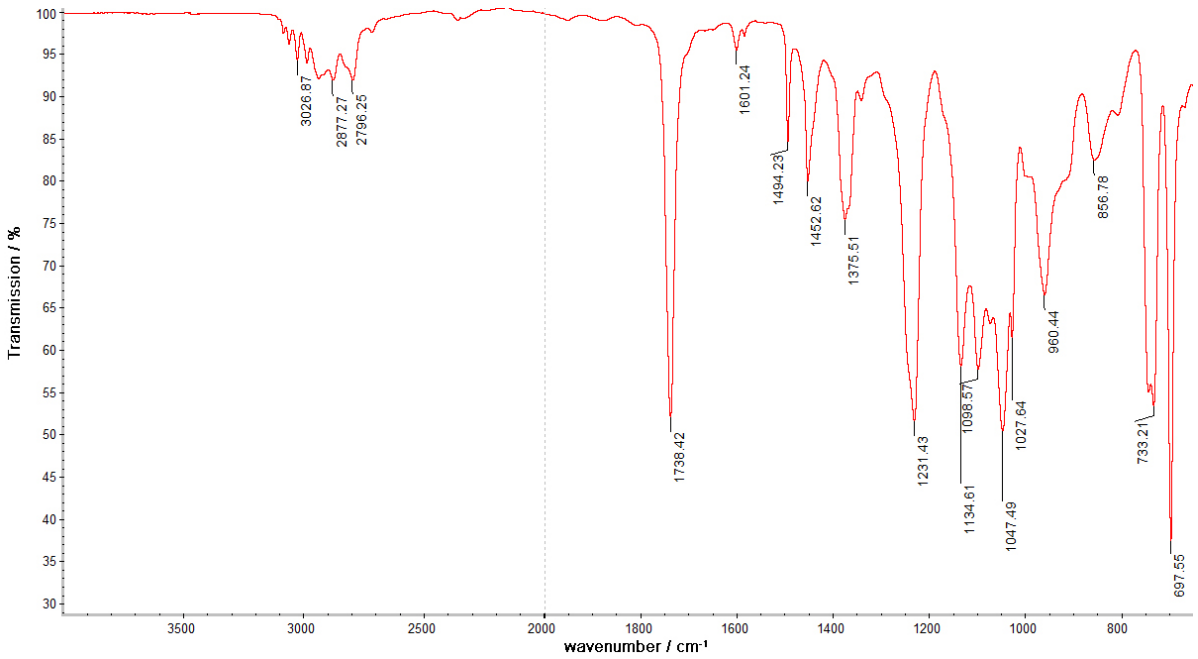

Figure S33. IR-spectrum of **3b**.

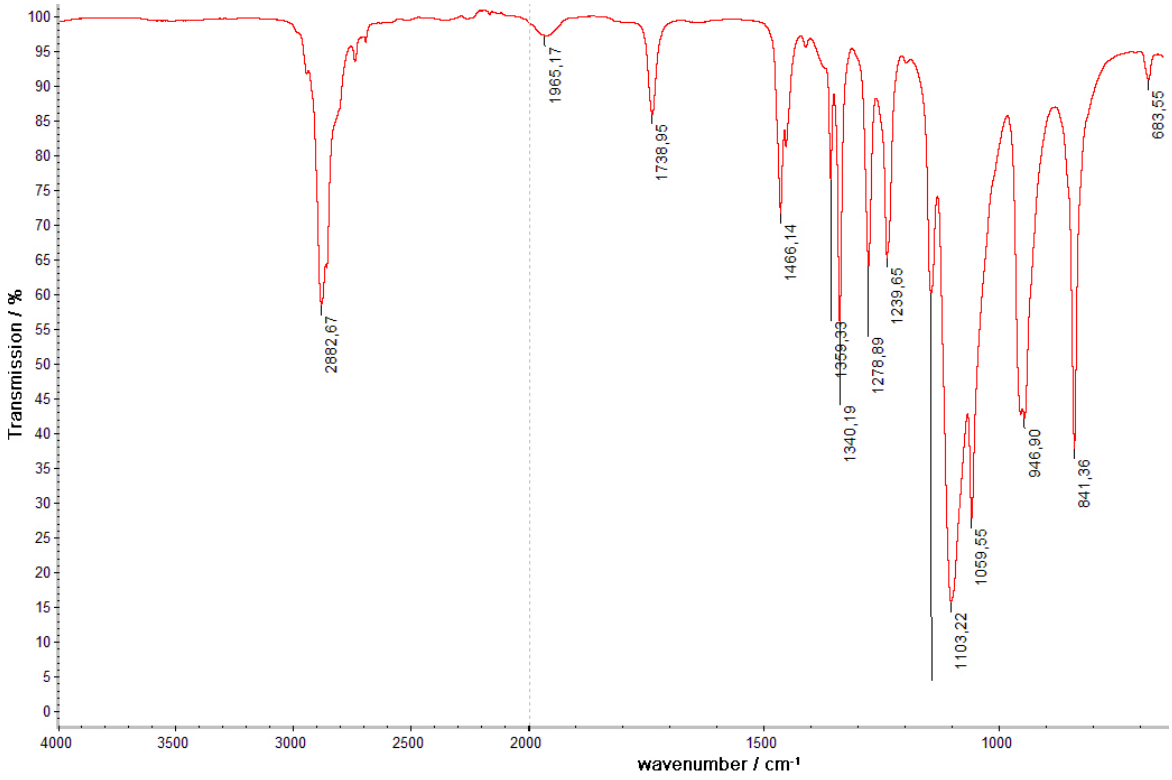

Figure S34. IR-spectrum of **3c**.

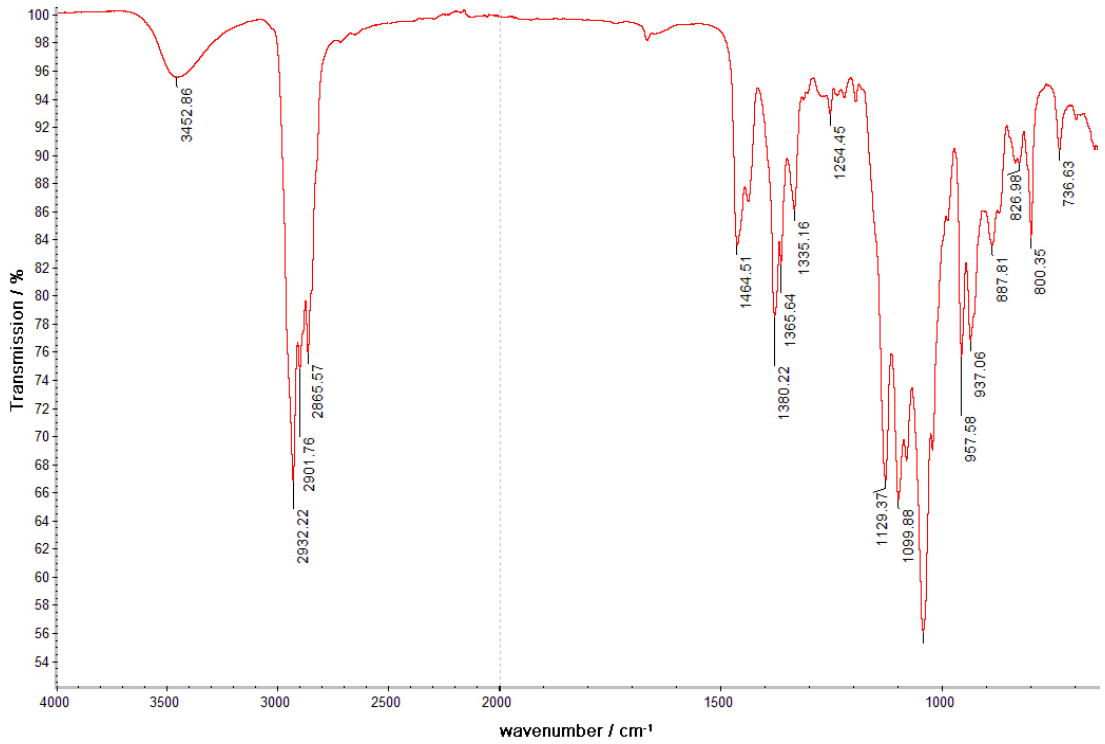

Figure S35. IR-spectrum of **4a**.

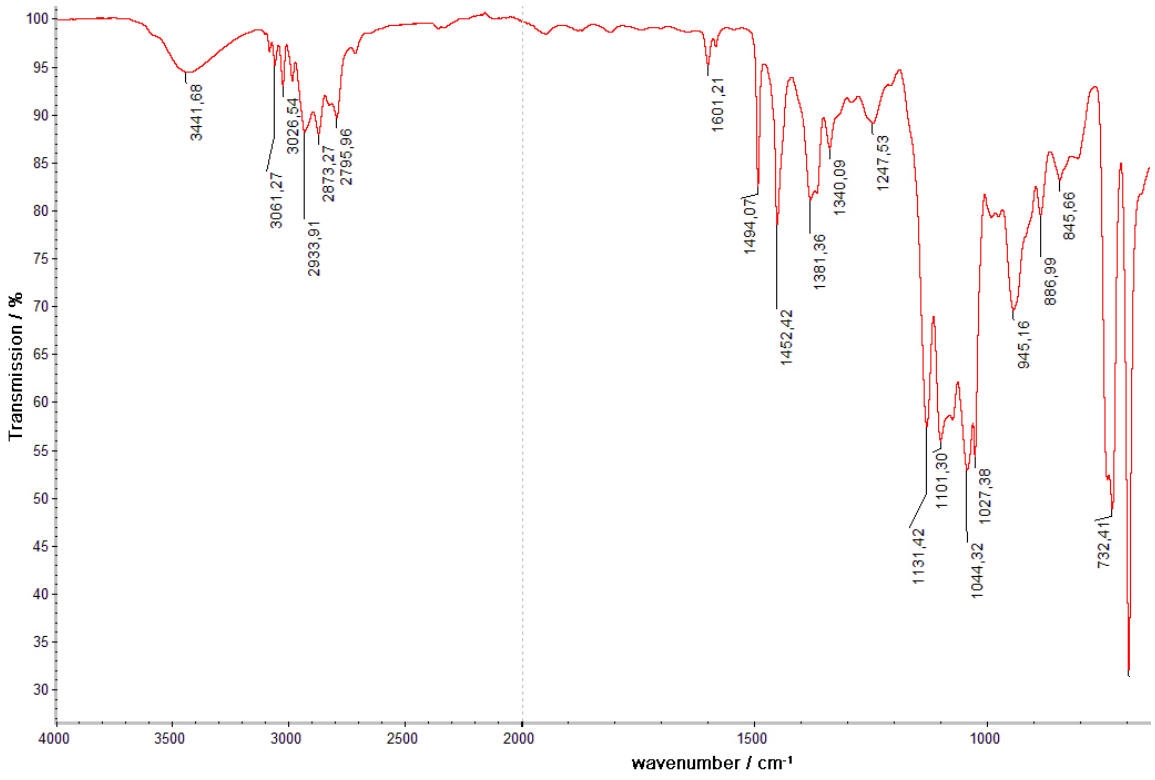

Figure S36. IR-spectrum of **4b**.

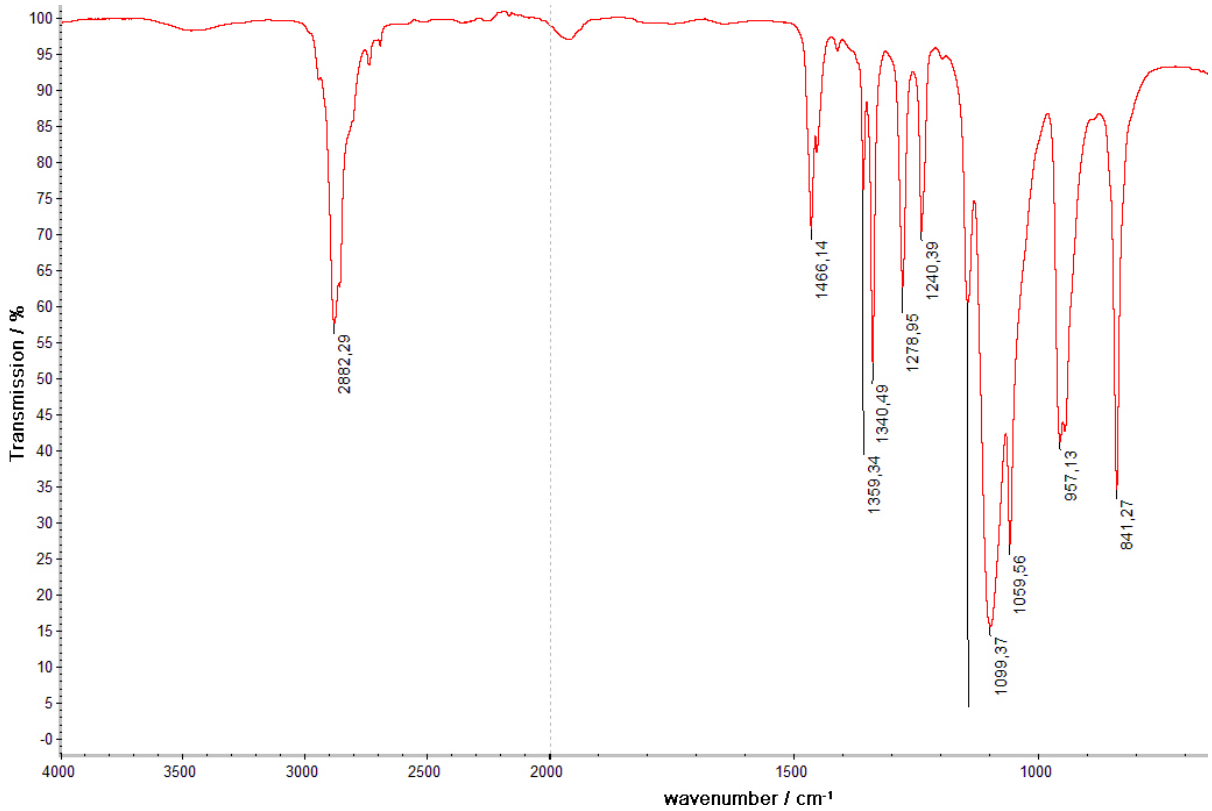

Figure S37. IR-spectrum of **4c**.

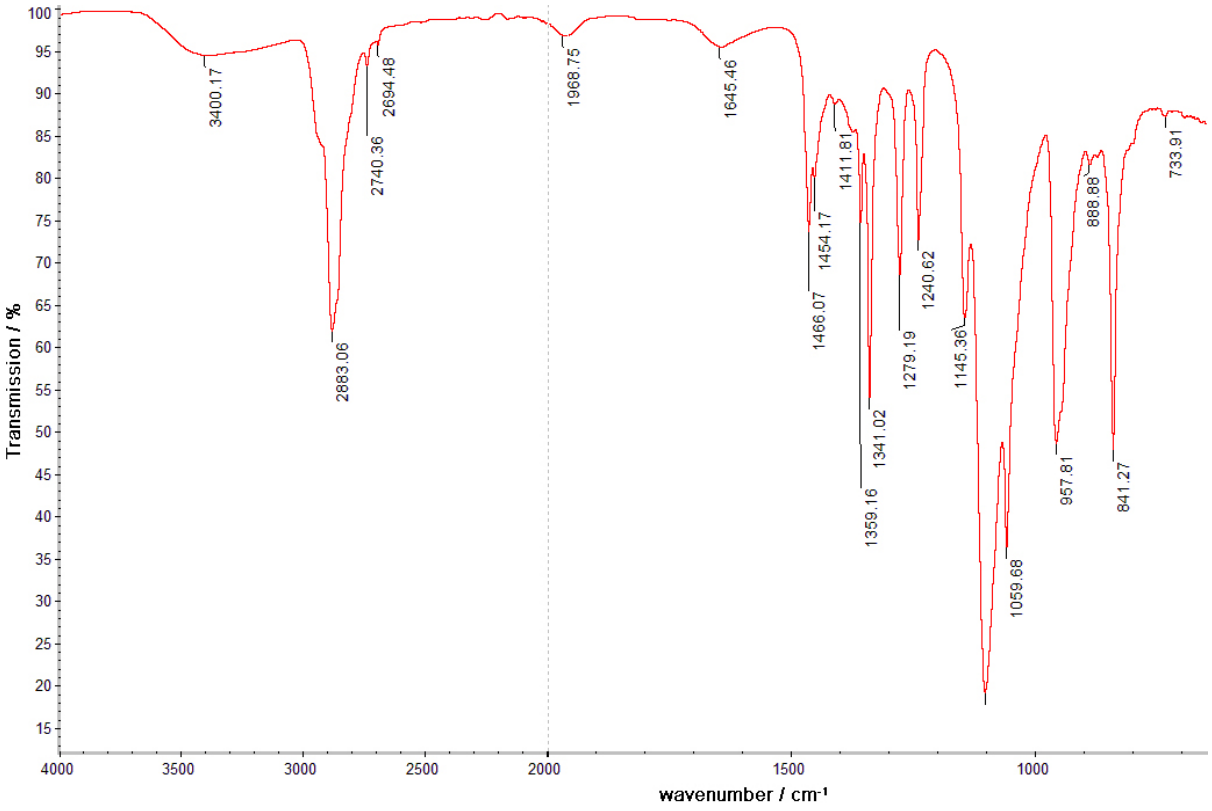

Figure S38. IR-spectrum of **5**.

4. MALDI TOF mass spectra

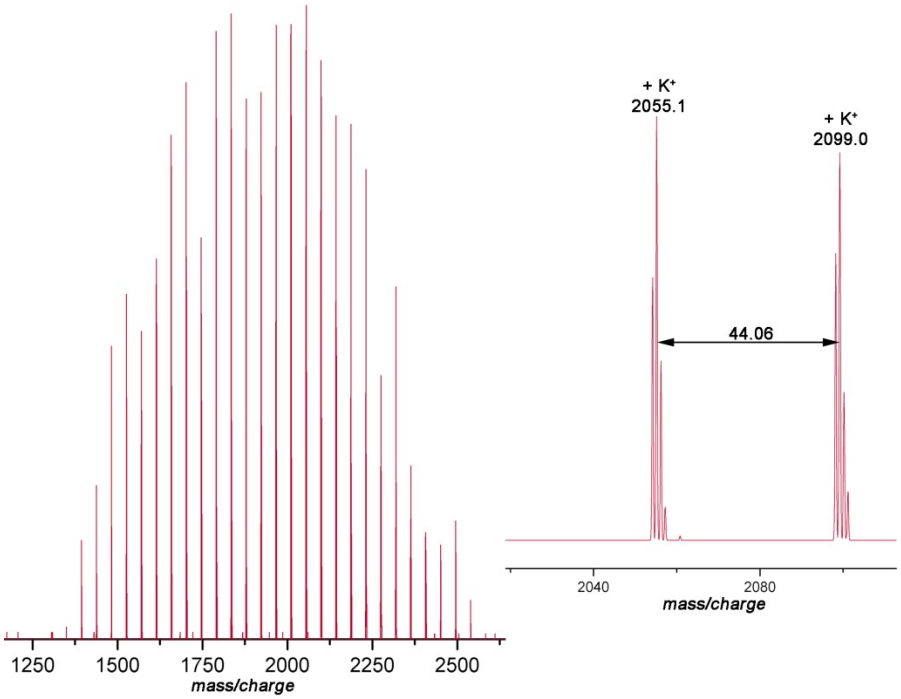

Figure S39. MALDI-ToF mass spectrum of **5** and detail (masses given for averaged signals, mass differences calculated from monoisotopic peaks). Matrix: CHCA. Salt: KTFA. Reflectron mode.
All mass-averaged peaks satisfied the following equation:

$$\boldsymbol{M_5(n) = M_{4a} + n \cdot M_{EO} + M_{K^+} = 474.8\frac{g}{mol} + n \cdot 44.05\frac{g}{mol} + 39.1\frac{g}{mol}}$$

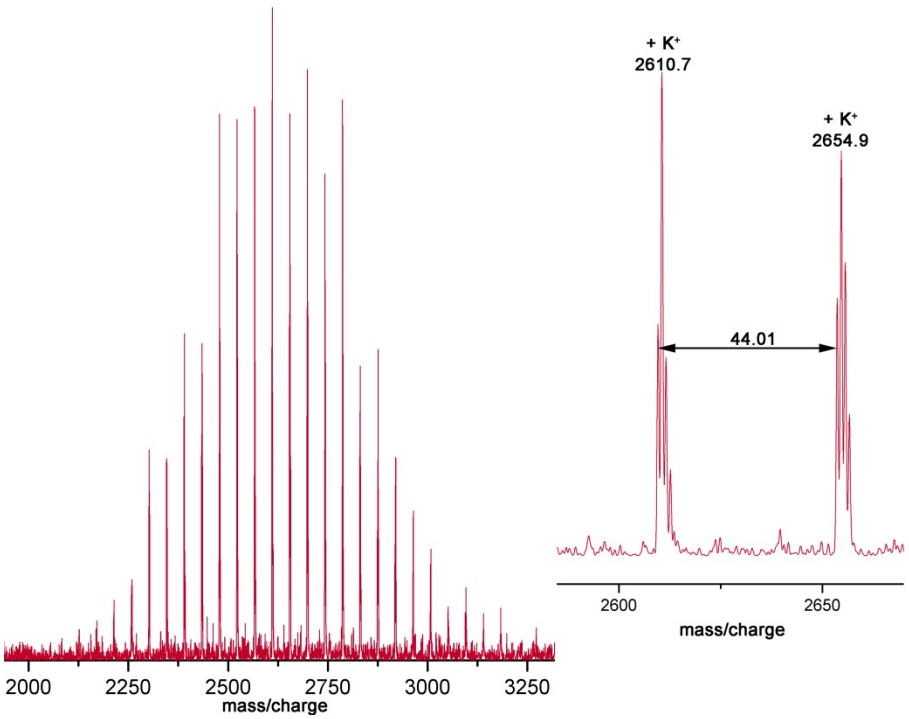

Figure S40. MALDI-ToF mass spectrum of $\mathbf{7_{50}}$ and detail (masses given for averaged signals, mass differences calculated from monoisotopic peaks). Matrix: CHCA. Salt: KTFA. Reflectron mode.
All mass-averaged peaks satisfied the following equation:

$$\boldsymbol{M_7(n) = M_{H_3N} + (3+n) \cdot M_{EO} + M_{K^+} = 17.0\frac{g}{mol} + (3+n) \cdot 44.05\frac{g}{mol} + 39.1\frac{g}{mol}}$$

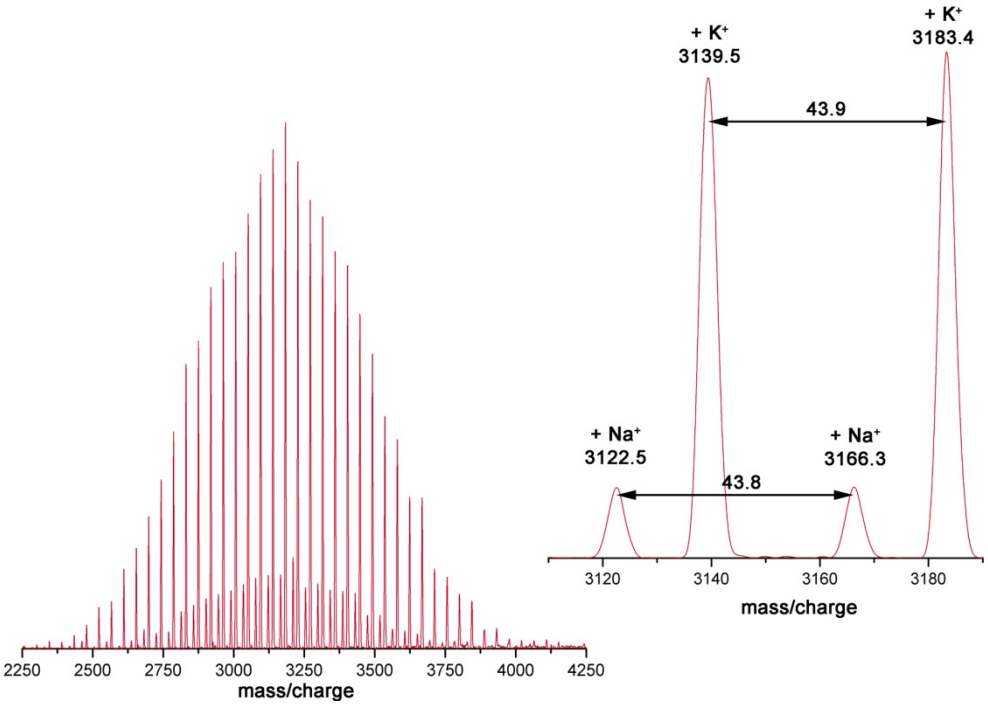

Figure S41. MALDI-ToF mass spectrum of $\mathbf{7}_{75}$ and detail (masses and differences given for averaged signals). Matrix: CHCA. Salt: KTFA. Reflectron mode.

All mass-averaged peaks satisfied the following equation.

$$\boldsymbol{M_7(n) = M_{H_3N} + (3+n)\cdot M_{EO} + M_{C^+} = 17.0\frac{g}{mol} + (3+n)\cdot 44.05\frac{g}{mol} + M_{C^+}}$$

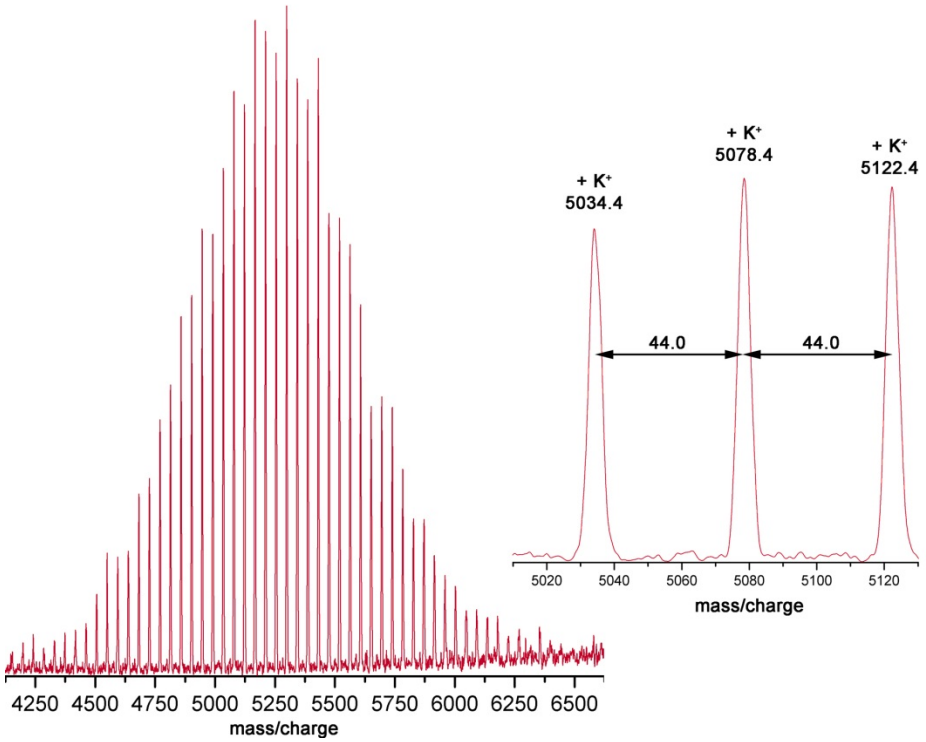

Figure S42. MALDI-ToF mass spectrum of $\mathbf{7}_{140}$ and detail (masses and differences given for averaged signals). Matrix: CHCA. Salt: KTFA. Reflectron mode.

All mass-averaged peaks satisfied the following equation:

$$\boldsymbol{M_7(n) = M_{H_3N} + (3+n)\cdot M_{EO} + M_{K^+} = 17.0\frac{g}{mol} + (3+n)\cdot 44.05\frac{g}{mol} + 39.1\frac{g}{mol}}$$

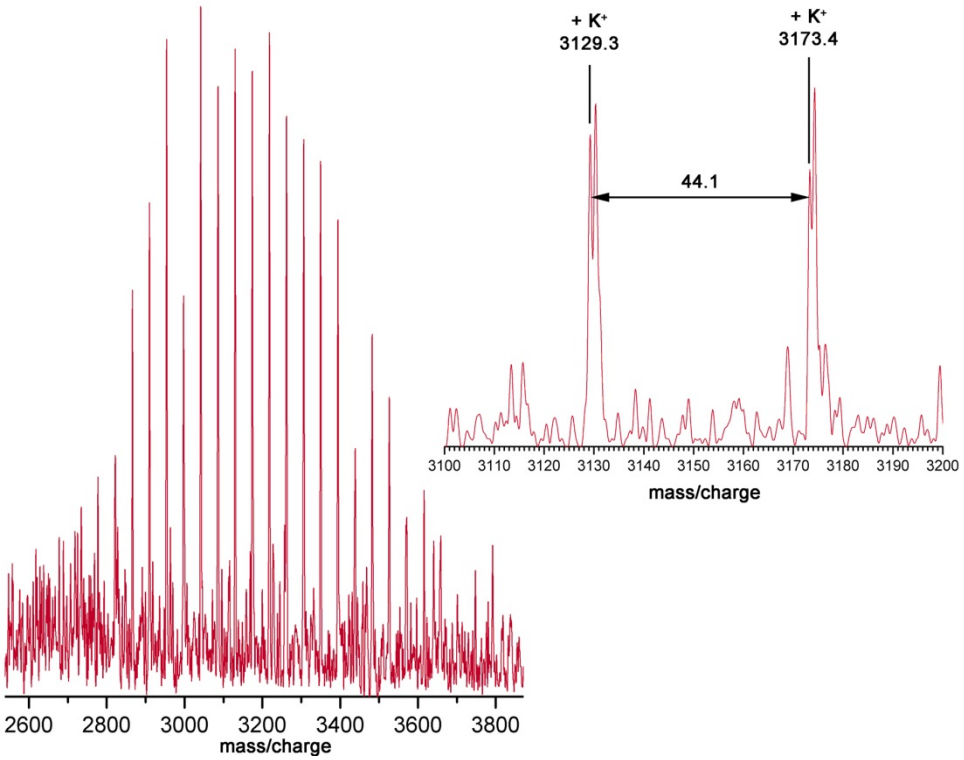

Figure S43. MALDI-ToF mass spectrum of **10** and detail (masses and difference given for monoisotopic peaks). Matrix: CHCA. Salt: KTFA. Reflectron mode.

5. SEC elugrams

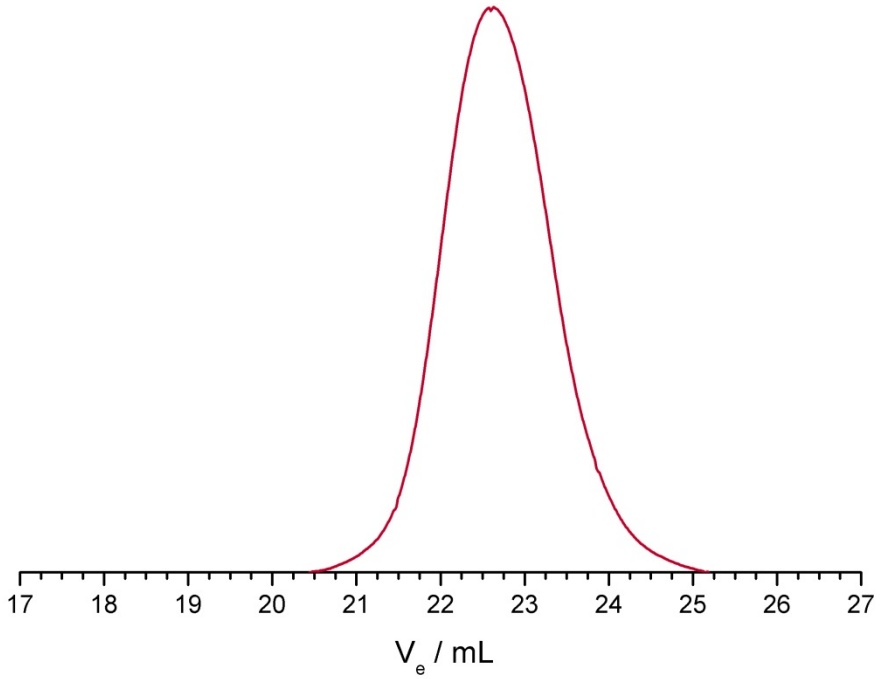

Figure S44. SEC elugram of **5**. M_n = 1690 g·mol^{-1}, *PDI* = 1.08. Number averaged molecular weight and polydispersity index obtained from calibration with PEO standards. RI detector channel, eluent: DMF containing 0.25 g·L^{-1} LiBr.

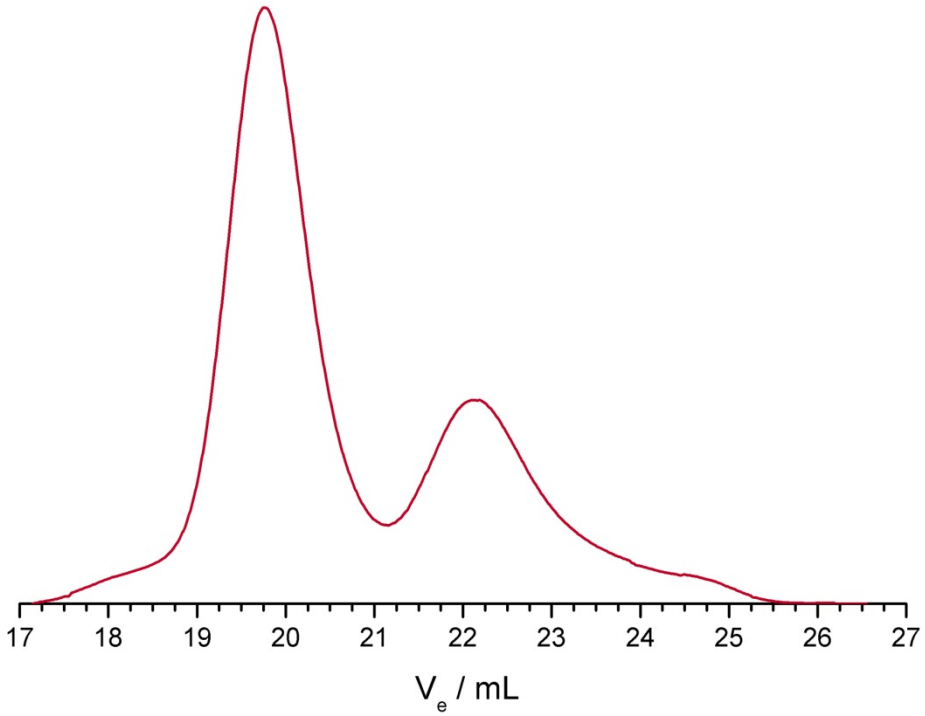

Figure S45. SEC elugram of $\mathbf{7}_{50}$. RI detector channel, eluent: DMF containing 0.25 g L^{-1} LiBr. *Note: Amino PEGs often revealed a broadening of the mass distribution in the SEC analysis (on our system) leading to an increase in the apparent M_w/M_n ratio (polydispersity index, PDI) and even to bimodal traces. This might be the result of interactions of the amino moiety with the poly(HEMA) columns of the size-exclusion chromatograph. Upon derivatization of the amino group, e.g. amide formation, the PDIs decreased significantly, confirming that the enhanced PDI-values were an artifact of the SEC-method.*

6. Spectra / elugrams of reaction kinetics

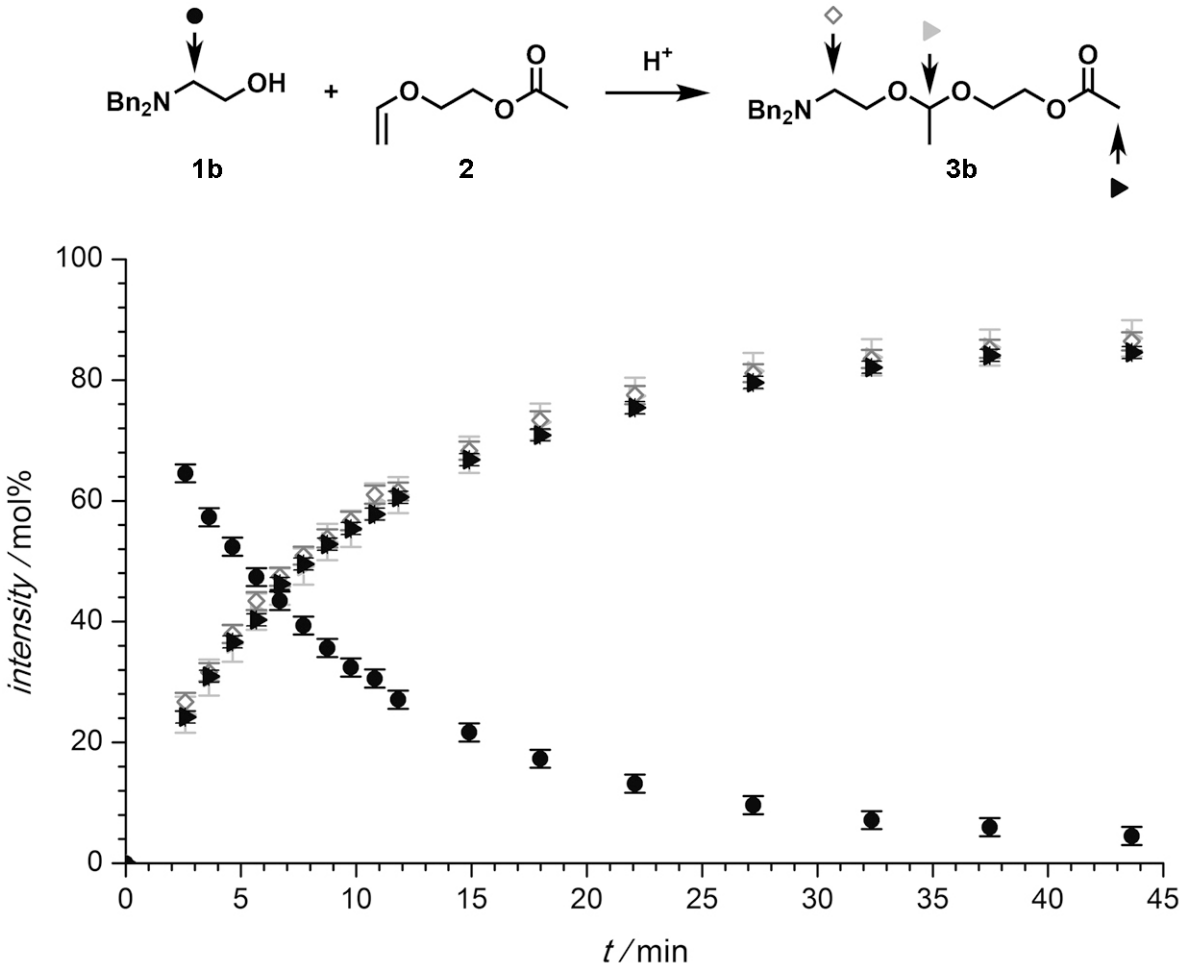

Figure S46. Reaction kinetics followed by 1H NMR spectroscopy in CDCl3 using 1.8 eq. of AcVE and 3 eq. of TFA. Exemplary, the normalized integral values of three peaks related to the dibenzylamino ethyl acetal **3b** as well as the methylene protons adjacent to dibenzylamino group of **1b** are plotted against time. Black triangles: Acetate methyl protons of **3b**. Grey triangles: Acetal methine proton of **3b**. Open diamonds: Methylene protons adjacent to dibenzylamino group of **3b**. Solid circles: Methylene protons adjacent to dibenzylamino group of **1b**. All integral values were referenced to the aromatic resonances.

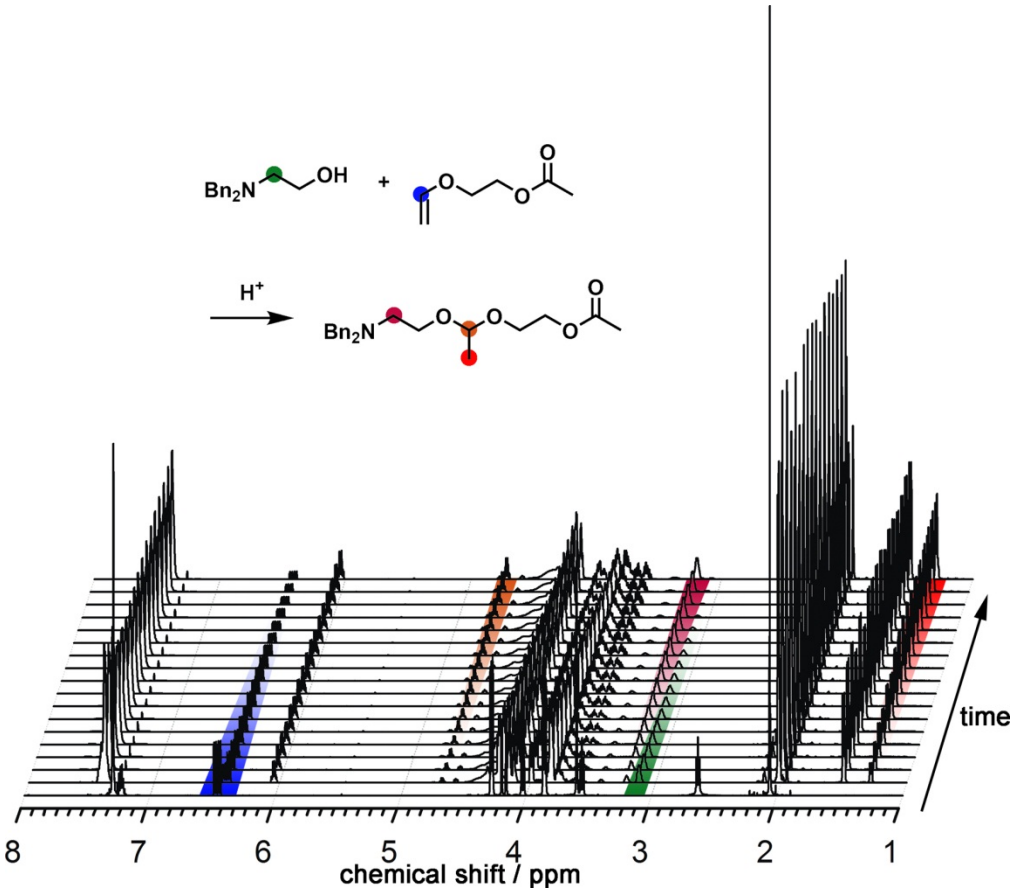

Figure S47. ^{1}H NMR spectra recorded of the reaction of dibenzylamino ethanol with acetoxyethyl vinyl ether (1.8 eq.) in CDCl3 with 3 eq. of TFA.

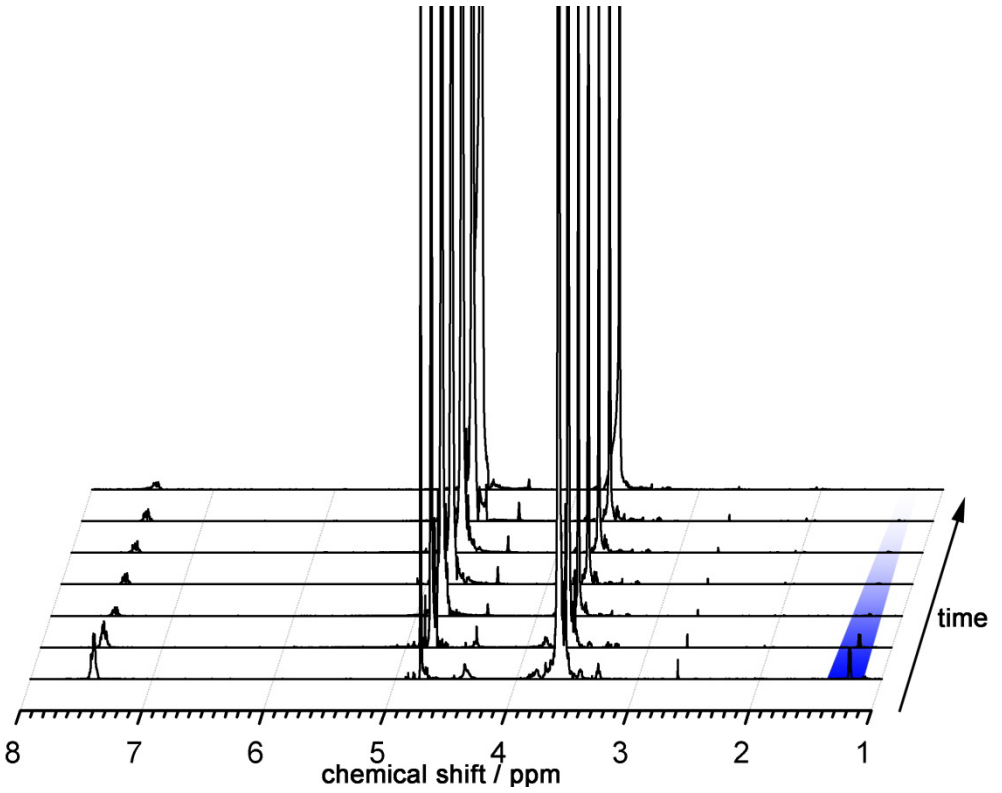

Figure S48. ^{1}H NMR spectra recorded of the acidic cleavage of $\mathbf{6}_{75}$ in D_2O acidified with D_2SO_4 (pD 2.4). Resonance of acetaldehyde acetal's methyl protons highlighted.

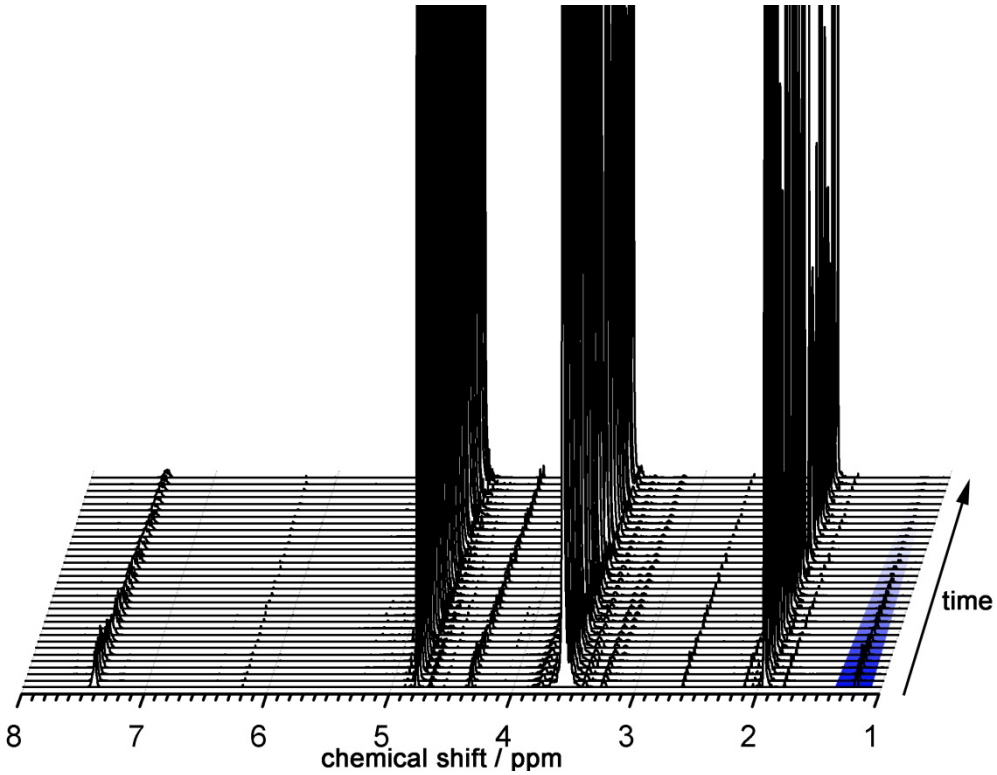

Figure S49. ^{1}H NMR spectra recorded of the acidic cleavage of $\mathbf{6}_{75}$ in deuterated aqueous acetate buffer solution (pD 4.4). Resonance of acetaldehyde acetal's methyl protons highlighted.

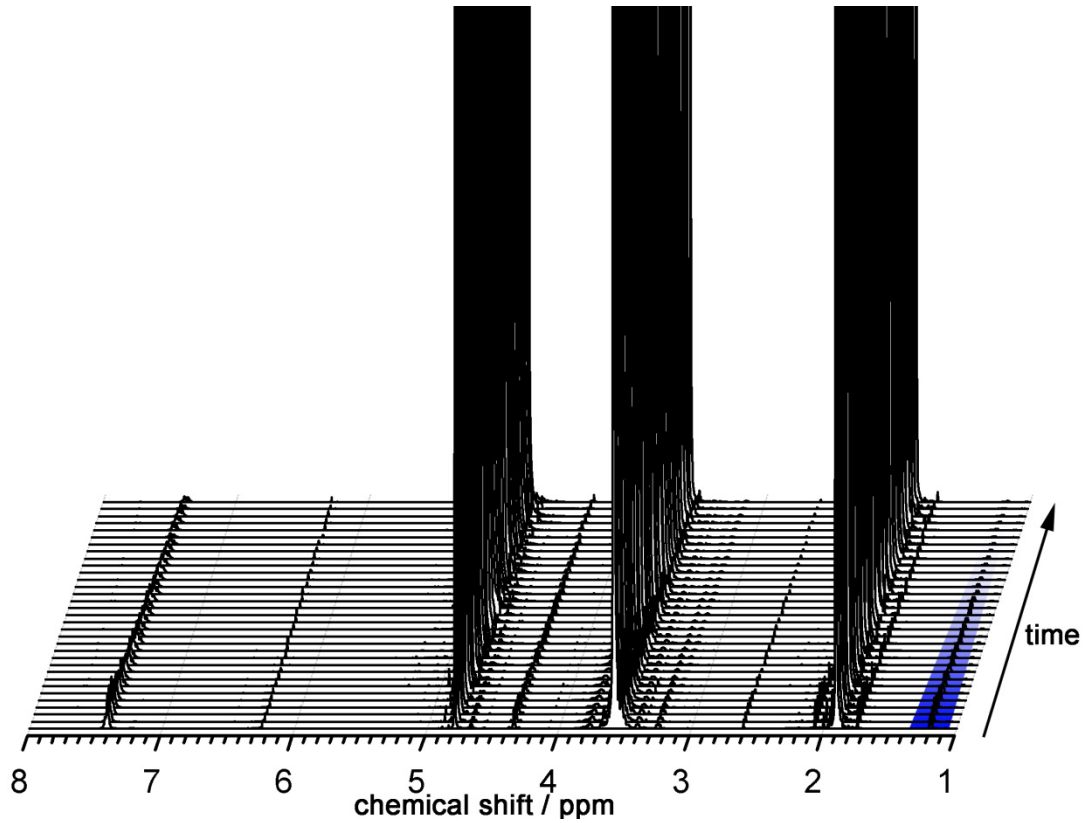

Figure S50. ^{1}H NMR spectra recorded of the acidic cleavage of $\mathbf{6}_{75}$ in deuterated aqueous acetate buffer solution (pD 4.9). Resonance of acetaldehyde acetal's methyl protons highlighted.

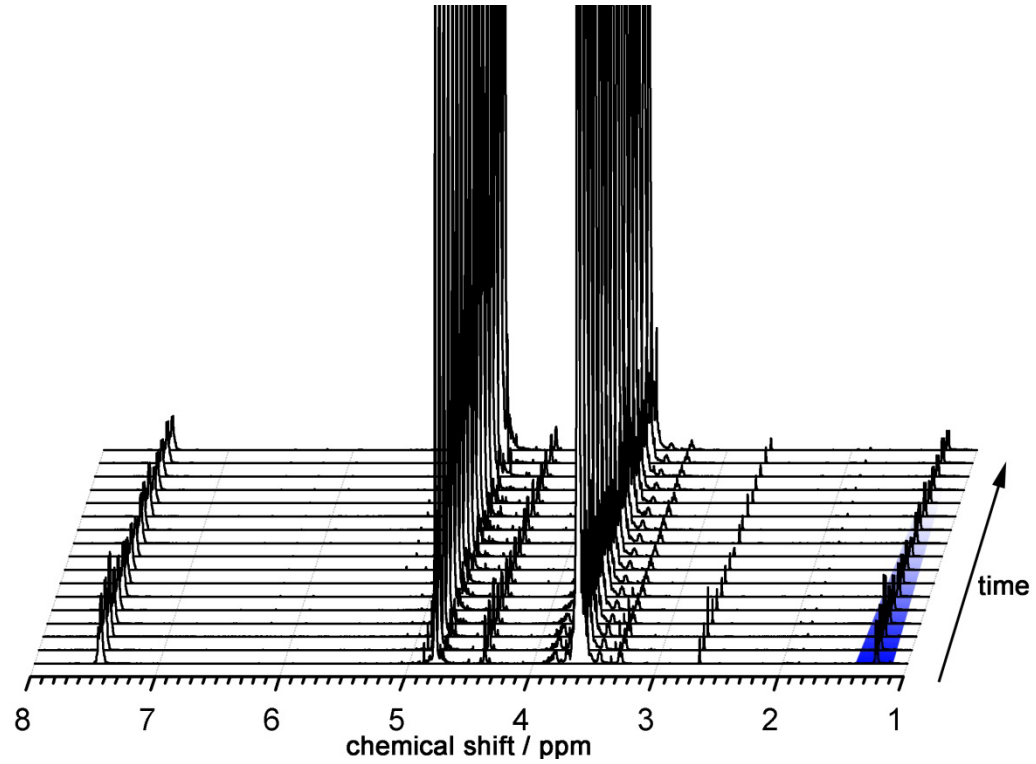

Figure S51. ^{1}H NMR spectra recorded of the acidic cleavage of $\mathbf{6}_{75}$ in deuterated aqueous phosphate buffer solution (pD 5.4). Resonance of acetaldehyde acetal's methyl protons highlighted.

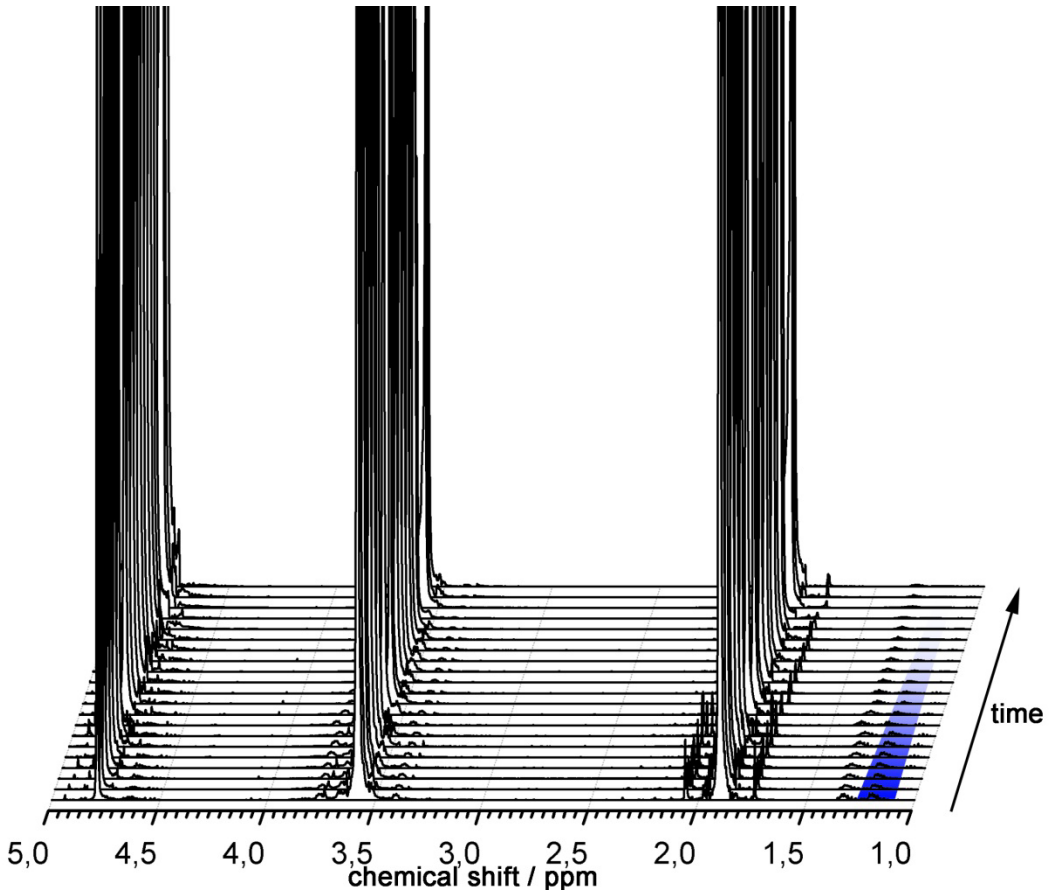

Figure S52. ^{1}H NMR spectra recorded of the acidic cleavage of **10** in deuterated aqueous acetate buffer solution (pD 4.9). Resonance of acetaldehyde acetal's methyl protons highlighted.

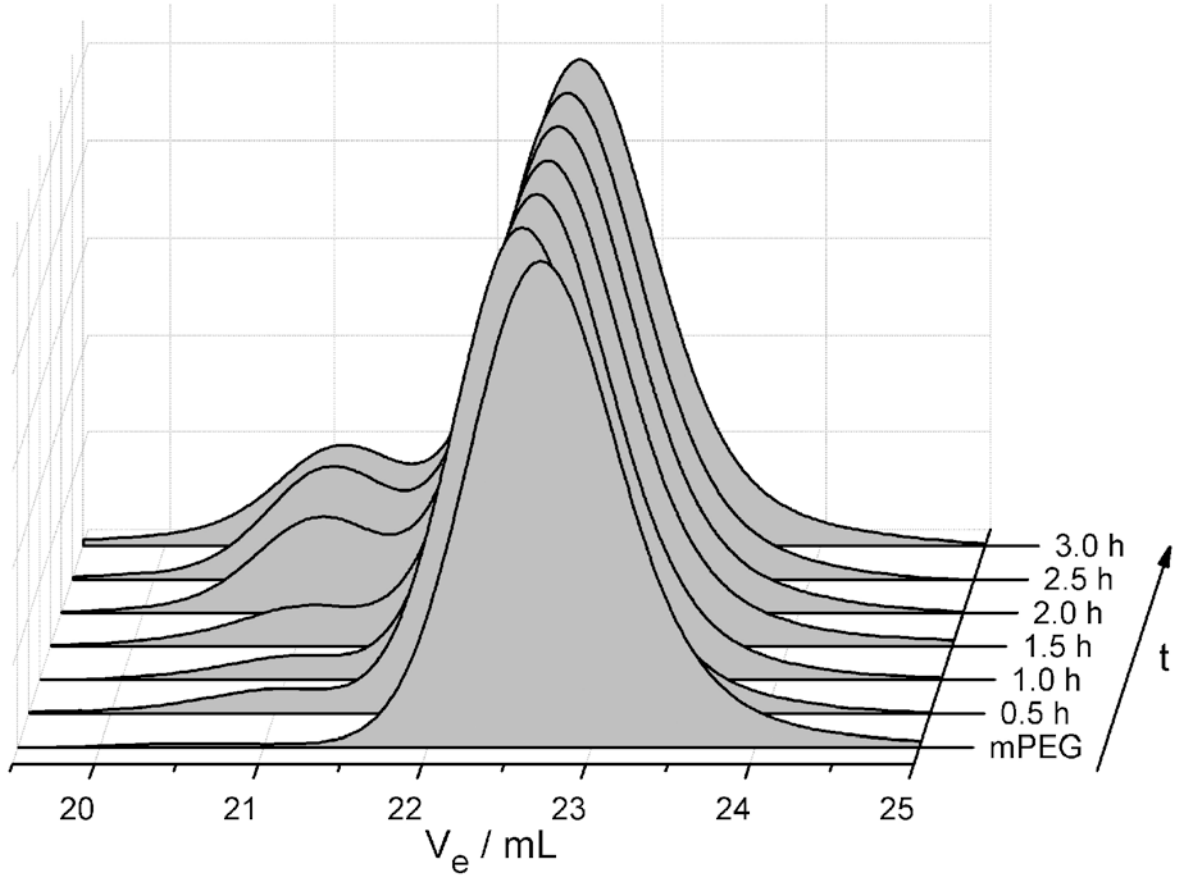

Figure S53. Reaction kinetics of the addition of mPEG (2 kg·mol^{-1}) to AcVE followed by SEC. Formation of symmetric di(mPEG) acetal observable as second mode at high molecular flank around V_e = 21 mL. RI detector channel, eluent: DMF containing 0.25 g·L^{-1} LiBr.

7. References

[1] P. K. Glasoe, F. A. Long, *J. Phys. Chem.* **1960**, *64*, 188.

[2] C. Dingels, F. Wurm, M. Wagner, H.-A. Klok, H. Frey, *Chem. Eur. J.* **2012**, *18*, 16828.

3.2 Synthesis of Heterofunctional Three-Arm Star-Shaped Poly(ethylene glycol)

Carsten Dingels,[1] *Frederik Wurm,*[2] *and Holger Frey**[1]

[1]Institut für Organische Chemie, Johannes Gutenberg-Universität Mainz, Duesbergweg 10–14, 55099 Mainz (Germany)

[2]Max-Planck-Institut für Polymerforschung, Ackermannweg 10, 55128 Mainz (Germany)

Unpublished results.

Abstract

The pharmacological properties of therapeutically interesting proteins can be improved by the covalent attachment of poly(ethylene glycol) (PEG) chains, a process also known as PEGylation. Branched PEGs have been found to be advantageous over their linear analogues, since they are less immunogenic, undergo slower proteolysis, exhibit higher in vitro bioactivities, and exhibit prolonged body residence times. However, none of these branched PEGs carry additional functionalities for the attachment of targeting moieties or labels. Herein, we present a straightforward route to α-amino ω_2-dihydroxyl three-arm star-shaped PEGs that are ideal candidates for the squaric acid mediated PEGylation. Further, we demonstrate by the use of a novel cleavable initiator for the anionic polymerization of ethylene oxide (EO) bearing a primary and a secondary hydroxyl group, that the rates of the initiation of the EO polymerization are independent on the nature of the alcohols.

Introduction

Therapeutically interesting proteins usually suffer from short body-residence times, since they undergo rapid proteolysis and often are immunogenic. The pharmacological properties of these proteins can be improved by the covalent attachment of poly(ethylene glycol) (PEG) chains,[1-6] a process also known as PEGylation and described first by Davis and coworkers.[7, 8] Besides the molecular weight of the fastened polyether,[9, 10] the *in vitro* bioactivity of PEGylated proteins, which is commonly reduced in comparison to the native derivatives and the blood-circulation times, depend on the PEG architecture. Especially the use of branched polymers drew a lot of attention, as their protein conjugates were less immunogenic, underwent slower proteolysis, and exhibited higher *in vitro* bioactivities as well as prolonged blood-circulation times than conjugates synthesized from linear PEGs.[11-15] These findings were assigned to a more effective shielding of the proteins by the branched PEGs, rather than to the different hydrodynamic radii of the resulting PEG/protein conjugates.[16] The most prominent branched PEG consists of two 20 kDa PEG monomethyl ether (mPEG) chains attached to both amino groups of a lysine active ester via urethane linkages and has been used to improve the pharmacological properties of several therapeutically interesting proteins.[11-13, 17-20] However, similar to other branched PEGs applied for protein PEGylation,[15, 21-29] the residual terminal functions of the polyethers are blocked as methyl ethers and the polymer chains cannot be derivatized at this position, which would be necessary to attach labels for tracking the fate of the polymer. Furthermore, Sherman et al. suggested that protein/PEG conjugates from α-activated ω-hydroxyl-PEGs, which were synthesized from PEG diols and subsequent isolation from divalent species via HPLC, might show a reduced loss of efficacy compared to the methylated derivatives.[30]

Herein, we report the straightforward synthesis of a heterofunctional three-arm star PEG carrying a single amino and two hydroxyl termini (Scheme 1), which can be applied for the recently presented squaric-acid-mediated PEGylation,[31, 32] and discuss the initiation rates of primary and secondary hydroxyl groups in the anionic ring-opening polymerization (AROP) of ethylene oxide (EO). An ether baed on glycerol was chosen as the branching unit, since it lasts the harsh AROP conditions and most probable yields a biocompatible material. This assumption was based on the biocompatibility of both glycerol and polyglycerol.[33, 34]

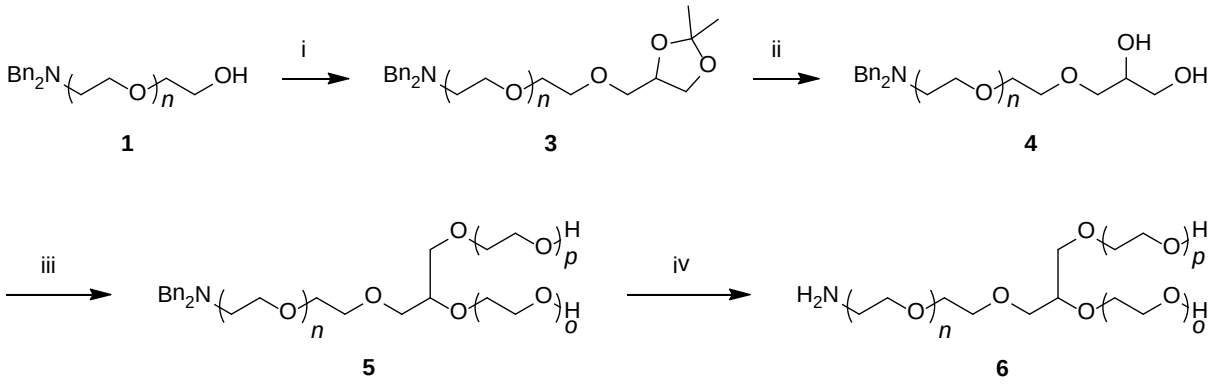

Scheme 1. Synthesis of heterofunctional three-arm star shaped PEG **6**. i) 2,2-Dimethyl-4-(*p*-tolylsulfonyl-oxymethyl)-1,3-dioxolane (**2**), NaOH, tetrahydrofuran (THF), tetrabutyl ammonium bromide (TBAB). ii) 1 M hydrochloric acid, THF. iii) 1. $CsOH{\cdot}H_2O$, C_6H_6, 90 °C, vacuum; 2. Tetrahydrofuran (THF), $m = o + p$ EO, 60 °C; 3. MeOH. iv) H_2, $Pd(OH)_2/C$, dioxane/water 1:1, 80 bar, 40 °C.

Experimental Section

Materials. All reagents and solvents were purchased from Acros Organics, Fluka or Sigma-Aldrich and were used without further purification unless stated otherwise. Ethylene glycol monovinyl ether was purchased from TCI Europe. Deuterated solvents were purchased from Deutero GmbH and stored over molecular sieves (except for deuterium oxide). Dibenzylamino ethanol,[35] 4-bromomethyl-2,2-dimethyl-1,3-dioxolane,[36] 2,2-dimethyl-4-trifluoromethane-sulfonyloxymethyl-1,3-dioxolane,[37] α-(*N,N*-dibenzylamino)-ω-hydroxy poly(ethylene glycol) (**1**),[31] and 1-(glycidyloxy)ethyl benzyloxethyl ether[38] were prepared according to known protocols. Dry THF used for the anionic ring-opening polymerization of ethylene oxide was dried and stored over sodium. Care must be taken when handling the highly toxic, flammable, and gaseous ethylene oxide.

Methods. 400 MHz spectra ^{1}H NMR spectra were either recorded on a Bruker ARX 400 or a Bruker Avance-II 400 with a 5mm BBO probes. 300 MHz spectra ^{1}H NMR spectra were recorded on a Bruker AC300 equipped with a 5mm dual ^{13}C probe and a B-ACS 60 auto sampler. All spectra were recorded with 32 scans at 294 K using a relaxation delay of 1 s unless stated otherwise and processed with MestReNova v6.1.1 software. Size-exclusion chromatography (SEC) measurements in DMF containing 0.25 $g{\cdot}L^{-1}$ of lithium bromide as additive were performed on an Agilent 1100 Series as an integrated instrument using PSS (Polymer Standards Service) HEMA column (106/105/104 g/mol), RI-detector, and UV-detector operating at 275 nm. Calibration was executed using poly(ethylene oxide) (PEO)

standards from PSS. Matrix-assisted laser desorption/ionization time-of-flight mass spectrometry (MALDI-ToF MS) measurements of all polymers were recorded on a Shimadzu Axima CFR MALDI-ToF MS mass spectrometer, equipped with a nitrogen laser delivering 3 ns laser pulses at 337 nm. α-Cyano hydroxyl cinnamic acid (CHCA) or dithranol was used as a matrix and potassium trifluoroacetate (KTFA) was added for ion formation. The analytes were dissolved in methanol at a concentration of 10 $g \cdot L^{-1}$. An aliquot (10 µL) was added to 10 µL of a solution (10 $g \cdot L^{-1}$) of the matrix and 1µL of a solution of the cationization agent. 1 µL of the mixture was applied on a multistage target, methanol evaporated, and a thin matrix/analyte film was formed. Mass spectra were measured on a Finnigan MAT 95 (field desorption, FD-MS).

Procedures. *2,2-Dimethyl-4-(p-tolylsulfonyloxymethyl)-1,3-dioxolane (2).* **2** was synthesized according to a modified version of a known protocol.[39] A solution of *p*-toluenesulfonyl chloride (89.0 g, 0.467 mol) in dry pyridine (160 mL) was placed in a dropping funnel and added drop-wise to freshly, over calcium hydride distilled solketal (51.6 g, 0.390 mol) in dry pyridine (40 mL) under argon atmosphere and continuous stirring at 0 °C. The resulting solution was allowed to come to room temperature slowly and was stirred over-night. Diethyl ether (200 mL) was added and the solution was subsequently washed with 1 m hydrochloric acid (440 mL), water (400 mL) and saturated sodium bicarbonate solution (400 mL). The organic layer was dried over sodium sulfate and filtered. **2** was obtained as colorless crystals (86.2 g, 0.301 mol, 77%) after recrystallizing twice from diethyl ether and subsequent drying *in vacuo*. *^1H NMR* (400 MHz, $CDCl_3$): δ [ppm] = 7.79 (d, 2H, J = 8.4 Hz, ortho CH_{Ar}), 7.35 (d, 2H, J = 8.4 Hz, meta CH_{Ar}), 4.34–4.19 (m, 1H, H-4), 4.15–3.91 (m, 3H, CH_2OTs and H-5a), 3.76 (dd, 1H, J = 8.8 Hz, 5.0 Hz, H-5b), 2.44 (s, 3H, Ar-CH_3), 1.33 (s, 3H, CH_3), 1.30 (s, 3H, CH_3).

α-(N,N-Dibenzylamino)-ω-(2,2-dimethyl-1,3-dioxolan-4-yl)methyl PEG (3). A mixture of sodium hydroxide (1.02 g, 25.6 mmol), tetrabutyl ammonium bromide (TBAB, 82.5 mg, 256 µmol), α-dibenzylamino-ω-hydroxy poly(ethylene glycol) (**1**, 4.67 g, 1.95 mmol), water (0.3 mL) and THF (0.75 mL) were heated in a closed flask to 55 °C for 1 h. Subsequently, **2** (6.66 g, 23.3 mmol) was added and the melt was stirred at that temperature for 5 d. Water was added and the mixture was extracted with dichloromethane (DCM) four times. The combined organic phases were dried over sodium sulfate, filtered and reduced to a small volume. The product was purified by precipitating from DCM in cold diethyl ether twice (3.87 g, 1.57 mmol, 80%).

^{1}H NMR (300 MHz, DMSO-d_6): δ [ppm] = 7.50-7.10 (m, 10H, CH_{Ar}), 4.24 – 4.09 (m, 1H, H-4), 3.97 (dd, 1H, J = 8.1 Hz, 6.5 Hz, H-5a), 3.90–3.08 (m, 189H, CH_2O and H-5b), 3.59 (s, 4H, CH_2Ph), 2.55 (t, 2H, J = 6.1 Hz, CH_2NBn_2), 1.31 (s, 3H, CH_3), 1.26 (s, 3H, CH_3).

α-(N,N-Dibenzylamino)-ω-2,3-dihydroxypropyl PEG (4). **3** (1.96 g, 0.794 mmol) was stirred in a solution of THF (5 mL) and 1 M hydrochloric acid (5 mL) for 24 h. After the pH was adjusted to 13 by the addition of caustic soda, half-concentrated brine (20 mL) was added and the solution was extracted four times with DCM. The combined organic phases were dried over sodium sulfate, filtered and reduced to a small volume. **4** was purified by precipitating from DCM in cold diethyl ether twice (1.65 g, 0.468 mmol, 86%). *^{1}H NMR* (400 MHz, DMSO-d_6): δ [ppm] = 7.41–7.15 (m, 10H, CH_{Ar}), 4.61 (d, 1H, J = 5.0 Hz, *sec* OH), 4.46 (t, 1H, J = 5.7 Hz, *prim* OH), 3.90–3.04 (m, 194H, CH_2O), 3.59 (s, 4H, CH_2Ph), 2.55 (t, 2H, J = 6.1 Hz, CH_2NBn_2).

α-(N,N-Dibenzylamino)-ω$_2$-dihydroxy PEG$_3$ (5). This protocol describes the polymerization initiated with $\mathbf{4}_{74}$. The macroinitiator $\mathbf{4}_{74}$ (950 mg, 0.275 mmol) was dissolved in benzene (10 mL) in a Schlenk flask equipped with a glass stir bar and dried by azeotropic distillation at 60 C in high vacuum overnight. Dry THF (20 mL) was cryo-transferred into the Flask which was subsequently flooded with argon. A solution of potassium naphthalenide in dry THF (0.35 mL, 0.5 M) was added via syringe and the solution was cooled to -80 °C. The hydrogen originating from the proton reduction as well as a small amount of THF was removed under reduced pressure. After ethylene oxide (1.1 mL) had been cryo-transferred via a graduated ampule to the initiator solution, the polymerization was carried out at 60 C for 2 days. **5** was isolated by repeated precipitation from dichloromethane in cold diethylether. *^{1}H NMR* (300 MHz, DMSO-d_6): δ [ppm] = 7.62–7.04 (m, 10H, CH_{Ar}), 4.72-4.47 (s, 2H, 2 OH), 4.12-2.86 (m, 388H, CH_2O), 2.55 (s, 2H, CH_2NBn_2).

α-Amino-ω$_2$-dihydroxyl PEG$_3$ (6). **5** was hydrogenated according to a protocol for the catalytic hydrogenation of *α-(N,N-Dibenzylamino)-ω-hydroxy-PEG*.[31] Yield: 61%.

1-(2-Hydroxypropyloxy)ethyl ethylene glycol ether (8). Palladium on activated charcoal (200 mg) was added to a solution of 1-(glycidyloxy)ethyl benzyloxethyl ether (**7**, 2.00 g, 7.93 mmol) in dry THF (40 mL). The mixture was placed under a hydrogen atmosphere in an autoclave at 40 bar and stirred for 72 h. Subsequently, the reaction mixture was filtered and the filter cake was washed with THF several times. The pure product (729 mg, 4.45 mmol, 56%) was obtained as a mixture of diastereomers upon removal of the solvent and subsequent column chromatography (eluent: petroleum ether/ethyl acetate/aceton 1:2:2 v/v/v). *^{1}H NMR* (400

MHz, DMSO-d_6): δ [ppm] = 4.68 (d, J = 5.3 Hz, 1H, H_3C-CHO_2), 4.59 (t, J = 5.4 Hz, 1H, *prim* OH), 4.57 (dd, J = 4.7 Hz, J = 2.9 Hz, 1H, *sec* OH), 3.74–3.63 (m, 1H, CH_3-CHOH-), 3.56–3.50 (m, 1H, $HOCH_2$-CH_a), 3.48 (dd, J = 10.3, J = 5.0 Hz, 2H, HO-CH_2), 3.42–3.37 (m, 1.5H, $HOCH_2$-CH_b + 0.5 MeCHOH-CH_a), 3.32–3.22 (m, 1H, 0.5 MeCHOH-CH_a + 0.5 MeCHOH-CH_b), 3.17 (dd, J = 9.6, 5.6 Hz, 1H, 0.5 MeCHOH-CH_b), 1.19 (d, J = 5.3 Hz, 1H, H_3C-CHO_2), 1.03 (dd, J = 6.3, 1.7 Hz, 3H, CH_3-CHOH-). *^{13}C NMR* (100.6 MHz, DMSO-d_6): δ [ppm] = 99.4 (1C, H_3C-CHO_2), 70.7 (1C, MeCHOH-CH_2), 66.7 (1C, $HOCH_2$-CH_2), 65.2 (1C, CH_3-CHOH-), 60.4 (1C, HO-CH_2), 20.4 (1C, CH_3-CHOH-), 19.8 (1C, H_3C-CHO_2). MS (FD-MS, MeOH): m/z = 89.2, 103.1, 165.1 $[M+H]^+$, 329.1 $[2M+H]^+$, 493.3 $[3M+H]^+$.

*Cleavable poly(ethylene glygol) (**9**).* The following protocol describes the synthesis of **9b** derived from 23% deprotonated **8**. **8** (171 mg, 1.04 mmol) was dissolved in benzene (6 mL) and placed in a dry Schlenk flask containing cesium hydroxide monohydrate (79 mg, 0.47 mmol). The solution was stirred for several hours at 60 °C under slightly reduced pressure. Benzene and reaction water were removed by distillation and subsequent drying at 40 °C under high vacuum. After dry THF (10 mL) had been cryo-transferred into the Schlenk flask, dry DMSO (2 mL) was added to the flask via a syringe. Ethylene oxide (5.0 g, 0.11 mol) was cryo-transferred via a graduated ampule into the initiator solution, the flask was closed tightly and the reaction mixture was stirred for 3 d at 40 °C. The polymer was precipitated from methanol in cold diethyl ether. Filtration and subsequent drying under reduced pressure gave **9** in quantitative yields. *^{1}H NMR* (300 MHz, DMSO-d_6): δ [ppm] = 4.69 (q, J = 5.1 Hz, 1H, H_3C-CHO_2), 4.58 (s, 2H, 2 OH), 3.92–3.11 (m, 413H, CH_2O), 1.19 (d, J = 5.3 Hz, 3H, H_3C-CHO_2), 1.06 (dd, J_{AB} = 6.2, 2.6 Hz, 3H, CH_3-CHOH-). Attention must be paid when working with the gaseous, toxic, and flammable ethylene oxide.

Results and Discussion

Synthesis of the macroinitiator. According to the synthetic pathway to heterofunctional three-arm star shaped poly(ethylene glycol)s presented in Scheme 1, amino-protected heterotelechelic α-(*N,N*-dibenzylamino)-ω-hydroxy poly(ethylene glycol)s (**1**) are required. Four well-defined polymers with different degrees of polymerization (P_n) $\mathbf{1}_{Pn}$ ($\mathbf{1}_{49}$, $\mathbf{1}_{74}$, $\mathbf{1}_{127}$, and

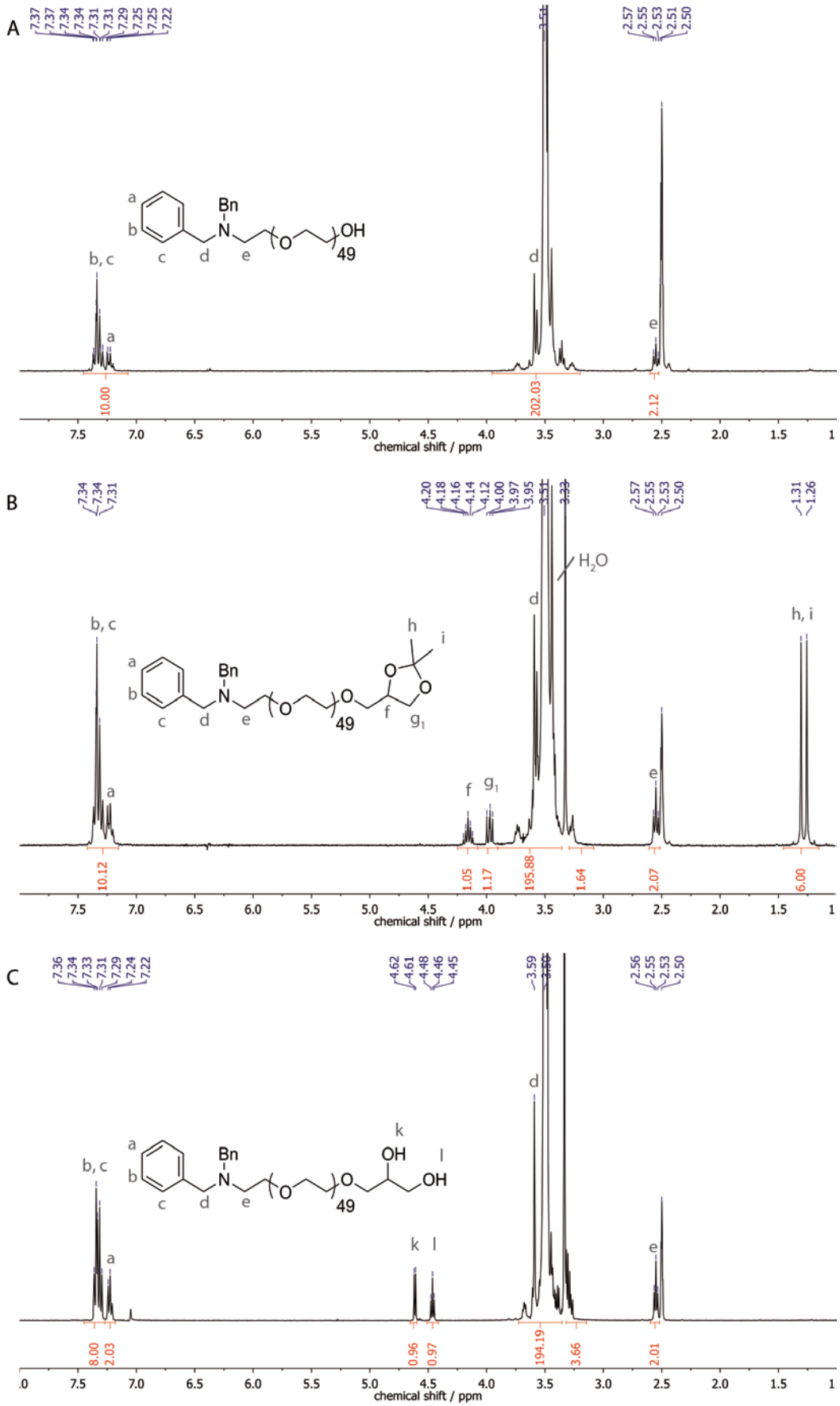

Figure 1. ^{1}H NMR spectra of the macroinitiator with P_n = 49 and its precursors recorded in DMSO-d_6. **A** $\mathbf{1}_{49}$ (300 MHz). **B** $\mathbf{3}_{49}$ (300 MHz). **C** $\mathbf{4}_{49}$ (400 MHz). Characteristic resonances are labeled.

$\mathbf{1}_{257}$) were synthesized in the molecular weight range of 2,000 g·mol^{-1} to 11,000 g·mol^{-1} with polydispersity indices (PDI, M_w/M_n) from 1.03 to 1.05, following a protocol published recently by our group and analyzed by standard characterization methods (^{1}H NMR spectroscopy, MALDI-TOF MS, and SEC).[31] The ^{1}H NMR and the mass spectra of $\mathbf{1}_{49}$ (along with its derivatives $\mathbf{3}_{49}$, and $\mathbf{4}_{49}$) are presented in Figures 1 and 2, respectively. The corresponding spectra of all the other polymers are provided in the Supporting Information. Unfortunately, MALDI-TOF MS analysis of most of the polymers with $P_n \geq 127$ resulted in unsatisfactory mass spectra, which either were poorly resolved or did not show any polymeric species, most probably due to the poorer desorbability resulting from the higher masses of theses polymers and the less accurate resolution of the spectrometer (compare Experimental Section) at higher molecular masses. SEC traces of all the macroinitiators and their precursors including $\mathbf{1}_{Pn}$ are shown in Figure 3.

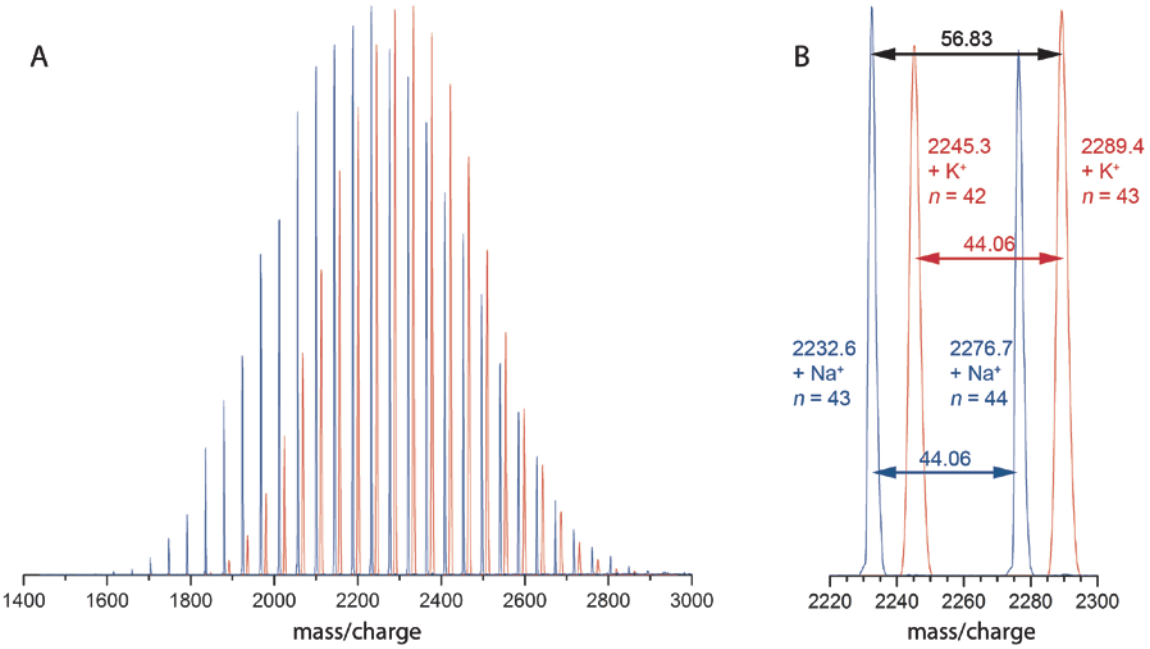

Figure 2. Superimposed MALDI-TOF mass spectra of $\mathbf{3}_{49}$ (red) and $\mathbf{4}_{49}$ (blue). **A** Full spectra. **B** Detail.

To yield **3**, the protected glycerol branching unit was added to **1** in a postpolymerization reaction via etherification with 2,2-dimethyl-4-(*p*-tolylsulfonyloxymethyl)-1,3-dioxolane (**2**), which was synthesized from solketal and *p*-toluenesulfonyl chloride by a modified version of a known protocol.[39] The isopropylidene protecting group was necessary to prevent uncontrolled etherification of the residual glycerol hydroxyls. It was removed form **3** efficiently in a THF/hydrochloric acid mixture. Attempts to synthesize **3** in a one-pot reaction by terminating

the *N,N*-dibenzylamino-ethanol-initiated EO polymerization with either **2**, 2,2-dimethyl-4-(trifluoromethanesulfonyloxymethyl)-1,3-dioxolane, or 4-bromomethyl-2,2-dimethyl-1,3-dioxolane did not result in polymers with completely converted terminal functionalities. Full conversions of both postpolymerization reactions, i.e., etherification and deprotection of the vicinal diol, were verified by end group analysis with and ^{1}H NMR spectroscopy and MALDI-TOF mass spectrometry.

Table 1. Polymers $\mathbf{1}_{Pn}$, $\mathbf{3}_{Pn}$, and $\mathbf{4}_{Pn}$, sorted by P_n.

Polymer	M_n[a] / g·mol^{-1}	M_n[b] / g·mol^{-1}	M_n[c] / g·mol^{-1}	M_w[c] / g·mol^{-1}	P_n[b]	PDI[c]
$\mathbf{1}_{49}$	2360	2400	1910	2000	49	1.05
$\mathbf{3}_{49}$	2510	2470	1770	1850	48	1.05
$\mathbf{4}_{49}$	2554	2430	2200	2340	48	1.06
$\mathbf{1}_{74}$	3360	3500	2740	2830	74	1.03
$\mathbf{3}_{74}$	3610	3660	2800	2920	75	1.04
$\mathbf{4}_{74}$	3460	3840[d]	2780	2880	80[d]	1.04
$\mathbf{1}_{127}$	5360	5940	5130	5380	127	1.05
$\mathbf{3}_{127}$	5990	5960	5000	5340	127	1.07
$\mathbf{4}_{127}$	5950	5960	5270	5650	128	1.07
$\mathbf{1}_{257}$	10400	11600	10100	10600	257	1.05
$\mathbf{3}_{257}$	11700	11200	8010	8700	247	1.09
$\mathbf{4}_{257}$	11700	11500	9480	10300	255	1.08

[a] Calculated. [b] Determined by ^{1}H NMR. [c] Determined by SEC, referenced to PEG standards. [d] NMR spectrum of poor quality.

From the NMR spectra of **3** (exemplary spectrum of $\mathbf{3}_{49}$ shown in Figure 1B) the degree of conversion of the etherification could be calculated by comparing the integrals of the resonances of the initiator (the aromatic signals or the peak of the methylene adjacent to the dibenzylamino group) to the area under the peaks of the 1,2-acetonide. The integral ratios of the PEG backbone signal (reduced by 5 protons, originating from the termini) to the initiator resonances yielded the degree of polymerizations, which were consistent with the corresponding precursor

polymers (Table 1). Complete removal of the isopropylidene protecting group was proven by the absence of the acetonide signal as well as the presence of the hydroxyl resonances in the proton NMR spectra (exemplary spectrum of $\mathbf{4}_{49}$ shown in Figure 1C).The results obtained from the NMR spectra were confirmed by the mass spectra, in which the polymeric species were either cationized with potassium or sodium ions. In Figure 2A the representative mass spectra of $\mathbf{3}_{49}$ and $\mathbf{4}_{49}$ are superimposed, exhibiting only the expected distributions of mass peaks. While the former was exclusively cationized with potassium, the latter was detected associated to sodium ions. The mass difference between molecules of $\mathbf{3}_{49}$ and $\mathbf{4}_{49}$ with the same degree of polymerization (Figure 2B) is consistent with the removal of the isopropylidene protecting group. MALDI-TOF spectra of the other polymers are provided in the Supporting Information. Unfortunately, from all PEGs with $P_n \geq 127$ a well-resolved mass spectrum was only obtained of $\mathbf{3}_{127}$.

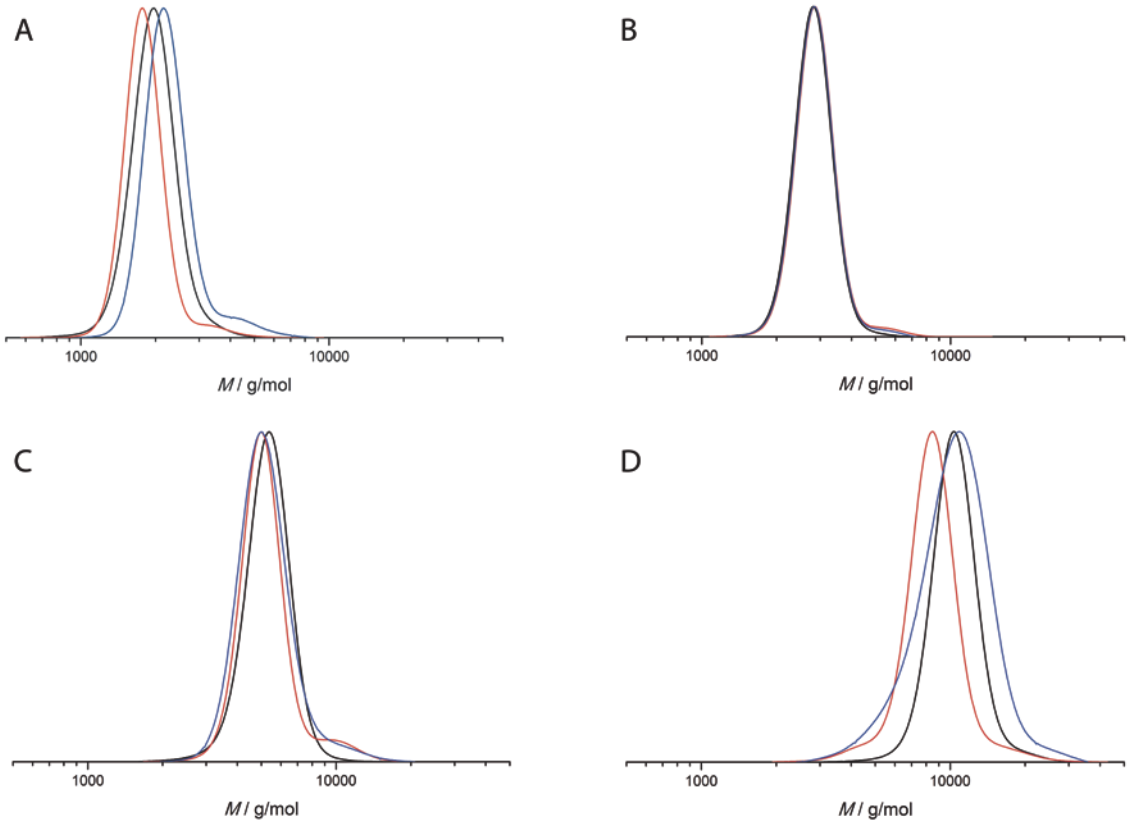

Figure 3. Molecular weight distributions of polymers $\mathbf{1}_{Pn}$ (black), $\mathbf{3}_{Pn}$ (red), and $\mathbf{4}_{Pn}$ (blue) referenced to PEG standards. **A** $P_n = 49$. **B** $P_n = 74$. **C** $P_n = 127$. **D** $P_n = 257$.

The size-exclusion chromatograms of $\mathbf{1}_{Pn}$, $\mathbf{3}_{Pn}$, and $\mathbf{4}_{Pn}$ (Figure 3) revealed well-defined polymers with PDIs in the range of 1.03-1.07 (Table 1). Solely the PEGs with the highest

degree of polymerization showed noteworthy broadening of their molecular weight distribution upon modification in the postpolymerization reactions (PDIs up to 1.09). Compared to the calculated molecular weights and the ones determined by ^{1}H NMR spectroscopy, the M_n values of all polymers were underestimated in SEC experiments. Since all samples were referenced to PEG diol standards, these values can be seen as a trend only. Therefore, the degrees of polymerization of all polymers were calculated from the ^{1}H NMR data.

Synthesis of the heterofunctional three-arm star polymers. The three-arm star polymers carrying a protected amino group were generated in a grafting-from approach using the polymeric vicinal diols **4** as macroinitiators for the anionic polymerization of EO. Since the smallest applicable amount of ethylene oxide in our setup is limited by the graduated ampule, which is used to condense the desired volume of EO for the polymerization, the batched masses of the high molecular weight initiators had to be on the order of one gram. To study the reaction conditions for the polymerization, two different initiators ($\mathbf{4}_{74}$ and $\mathbf{4}_{127}$) with different degrees of deprotonation were investigated: $\mathbf{4}_{74}$ was deprotonated with potassium naphthalenide by 32% and $\mathbf{4}_{127}$ was completely converted into the potassium dialkoxide.

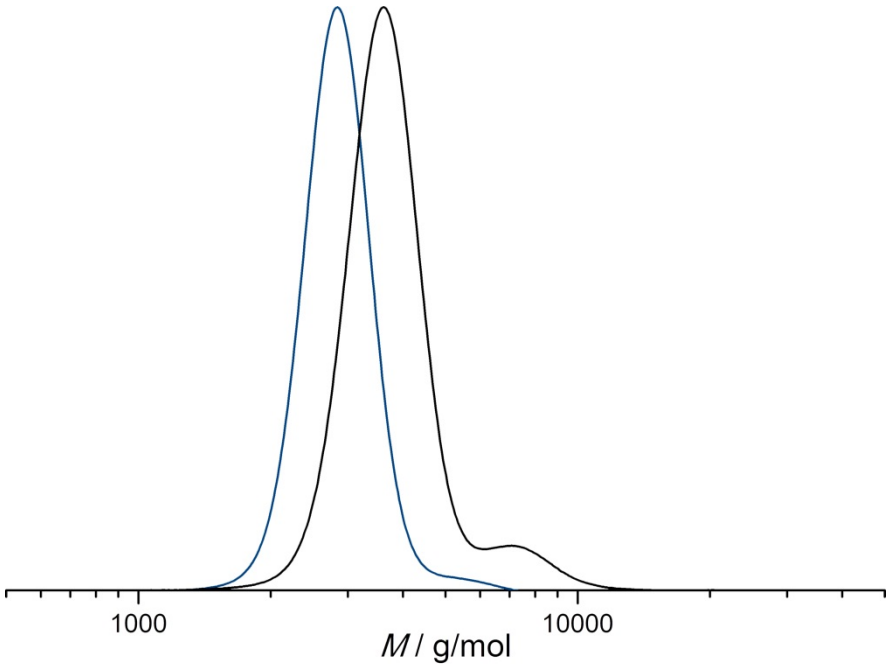

Figure 4. Size-exclusion chromatograms of the macroinitiator $\mathbf{4}_{74}$ (blue) and the corresponding star-shaped PEG $\mathbf{5}_{74}$ (black) referenced to PEG standards.

In SEC analysis (Figure 4), the three-arm star polymer α-(N,N-Dibenzylamino)-ω_2-dihydroxy PEG_3 derived from $\mathbf{4}_{74}$ ($\mathbf{5}_{74}$) showed a significant shift in the molecular weight

(M_n = 3610 g·mol^{-1}) compared to its precursor (M_n = 2780 g·mol^{-1}) indicating successful initiation of the polymerization. Even though the SEC trace exhibits a small high molecular weight mode, the polydispersity index is still low (1.07). The EO grafting was confirmed by the corresponding MALDI-TOF and NMR spectra. The superimposed spectra of the macroinitiator and the star-shaped PEG are shown in Figure 5. Both polymers were cationized with sodium or potassium ions. Especially the zoom-in (Figure 5B) displays that $\mathbf{5}_{74}$ possesses the same terminal groups as $\mathbf{4}_{74}$ and also has an incorporated glycerol unit, since the high-molecular-weight peaks of the initiator overlay perfectly with those of the star-shaped PEG. Although SEC and MALDI-TOF MS clearly reflect the molecular mass shift, the absolute molecular weight of $\mathbf{5}_{74}$ can only be determined from the ^{1}H NMR spectrum because in SEC the polymers are compared to linear PEG diol standards and in the mass spectrum species of higher masses are underestimated (mass-discrimination effect[40, 41]).

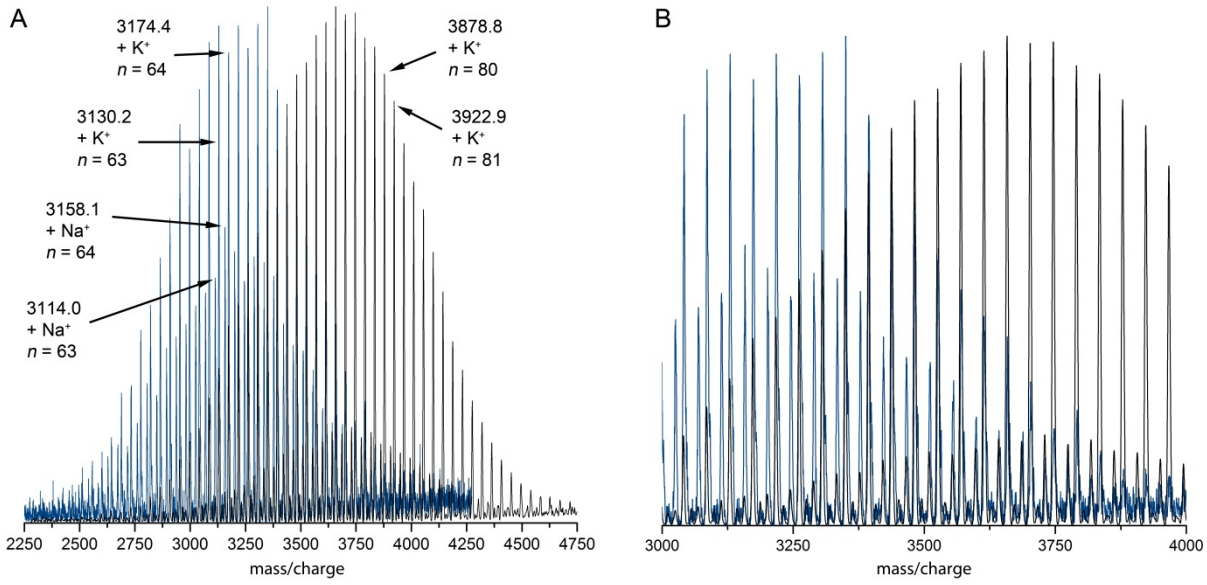

Figure 5. MALDI-TOF spectrum of the macroinitiator $\mathbf{4}_{74}$ (blue) and the star-shaped PEG $\mathbf{5}_{74}$ (black). **A** Superimposed spectra. **B** Detatil.

From the integral ratio of the backbone resonances around 3.5 ppm to the aromatic peaks around 7.4 ppm in the ^{1}H NMR spectrum of the star-shaped PEG (Figure 6), the degree of polymerization was calculated to P_n = 95 and the number-averaged molecular weight to M_n = 4520 g·mol^{-1}. This corresponds to an average addition of 21 ethylene oxide units per molecule or 10.5 units per arm. However, the theoretical increase in the degree of polymerization was 84, and hence only a conversion of 25% was reached. This was attributed to

the insufficient reaction time (2 d) which was obviously too short for the very low concentration of active chain ends.

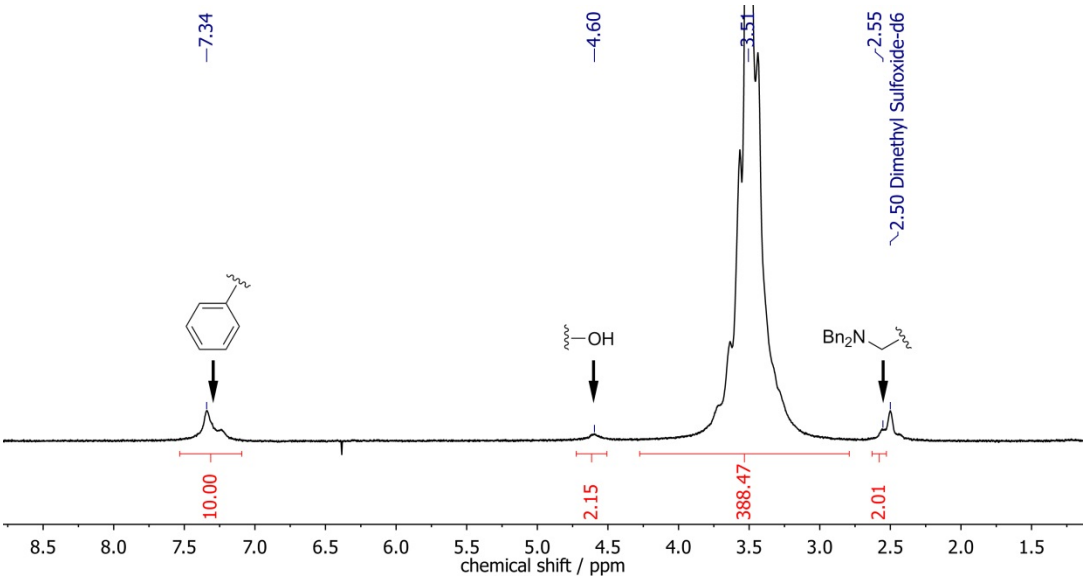

Figure 6. ^{1}H NMR spectrum (300 MHz) of $\mathbf{5}_{74}$ recorded in DMSO-d_6, T = 294 K.

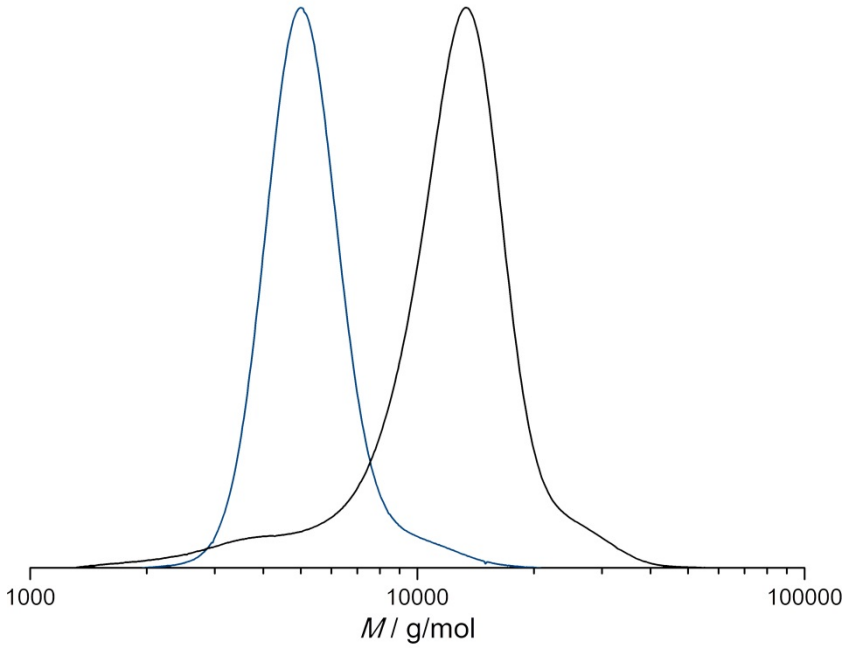

Figure 7. Size-exclusion chromatograms of the macroinitiator $\mathbf{4}_{127}$ (blue) and the corresponding star-shaped PEG $\mathbf{5}_{127}$ (black) referenced to PEG standards.

In contrast, the macroinitiator $\mathbf{4}_{127}$ was completely deprotonated and the polymerization was carried out for a longer time (4 d). From 406 theoretical monomer units, 353 (87%) were added according to the ^{1}H NMR spectrum recorded for the three-arm PEG $\mathbf{5}_{127}$ (SI, Figure S10. In result, the molecular weight of $\mathbf{5}_{127}$ was $M_{n,NMR}$ = 21500 g·mol^{-1}. The shift in the molecular weight referred to the macroinitiator was also detected by SEC. In Figure 7 the chromatograms

of both polymers are displayed. Note that the molecular mass of $\mathbf{5}_{127}$ is obviously underestimated by this method, since the molecules of the star-shaped PEG have smaller hydrodynamic radii compared to molecules of the linear standard polymer with the same degree of polymerization. However, the PDI increased to 1.20 after grafting of the additional PEG arms. This was mainly attributed to a small low-molecular-weight fraction which apparently did not initiate the EO polymerization. This is most probably due to aggregation of the divalent reactive sites of the initiator. The reaction conditions might be optimized to achieve full monomer conversion and to yield heterofunctional star-shaped PEGs with more narrowly distributed molecular weights.

The exploratory hydrogenation of the dibenzyl protected amino groups of the heterofunctional star-shaped PEGs was carried using $\mathbf{5}_{74}$ as a substrate. Full conversion to α-amino-ω_2-dihydroxyl PEG_3 (**6**) was confirmed by the absence of the aromatic resonances in the ^{1}H NMR spectrum (Figure 6). As we have reported earlier, amino group containing poly(ethylene glycol)s show an apparent broadening of the molecular weight distribution in SEC analysis on our system.[31, 42] We also observe this effect for the heterofunctional three-arm star-shaped PEG (SI, Figure S23).

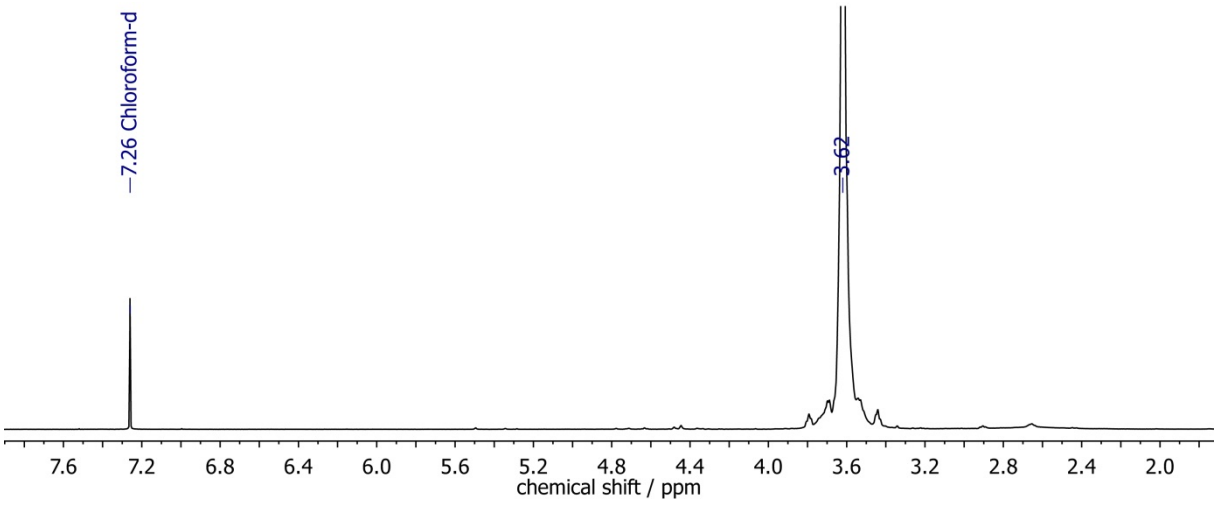

Figure 8. ^{1}H NMR spectrum (400 MHz) of **6** recorded in $CDCl_3$, T = 294 K, 16 scans.

Influence of the type of hydroxyl group on arm length. The presented synthetic strategy to heterofunctional star shaped PEGs involves the initiation of the AROP of EO with a divalent macroinitiator. Both initiation moieties differ chemically, since one is a primary and the other a secondary hydroxyl group. Although glycerol derivatives with hydroxyl groups of both

types have been used to initiate the anionic polymerization of ethylene oxide,[21, 43-47] the dependence of the nature of the hydroxyl group on the degree of polymerization of the corresponding PEG arm has barely been described. Grafting EO from propylene oxide (PO) capped hyperbranched poly(glycerol)s indicated sufficient reactivity of PO's secondary hydroxyl group for the complete initiation of these functionalities.[43] However, detailed investigation of this issue is not trivial since standard characterization methods such as NMR spectroscopy, IR spectroscopy, mass spectrometry, and size-exclusion chromatography give information on the degree of polymerization, hydrodynamic volume, conversion, and degree of incorporation of the initiator, but do not reveal the average number of EO units added to each of the chemically different initiation sites.

In order to study this particular question, we synthesized 1-(2-hydroxypropyloxy)ethyl ethylene glycol ether (HPEGE, **8**), a divalent AROP initiator carrying both, a primary and a secondary hydroxyl group, as well as build-in acid-degradable acetal junction. HPEGE was synthesized form 1-(glycidyloxy)ethyl benzyloxethyl ether (**7**) by catalytic perhydrogenation (Scheme 2). The PEG diol **9** resulting from HPEGE-initiated AROP of EO can be cleaved under acidic conditions. The obtained PEG fragments **10** and **11**, initiated by the ethylene glycol or the propylene glycol site, respectively, do not have to be separated, which would be almost impossible, and can be analyzed by SEC and MALDI-TOF mass spectrometry to disclose the difference in the initiation rates.

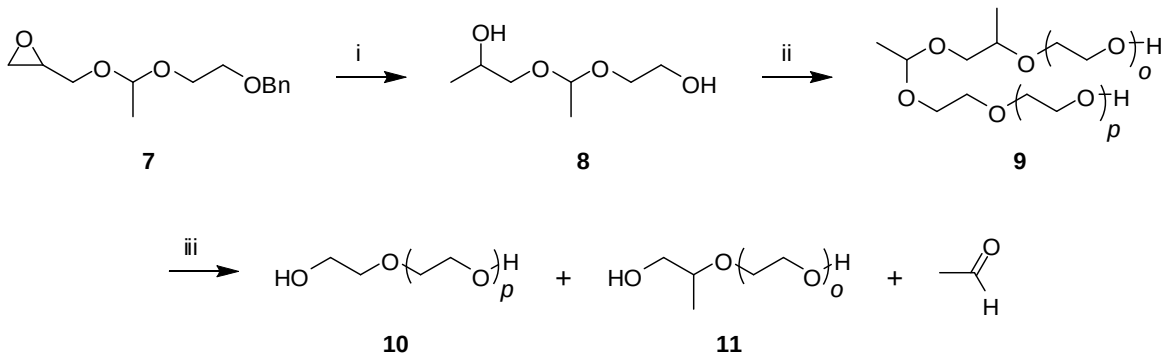

Scheme 2. Synthesis of cleavable poly(ethylene glycol) (**9**). i) H_2, Pd/C, THF, 40 bar, room temperature, 72 h. ii) 1. $CsOH{\cdot}H_2O$, C_6H_6, 90 °C, vacuum; 2. Tetrahydrofuran (THF), $m = o + p$ EO, 60 °C; 3. MeOH. iii) 1 M hydrochloric acid, THF.

HPEGE has been briefly identified as a byproduct in the synthesis of 1-(glycidyloxy)ethyl ethylene glycol ether (GEGE),[38] but has not been fully characterized yet. The conversion of **7** in favor of HPEGE was improved by using palladium on activated charcoal instead of Pearlman's

catalyst, by increasing the reaction time as well as the reaction pressure (p = 40 bar), and by conducting the reaction in dry THF. HPEGE was obtained as a mixture of its diastereomers and was characterized by NMR spectroscopy and mass spectrometry.

In the ^{1}H NMR spectrum of **8** (Figure 9) the characteristic acetaldehyde acetal signals (quadruplet at δ = 4.68 ppm and doublet at δ = 1.19 ppm) as well as the resonances of the hydroxyl protons and the propanyl's methyl group were easily identified. To assign the residual signals, a H,H-COSY (correlated spectroscopy) spectrum (SI, Figure S12) was recorded, which revealed three spin systems, i.e., the one of the aldehyde, the hydroxylethyl, and the hydroxylpropyl moiety. The assignment was confirmed by the ^{13}C NMR and ^{1}H, ^{13}C-HSQC NMR spectra of **8** (SI, Figures S11 and S13). In field-desorption mass spectrometry **8** was detected as protonated unimer, dimer and trimer. Since **8** can easily undergo intramolecular transacetalization when protonated, also the resulting protonated cyclic acetals 2-methyl-1,3-dioxolane and 2,4-dimethyl-1,3-dioxolane were detected in the mass spectrum at m/z = 89.2 and 103.1, respectively. These species were formed during the ionization process, because the NMR spectra gave no hint to their presence in the sample.

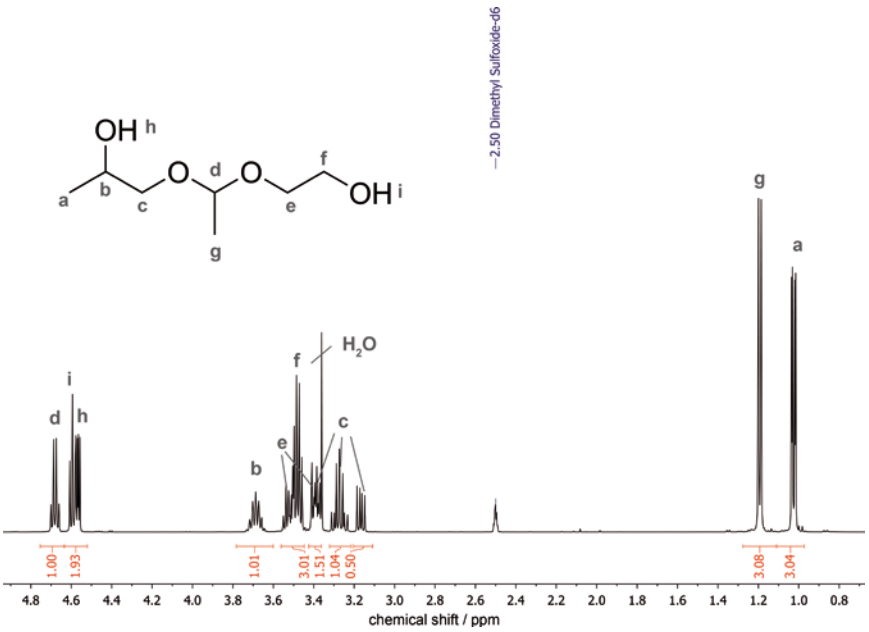

Figure 9. ^{1}H NMR spectrum (400 MHz) of HPEGE (**8**) recorded in DMSO-d$_6$, T = 294 K.

Two polymers **9** with molecular weights of around 5,000 g/mol were prepared from HPEGE deprotonated with either 24 mol% (**9a**) or 45 mol% (**9b**) of cesium hydroxide (resulting in 12% and 23% deprotonated hydroxyls, respectively) to investigate the influence of the degree of deprotonation on the chain length to either side of the initiator. The polymerization initiated by

the former was stirred 24 h longer than the second one to ensure full EO conversion. In the ^{1}H NMR spectra of both samples of **9** (SI, Figures S14 and S15), the resonances of the acetaldehyde acetal moiety and the methyl group of the propylene oxide unit proved the incorporation of the initiator into the polymers. From the integral ratios of these signals to the backbone peaks the degrees of polymerization and the molecular weights of the polyethers were determined, which agreed well with the theoretical values (Table 2).

Full incorporation of the initiator into **9a** was confirmed by the MALDI-TOF mass spectrum (SI, Figure S21), which showed the expected series of mass peaks cationized with potassium. SEC analysis (Figure 10A and SI, Figures S24) again yielded slightly underestimated molecular weights (Table 2). The molecular weight distribution of the polymer derived from the diol deprotonated to a lesser extend (**9a**) was slightly broader (1.08) than that of the one of the second polymer (**9b**, PDI = 1.06), which might be attributed to the slower initiation rates in the less basic system.

Table 2. Cleavable PEGs **9a** and **9b** as well as the corresponding hydrolysis producs **(10 + 11)a** and **(10 + 11)b**

Polymer	M_n[a] / g·mol^{-1}	M_n[b] / g·mol^{-1}	M_n[c] / g·mol^{-1}	M_w[c] / g·mol^{-1}	P_n[b]	PDI[c]
9a	4960	4750	4120	4460	104	1.08
9b	4960	5120	4460	4750	112	1.06
(10 + 11)a	2360[e]	2420[d]	2150[d]	2340[d]	53[d]	1.09[d]
(10 + 11)b	2540[e]	2640[d]	2330[d]	2480[d]	58[d]	1.06[d]

[a] Calculated. [b] Determined by ^{1}H NMR. [c] Determined by SEC, referenced to PEG standards. [d] Average values of mixture. [e] Calculated under assumption of symmetrical polymerization.

The product of the acidic cleavage of the acetal in the backbone of **9b** - a mixture of PEG diol (**10**) and α-(hydroxylisopropyl)-ω-hydroxy PEG (**11**) - yielded a monomodal SEC trace, that corresponded to a polymer with approximately half the molecular weight of **9b** (Figure 10A) and the PDI was still as low as 1.06. Symmetrical cleavage was also confirmed by MALDI-TOF MS (detail shown in Figure 10B, full spectrum provided in the SI). The distributions of both, **10** and **11**, were found superimposed in the expected molecular weight range around 2500 g/mol, although **10** was detected with a much higher intensity. However, the proton NMR spectrum of **10** and **11** (Figure 10C) proved equimolar presence of both PEG derivatives, since the hydroxyl

proton resonance of the hydroxylisopropyl moiety was clearly distinguishable from those of the other ones and the integration ratios were 1:3, respectively. Similar results were obtained from the degradation of **9a** (SI, Figure S16).

Due to the finding of a symmetrical cleavage of **9**, it can be concluded that both hydroxyl groups of **8**, primary and secondary, do not exhibit a significant difference in the rate of initiation in the AROP of EO under the investigated conditions. Also, this outcome is independent from the degree of initiator deprotonation. This further indicates that the initiation of anionic EO polymerization with the divalent PEG macroinitiators presented above actually afforded the targeted three-arm star polymer with indistinguishable lengths of the grafted arms.

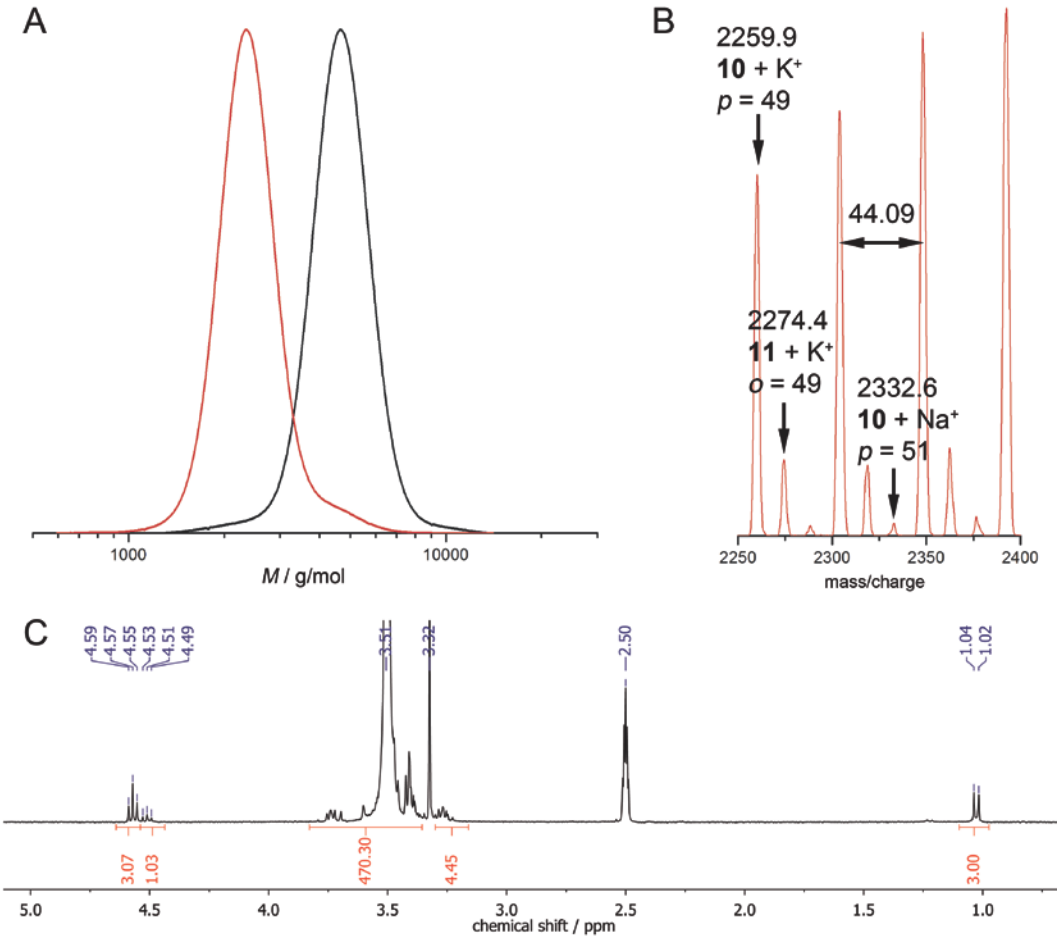

Figure 10. Characterization of the mixture of **10** and **11** derived from **9b**. **A** SEC traces of **9b** before (black) and after (red) cleavage referenced to PEG standards. **B** Detail of MALDI-TOF mass spectrum of **10** and **11**. **C** ^{1}H NMR spectrum (300 MHz) of **10** and **11** recorded in DMSO-d_6.

Conclusions

We have developed a straightforward synthetic route to heterofunctional three-arm star-shaped poly(ethylene glycol)s and have successfully demonstrated the synthesis of linear, divalent macroinitiators in the molecular weight range of 2,000-10,000 $g \cdot mol^{-1}$. Further, we synthesized two PEG stars carrying dibenzyl-protected amino groups by grafting two additional polyether arms from the initiators' vicinal diols. However, the conditions of this polymerization can probably be further optimized to obtain full monomer conversion and heterofunctional three-arm stars with narrowly distributed molecular weights. In an exploratory hydrogenation to yield α-amino-ω_2-dihydroxyl PEG_3 we have demonstrated the removal of the benzyl protecting groups. A possible application of these novel branched PEGs in the squaric acid mediated PEGylation of proteins and their effect on the blood circulation times as well as the bioactivities of the resulting PEG/protein conjugates are under current investigation.

In order to investigate the influence of the nature of the hydroxyls on the length of the PEG arms grafted from the initiators, we have developed and fully characterized a new AROP initiator that carries a primary as well as a secondary hydroxyl group separated by an acid-sensitive acetal moiety. By polymerizing ethylene oxide from this divalent initiator and subsequent hydrolysis of the acetal, we demonstrated that there is no investigable difference in the initiation rates of both types of hydroxyl groups in the AROP of EO.

References

[1] P. Caliceti, F. M. Veronese, *Adv. Drug Del. Rev.* **2003**, *55*, 1261.

[2] R. B. Greenwald, Y. H. Choe, J. McGuire, C. D. Conover, *Adv. Drug Del. Rev.* **2003**, *55*, 217.

[3] J. M. Harris, R. B. Chess, *Nat. Rev. Drug Discov.* **2003**, *2*, 214.

[4] F. M. Veronese, G. Pasut, *Drug Discovery Today* **2005**, *10*, 1451.

[5] G. Pasut, M. Sergi, F. M. Veronese, *Adv. Drug Del. Rev.* **2008**, *60*, 69.

[6] G. Pasut, F. M. Veronese, *Adv. Drug Del. Rev.* **2009**, *61*, 1177.

[7] A. Abuchowski, T. van Es, N. C. Palczuk, F. F. Davis, *J. Biol. Chem.* **1977**, *252*, 3578.

[8] A. Abuchowski, J. R. McCoy, N. C. Palczuk, T. van Es, F. F. Davis, *J. Biol. Chem.* **1977**, *252*, 3582.

[9] T. Yamaoka, Y. Tabata, Y. Ikada, *J. Pharm. Sci.* **1994**, *83*, 601.

[10] P. Bailon, W. Berthold, *Pharm. Sci. Technol. Today* **1998**, *1*, 352.

[11] C. Monfardini, O. Schiavon, P. Caliceti, M. Morpurgo, J. M. Harris, F. M. Veronese, *Bioconjugate Chem.* **1995**, *6*, 62.

[12] F. M. Veronese, C. Monfardini, P. Caliceti, O. Schiavon, M. D. Scrawen, D. Beer, *J. Controlled Release* **1996**, *40*, 199.

[13] F. M. Veronese, P. Caliceti, O. Schiavon, *J. Bioact. Compat. Polym.* **1997**, *12*, 196.

[14] R. Federico, A. Cona, P. Caliceti, F. M. Veronese, *J. Controlled Release* **2006**, *115*, 168.

[15] Y. Nojima, Y. Suzuki, K. Yoshida, F. Abe, T. Shiga, T. Takeuchi, A. Sugiyama, H. Shimizu, A. Sato, *Pharm. Res.* **2009**, *26*, 2125.

[16] C. J. Fee, *Biotechnol. Bioeng.* **2007**, *98*, 725.

[17] A. Basu, K. Yang, M. Wang, S. Liu, R. Chintala, T. Palm, H. Zhao, P. Peng, D. Wu, Z. Zhang, J. Hua, M.-C. Hsieh, J. Zhou, G. Petti, X. Li, A. Janjua, M. Mendez, J. Liu, C. Longley, Z. Zhang, M. Mehlig, V. Borowski, M. Viswanathan, D. Filpula, *Bioconjugate Chem.* **2006**, *17*, 618.

[18] J. Ramon, V. Saez, R. Baez, R. Aldana, E. Hardy, *Pharm. Res.* **2005**, *22*, 1374.

[19] P. Bailon, A. Palleroni, C. A. Schaffer, C. L. Spence, W.-J. Fung, J. E. Porter, G. K. Ehrlich, W. Pan, Z.-X. Xu, M. W. Modi, A. Farid, W. Berthold, M. Graves, *Bioconjugate Chem.* **2001**, *12*, 195.

[20] A. Takagi, N. Yamashita, T. Yoshioka, Y. Takaishi, K. Sano, H. Yamaguchi, A. Maeda, K. Saito, Y. Takakura, M. Hashida, *J. Controlled Release* **2007**, *119*, 271.

[21] Y. Yamamoto, H. Yoshioka, T. Takehana, S. Yoshimura, K. Kubo, K.-i. Nakamoto, *Polym. Prepr.* **2009**, *50*, 161.

[22] A. Martinez, A. Pendri, J. Xia, R. B. Greenwald, *Macromol. Chem. Phys.* **1997**, *198*, 2489.

[23] H. Zhao, K. Yang, A. Martinez, A. Basu, R. Chintala, H.-C. Liu, A. Janjua, M. Wang, D. Filpula, *Bioconjugate Chem.* **2006**, *17*, 341.

[24] B. N. Novikov, J. K. Grimsley, R. J. Kern, J. R. Wild, M. E. Wales, *J. Controlled Release* **2010**, *146*, 318.

[25] T. J. Rutkoski, J. A. Kink, L. E. Strong, R. T. Raines, *Cancer Biol. Ther.* **2011**, *12*, 208.

[26] T. H. Kim, H. H. Jiang, S. M. Lim, Y. S. Youn, K. Y. Choi, S. Lee, X. Chen, Y. Byun, K. C. Lee, *Bioconjugate Chem.* **2012**, *23*, 2214.

[27] N. W. Nairn, K. D. Shanebeck, A. Wang, T. J. Graddis, M. P. VanBrunt, K. C. Thornton, K. Grabstein, *Bioconjugate Chem.* **2012**, *23*, 2087.

[28] Y. Vugmeyster, C. A. Entrican, A. P. Joyce, R. F. Lawrence-Henderson, B. A. Leary, C. S. Mahoney, H. K. Patel, S. W. Raso, S. H. Olland, M. Hegen, X. Xu, *Bioconjugate Chem.* **2012**, *23*, 1452.

[29] V. L. Elliott, G. T. Edge, M. M. Phelan, L.-Y. Lian, R. Webster, R. F. Finn, B. K. Park, N. R. Kitteringham, *Mol. Pharm.* **2012**, *9*, 1291.

[30] M. R. Sherman, L. D. Williams, M. A. Sobczyk, S. J. Michaels, M. G. P. Saifer, *Bioconjugate Chem.* **2012**, *23*, 485.

[31] C. Dingels, F. Wurm, M. Wagner, H.-A. Klok, H. Frey, *Chem. Eur. J.* **2012**, *18*, 16828.

[32] F. Wurm, C. Dingels, H. Frey, H.-A. Klok, *Biomacromolecules* **2012**, *13*, 1161.

[33] R. K. Kainthan, J. Janzen, E. Levin, D. V. Devine, D. E. Brooks, *Biomacromolecules* **2006**, *7*, 703.

[34] M. Calderón, M. A. Quadir, S. K. Sharma, R. Haag, *Adv. Mater.* **2010**, *22*, 190.

[35] D. Dix, P. Imming, *Arch. Pharm.* **1995**, *328*, 203.

[36] S. Sugai, H. Ikawa, Y. Hasegawa, S. Yoshida, T. Kutsuma, S. Akaboshi, *Chem. Pharm. Bull.* **1984**, *32*, 967.

[37] S. Cassel, C. Debaig, T. Benvegnu, P. Chaimbault, M. Lafosse, D. Plusquellec, P. Rollin, *Eur. J. Org. Chem.* **2001**, *2001*, 875.

[38] C. Tonhauser, C. Schüll, C. Dingels, H. Frey, *ACS Macro Lett.* **2012**, *1*, 1094.

[39] H. R. Pfaendler, F. K. Maier, S. Klar, W. Göggelmann, *Liebigs Ann. Chem.* **1988**, *1988*, 449.

[40] D. C. Schriemer, L. Li, *Anal. Chem.* **1997**, *69*, 4169.

[41] D. C. Schriemer, L. Li, *Anal. Chem.* **1997**, *69*, 4176.

[42] C. Dingels, S. S. Müller, T. Steinbach, C. Tonhauser, H. Frey, *Biomacromolecules* **2013**, DOI: 10.1021/bm3016797.

[43] R. Knischka, P. J. Lutz, A. Sunder, R. Mülhaupt, H. Frey, *Macromolecules* **2000**, *33*, 315.

[44] X.-S. Feng, D. Taton, E. L. Chaikof, Y. Gnanou, *J. Am. Chem. Soc.* **2005**, *127*, 10956.

[45] L. M. v. Renterghem, X. Feng, D. Taton, Y. Gnanou, F. E. Du Prez, *Macromolecules* **2005**, *38*, 10609.

[46] X. Feng, D. Taton, E. L. Chaikof, Y. Gnanou, *Biomacromolecules* **2007**, *8*, 2374.

[47] X. Feng, E. L. Chaikof, C. Absalon, C. Drummond, D. Taton, Y. Gnanou, *Macromol. Rapid Commun.* **2011**, *32*, 1722.

Supporting Information

Synthesis of Heterofunctional Three-arm Star Shaped Poly(ethylene glycol)

Carsten Dingels, Frederik Wurm, and Holger Frey

Table of contents

1. Procedures

1.1 Acidic cleavage of **9**

9 (250 mg, 51.2µmol) was stirred in a mixture of methanol (1 mL) and hydrochloric acid (2 M, 1 mL) for several hours. The mixture was neutralized by the addition of caustic lye of soda and extracted 5 times with dichloromethane. The combined organic phases were dried over sodium sulfate and evaporated to a small volume. Precipitation in cold diethyl ether and subsequent drying yielded the cleaved polymer in almost quantitative yield.

2. NMR Spectra

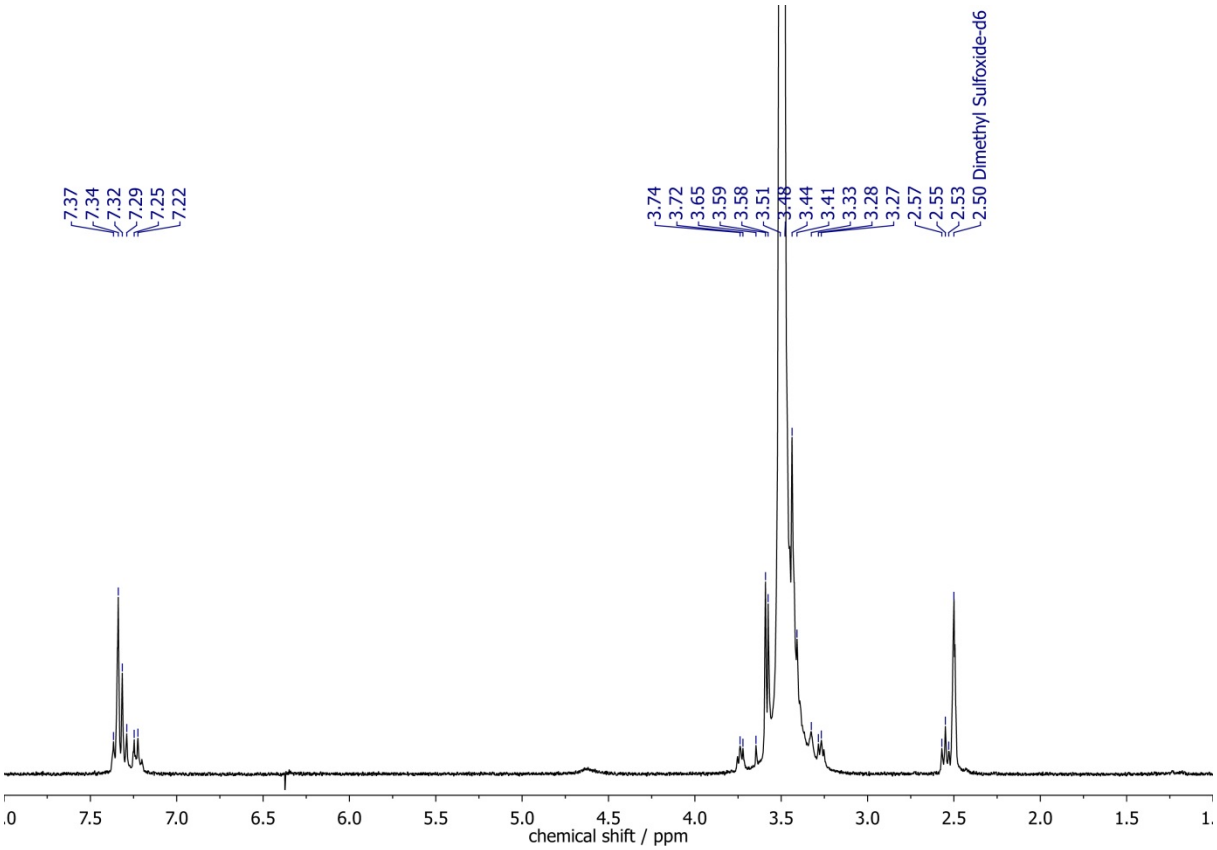

Figure S1. ^{1}H NMR spectrum (300 MHz) of $\mathbf{1}_{74}$ recorded in DMSO-d_6, T = 294 K.

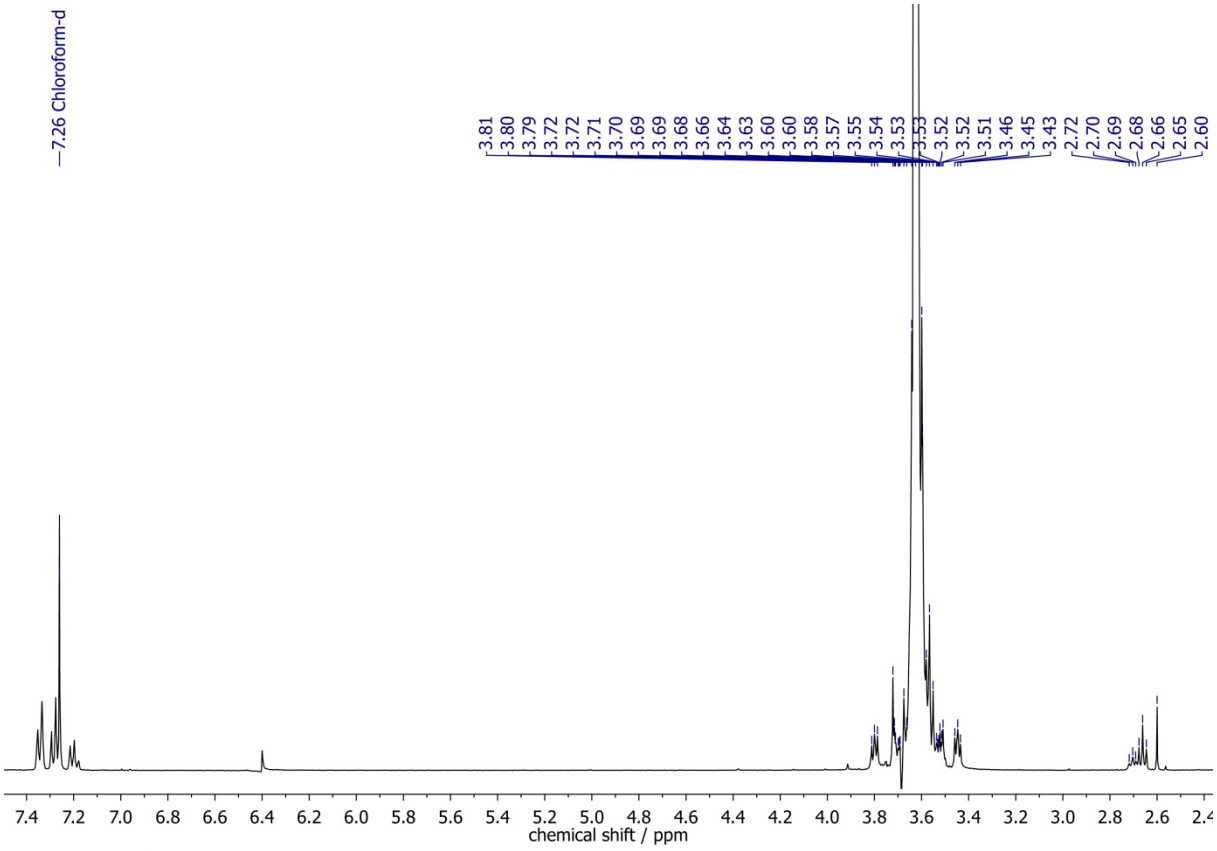

Figure S2. ^{1}H NMR spectrum (400 MHz) of $\mathbf{1}_{127}$ recorded in $CDCl_3$, T = 294 K.

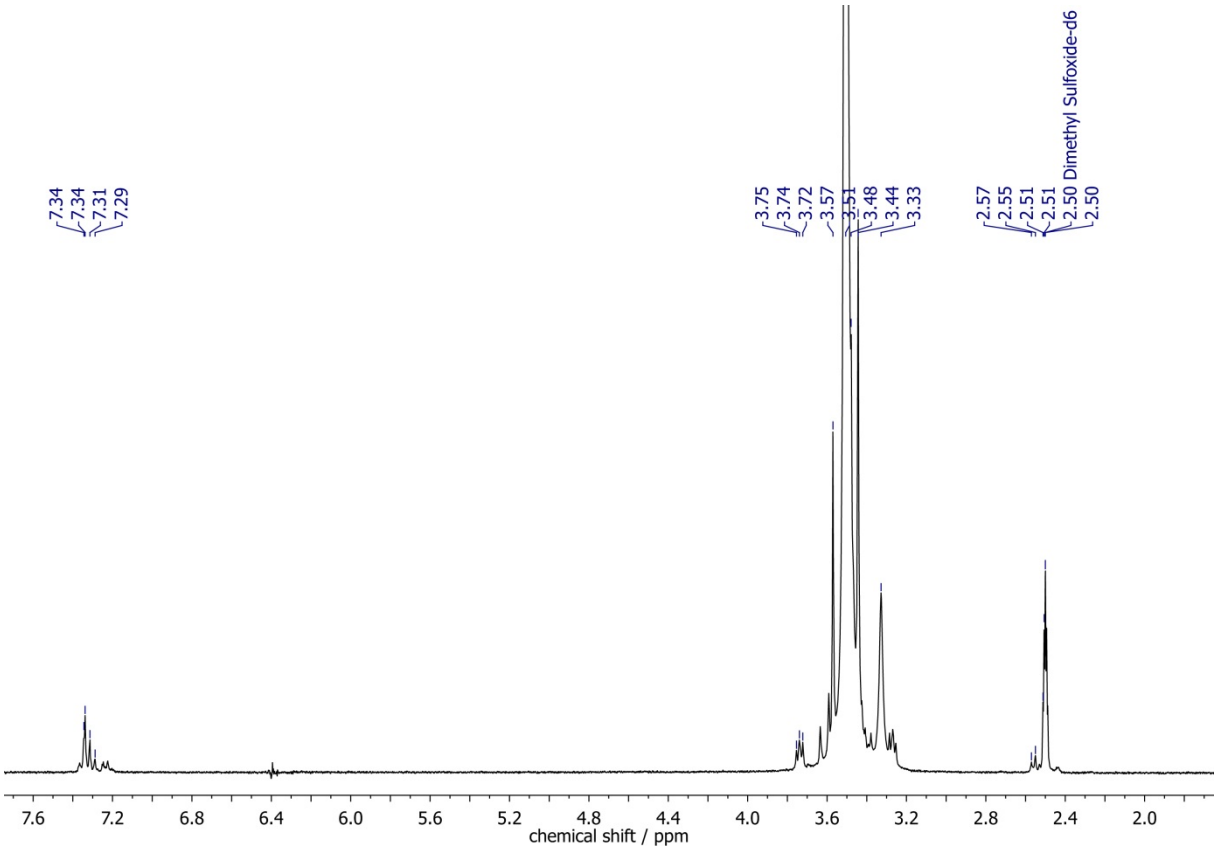

Figure S3. ^{1}H NMR spectrum (300 MHz) of $\mathbf{1}_{257}$ recorded in DMSO-d_6, T = 294 K.

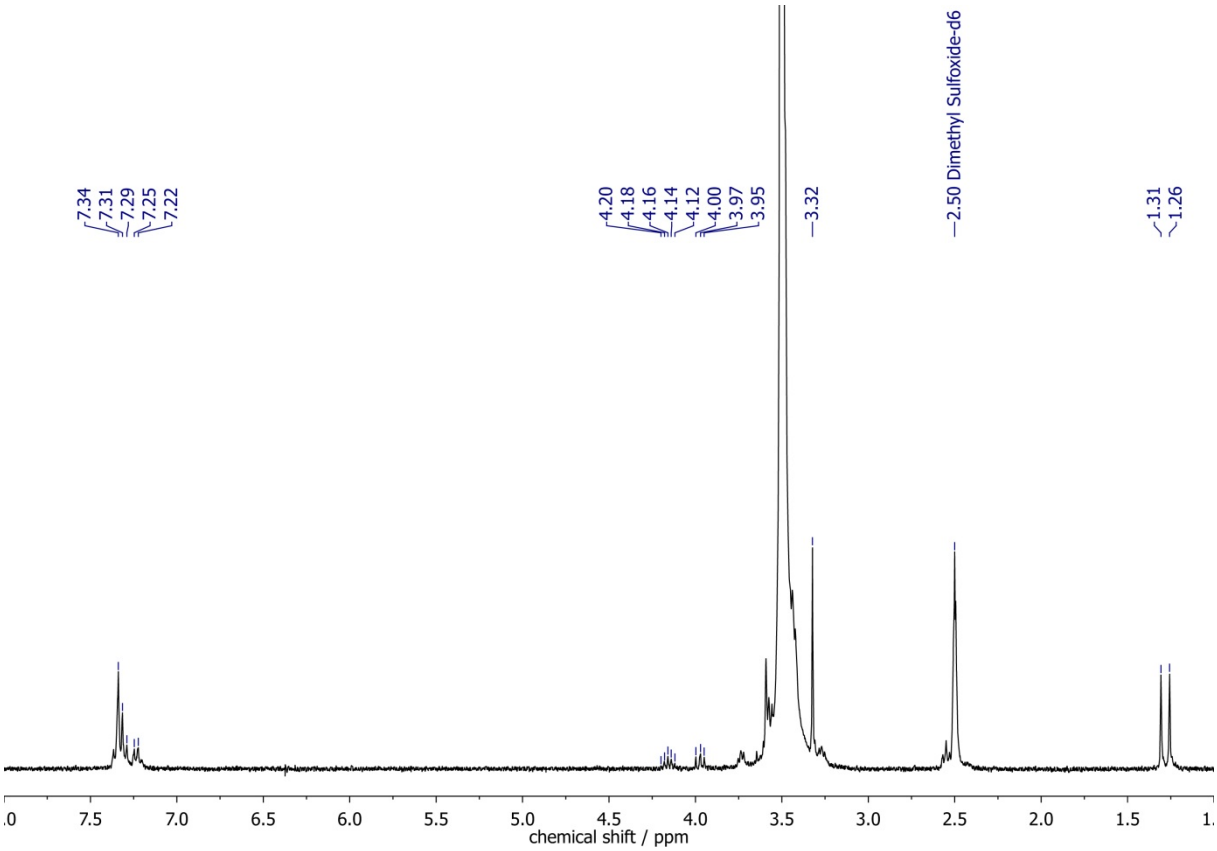

Figure S4. ^{1}H NMR spectrum (300 MHz) of $\mathbf{3}_{74}$ recorded in DMSO-d_6, T = 294 K.

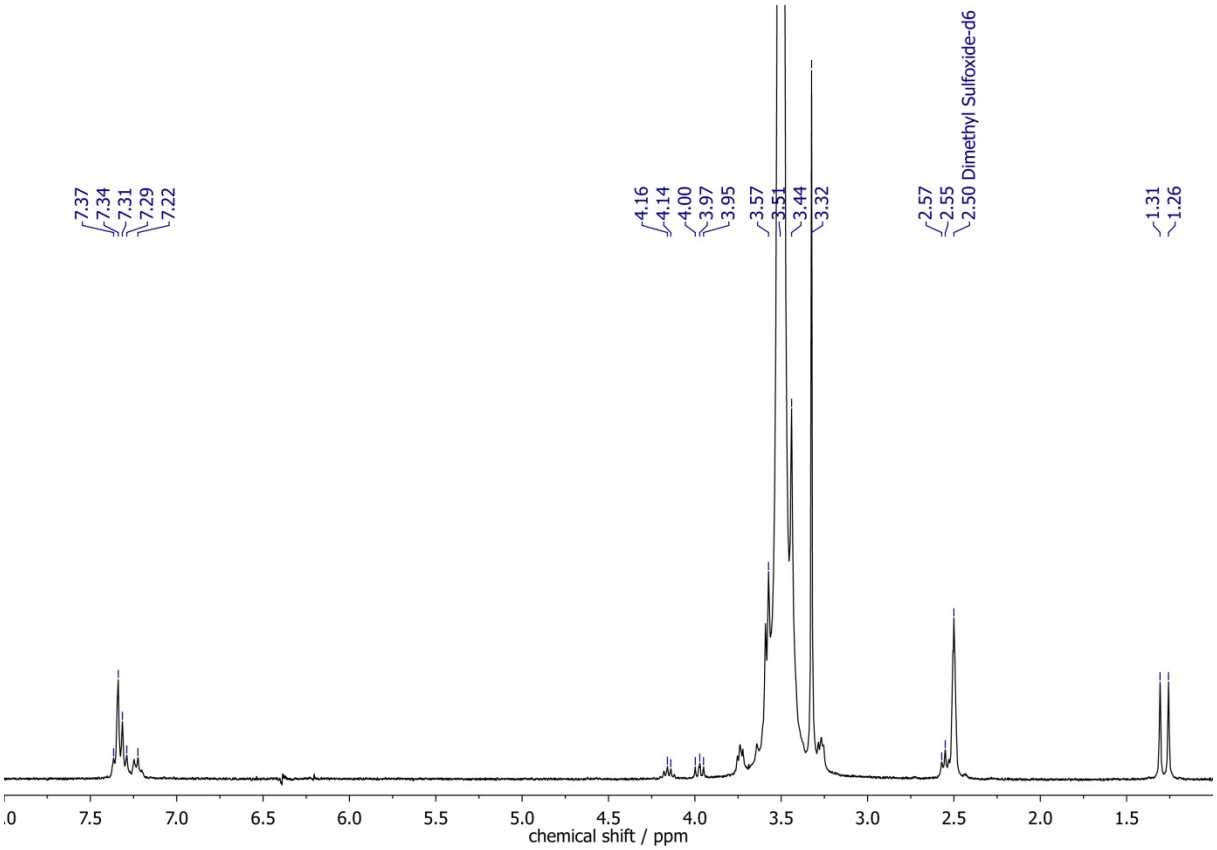

Figure S5. ^{1}H NMR spectrum (300 MHz) of $\mathbf{3}_{127}$ recorded in DMSO-d_6, T = 294 K.

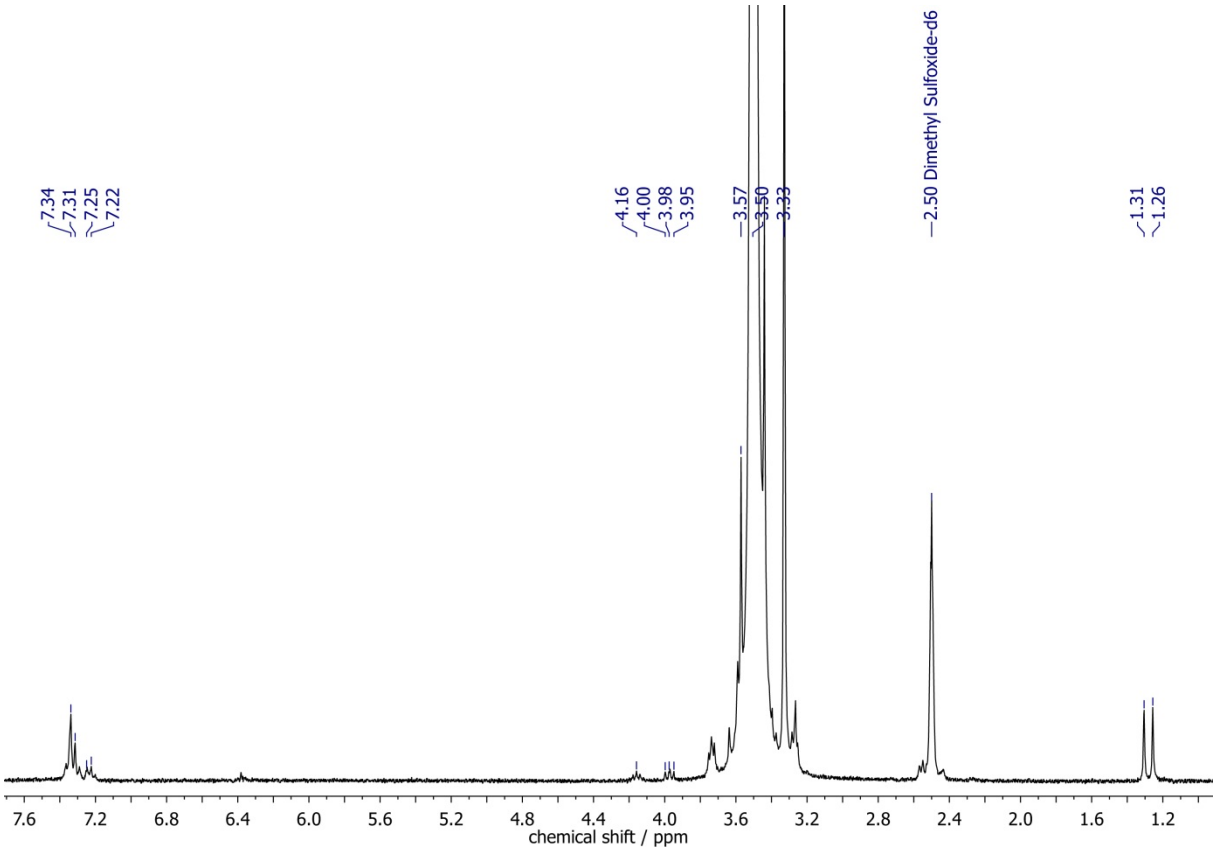

Figure S6. ^{1}H NMR spectrum (300 MHz) of $\mathbf{3}_{257}$ recorded in DMSO-d_6, T = 294 K.

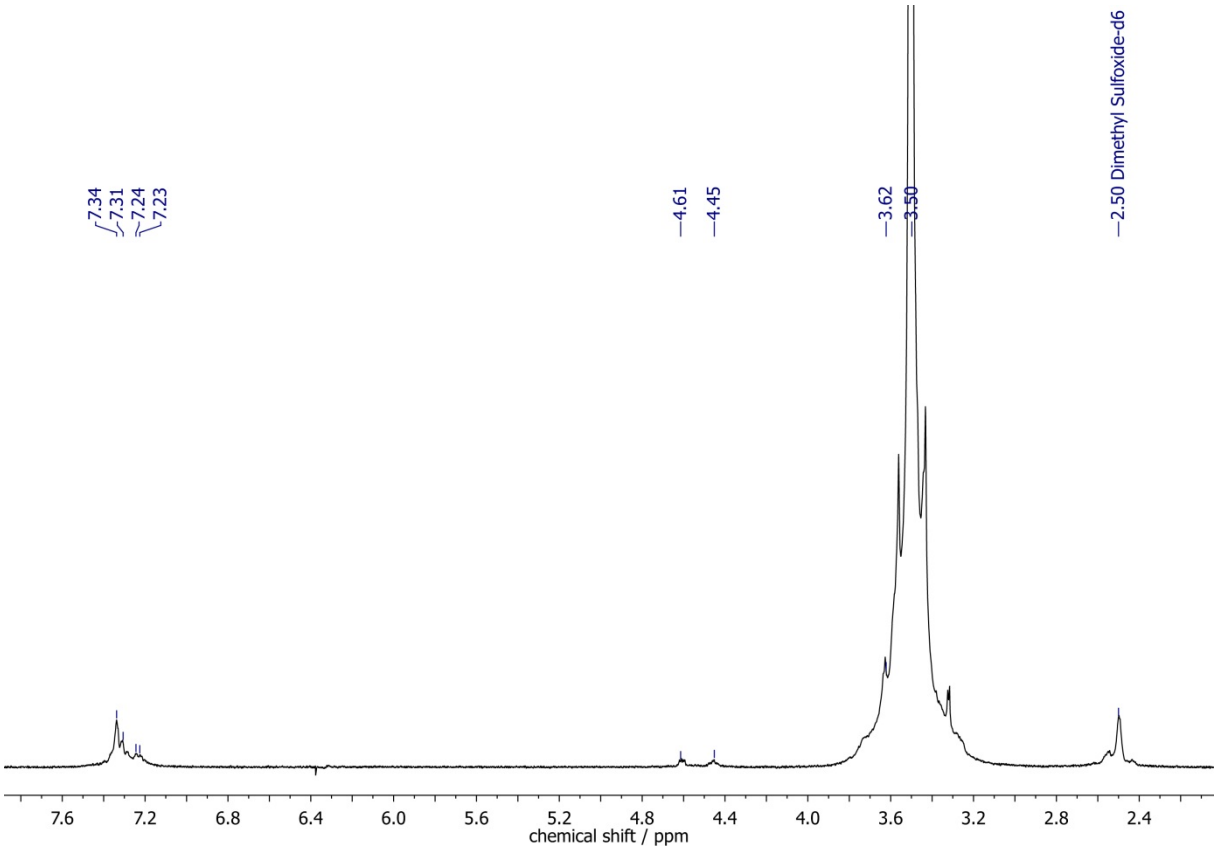

Figure S7. ^{1}H NMR spectrum (300 MHz) of $\mathbf{4}_{74}$ recorded in DMSO-d_6, T = 294 K.

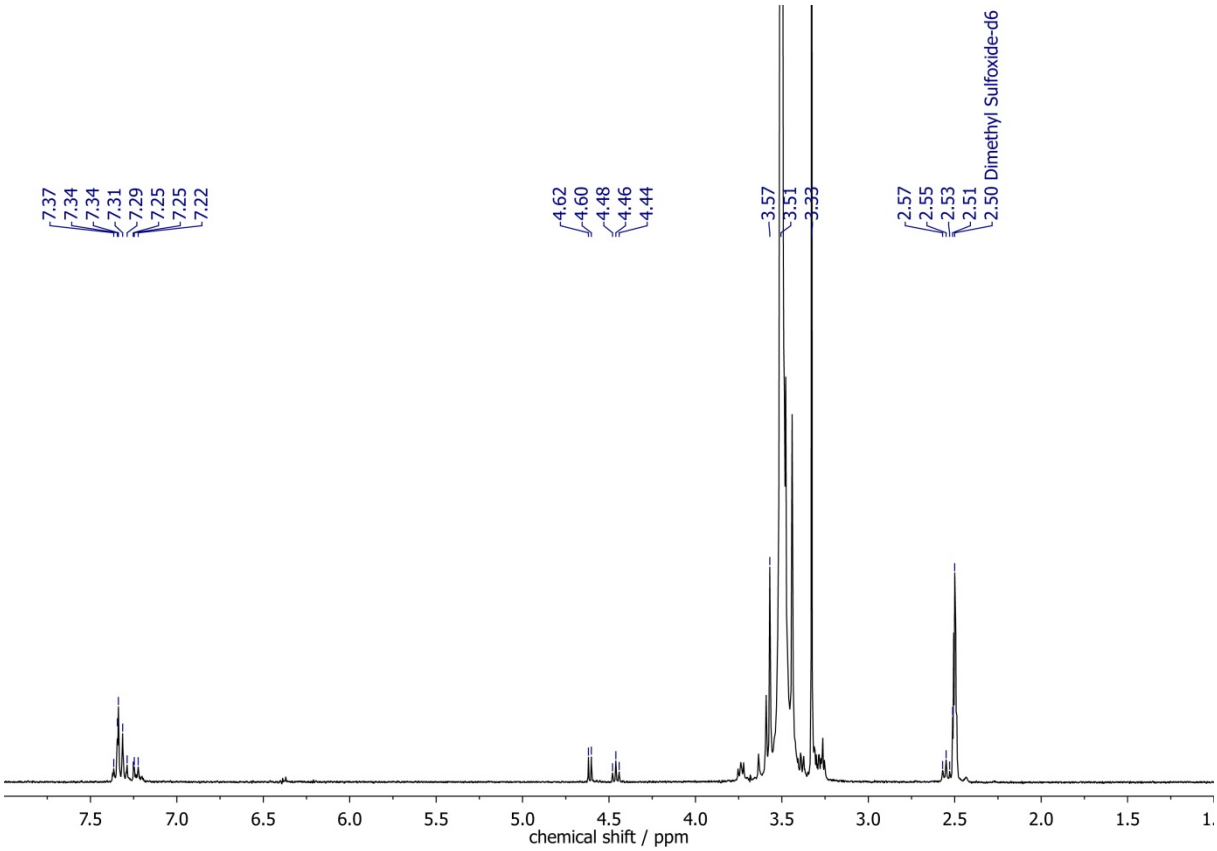

Figure S8. ^{1}H NMR spectrum (300 MHz) of $\mathbf{4}_{127}$ recorded in DMSO-d_6, T = 294 K.

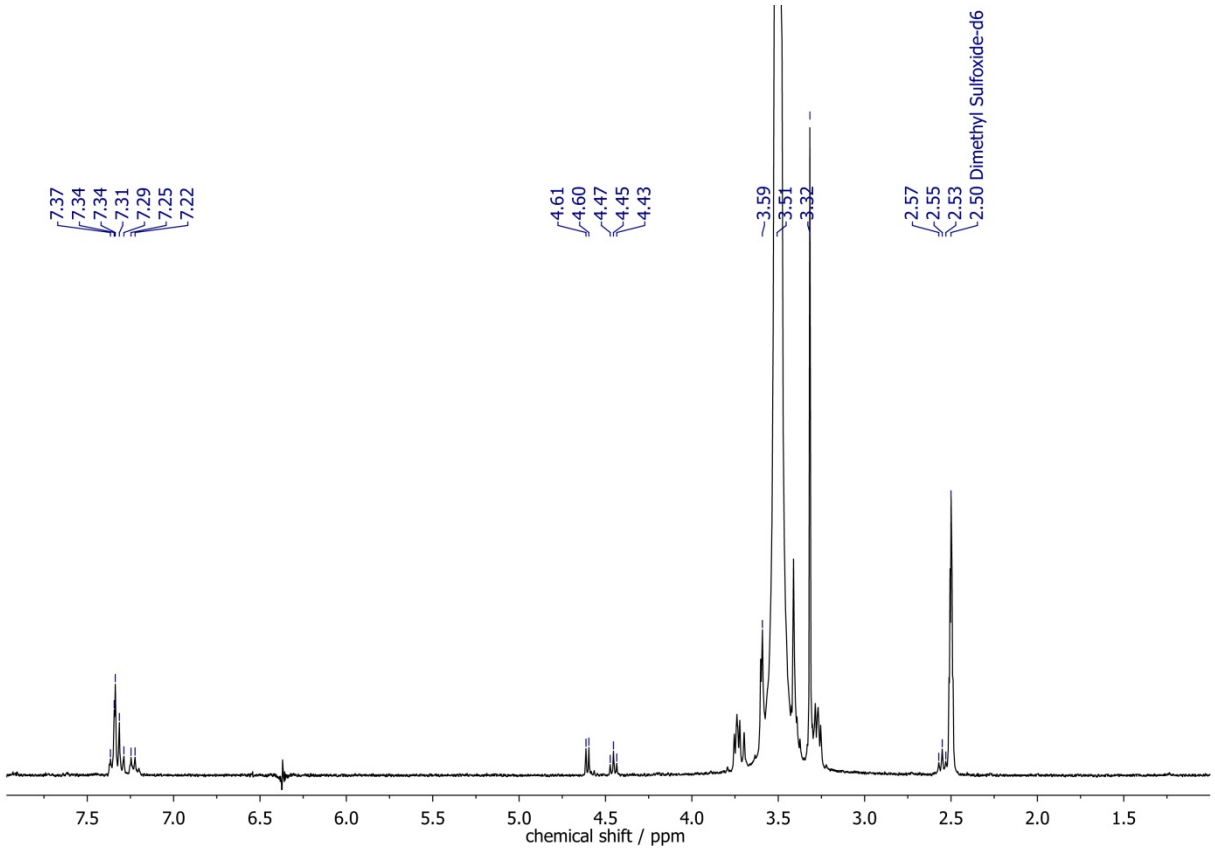

Figure S9. ^{1}H NMR spectrum (300 MHz) of $\mathbf{4}_{257}$ recorded in DMSO-d_6, T = 294 K.

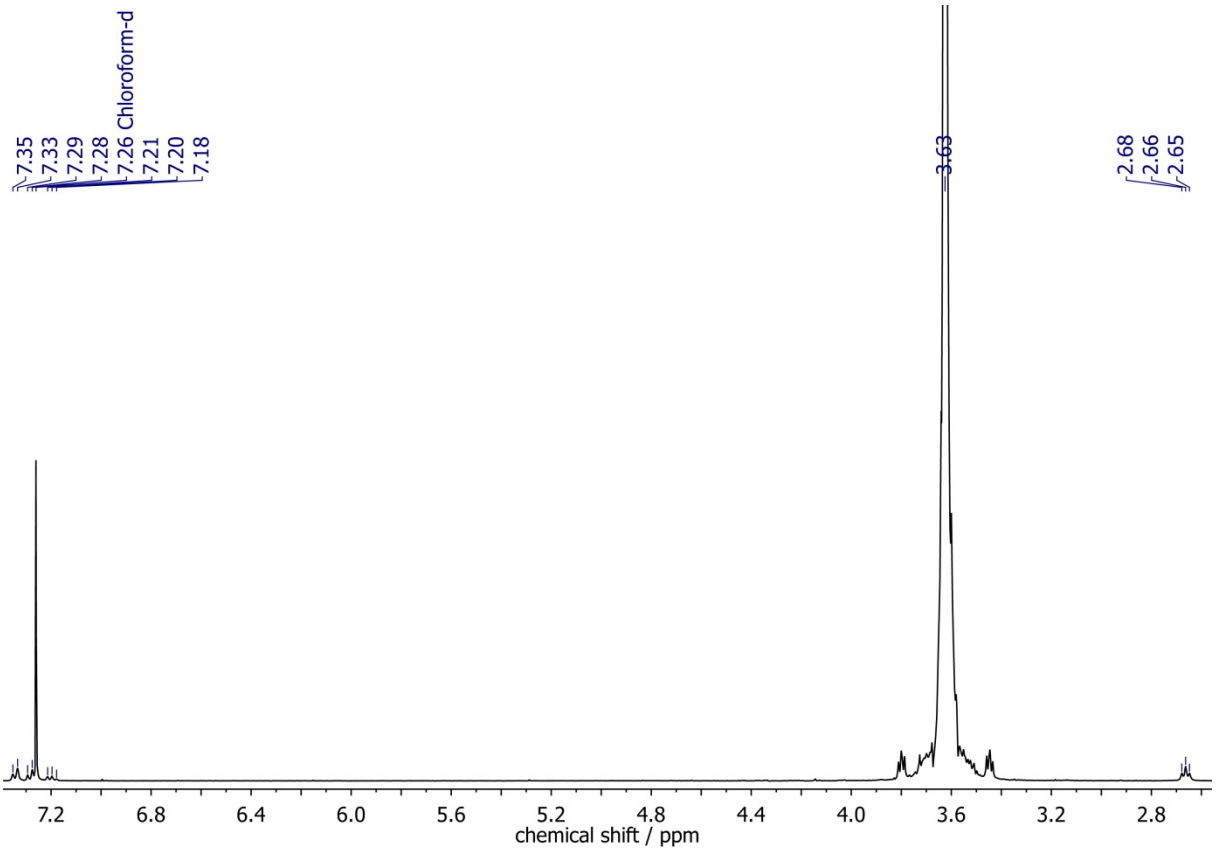

Figure S10. ^{1}H NMR spectrum (400 MHz) of $\mathbf{5}_{127}$ recorded in $CDCl_3$, T = 294 K, 16 scans.

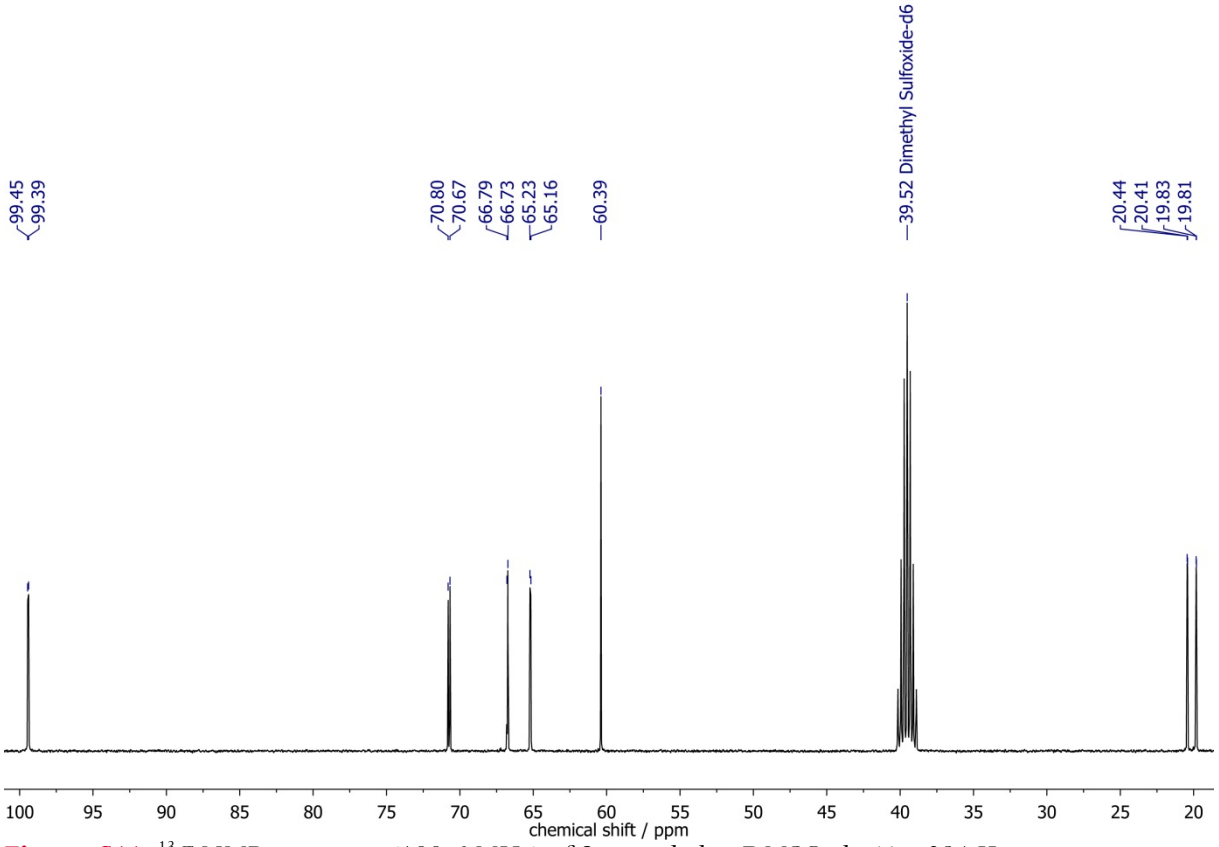

Figure S11. ^{13}C NMR spectrum (100.6 MHz) of **8** recorded in DMSO-d$_6$, T = 294 K.

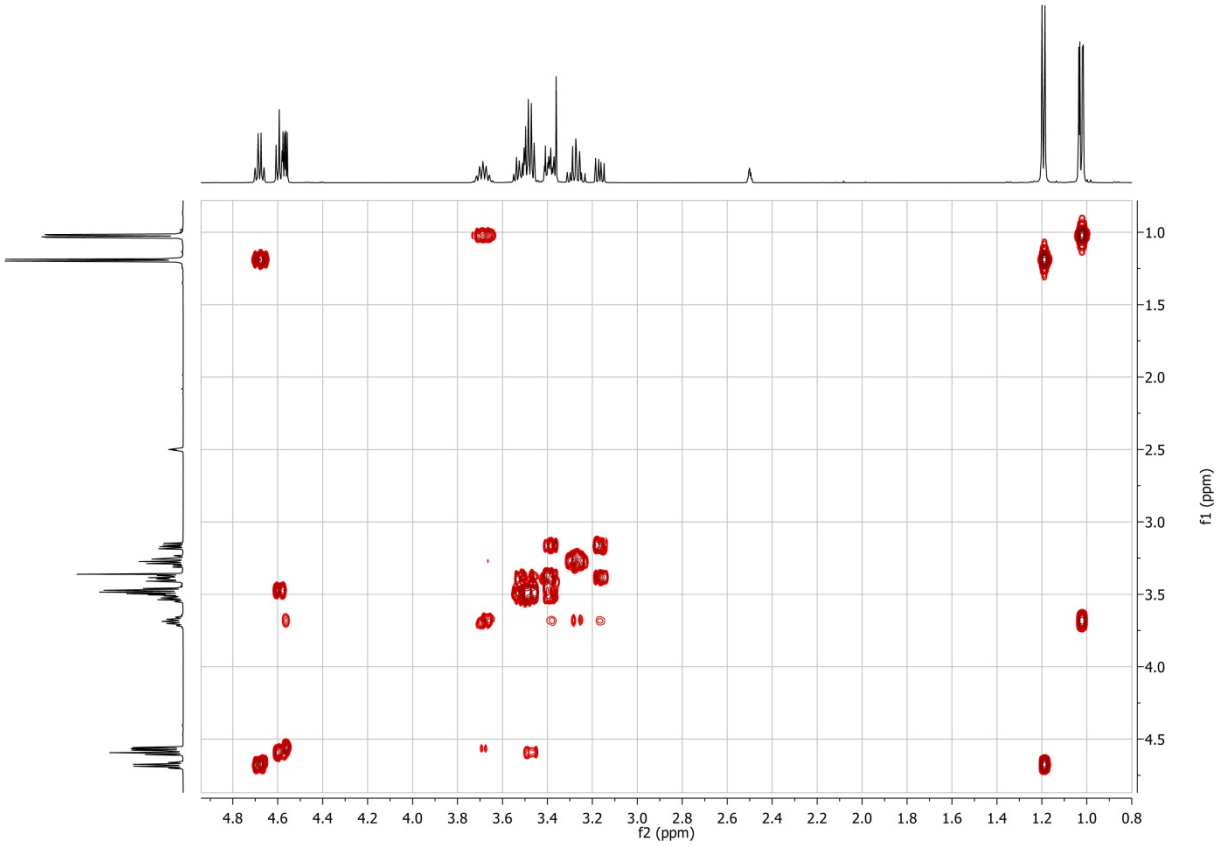

Figure S12. ^{1}H,^{1}H COSY NMR spectrum (400 MHz) of **8** recorded in DMSO-d$_6$, T = 294 K.

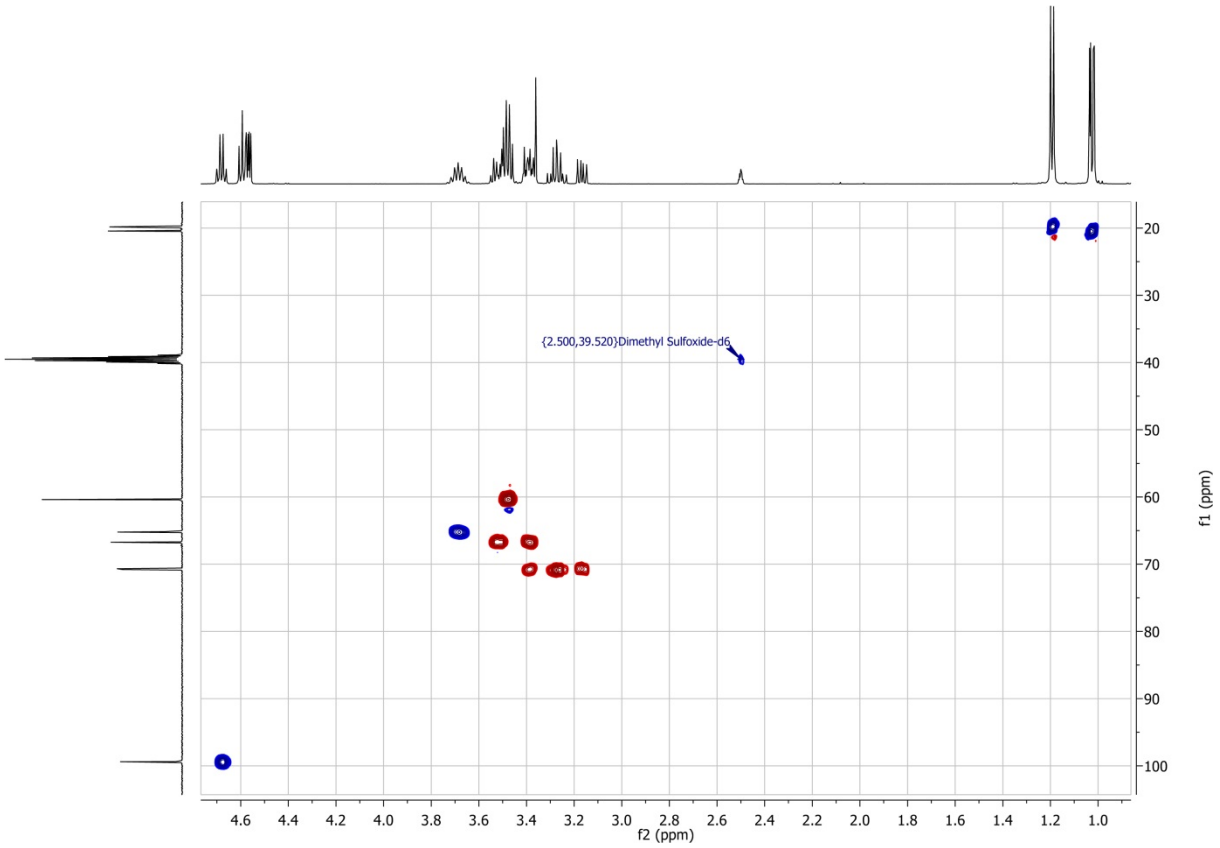

Figure S13. ^{1}H,^{13}C-HSQC NMR spectrum (400 MHz) of **8** recorded in DMSO-d$_6$, T = 294 K.

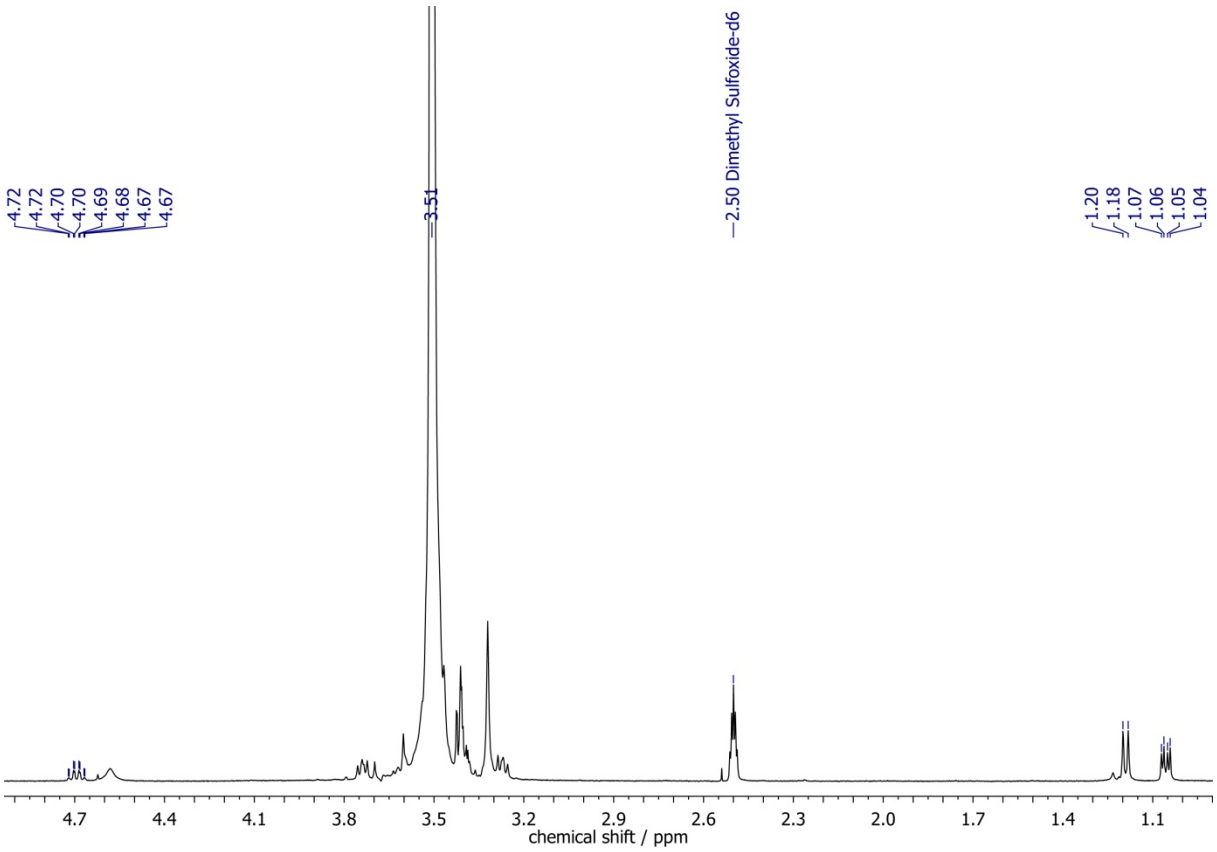

Figure S14. ^{1}H NMR spectrum (300 MHz) of **9a** recorded in DMSO-d$_6$, T = 294 K.

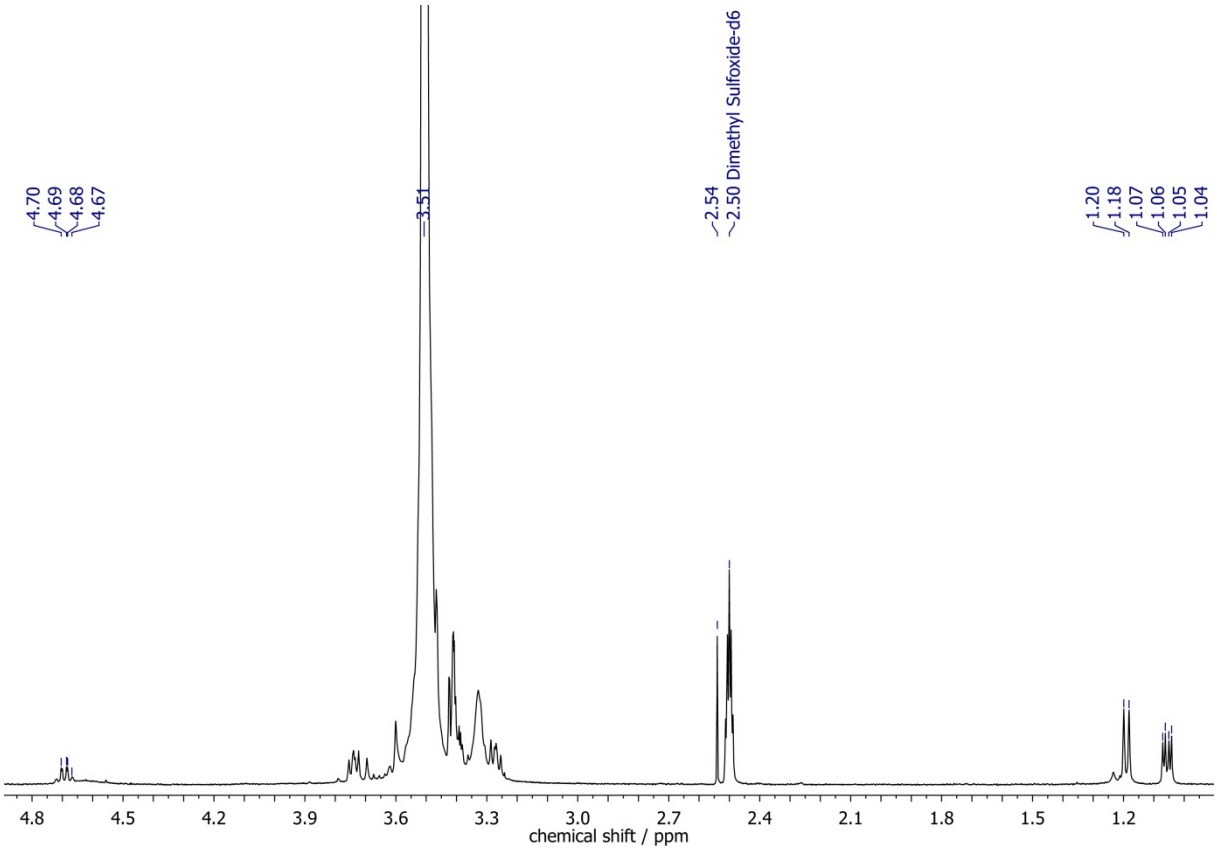

Figure S15. ^{1}H NMR spectrum (300 MHz) of **9b** recorded in DMSO-d_6, T = 294 K.

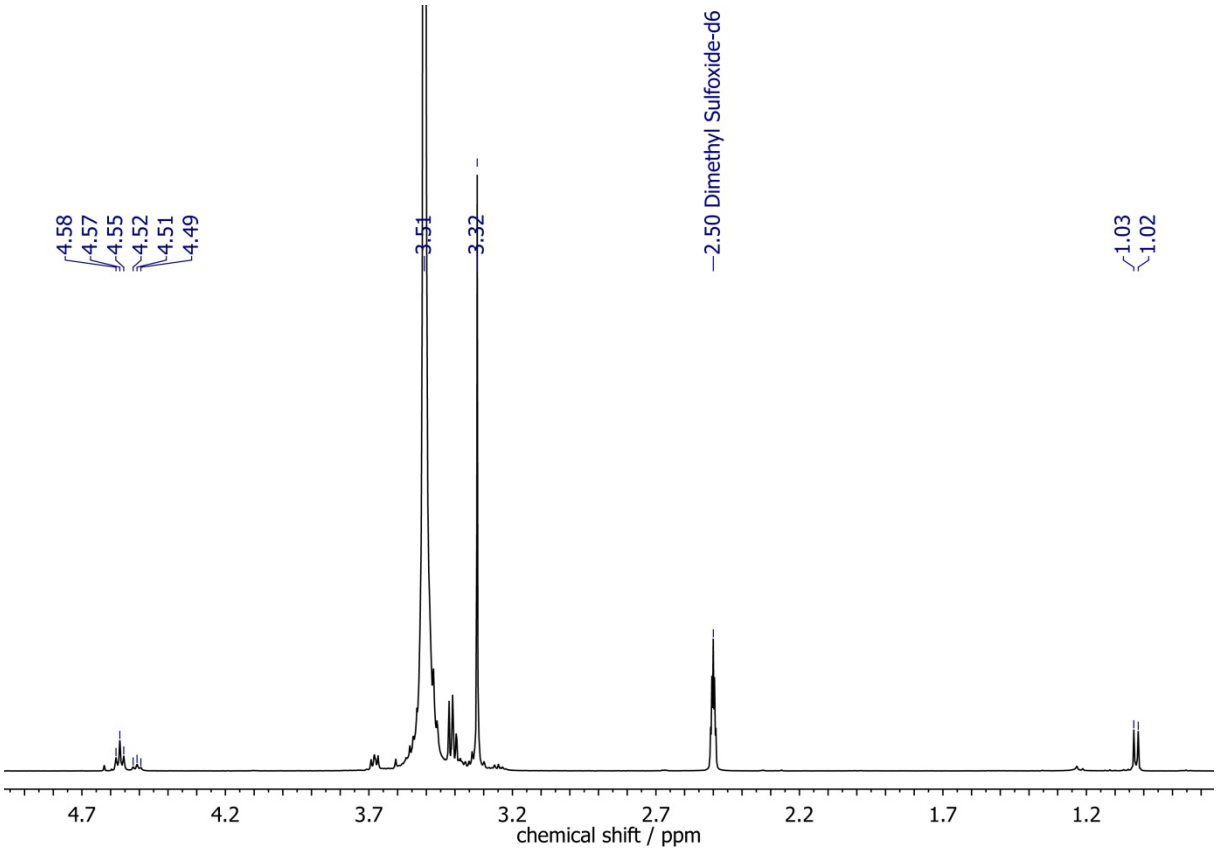

Figure S16. ^{1}H NMR spectrum (300 MHz) of mixture of **10** and **11** derived from **9a** recorded in DMSO-d_6, T = 294 K.

3. MALDI-TOF Mass Spectra

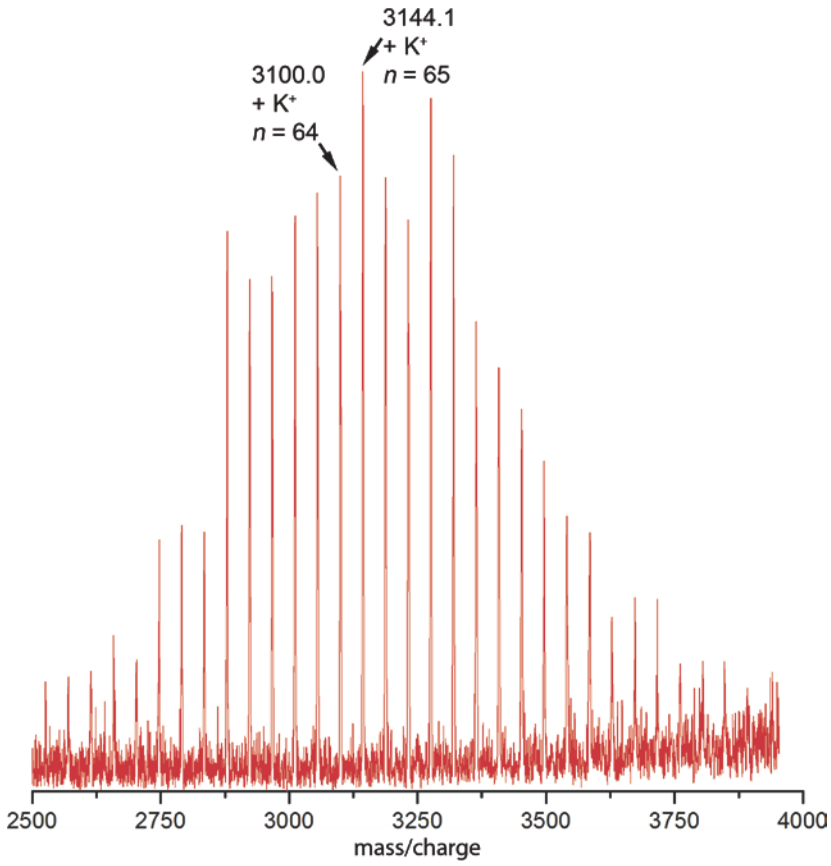

Figure S17. MALDI-TOF mass spectrum of $\mathbf{1}_{74}$. Matrix: CHCA. Salt: KTFA. Reflectron mode.

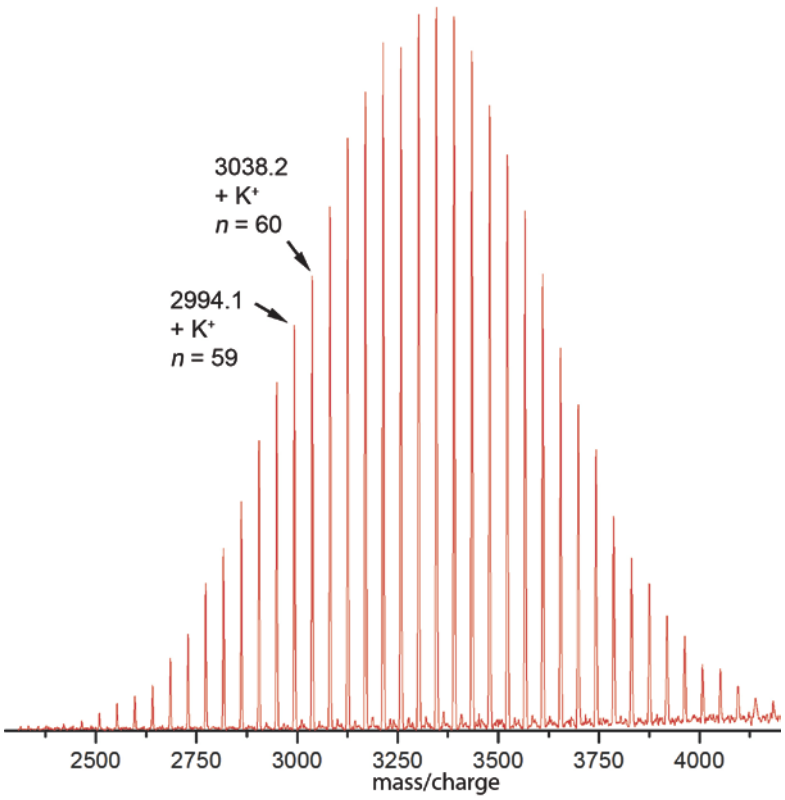

Figure S18. MALDI-TOF mass spectrum of $\mathbf{3}_{74}$. Matrix: CHCA. Salt: KTFA. Reflectron mode.

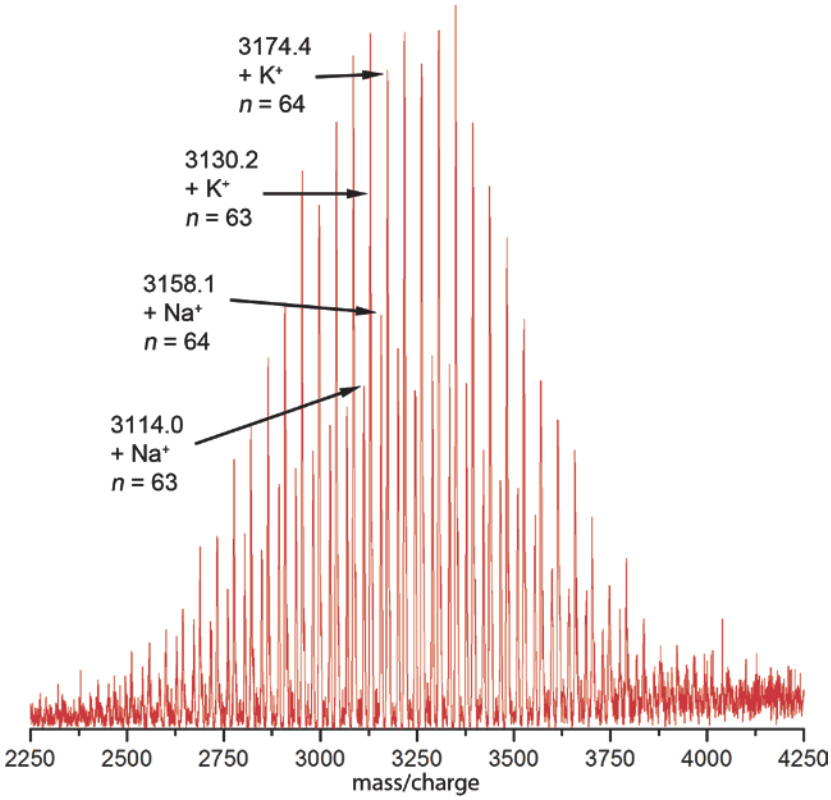

Figure S19. MALDI-TOF mass spectrum of $\mathbf{4}_{74}$. Matrix: CHCA. Salt: KTFA. Reflectron mode.

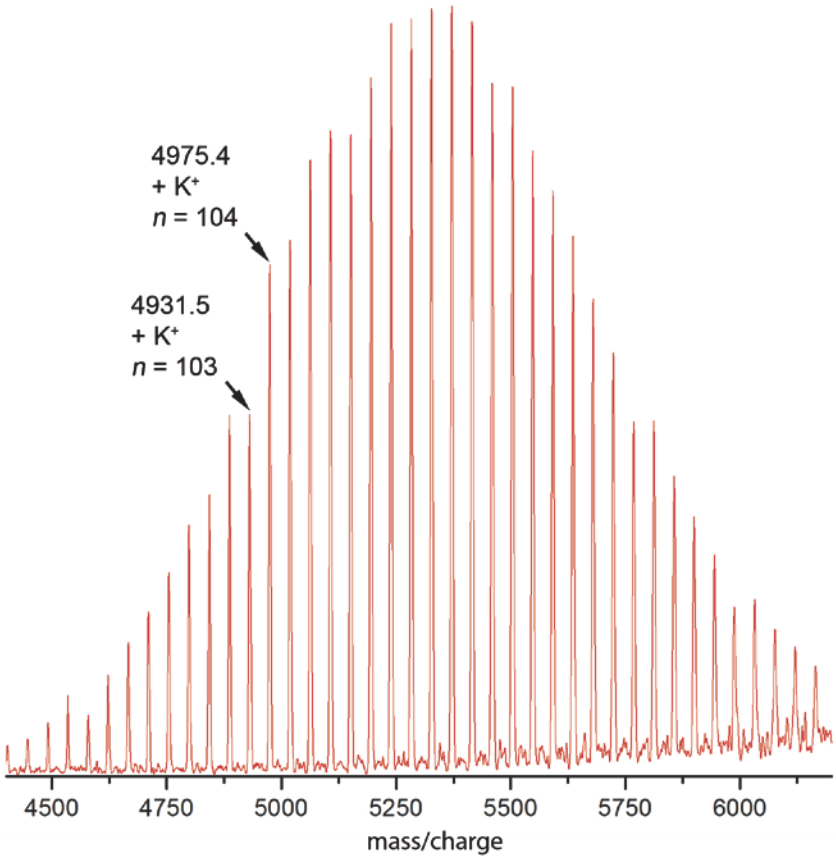

Figure S20. MALDI-TOF mass spectrum of $\mathbf{3}_{127}$. Matrix: CHCA. Salt: KTFA. Reflectron mode.

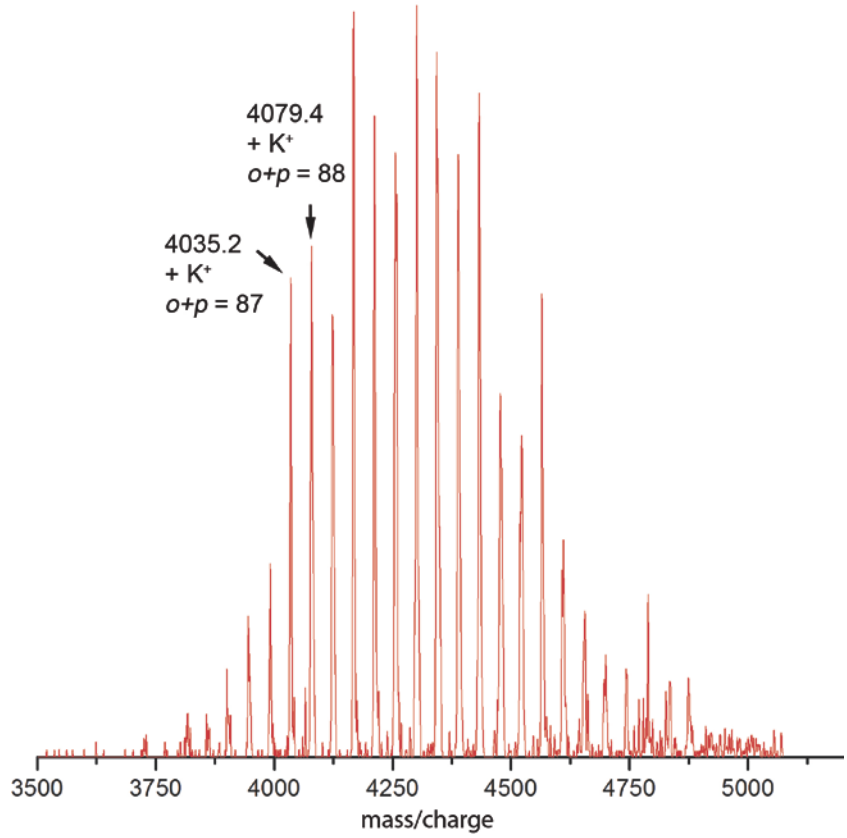

Figure S21. MALDI-TOF mass spectrum of **9a**. Matrix: CHCA. Salt: KTFA. Reflectron mode.

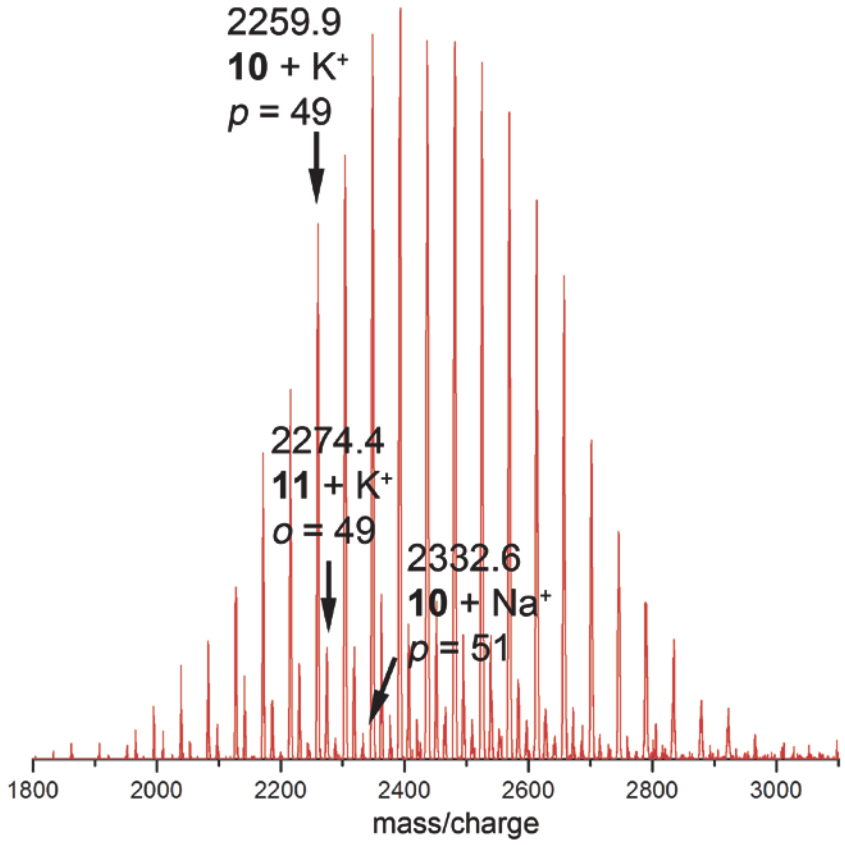

Figure S22. MALDI-TOF mass spectrum of **10** and **11** derived from **9b**. Matrix: CHCA. Salt: KTFA. Reflectron mode.

4. SEC traces

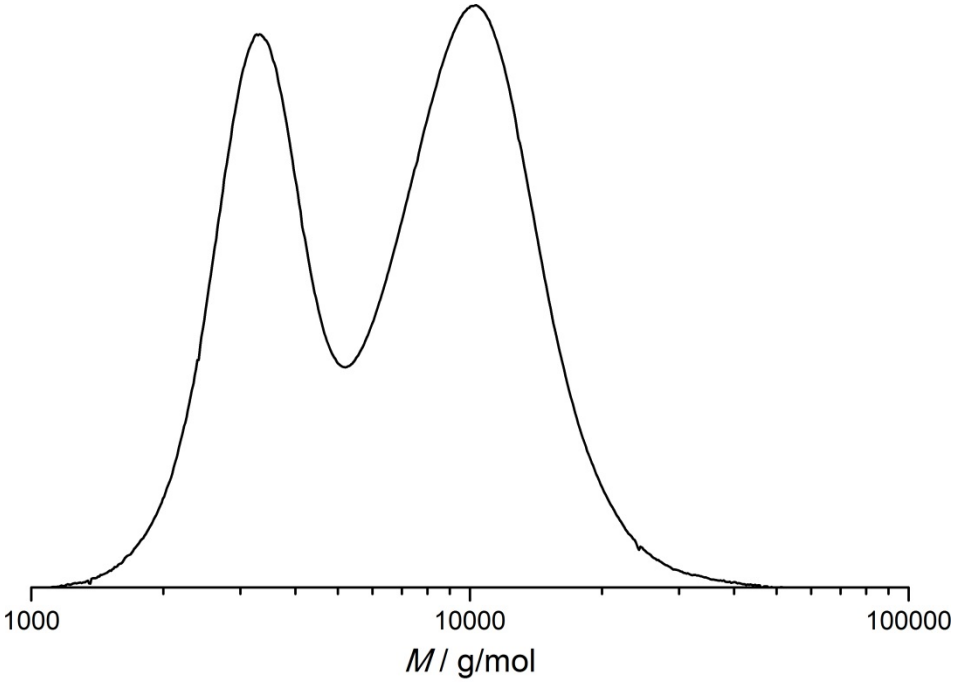

Figure S23. SEC traces of **6** referenced to PEG standards. Eluent: DMF, RI-Detector.

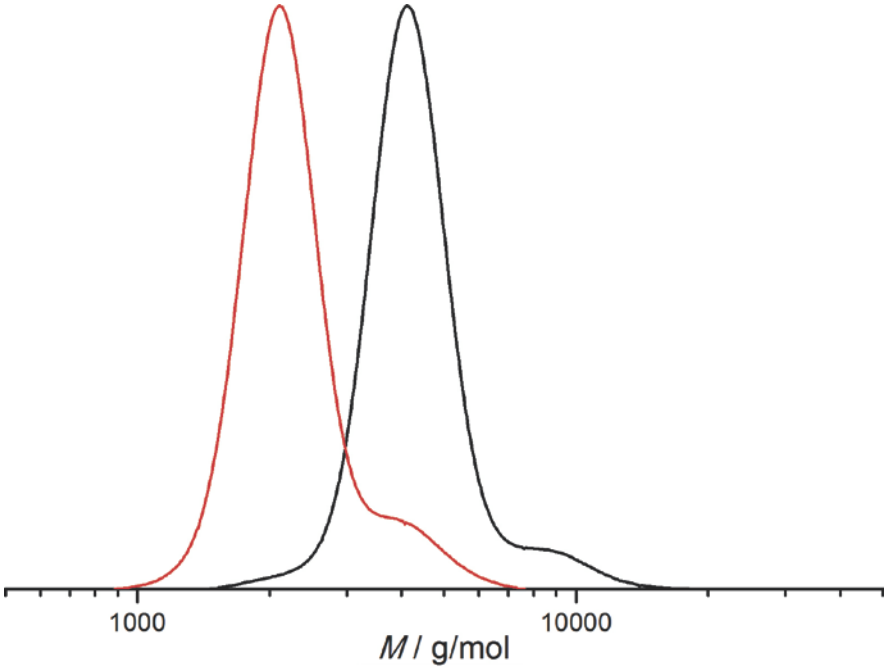

Figure S24. SEC traces of **9a** before (black) and after (red) cleavage referenced to PEG standards. Eluent: DMF, RI-Detector.

Appendix

A.1 α,ω_n-Heterotelechelic Hyperbranched Polyethers Solubilize Carbon Nanotubes

*Frederik Wurm, Anna Maria Hofmann, Anja Thomas, Carsten Dingels, and Holger Frey**

Institut für Organische Chemie, Makromolekulare Chemie, Johannes Gutenberg-Universität Mainz, Duesbergweg 10–14, 55099 Mainz (Germany)

Published in: *Macromol. Chem. Phys.* **2010**, *211*, 932-939.

Macromolecular Chemistry and Physics

Macromolecular Journals

Full Paper

α,ω_n-Heterotelechelic Hyperbranched Polyethers Solubilize Carbon Nanotubes[a]

Frederik Wurm, Anna Maria Hofmann, Anja Thomas, Carsten Dingels, Holger Frey*

The synthesis of novel linear-hyperbranched (*linhb*) polyether block copolymers based on poly(ethylene oxide) and branched poly(glycerol), bearing a single pyrene or myristyl moiety at the α-position of the linear chain is described. The polymers exhibit low polydispersity ($\overline{M}_w/\overline{M}_n < 1.3$) and controlled molecular weights ($\overline{M}_n = 5\,000\ g \cdot mol^{-1}$). The mainly hydrophilic block copolymers with multiple hydroxyl end groups readily dissolve multiwalled carbon nanotubes (MWCNTs) in water by mixing and subsequent sonification, resulting in noncovalent attachment of the *linhb* hybrid structure to the carbon nanotubes (CNTs). Transmission electron microscopy (TEM) was employed to visualize the solubilized nanotubes; after sulfation of the multiple hydroxyl groups the polymer layer was detected in the TEM images.

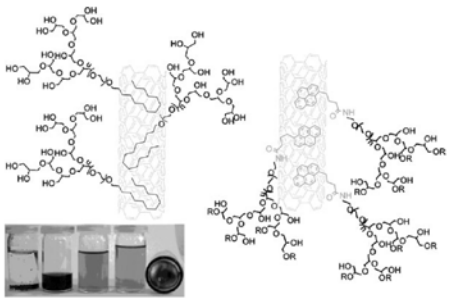

Introduction

Due to their unique physical, mechanical, and chemical properties, carbon nanotubes (CNTs) have attracted immense attention in recent years after their discovery in 1990.[1] However, their strong aggregation, resulting in insolubility in most common solvents is generally considered as a significant disadvantage for the use of CNTs. Particularly, their insolubility in water is one of the major concerns regarding their potential biomedical application[2] (e.g., for biosensors, drug delivery devices, and biomedical imaging).

F. Wurm, A. M. Hofmann, A. Thomas, C. Dingels, H. Frey
Institut für Organische Chemie, Makromolekulare Chemie, Johannes Gutenberg-Universität Mainz, Duesbergweg 10–14, D-55099 Mainz, Germany
E-mail: hfrey@uni-mainz.de

[a] Supporting information for this article is available at the bottom of the article's abstract page, which can be accessed from the journal's homepage at http://www.mcp-journal.de, or from the author.

In the last decade two main strategies have been developed to introduce (aqueous) solubility: covalent and noncovalent functionalization of CNTs. The covalent approach includes chemical modification[3] (e.g., halogenation, grafting of polymers, cycloaddition, etc.) to achieve sidewall functionalization, or defect site chemistry (e.g., oxidation[4]), allowing direct covalent attachment of substituents. Although chemical functionalization or modification provides a convenient opportunity for solubilizing CNTs, the major drawback is a shortening of the average tube length and surface destruction, resulting in a change in the electronic structure as well as product mixtures due to side reactions. The noncovalent functionalization is based on van der Waals (vdW) forces or π–π-stacking and thus offers the possibility of attaching solubilizing moieties without modification of the electronic structure of the tubes.[5] Several recent reports have shown that pyrene-carrying (linear) polymers,[6] oligothiophene-terminated poly(ethylene glycol) (PEG),[7] detergents,[8] or starch[9] can effectively solubilize CNTs in a supramolecular manner.

Only a few reports on the noncovalent attachment of hyperbranched (*hb*) polymers to nonmodified CNTs have

Macromol. Chem. Phys. **2010**, *211*, 932–939

InterScience

DOI: 10.1002/macp.200900652

been published very recently.[10] In the reported cases, hyperbranched materials of broad polydispersity with multiple interaction sites have been combined with the CNTs, achieving solubilization in organic solvents and water. However, to the best of our knowledge, there are no reports on the supramolecular attachment of specifically designed hyperbranched structures with a single, focal interaction moiety to multiwalled CNTs (MWCNTs). This is highly relevant, since the multifunctionality and compact globular structure of hyperbranched polymers give access to a wide range of modification reactions for further functionalization. Covalent grafting of *hb*-polyoxetanes and noncovalent adsorption of poly(phenylene vinylene)s on single-walled CNTs has also been reported.[11]

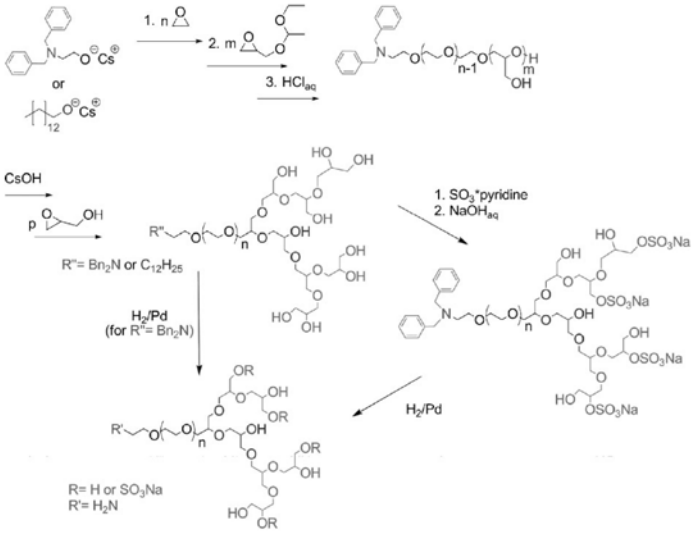

Scheme 1. Synthesis of α,ω_n-telechelics; a linear-hyperbranched polymer is obtained for $n > 1$, when omitting the polymerization of ethylene oxide ($n = 0$), a monoamino-hyperbranched polyglycerol homopolymer is formed.

Our group has investigated the ring-opening multibranching polymerization of glycidol that permits the controlled synthesis of *hb*-polyglycerol (*hb*PG) with polydispersities usually below 1.5 and adjustable molecular weights.[12] Polydispersity can be further reduced (<1.3) by using a two-step protocol for the synthesis of double-hydrophilic linear-hyperbranched (*linhb*) block copolymers based on PEG and *hb*PG that are merely built up from biocompatible segments avoiding any other linkages than aliphatic ethers.[13] In related works, amphiphilic derivatives with *hb*PG segments have also been developed.[14]

In order to obtain biocompatible conjugates of MWCNTs, PEG as one of the most important biocompatible, water-soluble polymers has been employed.[2,15] Its low toxicity, excellent solubility in aqueous solutions and extremely low immunogenicity and antigenicity as well as good pharmacokinetic and biodistribution behavior render PEG the polymer of choice for versatile biomedical applications.[15] The low intrinsic viscosity of *hb*PG and particularly its large number of derivatizable hydroxyl groups can provide advantages in pharmaceutical and medical fields compared to its linear analogs.[16] As expected from its structural similarity to PEG and polysaccharides, *hb*PG (at least up to $\overline{M}_n \approx 3\,000\ g \cdot mol^{-1}$) has been found to be as biocompatible as PEG.[16b]

In this paper we report different strategies for the supramolecular modification of MWCNTs with α,ω_n-heterotelechelic *linhb*-polyethers by (i) noncovalent pyrene-modified polymers in the α-position (π–π-stacking) or (ii) vdW interactions, based on myristyl alcohol as the respective initiator. In addition, first results of a novel covalent strategy relying on active esters attached to the CNTs are presented.

Experimental Part

Instrumentation

^{1}H, ^{13}C nuclear magnetic resonance spectra were recorded using a Bruker AC 300 or a Bruker AMX 400 spectrometer operated at 300 or 400 MHz for ^{1}H NMR, employing deuterated dimethylsulfoxide (DMSO) as a solvent. ^{13}C NMR spectra are referenced internally to solvent signals and were recorded at 100.15 MHz. FT-IR spectra were recorded on a Nicolet SDXC FT-IR spectrometer equipped with an ATR unit. SEC measurements in dimethylformamide (DMF) containing $0.25\ g \cdot L^{-1}$ of lithium bromide, an Agilent 1100 Series GPC Setup (gel permeation chromatography) was used as an integrated instrument, including a PSS HEMA column ($10^6/10^5/10^4\ g \cdot mol^{-1}$), a UV (254 nm), and RI detector. Calibration was carried out using poly(styrene) or poly(ethylene oxide) standards, provided by Polymer Standards Service. The eluent was used at 50 °C and at a flow rate of $1\ mL \cdot min^{-1}$. Matrix-assisted laser desorption and ionization time-of-flight (MALDI-TOF) measurements were performed on a Shimadzu Axima CFR MALDI-TOF mass spectrometer equipped with a nitrogen laser delivering 3 ns laser

Macromolecular
Chemistry and Physics

pulses at 337 nm. α-Cyano-4-hydroxycinnamic acid was used as matrix. Samples were prepared by dissolving the polymer in methanol at a concentration of 10 g · L^{-1}. A 10 μL aliquot of this solution was added to 10 μL of a 10 g · L^{-1} solution of the matrix and 1 μL of a solution of KTFA (0.1 M in methanol as cationization agent). A 1 μL aliquot of the mixture was applied to a multistage target to evaporate $CHCl_3$ and create a thin matrix/analyte film. The samples were measured in positive ion and in reflection mode of the spectrometer.

Reagents

Diglyme (99%, Acros), glycidol (99%, Acros), ethanolamine (98%, Acros), pyridine (99%, Acros) were purified by distillation from CaH_2 directly prior to use. Ethoxyethyl glycidyl ether (EEGE) or isopropylidene(glyceryl glycidyl ether) (IGG) was prepared as described in literature,[13,17] dried over CaH_2, and freshly distilled before used. The procedure for introduction of sulfate groups into hyperbranched poly(glycerol) can be found elsewhere and was adopted.[18] Sulfur trioxide pyridine complex (99%), pentafluorophenol (99%), benzyl bromide (99%), 1-pyrene-butyric acid (97%), myristyl alcohol (99%) was purchased from Aldrich and used as-received. MWCNTs were purchased from Aldrich and used as-received (outer diameter: 10–15 nm, length: 0.1–10 μm, >90% AS MWCNT), and "short" MWCNT (compare Figure S17) were obtained from Aldrich ("bucky tubes," as produced cylinders 7.5% MWCNT content).

Cesium hydroxide monohydrate, palladium on activated charcoal, potassium carbonate, *N,N'*-dicyclohexylcarbodiimide (DCC) was purchased from Acros and used as-received. Deuterated DMSO-d_6 was purchased from Deutero GmbH, dried, and stored over molecular sieves. Methanol and other solvents and reagents were purchased from Acros and used as-received, if not otherwise mentioned.

N,N-Dibenzyl-2-aminoethanol

A mixture of 2-aminoethanol (30 g, 0.5 mol), benzyl bromide (171.3 g, 1 mol), K_2CO_3 (276 g, 2 mol), and water (900 mL) was refluxed and vigorously stirred for 5 h. The organic phase was diluted with diethyl ether and separated from the aqueous layer. The organic phase was washed two times with water (each 100 mL, dried over Na_2SO_4), and evaporated to give 105 g of crude product as a pale yellow oil. The product was crystallized from 9:1 mixture pentane/ethyl acetate and recrystallized twice to form white crystals mp. 38 °C, 60 g (50%) ^{1}H NMR ($CDCl_3$): $\delta = 7.31–7.32$ (m, 10 H, Ar-H), 3.60 (s, 4 H, CH_2Ph), 3.57 (t, $J = 5.7$ Hz, 2H, CH_2OH), 2.65 (t, $J = 5.4$ Hz, 2H, CH_2CH_2OH). ^{13}C NMR ($CDCl_3$): $\delta = 54.7$ (CH_2N), 58.4 ($C_6H_5CH_2N$), 58.5 (CH_2OH), 127.2, 128.4, 129.0, 138.7 (aromatic carbons).

1-Pyrene-butyric Acid Pentafluorophenyl Ester

1-Pyrene-butyric acid (1 g, 3.47 mmol) was dissolved in a mixture of dry dichloromethane:dry pyridine (50:50, ca. 25 mL) at 50 °C, cooled to room temperature, and then pentafluorophenol (645 mg, 3.5 mmol) was added. The reaction mixture was cooled with an ice bath, and DCC (714 mg, 3.5 mmol) in dry dichloromethane (5 mL) was added dropwise within 30 min. The mixture was allowed to warm up to room temperature overnight. The DCU formed was removed (filtration) and washed with dichloromethane (10 mL). The combined solutions were concentrated and kept at room temperature for 5 h. A small amount of residual DCU was removed by filtration, the solvent was evaporated, and the crude mixture was purified via flash chromatography with dichloromethane as eluent. Yield: 90% after column, yellow crystalline powder. ^{1}H NMR (300 MHz, $CDCl_3$): $\delta = 8.32–7.88$ (m, aromat.), 3.50 (t, 2H), 4.31 (m, 1H, CHN methin.), 2.80 (t, 2H), 2.35 (q, 2H).

General Procedure for Anionic Polymerization

Linear Block Copolymers

N,N-Dibenzyl-2-aminoethanol or myristyl alcohol was dissolved in benzene in a Schlenk flask and a stoichiometric amount of cesium hydroxide monohydrate was added under argon. The mixture was stirred at 60 °C for 45 min and evacuated at 90 °C (10^{-2} mbar) for 2 h to remove benzene and water. The dry cesium alkoxide was dissolved in dry DMSO or toluene (20 wt.-%). In a separate setup, THF was cryo-transferred into a Schlenk flask from a dark purple colored sodium/benzophenon THF solution. Subsequently, ethylene oxide was first cryo-transferred to a graduated ampoule and then into the flask containing THF to produce a ca. 50 wt.-% solution. The solution was kept at 0 °C and the initiator was added via canula. The slightly yellow mixture was allowed to slowly warm up to room temperature and polymerization was performed for 1–2 d in vacuo at 40 °C. Subsequently the flask was filled with argon, the appropriate amount of EEGE or IGG was added with a syringe and temperature was raised to 80 °C for 12 h. The polymerization was terminated by addition of methanol and acidic ion exchange resin. Filtration and precipitation in cold diethyl ether resulted in the pure polymer. Yields: 95% quantitative.

For *N,N*-dibenzyl-2-aminoethanol as the respective initiator and EEGE as second monomer: ^{1}H NMR (300 MHz, $CDCl_3$): $\delta = 7.33$ (m, C_6H_5), 4.69 (br, acetal-H), 3.86–3.37 (polyether backbone), 2.32 (br, NCH_2Ph), 1.28–1.15 (br, CH_3 acetal).

For myristyl alcohol as the respective initiator and IGG as second monomer: ^{1}H NMR (300 MHz, $CDCl_3$): $\delta = 4.3$ (m, 1H, *CH* acetal), 4.07 (m, 1H), 3.86–3.37 (polyether backbone), 1.45 (br, CH_2 (initiator)), 1.44 (br, 3H, CH_3), 1.38 (br, 3H, CH_3), 1.23 (CH_2 (initiator)), 0.84 ppm (CH_3 (initiator)). 0.84 ppm and broad signals for the methylene groups at 1.23 and 1.45 ppm.

DPn of EEGE or IGG was determined by comparison of aromatic signals of the initiator and the methyl signals for PEEGE or PIGG block. Molecular weights were obtained by comparison of the aromatic protons with the polyether signals.

Deprotection to Linear Block Copolymers

The acetal protecting groups were removed by the addition of 1 M hydrochloric acid to a 20% solution of the polymer in ethanol and stirring for 30 min. Purification of the block copolymer was achieved by repetitive precipitation from a concentrated ethanolic solution in diethyl ether or by exhaustive dialysis in methanol using a dialysis tube with an MWCO of 1 000 g · mol^{-1}. Yields: 80–90%. The polymers with *N,N*-dibenzyl-2-aminoethanol as initiator are usually obtained as the respective ammonium chlorides; recovery of the free amine is achieved by addition of triethylamine during dialysis.

Macromol. Chem. Phys. **2010**, *211*, 932–939

Macromolecular Journals
DOI: 10.1002/macp.200900652

^{1}H NMR (300 MHz, DMSO-d_6): $\delta = 11.14$ (br, Bn_2NH^+), 7.62, 7.40 (br, C_6H_5), 4.59 (br, OH), 3.59–3.27 (polyether backbone), 2.46 (br, NCH_2Ph).

Hypergrafting to Linear-Hyperbranched Block Copolymers

The linear macroinitiator was placed in a Schlenk flask and dissolved in benzene (20 wt.-%). Subsequently the appropriate amount of cesium hydroxide monohydrate was added to achieve 30% of deprotonation of the hydroxyl groups along the backbone. After heating to 60 °C for 30 min and evacuation (10^{-2} mbar) at 90 °C for 2 h dry diglyme was added to produce a 20 wt.-% solution and the flask was placed in an ultrasonic bath for 15 min to ensure complete suspension of the macroinitiator. The mixture was heated to 100 °C and a 20 wt.-% solution of glycidol in dry diglyme was added slowly with a syringe over a period of ca. 12 h. The reaction was terminated by addition of an excess of methanol and an acidic cation exchange resin. The products were filtrated, concentrated, and precipitated into cold diethyl ether. The resulting material was dried in vacuo for 2 d at 40 °C. Yields: quantitative.

^{1}H NMR for *N,N*-dibenzyl-2-aminoethanol as initiator (300 MHz, DMSO-d_6): $\delta = 7.62$, 7.40 (br, C_6H_5), 4.79–4.42 (br, OH, different signals due to branched PG), 3.59–3.27 (polyether backbone), 2.46 (br, NCH_2Ph).

Hydrogenation of Linear-Hyperbranched Block Copolymers H_2N-Poly(ethylene oxide)-Block-Hyperbranched-poly(glycerol)

Under an argon atmosphere, 1 g *N,N*-dibenzyl-poly(ethylene oxide)-*block*-hyperbranched-poly(glycerol) was dissolved in methanol and palladium on activated charcoal (10%) was added. The vessel was flushed with hydrogen (8 bar) and the reaction was allowed to stir for 48–72 h at room temperature, completion of the reaction was monitored via ^{1}H NMR spectroscopy. The solution was filtered, concentrated, and precipitated into cold diethyl ether. Yields: quantitative.

^{1}H NMR (300 MHz, DMSO-d_6): $\delta = 4.79$–4.42 (br, OH, different signals due to branched PG), 3.59–3.27 (polyether backbone).

Synthesis of Sulfates 2a and 2b

The sulfation of the polymers 2a and 2b was performed according to the method described by Haag and coworkers.[18] (a) To a stirred solution of 500 mg polymer Bn_2NhbPG_{47} (6.7 mmol OH-groups) in 2 mL DMF was added dropwise a solution of 1.07 g (6.7 mmol) SO_3/pyridine complex in 7 mL DMF at 60 °C under an argon atmosphere. The reaction mixture was further stirred at 60 °C overnight. Distilled water (5 mL) was added to the cooled solution and immediately 1 M NaOH was added to reach a pH of at least 11. After concentration in vacuo the crude product was further purified by dialysis in water. Evaporation of the solvent gave the product as a yellow solid. Yield: 380 mg. FT-IR (ν, cm^{-1}): 3 439 (PG(OH)$_n$ stretch), 2 872 ($-CH_2-$ stretch (polyetherbackbone)), 1 653 (–C=C– stretch, aromatic), 1 458 ($-CH_2-$ deform.), 1 348 (–C–N– stretch), 1 219 ($-C-O-SO_3$), 1 068 (–C–O–C– stretch), 1 001 (–C–O–C– stretch), 939, 776 (=C–H deform.), 578.

Deprotection of the Polymer Sulfates

Under an argon atmosphere, the polymer sulfates were dissolved in water and acetic acid and palladium on activated charcoal (10%) was added. The vessel was flushed with hydrogen and the reaction was allowed to stir for 5 d at room temperature. The solution was centrifuged, filtered, and the solvent evaporated to obtain the product as a solid. Yields: quantitative.

^{1}H NMR (300 MHz, D_2O): $\delta = 4.7$–4.5 ($-CH_2OSO_3Na$), 4.35–3.35 (polyether backbone).

Coupling Reaction of α,ω_n-Heterotelechelic H_2N-Poly(ethylene oxide)-Block-Hyperbranched-poly(glycerol) with Pyrene

H_2N-poly(ethylene oxide)-*block*-hyperbranched-poly(glycerol) (0.2 g, $\overline{M}_n = 5\,200\ g \cdot mol^{-1}$, 0.038 mmol) was dissolved in 3 mL of degassed DMF and 50 µL of freshly distilled triethylamine was added under argon. Pyrenebutyric pentafluorophenol ester (32 mg, 0.071 mmol) was added and the reaction was allowed to stir for 24 h at room temperature. The excess PFP-ester was removed by repetitive precipitation from DMF into cold acetone or exhaustive dialysis in DMF (MWCO 1 000 $g \cdot mol^{-1}$). Yield: 0.2 g (quantitative).

^{1}H NMR (300 MHz, DMF-d_7): $\delta = 8.4$–7.9 (br, aromat.), 4.79–4.42 (br, OH, different signals due to branched PG), 3.59–3.27 (polyether backbone), 2.6–2.0 (br, CH_2).

Coupling Reaction of α,ω_n-Heterotelechelic Polymers with MWCNTs

Noncovalent

Pyrene-activated polymer (45 mg) and MWCNTs (2.8 mg) were suspended in 3 mL of water and mixed by sonification for 3 h. After sonification the deep black solution was filtered through a Kim-wipe filter to remove traces of undissolved material and evaporated to give the MWCNT–polymer conjugate in quantitative yield. Dialysis of the aqueous solution did not reduce the amount of conjugate, indicating complete adsorption of the block copolymers onto the tubes.

Covalent

Acid treated MWCNTs (200 mg) were heated in thionyl chloride (30 mL) to produce acyl chloride groups.[3] The MWCNT–acyl chloride was dissolved in anhydrous DMF, 0.6 g pentafluorophenol were added, and the resulting mixture was sonificated for 30 min and stirred at room temperature for additional 12 h. Filtration to remove the solvents and excess reagents gave the MWCNT-active-ester (MWCNT-PFP) as a black solid (Yield quantitative, degree of functionalization not determined) (Scheme 2).

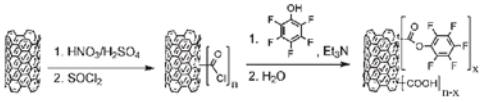

Scheme 2. Covalent modification of MWCNTs with PFP-active esters.

Macromolecular
Chemistry and Physics

Covalent Coupling of Amino-terminated Poly(ether)s to MWNCT-PFP

MWCNT-PFP (3.7 mg) and H_2NhbPG (60 mg) ($\overline{M}_n = 6\,500\ g \cdot mol^{-1}$) were dissolved in anhydrous DMF and triethylamine was added to obtain the free amine. The mixture was sonicated for 5 h and stirred at room temperature for additional 12 h; the mixture was filtrated to obtain a black solution of MWCNT-CO-NH-PG in DMF. Evaporation gave the black solid product (Yield compared to polymer 70–90%).

FTIR (ν, cm^{-1}): 3 406 (PG(OH)$_n$ stretch), 2 878 (–CH_2– stretch (polyether backbone)), 1 637 (C=O stretch), 1 458 (–CH_2– deform.), 1 115 (–C–O–C– stretch).

Results and Discussion

The anionic polymerization of epoxides conveniently allows the incorporation of several (functional) initiators that can be selectively addressed subsequent to the polymerization of glycidol to introduce specific α-moieties (compare Scheme 1). The selective attachment of *linhb* block copolymers to generate such nanocomposites via a single, specific α-functionality opens the way for several further modifications in the *hb*-periphery, such as conjugation with drugs or electroactive moieties. In a first account of our group, noncovalent bioconjugation of avidin was found to be feasible via biotinylated *linhb*- and *hb*-polyethers.[19] Several polymers have been synthesized via the protocol summarized in Scheme 1 (detailed characterization data can be found in Table 1 and the Supporting Information).

As an example for selective modification of the hyperbranched polyglycerol block, the OH-groups can be converted into sulfates to enhance water solubility and to introduce specific biological properties. This reaction proceeds smoothly in DMF via the pyridine complex of sulfur trioxide.[18] The degrees of functionalization obtained for the sulfated samples was determined via ^{1}H NMR and were found to be similar as reported for nonfunctional *hb*PG homopolymers previously (i.e., 45% sulfate groups were targeted and achieved).

In the α-position of the *linhb* polyethers the dibenzyl-protective group can be removed conveniently via catalytic hydrogenation, liberating the primary amino group. Quantitative pyrene modification was achieved by the pentafluorophenyl (PFP) active ester of pyrene butyric acid and monitored via MALDI-ToF spectrometry (cf. Scheme 3 and Figure 1B, SEC traces and NMR spectrum can be found in the Supporting Information).

Table 1. Characterization data of linear-hyperbranched block copolymers and hyperbranched poly(glycerol) homopolymers.

#	Compound	$\overline{M}_n$ [a]	PDI [a]	$\overline{M}_n$ [b]
1	Bn_2NPEG_{25} *lin*PG_5	1 500	1.06	1 400
2	Bn_2NPEG_{125} *lin*PG_{15}	6 300	1.05	6 500
1a	Bn_2NPEG_{25} *hb*PG_{50}	4 700	1.23	5 200
2a	Bn_2NPEG_{125} *hb*PG_{50}	8 400	1.19	9 600
1a*	H_2NPEG_{25} *hb*PG_{50}	4 700	1.25	5 200
2a*	H_2NPEG_{125} *hb*PG_{50}	8 200	1.18	9 600
3	Bn_2N*lin*PG_{15}	1 200	1.17	1 300
3a	Bn_2N*hb*PG_{80}	5 700	1.20	6 300
3a*	H_2N*hb*PG_{80}	6 400	1.21	6 300
4a	$C_{14}H_{29}O$-$PEG_{60}PGG_{15}$	4 800	1,08	5 000
4b	$C_{14}H_{29}O$-PEG_{60} *hb*PG_{40}	5 200	1.19	5 900

[a] Determined via size-exclusion chromatography in dimethylformamide versus polystyrene standards; [b] Determined via ^{1}H NMR spectroscopy in DMSO-d_6. *lin*PG: linear poly(glycerol), *hb*PG: hyperbranched poly(glycerol), PGG: poly(glyceryl glycidyl ether).

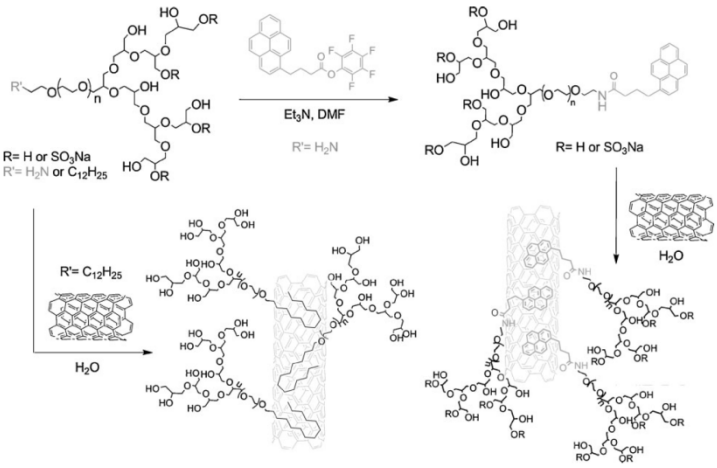

Scheme 3. Different strategies for noncovalent modification of MWCNT inducing water solubility. In α-position of the PEG-chains either a pyrene unit or a myristyl chain was attached.

Macromol. Chem. Phys. **2010**, *211*, 932–939

Macromolecular Journals
DOI: 10.1002/macp.200900652

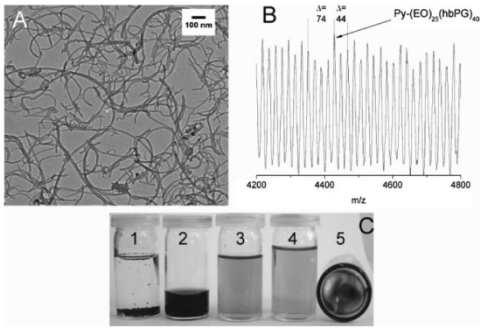

Figure 1. A: TEM image of an aqueous solution of pyrene-modified MWCNT. B: Section of MALDI-ToF of pyrene-modified PEG_{25}-*hb*PG_{40}. C: Images of aqueous MWCNT solutions: (1) Pristine MWCNT (not soluble), (2) myristyl-alcohol-modified PEG-*hb*PG ($c = 10\ g \cdot L^{-1}$), (3) pyrene-modified PEG_{120}-*hb*PG_{50} ($c = 0.3\ g \cdot L^{-1}$, strongly diluted for UV measurements), (4) covalently modified MWCNT (c approx. $0.1\ g \cdot L^{-1}$), and (5) film obtained after drying PEG_{25}-*hb*PG_{40}.

With this strategy no side reactions or interferences with the multiple OH-groups were detected. The introduction of myristyl alcohol can be achieved directly by employing this compound as an initiator for the polymerization of ethylene oxide (the respective MALDI-ToF spectrum can be found in the Supporting Information). These polymers are amphiphilic and form micelles in water, but readily solubilize MWCNTs. It is worth mentioning that the synthetic protocol for the myristyl alcohol-modified PEG-*hb*PG is based on a novel strategy for an amphiphilic, branched polyether. Furthermore, it has to be emphasized that no further derivatization is necessary and polydispersities and molecular weights can easily be tailored, keeping the polydispersity low. For the solubilization experiments a polymer consisting of $C_{14}H_{29}$-PEG_{60} *hb*PG_{40} ($\overline{M}_n = 5\,900\ g \cdot mol^{-1}$ PDI = 1.19) was applied. ^{1}H NMR spectra of different steps of the myristyl alcohol-based system are shown in Figure 2. The lower spectrum shows the first block "$C_{14}H_{29}$-PEG" with the respective broad signals for the initiator with a triplet for the methyl group at 0.84 ppm and broad signals for the methylene groups at 1.23 and 1.45 ppm. The middle spectrum is obtained from the protected linear precursor, here based on poly(isopropylidene(glyceryl glycidyl ether)), and the top spectrum was recorded for the final *linhb* block copolymer after hypergrafting with glycidol. The hyperbranched structure was confirmed via ^{13}C NMR analysis according to literature procedures[12] and is also visible in the ^{1}H NMR due to the different signals for the hydroxyl groups between 4 and 5 ppm.

Mixing of the pyrene-modified or myristyl alcohol-initiated block copolymers with MWCNT in water and

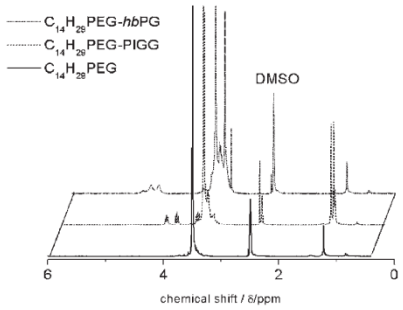

Figure 2. ^{1}H NMR spectra of myristyl alcohol-initiated PEG (bottom), $C_{14}H_{29}PEG_{60}$-$PIGG_{15}$ (middle), and the final product $C_{14}H_{29}PEG_{60}$-*hb*PG_{40} (top).

subsequent sonification for approximately 3 h resulted in deep black solutions that were stable over months. The sulfated block copolymers gave dark solutions, *albeit* with lower CNT content; we assume this is due to interference of the polyanion with the pyrene adsorption. Interestingly, for the sulfated polymers, transmission electron microscopy (TEM) investigation directly revealed the polymer layer on the MWCNTs due to the enhanced contrast of sulfur. Predominantly rod-like polymer micelles have been detected (Figure 1 and Supporting Information).

UV/vis, TGA, and TEM studies confirmed efficient solubilization of MWCNTs in water by the polyhydroxyl-functional polymers. Figure 3A shows a typical TEM image of the supramolecular water-solubilized MWCNTs that are present as discrete nanotube structures (for additional images, see Supporting Information). ^{1}H NMR spectra of the CNT–polymer conjugates showed broad signals and the signals for myristyl alcohol or pyrene, respectively, can be hardly detected due to interaction with the nantotubes.

As an alternative to the supramolecular strategy presented here, a covalent approach for water-soluble MWCNTs relies on the oxidation of the tubes via HNO_3/H_2SO_4 introducing multiple carboxylic acid functionalities

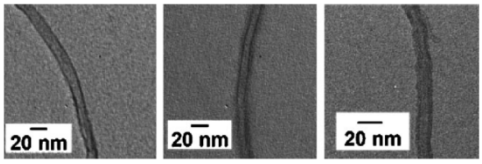

Figure 3. Transmission electron microscopy images of MWCNTs drop-cast from an aqueous solution (all samples were prepared with the same amount of MWCNTs). Left: $C_{14}H_{29}O$-PEG_{60} *hb*$PG_{40}(SO_4Na)_n$, middle: $C_{14}H_{29}O$-PEG_{60} *hb*PG_{40}, right: *hb*PG_{80}-@MWCNT (covalent).

that were reacted with thionyl chloride to form the acyl chlorides, and subsequently with pentafluorophenol to the respective active esters. The latter can react selectively with the polyethers carrying the amino group in the α-position in DMF. Also in this case stable, black aqueous solutions were formed after solvent exchange. This approach might be useful if the electronic properties of the tubes are not essential for a targeted application. However, the covalent approach is less controlled due to the harsh oxidation conditions (reaction scheme cf. Experimental Part). For this covalent solubilization approach shortened CNTs with a partly destroyed surface are detected via TEM, as expected. On the other hand, the novel covalent strategy relying on PFP-active esters may find useful application for other amine-containing polymers that will be investigated in the future.

How does the structure of the α,ω_n-block copolymers influence solubilization and surface coverage of the CNTs? TGA measurements show that by solubilizing CNTs with the *linhb* systems introduced in this work the amount of solubilized CNTs can be further increased in comparison to the *hb*-homopolymer, probably due to steric effects. This can be supported by TGA measurements for different block ratios, indicating the lowest MWCNT-incorporation, when the *hb*PG_{80} homopolymer ($\overline{M}_n = 6\,kg\cdot mol^{-1}$, PDI = 1.21) is used (Supporting Information).

Figure 3C shows images of the MWCNT solutions in water: (1) pristine MWCNT are insoluble in water; (2) myristyl alcohol-modified block copolymer solution ($c = 10\,g\cdot L^{-1}$); (3) pyrene-modified PEG_{125}-*hb*PG_{50} ($\overline{M}_n = 6\,kg\cdot mol^{-1}$, PDI = 1.14) ($c = 0.3\,g\cdot L^{-1}$, strongly diluted for UV measurements); and (4) covalently modified MWCNT (c approx. $0.1\,g\cdot L^{-1}$) showing a clear and stable CNT solution. Interestingly, a homogeneous film was obtained after drying of the MWCNTs modified with PEG_{25}-*hb*PG_{40} ($\overline{M}_n = 4.1\,kg\cdot mol^{-1}$, PDI = 1.25) due to the low T_g of *hb*PG (−30 °C) and suppression of the PEG melting point (Figure 3B-5).

Conclusion

We have presented a synthetic pathway for heterotelechelic *linhb* block copolymers bearing a single pyrene moiety or aliphatic chain (myristyl alcohol) in the α-position, permitting supramolecular solubilization of MWCNTs in water. The block copolymers exhibit rather narrow molecular weight distributions with $\overline{M}_w/\overline{M}_n < 1.3$ in all cases; for myristyl alcohol as the respective initiator, this protocol allows the synthesis of complex amphiphiles in only two steps, which readily dissolve MWCNTs in water. The homogeneous aqueous solutions were stable over months. Additionally, partial functionalization of the OH-groups in *hb*PG into sulfates has been achieved and the first supramolecular solubilization of MWCNTs with an *hb*-polyelectrolyte was presented. Further studies concerning modification, drug loading, and circulation times are under investigation. Preliminary data for a versatile covalent approach relying on the selectivity of PFP-active esters to amines has also been presented.

Acknowledgements: H.F. acknowledges the *Fonds der Chemischen Industrie* (FCI) for valuable financial support. A.M.H. is grateful to the graduate class of excellence "*POLYMAT*" in the context of the graduate school of excellence MAINZ for funding. H.F. acknowledges the *SFB 625* and the *German Science Foundation* (DFG) for valuable support.

Received: November 21, 2009; Published online: February 1, 2010; DOI: 10.1002/macp.200900652

Keywords: carbon nanotubes; hyperbranched polymers; linear dendritic block copolymers; poly(ethylene glycol); polyglycerol

[1] S. Iijima, *Nature* **1991**, *354*, 56.
[2] Z. Liu, S. Tabakman, K. Welsher, H. Dai, *Nano Res.* **2009**, *2*, 85.
[3] D. Tasis, N. Tagmatarchis, A. Bianco, M. Prato, *Chem. Rev.* **2006**, *106*, 1105.
[4] [4a] I. D. Rosca, F. Watari, M. Uo, T. Akaska, *Carbon* **2005**, *43*, 3124; [4b] J. Liu, A. G. Rinzler, H. J. Dai, J. H. Hafner, R. K. Bradley, P. J. Boul, A. Lu, T. Iverson, K. Shelimov, C. B. Huffman, F. Rodriguez-Macias, Y. S. Shon, T. R. Lee, D. T. Colbert, R. E. Smalley, *Science* **1998**, *280*, 1253; [4c] A. V. Ellis, M. R. Waterland, J. Quinton, *Chem. Lett.* **2007**, *36*, 1172.
[5] [5a] S. Meuer, L. Braun, R. Zentel, *Chem. Commun.* **2008**, 3166, DOI: 10.1039/b803099e; [5b] D. Tasis, N. Tagmatarchis, V. Georgakilas, M. Prato, *Chem. Eur. J.* **2003**, *9*, 4000; [5c] G. Prencipe, S. M. Tabakman, K. Welsher, Z. Liu, A. P. Goodwin, L. Zhang, J. Henry, H. Dai, *J. Am. Chem. Soc.* **2009**, *131*, 4783.
[6] [6a] G. J. Bahun, C. Wang, A. Adronov, *J. Polym. Sci. Part A: Polym. Chem.* **2006**, *44*, 1941; [6b] C.-H. Xue, R.-J. Zhou, M.-M. Shi, Y. Gao, G. Wu, X.-B. Zhang, H.-Z. Chen, M. Wang, *Nanotechnology* **2008**, *19*, 215604.
[7] J. U. Lee, J. Huh, K. H. Kim, C. Park, W. H. Jo, *Carbon* **2007**, *45*, 1051.
[8] M. F. Islam, E. Rojas, D. M. Bergey, A. T. Johnson, A. G. Yodh, *Nano Lett.* **2003**, *3*, 269.
[9] A. Star, D. W. Steuerman, J. R. Heath, J. F. Stoddart, *Angew. Chem.* **2002**, *114*, 2618.
[10] [10a] T. Ogoshi, T. Saito, T. A. Yamagishi, Y. Nakamoto, *Carbon* **2009**, *47*, 117; [10b] W. Zhou, S. Lv, W. Shi, *Eur. Polym. J.* **2008**, *44*, 587.
[11] [11a] Y. Xu, C. Gao, H. Kong, D. Yan, Y. Z. Jin, P. C. P. Watts, *Macromolecules* **2004**, *37*, 8846; [11b] A. Star, F. Stoddart, *Macromolecules* **2002**, *35*, 7516; [11c] J. Zhang, Y. Zheng, P. Yu, S. Mo, R. Wang, *Polymer* **2009**, *50*, 2953.
[12] [12a] A. Sunder, R. Hanselmann, H. Frey, R. Mülhaupt, *Macromolecules* **1999**, *32*, 4240; [12b] D. Wilms, F. Wurm, J. Nieberle, P. Böhm, U. Kemmer-Jonas, H. Frey, *Macromolecules* **2009**, *42*, 3230; [12c] E. Barriau, L. Pastor-Pérez, E. Berger-Nicoletti, A. F.

DOI: 10.1002/macp.200900652

M. Kilbinger, J. Pérez-Prieto, H. Frey, S.-E. Stiriba, *J. Polym. Sci., Polym. Chem.* **2008**, *46*, 2049. [12d] D. Wilms, J. Nieberle, J. Klos, H. Löwe, H. Frey, *Chem. Eng. Technol.* **2007**, *30*, 1519; [12e] D. Wilms, S. E. Stiriba, H. Frey, *Acc. Chem. Res.* **2009**, DOI: 10.1021/ar900158p. [12f] M. Calderon, M. A. Quadir, S. Sharma, R. Haag, *Adv. Mater.* **2009**, *22*, 190.

[13] [13a] F. Wurm, J. Nieberle, H. Frey, *Macromolecules* **2008**, *41*, 1184; [13b] F. Wurm, U. Kemmer-Jonas, H. Frey, *Polym. Int.* **2009**, *58*, 989.

[14] [14a] V. Istratov, H. Kautz, Y.-K. Kim, R. Schubert, H. Frey, *Tetrahedron* **2003**, *59*, 4017; [14b] A. Sunder, T. Bauer, R. Mülhaupt, H. Frey, *Macromolecules* **2000**, *33*, 1330; [14c] T. Demina, I. Grozdova, O. Krylova, A. Zhirnov, V. Istratov, H. Frey, H. Kautz, N. Melik-Nubarov, *Biochemistry* **2005**, *44*, 4042.

[15] [15a] S. Zalipsky, *Adv. Drug Delivery Rev*, **1995**, *16*, 157; [15b] E. W. Merrill, *Poly(ethylene glycol) Chemistry: Biotechnical and Biomedical Applications*, J. M. Harris, Ed., Plenum Press, New York 1992; [15c] M. J. Roberts, M. D. Bentley, J. M. Harris, *Adv. Drug Delivery Rev.* **2002**, *54*, 459.

[16] [16a] R. K. Kainthan, D. E. Brooks, *Biomaterials* **2007**, *28*, 4779; [16b] R. K. Kainthan, S. R. Hester, E. Levin, D. V. Devine, D. E. Brooks, *Biomaterials* **2007**, *28*, 4581.

[17] F. Wurm, J. Nieberle, H. Frey, *Macromolecules* **2008**, *41*, 1909.

[18] H. Türk, R. Haag, S. Alban, *Bioconjugate Chem.* **2004**, *15*, 162.

[19] F. Wurm, J. Klos, H. Räder, H. Frey, *J. Am. Chem. Soc.* **2009**, *131*, 7954.

A.2 PEG-based Multifunctional Polyethers with Highly Reactive Vinyl-Ether Side Chains for Click-Type Functionalization

Christine Mangold,[1, 2] *Carsten Dingels,*[2] *Boris Obermeier,*[2] *Holger Frey,**[2] *and Frederik Wurm**[3]

[1]Graduate School Materials Science in Mainz, Staudinger Weg 9, D-55128 Mainz, Germany

[2]Institute of Organic Chemistry, Organic and Macromolecular Chemistry, Duesbergweg 10-14, Johannes Gutenberg-Universität Mainz, D-55099 Mainz, Germany

[3]Institut des Materiaux, Laboratoire des Polymères, (EPFL), Bâtiment MXD, Station 12, Ecole Polytechnique Fédérale de Lausanne, CH-1015 Lausanne, Switzerland

Published in: *Macromolecules* **2011**, *44*, 6326.

Macromolecules

ARTICLE

pubs.acs.org/Macromolecules

PEG-based Multifunctional Polyethers with Highly Reactive Vinyl-Ether Side Chains for Click-Type Functionalization

Christine Mangold,[†,‡] Carsten Dingels,[‡] Boris Obermeier,[‡] Holger Frey,[*,‡] and Frederik Wurm[*,§]

[†]Graduate School Materials Science in Mainz, Staudinger Weg 9, D-55128 Mainz, Germany

[‡]Institute of Organic Chemistry, Organic and Macromolecular Chemistry, Duesbergweg 10-14, Johannes Gutenberg-Universität Mainz, D-55099 Mainz, Germany

[§]Institut des Matériaux, Laboratoire des Polymères, Batiment MXD, Station 12, Ecole Polytechnique Fédérale de Lausanne, CH-1015 Lausanne, Switzerland

Supporting Information

ABSTRACT:

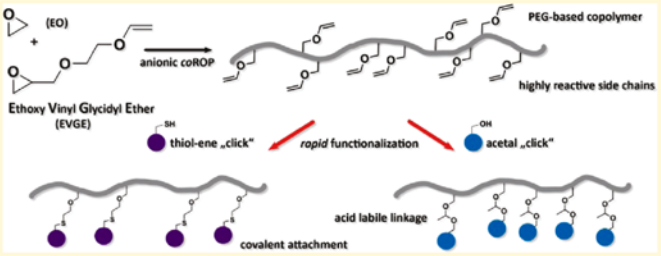

Introduction of highly reactive vinyl ether moieties along a poly(ethylene glycol) (PEG) backbone has been realized by copolymerization of the novel epoxide monomer ethoxy vinyl glycidyl ether (EVGE) with ethylene oxide (EO). A series of copolymers with varying structure (block and random) as well as EVGE comonomer content (5−100%) with molecular weights in the range of 3,900−13,200 g/mol and narrow molecular weight distributions (M_w/M_n = 1.06−1.20) has been synthesized and characterized with respect to their microstructure and thermal properties. The facile transformation of the vinyl ether side chains in click type reactions was verified by two different post polymerization modification reactions: (i) thiol−ene addition and (ii) acetal formation, employing various model compounds. Both strategies are very efficient, resulting in quantitative conversion. The rapid and complete acetal formation with alcohols results in an acid-labile bond and is thus highly interesting with respect to biomedical applications that require slow or controlled release of a drug, while the thiol−ene addition to a vinyl ether prevents cross-linking efficiently compared to other double bonds.

INTRODUCTION

The importance of multifunctional, biocompatible polymer structures is obvious, particularly with respect to binding and release of pharmacologically active agents. Poly(ethylene glycol) (PEG), which exhibits low toxicity and antigenicity,[1,2] is used in a broad variety of biomedical applications.[3,4] However, the use of PEG is limited by its low loading capacity in drug conjugation, particularly when used as support for low molecular weight drugs. One strategy to increase the functionality of PEG is the synthesis of star- or block copolymers, which often leads to amphiphilicity and requires multistep syntheses. Another, more recent approach for enhancing the functionality of PEG, but leaving the water-solubility and toxicity unchanged, is the random copolymerization with an epoxide comonomer bearing an additional functional group that in most cases has to be protected for the anionic ring-opening polymerization (AROP). The most popular protecting groups in AROP are acetals, such as ethoxy ethyl- (for OH-functionalities), as for example in the case of ethoxy ethyl glycidyl ether[5] (EEGE), a monomer which has been used in a number of reports for the copolymerization with ethylene oxide[6−8] either in a random[9−11] or block-like[12,13] manner to achieve linear and also more sophisticated structures.[14,15] Other functionalities introduced via the protected-monomer strategy are vicinal diols[16] or amino functionalities,[17] which were reported recently by our group. Currently, for the introduction of functionalities other than hydroxyl groups, different postpolymerization modifications are applied, which exceed a simple one-step deprotection reaction. A comprehensive overview of such reactions has been given by Li and Chau.[18]

Received: April 19, 2011
Revised: June 24, 2011
Published: July 22, 2011

dx.doi.org/10.1021/ma200898n | Macromolecules 2011, 44, 6326–6334

Scheme 1. Ethoxy Vinyl Glycidyl Ether (EVGE), Obtained via Phase Transfer Catalysis

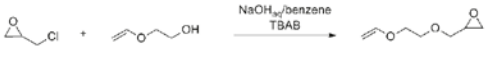

Functional macromolecules that permit facile and complete transformation of side chains play an important role in polymer science with respect to the attachment of drugs, catalyst structures or reagents.[19] To date, the only functional epoxide monomer that contains a stable functional group for AROP, is allyl glycidyl ether (AGE),[20,21] permitting the introduction of allyl groups. In the current report we present the novel comonomer ethoxy vinyl glycidyl ether (EVGE) for the AROP to introduce vinyl ethers attached randomly along a PEG chain. The monomer is accessible in a simple one-step reaction,[22] and purified by distillation (Scheme 1).

In a single previous work, this compound was used as a cross-linking reagent,[23] but to date, no reports on the AROP of the glycidyl ether have been reported. Since vinyl ethers are stable toward carbanionic[24] and oxyanionic[25] polymerization conditions, this monomer can be employed for AROP. In a recent first account we have demonstrated that EVGE can be homopolymerized and that multiple attachment of Grubbs' catalyst to the resulting structure is possible.[26] The vinyl ether group does not only offer the opportunity for thiol−ene functionalization reactions, but also for the attachment of any molecule possessing an alcohol. The latter modification results in an acetal which allows triggered release of a specified target in acidic conditions. This is a promising approach for the design of novel polymer therapeutics with releasable payloads. There are various examples in literature, where this principle has been realized, but usually multistep procedures are necessary.[27]

In the current publication we describe the random, anionic ring-opening copolymerization of EVGE with EO (Scheme 2). The resulting polyethers with vinyl ether side chains have been characterized with respect to their thermal behavior and their microstructure, particularly in view of the random incorporation of both comonomers. In addition, postpolymerization modifications were performed, i.e., thiol−ene functionalization with different model compounds, and the kinetics of the resulting acetal formation has been studied, employing ^{1}H NMR online measurements.

■ EXPERIMENTAL SECTION

Instrumentation. ^{1}H NMR spectra (300 and 400 MHz) and ^{13}C NMR spectra (75.5 MHz) were recorded using a Bruker AC300 or a Bruker AMX400. All spectra were referenced internally to residual proton signals of the deuterated solvent. For SEC measurements in DMF (containing 0.25 g/L of lithium bromide as an additive) an Agilent 1100 Series was used as an integrated instrument, including a PSS HEMA column ($10^6/10^5/10^4$ g/mol), a UV- (275 nm) and a RI-detector. Calibration was carried out using poly(ethylene oxide) standards provided by Polymer Standards Service. DSC measurements were performed using a Perkin-Elmer 7 series thermal analysis system and a Perkin-Elmer thermal analysis controller TAC 7/DX in the temperature range from −100 to +80 °C at heating rates of 10 K·min^{-1} under nitrogen.

Reagents. Solvents and reagents were purchased from Acros Organics, Sigma-Aldrich, or Fluka and used as received, unless otherwise stated. Chloroform-d_1, methanol-d_4, and DMSO-d_6 were purchased from Deutero GmbH. The two different initiators used, di(benzyl)aminoethanol and di(*p*-methoxybenzyl)aminoethanol, were synthesized as reported previously.[11,14]

Scheme 2. Synthesis of Random Copolymers of EO and EVGE by Simultaneous Reaction of Both Monomers with the Deprotonated Initiator

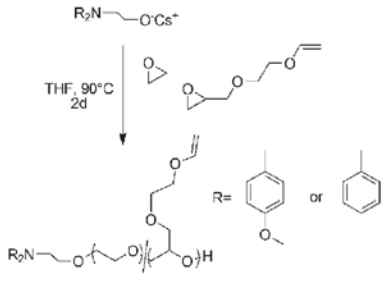

Ethoxy Vinyl Glycidyl Ether (EVGE). 2-(Vinyloxy)ethanol (10 g, 113.5 mmol) was placed in a 500 mL round-bottom flask and dissolved in a mixture of 50% aqueous NaOH (150 mL) and benzene (150 mL). To this mixture was added 3.5 g (11 mmol) of tetrabutylammonium bromide (TBAB), and the mixture was stirred quickly with a mechanical stirrer. Subsequently the reaction mixture was cooled with an ice bath, and epichlorohydrin (31.5 g, 340.5 mmol) was slowly added via a dropping funnel. After 24 h reaction time at room temperature, the organic phase was separated from the aqueous phase, washed several times with brine, dried, and concentrated *in vacuo* to remove benzene and the excess epichlorohydrin. The resulting slightly yellow residue was distilled under reduced pressure to yield the desired product as a colorless liquid, typically in 70−80% yield (11−13 g). ^{1}H NMR ($CDCl_3$, 300 MHz): δ (ppm) = 6.44 (1H, dd, CH_2=CH, J_1 = 14.3, J_2 = 7), 4.13 (1H, dd, CH_2=CH, J_1 = 14.3, J_2 = 2.2), 3.96 (1H, dd, CH_2=CH, J_1 = 7, J_2 = 2.2), 3.8−3.65 (4H, m, −O−CH_2−CH_2−O− and CH_2 (*glycidyl ether*)), 3.38 (2H, dd, CH_2 (*glycidyl ether*), J_1 = 11.8, J_2 = 5.9), 3.1 (1H, m, CH−*epoxide*), 2.74 (1H, dd, CH_2−*epoxide*, 1H, J_1 = 5, J_2 = 4.2), 2.56 (1H, dd, CH_2−*epoxide*, J_1 = 5.2, J_2 = 2.6).

General Procedure for the Copolymerization of EO and EVGE. *N*,*N*-Di(*p*-methoxy-benzyl)-2-amino ethanol was dissolved in benzene in a 250 mL-Schlenk flask, and 0.9 equiv of cesium hydroxide were added. The mixture was stirred under argon for 3 h at room temperature and evacuated at (10^{-2} mbar) for 12 h to remove benzene and water, forming the corresponding cesium alkoxide. Then 20 mL of dry THF was cryo-transferred into the Schlenk flask to dissolve the initiator-salt. EO was first cryo-transferred to a graduated ampule, and subsequently cryo-transferred into the flask containing the initiator in THF (at around −80 °C). The EVGE comonomer was added via syringe and the mixture was heated to 90 °C and stirred for 24−72 h. Precipitation in cold diethyl ether resulted in the pure copolymers. For polymers with a high fraction of EVGE, the polymer solution was dried *in vacuo*. Yields: 95% to quantitative. ^{1}H NMR (DMSO-d_6, 300 MHz): δ (ppm) = 7.24, 6.87 (8H, d, C_6H_4OMe) in the case of *p*-methoxybenzyl-; without methoxy-group: 7.40−7.15 (10H, m, aromatic), 6.48 (1H/EVGE-unit, dd, CH=CH_2), 4.16 (1H/EVGE-unit, dd, CH=CHH), 3.95 (1H/EVGE-unit, dd, CH=CHH), in the case of methoxy-benzyl: 3.74 (s, C_6H_4OMe), 3.68−3.34 (polyether backbone), 2.54 (2H, t, $Bn_2NCH_2CH_2O$−).

Block Copolymer Synthesis. A 2 g sample of mPEG-5000 was deprotonated with 0.9 equiv of CsOH·H_2O. The reaction water was removed by azeotropic distillation with benzene. The deprotonated polymer was dissolved in dry DMSO to give a 50% solution. Subsequently, EVGE was added to the mixture, and the polymerization was

Table 1. Characterization Data for All Copolymer Samples Prepared

no.	monomer feed composition	polymer composition[a]	M_n (NMR)[a]	M_n (SEC)[b]	PDI[b]
1	$MeOBn_2NP(EO_{100}$-*co*-$EVGE_{10})$	$MeOBn_2NP(EO_{104}$-*co*-$EVGE_6)$	5800	2400	1.06
2	$MeOBn_2NP(EO_{120}$-*co*-$EVGE_{10})$	$MeOBn_2NP(EO_{115}$-*co*-$EVGE_{11})$	6700	2500	1.08
3	$MeOBn_2NP(EO_{120}$-*co*-$EVGE_{30})$	$MeOBn_2NP(EO_{120}$-*co*-$EVGE_{30})$	9900	5130	1.08
4	$MeOBn_2NP(EO_{100}$-*co*-$EVGE_{30})$	$MeOBn_2NP(EO_{89}$-*co*-$EVGE_{30})$	8500	5100	1.11
5	$Bn_2NP(EO_{2.5}$-*co*-$EVGE_{2.5})$	$Bn_2NP(EO_{23}$-*co*-$EVGE_{2.5})$	4600	1600	1.20
6	$Bn_2NP(EO_{30}$-*co*-$EVGE_{90})$	$Bn_2NP(EO_{31}$-*co*-$EVGE_{80})$	13200	4000	1.20
7	$Bn_2NP(EO_2$-*co*-$EVGE_{20})$	$Bn_2NP(EO_2$-*co*-$EVGE_{15})$	2200	1600	1.15
8	$MeOP(EO_{114}$-*block*-$EVGE_{10})$	$MeOP(EO_{114}$-*block*-$EVGE_9)$	6300	4900	1.04
9	$Bn_2NP(EVGE_{30})$	$Bn_2NP(EVGE_{27})$	3900	2300	1.22

[a] Determined from ^{1}H NMR (300 MHz, $CDCl_3$-d_1). [b] Determined by SEC-RI in DMF.

allowed to proceed for 12 h at 90 °C. Precipitation in diethyl ether resulted in the pure block copolymer.

Polymer Modification: Thiol−Ene-Functionalization. 0.2 g of the respective copolymer were dissolved in 10 mL DMF and 0.5 to 10 eq. of benzyl mercaptan and 0.75 eq. of azobis(isobutyronitrile) (AIBN) with respect to the absolute number of vinyl ether groups, were added. After three freeze−pump−thaw cycles the reaction mixture was heated to 75 °C and stirred for 12 h. The reaction mixture was then dialyzed against THF/MeOH, using benzoylated tubings (MWCO 1500 g/mol), for 2 days. ^{1}H NMR ($CDCl_3$-d_1, 300 MHz): δ (ppm) = 7.39−7.10 (initiator and arom. side group), 4.15−3.36 (polyether backbone), 3.70 (s, benzylic), 2.57 (CH_2S−benzyl).

Polymer Modification: Acetal-Formation. A 0.2 g sample of the respective copolymer and 10 equiv of benzyl alcohol were placed in a round-bottom flask, and 0.01 equiv of *p*-toluenesulfonic acid (in relation to the absolute number of vinyl-ether bonds) was added at 0 °C. After 2 h of stirring at room temperature, the reaction was stopped by the addition of triethylamine, and the mixture was dialyzed against THF (MWCO= 1500 g/mol) for 24−48 h, to remove the residual benzyl alcohol and PTSA as well as NEt_3. ^{1}H NMR ($CDCl_3$-d_1, 300 MHz): δ (ppm) = 7.36−7.18 (initiator and arom. side-group), 6.80 (d, ini.), 4.82 (m, acetal-H), 4.54 (dd, benzyl-H), 3.68−3.34 (polyether backbone), 2.54 (2H, t, $Bn_2NCH_2CH_2O$−), 1.33 (d, CH_3).

^{1}H NMR Kinetics. A 30 mg sample of the copolymer was dissolved in 0.5 mL of deuterated methanol, and the first spectrum (t = 0) was recorded immediately. Then the respective amount of PTSA were dissolved in 0.2 mL of deuterated methanol and added to the polymer solution via syringe. After rapid mixing, ^{1}H NMR spectra were taken every minute (compare Figure 4).

■ RESULTS AND DISCUSSION

A. Synthesis of P(EO-*co*-EVGE) Copolymers, Characterization, and Thermal Properties. *Synthesis.* The copolymerization of two monomers with highly diverging boiling points requires special reaction conditions. The key for random incorporation of glycidyl ether comonomers is polymerization at an elevated temperature, which was proven in previous works for other glycidyl ethers.[11,15,16,18] To level the different reactivities of the monomers, the reaction mixture was rapidly heated to 90 °C in a sealed system under vacuum. All polymerizations were carried out in THF and stirred for at least 48 h to guarantee full conversion of both monomers. *N,N*-di(*p*-methoxy-benzyl)-2-amino ethanol and *N,N*-di(benzyl)-2-amino ethanol were used as the respective initiators, since they allow the facile determination of the molecular weight via ^{1}H NMR. The aromatic signals of the resulting end group do not interfere with other signals in the spectrum and therefore permit reliable integration of the ^{1}H NMR spectra for molecular weight determination. In addition, the protective groups can be removed to regenerate a primary amino group in the α-position of the polymer chain. The corresponding initiator was deprotonated with 0.9 equiv of $CsOH \cdot H_2O$, and the evolving water was azeotropically removed under vacuum in the presence of benzene. As the vinyl ether groups are highly reactive and unstable toward acidic media, the resulting copolymers were either purified by dialysis or precipitation in diethyl ether (for low EVGE-content, compare Experimental Section). Stirring the polymers with acidic ion-exchange resin to reprotonate the active species and to remove residual Cs^+ ions leads to the deprotected polymer with $-CH_2OCH_2CH_2OH$ side chains and a similar structure as linear poly(glycerol); thus, the vinyl ether side chain can also be regarded as an efficient protective group for hydroxyl groups in the AROP. It should also be mentioned here, that the use of acidic media in combination with heat and low pressure can result in cross-linked products for this system.

The EVGE comonomer content has been varied in a systematic manner from 5% to 100%, and Table 1 summarizes the results for the series of copolymers that were prepared in this study with respect to molecular weights and polydispersities. From a comparison of the composition of the monomer feed and the copolymer composition it can clearly be stated that the monomer feed corresponds to the incorporated EO/EVGE-ratio, as determined by ^{1}H NMR spectroscopy. The copolymers showed good water solubility up to 25% EVGE-content at room temperature, which is crucial for biomedical applications. A typical spectrum of a water-soluble copolymer in D_2O is displayed in Figure 1.

The resonances a, b, and c correspond to the vinyl ether groups, and by integration of these signals and comparison to the polyether backbone (3.18−3.79 ppm) and the aromatic end group signals (6.78−7.25 ppm) the copolymer composition can be calculated. The structural parameters given in Table 1 have been determined using ^{1}H NMR in $CDCl_3$-d_1 (additional ^{1}H and ^{13}C NMR spectra can be found in the Supporting Information)

The molecular weight distributions obtained from size exclusion chromatography (SEC) measurements (in DMF with PEG standards) were in the range of M_w/M_n= 1.06 to 1.22, as expected for oxyanionic polymerization. The resulting monomodal SEC traces are given in the Supporting Information (Figure S1). The deviation of the molecular weights obtained from NMR and SEC can be explained by the presence of the side-chains, since their mass does not contribute to the overall hydrodynamic radius in the same manner as an increase of the degree of polymerization does, and SEC was calibrated with PEG. Furthermore, incorporation of EVGE units leads to more hydrophobic copolymers, which changes the hydrodynamic

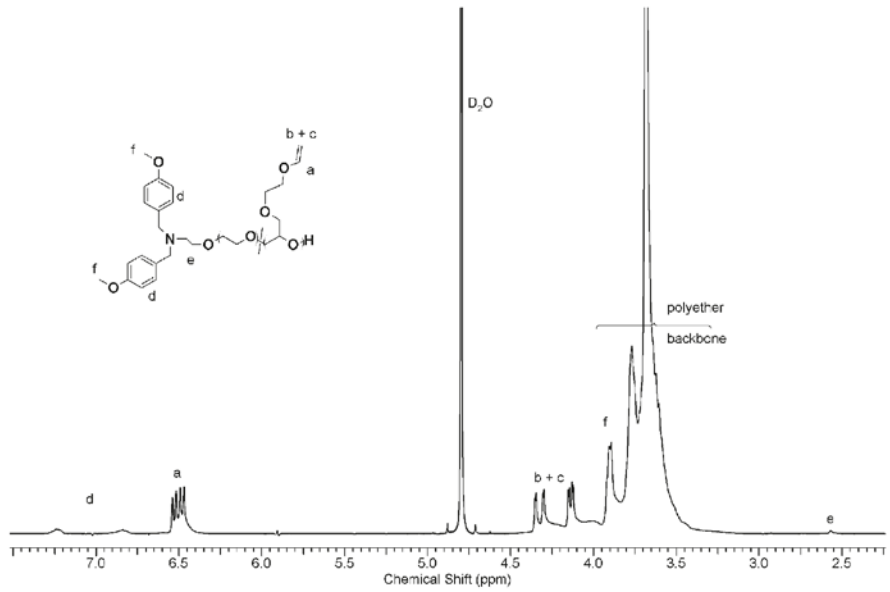

Figure 1. ^{1}H NMR spectra in D_2O-d_2 of P(EO_{120}-*co*-$EVGE_{30}$).

radius compared to the PEG-standards in DMF. The comparison reveals an average deviation factor of 2 for our setup.

^{13}C NMR Characterization (Triad Sequence Analysis). Random distribution of the vinyl ether side chains is essential for use of the EVGE/EO copolymers in any application. The influence of adjacent units on the methylene (and methine) carbon shift in ^{13}C NMR allows for the determination of the microstructure of copolymers. The resulting triad sequence distribution allows to investigate the distribution of two different monomers in the poly(ether) backbone and represents a well-established method for the characterization of copolymers based on propylene oxide and EO.[28] Recently, some other poly(ether)s have been investigated in this manner by our group (EEGE,[11] IGG (1,2-isopropylidene glyceryl glycidyl ether),[16] AGE and DBAG[17]). For all of these monomers and the novel monomer EVGE, this technique clearly evidence the random composition of such epoxide-based copolymers. Figure 2 displays the relevant region of the ^{13}C NMR spectra of several EO/EVGE copolymers, showing the resonances for the respective triads. For brevity, ethylene oxide units are referred to as "E", while EVGE units are abbreviated with "V". Both units have two different carbon atoms (a and b or a′ and b′), which are shifted in dependence of the adjacent monomer units.

In the ^{13}C NMR spectrum of all different copolymers (Figure 2), two regions can be analyzed to determine the distribution of the comonomers via triad analysis: (i) from 69 to 72 ppm and (ii) from 77 to 79 ppm, which stem from the carbon resonances of the polyether backbone. With the block copolymer (8% EVGE) in hand, all signals corresponding to the side group of EVGE (marked with I, II, and III) and the methine signal (cf. Figure 2B) can be unequivocally assigned. In addition, the signals of the methylene carbons (a and b) of the EO triads, which are marked with EEE, can be clearly identified. As expected, the spectra of the random copolymers differ significantly from the block copolymer MeOP-(EO_{114}-*block*-$EVGE_9$). With increasing EVGE-content several new resonances in the area of the side groups appear, but in addition new signals occur in the regions marked in gray in Figure 2A. These resonances overlap with the side group signals, rendering quantification difficult. However, from simulated ^{13}C NMR spectra (performed with ChemDraw Ultra 10.0), the triads can be assigned to the respective regions marked in gray. The signals in these regions increase steadily up to 65% EVGE incorporation, while the EEE-triad decreases to the same extent. In the spectrum with 88% EVGE, the signals of the EEE-triad vanish completely, in line with expectation.

Figure 2B gives a zoom into the area for the methine carbons of EVGE. In the case of the block copolymer, the methine-signal of the EVGE-unit (b′) is detected as a single signal (Figure 2B, bottom), which can be assigned to the VVV-triad of the PEVGE copolymer. In the case of the random copolymer with only 5% EVGE, the most probable environment for one EVGE unit are two EO units (EVE-triad), and the only signal which appears in the respective region can be assigned to this triad. With increasing incorporation of EVGE, other combinations become likely and at least two other signals appear at 78 ppm. The spectrum of $Bn_2NP(EO_2$-*co*-$EVGE_{15})$ (entry 8, Table 1) with 88% EVGE-content exhibits one major signal at the same position as it can be found in the block copolymer, which is again assigned to the VVV triad. The strongest evidence can be found by direct comparison of the two copolymers with approximately the same EVGE incorporation (8—9%), but varying internal structure. While in the block copolymer only four carbon resonances between 72 and 68 ppm are detected, the random copolymer exhibits a considerably more complicated spectrum. The occurrence of triad-signals confirms the random comonomer distribution.

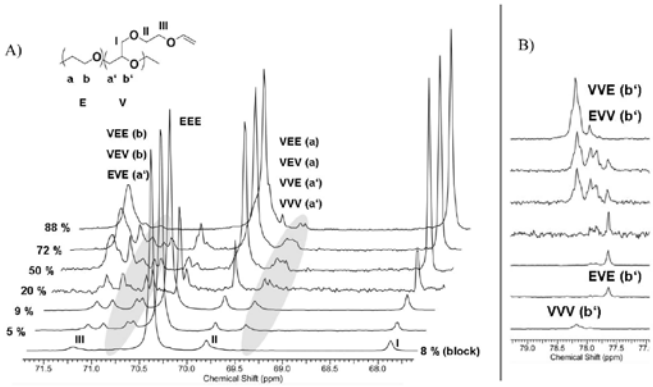

Figure 2. Typical ^{13}C NMR spectra in DMSO-d_6 of P(EO-*co*-EVGE) copolymers with varying EVGE fraction (in %), and a block copolymer (bottom) from (A) 67 to 72 ppm and (B) 77 to 79 ppm.

This result also is in line with previous works on other glycidyl ether copolymerizations with EO.[11,15−17]

Thermal Behavior. Characterization of the thermal properties was carried out via differential scanning calorimetry (DSC, heating rate 10 K/min). PEG with a molecular weight of 600 g/mol and higher is a crystalline polymer with a melting temperature, which is strongly dependent on the molecular weight of the polymer. PEG-600 has a melting range of 17−22 °C,[30] and with increasing M_w the T_m increases steadily until a maximum of 65 °C[29] is reached. PEVGE, on the other hand, exhibits an amorphous character and a low T_g (−63 °C, sample 9, Table 1). Incorporation of EVGE-units into the PEG-backbone leads to obvious morphology changes, as the copolymers are obtained as (i) white powder for 5% EVGE incorporation, (ii) sticky solid (at 10% EVGE-incorporation), and (iii) viscous liquids (with more than 25% EVGE incorporated). DSC measurements demonstrate that the polymers with a low content of EVGE (5, 10%) contain a crystalline fraction and show a melting point and related melting enthalpies (compare Table 2). As the number of EVGE monomer units increases, the crystalline domains disappear, and no melting point can be detected via DSC. On the basis of the assumption that the distribution of the EVGE units is completely random, the average number of adjacent EO units is 17 in the case of copolymer **1** and 10 in the case of copolymer **2**. The average length of homo-PEG units that is required to obtain a crystalline homopolymer is 13 (this corresponds to PEG-600).[30] Thus, the thermal characteristics reflect the random copolymer structure. The glass transition temperature of the copolymers, on the other hand, decreases only slightly, from −55 °C, to a T_g of −60 °C with increasing amount of EVGE. While a T_g of −55 °C (copolymer 1) can clearly be ascribed to the PEG-domains, the final T_g of copolymer 7 (88% EVGE) corresponds to the PEVGE nature, since the pure homopolymer of EVGE exhibits a T_g of −63 °C. The slight variation of the T_g can be ascribed to differing molecular weights.

Again, a block copolymer PEO-*b*-PEVGE was used to compare two polymers with similar EVGE content, but different structure. Comparing polymer **2** with polymer **8** (both with approximately 8−9% EVGE) clearly shows the presence of a crystalline fraction. However, the melting points differ strongly and the melting enthalpy in the random copolymer is reduced,

Table 2. Thermal Properties of Poly(ethylene glycol-*co*-ethoxy vinyl glycidyl ether) with Varying Amounts of EVGE Incorporated

no.	polymer composition	EVGE %	T_g[a]/°C	T_m[b]/°C	ΔH[c]/J/g
1	$MeOBn_2NP(EO_{104}$-*co*-$EVGE_6)$	5	−55	34	74
2	$MeOBn_2NP(EO_{115}$-*co*-$EVGE_{11})$	9	−59	16	47
3	$MeOBn_2NP(EO_{120}$-*co*-$EVGE_{30})$	20	−58	-	-
4	$MeOBn_2NP(EO_{89}$-*co*-$EVGE_{30})$	25	−58	-	-
5	$Bn_2NP(EO_{23}$-*co*-$EVGE_{25})$	52	−57	-	-
6	$Bn_2NP(EO_{31}$-*co*-$EVGE_{80})$	72	−60	-	-
7	$Bn_2NP(EO_2$-*co*-$EVGE_{15})$	88	−60	-	-
8	$MeOP(EO_{114}$-*block*-$EVGE_9)$	8	−55	54	103
9	$MeOBn_2NP(EVGE_{27})$	100	−63	-	-
10	mPEG-5000	0	*d*	61	175

[a] Glass transition temperature. Estimated error = 3 °C. [b] Melting temperature T_m: in °C. Estimated error = 3 °C. [c] Melting enthalpy determined by integration of the area under the melting peak. [d] Not detectable in this setup.

since the crystalline order is impeded by the presence of the comonomer, as expected. In summary, thermal properties mirror the random incorporation of EVGE into the polymer backbone.

B. "Click" Type Functionalization of the EVGE-Copolymers. Two different types of high-yield transformations have been studied that capitalize on the peculiar reactivity of the vinyl ether side chains of the EVGE comonomer units (Scheme 3).

Thiol−Ene Reaction. The functionalization of double-bond carrying polymers by thiol−ene "click" reactions has been studied intensively by several groups.[31−34] A major issue which has to be considered are undesired cross-linking reactions between the double bonds along the backbone. In the case of the thiol−ene reaction these can be successfully suppressed by using an excess of the thiol-containing component in the reaction mixture. This necessitates subsequent purification (i.e., dialysis) of the polymers to remove residual thiol. The term "click-reaction", with respect to polymer modification reactions has recently been subject of an intense discussion.[35] The general requirements of click reactions are high (close to complete) conversion, facile reaction conditions with easily available starting materials, preferably with no solvent involved, and

a simple isolation procedure. This general concept was expanded by the authors by introducing the concept of equimolarity, when a simple work-up procedure, such as precipitation, is not possible. This would imply that thiol−ene reactions are no "click-reactions" when employed for polymer modification. However, due to the stability of the vinyl ether radical, no cross-linking of the polymer chains occurs. This finding is in good agreement with prior reports on radical polymerization of vinyl ethers,[36] which only undergo copolymerization in the presence of a second vinyl monomer with electron withdrawing groups[37,38] or by the introduction of electron acceptors in proximity to the vinyl ether moiety.[39]

In principle, the Markovnikov as well as the anti-Markovnikov addition of the thiol-component is possible, but fundamental studies on thiol−ene reactions involving vinyl ethers have shown that due to the prealignment of the molecules by the oxygen−hydrogen interaction the anti-Markovnikov product is clearly favored over the Markovnikov product, leading to more uniform products compared to allyl-systems.[40] In addition, it should be mentioned that vinyl ethers do not exhibit double bond isomerization, which can be found for the allyl analogues.[41,20]

Benzyl mercaptan was chosen as a model compound, since it allows the facile assignment of the relevant resonances in ^{1}H NMR spectroscopy. The reaction was carried out overnight in DMF at 75 °C and after work-up by dialysis (to remove residual DMF) the successful transformation of the vinyl ether can be observed by the (partial) disappearance of the resonances at 6.48, 4.16, and 3.95 ppm, while new resonances are detected due to formation of the thio ether structure. These are, e.g., for mercaptobenzyl alcohol in the aromatic region (c 7.34 ppm), at 3.70 (deriving from the benzylic protons), and at 2.57 ppm - (corresponding to CH_2 adjacent to the thioether bond, Figure 3). The comparison of the thio ether signals with the poly(ether) backbone and the initial amount of vinyl ether side chains allows

Scheme 3. Polymer Modification Reactions Employing (i) the Thiol−Ene Reaction with thiols and (ii) Acetal Formation with Alcohols

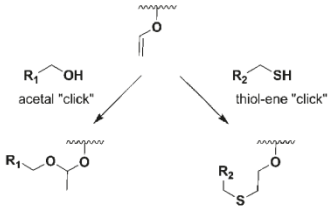

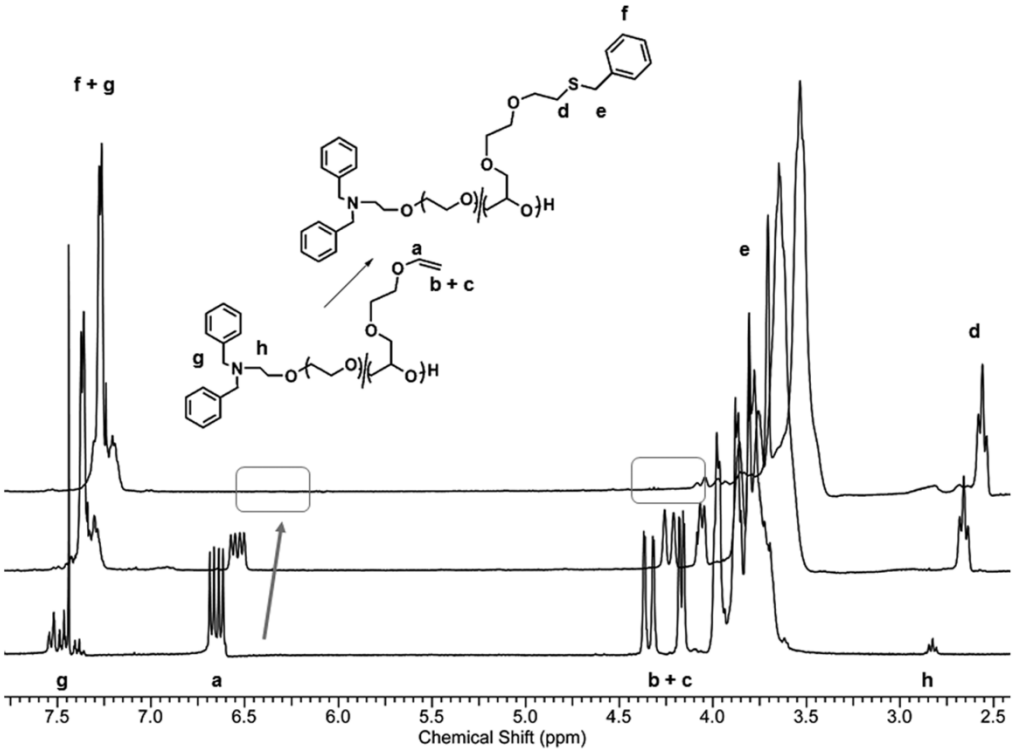

Figure 3. Copolymer **5** in $CDCl_3$-d_1 ($Bn_2P(EO_{23}$-*co*-$EVGE_{25})$) before and after the thiol−ene click reaction with 0.5 and 10 equiv of added thiol (scale bar corresponds to the top spectrum).

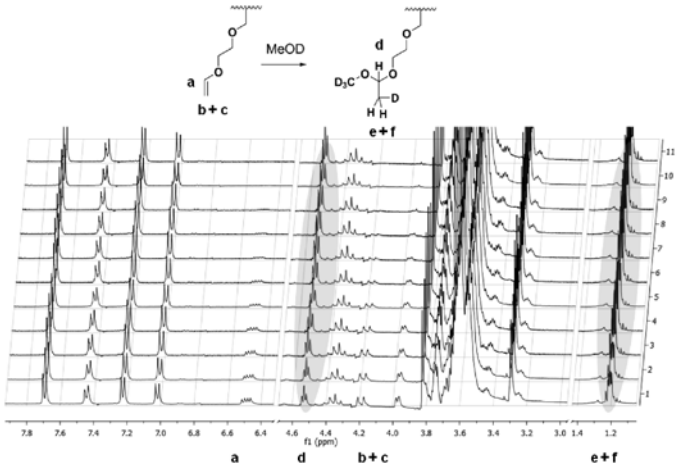

Figure 4. Reaction of copolymer **1** with MeOD-d_4 (4.92 and 3.31 ppm), in the presence of PTSA (7.75, 7.28, and 2.41 ppm). For clarity only, the relevant part of the spectrum is shown, additional spectra with the whole ppm range can be found in the Supporting Information.

to determine the conversion of the vinyl ether moieties. This demonstrates that attachment of small molecules to the vinyl ether side chains is possible and can in principle be employed for any compound bearing a thiol moiety. Since cross-linking reactions do not occur, it is possible to attach less than one equivalent of the thiol component and this implies that (i) this post polymerization reaction is a real "click reaction" and (ii) the remaining double bonds can be used for further functionalization reactions (compare Figure S7, Supporting Information), which is highly interesting with respect to future applications.

Acetal-Formation as a Click-Type Polymer Modification. The general requirements for click reactions and the currently considered criteria for polymer modification reactions have been discussed in the previous section. The first three criteria (high conversion, facile reaction conditions, easily available starting materials) are all met by the acetal formation reaction by addition of an alcohol to a vinyl ether. However, the criteria equimolarity, facile work-up procedure as well as stable end-products, are not fulfilled. The formation of acetals based on vinyl ethers and alcohols is generally fast and proceeds selectively in the absence of water. In the case of low molecular weight compounds, the acetal bond is generated under acidic catalysis from the respective alcohol and the vinyl ether within several minutes without any side-products. Compared to other polymer modification reactions this method allows the facile, rapid and quantitative attachment of alcohols via a pH-labile acetal bond.

Benzyl alcohol was chosen as a model compound and PTSA was added as a catalyst. The reaction was monitored via ^{1}H NMR, following the disappearance of the vinyl ether signals (compare Supporting Information, Figure S5, parts a, b, and c) and the emerging signals at 4.82 (d, acetal), 4.54 (e, benzyl), and 1.33 (f, CH_3) ppm. From a comparison of the acetalic proton and the CH_3-group integrals to the initial amount of vinyl ether side chains, it can clearly be concluded that this reaction is quantitative and no detectable side reactions occur. Removal of the acidic catalyst was most efficient via dialysis against THF/NEt_3. The precipitation of the product in diethyl ether does not guarantee complete removal of the *p*-toluenesulfonic acid (PTSA) and, moreover, cross-linking by trans-acetalization can occur (compare above).

Since the transformation of the vinyl ether groups was found to be very fast, the reaction was investigated by online ^{1}H NMR kinetics (Figure 4). For the respective measurements, the polymer was dissolved in deuterated methanol, which served both as a solvent and as a reactant. The catalyst was dissolved in MeOD separately. After addition of the acid to the polymer solution NMR-spectra were measured in intervals of 30 s.

Since the lock and shim process requires approximately 3−5 min, the resonance for the acetal proton is already present in the first spectrum. The corresponding signal can be discerned at 4.59 ppm (d) and the corresponding methyl-group signal at 1.26 ppm (e + f). Nevertheless, the reaction can be followed by monitoring the disappearance of the vinyl ether signals at 6.54 (a), 4.26 and 2.04 ppm (b + c). The reaction reached 99% conversion of the vinyl ether bonds within 10 min. Note: Even in the presence of trace amounts of water, which is due to the crystallization water of PTSA (not dried prior to the experiment) no cleavage of the acetal bond is found. If the acetal had been opened, the respective resonances for acetaldehyde around 9 ppm (aldehyde) and 2 ppm (methyl-group) would have been detectable. Here, acetal formation at the multifunctional PEG copolymers can be described by first order kinetics, since one of the reagents serves as the solvent and thus the concentration is constant throughout the reaction. A plot of converted vinyl ether groups versus reaction time (shown in Figure 5) supports this assumption.

The first spectrum from the NMR experiment was obtained at already 61% conversion after approximately 3 min. Nevertheless, it is possible to assign these values with an exponential fit and estimate the half-life time of the vinyl ether moieties to ca. 80 s. This value depends on the reaction conditions and has to be treated with care, since every alcohol will show a different behavior and methanol was used as a solvent in this case. In addition, both the concentration of the catalyst and of the alcohol

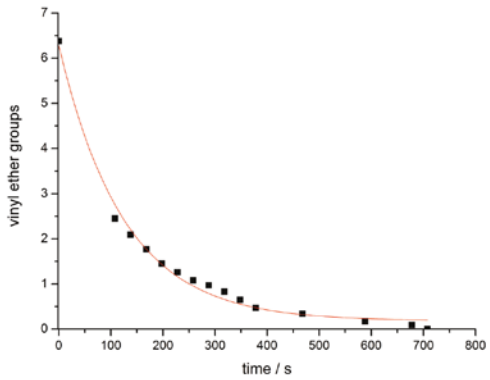

Figure 5. Conversion of vinyl ether groups versus time for the reaction of copolymer **1** with MeOD-d_4. Key: black squares, measured values; red line, exponential fit (Origin 7).

represent key parameters for this reaction. Additional measurements were carried out, and the respective spectra are given in the Supporting Information. A comparison of the two kinetics conducted shows that reducing the amount of catalyst/vinyl ether ratio from 1:2.5 to 1:20 prolongs the half-life time from 80 to 180 s. The reaction time and conditions will have to be adjusted according to the respective molecule. Further work on a broad range of alcohols is currently in progress.

In summary, these results clearly evidence that the acetal formation at the polymer backbone is a very rapid and selective transformation for polymer modification. In direct comparison with other polymer modification methods, it is facile, leads to high conversion, can be used to attach a variety of molecules bearing a hydroxyl functionality and is therefore as valuable as the widespread thiol—ene modification. It was also proven that in the presence of diluted acids the attached molecules can be released. This allows the attachment of drugs or biomolecules and the triggered release of them in slightly acidic media, as present, e.g., in lysosomes. The use of these materials in biomedical applications is subject of ongoing studies in our group.

CONCLUSION

The importance of functional and biocompatible polymers has increased steadily during the past decade. The materials are obtained either by radical polymerization techniques or end group modification of commercial PEG. Another, straightforward strategy for introducing a broad range of functionalities into the biocompatible PEG backbone is the direct copolymerization of functional comonomers with EO.[42] In this work, we have introduced the novel monomer EVGE with a vinyl ether group, which copolymerizes with EO in a controlled and random manner. The random distribution of the EVGE comonomer units in the PEG backbone was proven by NMR and DSC measurements. PEG copolymers with up to 25% vinylether content are soluble in aqueous solution, which opens manifold possibilities for biomedical applications.

The PEG-based multifunctional polymers can be derivatized in different ways: (i) by reaction with a thiol a side-chain polythioether is generated and (ii) the reaction with any alcohol results in a side-chain polyacetal. This has been demonstrated by different model reactions and by kinetic NMR measurements. The first transformation results in the stable, covalent attachment of thiols to the PEG-based copolymer, avoiding cross-linking, which represents a hard to exclude side reaction for comparable allyl bonds in poly(allyl glycidyl ether).[20,41] Thus, this feature represents a significant advantage over the allyl glycidyl ether (AGE) monomer which has been reported to permit sequential "click" reactions to multifunctional polymers in previous studies.

In addition, the rapid acetal formation (ii), which has, to the best of our knowledge not been applied in a postpolymerization protocol, is highly interesting with respect to polymer therapeutics or hydrogels, due to the facile release of the alcohol in acidic media. In ongoing studies the suitability of these postpolymerization reactions with respect to the attachment of proteins or low molecular weight drugs is investigated and will be presented in near future.

ASSOCIATED CONTENT

Supporting Information. Additional characterization data (Figures S1—S7). This material is available free of charge via the Internet at http://pubs.acs.org.

AUTHOR INFORMATION

Corresponding Author

*E-mail: (H.F.) hfrey@uni-mainz.de; (F.W.) frederik.wurm@epfl.ch.

ACKNOWLEDGMENT

The authors thank Alina Mohr for technical assistance. C.M. is a recipient of a fellowship through funding of the Excellence Initiative (DFG/GSC 266). C.D. is grateful to MPGC for a scholarship and financial support. B.O. acknowledges the Fonds der Chemischen Industrie for a scholarship. F.W. thanks the Alexander-von-Humboldt foundation for a fellowship. H.F. acknowledges the SFB 625 of the DFG (German Science Foundation) for valuable support.

REFERENCES

(1) Harris, J. M. *Poly(ethylene glycol) Chemistry: Biotechnical and Biomedical Applications*; Plenum Press: New York, 1992.
(2) Harris, J. M.; Zalipsky, S., *Poly(ethylene glycol) - Chemistry and Biological Applications*. American Chemical Society: Washington, DC, 1997.
(3) Abuchowski, A.; Vanes, T.; Palczuk, N. C.; Davis, F. F. *J. Biol. Chem.* **1977**, *252*, 3578–3581.
(4) Davis, F. F. *Adv. Drug Delivery Rev.* **2002**, *54*, 457–458.
(5) Fitton, A.; Hill, J.; Jane, D.; Miller, R. *Synthesis* **1987**, 1140–1142.
(6) Taton, D.; Le Borgne, A.; Sepulchre, M.; Spassky, N. *Macromol. Chem. Phys.* **1994**, *195*, 139–148.
(7) Halacheva, S.; Rangelov, S.; Tsvetanov, C. *Macromolecules* **2006**, *39*, 6845–6852.
(8) Dworak, A.; Panchev, I.; Trzebicka, B.; Walach, W. *Macromol. Symp.* **2000**, *153*, 233–242.
(9) Pang, X.; Jing, R.; Huang, J. *Polymer* **2008**, *49*, 893–900.
(10) Yu, Z.; Li, P.; Huang, J. *J. Polym. Sci., Part A: Polym. Chem.* **2006**, *44*, 4361–4371.
(11) Mangold, C.; Wurm, F.; Obermeier, B.; Frey, H. *Macromol. Rapid Commun.* **2010**, *31*, 258–264.
(12) Dworak, A.; Baran, G.; Trzebicka, B.; Walach, W. *React. Funct. Polym.* **1999**, *42*, 31–36.

(13) Dimitrov, P.; Hasan, E.; Rangelov, S.; Trzebicka, B.; Dworak, A.; Tsvetanov, C. B. *Polymer* **2002**, *43*, 7171–7178.
(14) Wurm, F.; Räder, H. J.; Frey, H. *J. Am. Chem. Soc.* **2009**, *131*, 7954–7955.
(15) Wurm, F.; Kemmer-Jonas, U.; Frey, H. *Polym. Int.* **2009**, *58*, 989–995.
(16) Mangold, C.; Wurm, F.; Obermeier, B.; Frey, H. *Macromolecules* **2010**, *43*, 8511–8518.
(17) Obermeier, B.; Wurm, F.; Frey, H. *Macromolecules* **2010**, *43*, 2244–2251.
(18) Li, Z.; Chau, Y. *Bioconjugate Chem.* **2009**, *20*, 780–789.
(19) Gauthier, M. A.; Gibson, M. I.; Klok, H.-A. *Angew. Chem.* **2009**, *121*, 50–60.
(20) Obermeier, B.; Frey, H. *Bioconjugate Chem.* **2011**, *22*, 436–444.
(21) (a) Wurm, F.; Schüle, H.; Frey, H. *Macromolecules* **2008**, *41*, 9602–9611. (b) Sunder, A.; Türk, H.; Haag, R.; Frey, H. *Macromolecules* **2000**, *33*, 7682.
(22) Belozerov, L. E.; Stankevich, V. K.; Ezhova, L. N.; Balakhchi, G. K.; Trofimov, B. A. *Russ. J. Appl. Chem.* **1994**, *67*, 1231–1232.
(23) Annenkov, V. V.; Levina, A. S.; Danilovtseva, E. N.; Filina, E. A.; Mikhaleva, E. A.; Zarytova, V. F. *Russ. J. Bioorg. Chem.* **2006**, 32460–467.
(24) Ruckenstein, E.; Zhang, H. *Polym. Bull.* **2001**, *47*, 113–119.
(25) Wurm, F.; König, H. M.; Hilf, S.; Kilbinger, A. F. M. *J. Am. Chem. Soc.* **2008**, *130*, 5876–5877.
(26) (a) .Janus micelles from polyether block copolymers.Wurm, F.; Mangold, C.; Kilbinger, A. F. M. *Polym. Prepr. (Am. Chem. Soc., Div. Polym. Chem.)* , **2010**, *51* (1), 322—323. (b) Mangold, C.; Wurm, F.; Kilbinger, A. F. M. *Non-Conventional Functional Block Copolymers*; ACS Symposium Series 1066; American Chemical Society: Washington, DC, 2011; Chapter 8, pp 103—115.
(27) Vetvicka, D.; Hruby, M.; Hovorka, O.; Etrych, T.; Vetrik, M.; Kovar, L.; Kovar, M.; Ulbrich, K.; Rihova, B. *Bioconjugate Chem.* **2009**, *20*, 2090–2097.
(28) Hamaide, T.; Goux, A.; Llauro, M. F.; Spitz, R.; Guyot, A. *Angew. Makromol. Chem.* **1996**, *237*, 55–57.
(29) Mandelkern, L. *Chem. Rev.* **1956**, *56*, 903–958.
(30) Henning, T. *SOFW J.* **2001**, *127*, 28–35.
(31) Herczynska, L.; Lestel, L.; Boileau, S.; Chojnowski, J.; Polowinski, S. *Eur. Polym. J.* **1999**, *35*, 1115–1122.
(32) Gress, A.; Volkel, A.; Schlaad, H. *Macromolecules* **2007**, *40*, 7928–7933.
(33) Romani, F.; Passaglia, E.; Aglietto, M.; Ruggeri, G. *Macromol. Chem. Phys.* **1999**, *200*, 524–530.
(34) Passaglia, E.; Donati, F. *Polymer* **2007**, *48*, 35–42.
(35) Barner-Kowollik, C.; Du Prez, F. E.; Espeel, P.; Hawker, C. J.; Junkers, T.; Schlaad, H.; van Camp, W. *Angew. Chem., Int. Ed.* **2011**, *50*, 60–62.
(36) Eri Mishima, E.; Yamago, S. *Macromol. Rapid Commun.* **2011**, *32*, 893–898.
(37) Stille, J. K.; Chung, D. C. *Macromolecules* **1975**, *8*, 114–121.
(38) Meskini, A.; Raihane, M.; Ameduri, B. *Macromolecules* **2009**, *42*, 3532–3539.
(39) Lee, J.-Y.; Kim, M.-J.; Jin, M.-K.; Ahn, M.-R. *Bull. Korean Chem. Soc.* **1999**, *20*, 1355–1358.
(40) Lou, F.-W.; Xu, J.-M.; Liu, B.-K.; Wu, Q.; Pan, Q.; Lin, X.-F. *Tetrahedron Lett.* **2007**, *48*, 8815–8818.
(41) Koyama, Y.; Umehara, M.; Mizuno, A.; Itaba, M.; Yasukouchi, T.; Natsume, K.; Suginaka, A.; Watanabe, K. *Bioconjugate Chem.* **1996**, *7*, 298–301.
(42) Obermeier, B.; Wurm, F.; Mangold, C.; Frey, H. *Angew. Chem., Int. Ed.* **2011**, published on the web, DOI: 10.1002/anie.2011.00027.

A.3 Squaric Acid Mediated Synthesis and Biological Activity of a Library of Linear and Hyperbranched Poly(Glycerol)–Protein Conjugates

Frederik Wurm,[1] Carsten Dingels,[2] Holger Frey,[2] and Harm-Anton Klok[1]*

[1]École Polytechnique Fédérale de Lausanne (EPFL), Institut des Matériaux and Institut des Sciences et Ingénierie Chimiques, Laboratoire des Polymères, Bâtiment MXD, Station 12, CH-1015 Lausanne, Switzerland

[1]Department of Organic and Macromolecular Chemistry, Johannes Gutenberg-Universität Mainz, Duesbergweg 10-14; 55099 Mainz, Germany

Published in: *Biomacromolecules* **2012**, *13*, 1161.

BioMACROMOLECULES

Article

pubs.acs.org/Biomac

Squaric Acid Mediated Synthesis and Biological Activity of a Library of Linear and Hyperbranched Poly(Glycerol)−Protein Conjugates

Frederik Wurm,[†] Carsten Dingels,[‡] Holger Frey,[‡] and Harm-Anton Klok*[,†]

[†]École Polytechnique Fédérale de Lausanne (EPFL), Institut des Matériaux and Institut des Sciences et Ingénierie Chimiques, Laboratoire des Polymères, Bâtiment MXD, Station 12, CH-1015 Lausanne, Switzerland

[‡]Department of Organic and Macromolecular Chemistry, Johannes Gutenberg-Universität Mainz, Duesbergweg 10-14; 55099 Mainz, Germany

Supporting Information

ABSTRACT: Polymer−protein conjugates generated from side chain functional synthetic polymers are attractive because they can be easily further modified with, for example, labeling groups or targeting ligands. The residue specific modification of proteins with side chain functional synthetic polymers using the traditional coupling strategies may be compromised due to the nonorthogonality of the side-chain and chain-end functional groups of the synthetic polymer, which may lead to side reactions. This study explores the feasibility of the squaric acid diethyl ester mediated coupling as an amine selective, hydroxyl tolerant, and hydrolysis insensitive route for the preparation of side-chain functional, hydroxyl-containing, polymer−protein conjugates. The hydroxyl side chain functional polymers selected for this study are a library of amine end-functional, linear, midfunctional, hyperbranched, and linear-block-hyperbranched polyglycerol (PG) copolymers. These synthetic polymers have been used to prepare a diverse library of BSA and lysozyme polymer conjugates. In addition to exploring the scope and limitations of the squaric acid diethylester-mediated coupling strategy, the use of the library of polyglycerol copolymers also allows to systematically study the influence of molecular weight and architecture of the synthetic polymer on the biological activity of the protein. Comparison of the activity of PG−lysozyme conjugates generated from relatively low molecular weight PG copolymers did not reveal any obvious structure−activity relationships. Evaluation of the activity of conjugates composed of PG copolymers with molecular weights of 10000 or 20000 g/mol, however, indicated significantly higher activities of conjugates prepared from midfunctional synthetic polymers as compared to linear polymers of similar molecular weight.

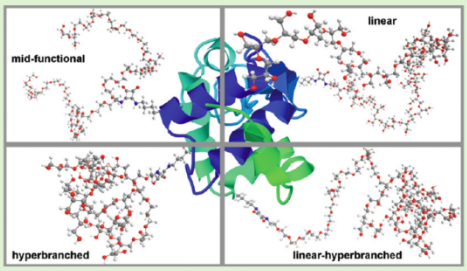

INTRODUCTION

In recent years, with the discovery of novel pharmaceutically active peptides and proteins, a novel field of human therapy is rapidly evolving based on complex biopolymers.[1] A drawback of protein-based "biotherapeutics" is their fast degradation in the human body by both the digestive system and the circulatory system, that is, they are rapidly removed by proteolytic digestion and renal excretion.[2,3] In the last decades, the covalent attachment of synthetic macromolecules has proven to be an effective strategy to improve protein stability, reduce immunogenicity, extend plasma half-life times, and increase solubility.[4]

Seminal work has been conducted in the 1970s by Davis and Abuchowski, who found that covalent attachment of poly(ethylene glycol) (PEG) to bovine serum albumin (BSA) and bovine liver catalase resulted in reduced immunogenicity and increased blood circulation times.[5,6] To date, among a variety of other water-soluble and biocompatible polymers, PEG is still the most frequently used for the modification of peptides and proteins. In more recent work, it has been demonstrated that the use of "branched" PEG-structures, that is, PEG derivatives with a single branching point bearing the protein-reactive group in the center of a linear polymer chain leads to improved circulation times as compared to conjugates based on linear PEG chains.[7] Today, several FDA-approved PEGylated proteins are used for the treatment of cancer, hepatitis C, anemia, and diabetes.[8,9] A commercial therapeutic for the treatment of hepatitis C ("PEGASYS, Roche") is available that relies on a midfunctional PEG coupled to interferon α-2a.[10]

Although it is a highly valuable concept, protein PEGylation also has several limitations: (i) linear PEG only possesses two functional groups at the polymer chain ends, which restricts the possibilities for further functionalization and the preparation of multiprotein conjugates, and (ii) PEGylation often leads to a loss of protein activity.[11] The development of strategies to overcome these limitations and that allow access to protein−polymer

Received: January 19, 2012
Revised: February 19, 2012
Published: March 1, 2012

conjugates with superior properties is a very topical and active field of research.

One approach to generate "PEG-like" polymers with a large number of functional groups is based on the controlled radical polymerization of appropriate side-chain functional (meth)-acrylates, such as 2-hydroxyethyl(meth)acrylate, poly(ethylene glycol)(meth)acrylate, or 2-hydroxypropylmethacrylamide.[12−14] These polymers can be conjugated to the peptide or protein of interest via a "grafting from" or a "grafting to" approach to the respective amino acid residues.[14,15] Another interesting class of PEG-like polymers, which, however, so far has been barely explored for the synthesis of protein–polymer conjugates, are polyglycerols (PGs).[16] PGs are attractive because they are biocompatible and nontoxic,[17,18] as well as more protein-resistant and thermally and oxidatively stable as compared to PEG.[19] PG can be obtained via ring-opening polymerization of glycidol or glycidyl ethers in a controlled manner.[18−22] Depending on the type of monomer used and the polymerization conditions applied, both linear and (hyper)branched PGs can be synthesized. This is attractive as it allows access to libraries of chemically identical but structurally different PG analogues, which may be valuable to investigate the influence of polymer architecture on the properties of polymer–protein conjugates.

In many instances, PEGylation is aimed at modifying amine groups of the peptide/protein of interest. Traditionally, site-selective modification of amine groups is accomplished by using, for example, *N*-hydroxysuccinimide (NHS), 4-nitrophenyl chloroformate, or similar end-functionalized PEG derivatives.[15,23] While these approaches work well for a large variety of synthetic polymers, they cannot be applied to side-chain (hydroxy) functional polymers such as PG, because the classical active esters are susceptible to concurrent transesterification and hydrolysis. Lysine-selective protein modification with PG (co)polymers requires protein-reactive groups that are tolerant toward hydroxy groups and have extended hydrolysis half-lives. One example of an amine-reactive, hydroxy-tolerant activation group is the thiazolidine-2-thione group. This activating group, which has been successfully used by Tao et al. for the synthesis of PHPMA–protein conjugates,[12] has a hydrolysis half-life of several hours as compared to minutes for NHS esters.[24,25] The thiazolidine-2-thione group, however, has been reported to undergo side reactions with thiol groups.[25] Another potentially interesting class of reagents to allow amine-selective modification of proteins are squaric acid dialkyl esters, such as squaric acid diethyl ester (SADE). While SADE has found widespread use for glycosylation[26−28] or other coupling reactions between low molecular weight compounds,[29,30] it has not been explored for the preparation of synthetic polymer–protein conjugates. Squaric acid dialkyl esters react selectively with amine groups at pH 7 and room temperature without interference of transesterification or hydrolysis reactions.[30] Due to the lower reactivity of the reaction product as compared to the starting material, only squaric acid ester monoamides are formed, which can be isolated and characterized. Under more basic reaction conditions (pH 9), the ester amide intermediates can then be conjugated to another amine functional compound in a second amine-selective and hydroxy-tolerant reaction,[26] which makes the squaric acid mediated coupling a potentially attractive approach to synthesize PG and other side chain functional (co)polymer–protein conjugates.

In a recent study, we have explored the one-step activation of amino poly(ethylene glycol)s (PEGs) with squaric acid diethyl ester and investigated the reactivity and chemoselectivity of these PEG derivatives toward the amine-selective modification of α-amino acids and proteins.[31] The present study is aimed at further exploring and expanding the scope of this approach and (i) explores the feasibility of the squaric acid mediated coupling for the synthesis of side-chain functional synthetic polymer (specifically, linear and hyperbranched polyglycerol)–protein conjugates; (ii) uses the versatility of the glycidol ring-opening polymerization to generate an architecturally diverse library of PG–protein conjugates; and (iii) evaluates the biological activity of these polymer–protein hybrids (Scheme 1).

Scheme 1. (Top) Squaric Acid Mediated Coupling of PG (Co)Polymers to Proteins; (Bottom) Schematic Representation of the Architecturally Different Protein–Polymer Conjugates Prepared and Investigated in This Study

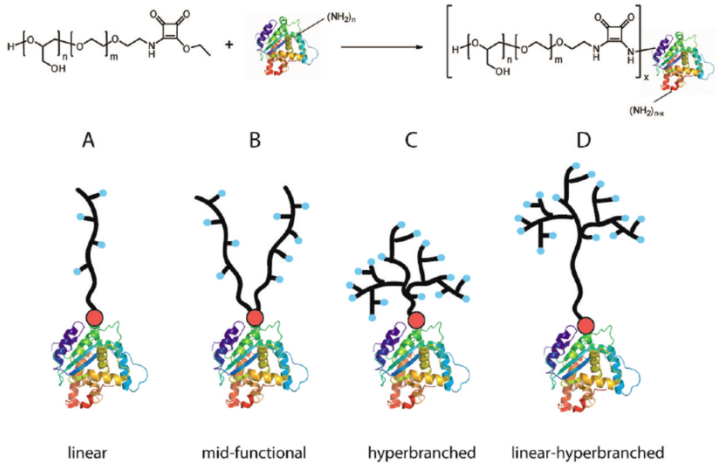

EXPERIMENTAL SECTION

Materials. Ethylene oxide (Fluka 99%), glycidol (Acros 96%), cesium hydroxide monohydrate (99.95% Aldrich), ethyl vinyl ether (98% Aldrich), ethanolamine (99% Acros), serinol (2-amino-1,3-propanediol, 98%, Acros), *p*-methoxybenzylalcohol (98% Acros), phosphorus tribromide (phosphorus tribromide, 1.0 M solution in dichloromethane, AcroSeal), potassium carbonate (99+% Acros), palladium on activated charcoal (10%Pd, Aldrich), benzene (99% Acros), lysozyme (90%), bovine serum albumin (98%), *Micrococcus lysodeikticus* (lyophilized cells), and ninhydrin reagent were purchased from Aldrich and used as received. Squaric acid diethyl ester was purchased from VWR and used as received. α-Amino-ω-methoxy-poly(ethylene glycol)s were purchased from IRIS Biotech and used as received. DMSO-d_6 and $CDCl_3$ were purchased from Deutero GmbH. Ethoxy ethyl glycidyl ether was prepared as described by Fitton et al.,[32] dried over CaH_2, and freshly distilled before use. Ethylene oxide and glycidol were distilled from CaH_2 before use. *p*-Methoxybenzylbromide was synthesized as described previously.[33] All other reagents and solvents were purchased from Aldrich and used as received, if not otherwise mentioned.

Methods. ^{1}H NMR spectra were recorded using either a Bruker AC 300 (300 MHz spectra) or a Bruker AMX 400 instrument (400 MHz spectra). All spectra were referenced internally to the residual proton signals of the deuterated solvent. SEC analysis in water was carried out on a Viscotek TDA 300 instrument equipped with a MetaChem degasser, a Visotek VE 1121 SEC solvent pump, and a VE 5200 SEC autosampler. A 9:1 mixture of phosphate buffer (0.1 M, pH = 6.5)/methanol was used as a mobile phase. Samples were eluted at 25 °C and at a flow rate of 0.5 mL·min^{-1} over Shodex OHpak 804 and 805 columns. Sample elution was monitored using a triple detection setup and absolute molecular weights were determined via light scattering. For SEC measurements in DMF (containing 0.25 g/L of lithium bromide as an additive), an Agilent 1100 Series instrument equipped with a PSS HEMA column (106/105/104 g/mol), a UV (275 nm), and a RI detector was used. Calibration was carried out using poly(ethylene oxide) standards provided by Polymer Standards Service. MALDI-ToF mass spectrometry was performed on a Shimadzu Axima CFR MALDI-ToF MS mass spectrometer equipped with a nitrogen laser delivering 3 ns laser pulses at 337 nm. α-Cyano-hydroxycinnamic acid (CHCA) was used as a matrix and potassium triflate was added to facilitate ionization of polymer samples. SDS-PAGE was carried out with 4−20% Tris-HCl gels (Biorad, 0.75 mm, 10 well). Reverse phase HPLC was performed on a Grace Vydac C4-protein column using a modular setup from JASCO equipped with a quaternary gradient pump PU-2089plus, autosampler AS-2055plus, UV-detector UV-2075plus, and a column oven (25 °C) CO-2060plus. Gradient elution was carried out at a flow rate of 0.5 mL/min with a mobile phase A (99.9% H_2O, 0.01% TFA) and a mobile phase B (99.9% acetonitrile, 0.01% TFA). The gradient sequence (B) was 5−100% from 0−60 min, 100% from 60−80 min, 100−5% from 80−110 min. Sample elution was monitored at a UV absorbance of 280 nm. Ninhydrin test: A solution of the analyte was dropped onto a silica gel TLC plate, dipped into the solution, and dried with a heatgun; a positive test was indicated by a color change.

Procedures. *N,N-Di(p-methoxybenzyl)aminoethanol (1).* Freshly distilled *p*-methoxybenzyl bromide (7.5 g, 37.5 mmol), ethanolamine (1.15 g, 18.5 mmol), and potassium carbonate (7 g, 50 mmol) were mixed in about 80 mL of DMF and refluxed for 24 h. After the reaction mixture was allowed to cool to room temperature, the solution was filtered and diethyl ether (ca. 200 mL) was added. The organic phase was then washed with water and a saturated $NaHCO_3$ solution and dried with $MgSO_4$. The organic phase was dried and concentrated in vacuo to afford a highly viscous liquid. The crude product was purified by column chromatography using ethyl acetate and petrol ether (6:4) as eluent. Yield: 4.5 g (80%). ^{1}H NMR (300 MHz, DMSO): δ (ppm) 7.26−6.85 (8H, aromatic), 4.33 (t, J = 6 Hz 1H, OH), 3.72 (s, 6H, OCH_3), 3.47 (s, 4H, NCH_2Ph), 3.44 (t, J = 6 Hz, 2H, CH_2OH), 2.65 (t, J = 6 Hz, 2H, NCH_2). ESI-MS: 302.5 (MH^+), 324.8 (MNa^+).

N,N-Di(p-methoxybenzyl)serinol (2). Compound **2** was synthesized as above with the following ratios: serinol (1.13 g, 12.4 mmol), *p*-methoxybenzyl bromide (5.03 g, 25 mmol), potassium carbonate (4.8 g, 35 mmol), and 80 mL DMF. Yield: (3.1 g, 78%). ^{1}H NMR (300 MHz, DMSO): δ (ppm) 7.23−6.84 (8H, aromatic), 4.28 (br, 2H, OH), 3.70 (s, 6H, OCH_3), 3.62 (s, 4H, NCH_2Ph), 3.54 (m, 2H, CH_2OH), 2.66 (t, J = 6 Hz, 1H, NCH). ESI-MS: 322.8 (MH^+).

General Procedure for the Synthesis of Linear Poly(ethoxy ethyl glycidyl ether) (Co)Polymers. The appropriate initiator (ca. 100 mg) was placed in a Schlenk flask and dissolved in benzene (ca. 5 mL) under an argon atmosphere. Cesium hydroxide monohydrate was introduced to achieve a degree of deprotonation of 50%. The mixture was stirred at 60 °C over a period of 45 min and then heated to 80−90 °C in vacuo for 2 h to remove the formed water and benzene azeotropically. In a separate setup, first dry THF, and the respective monomers (ethylene oxide or ethoxy ethyl glycidyl ether (EEGE), predried over CaH_2) were distilled into a Schlenk flask equipped with a stir bar, a Teflon tap, and a rubber septum. The flask was closed under vacuum and the cesium salt of the initiator was added dissolved in dry DMSO to afford about a 10 wt % solution of the monomer(s) in a 9:1 mixture of THF and DMSO. The reaction mixture was directly heated to 70 °C in static vacuo over a period of 20 h and quenched by the addition of about 20 mL of methanol and 0.5 g acidic ion-exchange resin. After that, the solution was filtered, concentrated, and precipitated into diethyl ether/acetone (70:30) first and subsequently in pure diethyl ether to yield the final polymer after drying in a yield typically between 90% to quantitative. Note: PEEGE-homopolymers were filtered and precipitated twice into water. ^{1}H NMR (for PEG-*co*-PEEGE and PEG-*b*-PEEGE in DMSO-d_6, 300 MHz): 7.22−6.82 (8H, aromatic signals from the initiator), 4.64 (br s, acetal H), 3.69 (s, 6H, MeO-C_6H_4-), 3.64−3.18 (br, -CH_2-$CH_{(2)}$O- (backbone), and -O-CH_2-CH_3 (side chain)), 1.25−0.9 (-O-CH_2-CH_3 and -CH-CH_3).

Removal of the Acetal Protective Groups. The PEEGE-containing (co)polymer was dissolved in methanol (ca. 20 wt %) and the same volume of 1 N HCl was added. The mixture was stirred at room temperature overnight, concentrated in vacuo and precipitated three times into diethyl ether. The isolated yields ranged between 80 and 90% in all cases. ^{1}H NMR (DMSO-d_6, 300 MHz): 10.57 (s, 1H, *H*-N^+R_3), 7.54−6.97 (8H, aromatic signals from the initiator), 4.27 (br s, OH, intensity and chemical shift can vary), 3.75 (s, 6H, MeO-C_6H_4-), 3.64−3.18 (br, -CH_2-$CH_{(2)}$O- (backbone)).

Hypergrafting of Glycidol. The linear precursor polymer was dissolved (or suspended) in benzene at a concentration of about 20 wt %. Cesium hydroxide monohydrate was added (to achieve a degree of deprotonation of 20%) and the mixture was allowed to react at 60 °C for 60 min. The formed water and benzene were removed azeotropically at 90 °C over a period of 90 min. After that, the activated macroinitiator was suspended in dry diglyme (ca. 20 wt %), heated to 90 °C, and freshly distilled glycidol (amount depends on the targeted degree of polymerization) in dry diglyme was added slowly with a syringe pump over a period of 5−8 h. The reaction was terminated by the addition of 20 mL methanol and 0.5 g acidic ion-exchange resin, filtered, concentrated in vacuo, and precipitated into a 10-fold excess of diethyl ether to afford the desired polymer in quantitative yield.

Hydrogenation (General Procedure). A hydrogenation vessel was charged with the polymer (ca. 1 g) dissolved in degassed methanol (ca. 20 mL) and palladium on activated charcoal (ca. 100−200 mg) was added under a stream of argon. The vessel was closed, pressurized with hydrogen (8 bar) and stirred at room temperature until no residual aromatic signals could be detected by ^{1}H NMR spectroscopy (typically 24−48 h were necessary to achieve complete conversion). After completion of the reaction, workup was done by purging the reaction vessel with argon and filtration over Celite to remove the catalyst and washed with about 100 mL of methanol. The filtrate was then concentrated to about 5 mL, precipitated into cold diethyl ether and dried. ^{1}H NMR (DMSO-d_6, 300 MHz): 5.0−3.80 (br, OH, intensity and chemical shift can vary), 3.64−3.10 (br, -CH_2-$CH_{(2)}$O- (backbone)).

General Procedure for the Polymer Chain End Modification with Squaric Acid Diethyl Ester. The polymer (0.05 mmol) was dissolved in ethanol (15 mL) and pyridine was added (ca. 20 mg). To this mixture a 5-fold molar excess of squaric acid diethyl ester (SADE, 0.25 mmol, 43 mg) was added with a microliter syringe and the mixture was gently shaken at room temperature over a period of 16 h. The solution

Scheme 2. Synthesis of Different Monoamino Polyethers Based on Polyethylene Glycol (PEG) and Polyglycerol (PG) with Varying Architecture[a]

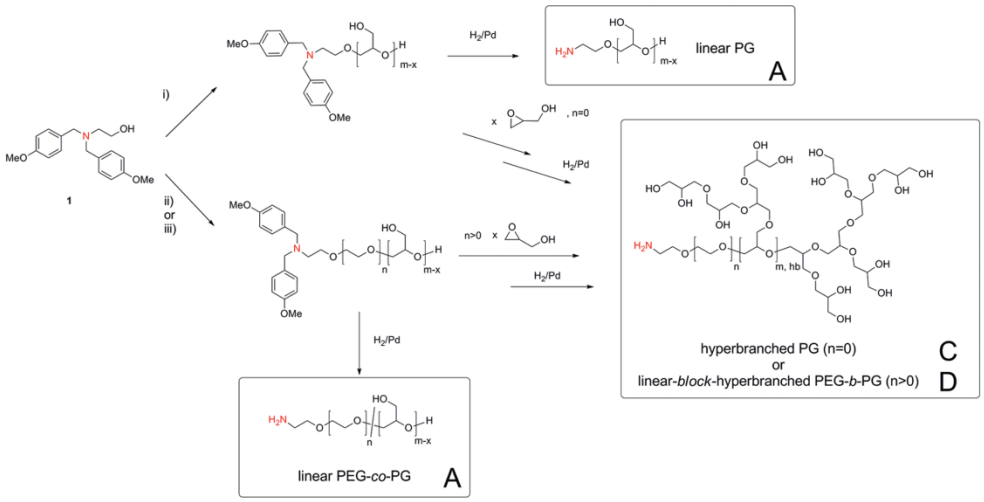

[a](i) 1. CsOH·H_2O, vacuo; 2. ethoxyethyl glycidyl ether; 3. HCl/MeOH. (ii) 1. CsOH·H_2O, vacuo; 2. ethylene oxide and ethoxyethyl glycidyl ether; 3. HCl/MeOH. (iii) 1. CsOH·H_2O, vacuo; 2. ethylene oxide; 3. ethoxyethyl glycidyl ether; 4. HCl/MeOH.

Scheme 3. Synthesis of Mid-Functional Poly(ethylene glycol-*co*-glycerol)s Starting from Di(*p*-methoxybenzyl)serinol (2)[a]

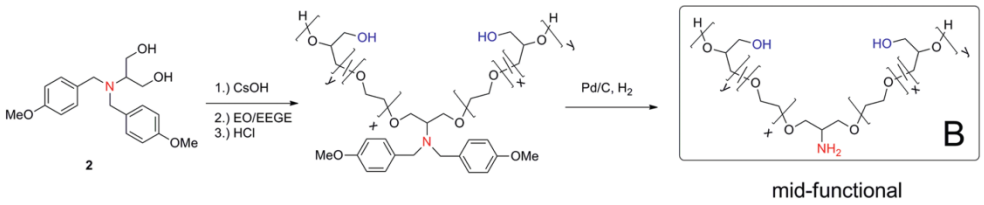

[a]EO: ethylene oxide; EEGE: ethoxyethyl glycidyl ether.

was concentrated in vacuo (taking care to keep the temperature below 60 °C to prevent transesterification) and precipitated four times into diethyl ether. Typical yields are between 85 and 95%. ^{1}H NMR (DMSO-d_6, 300 MHz): 8.7−8.4 (1H *H*-N-, two amide signals), 4.6 (br, 2H, −O-CH_2-CH$_3$), 3.64−3.18 (br, -CH_2-C$H_{(2)}$O- (backbone)), 1.4 (br, 3H, -O-CH$_2$-CH_3).

General Procedure for Squaric Acid Mediated Protein Conjugation. BSA or lysozyme was dissolved in a 3:1 mixture of borate buffer (0.01 M, pH = 9.1) and DMSO to yield a final protein concentration of 1 g/L. The calculated amount of polymer (for BSA, 9 equiv, or for lysozyme, 1−7 equiv) was added to the protein solution and the reaction mixture was gently shaken over a period of 20 h at room temperature. Samples were taken from the reaction mixture and dialyzed against deionized water (molecular weight cutoff of 1000 g/mol) to remove salts and DMSO and were analyzed by SDS-PAGE to monitor the conjugation reaction. Purification of the remaining solution was achieved by dialysis against deionized water for 48 h (depending on the molecular weight of the polymer, dialysis membranes with molecular weight cutoff between 15000 and 100000 g/mol were used for lysozyme conjugates, while all BSA conjugates were dialyzed against a molecular weight cutoff of 50000 g/mol), and subsequently freeze-dried. Yield: 95% quantitative (compared to protein).

Lysozyme Activity Measurements. The activity of the lysozyme conjugates was tested using *Micrococcus lysodeikticus* (Ml) cells as substrate. *Micrococcus lysodeikticus* cells (17 mg) were suspended in sodium acetate buffer (45 mL, pH = 5, 50 mM) and an aliquot of 3 mL was transferred into a UV cuvette. The initial absorbance at 450 nm was defined as baseline. Subsequently, 5 μL of a 1 g/L (protein) solution of the appropriate polymer−protein conjugate in borate buffer/DMSO (3:1) was added, the resulting solution mixed, and the absorption at 450 nm was recorded as a function of time during a period of 3 min. The activity of the conjugate is reported as a percentage compared to unmodified lysozyme with activity of 100%. The reported activities are the average of three independent experiments.

RESULTS AND DISCUSSION

Polymer Synthesis. A library of different poly(glycerol) (PG) and poly(ethylene glycol-*co*-glycidol) copolymers was synthesized via anionic polymerization as outlined in Schemes 2 and 3. The library consists of linear PG and linear poly(ethylene glycol-*co*-glycerol) copolymers (series A), midfunctional PEG-*co*-PG copolymers (series B), hyperbranched PG (series C), and linear-*block*-hyperbranched PEG-*b*-*hb*PG copolymers (series D; Scheme 1).

Di(*p*-methoxybenzyl)aminoethanol (**1**) was used as the initiator for the synthesis of linear, linear-hyperbranched, and hyperbranched polymers,[16,34] while di(*p*-methoxybenzyl)-serinol (**2**) was used as initiator for the preparation of midfunctional polymers. In the random copolymers the glycidol content was adjusted to 10%. The molecular weights were varied by the monomer: initiator ratio and several well-defined polymers (M_w/M_n = 1.05−1.15 for the linear polymers, respectively, 1.20−1.50 for the hyperbranched polymers) with variation in architecture and molecular weight were obtained. For the synthesis of linear PG and poly(ethylene glycol-*co*-glycerol) copolymers, ethoxy ethyl glycidyl ether[32] was used as the monomer, which was deprotected after polymerization by diluted hydrochloric acid to release the hydroxyl groups (see Supporting Information, Figure S1 for a representative MALDI ToF mass spectrum). Hyperbranched PG was synthesized via a slow-monomer addition hypergrafting protocol onto linear PG as reported previously.[16,35] For all synthesized polymers, the di(*p*-methoxybenzyl) protected amino group was released in a final step by catalytic hydrogenation at a hydrogen pressure of about 8 bar with palladium on activated charcoal as a catalyst. The end point of the reaction was determined by ^{1}H NMR spectroscopy monitoring the disappearance of the aromatic signals of the protective group. After completion of the reaction, all polymers showed a positive ninhydrin test. The resulting amino-functionalized PG (co)polymers were characterized by ^{1}H NMR spectroscopy, SEC and MALDI ToF mass spectrometry. ^{1}H NMR spectra of several selected polymers are included in the Supporting Information (Figure S2−S5). Table 1 lists the molecular weights of the different polymers as determined from ^{1}H NMR spectroscopy and SEC. Generally, the experimentally determined molecular weights were in good agreement with those expected based on the monomer: initiator ratio, which illustrates the living nature of the anionic ring-opening polymerization.

Synthesis of Protein-Reactive Poly(glycerol) (Co)-Polymers. To allow protein modification, the PG (co)polymers shown in Schemes 2 and 3 need to be further modified with an appropriate protein reactive functional group. The specific aim of this study was to explore the squaric acid mediated coupling strategy for the synthesis of PG (co)polymer−protein conjugates. The synthesis of the protein-reactive, squaric acid modified PG (co)polymers is outlined in Scheme 4.

In a first series of test reactions, the conditions for the reaction outlined in Scheme 4 were optimized with respect to the molar excess of SADE to minimize the formation of the bisamide analogue. These experiments were carried out with commercially available monoamino poly(ethylene glycol)s with molecular weights of 750, 2000, 5000, and 10000 g/mol. In general, dimerization by the formation of the diamide is unlikely because the reactivity of the diester is much higher compared to the ester amide. However, because during the deprotection of the acetal functionalized prepolymers the corresponding ammonium salts are formed, pyridine was added for neutralization during the SADE modification, which may facilitate dimerization.[36] When 5 equiv of SADE were used, the MALDI-ToF spectra indicated that no coupling takes places for polymers with a molecular weight of 2000 g/mol and higher and that quantitative end-capping is guaranteed. Low molecular weight mPEG$_{17}$ (M_n = 800 g/mol) showed a slight tendency for dimerization (ca. 10% as estimated from MALDI ToF mass spectrometry; see Supporting Information, Figures S6 and S7). However, because they do not participate in the protein modification reaction, dimerized polymer impurities are uncritical and easily removed via dialysis after the conjugation reaction.

Modification of the amino-functionalized PG (co)polymers using the conditions established above proceeded quantitatively as indicated by a negative ninhydrin test. The resulting SADE-modified PG (co)polymers were further characterized with MALDI-ToF mass spectrometry and ^{1}H NMR spectroscopy. As a typical example, Figures 1 and 2 show the MALDI-ToF mass spectrum and the ^{1}H NMR spectrum, respectively, of a midfunctional poly(ethylene glycol-*co*-glycerol) copolymer (mid-P(EG$_{100}$-*co*-G)$_8$). The MALDI-ToF mass spectrum shows the typical distribution of a copolymer with all possible linear combinations of

Table 1. Molecular Weight Characteristics of the Poly(glycerol) (Co)Polymers Investigated in this Study

series[a]	sample code[b]	$M_{n,th}$[c] (g/mol)	$M_{n,NMR}$[d] (g/mol)	$M_{n,SEC}$[e] (g/mol)	M_w/M_n[e] (−)
A	lin-PG$_{35}$	2500	2600	1900	1.12
	lin-PG$_{74}$	5000	5500	5200	1.18
	lin-P(EG$_{41}$-*co*-G$_3$)	2000	2000	2200	1.05
	lin-P(EG$_{102}$-*co*-G$_7$)	5000	4500	3400	1.05
	lin-P(EG$_{204}$-*co*-G$_{14}$)	10000	10000	7600	1.07
	lin-P(EG$_{407}$-*co*-G$_{28}$)	20000	19400	14800	1.12
B	mid-PG$_{30}$	2000	2200	1700	1.09
	mid-PG$_{68}$	5000	5500	4600	1.11
	mid-P(EG$_{41}$-*co*-G$_3$)	2000	2000	1800	1.04
	mid-P(EG$_{100}$-*co*-G$_8$)	4000	3400	3000	1.09
	mid-P(EG$_{205}$-*co*-G$_{14}$)	10000	9800	6500	1.12
	mid-P(EG$_{367}$-*co*-G$_{24}$)	20000	18000	13700	1.15
C	hb-PG$_{35}$	2500	2600	2500	1.30
	hb-PG$_{65}$	5000	4800	4400	1.28
	hb-PG$_{86}$	8000	6400	6000	1.52
	hb-PG$_{203}$	15000	15000	13200	1.39
D	PEG$_{23}$-*b*-hbPG$_{28}$	3000	2800	2710	1.26
	PEG$_{32}$-*b*-hbPG$_{14}$	4500	3300	2900	1.18
	PEG$_{350}$-*b*-hbPG$_{40}$	5500	5200	5000	1.20

[a]Compare Scheme 1. [b]Subscripts indicate the number-average degree of polymerization determined via ^{1}H NMR. [c]Theoretical number-average molecular weight calculated from the initial monomer/initiator ratio. [d]Experimentally determined number-average molecular weight via ^{1}H NMR. [e]Experimentally determined number-average molecular weight (M_n) and polydispersity (M_w/M_n) via SEC in DMF vs poly(ethylene oxide) standards.

Scheme 4. Polymer Modification with Squaric Acid Diethyl Ester to Form a Protein-Reactive Polymer-Squaric Ethylester-Amide (Polymer-SEA)

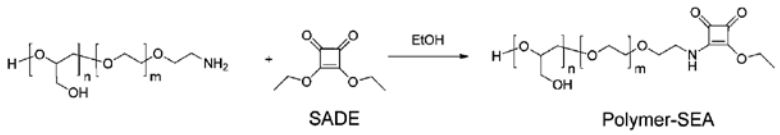

dx.doi.org/10.1021/bm300103u | Biomacromolecules 2012, 13, 1161−1171

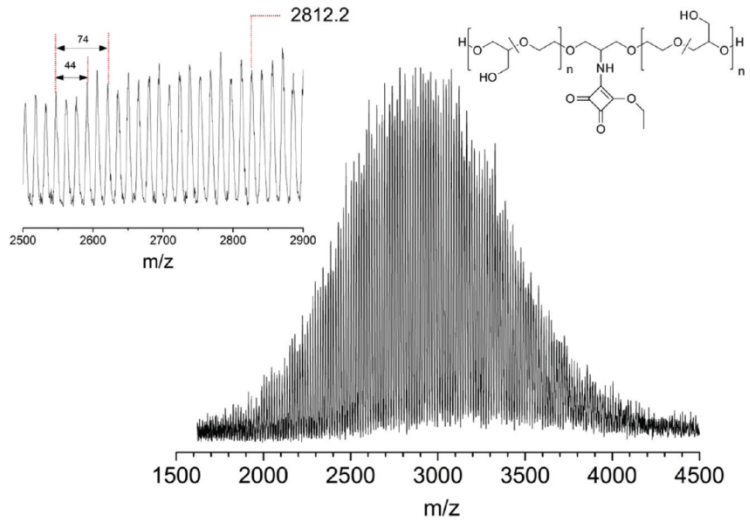

Figure 1. MALDI-ToF mass spectrum of a midfunctional random copolymer of PEG and PG (midP(EG_{100}-*co*-G_8)) modified with squaric acid ethyl ester (M_n = 3400 g/mol (NMR)). The mass indicated in the insert at 2812 corresponds to the sum formula of P(EG_{50}-*co*-G_5).

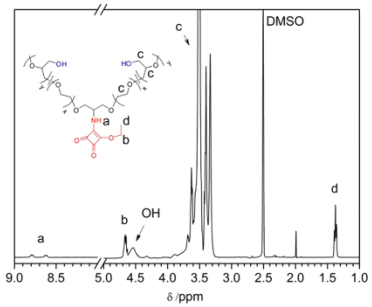

Figure 2. ^{1}H NMR spectrum of a squaric acid activated midfunctional random copolymer of PEG and PG (mid-P(EG_{100}-*co*-G_8)).

both monomer masses (44 for ethylene glycol and 74 for glycerol). The inset in Figure 1 only reveals a single distribution of species, which can be assigned to the SADE-modified polymer.

The ^{1}H NMR spectrum in Figure 2 reveals the characteristic squaric acid ethyl ester resonances at 1.37 (-CH_3) and 4.66 ppm (-CH_2-), respectively (note: the methylene resonance at 4.66 ppm is not visible in every sample due to possible overlap with the OH resonances of the polyol), as well as signals due to the polymer backbone between about 3.3 and 3.8 ppm and an amide resonance at 8.6 and 8.8 ppm. The splitting of the amide signal into two resonances has been reported before for low molecular weight squaric acid derivatives and is a result of the rotational barrier across the rigid cyclobutene carbon nitrogen bond and the different chemical environment of the proton provided by the *syn* rotamer and the corresponding *anti* form.[37]

Protein Conjugation. BSA was selected as a model protein to explore the squaric acid mediated polymer conjugation. BSA contains 59 lysine residues[38] of which 30–35 are accessible for polymer modification.[39] In a first set of experiments, several BSA–polymer conjugates were prepared by dissolving the protein in a 3:1 (v/v) mixture of borate buffer (ca. 1–3 g/L, pH = 9.1, 10 mM) and DMSO and adding an 8-fold excess of the SAE-activated polymer (Scheme 5). The mixture was gently shaken overnight at room temperature and the reaction product purified via dialysis.

The BSA–PG conjugates were first characterized by SEC. The results of these analyses are summarized in Table 2. The number of conjugated polymer chains per protein was calculated from RALS detection after determination of the apparent dn/dc and by considering the known molecular weight of BSA and the conjugated PG (co)polymer. In addition to the PG conjugates, Table 2 also lists the characteristics of two PEG conjugates that were obtained by reacting BSA with a 10-fold excess of squaric acid monoamide functionalized PEG. For the lower molecular weight P(E)G (co)polymers, Table 2 reveals excellent agreement between the expected and experimentally determined degree of P(E)Gylation. Increasing the molecular weight of the synthetic polymer generally results in a decrease in the experimentally determined degree of P(E)Gylation as compared to the expected value. Similar findings have been reported previously for other systems and were ascribed to decreasing end group reactivity and steric crowding at the protein with increasing molecular weight of the polymer.[13] The SEC experiments further revealed that the Mark–Houwink α-parameter of the PG-protein conjugates was influenced by the polymer architecture. All conjugates with linear polymers showed a value of about α = 0.33, which is an often found value for a star-branched polymer,[40] while conjugates prepared with midfunctional or hyperbranched polymers showed lower α values in the range of 0.19–0.24, that is, are more branched. The lowest α values (0.11–0.13) are observed for the *hb*PG and linear-hyperbranched block copolymer conjugates.

Scheme 5. Conjugation of Squaric Acid Modified PG (Co)Polymers to Lysine Residues of a Protein

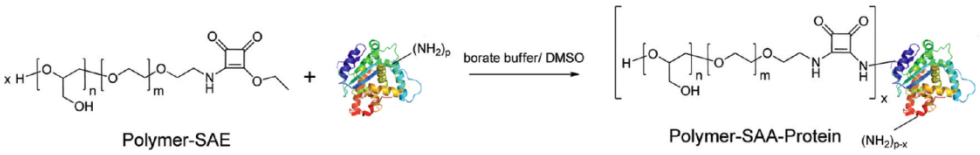

Table 2. Characteristics of the BSA–Polymer Conjugates Prepared in This Study

sample code	M_n[a] (g/mol)	M_w/M_n[a] (–)	dn/dc[a] (mL/g)	α[a] (–)	N_{th}[b]	N_{SEC}[c]
BSA	64400	1.08	0.16	0.16	0	0
BSA-$(PEG_{44})_n$	87000	1.17	0.14	0.36	10	9.8
BSA-$(PEG_{113})_n$	112250	1.12	0.13	0.38	10	9.3
BSA-(lin-P(EG_{41}-*co*-G_3)$_n$	83100	1.11	0.14	0.29	8	8.6
BSA-(lin-P(EG_{102}-*co*-G_7)$_n$	106000	1.22	0.12	0.32	8	8
BSA-(lin-P(EG_{204}-*co*-G_{14})$_n$	123000	1.13	0.10	0.33	8	6
BSA-(lin-P(EG_{407}-*co*-G_{28})$_n$	158 000	1.10	0.10	0.33	8	4.6
BSA-(mid-P(EG_{100}-*co*-G_8)$_n$	97 300	1.08	0.12	0.24	8	6.3
BSA-(mid-P(EG_{205}-*co*-G_{14})$_n$	114 000	1.11	0.12	0.19	8	5
BSA-$(hbPG_{35})_n$	83 000	1.09	0.11	0.11	8	6.8
BSA-(PEG_{13}-*b*-$hbPG_{28}$)$_n$	88 700	1.10	0.13	0.13	8	8.1

[a]Number average molecular weight (M_n), polydispersity index (M_w/M_n), refractive index increment (dn/dc), and Mark–Houwink parameter (α) determined by triple-detection SEC in water (phosphate buffer, pH = 6.5, 0.1 M)/methanol (9:1). [b]Expected number of polymer chains conjugated per protein. [c]Average number of polymer chains per protein as detected from SEC.

The dn/dc values of the conjugates are approaching those of the pure polymers with increasing mass percentage of the polymer in the conjugate (note: the dn/dc for *hb*PG was found to be 0.11 cm^3/g under these conditions and is close to the literature value of 0.12 in aqueous $NaNO_3$[17]).

To further corroborate the GPC analyses, the BSA conjugates were also analyzed by gel electrophoresis. Figure 3 summarizes the results of these experiments. The gels in Figure 3 were run using unpurified conjugation mixtures, which were only dialyzed to remove excess salt and DMSO before electrophoresis. The results of these experiments confirm the absence of free, unmodified BSA, which underlines the efficiency of the conjugation reaction under the investigated reaction conditions. Furthermore, the gel electrophoresis experiments indicate that the apparent molecular weight of the conjugates shifts to higher values with increasing molecular weight of the conjugated synthetic polymer.

In a second series of conjugation experiments, the enzyme lysozyme was chosen as substrate for the modification with the PG–(co)polymers. Lysozyme was selected as it is a convenient model protein to assess the influence of PG-conjugation on biological activity (vide infra). In contrast to the BSA modification experiments discussed above, which were carried out with a large excess of PG, the objective of the lysozyme modification experiments was to control the degree of modification by adjusting the relative quantity of squaric acid activated PG

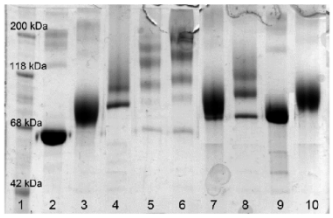

Figure 3. SDS-PAGE (12%) of BSA–polyether conjugates: (Lane 1) molecular weight markers; (Lane 2) BSA; (Lane 3) BSA-(lin-P(EG_{41}-*co*-G_3)$_n$); (Lane 4) BSA-(lin-P(EG_{102}-*co*-G_7)$_n$); (Lane 5) BSA-(lin-P(EG_{204}-*co*-G_{14})$_n$); (Lane 6) BSA-(lin-P(EG_{407}-*co*-G_{28})$_n$); (Lane 7) BSA-(mid-P(EG_{41}-*co*-G_3)$_n$); (Lane 8) BSA-(mid-P(EG_{205}-*co*-G_{14})$_n$); (Lane 9) BSA-$(hbPG_{35})_n$; (Lane 10) BSA-(PEG_{13}-*b*-$hbPG_{28}$)$_n$.

and lysozyme during the conjugation reaction. Lysozyme contains seven amine groups that are available for polymer modification: six lysine residues and the *N*-terminal amine group. To investigate to which extent the degree of polymer modification can be controlled, first a series of screening experiments with squaric acid activated α-methoxy-ω-amino poly(ethylene glycol)s (mPEG) with molecular weights of 750, 2000, 5000, and 10000 g/mol was carried out. In these experiments, varying equivalents of squaric acid activated mPEG were reacted with lysozyme at pH 9.1 in a 9:1 (v/v) borate buffer: DMSO mixture and the degree of PEGylation investigated via MALDI ToF mass spectrometry and electrophoresis (see Supporting Information, Figures S8–S11). In all cases, MALDI ToF mass spectrometry revealed a mixture of conjugates with different degrees of PEGylation. Up to a targeted degree of PEGylation of 4 and using PEG derivatives with molecular weights of 750 or 2000 g/mol, the MALDI ToF mass spectra suggest relatively good control over the number of conjugated PEG chains. Increasing the mPEG/lysozyme ratio from 4:1 to 5:1 for a squaric acid activated mPEG derivative with a molecular weight of 2000 g/mol, in contrast, was not found to result in a significant further improvement in the degree of PEGylation (see Figure S9). Further increasing the PEG molecular weight to 5000 g/mol made it more difficult to generate lysozyme–polymer conjugates where the degree of PEGylation corresponds to the used stoichiometry of amine reactive PEG and lysozyme (Figure S10).

Based on the results of the screening experiments discussed above, a series of polyglycerol (co)polymer–lysozyme conjugates were prepared with a targeted degree of modification of 3. As an example, Figure 4 shows the MALDI-ToF mass spectrum of lysozyme and the corresponding midfunctional P(EG_{100}-*co*-G_8) conjugate. The mass spectrum confirms the successful conjugation and reveals multiple distributions, which are due to multiple charged and multimeric species as is expected for protein analysis by MALDI ToF mass spectrometry.

dx.doi.org/10.1021/bm300103u | *Biomacromolecules* 2012, 13, 1161–1171

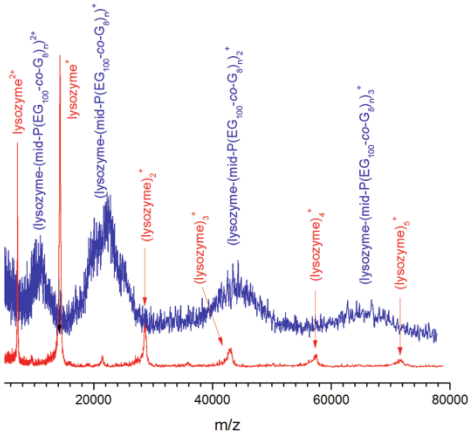

Figure 4. MALDI-ToF mass spectra of lysozyme (red) and a conjugate of lysozyme and midfunctional P(EG_{100}-*co*-G_8) (blue).

Figure 5 shows the results of the SDS-PAGE analysis of a series of lysozyme-polyglycerol (co)polymer conjugates that were prepared using a 3-fold molar excess of the protein-reactive polymer relative to lysozyme. These experiments were carried out with samples taken from the crude, unpurified reaction mixture. Figure 5A,B show the results for different lysozyme conjugates prepared with linear and midfunctional polyglycerol (co)polymers at a polymer/lysozyme ratio of 3:1 and demonstrate the success of the conjugation reaction in all cases. In most cases a small amount of free protein can be detected in the unpurified conjugation mixture together with a distribution of conjugates with a variable number of polymers attached to the protein. If a 3-fold molar excess of two architecturally different copolymers with similar molecular weights is used (cf. lin-P(EG_{204}-*co*-G_{14}; Figure 5A, Lane 5) and mid-P(EG_{205}-*co*-G_{14}) (Figure 5A, Lane 10)), one can clearly see that the apparent molecular weights of the resulting conjugates determined via SDS-PAGE are very similar. Further increasing the molecular weight of the synthetic polymer (see, e.g., lin-P(EG_{407}-*co*-G_{28}), Lane 6) results in a shift to higher apparent molecular weights.

In addition to lysozyme conjugates in which only a part of the available amine groups was modified, another series of conjugation experiments was performed that was aimed at complete modification of the lysozyme amine groups. Figure 6 shows SDS-PAGE analysis of lysozyme that was that was reacted with 10 or 20 equiv of a linear (Lane 3), midfunctional (Lane 2), or linear-hyperbranched polyglycerol derivative (Lane 1) of a molecular weight of about 2000−2700 g/mol as well as different hyperbranched polyglycerol−lysozyme conjugates (Lanes 4−7). As expected for the complete modification of lysozyme, SDS analysis of the $hbPG_{35}$ conjugate (Lane 7) reveals a single broad band. In contrast, for hbPGs with higher molecular weight, that is, 4800, 6400, and 15000 g/mol, conjugation is observed (which is detected by SDS-PAGE (Figure 6, Lanes 4−6)) but the resulting conjugates show a broader distribution of molecular weights. This may be due to steric reasons as the protein-reactive SA ester amide is located at the core of the hyperbranched polymer and probably less accessible compared to linear polymers, so that only low

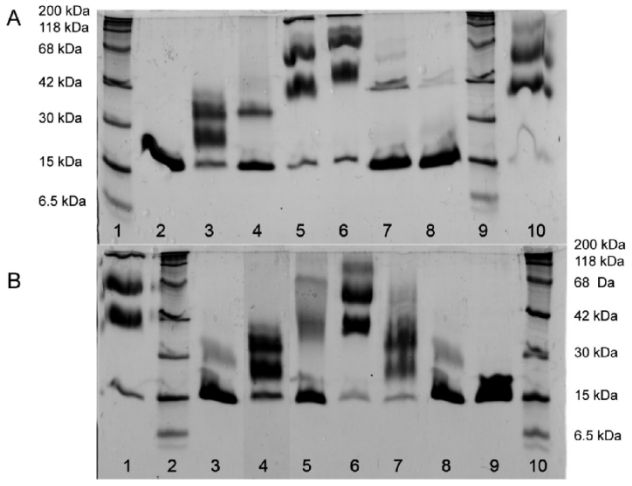

Figure 5. SDS PAGE of (A): (Lane 1) molecular weight markers; (Lane 2) lysozyme; (Lane 3) lin-P(EG_{41}-*co*-G_3) (2000 g/mol, 3 equiv); (Lane 4) lin-P(EG_{102}-*co*-G_7) (4500 g/mol, 3 equiv); (Lane 5) lin-P(EG_{204}-*co*-G_{14}) (10000 g/mol, 3 equiv); (Lane 6) lin-P(EG_{407}-*co*-G_{28}) (19400 g/mol, 3 equiv); (Lane 7) $linPG_{35}$ (2600 g/mol, 2 equiv); (Lane 8) $linPG_{74}$ (5500 g/mol, 2 equiv); (Lane 9) molecular weight markers; and (Lane 10) mid-P(EG_{205}-*co*-G_{14}) (9800 g/mol, 3 equiv); (B): (Lane 1) lin-P(EG_{204}-*co*-G_{14}) (10000 g/mol, 3 equiv); (Lane 2) molecular weight markers; (Lane 3) mid-P(EG_{41}-*co*-G_3) (2000 g/mol, 3 equiv); (Lane 4) mid-P(EG_{100}-*co*-G_8) (3400/mol, 3 equiv); (Lane 5) mid-P(EG_{205}-*co*-G_{14}) (9800 g/mol, 3 equiv); (Lane 6) mid-P(EG_{367}-*co*-G_{24}) (18000 g/mol, 3 equiv); (Lane 7) mid-PG_{68} (5500 g/mol, 3 equiv); (Lane 8) mid-PG_{30} (2200 g/mol, 3 equiv); (Lane 9) lysozyme; and (Lane 10) molecular weight markers.

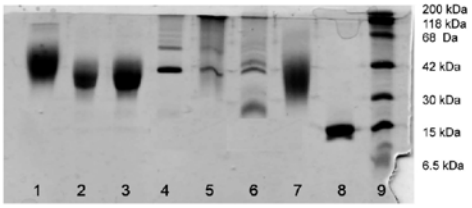

Figure 6. SDS-PAGE analysis of lysozyme conjugates prepared with (Lane 1) PEG_{13}-*b*-$hbPG_{28}$ (2800 g/mol, 20 equiv); (Lane 2) mid-P(EG_{41}-*co*-G_3) (2000 g/mol, 20 equiv); (Lane 3) lin-P(EG_{41}-*co*-G_3) (2000 g/mol, 20 equiv); (Lane 4) $hbPG_{203}$ (15000 g/mol, 10 equiv); (Lane 5) $hbPG_{86}$ (6400 g/mol, 10 equiv); (Lane 6) $hbPG_{65}$ (4800 g/mol, 10 equiv); (Lane 7) $hbPG_{35}$ (2500 g/mol, 10 equiv); (Lane 8) lysozyme; (Lane 9) molecular weight markers.

molecular weight polymers react with lysozyme while the larger ones do not react. Conjugation of $hbPG_{203}$ results in quite sharp bands on the SDS PAGE, which probably represent lysozyme was modified with one and two polymer chains (Lane 4) as the main product. In addition several other conjugates can be detected even with very high molecular weight, which do not penetrate into the gel.

Enzymatic Activity. The activity of a series of PEG and PG (co)polymer-lysozyme conjugates was investigated against *Micrococcus lysodeikticus* (Ml) cells.[41] Prior to the activity measurements, all conjugates were purified by exhaustive dialysis to remove unmodified lysozyme. Gel electrophoresis, HPLC and GPC analysis results of the purified conjugates are included in the Supporting Information (Figures S12–S17). The activity of the conjugates was measured in acetate buffer at pH = 5 (50 mM) as lysozyme has its highest activity at pH = 5.[42] The results are summarized in Table 3.

All polymer–lysozyme conjugates show a loss of activity as compared to unmodified lysozyme as it has been reported in literature for other lysozyme–polymer conjugates.[13,42] From the activity data, three general conclusions can be drawn: (i) the more polymer chains (of a given molecular weight) are conjugated to lysozyme the more the activity is decreased; (ii) at any given degree of modification, the activity of the conjugates (of the same polymer-type) decreases as the molecular weight of the conjugated polymer increases; (iii) only at high PG (co)polymer molecular weights, lysozyme activity appears to be significantly influenced by polymer architecture.

To illustrate the first conclusion, if five PEG_{17} chains (M_n = 800 g/mol) were conjugated, the residual activity was found to be 18 ± 2%. For lysozyme modified with 5 equiv PEG_{44} (M_n = 2100 g/mol), the activity was reduced further to 3.8 ± 1.2% and essentially no activity was observed when in average five chains PEG_{113} (M_n = 5100 g/mol) were conjugated to lysozyme (residual activity 0.5 ± 1%). When all amine groups of lysozyme were P(E)Gylated (use of 20-fold molar excess of the polymer), no residual activity was detected for most conjugates (data not shown), which is also in agreement with other studies that have been reported on various polymers.[11] The influence of the degree modification on enzymatic activity is also obvious from the results on the *hb*PG_{35} conjugates. The activity of these conjugates decreases from 93 to 31% upon increasing the degree of P(E)Gylation from 1 to 5.

The influence of polymer molecular weight at a given degree of P(E)Gylation on the activity is most apparent from the

Table 3. Comparison of the Activities of Different Lysozyme Conjugates

conjugated polymer	$M_{n,polymer}$ (g/mol)[a]	$N_{polymer}$[b]	activity[c]
PEG_{17}	800	3	99 ± 3.0
PEG_{17}	800	5	18 ± 0.6
PEG_{44}	2100	3	71 ± 2.0
PEG_{44}	2100	5	2.8 ± 0.4
PEG_{113}	5100	3	41 ± 1.0
PEG_{113}	5100	5	0.5 ± 0.4
PEG_{226}	10100	3	25 ± 1.9
lin-P(EG_{41}-*co*-G_3)	2000	3	71 ± 2.4
lin-P(EG_{102}-*co*-G_7)	4500	3	62 ± 1.0
lin-P(EG_{204}-*co*-G_{14})	10000	3	28 ± 2.3
lin-P(EG_{407}-*co*-G_{28})	19400	3	23 ± 0.9
lin-PG_{35}	2600	3	67 ± 2.5
lin-PG_{78}	5500	3	52 ± 2.1
mid-P(EG_{41}-*co*-G_3)	2000	3	78 ± 2.0
mid-P(EG_{100}-*co*-G_8)	3400	3	67 ± 1.7
mid-P(EG_{205}-*co*-G_{14})	9800	3	57 ± 2.0
mid-P(EG_{367}-*co*-G_{24})	18000	3	34 ± 1.7
PEG_{13}-*b*-$hbPG_{28}$	2700	3	79 ± 1.1
PEG_{32}-*b*-$hbPG_{14}$	3300	3	58 ± 1.2
PEG_{50}-*b*-$hbPG_{40}$	5200	3	51 ± 1.3
$hbPG_{35}$	2500	1	93 ± 1.0
$hbPG_{35}$	2500	2	85 ± 2.0
$hbPG_{35}$	2500	3	60 ± 1.0
$hbPG_{35}$	2500	5	31 ± 5.0

[a]Number average molecular weight (M_n) determined via ^{1}H NMR. [b]Ratio polymer/protein used in the reaction. [c]Activity measured against *Micrococcus lysodeikticus* cells in percent compared to unmodified lysozyme.

results obtained on the lin-P(EG-*co*-G) and mid-P(EG-*co*-G) lysozyme conjugates. For both families of conjugates, the enzymatic activity was found to decrease from 71% (lin-P(EG-*co*-G)), respectively, 78% (mid-P(EG-*co*-G)) to 23% (lin-P(EG-*co*-G)), and 34% (mid-P(EG-*co*-G)) upon increasing the molecular weight of the conjugated polymer from 2000 to ~20000 g/mol.

In several studies, the influence of polymer architecture on the biological activity of polymer–protein conjugates has been reported. Tao et al., for example, reported a 2.5 times higher activity of a polymer–protein conjugate consisting of a mid-functional PHPMA (28.5% residual activity) as compared to the linear counterpart (11.5%) of comparable molecular weight (ca. 9000 g/mol).[12] However, the compared protein conjugates differed in the number of attached polymer chains (1.6 for the midfunctional vs 3.1 for the linear), which makes an architectural comparison difficult. Another example was given for uricase, which was PEGylated with a 10000 g/mol linear or midfunctional PEG by Veronese et al.[7] The authors found a residual activity of 29% for linear PEG and 70% for midfunctional PEG. On a first sight, comparison of the enzymatic activities of the conjugates listed in Table 3 that have identical degrees of modification but are generated from architecturally different P(E)G copolymers of comparable molecular weight does not provide any very obvious hints as to possible structure–activity relationships. For example, at a degree of modification of 3 and a polymer molecular weight of ≈2000 g/mol, the PEG_{44} conjugate shows a relative activity of 71% as compared to 71, 78, 79, and 60% for the comparable lin-P(EG_{41}-*co*-G_3), mid-P(EG_{41}-*co*-G_3), PEG_{13}-*b*-$hbPG_{28}$, and $hbPG_{35}$ conjugates. At a similar degree

dx.doi.org/10.1021/bm300103u | *Biomacromolecules* 2012, 13, 1161–1171

of modification but using polymers with a molecular weight of ≈5000 g/mol, the relative activities of the PEG_{113}, lin-P(EG_{102}-*co*-G_7), and PEG_{50}-*b*-hbPG_{40} were determined as 41, 62, and 51%. While possible effects of the P(E)G architecture on the activity of the low molecular weight polymer conjugates seem to be relatively minor, comparison of the activities of the higher molecular weight P(E)G conjugates does reveal some interesting insights. From the three conjugates that contain three copies of a P(E)G copolymer with a molecular weight of ~10000 g/mol, the residual activity of the mid-P(EG_{205}-*co*-G_{14}) conjugate is two times higher than those of the PEG_{226} and lin-P(EG_{204}-G_{14}) conjugates. Also, comparison of the lin-P(EG_{407}-*co*-G_{28}) and mid-P(EG_{367}-*co*-G_{24}) conjugates, which consists of synthetic polymers of comparable molecular weights, shows a 1.5 times higher residual activity of the mid-functional as compared to the linear P(E)G copolymer conjugate. These observations are in agreement with earlier studies (vide supra)[7,12] and indicate that, at similar molecular weights, the use of a midfunctional, water-soluble polymer is advantageous to minimize the loss of enzymatic activity as compared to the use of the corresponding linear polymer.

CONCLUSIONS

This contribution has successfully demonstrated the feasibility of the squaric acid dialkyl ester mediated amine selective modification of proteins with amine end functionalized, side chain functional synthetic polymers. The synthetic polymers investigated in this study were amine end-functionalized polyglycerol (PG) copolymers obtained via ring-opening polymerization of glycidol derivatives and ethylene oxide. The anionic ring-opening polymerization of glycidol is a versatile synthetic strategy that was used to prepare a library of linear, midfunctional, hyperbranched, and linear-block-hyperbranched PG copolymers. Whereas the efficiency of traditional approaches to couple such hydroxyl side chain functional polymers to proteins can be compromised by concurrent transesterification and hydrolysis reactions, the squaric acid diethylester strategy presented herein combines a high amine selectivity with low susceptibility to hydrolysis, which enables the amine selective protein conjugation of side chain hydroxyl functionalized PG copolymers. For the experiments in this study, BSA and lysozyme were used as model proteins. Varying the relative amounts of squaric acid diethylester activated polymer to protein allowed to control the degree of modification of these proteins. The library of PG−lysozyme conjugates was used to investigate the possible effects of the architecture of the PG copolymers on the enzymatic activity of the PG−lysozyme conjugates. Comparison of the activity of PG−lysozyme conjugates generated from relatively low molecular weight PG copolymers (<5000 g/mol) did not reveal any obvious structure−activity relationships. Evaluation of the activity of conjugates composed of PG copolymers with molecular weights of 10000 or 20000 g/mol, however, indicated significantly higher activities of conjugates prepared from midfunctional synthetic polymers as compared to linear polymers of similar molecular weight. The squaric acid diethyl ester mediated protein conjugation presented here allows unprecedented access to side chain functional synthetic polymer−protein hybrid conjugates and may prove particularly useful for the generation of polymer−protein hybrids modified with labeling groups or targeting ligands for biological or medical applications. Combined with the versatility of the glycidol ring-opening polymerization, this unique coupling strategy opens the way to a broad architectural variety of polymer−protein conjugates and allows to engineer the architecture of the synthetic polymer such as to minimize loss of enzymatic activity in the resulting modified proteins.

ASSOCIATED CONTENT

Supporting Information

Additional NMR, mass spectrometry, and SDS PAGE analysis. This material is available free of charge via the Internet at http://pubs.acs.org.

AUTHOR INFORMATION

Corresponding Author

*E-mail: harm-anton.klok@epfl.ch.

Notes

The authors declare no competing financial interest.

ACKNOWLEDGMENTS

F.W. is grateful to the Alexander von Humboldt Stiftung for a Feodor Lynen fellowship. C.D. is a recipient of a fellowship of the Max Planck Graduate Center mit der Johannes Gutenberg-Universität Mainz (MPGC). This work was partially supported by the NCCR Nanoscale Science (H.-A.K.)

REFERENCES

(1) James, E. T. *Adv. Drug Delivery Rev.* **1993**, *10*, 247−299.
(2) Putney, S. D.; Burke, P. A. *Nat. Biotechnol.* **1998**, *16*, 153−157.
(3) Veronese, F. M.; Pasut, G. *Drug Discovery Today* **2005**, *10*, 1451−1458.
(4) Caliceti, P.; Veronese, F. M. *Adv. Drug Delivery Rev.* **2003**, *55*, 1261−1277.
(5) Abuchowski, A.; van Es, T.; Palczuk, N. C.; Davis, F. F. *J. Biol. Chem.* **1977**, *252*, 3578−3581.
(6) Abuchowski, A.; McCoy, J. R.; Palczuk, N. C.; Es, T. v.; Davis, F. F. *J. Biol. Chem.* **1977**, *252*, 3582−3586.
(7) Veronese, F. M.; Caliceti, P.; Schiavon, O. *J. Bioact. Compat. Polym.* **1997**, *12*, 196−207.
(8) Pasut, G.; Veronese, F. M. *Prog. Polym. Sci.* **2007**, *32*, 933−961.
(9) Alconcel, S. N. S.; Baas, A. S.; Maynard, H. D. *Polym. Chem.* **2011**, *2*, 1442−1448.
(10) Bailon, P.; Palleroni, A.; Schaffer, C. A.; Spence, C. L.; Fung, W.-J.; Porter, J. E.; Ehrlich, G. K.; Pan, W.; Xu, Z.-X.; Modi, M. W.; Farid, A.; Berthold, W.; Graves, M. *Bioconjugate Chem.* **2001**, *12*, 195−202.
(11) Gauthier, M. A.; Klok, H.-A. *Polym. Chem.* **2010**, *1*, 1352−1373.
(12) Tao, L.; Xu, J.; Gell, D.; Davis, T. P. *Macromolecules* **2010**, *43*, 3721−3727.
(13) Tao, L.; Liu, J.; Davis, T. P. *Biomacromolecules* **2009**, *10*, 2847−2851.
(14) Broyer, R. M.; Grover, G. N.; Maynard, H. D. *Chem. Commun.* **2011**, 2212−2226.
(15) Gauthier, M. A.; Klok, H.-A. *Chem. Commun.* **2008**, 2591−2611.
(16) Wurm, F.; Klos, J.; Räder, H. J.; Frey, H. *J. Am. Chem. Soc.* **2009**, *131*, 7954−7955.
(17) Kainthan, R. K.; Brooks, D. E. *Biomaterials* **2007**, *28*, 4779−4787.
(18) Wilms, D.; Stiriba, S.-E.; Frey, H. *Acc. Chem. Res.* **2009**, *43*, 129−141.
(19) Siegers, C.; Biesalski, M.; Haag, R. *Chem.—Eur. J.* **2004**, *10*, 2831−2838.
(20) Dworak, A.; Walach, W.; Trzebicka, B. *Macromol. Chem. Phys.* **1995**, *196*, 1963−1970.
(21) Kainthan, R. K.; Muliawan, E. B.; Hatzikiriakos, S. G.; Brooks, D. E. *Macromolecules* **2006**, *39*, 7708−7717.
(22) Sunder, A.; Hanselmann, R.; Frey, H.; Mulhaupt, R. *Macromolecules* **1999**, *32*, 4240−4246.
(23) Roberts, M. J.; Bentley, M. D.; Harris, J. M. *Adv. Drug Delivery Rev.* **2002**, *54*, 459−476.

(24) Greenwald, R. B.; Pendri, A.; Martinez, A.; Gilbert, C.; Bradley, P. *Bioconjugate Chem.* **1996**, *7*, 638−641.
(25) Subr, V.; Ulbrich, K. *React. Funct. Polym.* **2006**, *66*, 1525−1538.
(26) Hou, S.-j.; Saksena, R.; Kovác, P. *Carbohydr. Res.* **2008**, *343*, 196−210.
(27) Izumi, M.; Okumura, S.; Yuasa, H.; Hashimoto, H. *J. Carbohydr. Chem.* **2003**, *22*, 317−329.
(28) Yan, H.; Aguilar, A. L.; Zhao, Y. *Bioorg. Med. Chem. Lett.* **2007**, *17*, 6535−6538.
(29) Sejwal, P.; Han, Y.; Shah, A.; Luk, Y.-Y. *Org. Lett.* **2007**, *9*, 4897−4900.
(30) Tietze, L. F.; Arlt, M.; Beller, M.; Glüsenkamp, K. H.; Jähde, E.; Rajewsky, M. F. *Chem. Ber.* **1991**, *124*, 1215−1221.
(31) Dingels, C.; Wurm, F.; Klok, H.-A.; Frey, H. submitted for publication.
(32) Fitton, A. O.; Hill, J.; Jane, D. E.; Millar, R. *Synthesis* **1987**, *1140*, 1142.
(33) Zhang, W.; Go, M. L. *Eur. J. Med. Chem.* **2007**, *42*, 841−850.
(34) Mangold, C.; Wurm, F.; Obermeier, B.; Frey, H. *Macromol. Rapid Commun.* **2010**, *31*, 258−264.
(35) Wurm, F.; Nieberle, J.; Frey, H. *Macromolecules* **2008**, *41*, 1184−1188.
(36) Schmidt, A. H. *Synthesis* **1980**, 961−994.
(37) Rotger, M. C.; Pina, M. N.; Frontera, A.; Martorell, G.; Ballester, P.; Deyà, P. M.; Costa, A. *J. Org. Chem.* **2004**, *69*, 2302−2308.
(38) Hirayama, K.; Akashi, S.; Furuya, M.; Fukuhara, K.-I. *Biochem. Biophys. Res. Commun.* **1990**, *173*, 639−646.
(39) Van Regenmortel, M. H. V., Briand, J. P., Müller, S.; Plaué, S. *Synthetic Polypeptides as Antigens*; Elsevier: Amsterdam, 1988; Vol. *19*.
(40) Held, D.; Müller, A. H. E. *Macromol. Symp.* **2000**, *157*, 225−238.
(41) Salton, M. R. J. *Nature* **1952**, *170*, 746−747.
(42) Nodake, Y.; Yamasaki, N. *Biosci. Biotechnol. Biochem.* **2000**, *64*, 767−774.

A.4 *N*,*N*-Diallylglycidylamine: A Key Monomer for Amino-Functional Poly(ethylene glycol) Architectures

Valerie S. Reuß,[1,2] *Boris Obermeier,*[1] *Carsten Dingels,*[1] *and Holger Frey**[1]

[1]Department of Organic Chemistry, Johannes Gutenberg-Universität Mainz, Duesbergweg 10-14, 55099 Mainz, Germany

[2]Graduate School "Materials Science in Mainz", Staudingerweg 9, 55099 Mainz, Germany

Published in: *Macromolecules* **2012**, *45*,4581.

Macromolecules

Article

pubs.acs.org/Macromolecules

N,N-Diallylglycidylamine: A Key Monomer for Amino-Functional Poly(ethylene glycol) Architectures

Valerie S. Reuss,[†,‡] Boris Obermeier,[†] Carsten Dingels,[†] and Holger Frey*[,†]

[†]Department of Organic Chemistry, Johannes Gutenberg-Universität Mainz, Duesbergweg 10-14, 55099 Mainz, Germany

[‡]Graduate School "Materials Science in Mainz", Staudingerweg 9, 55099 Mainz, Germany

Supporting Information

ABSTRACT: The first application of *N,N*-diallylglycidylamine (DAGA) as a monomer for anionic ring-opening polymerization is presented. The monomer is obtained in a one-step procedure using epichlorohydrin and *N,N*-diallylamine. Both random and block copolymers consisting of poly(ethylene glycol) and poly(*N,N*-diallylglycidylamine) with adjusted DAGA ratios from 2.5 to 24% have been prepared, yielding well-defined materials with low polydispersities (M_w/M_n) in the range 1.04−1.19. Molecular weights ranged between 2600 and 10 300 g mol^{-1}. Isomerization of allylamine to enamine structures during polymerization depending on time, temperature, and counterion has been realized. The kinetics of the formation of the copolymer structure obtained by random copolymerization was investigated, using time-resolved ^{1}H NMR measurements and ^{13}C NMR triad sequence analysis. A tapered character of the monomer incorporation was revealed in the course of the concurrent copolymerization of EO and DAGA. The thermal behavior of the copolymers in both bulk and aqueous solution has been studied, revealing LCSTs in the range 29−94 °C. Quantitative removal of protective groups via double-bond isomerization mediated by Wilkinson's catalyst and subsequent acidic hydrolysis yielded multiamino-functional PEG copolymers with tapered or block structure. Accessibility of liberated primary amines for further transformation was demonstrated in a model reaction by derivatization with acetic anhydride. In contrast to previous approaches, the DAGA monomer permits the synthesis of block copolymers with PEG block combined with multiamino-functional polyether block.

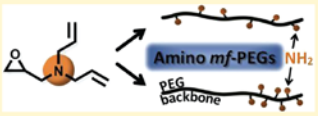

INTRODUCTION

Poly(ethylene glycol) (PEG) and its derivatives represent a highly versatile class of polyethers, covering applications from fields as diverse as biomedicine to nonionic surfactants and soluble polymeric supports for catalysts and reagents.[1−16] Approved by the US-American Food and Drug Administration (FDA) for use in the human body,[17] PEG combines excellent solubility in both water and organic solvents with biocompatibility; showing no immunogenicity, antigenicity, or toxicity.[18] These properties are accompanied by high flexibility and pronounced hydration of the main chain. As a result, PEG has left behind its former task as a simple additive in cosmetic and skin care formulations, now being the "gold standard" for use in sophisticated biomedical applications such as "PEGylation" of pharmaceutically active drugs and peptides.[18−32,67]

A drawback for both pharmaceutical and polymeric support-related applications is the low number of functional groups at the PEG backbone, namely the two end groups. Their nature can be varied by the choice of initiator, end-capping agent, or postpolymerization transformation reactions. As an example, amino end-functionalized PEG is accessible through the use of benzyl-protected 2-aminoethanol as an initiator and subsequent hydrogenation[33] and is also commercially available (e.g., Jeffamines).[34]

Multifunctionality can be realized by copolymerization of ethylene oxide (EO) with an epoxide derivative bearing a (protected) functional group, resulting in structures known as *mf*-PEGs (multifunctional PEGs).[35] The synthesis of functional aliphatic polyethers has been first reported by Taton et al.[36] in the mid-1990s, employing an acetal-protected glycidyl derivative (ethoxy ethyl glycidyl ether, EEGE), releasing hydroxyl groups at the chain upon acidic work-up to generate linear polyglycerol. This increased number of addressable moieties allows for the conjugation of an enlarged number of catalysts or active compounds, labels, and targeting molecules to a single polymer chain.[37]

Few concepts for multiple incorporation of amino groups at a PEG-based backbone have been presented to date. Starting from anionic copolymerization of EO and allyl glycidyl ether (AGE), Koyama et al.[38] were the first to obtain amino functionalities via thiol−ene click of 2-aminoethanethiol to allylic double bonds, a methodology that has been adapted in many other published studies since.[29,31,39] Employing the monomer-activated anionic polymerization concept,[40] Möller and co-workers[41] recently obtained poly(glycidylamine) and copolymers thereof in a multistep synthesis by nucleophilic substitution of poly(epichlorohydrin) with an azide and subsequent reduction.

As a further development of the concept of polymerization of protected glycidyl ether derivatives, the use of *N,N*-dibenzylamino glycidol (DBAG) as a comonomer in anionic ring-opening polymerization (AROP) has been introduced in a

Received: February 12, 2012
Revised: April 26, 2012
Published: May 21, 2012

dx.doi.org/10.1021/ma300292m | Macromolecules 2012, 45, 4581−4589

recent work by our group.[42] Here, liberation of the amine is achieved by hydrogenation of the benzyl protecting groups, releasing the glycidylamine (GA) repeating units. Unfortunately, the success of this approach has been somewhat hampered by the heterogeneous nature of the deprotection reaction, not only resulting in prolonged reaction times and lowered yields but furthermore preventing the synthesis of amino-functional block copolymers PEG-*b*-PGA.

Herein, we present the first study of *N,N*-diallylglycidylamine (DAGA) as a comonomer for the straightforward preparation of well-defined *mf*-PEGs with varying content and incorporation sequence, including amino-functional block copolymers (Scheme 1).

Scheme 1. Synthetic Strategy for the Copolymerization of EO and DAGA (top), Diblock Copolymer Preparation of mPEG-*b*-PDAGA As Well As PDAGA Homopolymer Synthesis (bottom) via Anionic Ring-Opening Polymerization

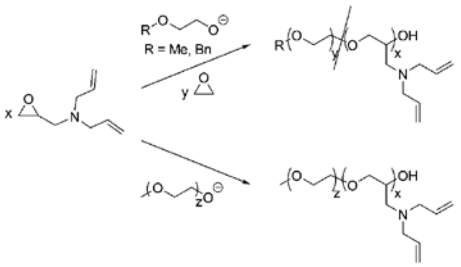

The monomer can be prepared in a one-step procedure starting from commercially available reagents. This approach represents a major improvement of the above-mentioned concept of glycidyl amine derivatives and relies on an alternative deprotection route, providing fast access to copolymers with ethylene oxide and poly(ethylene glycol) monomethyl ether exhibiting multiple amino functionalities. The block structures are interesting with regard to polymer-supported catalytic systems and for bioconjugation.

EXPERIMENTAL SECTION

Instrumentation. ^{1}H NMR spectra (300 and 400 MHz) and ^{13}C NMR spectra (75.5 MHz) were recorded using a Bruker AC300 or a Bruker AMX400 spectrometer. All spectra were referenced internally to residual proton signals of the deuterated solvent. For SEC measurements in DMF (containing 0.25 g/L of lithium bromide as an additive) an Agilent 1100 Series was used as an integrated instrument, including a PSS HEMA column ($10^6/10^5/10^4$ g mol^{-1}), a UV (275 nm) detector, and a RI detector. Calibration was carried out using poly(ethylene oxide) standards provided by Polymer Standards Service. DSC measurements were performed using a PerkinElmer DSC 8500 with PerkinElmer CLN2 in the temperature range from −100 to 100 °C at heating rates of 10 K min^{-1} under nitrogen. Cloud points were determined in deionized water at a concentration of 20 mg mL^{-1} and observed by optical transmittance of a light beam (λ = 670 nm). The measurements were performed in a Tepper turbidimeter TP1. The intensities of the transmitted light were recorded versus the temperature of the sample cell. The heating/cooling rate was 1 K min^{-1}. The cloud point temperatures of the sharp transitions from translucent to opaque solutions were defined as the values measured at 50% transmittance.

Reagents. Poly(ethylene glycol) monomethyl ether (mPEG 5000, M_n = 5000 g mol^{-1}) was purchased from Fluka. Diallylamine, epichlorohydrin (99%), sodium hydroxide, and ethylene oxide (99.5%) as well as dimethyl sulfoxide (puriss, over molecular sieve), tetrahydrofuran (puriss, over molecular sieve), and toluene (puriss, over molecular sieve) were purchased from Aldrich. Deuterated chloroform-d_1 and DMSO-d_6 were purchased from Deutero GmbH. All other solvents and reagents were purchased from Acros Organics.

Synthesis of *N,N*-Diallylglycidylamine (DAGA: *N,N*-Diallyl-(2,3-epoxypropyl)amine). 118 g of diallylamine (1.21 mol, 1 equiv) and 118 g of epichlorohydrin (1.28 mol, 1.05 equiv) were combined. A 50 wt % aqueous solution of 85 g of NaOH (2.12 mol, 1.75 equiv) was added, and the two-phase mixture was vigorously stirred overnight. After centrifugation (10 min, 4500 min^{-1}) and careful separation of the layers, the organic layer was dried over $MgSO_4$. Fractionating distillation from CaH_2 (8×10^{-2} mbar, 54 °C) afforded the product as a colorless liquid. The monomer was stored under argon at 8 °C and cryo-transferred from CaH_2 prior to polymerization. Yield: 80−91%. ^{1}H NMR (400 MHz, DMSO-d_6): δ [ppm] = 5.95−5.70 (m, 2H, CH=), 5.30−4.95 (m, 4H, CH_2=), 3.22−3.02 (m, 4H, N−CH_2−CH=), 3.01−2.95 (m, 1H, CH_{ring}), 2.70−2.62 (m, 2H, $CH'H''_{ring}$ and $CH'H''$−N), 2.45−2.40 (dd, 1H, $CH'H''_{ring}$), 2.38−2.29 (dd, 1H, $CH'H''$−N). ^{13}C NMR (75.5 MHz, $CDCl_3$): δ [ppm] = 135.37 (CH=), 117.66 (CH_2=), 57.34 (CH_2−N), 55.69 (N−CH_2−CH=), 50.72 (CH_{ring}), 45.22 (CH_{2ring}).

Homopolymerization. In a dry Schlenk flask under argon atmosphere, 21 mg of cesium hydroxide monohydrate (0.13 mmol, 1 equiv) was suspended in 5 mL of benzene. 10 mg of 2-methoxyethanol (0.13 mmol, 1 equiv) was added. Stirring at 60 °C for 30 min and evacuation at 90 °C for 3 h afforded the cesium alkoxide. 1 g of DAGA (6.5 mmol, 50 equiv) was added, and polymerization was performed at 90 °C for 12 h. Polymerization was terminated by addition of 0.3 mL of methanol. Unreacted monomer and solvent were removed in high vacuum at 60 °C under stirring. The polymer was dissolved in chloroform, filtrated to remove salts, and dried in high vacuum. Yield: 41%.

Block Copolymer Synthesis (mPEG-*b*-PDAGA). 2 g of mPEG 5000 (0.4 mmol, 1 equiv), 60 mg of cesium hydroxide monohydrate (0.36 mmol, 0.9 equiv), and 10 mL of benzene were added sequentially to a dry Schlenk flask under argon atmosphere. Stirring at 60 °C for 30 min and evacuation at 90 °C for 3 h afforded the partially deprotonated macroinitiator. The respective amount of DAGA was syringed in, and the reaction mixture was stirred for 12 h. After addition of 0.3 mL of methanol and cooling, the polymer was dissolved in chloroform and filtrated to remove salts. The solvents were removed under reduced pressure. Precipitation from methanol into cold diethyl ether and drying in high vacuum afforded the block copolymer. Yields >93%. For block copolymer synthesis using alternative deprotonating agents, mPEG was twice dissolved in benzene and dried at 70 °C under high vacuum prior to addition of potassium methoxide or sodium hydride, respectively. The subsequent deprotonation and evacuation steps were carried out as described above.

Copolymerization of Ethylene Oxide with *N,N*-Diallylglycidylamine (PEG-*co*-PDAGA). For PEG_{95}-*co*-$PDAGA_5$: In a dry Schlenk flask under argon atmosphere, 177 mg of cesium hydroxide monohydrate (1.05 mmol, 1 equiv) was suspended in 5 mL of benzene. After addition of 80 mg of 2-methoxyethanol (1.05 mmol, 1 equiv) the mixture was stirred at 60 °C for 30 min and evacuated at 90 °C for 3 h, affording the cesium alkoxide. 5 mL of DMSO and ~30 mL of THF were added to the evacuated flask. The flask was cooled to −80 °C, and 5 mL of ethylene oxide (100 mmol, 95 equiv) was cryo-transferred from a graduated ampule. 812 mg of DAGA (5.3 mmol, 5 equiv) was injected. Polymerization was performed at 40 °C for 12 h. Copolymerization with 20% DAGA was performed without THF. Polymerizations were terminated by addition of methanol. For DAGA contents up to 10%, filtration, removal of THF under reduced pressure, and precipitation in cold diethyl ether resulted in the pure polymer. For higher DAGA contents, dialysis in methanol was carried out (MWCO = 1000 g mol^{-1}). Polymers were dried at 40 °C in high

dx.doi.org/10.1021/ma300292m | *Macromolecules* 2012, 45, 4581−4589

vacuum or dissolved in water and lyophilized to give pale yellow to brownish yellow materials in good yields (>80%). Polymers were stored under argon at −27 °C. Because of limited shelf life of the polymers and observed gelation effects, deprotection steps were carried out soon after synthesis.

Isomerization of Double Bonds. Under an argon atmosphere, 300 mg of diallyl-protected polymer was dissolved in 5 mL of dry toluene. The solution was degassed by three freeze−pump−thaw cycles. 2 mol % of Wilkinson's catalyst was added followed by another three freeze−pump−thaw cycle. The mixture was refluxed for 2 h. After cooling, precipitation in cold diethyl ether and centrifugation afforded the polymer with completely isomerized double bonds. Yields: 85−90%.

Release of Amino Functionalities. The polymer with isomerized double bonds was dissolved in toluene and subsequently acidic ion-exchange resin (Dowex 50WX8), and water was added. While stirring at 85 °C for 2 h, some liquid was distilled off the reaction mixture to allow propanal to escape and avoid possible imine formation. Filtration, removal of solvents under reduced pressure, precipitation from toluene into cold diethyl ether, and centrifugation afforded the amino-multifunctional materials in almost quantitative yields.

One-Pot Isomerization and Removal of Allyl Groups. The two deprotection steps can also be carried out in a one-pot procedure, omitting the purification step after isomerization of the allyl to propenyl moieties. Instead of precipitation of the polymer, water and acidic ion-exchange resin are added directly to the reaction mixture. The polymer is worked up in the same way as mentioned above, yielding the amino-multifunctional materials.

Derivatization of Amino Functionalities with Acetic Anhydride. The reaction was carried out according to a literature procedure.[42]

■ RESULTS AND DISCUSSION

Monomer Synthesis. The synthesis of allyl-protected comonomer *N,N*-diallylglycidylamine (DAGA) was accomplished in a facile one-step procedure (Scheme 2). Starting from commercially available epichlorohydrin and diallylamine in presence of a 50 wt % aqueous solution of sodium hydroxide, DAGA is obtained without observation of residual diallyl-3-chloro-2-hydroxypropylamine or isomerization of the double bonds in ^{1}H NMR spectroscopy. In addition, the aqueous conditions permit to avoid the use of organic solvents and thus reduce environmental impact and cost. By modification and optimization of a literature procedure,[43] good yields (>80%) were realized despite the rigorous monomer purification steps required for the ensuing oxyanionic polymerization. Detailed characterization including 2D NMR studies and mass spectrometry has been carried out (see Supporting Information). This compound has recently become commercially available.[68]

Scheme 2. Synthesis of the Allyl-Protected Amino-Functional Epoxide Monomer *N,N*-Diallylglycidylamine (DAGA)

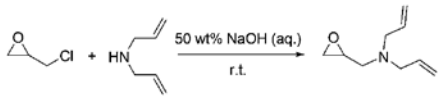

Synthesis of Block Copolymers mPEG-*b*-PDAGA. Preparation of the macroinitiators was achieved using commercially available mPEG (M_n = 2000 or 5000 g mol^{-1}) and cesium hydroxide monohydrate (Scheme 1) as an initiator system. Block copolymer synthesis was carried out at 90 °C for 12 h. Compared with the macroinitiator, SEC analysis showed a shift toward higher molecular weights as well as monomodal molecular weight distributions with low polydispersity indices in the range 1.04−1.11. As can be seen from Table 1 (runs 2−5), the obtained degrees of polymerization were usually somewhat lower than anticipated. This may be attributed to transfer reactions, a known limiting parameter in alkali metal-mediated anionic ring-opening polymerization of epoxides.[42,44] A detailed study of transfer to the monomer has been carried out, based on NMR spectroscopy and SEC (for detailed discussion see Supporting Information). Whereas chain transfer appears to play a limited role in block copolymer synthesis, its influence is small in the concurrent copolymerization of both comonomers.

Table 1. Characterization Data for Polymers comprised of Ethylene Oxide (EO) and *N,N*-Diallylglycidylamine (DAGA) Obtained from ^{1}H NMR Spectroscopy and SEC[a]

no.	composition (NMR)	DAGA[b]/%	$M_{n,NMR}$[b]/ g mol^{-1}	$M_{n,SEC}$[c]/ g mol^{-1}	M_w/M_n[c]
1	$PDAGA_{20}$	100	3000	1400	1.20
2	$mPEG_{45}$-*b*-$PDAGA_{10}$		3500	3200	1.08
3	$mPEG_{113}$-*b*-$PDAGA_5$		6000	4500	1.05
4	$mPEG_{113}$-*b*-$PDAGA_{15}$		7300	5200	1.04
5	$mPEG_{113}$-*b*-$PDAGA_{17}$		7600	6300	1.11
6	PEG_{98}-*co*-$PDAGA_3$	2.5	4700	3800	1.08
7	PEG_{154}-*co*-$PDAGA_8$	5	7400	5100	1.08
8	PEG_{160}-*co*-$PDAGA_{11}$	6	8800	5800	1.11
9	PEG_{113}-*co*-$PDAGA_{10}$	8	6500	3400	1.19
10	PEG_{42}-*co*-$PDAGA_4$	9	2600	1800	1.18
11	PEG_{128}-*co*-$PDAGA_{30}$	19	10300	3800	1.13
12	PEG_{90}-*co*-$PDAGA_{28}$	24	8200	2800	1.08

[a]For SEC elugrams see Figures S5 and S6 in the Supporting Information. [b]Calculated from ^{1}H NMR spectra. [c]Determined by SEC-RI in DMF.

During block copolymer formation, partial isomerization of the double bonds from allyl to *cis*- and *trans*-propenyl moieties was observed. This behavior is known from allylamines under harsh basic conditions.[45−47] The degree of isomerization was calculated using ^{1}H NMR, comparing the integrals of the signals representing all incorporated DAGA units (signals a and b in Figure 6, (1)), with those representing the propenyl groups (signal d in Figure 6, (1)). It was shown to depend on both temperature and counterion. We assume isomerization to take place at DAGA units positioned at the propagating chain end only (see online 1H NMR kinetics section).

Using initiators deprotonated by cesium hydroxide monohydrate, the degree of isomerization increased with temperature, from 5% at 70 °C to 53% at 100 °C. This finding is in agreement with observations on double-bond isomerization in allyl glycidyl ether polymerization made by Lee et al.,[48] although one has to note that in the case of DAGA both *cis*- and *trans*-isomers are formed with no observable trend

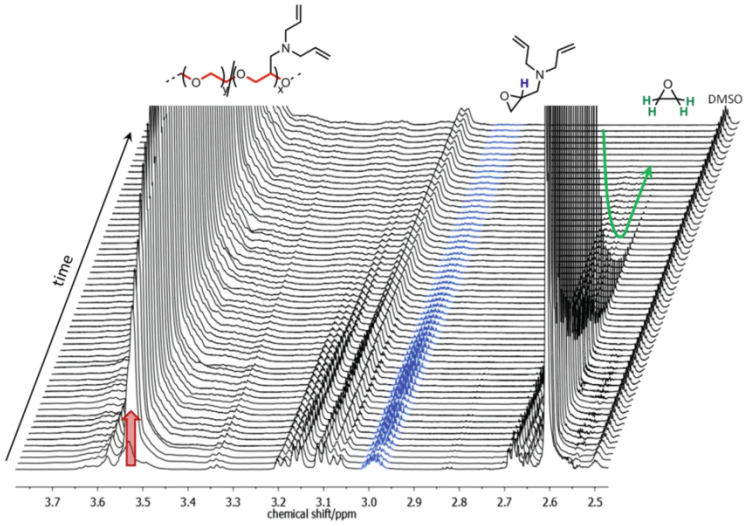

Figure 1. Time-resolved 400 MHz ^{1}H NMR spectra for random copolymerization of EO and DAGA (16%) at 40 °C with highlighted signals for polymer backbone and comonomers.

concerning a relationship between *cis*/*trans* ratio and temperature.

Maintaining the reaction temperature constant at 90 °C and using different deprotonating agents, viz. sodium hydride, potassium methoxide, and cesium hydroxide monohydrate, a dependence of the degree of isomerization on the counterion was revealed. While both potassium and cesium led to an isomerization degree of 39%, the presence of the counterion sodium resulted in no change of double-bond structure at all according to ^{1}H NMR characterization. One may speculate whether this might be caused by sodium lacking any d-orbitals, thereby impeding excessive interaction of the alkali metal cation with the lone pair of nitrogen and π-orbitals of the double bond. From another point of view, the character of the ion pair alkali metal ion−alkoxide might serve as an explanation. Sodium (Na^+) is smaller and better solvated compared to its larger, less solvated homologues (K^+, Cs^+). Because of lower interaction and larger distance between counterion and propagating chain end, one may assume that interaction of a sodium cation with terminal DAGA units is less likely, resulting in a pronounced decrease in tendency for isomerization.

By tuning both parameters—temperature and counterion—the amount of isomerized double bonds can be adjusted. Deprotection of amino groups carrying propenyl groups is achieved via acidic hydrolysis, leaving the remaining *N*-allyl moieties unaltered. Following this strategy, double functional polymers with adjustable number and ratio of primary amino groups to terminal allylic double bonds are easily obtained in one pot, offering an alternative to the hydroxy- and allyl-functional polyethers presented by Hawker and co-workers.[48]

Concurrent Anionic Ring-Opening Polymerization of EO and DAGA. Based on initiation of the cesium salt of 2-methoxyethanol or 2-benzyloxyethanol, DAGA was copolymerized with EO concurrently. Analytical data of the obtained copolymers are summarized in Table 1. Determination of absolute molecular weights using ^{1}H NMR spectra revealed elevated molecular weights compared to the targeted values, especially when using 2-methoxyethanol as an initiator. This may be attributed to incomplete dissolution of the cesium alkoxide even in DMSO, resulting in a reduced actual initiator concentration. Because of a certain signal overlap, the error of NMR determination is estimated to be ±10%. While keeping the number of repeating units constant, an increase in DAGA content corresponds to a higher molecular weight due to the mass of the side chains (e.g., 24 mol % DAGA add up to 52 wt %). Additionally, this leads to an increased hydrophobicity of the polymer chain as compared to the PEG standards used for SEC measurements. Thus, underestimation of molecular weights in SEC measurements becomes more pronounced with increasing DAGA fraction.

Online ^{1}H NMR Copolymerization Kinetics. In order to disclose the copolymer microstructure and distribution of functional groups at the backbone, online polymerization monitoring was carried out, recording ^{1}H NMR spectra of a reaction mixture in DMSO-d_6 in a conventional NMR tube sealed under high vacuum in intervals of 30 s.[42] In order to permit precise determination of the degree of polymerization, 2-benzyloxyethanol was used as an initiator, providing five protons in the aromatic region well-suited for integration and referencing purposes. The polymerization was conducted in a preheated NMR spectrometer with a DAGA fraction of 16%. Within the course of preceding studies, copolymerization temperature was not found to exert any remarkable influence on relative reactivities of epoxide monomers in anionic ring-opening polymerization;[33,42] hence, it was fixed to 40 °C in order to mimic polymerization conditions in the flask.

Monomer consumption and changes in the remaining monomer composition were followed by integration of the respective signals (Figure 1). EO consumption was monitored by integration of the methylene signal (4H, 2.61 ppm). DAGA

conversion could be determined by comparison of the signal generated by the methine proton of the epoxide ring (e, 1H, 3.02−2.93 ppm) (representing monomeric DAGA) with the combined signal of methine protons of the double bond (a and b, 2H, 6.00−5.50 ppm), representing the total amount of DAGA present. Finally, growth of the polymer backbone was observed by an evolving signal at around 3.5 ppm.

The copolymerization was found to proceed rapidly at 40 °C, with >95% total conversion after 63 min (Figure 2). Because of

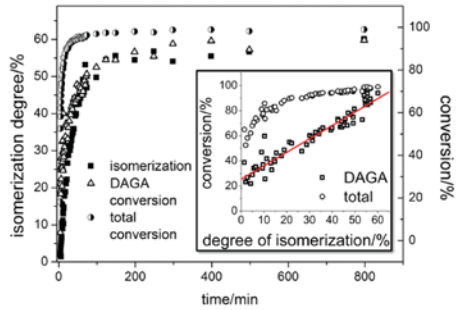

Figure 2. Monomer conversion and degree of isomerization versus time plots for copolymerization of ethylene oxide and *N,N*-diallylglycidylamine (16%) at 40 °C in DMSO-d_6. Inset: plot of total and DAGA conversion versus isomerization degree. Spheres: total conversion; squares: DAGA conversion; red line: linear fit of experimental data of DAGA conversion.

the asymmetry of the sealed NMR tube, spinning is not possible in this method. Nevertheless, the obtained polymer exhibited a narrow molecular weight distribution (M_w/M_n = 1.12, DMF, RI detection, PEG standards; Figure S18), pointing to negligible mixing and diffusion issues. Furthermore, virtually nonexistent chain transfer can be assumed for these reaction conditions (cf. Supporting Information).

Tracing the evolution of monomer feed composition (Figure 3) in the initial stages of polymerization, the data show that EO becomes incorporated into the growing polymer chain more rapidly than DAGA. The DAGA fraction remains slightly below the corresponding initial monomer feed ratio of 16%, reaching

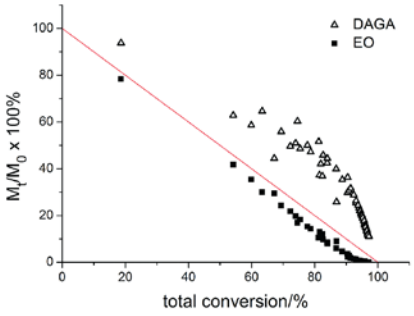

Figure 3. Percentage of initial monomer concentration of ethylene oxide and *N,N*-diallylglycidylamine (16%) versus total conversion for copolymerization at 40 °C in DMSO-d_6.

this value toward the end of the reaction. In conclusion, copolymers with a tapered structure are obtained.

Online monitoring of the polymerization also allows for a more detailed analysis of the 1,3-hydrogen shift, leading to isomerization of *N*-allyl to *N*-propenyl moieties. Comparing the emergence of isomerized double bonds with the conversion of the DAGA monomer over time, both processes seem to take place simultaneously (Figure 2). The linear relationship between the degree of isomerization and DAGA conversion (Figure 2, inset) is not found when comparing to total conversion of this copolymerization. Additionally, further heating of the reaction mixture does not change the degree of isomerization significantly. Accounting for the above-mentioned results on the influence of counterions on isomerization during block copolymer formation, it can be assumed that double-bond isomerization takes place at DAGA units located at the living terminus of a polymer chain only. We assume that interaction of comonomer allyl side chains with the alkali metal ions is involved in this process.

^{13}C NMR Characterization of Copolymer Microstructure. Detailed characterization of the random copolymer microstructures also demands ^{13}C NMR triad analysis. The relevant regions of the spectra are highlighted in Figure 4. On

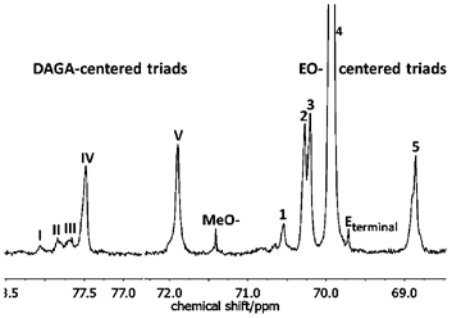

Figure 4. ^{13}C NMR spectrum (75.5 MHz, DMSO-d_6) of PEG_{128}-*co*-$PDAGA_{30}$ (19% comonomer; run 11, Table 1), regions characteristic for DAGA CH (I−IV) and CH_2 (V) backbone signals and EO CH_2 backbone signals. Signal assignment: (I) D-D_b-D, (II) D-D_b-E, (III) E-D_b-D, (IV) E-D_b-E, (V) E-D_a-E; (1) D-E_b-D, (2) D-E_b-E, (3) E-E_b-D, (4) E-E_a-E + E-E_b-E, (5) D-E_a-D + D-E_a-E; (MeO−) initiator signal, ($E_{terminal}$) E_b−OH.

the left-hand side of the figure, signals generated by the carbon atoms in DAGA (D)-centered triads are found while EO (E)-centered triads are located on the right (complete ^{13}C NMR data are available from the Supporting Information, Figure S7). Peak assignment was performed with reference to literature data on random EO/oxirane copolymers[42,49−51] and comparison with block- and homopolymers as well as calculated spectra. Nomenclature of the carbon atoms was adopted from cited work,[42,49−51] a and b representing first and second $CH_{(2)}$ groups of central monomer units, respectively. Upon incorporation of increasing DAGA amounts, signal splitting of the tertiary carbon peak at 77.5 ppm becomes increasingly pronounced, indicating a parallel existence of a mixture of possible triads. Taking a closer look at the triad distribution, their abundance can be roughly sorted in E-D-E > D-D-E ≅ E-D-D > D-D-D, although inverse gated experiments were not

dx.doi.org/10.1021/ma300292m | *Macromolecules* 2012, 45, 4581−4589

carried out due to considerable signal overlap. This order equals the sequence one would expect from random or gradient copolymers. Together with an increasing intensity of the E-D_a-E triad signal with increasing DAGA content, ^{13}C NMR supports absence of a copolymer composed of blocky segments.

Thermal Behavior. In order to further evaluate the properties of the copolymers PEG-*co*-PDAGA and to confirm the conclusions on the microstructure of the polymer chains, their thermal behavior in bulk and in aqueous solution was studied by means of differential scanning calorimetry (DSC) and turbidimetric measurements.

PEG and its copolymers are known to exhibit lower critical solution temperature (LCST) behavior in water (Figure 5).[13,52−62,69−71] The LCSTs found were in the range of 29−94 °C, depending on the amount of the apolar DAGA monomer in the chain (cf. Table 2). Plotting the cloud points of PEG-*co*-PDAGA copolymers over the incorporated DAGA fraction results in a linear correlation (Figure S9, Supporting Information). Thus, the temperature at which the sharp transition from translucent to opaque takes place can be tailored by variation of comonomer fractions in the polymer. Fitting of the experimental data and interpolation of the data to a comonomer content of 0%, i.e. PEG homopolymer, results in a theoretical cloud point of 89 °C. This value differs considerably from the literature value for PEG of comparable molecular weight.[52,62] Taking analyses of ^1H NMR online kinetic measurements as well as previous work on LCST behavior of random PEG-based structures[54] into account, this can be understood as further support for our assumption that this shifted linear behavior is induced by a compositional drift in the chain.

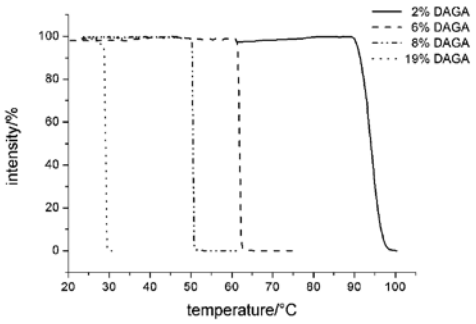

Figure 5. Transmitted laser light intensity plotted versus solution temperature for PEG-*co*-PDAGA copolymers in aqueous solution, c = 20 mg mL^{-1}.

Concerning bulk properties, the PEG homopolymer is a highly crystalline material. Examining the behavior of PEG-*co*-PDAGA in bulk visually, going from 2% to 24% comonomer content, the materials' appearance changes from a powder to highly viscous liquids at room temperature. DSC measurements reveal gradually decreasing glass transition temperatures, melting temperatures, and melting enthalpies for increasing amounts of DAGA present in the polymer. An interesting feature of these measurements is that linear interpolation of the melting point data to a comonomer content of 0% is in excellent agreement with data reported for mPEG 5000 (Table 2).[63] If a block-type structure had been obtained from the copolymerization reaction, one would expect a melting point for the PEG segments close to the melting point of PEG. The linear, gradual character of the decrease of the melting point is another indication that DAGA is incorporated throughout the polymer chain in a gradient manner, without the occurrence of prolonged stretches of EO repeating units.

Deprotection and Release of Amino Functionalities. The general pathway for the cleavage of *N*-allyl protecting groups includes two steps (Scheme 3): Quantitative isomerization of the allylamine into an enamine, fostered by the favorable equilibrium between these systems and subsequent

Scheme 3. Synthetic Scheme for Isomerization and Cleavage of *N*-Allyl Protecting Groups as Well as Subsequent Reaction of Amino Groups with Acetic Anhydride

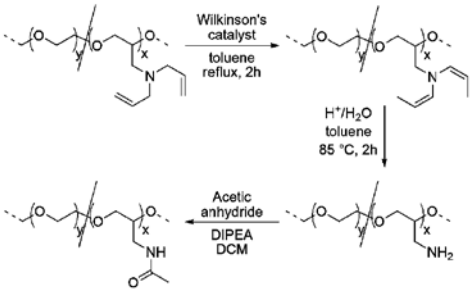

Table 2. Thermal Properties of Copolymers PEG-*co*-PDAGA in Bulk and Aqueous Solution obtained from Differential Scanning Calorimetry (DSC) and Turbidimetry (/ Not Determined; − Not Existent)

composition (NMR)	DAGA[a]/%	cp/°C	T_g[c]/°C	T_{rc}[d]/°C	T_m[e]/°C	ΔH^f/J g^{-1}
$mPEG_{113}$	0	−[g]	−65.0[h]	−	53.2[i]	195.1[i]
PEG_{136}-*co*-$PDAGA_3$	2	94.0	/	/	/	/
PEG_{98}-*co*-$PDAGA_3$	2.5	/	−55.9	−	41.8	97.6
PEG_{160}-*co*-$PDAGA_{11}$	6	62.0	−61.7	−	36.8	64.9
PEG_{294}-*co*-$PDAGA_{14}$	7	/	−64.5	−	34.9	61.1
PEG_{113}-*co*-$PDAGA_{10}$	8	50.5	/	/	/	/
PEG_{128}-*co*-$PDAGA_{50}$	19	29.0	−69.2	−41.6	−5.0	19.4

[a]Percentage of comonomer incorporated, determined from ^1H NMR. [b]c = 20 mg mL^{-1}. [c]Glass transition temperature. [d]Recrystallization temperature. [e]Melting temperature. [f]Melting enthalpy, determined via integration of the melting signal. [g]No cloud point observed under chosen conditions (20 mg mL^{-1}, 20−100 °C, 1 K min^{-1}). [h]Taken from the literature.[64] [i]Taken from the literature.[63]

dx.doi.org/10.1021/ma300292m | *Macromolecules* 2012, 45, 4581−4589

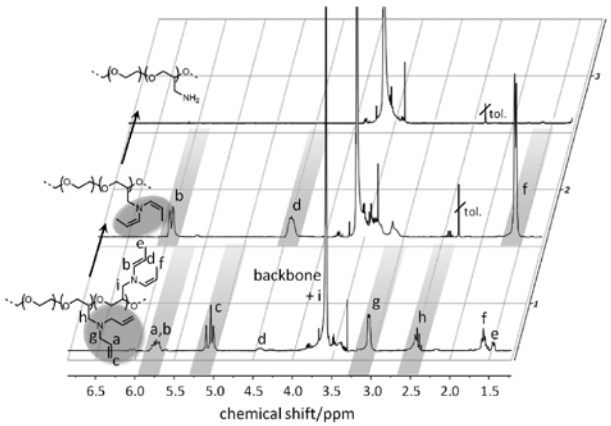

Figure 6. ^{1}H NMR spectra (300 MHz, $CDCl_3$) of a block copolymer of poly(ethylene glycol) monomethyl ether and *N,N*-diallylglycidylamine (1) after polymerization, (2) after isomerization of the double bonds with Wilkinson's catalyst ($RhCl(PPh_3)_3$), and (3) after liberation of the primary amino groups via acidic hydrolysis.

cleavage of the enamine upon hydrolysis.[45,65] For both gradient and block copolymers, Wilkinson's catalyst [$RhCl(PPh_3)_3$] effected full isomerization of the double bonds, as concluded from ^{1}H NMR. Interestingly, only the *cis* isomer has been observed after this treatment. This might be explained by an initial coordination of the transition metal center of the complex to a nitrogen lone pair, followed by a 1,3-hydrogen shift via a π-allyl intermediate formed by oxidative addition of the allylic C−H bond to the metal and a consecutive final reductive elimination step.

Subsequent treatment of the material under acidic hydrolysis conditions results in formal substitution of all propenyl groups by hydrogen, thus yielding the desired amine functionalities at the poly(ethylene glycol)−poly(glycidyl amine) (PEG−PGA) copolymer chain. It has proven beneficial to remove a small portion of the solvents via distillation in order to strip off evolving propanal from the reaction mixture, thus avoiding imine formation. Successful hydrolysis in high yields (>85%) can be deduced from ^{1}H NMR spectra due to the absence of allyl or propenyl signals (a−g; Figure 6), supported qualitatively by ninhydrin tests (Figure S8, Supporting Information).[66] Liberation of the amines, including isomerization and hydrolysis, can also be carried out in a one-pot procedure without necessity for an intermediate work-up of the isomerized polymer. Facile deprotection is considered a key feature of the new comonomer DAGA.

Accessibility of the primary amino groups at the PEG chains for further modification was demonstrated by derivatization with acetic anhydride. In ^{1}H NMR, the emergence of the additional methyl group could be observed. Comparison of SEC elugrams of PEG-*co*-PDAGA as well as PEG-*co*-PGA reacted with acetic anhydride results in preservation of the molecular weight and retained low polydispersity (Figure S10, Supporting Information).

■ CONCLUSIONS

We have described the first application of the allyl-protected amino-functional epoxide monomer *N,N*-diallylglycidylamine (DAGA) for use in anionic ring-opening copolymerization with ethylene oxide, resulting in well-defined random and block copolymer structures. The fraction of amino-functional comonomer was varied from 2.5 to 24%, and the resulting copolymer microstructure was studied by online ^{1}H NMR monitoring, ^{13}C NMR triad analysis, differential scanning calorimetry, and turbidimetry. Formation of block-like structures could be excluded, although a certain gradient character of the composition was observed in the course of the copolymerization. Facile deprotection in a two-step one-pot procedure via isomerization of allylamine to enamine moieties and subsequent acidic hydrolysis was demonstrated, independent of the copolymer structure. The obtained primary amines were derivatized using acetic anhydride in a model reaction, proving accessibility for coupling reactions.

Compared to the earlier concept of *N,N*-dibenzyl protecting groups,[42] this approach possesses major advantages for the preparation of multiamino-functional poly(ethylene glycol)s via protected glycidylamines: (i) the monomer, DAGA, can be obtained in a facile one-step procedure on a large scale, (ii) time for deprotection is reduced from 1 to 8 days to 4 h, (iii) yields improved from 30 to 50% to over 85%, and (iv) most importantly, the synthesis grants first time access not only to gradient but also to block copolymers of ethylene oxide and glycidylamine with narrow polydispersities via living AROP.

The obtained materials offer intriguing potential regarding new architectural possibilities and applications in biomedicine as hybrid materials and cross-linkers. Furthermore, in the field of homogeneous polymer-supported catalysts and reagents, multiple amino groups may serve as anchors for active compounds, while the PEG block ensures easy separation of low-molecular-weight product and polymer-bound reagent via precipitation or dialysis.

■ ASSOCIATED CONTENT

Supporting Information

Additional data, SEC elugrams, and NMR spectra. This material is available free of charge via the Internet at http://pubs.acs.org.

AUTHOR INFORMATION

Corresponding Author

*E-mail: hfrey@uni-mainz.de.

Notes

The authors declare no competing financial interest.

ACKNOWLEDGMENTS

We thank Dr. Mihail Mondeshki for NMR measurements and Dennis Sauer and Colin Drabe for technical assistance. V.S.R. and B.O. are grateful to the Fonds der Chemischen Industrie (FCI) for a fellowship and to the Graduate School "Materials Science in Mainz" for funding. V.S.R. acknowledges valuable financial support from the Gutenberg-Akademie der Johannes Gutenberg-Universität Mainz. C.D. is thankful to the Max Planck Graduate Center mit der Johannes Gutenberg-Universität Mainz for a fellowship.

REFERENCES

(1) Feng, C.; Lu, C.; Chen, Z.; Dong, N.; Shi, J.; Yang, G. *J. Heterocycl. Chem.* **2010**, *47*, 671−676.
(2) Gravert, D. J.; Janda, K. D. *Chem. Rev.* **1997**, *97*, 489−510.
(3) Huang, Y.; Lu, C.; Chen, Z.; Yang, G. *J. Heterocycl. Chem.* **2007**, *44*, 1421−1424.
(4) Osburn, P. L.; Bergbreiter, D. E. *Prog. Polym. Sci.* **2001**, *26*, 2015−2081.
(5) Porcheddu, A.; Ruda, G. F.; Sega, A.; Taddei, M. *Eur. J. Org. Chem.* **2003**, *2003*, 907−912.
(6) Rao, Z.; Peng, H.; Yang, G.; Chen, Z. *Comb. Chem. High Throughput Screening* **2006**, *9*, 743−746.
(7) Toy, P. H.; Janda, K. D. *Acc. Chem. Res.* **2000**, *33*, 546−554.
(8) Xiang, F.-Y.; Lu, C.-F.; Yang, G.-C.; Chen, Z.-X. *Chin. J. Chem.* **2008**, *26*, 543−546.
(9) Yan, X.; Yu, J.; Ye, R.; Chen, Z.; Yang, G. *Lett. Org. Chem.* **2007**, *4*, 239−241.
(10) Yang, G.; Chen, Z.; Zhang, H. *Green Chem.* **2003**, *5*, 441−442.
(11) Yang, G.-C.; Chen, Z.-X.; Zhang, Z.-J. *React. Funct. Polym.* **2002**, *51*, 1−6.
(12) Zhang, H.; Yang, G.; Chen, J.; Chen, Z. *Synthesis* **2004**, 3055−3059.
(13) Dickerson, T. J.; Reed, N. N.; Janda, K. D. *Chem. Rev.* **2002**, *102*, 3325−3344.
(14) Grinberg, S.; Kasyanov, V.; Srinivas, B. *React. Funct. Polym.* **1997**, *34*, 53−63.
(15) Terashima, T.; Ouchi, M.; Ando, T.; Sawamoto, M. *Polym. J.* **2011**, *43*, 770−777.
(16) Xiang, F.; Zhang, S.; Lu, C.; Chen, Z.; Yang, G. *Synth. Commun.* **2008**, *38*, 953−960.
(17) Fuertges, F.; Abuchowski, A. *J. Controlled Release* **1990**, *11*, 139−148.
(18) Pasut, G.; Veronese, F. M. *Adv. Drug Delivery Rev.* **2009**, *61*, 1177−1188.
(19) Levy, Y.; Hershfield, M. S.; Fernandez-Mejia, C.; Polmar, S. H.; Scudiery, D.; Berger, M.; Sorensen, R. U. *J. Pediatr.* **1988**, *113*, 312−317.
(20) Graham, M. L. *Adv. Drug Delivery Rev.* **2003**, *55*, 1293−1302.
(21) Kinstler, O.; Molineux, G.; Treuheit, M.; Ladd, D.; Gegg, C. *Adv. Drug Delivery Rev.* **2002**, *54*, 477−485.
(22) Rajender Reddy, K.; Modi, M. W.; Pedder, S. *Adv. Drug Delivery Rev.* **2002**, *54*, 571−586.
(23) Wang, Y.-S.; Youngster, S.; Grace, M.; Bausch, J.; Bordens, R.; Wyss, D. F. *Adv. Drug Delivery Rev.* **2002**, *54*, 547−570.
(24) Knop, K.; Hoogenboom, R.; Fischer, D.; Schubert, U. S. *Angew. Chem., Int. Ed.* **2010**, *49*, 6288−6308.
(25) Li, Z.; Chau, Y. *Bioconjugate Chem.* **2009**, *20*, 780−789.
(26) Zhou, P.; Li, Z.; Chau, Y. *Eur. J. Pharm. Sci.* **2010**, *41*, 464−472.
(27) Hrubý, M.; Koňák, Č.; Ulbrich, K. *J. Appl. Polym. Sci.* **2005**, *95*, 201−211.
(28) Hrubý, M.; Koňák, Č.; Ulbrich, K. *J. Controlled Release* **2005**, *103*, 137−148.
(29) Vetvicka, D.; Hruby, M.; Hovorka, O.; Etrych, T.; Vetrik, M.; Kovar, L.; Kovar, M.; Ulbrich, K.; Rihova, B. *Bioconjugate Chem.* **2009**, *20*, 2090−2097.
(30) Koyama, Y.; Yamashita, M.; Iida-Tanaka, N.; Ito, T. *Biomacromolecules* **2006**, *7*, 1274−1279.
(31) Sakae, M.; Ito, T.; Yoshihara, C.; Iida-Tanaka, N.; Yanagie, H.; Eriguchi, M.; Koyama, Y. *Biomed. Pharmacother.* **2008**, *62*, 448−453.
(32) Yoshihara, C.; Shew, C.-Y.; Ito, T.; Koyama, Y. *Biophys. J.* **2010**, *98*, 1257−1266.
(33) Mangold, C.; Wurm, F.; Obermeier, B.; Frey, H. *Macromolecules* **2010**, *43*, 8511−8518.
(34) Jeffamines are distributed by Huntsman International LLC.
(35) Obermeier, B.; Wurm, F.; Mangold, C.; Frey, H. *Angew. Chem., Int. Ed.* **2011**, *50*, 7988−7997.
(36) Taton, D.; Le Borgne, A.; Sepulchre, M.; Spassky, N. *Macromol. Chem. Phys.* **1994**, *195*, 139−148.
(37) Ringsdorf, H. *J. Polym. Sci., Polym. Symp.* **1975**, *51*, 135−153.
(38) Koyama, Y.; Umehara, M.; Mizuno, A.; Itaba, M.; Yasukouchi, T.; Natsume, K.; Suginaka, A.; Watanabe, K. *Bioconjugate Chem.* **1996**, *7*, 298−301.
(39) Obermeier, B.; Frey, H. *Bioconjugate Chem.* **2011**, *22*, 436−444.
(40) Gervais, M.; Brocas, A.-L.; Cendejas, G.; Deffieux, A.; Carlotti, S. *Macromolecules* **2010**, *43*, 1778−1784.
(41) Meyer, J.; Keul, H.; Möller, M. *Macromolecules* **2011**, *44*, 4082−4091.
(42) Obermeier, B.; Wurm, F.; Frey, H. *Macromolecules* **2010**, *43*, 2244−2251.
(43) Failla, L.; Massaroli, G.; Scuri, R.; Signorelli, G. *Farmaco Sci.* **1964**, *19*, 269−285.
(44) Hans, M.; Keul, H.; Möller, M. *Polymer* **2009**, *50*, 1103−1108.
(45) Escoubet, S.; Gastaldi, S.; Bertrand, M. *Eur. J. Org. Chem.* **2005**, *2005*, 3855−3873.
(46) Price, C. C.; Snyder, W. E. *Tetrahedron Lett.* **1962**, *3*, 69−73.
(47) Musorin, G. K. *Russ. J. Org. Chem.* **2003**, *39*, 915−918.
(48) Lee, B. F.; Kade, M. J.; Chute, J. A.; Gupta, N.; Campos, L. M.; Fredrickson, G. H.; Kramer, E. J.; Lynd, N. A.; Hawker, C. J. *J. Polym. Sci., Part A: Polym. Chem.* **2011**, *49*, 4498−4504.
(49) Hamaide, T.; Goux, A.; Llauro, M.-F.; Spitz, R.; Guyot, A. *Angew. Makromol. Chem.* **1996**, *237*, 55−77.
(50) Heatley, F.; Yu, G.; Booth, C.; Blease, T. G. *Eur. Polym. J.* **1991**, *27*, 573−579.
(51) Rejsek, V.; Sauvanier, D.; Billouard, C.; Desbois, P.; Deffieux, A.; Carlotti, S. *Macromolecules* **2007**, *40*, 6510−6514.
(52) Saeki, S.; Kuwahara, N.; Nakata, M.; Kaneko, M. *Polymer* **1976**, *17*, 685−689.
(53) Kjellander, R.; Florin, E. *J. Chem. Soc., Faraday Trans. 1* **1981**, *77*, 2053−2077.
(54) Mangold, C.; Obermeier, B.; Wurm, F.; Frey, H. *Macromol. Rapid Commun.* **2011**, *32*, 1930−1934.
(55) Louai, A.; Sarazin, D.; Pollet, G.; François, J.; Moreaux, F. *Polymer* **1991**, *32*, 703−712.
(56) Persson, J.; Johansson, H.-O.; Tjerneld, F. *Ind. Eng. Chem. Res.* **2000**, *39*, 2788−2796.
(57) Kurzbach, D.; Reh, M. N.; Hinderberger, D. *ChemPhysChem* **2011**, *12*, 3566−3572.
(58) Dworak, A.; Trzebicka, B.; Walach, W.; Utrata, A.; Tsvetanov, C. *Macromol. Symp.* **2004**, *210*, 419−426.
(59) Halacheva, S.; Rangelov, S.; Tsvetanov, C. *Macromolecules* **2006**, *39*, 6845−6852.
(60) Dilip, M.; Griffin, S. T.; Spear, S. K.; Rodríguez, H.; Rijksen, C.; Rogers, R. D. *Ind. Eng. Chem. Res.* **2010**, *49*, 2371−2379.
(61) Dormidontova, E. E. *Macromolecules* **2004**, *37*, 7747−7761.
(62) Bailey, F. E.; Callard, R. W. *J. Appl. Polym. Sci.* **1959**, *1*, 56−62.
(63) Yan, J.; Ye, Z.; Chen, M.; Liu, Z.; Xiao, Y.; Zhang, Y.; Zhou, Y.; Tan, W.; Lang, M. *Biomacromolecules* **2011**, *12*, 2562−2572.

(64) Brandrup, J.; Immergut, E. H.; Grulke, E. A. *Polymer Handbook*, 4th ed.; Wiley-Interscience: New York, 1999; p VI-253.
(65) Krompiec, S.; Krompiec, M.; Penczek, R.; Ignasiak, H. *Coord. Chem. Rev.* **2008**, *252*, 1819−1841.
(66) Schwetlick, K. In *Organikum*, 21st ed.; Wiley-VCH: Weinheim, 2001; p 695.
(67) Dingels, C.; Schömer, M.; Frey, H. *Chem. Unserer Zeit* **2011**, *45*, 338−349.
(68) N,N-Diallyl-N-(oxiran-2-ylmethyl)amine is available from Evoblocks, Inc. (catalog number EB14321).
(69) Chen, H.; Jia, Z.; Yan, D.; Zhu, X. *Macromol. Chem. Phys.* **2007**, *208*, 1637−1645.
(70) Jia, Z.; Chen, H.; Zhu, X.; Yan, D. *J. Am. Chem. Soc.* **2006**, *128*, 8144−8145.
(71) Zhou, Y.; Yan, D.; Dong, W.; Tian, Y. *J. Phys. Chem. B* **2007**, *111*, 1262−1270.

A.5 Branched Acid-Degradable, Biocompatible Polyether Copolymers via Anionic Ring-Opening Polymerization Using an Epoxide Inimer

Chistine Tonhauser,[1, 2] Christoph Schüll,[1, 2] Carsten Dingels,[2] and Holger Frey*[2]

[1]Graduate School Materials Science in Mainz, Staudingerweg 9, 55128 Mainz, Germany

[2]Institute of Organic Chemistry, Organic and Macromolecular Chemistry, Duesbergweg 10-14, Johannes Gutenberg-University Mainz, 55099 Mainz, Germany

Published in: *ACS Macro Lett.* **2012**, *1,* 1094.

ACS Macro Letters

Letter

pubs.acs.org/macroletters

Branched Acid-Degradable, Biocompatible Polyether Copolymers via Anionic Ring-Opening Polymerization Using an Epoxide Inimer

Christine Tonhauser,[†,‡] Christoph Schüll,[†,‡] Carsten Dingels,[‡] and Holger Frey*[,‡]

[†]Graduate School Materials Science in Mainz, Staudingerweg 9, 55128 Mainz, Germany

[‡]Institute of Organic Chemistry, Organic and Macromolecular Chemistry, Duesbergweg 10-14, Johannes Gutenberg-University Mainz, 55099 Mainz, Germany

Supporting Information

ABSTRACT: The introduction of acid-degradable acetal moieties into a hyperbranched polyether backbone has been achieved by the design of a novel epoxide-based degradable inimer. This new monomer, namely, 1-(glycidyloxy)ethyl ethylene glycol ether (GEGE), has been copolymerized in the anionic ring-opening polymerization (AROP) with ethylene oxide (EO) or glycidol (G), respectively, yielding branched polyethers, that is, P(EO-*co*-GEGE) and P(G-*co*-GEGE), that possess an adjustable amount of acid-cleavable acetal units. In addition, a novel class of multiarm star copolymers P(G-*co*-GEGE-*g*-EO) with acid-labile polyether core and PEG side chains was synthesized by using the P(G-*co*-GEGE) copolymers as multifunctional macroinitiators for AROP of EO. The new materials have been characterized in a detailed manner, revealing narrow to moderate molecular weight distributions. The degradation of these polymers under acidic conditions was characterized via SEC and ^{1}H NMR spectroscopy.

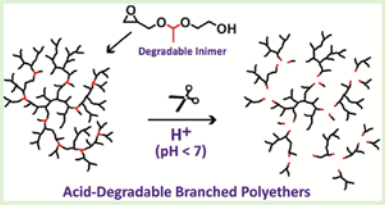

The use of biocompatible, nondegradable polymers in biomedical stealth applications, such as PEGylation,[1] is a well-established concept, which is widely explored in academia, but also finds increasing application in the pharmaceutical industry. A well-known example is Pegasys, which is PEGylated interferon used for the treatment of hepatitis C.[2] Although PEGylation and similar concepts based on linking polymers with protein or drugs are of increasing importance in future biomedical applications, the use of polymer−drug (or polymer−protein) conjugates is currently limited to a maximum molecular weight (40000 g/mol for PEG), as PEG can accumulate in the human body at higher molecular weight.[3] It is an important challenge to develop biocompatible polymers that degrade under physiological conditions. An acidic degradation mechanism of the respective polymer is favored.[4,5] Synthetic routes for acid-degradable PEG have been described in a few works to date, employing varying synthetic strategies. All of these routes rely on postpolymerization reactions,[6] and commonly an acetal moiety is used to guarantee the acid labile character. The most prominent example of an acid-labile PEG is "APEG", developed by Brocchini and Duncan, which is obtained by the acid-catalyzed reaction of diols and vinyl-ether moieties.[7] An unavoidable drawback for this interesting material is the rather broad molecular weight distribution due to the polycondensation kinetics involved.[8,9] Another approach was developed by Taton and co-workers,[10] who designed acid degradable PEG-based arborescent polymers. To this end, however, a demanding reaction sequence is required, comparable to a dendrimer synthesis. A similar concept was studied by Hawker et al.[11]

In this report, a novel acetal-containing inimer, namely, 1-(glycidyloxy)ethyl ethylene glycol ether (GEGE), and its use as a latent AB_2 monomer is described (Figure 1). Copolymerization with ethylene oxide (EO) and glycidol (G) yields long-chain branched and hyperbranched polyether polyols. In addition, PEO chains were grafted from P(G_n-*co*-$GEGE_{m}$) core molecules to obtain multiarm star polymers. The obtained polymer architectures were characterized using SEC and NMR spectroscopy and have been probed with respect to their

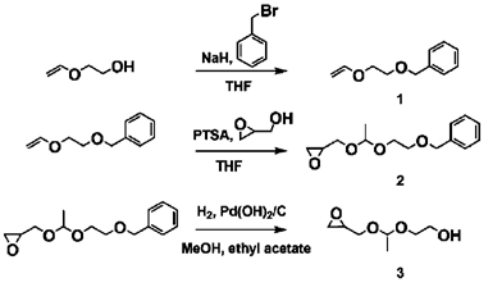

Figure 1. Strategy for the synthesis of the epoxide inimer 1-(glycidyloxy)ethyl ethylene glycol ether (GEGE), 3.

Received: May 25, 2012
Accepted: August 13, 2012

   dx.doi.org/10.1021/mz300265z | *ACS Macro Lett.* 2012, 1, 1094−1097

degradability, revealing a strong pH-dependence of the degradation kinetics.

A major challenge in synthesizing a PEG/PG-based polymer with base stable[12−15] but acid labile groups in the backbone in a single reaction step is the design of a suitable monomer (Figure 1). For the introduction of labile groups into a polyether backbone a so-called "degradable inimer" is required. The respective concept was first presented by Matyjaszewski et al. for vinyl monomers,[16,17] but has been hardly explored to date. In Figure 2, the ^{1}H NMR spectrum of GEGE is displayed. All

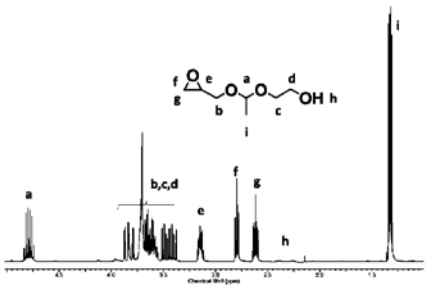

Figure 2. ^{1}H NMR spectrum of 1-(glycidyloxy)ethyl ethylene glycol ether in $CDCl_3$ (300 MHz).

signals can be assigned to the respective protons, verifying the structure of the novel compound.[14,19] Three different branched polyether architectures have been synthesized using GEGE as a key building block: (i) long-chain branched (P(EO_n-*co*-$GEGE_m$)), (ii) hyperbranched (P(G_n-*co*-$GEGE_m$)), and (iii) multiarm star (P(G_n-*co*-$GEGE_m$-*g*-EO_k)) polyethers. An overview of the different polymer topologies synthesized is given in Figure 3. Corresponding characterization data of all polymers are given in Table 1.

[P(EO-*co*-GEGE)]: For the copolymerization of GEGE with EO, the alkoxide of *N*,*N*-di(*p*-methoxy)-benzyl tris-(hydroxymethyl) aminomethane ((MeOBn$_2$)NTRIS) was prepared.[14,18,20−24] In all cases, narrow molecular weight distributions were obtained (M_w/M_n < 1.3), considering the branched structure of the product. The molecular weights of the polymers prepared ranged between 1800 and 2200 g mol^{-1}. The amount of GEGE in the monomer feed was varied from 5 to 20 mol %, which could be confirmed via ^{1}H NMR spectroscopy for the resulting copolymers. In contrast to previous works, no slow monomer addition (SMA) could be employed. For experimental reasons, there is no possibility to introduce the gaseous, toxic EO (bp 11 °C) steadily into a reaction flask with an inside temperature of 60 °C without severe safety issues. Therefore, both monomers were added to the initiator salt in a one-pot reaction, in analogy to a previously described procedure.[18] Because GEGE is an inimer, the formation of small oligomer side products was observed. In addition, the targeted molecular weight does not correspond to the obtained molecular weight.[18] These expected drawbacks given by the utilization of ethylene oxide as a comonomer are avoided, when employing glycidol as a comonomer (see the following paragraph). However, it is important to show that in principle copolymerization of GEGE with EO is feasible, given the high acceptance of PEG for biomedical stealth applications.

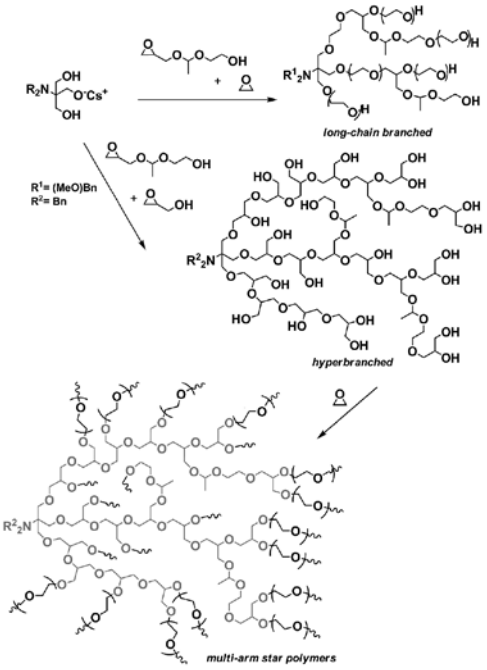

Figure 3. Overview of the different copolymerization routes developed based on the GEGE monomer.

Table 1. Overview on the Different Polymers Synthesized

No.	formula (NMR)	% GEGE (NMR)	M_n g/mol (NMR)	M_n g/mol (SEC)[a]	PDI (SEC)[a]
1	P(EO_{129}-*co*-$GEGE_8$)	5.8	6900	2200	1.3
2	P(EO_{129}-*co*-$GEGE_{13}$)	9.2	7800	2400	1.4
3	P(EO_{132}-*co*-$GEGE_{15}$)	10.3	8200	1800	1.3
4	P(G_{58}-*co*-$GEGE_4$)	6.4	4900	2300	1.9
5	P(G_{34}-*co*-$GEGE_{11}$)	24.4	4300	2400	1.8
6	P(G_{20}-*co*-$GEGE_{19}$)	38.7	4100	3100	1.6
7	P4-*g*-EO_{147}	5.7	10700	5800	1.4
8	P6-*g*-EO_{153}	9.8	10800	5200	1.6

[a]Obtained from the RI signal vs PEO standards.

[P(G-*co*-GEGE)]: On the other hand, the structural analogy of glycidol and GEGE allows for the controlled incorporation of GEGE into the hyperbranched polyglycerol[18,22] (*hb*PG) structure. PG is biocompatible, independent of architecture and molecular weight.[25−27] By SMA of a mixture of glycidol and GEGE in high dilution to the partially deprotonated initiator Bn$_2$TRIS, several (P(G-*co*-GEGE)) copolymers have been synthesized.

The molecular weight of the hyperbranched copolymers was characterized using SEC and ^{1}H NMR spectroscopy. In the ^{1}H NMR spectrum, the incorporation of GEGE into *hb*PG can be

quantified by comparing the integrals of the initiator (7.44–7.07 ppm), the signal of the acetal proton of GEGE (4.82 ppm) and the methyl group (1.35 ppm; Supporting Information (SI)). Overall, we find good agreement between the targeted values and the data obtained by NMR spectroscopy for all polymers (GEGE content of 5–38%). This is in accordance with the control over the copolymerization reaction in contrast to the above-mentioned findings for the copolymerization with EO. Because no oligomer side products were found, full conversion of the benzyl-protected amine initiator can be assumed. Thus, the number average molecular weight of the polymers can be calculated from a comparison of the signals of the initiator and the polyether backbone (4.11–3.42 ppm). In the SEC analysis, the molecular weight is usually underestimated, compared to results from ^{1}H NMR and the targeted values, due to the branched architecture and the presence of multiple hydroxyl functionalities. The copolymers show narrow to moderate PDIs (M_w/M_n = 1.6–1.9), with a monomodal distribution (Figure S4). These values are slightly higher than for conventional *hb*PG polymers, but still acceptable for some biomedical applications.[9] Although the use of glycidol as a comonomer resulted in controlled polymerization conditions, the maximum molecular weight that can be achieved is still limited. An additional class of degradable polymers has been synthesized and is discussed in detail in the following paragraph.

[P(G-*co*-GEGE-*g*-EO)]: Due to the limitation in achievable molecular weights of P(G-*co*-GEGE) (around 2000 g/mol) and P(EO-*co*-GEGE) (2000–3000 g/mol), poly(ethylene glycol) (PEG) was grafted from P(G-GEGE). The use of PG as a core for the synthesis of multiarm-star polymers with a polyether structure has been described previously by our group.[28−30] The molecular weight increase from sample **6** to sample **8** can be verified by SEC and NMR, which is displayed in the SI. The PEO multiarm star polymers exhibit molecular weights exceeding 10000 g/mol. NMR spectra can be measured in $CDCl_3$ and the solubility in this solvent confirms successful grafting of PEG. The PDIs obtained from SEC remain constant and are in line with the hyperbranched precursors (M_w/M_n < 1.6). A considerable deviation of the molecular weights obtained from NMR and the molecular weight obtained by SEC is observed. Besides enhancing the molecular weight of the polymers, grafting of PEG chains onto the branched polyethers also results in larger fragments formed during the degradation process of the copolymers.

To demonstrate that the acetal containing polyethers are stable in aqueous solution at neutral pH (pH = 7) at room temperature, polymer **2** was kept in D_2O for several weeks without observable degradation (compare SI). The absence of acetaldehyde, which would be formed during degradation of the polymers and would be observable at 2.12 and 9.58 ppm in D_2O (compare degradation kinetics), verifies the excellent stability of the polymers in neutral aqueous solution. Studying the degradation using SEC only does not allow for a quantitative investigation of the degradation kinetics, because the intensity of the RI signals is not only related to the polymer concentration but is also dependent on the molecular weight of the fragments. Therefore, we employed ^{1}H NMR spectroscopy in deuterated water at different pH values to determine the degradation behavior. All samples were kept at 37 °C to mimic physiological conditions. Sample **6** was measured in acidic D_2O (pH 4). A clear decrease of the acetal group concentration was observed within the first 8 h (Figure S11), but after 50%, the degradation stagnated completely. This was explained by the presence of acetaldehyde, which is formed during the degradation process. Due to the boiling point of 20 °C it should be released from the NMR tube, but due to the small surface area and the good water solubility of acetaldehyde, it was found to remain within the solution and prevented further degradation due to the resulting acetalization/hydrolysis equilibrium. Thus, the setup for degradation studies had to be changed and the samples were stirred in a round-bottom flask. In this case, full degradation of the polymers is observed, without stagnation. As expected, a strong dependence of the degradation kinetics on the pH is observed (Figure 4). When

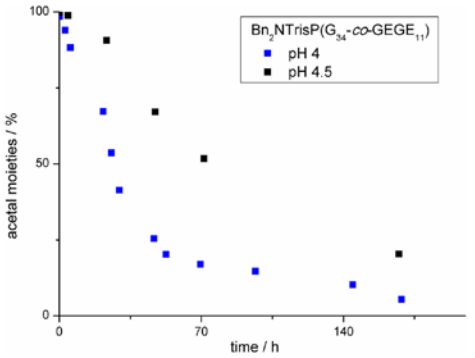

Figure 4. Decreasing acetal content dependent on pH reflects degradation of the acetal-containing polyethers.

an exponential decay to fit the slopes is used, the half-life time of the acetal groups can be calculated using Origin software (Figure S13). At pH 4.5, $t_{1/2}$ is approximately 76 h, while at pH 4, $t_{1/2}$ is less than half this value with 26 h.

With respect to biomedical applications, these materials appear to be interesting, because no degradation is observed at pH 7 or higher, guaranteeing storage stability. This means that in the bloodstream no molecular weight loss of the polyethers would be expected. However, in tissues with lower pH value, a decrease in the molecular weight and therefore an increase in the activity of the drug/protein attached should be observed. Covalent attachment of multiple reactive molecules (proteins or drugs) to the hydroxyl end groups is currently under investigation.

To the best of our knowledge, this represents the first synthesis of an acetal-containing epoxide inimer. The polymers obtained are promising in view of the combination of two properties, degradability and the biocompatibility, typical for aliphatic polyethers. Probing the degradability of the novel compounds revealed a strong pH-dependence of the half-life time of these polymers. Toxicity tests for the new materials are currently under way. We believe that acid labile materials mark a promising further development step for PEG and PG-based polyether structures for pharmaceutical application.

■ ASSOCIATED CONTENT

Supporting Information

Experimental details and additional supporting figures. This material is available free of charge via the Internet at http://pubs.acs.org.

AUTHOR INFORMATION

Corresponding Author

*E-mail: hfrey@uni-mainz.de.

Notes

The authors declare no competing financial interest.

ACKNOWLEDGMENTS

The authors thank Alina Mohr, Tim Dumslaff, Jochen Willersinn, and Margarete Deptolla for technical assistance. C.M. and C.S. are recipients of a fellowship through funding of the Excellence Initiative (DFG/GSC 266). C.D. is grateful to the Max Planck Graduate Center with the Johannes Gutenberg-Universität Mainz (MPGC) for a fellowship. H.F. acknowledges the Fonds der Chemischen Industrie and the SFB 625 for support.

REFERENCES

(1) Abuchowski, A.; McCoy, J. R.; Palczuk, N. C.; van Es, T.; Davis, F. F. *J. Biol. Chem.* **1977**, *252* (11), 3582−3586.
(2) Bailon, P.; Palleroni, A.; Schaffer, C. A.; Spence, C. L.; Fung, W.-J.; Porter, J. E.; Ehrlich, G. K.; Pan, W.; Xu, Z.-X.; Modi, M. W.; Farid, A.; Berthold, W.; Graves, M. *Bioconjugate Chem.* **2001**, *12* (2), 195−202.
(3) Knop, K.; Hoogenboom, R.; Fischer, D.; Schubert, U. S. *Angew. Chem.* **2010**, *122* (36), 6430−6452.
(4) Braunová, A.; Pechar, M.; Laga, R.; Ulbrich, K. *Macromol. Chem. Phys.* **2007**, *208* (24), 2642−2653.
(5) Tannock, I. F.; Rotin, D. *Cancer Res.* **1989**, *49* (16), 4373−4384.
(6) Reid, B.; Tzeng, S.; Warren, A.; Kozielski, K.; Elisseeff, J. *Macromolecules* **2010**, *43* (23), 9588−9590.
(7) Rickerby, J.; Prabhakar, R.; Ali, M.; Knowles, J.; Brocchini, S. *J. Mater. Chem.* **2005**, *15* (18), 1849−1856.
(8) Tomlinson, R.; Heller, J.; Brocchini, S.; Duncan, R. *Bioconjugate Chem.* **2003**, *14* (6), 1096−1106.
(9) Tomlinson, R.; Klee, M.; Garrett, S.; Heller, J.; Duncan, R.; Brocchini, S. *Macromolecules* **2002**, *35* (2), 473−480.
(10) Feng, X.; Chaikof, E. L.; Absalon, C.; Drummond, C.; Taton, D.; Gnanou, Y. *Macromol. Rapid Commun.* **2011**, *32* (21), 1722−1728.
(11) Satoh, K.; Poelma, J. E.; Campos, L. M.; Stahl, B.; Hawker, C. J. *Polym. Chem.* **2012**, *3*, 1890−1898.
(12) Tonhauser, C.; Wilms, D.; Wurm, F.; Berger-Nicoletti, E.; Maskos, M.; Löwe, H.; Frey, H. *Macromolecules* **2010**, *43* (13), 5582−5588.
(13) Hans, M.; Keul, H.; Möller, M. *Polymer* **2009**, *50* (5), 1103−1108.
(14) Mangold, C.; Wurm, F.; Obermeier, B.; Frey, H. *Macromol. Rapid Commun.* **2010**, *31* (3), 258−264.
(15) Gervais, M.; Brocas, A.-L.; Cendejas, G.; Deffieux, A.; Carlotti, S. *Macromolecules* **2010**, *43* (4), 1778−1784.
(16) Tsarevsky, N. V.; Huang, J.; Matyjaszewski, K. *J. Polym. Sci., Part A: Polym. Chem.* **2009**, *47* (24), 6839−6851.
(17) Rikkou-Kalourkoti, M.; Matyjaszewski, K.; Patrickios, C. S. *Macromolecules* **2012**, *45* (3), 1313−1320.
(18) Wilms, D.; Schömer, M.; Wurm, F.; Hermanns, M. I.; Kirkpatrick, C. J.; Frey, H. *Macromol. Rapid Commun.* **2010**, *31* (20), 1811−1815.
(19) Fitton, A. O.; Hill, J.; Jane, D. E.; Millar, R. *Synthesis* **1987**, *12*, 1140−1142.
(20) Burakowska, E.; Haag, R. *Macromolecules* **2009**, *42* (15), 5545−5550.
(21) Mangold, C.; Wurm, F.; Obermeier, B.; Frey, H. *Macromolecules* **2010**, *43* (20), 8511−8518.
(22) Sunder, A.; Hanselmann, R.; Frey, H.; Mülhaupt, R. *Macromolecules* **1999**, *32* (13), 4240−4246.
(23) Hanselmann, R.; Hölter, D.; Frey, H. *Macromolecules* **1998**, *31* (12), 3790−3801.
(24) Sunder, A.; Türk, H.; Haag, R.; Frey, H. *Macromolecules* **2000**, *33* (21), 7682−7692.
(25) Kainthan, R. K.; Janzen, J.; Levin, E.; Devine, D. V.; Brooks, D. E. *Biomacromolecules* **2006**, *7* (3), 703−709.
(26) Kainthan, R. K.; Hester, S. R.; Levin, E.; Devine, D. V.; Brooks, D. E. *Biomaterials* **2007**, *28* (31), 4581−4590.
(27) Kainthan, R. K.; Brooks, D. E. *Biomaterials* **2007**, *28* (32), 4779−4787.
(28) Doycheva, M.; Berger-Nicoletti, E.; Wurm, F.; Frey, H. *Macromol. Chem. Phys.* **2010**, *211* (1), 35−44.
(29) Knischka, R.; Lutz, P. J.; Sunder, A.; Mülhaupt, R.; Frey, H. *Macromolecules* **2000**, *33* (2), 315−320.
(30) Sunder, A.; Mülhaupt, R.; Frey, H. *Macromolecules* **2000**, *33* (2), 309−314.

A.6 Ferrocenyl Glycidyl Ether: A Versatile Ferrocene Monomer for Copolymerization with Ethylene Oxide to Water-Soluble, Thermo-Responsive Copolymers

Christine Tonhauser,[1, 2] *Arda Alkan,*[2, 3] *Martina Schömer,*[2] *Carsten Dingels,*[2] *Sandra Ritz,*[3] *Volker Mailänder,*[3] *Holger Frey,*[2] *Frederik Wurm**[3]

[1]Graduate School Materials Science in Mainz, Staudingerweg 9, D-55128 Mainz, Germany

[2]Institute of Organic Chemistry, Organic and Macromolecular Chemistry, Duesbergweg 10-14, Johannes Gutenberg-University Mainz (JGU), D-55099 Mainz, Germany

[3]Max Plack Institute or Polymer Research (MPI-P), Ackermannweg 10, D-55128 Mainz, Germany

Accepted for publication in: *Macromolecules* **2013**, DOI: 10.1021/ma302241w.

Note: The following pages contain the galley proofs of this article, which differ in minor details from the final version.

cxs00 | ACSJCA | JCA10.0.1465/W Unicode | research.3f (R3.4.i1:3887 | 2.0 alpha 39) 2012/09/13 09:54:00 | PROD-JCA1 | rq_858376 | 12/10/2012 14:55:07 | 9

Macromolecules

Article

pubs.acs.org/Macromolecules

Ferrocenyl Glycidyl Ether: A Versatile Ferrocene Monomer for Copolymerization with Ethylene Oxide to Water-Soluble, Thermoresponsive Copolymers

Christine Tonhauser,[†,‡] Arda Alkan,[‡,§] Martina Schömer,[‡] Carsten Dingels,[‡] Sandra Ritz,[§] Volker Mailänder,[§] Holger Frey,[‡] and Frederik R. Wurm*[,§]

[†]Graduate School Materials Science in Mainz, Staudinger Weg 9, D-55128 Mainz, Germany

[‡]Institute of Organic Chemistry, Organic and Macromolecular Chemistry, Duesbergweg 10-14, Johannes Gutenberg-Universität Mainz (JGU), D-55128 Mainz, Germany

[§]Max-Planck Institute for Polymer Research (MPI-P), Ackermannweg 10, D-55128 Mainz, Germany

Supporting Information

ABSTRACT: The first ferrocene-containing epoxide monomer, ferrocenyl glycidyl ether (fcGE), is introduced. The monomer has been copolymerized with ethylene oxide (EO). This leads to electroactive, water-soluble, and thermoresponsive poly(ethylene glycol) (PEG) derived copolyethers. Anionic homo- and copolymerization of fcGE with EO was possible. Molecular weights could be varied from 2000 to 10 000 g mol^{-1}, resulting in polymers with narrow molecular weight distribution (M_w/M_n = 1.07−1.20). The ferrocene (fc) content was varied from 3 to 30 mol %, obtaining water-soluble materials up to 10 mol % incorporation of the apolar ferrocenyl comonomer. Despite the steric bulk of fcGE, random copolymers were obtained, as confirmed via detailed ^{1}H NMR kinetic measurements as well as ^{13}C NMR studies of the polymer microstructure, including detailed triad characterization. In addition, the poly(fcGE) homopolymer has been prepared. All water-soluble copolyethers with fc side chains exhibited a lower critical solution temperature (LCST) in the range 7.2−82.2 °C in aqueous solution, depending on the amount of fcGE incorporated. The LCST is further tunable by oxidation/reduction of ferrocene, as demonstrated by cyclic voltammetry. Investigation of the electrochemical properties by cyclovoltammetry revealed that the iron centers can be oxidized reversibly. Further, to evaluate the potential for biomedical application, cell viability tests of the fc-containing PEG copolymers were performed on a human cervical cancer cell line (HeLa), revealing good biocompatibility only in the case of low amounts of fcGE incorporated (below 5%). Significant cytotoxic behavior was observed with fcGE content exceeding 5%. The ferrocene-substituted copolyethers are promising for novel redox sensors and create new options for the field of organometallic (co)polymers in general.

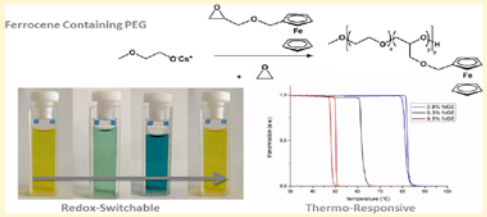

INTRODUCTION

Ferrocene (fc)-containing polymers[1] are interesting materials because of their unique physical and chemical properties such as redox-[2] and/or stimuli-responsive behavior.[3,4] Fc derivatives are used in (electro)catalysis[5] and in nonlinear optical polymers.[6] In addition, fc-containing materials may also become important for biomedical uses, since ferrocenyl moieties exhibit antineoplastic properties,[7,8] and the redox potential enables their utilization as amperometric glucose sensors.[9] Ferrocenyl groups can be incorporated into polymers either in the side chains or in the polymer backbone.[10−13] To date, the introduction of ferrocene units in polymers has relied mainly on two monomer structures, namely ferrocenophanes and vinylferrocene. Manners and co-workers introduced and intensively studied the controlled ring-opening polymerization of metallocenophanes[14,15] leading to poly(metallocenes) via different polymerization techniques and with variable bridging elements.[1] These elegant works rely on strict Schlenk techniques during monomer preparation, and the resulting polymers are usually not water-soluble. Therefore, they have to be converted into water-soluble derivatives via postpolymerization modification in most cases.[16]

The field of ferrocene side group polymers is currently dominated by monomers such as the above-mentioned vinylferrocene[12] but also ferrocenylmethyl (meth)acrylate.[13,17−19] Very recently, a series of (meth)acrylate (MA)-based monomers with varying spacers between fc and the MA unit have been introduced by Laschewsky and co-workers.[20] Other fruitful approaches to incorporate fc moieties in polymers are polymerization by hydrosilylation[21,22] or the

Received: October 29, 2012
Revised: December 5, 2012

dx.doi.org/10.1021/ma302241w | Macromolecules XXXX, XXX, XXX−XXX

introduction of amide linkages subsequent to the polymerization.[23]

Most of the above-mentioned strategies result in organo-soluble materials. Water-soluble fc-containing polymers have been reported in very few publications only. These approaches rely on the synthesis of block copolymers carrying highly hydrophilic segments, such as poly(2-(*N*,*N*-dimethylamino)-ethyl methacrylate) (at pH 8)[24] or poly(ethylene glycol) (PEG) attached to the fc-containing block.[25−27] Another approach capitalizes on the polymerization of fc-containing monomers with hydrophilic side chains, such as oligo(ethylene glycol)[28] or poly(electrolytes),[29,30] which lead to aqueous solubility with decreased aggregation behavior.

A versatile, yet unexplored approach is the random (co)polymerization of designed fc-based monomers with a hydrophilic comonomer, resulting in water-soluble (random) copolymers. Herein we present the first ferrocene-containing epoxide monomer that can be copolymerized and incorporated into polyether structures that differ significantly from all other fc-containing polymers reported to date. In this context we also present water-soluble poly(ethylene glycol) (PEG)-based copolymers bearing ferrocenyl side chains randomly distributed at the polyether backbone. The synthesis is based on the anionic homo- and copolymerization of ferrocenyl glycidyl ether (fcGE, **1**). Copolymerization was carried out with ethylene oxide, since PEG is an important water-soluble polymer (Scheme 1).

Scheme 1. Synthesis of Poly(ferrocenyl glycidyl ether) and Poly(ethylene glycol-*co*-ferrocenyl glycidyl ether) Homo- and Copolymers by Anionic Ring-Opening Polymerization

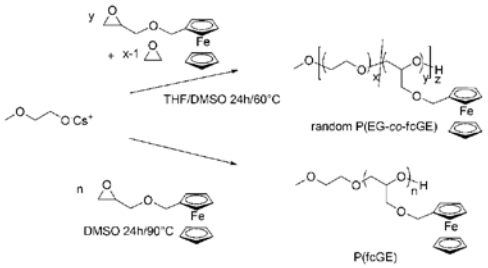

The polymers synthesized in this study have been investigated with respect to their properties, particularly aqueous solubility, thermoresponsive behavior,[31] and cytotoxicity as a function of the ferrocene content in the polyether. An interesting finding is that all water-soluble copolymers exhibit an LCST behavior. This LCST can be tailored by the fc content and further tuned by oxidation/reduction of the iron centers, resulting in multiresponsive structures.[32]

■ EXPERIMENTAL SECTION

Instrumentation. ^{1}H NMR spectra (300 and 400 MHz) and ^{13}C NMR spectra (75.5 MHz) were recorded using a Bruker AC300 or a Bruker AMX400. All spectra were referenced internally to residual proton signals of the deuterated solvent. For SEC measurements in DMF (containing 0.25 g/L of lithium bromide as an additive) an Agilent 1100 Series was used as an integrated instrument, including a PSS HEMA column ($10^6/10^5/10^4$ g/mol), a UV detector (275 nm), and a RI detector at a flow rate of 1 mL/min at 40 °C. Calibration was carried out using poly(ethylene oxide) standards provided by Polymer Standards Service. DSC measurements were performed using a PerkinElmer 7 series thermal analysis system and a PerkinElmer thermal analysis controller TAC 7/DX in the temperature range from −100 to 80 °C. Heating rates of 10 K min^{-1} were employed under nitrogen. Cloud points were determined in deionized water and observed by optical transmittance of a light beam (λ = 632 nm) through a 1 cm sample quartz cell. The measurements were performed in a Jasco V-630 photospectrometer with a Jasco ETC-717 Peltier element. The intensity of the transmitted light was recorded versus the temperature of the sample cell. The heating/cooling rate was 1 °C min^{-1}, and values were recorded every 0.1 °C. Cyclic voltammetry (CV) was performed using a BAS CV-50 W potentiostat using dichloromethane as a solvent under an inert atmosphere (N_2). The supporting electrolyte was tetrabutylammonium hexafluorophosphate (TBAH [0.1 M]). All experiments were performed at 25 °C in a conventional three-electrode cell, using a platinum working electrode (A 1/4 0.02 cm^2). All potentials are referred to a saturated calomel reference electrode (SCE). A coiled platinum wire was used as counter electrode.

Reagents. Solvents and reagents were purchased from Acros Organics, Sigma-Aldrich, or Fluka and used as received, unless otherwise stated. Chloroform-d_1, methanol-d_4, and DMSO-d_6 were purchased from Deutero GmbH. Ferrocenecarboxaldehyde and ferrocenemethanol were synthesized according to reported procedures.[33]

Synthesis. *Ferrocenyl Glycidyl Ether (fcGE, 1).* A synthesis pathway was developed relying on transformations known for other oxiranes.[34] In a typical reaction 5 g of ferrocenemethanol (23 mmol) was placed in a round-bottom flask, and 100 mL of benzene and 100 mL of a 50% NaOH solution were added. 1 g of tetrabutylammonium bromide (TBAB) was added as a phase transfer catalyst. To this mixture an excess of epichlorohydrin (4.3 g, 46 mmol) was added, while cooling the reaction mixture with ice. The solution was allowed to warm up to room temperature and rapidly stirred for 24 h. The progress of the reaction was followed by thin layer chromatography. The organic phase was washed with brine and $NaHCO_3$ solution, and the solvent was removed under vacuum. The crude product was purified by column chromatography using ethyl acetate and petroleum ether (3:7) as eluents. Besides the desired product (ferrocenyl glycidyl ether; R_f = 0.5), unreacted starting material (ferrocenemethanol; R_f = 0.2) was recovered and reused. The product was obtained as orange solid in typical yields of 70−80%. ^{1}H NMR (300 MHz, C_6D_6): δ (ppm) = 4.27−4.13 (m, 4 H, cp), 3.97 (d, 7 H, cp and CH_2-cp), 3.48−3.43 (dd, 1 H, CHCH*H*O), 3.20−3.14 (dd, 1 H, CHC*H*HO), 2.87 (q, 1 H, methine), 2.29−2.17 (m, 2 H, epoxide). The synthetic strategy is shown in Scheme 2. For a detailed assignment of the signals compare Figure 1 and Figures S1−S5 in the Supporting Information.

Scheme 2. Sequence for the Synthesis of the Novel Epoxide Monomer Ferrocenyl Glycidyl Ether (1, fcGE)

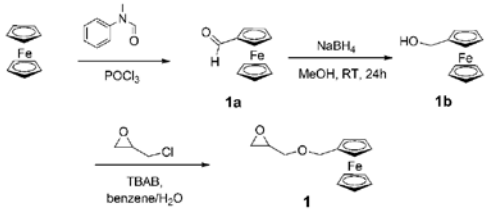

General Procedure for the Copolymerization of fcGE with EO: (P(EO-co-fcGE). Methoxyethanol and 0.9 equiv of cesium hydroxide monohydrate were placed in a 250 mL Schlenk flask, and benzene was added. The mixture was stirred at 60 °C under an argon atmosphere for 1 h and evacuated at 60 °C (10^{-2} mbar) for 12 h to remove benzene and water to generate the corresponding cesium alkoxide. Subsequently, ~20 mL of dry THF was cryo-transferred into the

dx.doi.org/10.1021/ma302241w | *Macromolecules* XXXX, XXX, XXX−XXX

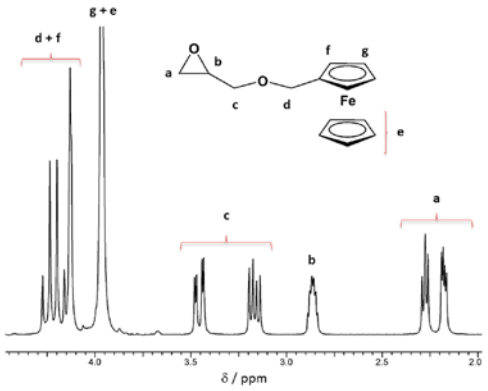

Figure 1. Detailed assignment of ^{1}H NMR resonances of ferrocenyl glycidyl ether (**1**) (measured in benzene-d_6).

Schlenk flask. EO was cryo-transferred to a graduated ampule and then cryo-transferred into the reaction flask containing the initiator in THF. Then, the second comonomer, fcGE, was added via syringe in a 50 wt % solution in anhydrous DMSO. The mixture was heated to 60 °C and stirred for at least 12−24 h. The copolymer solution was dried *in vacuo* and precipitated into cold diethyl ether to remove residual DMSO or dialyzed against deionized water (MWCO 1000 g/mol). The copolymer was obtained as an orange powder or viscous liquid depending on the fc content. Yields: 60−90%. ^{1}H NMR (300 MHz, DMSO-d_6): δ (ppm) = 4.24−4.16 (m, 4 H, cp), 4.07 (d, 7 H, cp and CH_2-cp), 3.68−3.45 (br, polyether backbone), 3.33 (*s*, 3 H, CH_3). For a detailed assignment compare Supporting Information Figure S6.

^{1}H NMR Kinetics. In a conventional NMR tube, a DMSO-d_6 solution of the initiator benzyl alcohol (deprotonated with 0.9 equiv of cesium hydroxide monohydrate) and a mixture of EO and fcGE in DMSO-d_6 were separately frozen under an argon atmosphere. High vacuum was applied, and the tube was flame-sealed while the solutions were kept frozen. To reduce the necessary time for locking and shimming of the polymerization mixture, a sample of the pure monomer mixture was measured in advance at the relevant temperature. Immediately after melting and mixing, the first spectrum was recorded. The temperature was kept at 40 °C. Sample spinning was turned off. Intervals between two measurements were 30 s (see also Figure S7).

Cell Viability Studies. The effect of fc-containing PEG copolymers on the viability of a human cervical cancer cell line (HeLa cells) was measured with a commercial luminescence assay CellTiter-Glo (Promega, Germany). The assay was based on the enzymatic reaction of luciferase transferring luciferin and ATP, supplied by the living cells, to oxyluciferin, resulting in luminescence. The luminescence is used as a measure of cell proliferation and cytotoxicity.

HeLa cells were cultured in Dulbeccós modified eagle medium (DMEM), supplemented with 10% FCS, 100 units penicillin, and 100 mg mL^{-1} streptomycin, 2 × 10^{-3} M L-glutamine (all from Invitrogen, Germany). Cells were grown in a humidified incubator at 37 °C and 5% CO_2. For determining the cell viability, HeLa cells were seeded at a density of 20 000 cells cm^{-2} (6 × 10^4 cells mL^{-1}) in 96-well plates (black, opaque-walled, Corning, Netherlands). FcGE copolymers (100 mg/mL) were dissolved in sterile water (Ampuwa , pH 7.4, Fresenius Kabi, Germany), and the indicated concentrations were produced by a serial dilution in cell culture medium (DMEM, 10% FCS). After 24 h, the culture medium was replaced by fcGE copolymer supplemented medium (200 μL, DMEM, 10% FCS) or medium without compound (DMEM, 10% FCS) as a specific control for 100% cell viability. The cells were treated for 24 or 48 h, and the number of viable cells was determined by the CellTiter-Glo assay following the manufacturer's instructions. Briefly, cell culture medium with compound was replaced by 100 μL CellTiter-Glo reagent. The 96-well plates were mixed for 2 min and incubated for 10 min at room temperature. During this time, the cytosolic ATP was released for the enzymatic reaction. The luminescence was detected with a plate reader (Infinite M1000, Tecan, Germany) using i-control software (Tecan, Germany). The values represent the mean ± SD of four replicates and were plotted relative to the untreated cells.

RESULTS AND DISCUSSION

A. Monomer and Polymer Synthesis. Water-soluble fc-containing (co)polymers with aliphatic polyether backbone are of interest for sensing, electrochemical, or potentially also biomedical fields and many other applications. The incorporation of fc into a water-soluble polymer backbone (viz. PEG) has been targeted by oxyanionic copolymerization of the newly designed monomer (**1**) with EO. The resulting copolymers were studied with respect to preservation of the metallocene during the anionic ring-opening polymerization of the oxirane. The monomer (fcGE, **1**) was synthesized in a three-step protocol (Scheme 2), starting with a Vilsmeier synthesis to generate ferrocenecarboxaldehyde (**1a**). The aldehyde was reduced into the corresponding alcohol (ferrocenemethanol (**1b**)) with $NaBH_4$, which was subsequently used in a phase-transfer-catalyzed nucleophilic substitution reaction with epichlorohydrin to yield fcGE similar to the synthetic protocols of other previously described glycidyl ethers (GEs)[34,35] (note: **1a** and **1b** are also commercially available). The monomer was obtained in overall good yields (up to 80%) and purified by column chromatography.

Figure 1 shows the ^{1}H NMR spectrum of **1** in benzene-d_6 (Figure S1 shows the ^{1}H NMR in DMSO-d_6). Unequivocal signal assignments were obtained using 2D NMR techniques (Figures S3−S5). ^{13}C NMR spectra with the respective assignments can also be found in the Supporting Information (Figure S2).

The (co)polymer synthesis was carried out similar to previous works on poly(ether) copolymers.[36−39] The cesium salt of methoxyethanol was used as the respective initiator, and a mixture of THF and DMSO as well as a reaction time of 12−24 h were found to represent the best suited polymerization conditions with respect to complete conversion. When exceeding an fc content of 10% incorporation into the PEG backbone, the copolymers were no longer soluble in water (at room temperature); therefore, the focus was placed on copolymers with limited fc content in the current work to obtain hydrophilic materials and to guarantee a certain degree of aqueous solubility. The homopolymer of fcGE is insoluble in water. All polymers synthesized in this study exhibited narrow molecular weight distributions (in the range of M_w/M_n = 1.07−1.20, compare Table 1) and monomodal SEC traces (compare Figure 2). This confirms that fc is stable toward the highly basic conditions applied during the anionic polymerization, and no undesired side reactions that would lead to cross-linking, occur. UV/vis spectra (Supporting Information) also prove the incorporation of fc with the characteristic absorption band at ca. 450 nm. The stability of fc during polymerization may be expected, since other fc-based monomers have also been used in (carb)anionic polymerizations in recent works.[12]

Molecular weights of the (co)polymers as well as the comonomer content were determined by ^{1}H NMR spectroscopy and are in agreement with theory. The methyl group of the initiator (at 3.28 ppm) can be used as a reference signal and

Table 1. Molecular Weight Data for the Ferrocene-Containing (Co)polymers Synthesized in This Study by Anionic ROP

no.	formula[a]	fcGE/(fcGE + EG) (%)	M_n[a] (g/mol)	M_n[b] (g/mol)	PDI[b]
P1	MeOP(EG_{99}-*co*-$fcGE_3$)	2.8	5200	4700	1.10
P2	MeOP(EG_{193}-*co*-$fcGE_6$)	2.9	10200	8100	1.20
P3	MeOP(EG_{64}-*co*-$fcGE_4$)	6.3	3900	2600	1.07
P4	MeOP(EG_{73}-*co*-$fcGE_6$)	7.1	4800	2200	1.14
P5	MeOP(EG_{36}-*co*-$fcGE_4$)	9.5	2500	2300	1.16
P6	MeOP(EO_{50}-*co*-$fcGE_6$)	10.6	3850	2100	1.10
P7	MeOP(EG_{28}-*co*-$fcGE_{11}$)	28	4200	2200	1.15
P8	MeOP($fcGE)_{17}$	100	4800	1300	1.17

[a]Determined via end-group analysis from ^{1}H NMR spectroscopy in DMSO-d_6. [b]Determined from size exclusion chromatography in DMF vs PEG standards using the RI-signal detection.

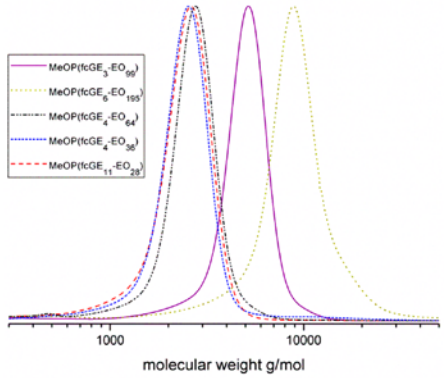

Figure 2. SEC traces (DMF, RI detection, 1 mL/min, 40 °C) of different P(EG-*co*-fcGE) copolymers, showing monomodal molecular weight distributions and low PDIs. Characterization data are summarized in Table 1.

is compared to the integral of the resonances of the polyether backbone between 3.68 and 3.45 ppm as well as the signals resulting from the cyclopentadienyl (cp) rings of fc at 4.24–4.16 and 4.07 ppm (Figure S6). The determined molecular weights correspond to the theoretical values based on the amount of initiator employed and are in good agreement with the conditions for a living anionic polymerization even with the sterically demanding fcGE.

The comonomer distribution and microstructure of the copolymer chains can be determined via the triad sequence distribution from ^{13}C NMR spectroscopy with different amounts of fcGE incorporated into the PEG backbone (Figure 3). For abbreviations, EO units are named "E", while the glycidyl ether signals of fcGE are named "G"; other carbon centers stemming from the cyclopentadienyl groups are marked with an "fc". The hompolymer of fcGE (100% in Figure 3, P8) allowed for the signal assignment of the GGG triad. For the copolymers, it can be clearly detected that the integral of the EEE triad decreases with increasing amount of fcGE incorporated (signal EEE, Figure 3). In addition, the resonance for the tertiary carbon of fcGE (b′) is detected at 78.3 ppm for the homopolymer (GGG), while the copolymers show additional signals, i.e., the EGE triad at ca. 77.7 ppm and with increasing amount of fcGE also the presence of GGE, EGG, and GGG triads. This effect is also visible for the substituted carbon at the cp ring (at ca. 85 ppm) that splits up for higher comonomer content (see Supporting Information). The triad sequence distribution indicates random incorporation of fcGE into the PEG backbone.

An overview of all polymer samples prepared is given in Table 1. A comparison of the molecular weights determined via end-group analysis from ^{1}H NMR spectroscopy and SEC measurements shows a considerable difference of the two values. This can be ascribed to the high molecular weight of the fc side chains changing the hydrodynamic radii during the SEC experiment only slightly compared to PEG. Thus, calibration vs linear PEG standards underestimates the molecular weights. In most of the cases an increasing content of fcGE in the copolymer leads to an increasing deviation during the SEC experiment. This effect was already observed for other P(EG-*co*-glycidyl ether) copolymers.[40] SEC equipped with a UV detector also confirms the incorporation of fc, as all polymers exhibit a strong absorption and are yellow to orange materials.

MALDI ToF mass spectrometry gives further insight into the copolymer microstructure. The MALDI ToF spectrum of the fcGE homopolymer shows a single distribution with a distance of 272 Da for the monomer (see Figure S15). For the copolymers, MALDI ToF mass spectrometry reveals the incorporation of both monomers into the polymer (Figure 4). A linear combination of the molecular weights of both monomers can be detected throughout the whole apparent molecular weight distribution (also compare Figure S8), as expected for a copolymer (M(EO) = 44 Da, M(fcGE) = 272 Da), supporting the incorporation of the two monomers into the polymer backbone.

Copolymerization Kinetics via ^{1}H NMR Spectroscopy. To confirm the random nature of the copolymerization of EO and fcGE in the anionic polymerization, ^{13}C NMR triad statistics has been determined (see above), and further detailed characterization of the evolution of the copolymer structure during the reaction was carried out, following the polymerization kinetics via *in situ* ^{1}H NMR spectroscopy. An experimental procedure[36] recently developed in our group was adapted for the comonomer pair EO/fcGE. Briefly, a DMSO-d_6 solution of the initiator and a mixture of fcGE (10 mol %) and EO (90 mol %) in DMSO-d_6 were separately transferred into a NMR tube under an argon atmosphere and quickly frozen with liquid nitrogen cooling. The cold NMR tube was evacuated and flame-sealed, and the polymerization was subsequently initiated by warming the tube to 40 °C in the NMR spectrometer. The growth of the polymer backbone as well as the consumption of both monomers was followed *in situ* by the decrease of the epoxide signals located at 2.61 ppm for the methylene protons of EO and at 3.07 ppm for the methine proton of fcGE, respectively (compare Figure S7). All signals are normalized to the 11 protons of the ferrocenyl methyl moiety (d–g) that remain constant during the reaction. Because of the overlap of the EO proton signal with the fcGE proton a (cf. Figures S1 and S7) and the residual DMSO signal, the value has to be corrected with the corresponding peak intensities. The intensity of the DMSO peak was determined from the last spectra recorded in which all EO and fcGE had reacted, and therefore no superposition of the mentioned peaks was observed, allowing the determination of the absolute value for the DMSO integral.

dx.doi.org/10.1021/ma302241w | *Macromolecules* XXXX, XXX, XXX−XXX

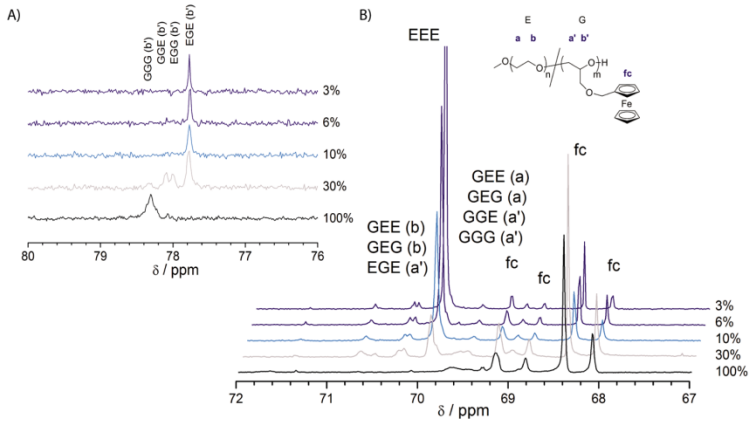

Figure 3. Zoom into typical ^{13}C NMR spectra of several copolymers of ethylene oxide and ferrocenyl glycidyl ether and the homopolymer of ferrocenyl glycidyl ether (in DMSO-d_6). The triad signals are highlighted, indicating a random distribution of ferrocenyl glycidyl ether units at the PEG backbone.

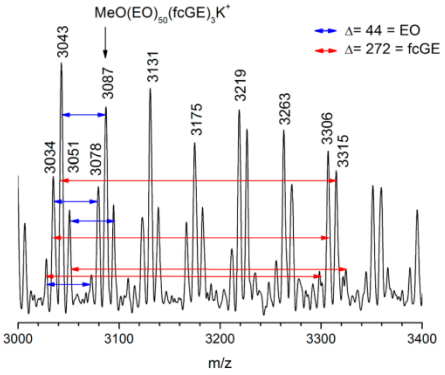

Figure 4. Zoom-in of the MALDI-ToF mass spectrum of sample **P7** showing linear combinations of the molecular masses of both comonomers (ethylene oxide M = 44 Da and ferrocenyl glycidyl ether M = 272 Da) proving that both are incorporated into the copolymer.

f5

Figure 5a shows a representative example for the monomer conversion in the course of the polymerization with comonomer content of 10% fcGE. The copolymerization at 40 °C requires ~8 h to completion. From earlier copolymerization studies it is known that the relative reactivity of the comonomers is independent of the temperature.[35,36]

Figure 5b illustrates the evolution of monomer feed composition during polymerization, revealing concurrent incorporation of fcGE and EO into the growing polymer chain during the whole reaction time. Throughout the polymerization, the molar ratio of fcGE and EO units in the polymer chain remains constant, and there is no deviation from the initial ratio of the comonomer feed. Unexpectedly, the sterically demanding fc moiety does not lower the reactivity of the glycidyl ether structure. This evidence unambiguously the formation of random copolymers of EO and fcGE by anionic

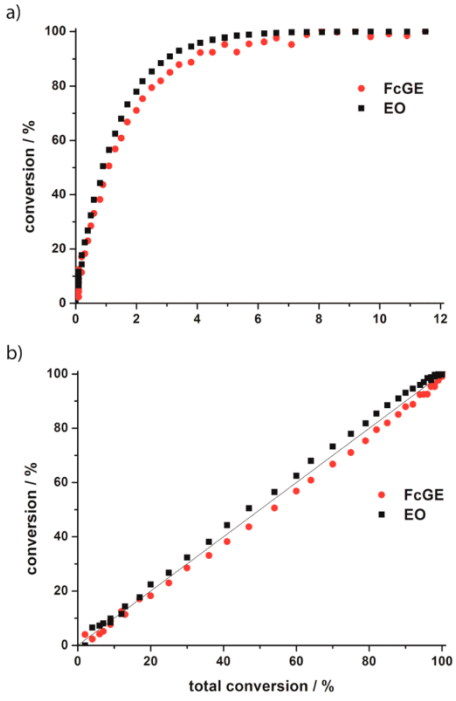

Figure 5. (a) Monomer conversion versus time plot for copolymerization of EO with fcGE ether (10%) at 40 °C measured via ^1H NMR kinetics in DMSO-d_6. (b) Percentage of monomer conversion of EO and fcGE versus total monomer conversion for copolymerization at 40 °C measured via ^1H NMR kinetics in DMSO-d_6.

dx.doi.org/10.1021/ma302241w | Macromolecules XXXX, XXX, XXX−XXX

copolymerization under the copolymerization conditions studied and is in line with the results of the microstructure characterization, i.e., the triad analysis described before.

B. Materials Properties of the PEG-*co*-PfcGE Copolymers. *Thermal Analysis.* Thermal analysis of all copolymers was carried out using differential scanning calorimetry (DSC). The copolymers prepared in this study show variable molecular weight which has to be taken into account when analyzing the results. Most of the samples, however, have a molecular weight (as determined by NMR) of around 5000 g/mol, making a comparison possible and also the other samples with different molecular weight and chain length still follow the expected trends (the results are summarized in Table 2): (1) The glass

Table 2. Thermal Data of the Copolymers Synthesized in This Study As Determined via Differential Scanning Calorimetry (DSC)

no.	formula	fcGE/(fcGE + EO) (%)	T_g[a] (°C)	T_m[b] (°C)	ΔH[c] (J/g)
P1	MeOP(EG$_{98}$-*co*-fcGE$_3$)	2.8	−56	43	82
P2	MeOP(EG$_{195}$-*co*-fcGE$_6$)	2.9	−54	42	72
P3	MeOP(EG$_{61}$-*co*-fcGE$_4$)	6.3	−56	27	48
P4	MeOP(EO$_{73}$-*co*-fcGE$_6$)	7.1	−58	16	27
P5	MeOP(EG$_{36}$-*co*-fcGE$_4$)	9.5	−59	14	40
P6	MeOP(EO$_{50}$-*co*-fcGE$_6$)	10.6	−51	8	6
P7	MeOP(EG$_{28}$-*co*-fcGE$_{11}$)	28	−49		

[a]Glass transition temperature T_g. [b]Melting temperature T_m. [c]Melting enthalpy determined by integration of the melting peak.

transition temperatures (T_g) for most copolymers determined are close to the value of PEG (−56 °C) because these copolymers consist of a major fraction of PEG. Only in the case of copolymers **P6** and **P7**, a slight increase of the T_g can be observed (which could be also attributed to a different chain length and molecular weight). These rather low T_g's, however, can be attributed to the aliphatic polyether backbone structure with its high flexibility, resulting in amorphous, low-T_g materials, even with a high fc content. (2) Considering the melting behavior of the copolymers, a clear trend is observed. PEG is a crystalline material with a melting temperature of 65 °C.[41] The degree of crystallization of the copolymers is gradually lowered with increasing incorporation of the comonomer, since the fc side chains disturb the crystallization of the PEG domains. This is also visible with the naked eye, as the copolymers are either obtained as orange powders for low fc content or deep orange, sticky solids for higher amounts of fcGE or the poly(fcGE) homopolymer. In a previous work it was estimated that ~13 adjacent EO units are needed (i.e., PEG with a molecular weight of 600 g/mol)[35,42] to observe crystallization in random PEG copolymer structures, which is still the case for copolymer **P5** (with an average of ca. 10 adjacent EO units) but not observable for copolymer **P7**. An incorporation of 28% of comonomer is required to completely suppress the crystallization of the PEG chains. The gradual change of the thermal behavior of the copolymers mirrors the random comonomer distribution in the polymer backbone in addition to the NMR kinetics and the triad abundance observed in ^{13}C NMR spectra.

Lower Critical Solution Temperature (LCST) Behavior. Very recently, we have been able to demonstrate that different copolymers based on EO and varied concentration of hydrophobic glycidyl ether comonomers exhibit tunable thermoresponsive behavior over a broad temperature range.[31] It was demonstrated that the LCST can be varied by two different parameters, the first (i) being the comonomer hydrophobicity and the second (ii) the comonomer content. With increasing content of hydrophobic comonomer and with increasing hydrophobicity of the comonomer the LCST is lowered gradually, as it is expected. Also for the herein reported fcGE copolymers an LCST behavior was detected. All polymers were investigated at a concentration of 5 g/L, and the results are summarized in Table 3. The cloud points of the aqueous

Table 3. Lower Critical Solution Temperature Values of Different P(EO-*co*-fcGE) Copolymers Determined by Turbidity Measurements

no.	formula[a]	fcGE/(fcGE + EO)[a] (%)	LCST[b] (°C)
P1	MeOP(EG$_{98}$-*co*-fcGE$_3$)	2.8	82.2
P2	MeOP(EG$_{195}$-*co*-fcGE$_6$)	2.9	69.1
P3	MeOP(EG$_{61}$-*co*-fcGE$_4$)	6.3	61.8
P4	MeOP(EO$_{73}$-*co*-fcGE$_6$)	7.1	37.7
P5	MeOP(EG$_{36}$-*co*-fcGE$_4$)	9.5	50.0
P6	MeOP(EO$_{50}$-*co*-fcGE$_6$)	10.6	7.2
P7	MeOP(EG$_{28}$-*co*-fcGE$_{11}$)	28	
P8	MeOP(fcGE)$_{17}$	100	

[a]Obtained from ^{1}H NMR spectroscopy. [b]For a 5 mg mL^{-1} solution of the copolymer in deionized water.

polymer solutions have been measured by monitoring the transmittance of a light beam (wavelength 632 nm) through a 1 cm quartz sample cell at a heating (cooling) rate of 1 °C min^{-1}. The cloud point temperatures of the very sharp transitions from translucent to opaque solutions were defined as the value measured at 50% transmittance. The respective graphs of the turbidimetry measurements can be found in the Supporting Information (Figure S9).

The LCST values of different copolymers with similar molecular weights have been plotted against the comonomer content. A linear relationship between comonomer content and cloud point is observed. A comparison of the slope of the fitted line with the values from the literature[31] indicates the degree of hydrophobicity of fcGE compared to other glycidyl ethers. It was found that the slope of the line and therefore the hydrophobicity of ferrocenyl glycidyl ether are situated between ethoxy vinyl glycidyl ether[35] and dibenzylamino gycidol.[31,36] Furthermore, it was found that in the case of perfectly random copolymers the interception with the *y*-axis is situated at around 100 °C, as it is also present in PEG homopolymers (Figure S10). For the fcGE-containing copolymers the interception was found to be at 94 ± 6 °C, which again suggests a random distribution of fcGE units in the chain, as proven by NMR studies (see above). The LCST for the P(EG-*co*-fcGE) copolymers could be varied from 82.2 °C for 2.8% fcGE to 7.2 °C for 10.6% incorporation (at similar molecular weights). It has to be kept in mind that the LCST of a polymer also depends on the molecular weight.[43] This effect is also detectable in the investigated copolymer library. For example, for polymers **P1** and **P2** the fcGE content is almost the same; however the LCST of **P3** (M_n(NMR) = 10 200 g/mol) is with 69.1 °C much lower than for **P1** with 82.2 °C having ca. half of the molecular weight (M_n (NMR) = 5200 g/mol).

In contrast to all other PEG copolymers investigated before, fc-containing PEGs offer a further possibility to tune the cloud points of a given polymer by an external stimulus. This was

demonstrated with two different experiments: First, fine-tuning of the LCST was achieved by supramolecular complexation and, second, by using the redox properties of fc.

It is well-known from the literature that β-cyclodextrin (β-CD)[43] forms inclusion complexes with fc which should be also generated upon the addition of β-CD to the herein presented copolymers. The addition of β-CD led to a shift of the respective LCST to slightly higher values due to the presence of the hydrophilic β-CD. For **P3**, for example, an increase of the LCST from 61.8 to ca. 68 °C was observed. This unexpected small influence on the cloud point (increase by ca. 5 °C) can most probably be ascribed to the temperature dependence of this host−guest complex[44] as well as to steric reasons (experimental results in the Supporting Information, Figure S11).[45] However, the host−guest complexation without a significant influence on the LCST could be used to tailor micellization or to attach dyes or labels in a noncovalent manner; this is currently under further investigation.

In a second approach, the influence of the oxidation of the fc moieties on the LCST was investigated. A strong influence on the LCST was observed after the oxidation to the poly(ferrocenium)-PEGs with silver(I) triflate ($AgCF_3SO_3$). Upon addition of the oxidizing agent, the yellow color vanished and a greenish to blue solution resulted, depending on the amount of oxidizing agent (compare Figure S12) and the formation of silver(0). After filtration from the precipitate, the clear solutions were measured in turbidimetry experiments. With increasing fc-oxidation level, higher LCST values were detected, until finally a fully water-soluble polymer without LCST behavior was obtained (compare Figure 6). Finally, this effect is reversible by

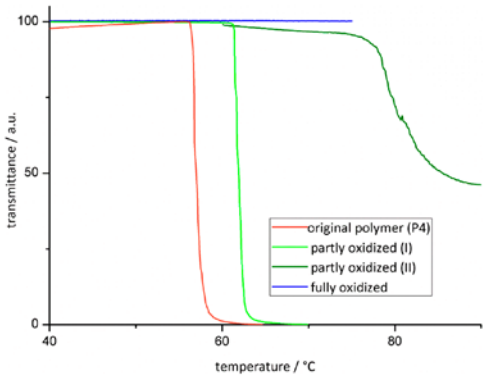

Figure 6. Turbidity measurements of **P5** upon oxidation. By the addition of oxidizing agents the LCST of the starting polymer (P5, red) can be altered (green) until finally the thermoresponsive behavior disappears (blue).

the reduction of the iron center using sodium thiosulfate ($Na_2S_2O_3$). The LCST values obtained after reduction reached similar values as for the pristine solutions, although it is important to mention that the salt concentration may have an influence on the absolute LCST ("salting out effect").[46] Intense studies on the direct correlation of the oxidation state and the LCST behavior are currently under way.

Cyclic Voltammetry Measurements. Fc can be oxidized reversibly by applying a cyclic potential, and this redox-active behavior can be studied by cyclic voltammetry.[47] We investigated two copolymers with different fc content with cyclic voltammetry. The copolymer samples **P1** and **P7** with the lowest and the highest amount of fc incorporated have been dissolved in dichloromethane with 0.1 M conducting salt (tetrabutylammonium hexafluorophosphate) at a concentration of 5 g/L. Figure 7 shows the cyclic voltammogram of both

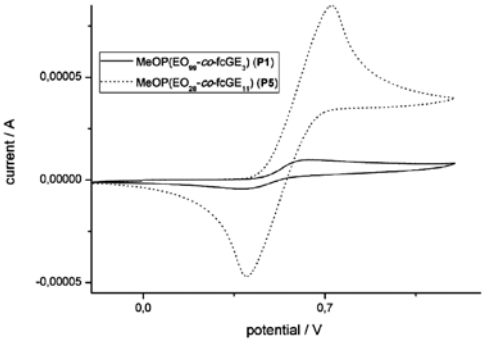

Figure 7. Cyclic voltammogram of **P1** and **P7** at a scan rate of 0.5 V/s.

polymers at a scan rate of 0.5 V/s. It can be seen that at a similar weight fraction (targeted: 5 mg/mL) different maximum currents can be detected. For **P1**, 5 g/L correspond to 2.9×10^{-6} mol of fc units/mL, while for **P7** 5 g/L correspond to 1.31×10^{-5} mol of fc units/mL, which is in accordance with the different maximum currents observed. Another important information that can be obtained from the cyclic voltammogram is that in this case oxidation is a homogeneous process, and no stepwise oxidation is observed, as for example reported for poly(ferrocenylsilane)s; i.e., the fc units are separated and do not communicate.[48]

C. Cell Viability Studies. Cell viability of the PEG copolymers represents an important feature of the materials properties with respect to potential applications in the biomedical field. PEG is used in many biomedical applications due to its low toxicity and immunogenicity. Further, it was shown recently that many P(EG-*co*-GE)s exhibit similarly low toxicity as PEG.[49] In this context we were interested in the effect of the fc moieties at the PEG backbone on the cytotoxicity of these materials, since ferrocenium salts are known to be cytostatic and have recently been investigated with respect to their potential use in anticancer therapy.[50,51]

The toxicity of the P(EG-*co*-fcGE) copolymers was investigated against a human cervical cancer cell line (HeLa) from a concentration range of 1−1000 μg mL^{-1} by measuring the ATP content of viable cells in relation to untreated cells. The results are displayed in Figure 8. While the two copolymers with less than 5 mol % fcGE units showed good biocompatibility comparable to the PEG homopolymer, the two copolymers with higher fcGE incorporation (6.3 and 9.5%) are clearly cytotoxic for concentrations exceeding 10 μg mL^{-1}.

With respect to biomedical applications these novel water-soluble polymers might be interesting for PEGylation[52]-like applications, enabling tracking of the polymer molecules due to the fc moieties, provided polymers with low iron content and low toxicity are used. In contrast, copolyethers with high ferrocene content might be interesting for applications as

dx.doi.org/10.1021/ma302241w | Macromolecules XXXX, XXX, XXX−XXX

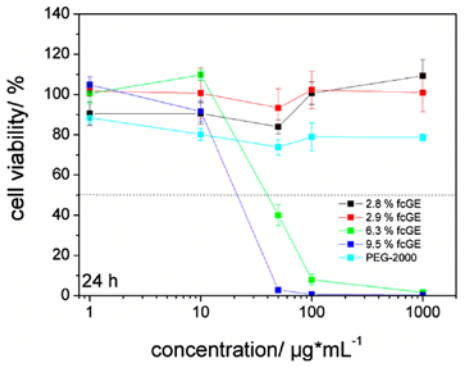

Figure 8. Cell viability of HeLa cells treated with fc-containing PEG copolymers after 24 h of incubation. Untreated cells were set to 100%. The experiment was carried out as four independent replicates.

polymeric cytotoxic agents. Further studies of this issue are in progress and will be reported soon.

■ CONCLUSION

A new ferrocene-containing epoxide monomer, namely ferrocenyl glycidyl ether, has been prepared, and its homo- and copolymerization behaviors with ethylene oxide have been studied. This represents the first synthesis ferrocene-containing polyether structures via anionic polymerization and of water-soluble polyether-based ferrocene containing polymer with a PEG-like structure. Homopolymerization of the sterically demanding fcGE was accomplished, and also anionic *co*-ROP of EO and the fcGE monomer, affording random copolymers with narrow molecular weight distributions, have been established. The random microstructure of the materials is supported by detailed kinetic characterization data of the polymerization with *in situ* ^{1}H NMR spectroscopy and further triad sequence analyses via ^{13}C NMR. The novel monomer fcGE broadens the field of ferrocene-containing monomers and polymers toward polyethers and may be viewed as the first epoxide analogue of vinylferrocene. Further, the thermal properties also support random incorporation of fcGE into the PEG backbone. As expected, the degree of crystallization is reduced with increasing fcGE content. The homopolymer of fcGE is an amorphous material. The copolymers exhibit thermoresponsive behavior in water with tunable LCSTs in the range 82.2 to 7.2 °C. The LCST can be further tailored either by the addition of β-cyclodextrin to form inclusion complexes or by oxidation/reduction of the fc moieties.

The cytotoxicity of these materials has been investigated against HeLa cells. It was found that for a low amount of fc moieties (ca. 3%) the polymers are comparable to PEG in their toxicity, while higher fc concentrations lead to strongly cytotoxic behavior. We believe that these PEG-derived copolymers with pending ferrocene units possess intriguing potential for application in various fields, e.g., for sensing, detection, and as potential polymer therapeutics, as one can easily detect the iron centers of the ferrocene unit.

■ ASSOCIATED CONTENT

Supporting Information

Figures S1−S15. This material is available free of charge via the Internet at http://pubs.acs.org.

■ AUTHOR INFORMATION

Corresponding Author

*E-mail wurm@mpip-mainz.mpg.de, Ph 0049 6131 379 502, Fax 0049 6131 370 330.

Notes

The authors declare no competing financial interest.

■ ACKNOWLEDGMENTS

C.T. is recipient of a fellowship through funding of the German Excellence Initiative (DFG/GSC 266). M.S. and C.D. are grateful to the Max Planck Graduate Center with the Johannes Gutenberg-Universität Mainz (MPGC) for fellowships and financial support. H.F. acknowledges the Fonds der Chemischen Industrie and the SFB 625 for support. F.W. thanks the Alexander-von-Humboldt foundation for a fellowship.

■ REFERENCES

(1) Nguyen, P.; Gomez-Elipe, P.; Manners, I. *Chem. Rev.* **1999**, *99* (6), 1515−1548.
(2) Frede, M.; Steckhan, E. *Tetrahedron Lett.* **1991**, *32* (38), 5063−5066.
(3) Arimoto, F. S.; Haven, A. C. *J. Am. Chem. Soc.* **1955**, *77* (23), 6295−6297.
(4) Eloi, J.-C.; Rider, D. A.; Cambridge, G.; Whittell, G. R.; Winnik, M. A.; Manners, I. *J. Am. Chem. Soc.* **2011**, *133* (23), 8903−8913.
(5) Durkee, D. A.; Eitouni, H. B.; Gomez, E. D.; Ellsworth, M. W.; Bell, A. T.; Balsara, N. P. *Adv. Mater.* **2005**, *17* (16), 2003−2006.
(6) Wright, M. E.; Toplikar, E. G.; Kubin, R. F.; Seltzer, M. D. *Macromolecules* **1992**, *25* (6), 1838−1839.
(7) Top, S.; Dauer, B. n. d.; Vaissermann, J.; Jaouen, G. R. *J. Organomet. Chem.* **1997**, *541* (1−2), 355−361.
(8) Top, S.; Vessières, A.; Leclercq, G.; Quivy, J.; Tang, J.; Vaissermann, J.; Huché, M.; Jaouen, G. *Chem.—Eur. J.* **2003**, *9* (21), 5223−5236.
(9) Foulds, N. C.; Lowe, C. R. *Anal. Chem.* **1988**, *60* (22), 2473−2478.
(10) Rehahn, M. Organic-Inorganic Hybrid Polymers. In *Synthesis of Polymers*; Schlüter, A.-D., Ed.; Wiley-VCH: Weinheim, Germany, 1999; p 319.
(11) Gallei, M.; Schmidt, B. V. K. J.; Klein, R.; Rehahn, M. *Macromol. Rapid Commun.* **2009**, *30* (17), 1463−1469.
(12) Gallei, M.; Klein, R.; Rehahn, M. *Macromolecules* **2010**, *43* (4), 1844−1854.
(13) Gallei, M.; Tockner, S.; Klein, R.; Rehahn, M. *Macromol. Rapid Commun.* **2010**, *31* (9−10), 889−896.
(14) Foucher, D. A.; Tang, B. Z.; Manners, I. *J. Am. Chem. Soc.* **1992**, *114* (15), 6246−6248.
(15) Manners, I. *Can. J. Chem.* **1998**, *76* (4), 371−381.
(16) Wang, Z.; Masson, G.; Peiris, F. C.; Ozin, G. A.; Manners, I. *Chem.—Eur. J.* **2007**, *13* (33), 9372−9383.
(17) Pittman, C. U.; Lai, J. C.; Vanderpool, D. P. *Macromolecules* **1970**, *3* (1), 105−107.
(18) Pittman, C. U.; Hirao, A. *J. Polym. Sci., Polym. Chem. Ed.* **1977**, *15* (7), 1677−1686.
(19) Pittman, C. U.; Hirao, A. *J. Polym. Sci., Polym. Chem. Ed.* **1978**, *16* (6), 1197−1209.
(20) Herfurth, C.; Voll, D.; Buller, J.; Weiss, J.; Barner-Kowollik, C.; Laschewsky, A. *J. Polym. Sci., Part A: Polym. Chem.* **2012**, *50* (1), 108−118.
(21) Wurm, F.; Villanueva, F. J. L.; Frey, H. *J. Polym. Sci., Part A: Polym. Chem.* **2009**, *47* (10), 2518−2528.

(22) Hale, P. D.; Boguslavsky, L. I.; Inagaki, T.; Lee, H. S.; Skotheim, T. A.; Karan, H. I.; Okamoto, Y. *Mol. Cryst. Liq. Cryst.* **1990**, *190* (1), 251−258.

(23) Swarts, J. C. *Macromol. Symp.* **2002**, *186* (1), 123−128.

(24) Wang, X.-S.; Winnik, M. A.; Manners, I. *Macromol. Rapid Commun.* **2002**, *23* (3), 210−213.

(25) Gohy, J.-F.; Lohmeijer, B. G. G.; Alexeev, A.; Wang, X.-S.; Manners, I.; Winnik, M. A.; Schubert, U. S. *Chem.—Eur. J.* **2004**, *10* (17), 4315−4323.

(26) Resendes, R.; Massey, J.; Dorn, H.; Winnik, M. A.; Manners, I. *Macromolecules* **2000**, *33* (1), 8−10.

(27) Tonhauser, C.; Mazurowski, M.; Rehahn, M.; Gallei, M.; Frey, H. *Macromolecules* **2012**, *45* (8), 3409−3418.

(28) Power-Billard, K. N.; Manners, I. *Macromolecules* **1999**, *33* (1), 26−31.

(29) Power-Billard, K. N.; Spontak, R. J.; Manners, I. *Angew. Chem., Int. Ed.* **2004**, *43* (10), 1260−1264.

(30) Yang, W.; Zhou, H.; Sun, C. *Macromol. Rapid Commun.* **2007**, *28* (3), 265−270.

(31) Mangold, C.; Obermeier, B.; Wurm, F.; Frey, H. *Macromol. Rapid Commun.* **2011**, *32* (23), 1930−1934.

(32) Schattling, P.; Jochum, F. D.; Theato, P. *Chem. Commun.* **2011**, *47*, 31.

(33) Broadhead, G. D.; Osgerby, J. M.; Pauson, P. L. *J. Chem. Soc.* **1958**, 650−656.

(34) Wurm, F.; Nieberle, J.; Frey, H. *Macromolecules* **2008**, *41* (6), 1909−1911.

(35) Mangold, C.; Dingels, C.; Obermeier, B.; Frey, H.; Wurm, F. *Macromolecules* **2011**, *44* (16), 6326−6334.

(36) Obermeier, B.; Wurm, F.; Frey, H. *Macromolecules* **2010**, *43* (5), 2244−2251.

(37) Mangold, C.; Wurm, F.; Obermeier, B.; Frey, H. *Macromolecules* **2010**, *43* (20), 8511−8518.

(38) Mangold, C.; Wurm, F.; Obermeier, B.; Frey, H. *Macromol. Rapid Commun.* **2010**, *31* (3), 258−264.

(39) Obermeier, B.; Frey, H. *Bioconjugate Chem.* **2011**, *22* (3), 436−444.

(40) Obermeier, B.; Wurm, F.; Mangold, C.; Frey, H. *Angew. Chem., Int. Ed.* **2011**, *50* (35), 7988−7997.

(41) Fuller, C. S. *Chem. Rev.* **1940**, *26* (2), 143−167.

(42) Henning, T. *SOFW J.* **2001**, *127*, 28−35.

(43) Zhang, Y.; Furyk, S.; Sagle, L. B.; Cho, Y.; Bergbreiter, D. E.; Cremer, P. S. *J. Phys. Chem. C* **2007**, *111* (25), 8916−8924.

(44) Rekharsky, M. V.; Inoue, Y. *Chem. Rev.* **1998**, *98* (5), 1875−1918.

(45) Giannotti, M.; Lv, H.; Ma, Y.; Steenvoorden, M.; Overweg, A.; Roerdink, M.; Hempenius, M.; Vancso, G. *J. Inorg. Organomet. Polym. Mater.* **2005**, *15* (4), 527−540.

(46) Zhang, Y.; Furyk, S.; Bergbreiter, D. E.; Cremer, P. S. *J. Am. Chem. Soc.* **2005**, *127* (41), 14505−14510.

(47) Rulkens, R.; Lough, A. J.; Manners, I.; Lovelace, S. R.; Grant, C.; Geiger, W. E. *J. Am. Chem. Soc.* **1996**, *118* (50), 12683−12695.

(48) Whittell, G. R.; Manners, I. *Adv. Mater.* **2007**, *19* (21), 3439−3468.

(49) Mangold, C.; Richard, O.; Frey, H.; Wurm, F. M.; Wurm, F. Submitted, 2012.

(50) Wasczcak, M. D.; Lee, C. C.; Hall, I. H.; Carroll, P. J.; Sneddon, L. G. *Angew. Chem.* **1997**, *109* (20), 2300−2302.

(51) Köpf-Maier, P.; Köpf, H.; Neuse, E. W.; Köpf, H. *Angew. Chem.* **1984**, *96* (6), 446−447.

(52) Abuchowski, A.; McCoy, J. R.; Palczuk, N. C.; van Es, T.; Davis, F. F. *J. Biol. Chem.* **1977**, *252* (11), 3582−3586.

A.7 List of Publications

Journal Articles

From Biocompatible to Biodegradable: Poly(ethylene glycol)s With In-Chain Cleavable Linkages
C. Dingels, H. Frey, **2012**, *submitted*.

A Universal Concept for the Implementation of a Single Cleavable Unit at Tunable Position in Functional Poly(ethylene glycol)s
C. Dingels, S. S. Müller, T. Steinbach, C. Tonhauser, H. Frey, *Biomacromolecules* **2013**, DOI: 10.1021/bm3016797.

Ferrocenyl Glycidyl Ether: A Versatile Ferrocene Monomer for Copolymerization with Ethylene Oxide to Water-Soluble, Thermo-Responsive Copolymers
C. Tonhauser, A. Alkan, M. Schömer, **C. Dingels**, S. Ritz, V. Mailänder, H. Frey, F. Wurm, M*acromolecules* **2013**, DOI: 10.1021/ma302241w.

Squaric Acid Mediated Chemoselective PEGylation of Proteins: Reactivity of Single-Step Activated α-Amino Poly(ethylene glycol)s
C. Dingels, F. Wurm, M. Wagner, H.-A. Klok, H. Frey, *Chem. Eur. J.* **2012**, *18*, 16828.

Branched Acid-Degradable, Biocompatible Polyether Copolymers via Anionic Ring-Opening Polymerization Using an Epoxide Inimer
C. Tonhauser, C. Schüll, **C. Dingels**, H. Frey, *ACS Macro Lett.* **2012**, *1*, 1094.

N,N-Diallylglycidylamine: A Key Monomer for Amino-Functional Poly(ethylene glycol) Architectures
V. S. Reuss, B. Obermeier, **C. Dingels**, H. Frey, *Macromolecules* **2012**, *45*, 4581.

Squaric Acid Mediated Synthesis and Biological Activity of a Library of Linear and Hyperbranched Poly(Glycerol)-Protein Conjugates
F. Wurm, **C. Dingels**, H. Frey, H.-A. Klok, *Biomacromolecules* **2012**, *13*, 1161.

Die vielen Gesichter des Poly(ethylenglykol)s
C. Dingels, M. Schömer, H. Frey, *Chem. unserer Zeit* **2011**, *45*, 338.

PEG-based Multifunctional Polyethers with Highly Reactive Vinyl-Ether Side Chains for Click-Type Functionalization
C. Mangold, **C. Dingels**, B. Obermeier, H. Frey, F. Wurm, *Macromolecules* **2011**, *44*, 6326.

α,ω_n-Heterotelechelic Hyperbranched Polyethers Solubilize Carbon Nanotubes
F. Wurm, A. M. Hofmann, A. Thomas, **C. Dingels**, H. Frey, *Macromol. Chem. Phys.* **2010**, *211*, 932.

Template Syntheses of Iron(II) Complexes Containing Chiral P-N-N-P and P-N-N Ligands
A. A. Mikhailine, E. Kim, **C. Dingels**, A. J. Lough, R. H. Morris, *Inorg. Chem.* **2008**, *47*, 6587.

Conference Contributions

From Inert to Labile: Well-Defined Functional pH-sensitive Poly(ethylene glycol)s
C. Dingels, S. S. Müller, T. Steinbach, C. Tonhauser, H. Frey
Smart Polymers, Oct 2012, Mainz.

Heterofunctional poly(ethylene glycol)s with a single cleavable moiety for bioconjugation
C. Dingels, C. Mangold, H. Frey, *Polym. Prepr. (Am. Chem. Soc., Div. Polym. Chem.)* **2012**, *53*, 586.
243rd ACS National Meeting & Exposition, Mar 2012, San Diego, CA, United States.

Squaric acid mediated bioconjugation: 20 years after
T. Steinbach, **C. Dingels**, F. Wurm
243rd ACS National Meeting & Exposition, Mar 2012, San Diego, CA, United States.

Novel polyethers carrying multiple vinyl ether side chains rom anionic ring-opening polymerization
C. Mangold, **C. Dingels**, B. Obermeier, F. Wurm, H. Frey
International Symposium on Ionic Polymerization, Jul 2011, Akron, OH, United States.

Synthesis and Characterization of in-chain functionalized amphiphilic block copolymers by anionic polymerization
C. Tonhauser, B. Obermeier, C. Mangold, **C. Dingels**, H. Frey
International Symposium on Ionic Polymerization, Jul 2011, Akron, OH, United States.

Squaric acid ester amido mPEGs: New reagents for the PEGylation of proteins
C. Dingels, F. Wurm, H.-A. Klok, H. Frey, *Polym. Prepr. (Am. Chem. Soc., Div. Polym. Chem.)* **2011**, *52*, 154.
241st ACS National Meeting & Exposition, Mar 2011, Anaheim, CA, United States.